

Synthesis and Reactivity of Hypersilylsilylene and Catalytic Applications of Organosilicon and Lithium Compounds

by
Milan Kumar Bisai

10CC15A26020

A thesis submitted to the
Academy of Scientific & Innovative Research
for the award of the degree of
DOCTOR OF PHILOSOPHY
in
SCIENCE

Under the supervision of
Dr. Sakya Singha Sen



CSIR-National Chemical Laboratory, Pune



Academy of Scientific and Innovative Research
AcSIR Headquarters, CSIR-HRDC campus
Sector 19, Kamla Nehru Nagar,
Ghaziabad, U.P. – 201 002, India

December - 2020

Certificate

This is to certify that the work incorporated in this Ph.D. thesis entitled, “Synthesis and Reactivity of Hypersilylsilylene and Catalytic Applications of Organosilicon and Lithium Compounds” submitted by Milan Kumar Bisai to the Academy of Scientific and Innovative Research (AcSIR) in fulfillment of the requirements for the award of the Degree of the Doctor of Philosophy in Science, embodies original research work carried-out by the student. We, further certify that this work has not been submitted to any other University or Institution in part or full for the award of any degree or diploma. Research material(s) obtained from other source(s) and used in this research work has/have been duly acknowledged in the thesis. Image(s), illustration(s), figure(s), table(s) etc., used in the thesis from other source(s), have also been duly cited and acknowledged.



(Signature of Student)

Milan Kumar Bisai

Date: 07/12/2020



(Signature of Supervisor)

Dr. Sakya Singha Sen

Date: 07/12/2020

STATEMENTS OF ACADEMIC INTEGRITY

I, Milan Kumar Bisai, a Ph.D. student of the Academy of Scientific and Innovative Research (AcSIR) with Registration No. 10CC15A26020 hereby undertake that the thesis entitled “Synthesis and Reactivity of Hypersilylsilylene and Catalytic Applications of Organosilicon and Lithium Compounds” has been prepared by me and that the document reports original work carried out by me and is free of any plagiarism in compliance with the UGC Regulations on “*Promotion of Academic Integrity and Prevention of Plagiarism in Higher Educational Institutions (2018)*” and the CSIR Guidelines for “*Ethics in Research and in Governance (2020)*”.



Signature of the Student

Date : 07/12/2020

Place : Pune

It is hereby certified that the work done by the student, under my/our supervision, is plagiarism-free in accordance with the UGC Regulations on “*Promotion of Academic Integrity and Prevention of Plagiarism in Higher Educational Institutions (2018)*” and the CSIR Guidelines for “*Ethics in Research and in Governance (2020)*”.

NA

Signature of the Co-supervisor (if any)

Name :

Date :

Place :



Signature of the Supervisor

Name : Dr. Sakya Singha Sen

Date : 07/12/2020

Place : Pune

*This dissertation is dedicated to
my beloved parents*



Acknowledgement

The process of earning a doctorate and writing a dissertation is long and arduous, and it is certainly would not have been possible without close association with many people. I take this opportunity to express my deepest gratitude to the people whose immense support made my academic journey successful. However, mentioning is not sufficient to thank them in the right way.

It gives me immense pleasure and pride to express my sincere gratitude and respect to my supervisor, Dr. Sakya Singha Sen, for constant assistance, inspiring guidance, tremendous support, and constructive criticism throughout my Ph.D. journey. I still remember our meeting at the beginning of my research career when I had no clue where my Ph.D. and, consequently, my life is heading. His encouragement and belief in me in that meeting showed a new hope, made me realize that doing a Ph.D. in an uncommon field is not impossible, rather more thrilling. Since that day, my life took a decisive turn and significant boost, I started enjoying my new research area, and I never looked back. I feel incredibly fortunate for the freedom rendered by him in the laboratory to fulfill my dream with proper planning and the research's execution. Again, I will always be an avid fan of his down to earth nature and excellent communication skills.

I want to convey my sincere thanks to my Doctoral Advisory Committee members, Dr. Sapna Rabindranathan, Dr. Kumar Vanka, Dr. Samir H. Chikkali, and Dr. E Balaraman. Their valuable suggestions and encouragement during my Ph.D. helped me to widen my research from various perspectives.

I am grateful to Prof. A. K. Nangia (Director, CSIR-NCL), Prof. S. Pal (Former Director, CSIR-NCL), Dr. D. Srinivas (Former Head, Catalysis and Inorganic Chemistry Division), Dr. C. S. Gopinath (Head, Catalysis and Inorganic Chemistry Division) for giving me this opportunity and providing all necessary infrastructure and facilities to carry out my research work. I want to acknowledge all the support from the office staff of the Catalysis and Inorganic Chemistry Division. I am also thankful to the Council of Scientific & Industrial Research (CSIR), New Delhi, for the financial assistance to pursue my research at CSIR-NCL, Pune.

My sincere thanks to Dr. Amitava Das, Dr. Sayam Sen Gupta, Dr. Rahul Banerjee, Dr. Sayan Bagchi, Dr. Benudhar Punji, Dr. J. Nithyanandhan, Dr. Udaya Kiran Marelli, Dr. C. V. Ramana, Dr. B. L. V. Prasad, Dr. T. Raja, Dr. V. C. Prabhakaran, Dr. Arup Kumar Rath, Dr. Janardan Kundu, Mrs. Kohle, Mr. Iyer, Mr. Purushothaman, Library staff, Student academic office staff and all other scientists of NCL for their motivation, constant encouragement, and support.

Furthermore, I extend my thanks to our collaborators Dr. Kumar Vanka and his doctoral students Tamal Da, Ruchi, Vipin, for their valuable suggestions and kind cooperation in theoretical calculations. My sincere thanks to Dr. Rajesh Gonnade and his group members Dr. Ekta, Dr. Samir, Dr. Shridhar, Dr. Veer, Christy, Tabrez, and Bhupender, for single-crystal X-ray diffraction measurements. Mrs. Shantakumari and her students for the help in HRMS analysis, and Mrs. Ansanas for elemental analysis. I would also like to thank Dr. Sapna Ravindranathan, Dr. Udaya Kiran Mareli, and Dr. T. G. Ajithkumar and their team Dinesh, Satish, Meenakshi, Deepali, for NMR facilities.

I want to express great appreciation to Dr. Shabana Khan and her doctoral students Dr. Shiv Pal, Dr. Neha, Rajarshi da, Nasrina di, Javed, Vikas, Nilanjana, Mousakhi from IISER-Pune for their kind help and support.

I am immensely grateful to Prof. K. N. Singh from BHU for the opportunity to join his team as an M.Sc. intern, for access to the laboratory and research facilities. I would also like to acknowledge the teachers I learned from since childhood; I would not have been here without their guidance, blessings, and support.

I was very fortunate to work with a fantastic group of colleagues in the Sen Lab. It has been a great learning experience for me through our group seminars. It is my pleasure to thank all my past and present lab mates Dr. Sandeep, Dr. Swamy, Sanjukta, Gargi, Rohit, Kritika, Ajith, Vishal, Dr. Moumita, Dr. Yuvaraj, Kajal, and Biplab, for devoting their precious time, helping hand and many valuable suggestions.

Beyond the lab, many well-wishers from CSIR-NCL and outside made my journey more comfortable. I want to acknowledge my senior colleagues for their helping hands and friendly affection, including Dr. Bharat, Dr. Rahul, Dr. Neetu, Dr. Pramod, Dr. Pravat, Dr. Krishanu, Dr. Hridayesh, Dr. Monalisa, Dr. Arunava, Dr. Manik, Dr. Sudip, Dr. Atreyee, Dr. Atanu, Dr. Suman Chandra, Dr. Santanu, Dr. Manoj, Dr. Santigopal, Dr. Subrata, Dr. Bikash, Dr. Suwendu, Dr. Arjun, Dr. Mohitosh, Dr. Shaibal, Dr. Siba, Dr. Manjur, Dr. Som, Dr. Indra, Dr. Vinod, Dr. Garima, Dr. Shahoo, Dr. Rana, Dr. Bipul, Dr. Shrikant, Dr. Goudappa, Dr. Pranab, Dr. Sagar, Dr. Shrikant Reddy, Prasenjit da, Debu da, Tapas da, Subhrashish da, Sutanu da, Sayantan Paul, Rahul da, Bittu da, Sandipan da, Abhijit da, Anagh da, Ashish da, Sayantan da, Ujjal da, Anupam da, Sourik da, Deborin da, Shushil, Ranga Rajan, Anup, Deerendra, Praveen throughout my tenure. No words are sufficient to acknowledge my prized friends and juniors in and out of NCL who have helped me at various stages of my work in NCL. I wish to thank Utsav, Suman, Soutick, Ranjan, Aditi, Vishwa, Ankit, Ashish, Anupam, Ketan, Naru, Himadri, Rahul, Anirban, Rohit, Suryadev, Srijan, Abdul, Nirsad, Pranoy, Nitai, Argha, Vinita, Priyanka, Chandan, Asif, Akash, Shailja, Soumya, and many others for making this journey so fantastic. I am lucky to have such a big family and always enjoy their company, and they are my strength for many things.

There are no words to express my gratitude and immense love to my family, my parents “Narayan Chandra Bisai” and “Mrityika Rani Bisai” and my younger sister “Moni” for their love, support, inspiration, and sacrifice. My father’s and mother’s prayer, relentless hard work, and constant struggle to overcome the life’s odds inspired me to pursue life with great ambition. I must thank my friend, critic, and better half “Sujata” for her understanding and love. Her support and encouragement boosted up my confidence and made this possible.

I am indebted to the eminent scientific community whose achievements are a constant source of inspiration for me. Above all, I extend my gratitude’s to the Almighty God for giving me the wisdom, health, and strength to undertake this research work and enabling me to its completion.

..... Milan

CONTENT OF THE THESIS

Content	Page No.
Abbreviations	iv
General remarks	vi
Synopsis	vii
Chapter 1:	
General Introduction	1-27
1.1 A brief history of silylene: Divalent silicon compound	2
1.1.1 Two coordinate silylenes	3
1.1.1.1 N-Heterocyclic silylenes (NHSis)	3
1.1.1.2 Carbocyclic silylenes	5
1.1.1.3 C,N-Stabilized cyclic silylenes	5
1.1.1.4 Acyclic silylenes	6
1.1.2 Three coordinated silylens	7
1.2 Main group compounds as an alternative to the transition metal complex	8
1.2.1 Small molecule activation	9
1.2.2 Main group compounds in homogeneous catalysis	12
1.2.2.1 Hydroboration	14
1.2.2.1.1 Hydroboration of carbonyl compounds	14
1.2.2.1.2 Hydroboration of imine, nitrile and carbodiimide	16
1.2.2.1.3 Hydroboration of alkene and alkyne	16
1.2.2.2 Cyanosilylation	17
1.3. Aim and outline of the thesis	18
1.4 References	19
Chapter 2:	
Synthesis and Reactivity of a Hypersilylsilylene	28-58
2.1 Introduction	29

2.2 Synthesis and characterization of hypersilylsilylene	30
2.3 Reaction of hypersilylsilylene with Me ₃ NO	33
2.4 Reaction with heavier chalcogens (S, Se, Te)	36
2.5 Reaction with acetone	38
2.6 Diverse reactivity of hypersilylsilylene with boranes	41
2.7 Reaction with organic azide: Synthesis of silaimines	45
2.8 Reaction with disubstituted chlorophosphines	47
2.9 Conclusion	53
2.10 References	53

Chapter 3:

Amidinato Silane for Catalytic Hydroboration of Aldehydes and Aldimines	59-73
3.1 Introduction	60
3.2 Hydroboration of aldehydes	61
3.3 Mechanistic investigations for the hydroboration of aldehydes	64
3.4 Hydroboration of aldimine	66
3.5 Mechanistic investigations for the hydroboration of aldimines	68
3.6 Conclusion	70
3.7 References	71

Chapter 4:

Easily Accessible Lithium Compounds Catalyzed Hydroboration and Cyanosilylation of Aldehydes, Ketones, Esters, Amides and Carbodiimides	74-110
4.1 Easily accessible lithium compound catalyzed mild and facile hydroboration and cyanosilylation of aldehydes and ketones	75-91
4.1.1 Introduction	75
4.1.2 Hydroboration of aldehydes and ketones	76
4.1.3 Competitive experiment for aldehyde/ketone hydroboration—a selectivity study	83
4.1.4 Mechanistic investigations	84
4.1.5 Cyanosilylation of aldehydes and ketones	88

4.1.6 Conclusion	91
4.2 Lithium Compounds as Swiss-Army-Knife Hydroboration Catalysts: Reduction of Amides, Esters and Carbodiimides	91-108
4.2.1 Introduction	91
4.2.2 Hydroboration of esters	93
4.2.3 Hydroboration of amides	94
4.2.4 Mechanistic investigations for the hydroboration of primary amides	99
4.2.5 Hydroboration of carbodiimide	102
4.1.6 Conclusion	105
4.3 References	106
 Chapter 5:	
Beyond Carbonyl Reduction: Lithium Compounds Catalyzed Hydroboration of Alkenes and Alkynes with Anti-Markovnikov Selectivity	111-122
5.1: Introduction	111
5.2 Hydroboration of alkene and alkyne	112
5.3 Hydroboration of terpenes	116
5.4 Regio- and chemo-selective study	117
5.5 Mechanistic investigations	118
5.6 Conclusion	120
5.7 References	120
 Appendix: Experimental details, NMR and crystal data	123-223

Abbreviations

Units and standard terms

BDE	Bond Dissociation Energy
°C	Degree Centigrade
DFT	Density Functional Theory
mg	Milligram
h	Hour
mL	Milliliter
Hz	Hertz
min	Minute
mmol	Millimole
NPA	Natural Population Analysis
ppm	Parts per million
%	Percentage
Mp	Melting Point
Calcd.	Calculated
CCDC	Cambridge Crystallographic Data Centre
CIF	Crystallographic Information file

Chemical Notations

Ar	Aryl
Me	Methyl
Et	Ethyl
Ph	Phenyl
Ad	Adamentyl
Dipp	Diisopropylaniline
<i>i</i> Pr	Isopropyl
<i>t</i> Bu	Tertiary butyl
MeOH	Methanol

MeCN	Acetonitrile
THF	Tetrahydrofuran
DCM	Dichloromethane
CDCl ₃	Deuterated chloroform
C ₆ D ₆	Deuterated benzene
DMSO-d ₆	Deuterated dimethyl sulfoxide
HBpin	Pinacolborane
TMSCN	Trimethylsilyl cyanide
TMSCl	Trimethylsilylchloride
<i>n</i> -BuLi	<i>n</i> -butyllithium
NHC	<i>N</i> -Heterocyclic carbene
NHSi	<i>N</i> -Heterocyclic silylene


Other Notations

δ	Chemical shift
J	Coupling constant in NMR
HRMS	High Resolution Mass Spectrometry
NMR	Nuclear Magnetic Resonance
rt	Room temperature
XRD	X-Ray Diffraction
equiv.	Equivalents
VT	Variable temperature

General remarks

- ❖ All chemicals were purchased from commercial sources and used without further purification.
- ❖ All reactions were carried out under inert atmosphere following standard procedures using Schlenk techniques and glovebox.
- ❖ The solvent used were purified by an MBRAUN solvent purification system MBSPS-800 and further dried by activated molecular sieves prior to use.
- ❖ Column chromatography was performed on silica gel (100-200 mesh size).
- ❖ Deuterated solvents for NMR spectroscopic analyses were used as received. All ^1H , ^{13}C , ^{19}F , ^{29}Si and ^{11}B NMR analysis were obtained using a Bruker or JEOL 200 MHz, 400 MHz or 500 MHz spectrometers. Coupling constants were measured in Hertz. All chemical shifts are quoted in ppm, relative to TMS, using the residual solvent peak as a reference standard.
- ❖ HRMS spectra were recorded at UHPLC-MS (Q-exactive-Orbitrap Mass Spectrometer) using electron spray ionization [(ESI+, +/- 5kV), solvent medium: acetonitrile and methanol] technique and mass values are expressed as m/z. GC-HRMS (EI) was recorded in Agilent 7200 Accurate-mass-Q-TOF.
- ❖ All the reported melting points are uncorrected and were recorded using Stuart SMP-30 melting point apparatus.
- ❖ Chemical nomenclature (IUPAC) and structures were generated using ChemDraw Professional 15.1.

Synopsis

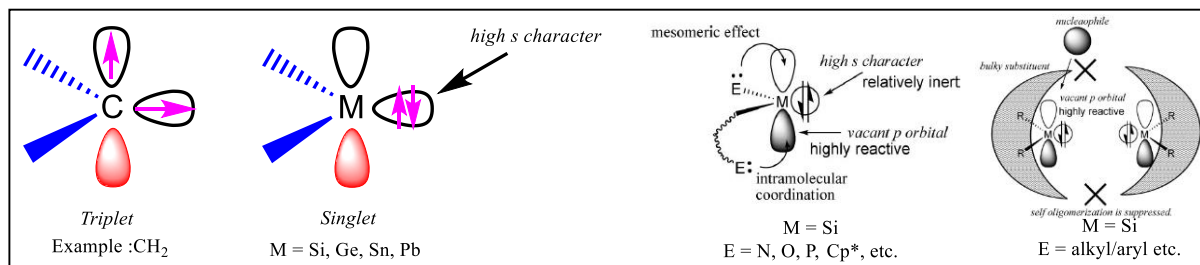
 Synopsis of the Thesis to be submitted to the Academy of Scientific and Innovative Research for Award of the Degree of Doctor of Philosophy in Chemistry	
Name of the Candidate	Milan Kumar Bisai
Degree Enrollment No. and Date	PhD in Chemical Science (10CC15A26020) August 2015
Title of the Thesis	Synthesis and Reactivity of Hypersilylsilylene and Catalytic Applications of Organosilicon and Lithium Compounds
Research Supervisor	Dr. Sakya Singha Sen (CSIR-NCL Pune)

Keywords: Hypersilylsilylene, Amidinato silane, Hydroboration, Cyanosilylation.

This thesis presents the synthesis and reactivity of a hypersilylsilylene and catalytic applications of organosilicon and lithium compounds. Thesis comprised of total five chapters and out of which first one is the general introduction part. First chapter describes the development of the chemistry of silylene and application of main group compounds in small molecule activation and catalysis with recent literature precedence. Whereas the next four chapters are working chapters and mainly based on the synthesis and reactivity of a hypersilylsilylene and catalytic reduction of unsaturated compounds using organosilicon and lithium compounds. The second chapter shows the synthetic protocol of hypersilylsilylene and its applications for various small molecules activation including boranes, organic azides and chlorophosphines. In the third chapter, a neutral penta-coordinated amidinato silane was shown as first reported Si(IV) compounds for catalytic hydroboration of aldehydes and aldimines under mild condition. We also discussed the usefulness of three very simple and easily accessible lithium compound having different electronegative substituents for the catalytic hydroboration and cyanosilylation of aldehydes and ketones under ambient condition, this was explained in fourth chapter of the thesis. And in addition, this catalytic activity was extended further for the other less activated and more important unsaturated compounds such as esters, amides and carbodiimides. On the other hand, the fifth chapter explores the effectiveness of the same lithium compounds for the selective anti-Markovnikov hydroboration of alkenes and alkynes. This catalytic process was extended for the reduction of biologically important terpenes.

Chapter 1: General Introduction

Since the journey of organosilicon chemistry in late 19th century, silicon has become a crucial element in research and application over the past few decades. In this regard, the chemistry of low valent silicon compounds, namely silylenes continues to be a thriving and rapidly developing area in synthetic chemistry, driven primarily by the fundamental studies of structure and bonding but also encompassing more reactivity studies. Although silicon is the heavier congeners of carbon but their molecular and electronic features are different. As a result, unlike the triplet state of methylene (CH_2), heavier analogues like SiH_2 , GeH_2 , SnH_2 & PbH_2 shows singlet ground state due to the large energy gap and spatial difference between the s- and p- orbitals. Silylenes shows ambiphilic nature due to the presence of a vacant $3p_z$ orbital and a lone pair of electrons (Scheme 1). In contrast to lighter congener, the development of the chemistry of silylene is in early stage, primarily due to lack of suitable synthetic protocol and their extreme reactivity. The breakthrough in the chemistry of stable Si(II) compounds came with the isolation of silicocene by Jutzi et al. and first N-heterocyclic silylene (NHSi) by Denk and coworkers with the delicate balance of suitable electronic and steric stabilization. For the electronic support, donor atom of the associated ligand donates lone pair of electrons into a vacant coordination site of the central Si(II) atom to minimize the electrophilicity. On the other hand, kinetic stabilization provides the shielding to the vacant orbital of Si(II) center from nucleophilic attack or solvent molecules with sufficient sterics of attached bulky ligands. And therefore, it stabilizes the corresponding monomeric units and suppresses the possibility of dimerization or oligomerization.



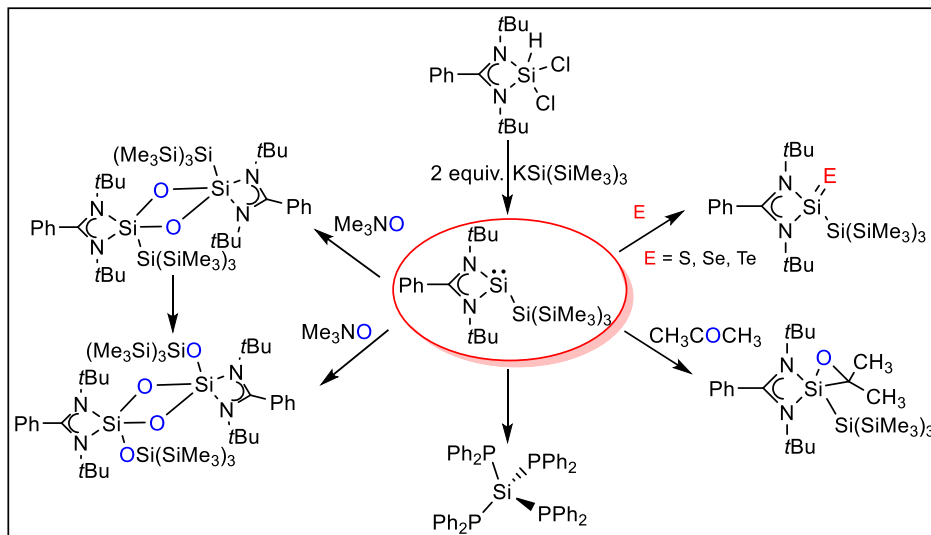
Scheme 1. Outlook of molecular and electronic features and stabilization of metallylenes.

After successful stabilization or isolation of such low valent main group compounds, the obvious next attempt is their reactivity studies. The recent progress reveals that low valent main group compound has potential to mimic the reactivity of the traditional transition metal. For example, two-coordinate acyclic silylenes reported from Aldridge's group were known to cleave both

dihydrogen and ammonia under mild reaction condition. Moreover, plenty of earth abundant or easily accessible main group compounds has been reported so far for the small molecule activation and catalytic transformation. Inspired from such results we have synthesized a unique three coordinate benz-amidinate silylene with hypersilyl substituents, lacking of extra π -donor group. Furthermore, the reactivity of prepared silylene, organosilicon compound and readily accessible lithium compound has been tested for small molecule activation and further catalytic application in important organic transformations.

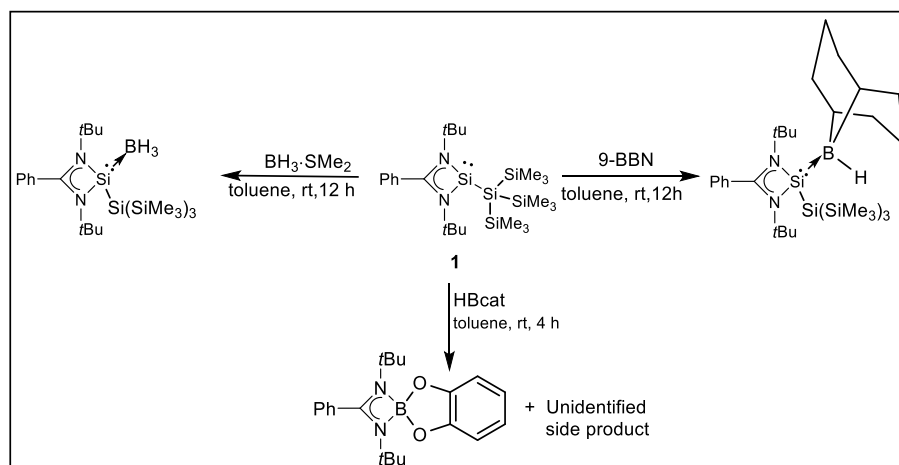
Chapter 2: Synthesis and Reactivity of a Hypersilylsilylene

The most extensively studied silylenes is the benzamidinato-stabilized silylene of composition $LSiX$ [$L = PhC(NtBu)_2$] presumably because of their ease of synthesis and thermal stability. However, a closer look would reveal that the majority of amidinatosilylenes contain an electron-rich π -donating functionalized group (X) such as Cl, Br, *OiPr*, NR_2 [$R = Ph, Cy, iPr, SiMe_3$], $P(SiMe_3)_2$], etc. Replacement of the π -donor ligand with a σ -donor group may reduce the highest occupied molecular orbital (HOMO)–lowest unoccupied molecular orbital (LUMO) gap, but this would add more synthetic challenges. While silylenes with π -donating ligands have not been reported for dihydrogen activation, the silylenes lacking π -donor ligands are found to split dihydrogen in a facile manner, which can be attributed to a decrease of π donation, leading to a reduction in the HOMO–LUMO gap. This significant result led us to study the synthesis of tris(trimethylsilyl)silylamidinosilylene from $PhC(NtBu)_2SiHCl_2$ with $K\{Si(SiMe_3)_3\}$ in more than 90% yield and further utilization for the small molecule activation (Scheme 2). Subsequent to the synthesis of the silylene, series of reactions with Me_3NO , S, Se, and Te were performed. While siloxane derivatives are obtained from reactions with Me_3NO , silachalcogenones with Si=E bonds are formed with other chalcogens. The reaction of hypersilylsilylene with acetone affords the first structurally authenticated silaoxirane derivative. On the other hand, the reaction of chlorodiarylphosphine with hypersilylsilylene has led to the formation of a novel tetraphosphinosilane in good yield. The four-coordinating phosphine site of the tetraphosphinosilane provides a platform for the synthesis of metal complexes and further opportunity in catalysis studies.



Scheme 2. Synthesis and reactivity of hypersilylsilylene.

Furthermore, the reactivity of hypersilylsilylene has been tested with some commercially available boranes and corresponding products have been synthesized and characterized successively. Depending on the Lewis acidity of boranes and substituent attached to the boron center, anomalous reactivities has been found with hypersilylsilylene (Scheme 3).

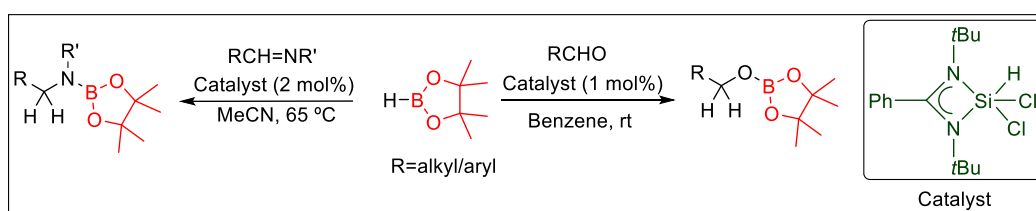


Scheme 3. Reactivity of hypersilylsilylene with boranes.

Also, silaimines, the heavier analogous of imines have been synthesized by the reaction of hypersilylsilylene with organic azides and their further reactivity has been tested with boranes.

Chapter 3: Amidinato Silane for Catalytic Hydroboration of Aldehydes and Aldimines

Among the full gamut of single site neutral compounds reported for transition metal free hydroboration of aldehydes and ketones, there is one element missing that one might have expected to be there: silicon. Being isosteres of carbon and owing to their larger covalent radius, electropositive nature, low toxicity and relative abundance, silicon compounds are highly sought after as single component catalysts because a catalytic cycle based on silicon could be sustainable, economical and green. Silylium ion promoted catalytic imine reduction and Diels–Alder reactions, and bis(perfluorocatecholato)silane [Si(catF)₂] catalyzed aldehyde hydrosilylation have been reported, illustrating the potential of silicon compounds as catalysts. Besides, there are recent theoretical and experimental reports on formylation of amines using a combination of CO₂ and a silane as the formylating reagent. This is due to the silicon atom to expand its valance shell, giving rise to five- or six-coordinate intermediate, which is of great interest in terms of catalysis. In this chapter, we present the catalytic potential of previously reported benz-amidinato dichlorosilane [PhC(NtBu)₂SiHCl₂], for the hydroboration of aldehydes and aldimines with very good chemo selectivity in excellent yield (Scheme 4). Our result reports various functional group tolerance throughout the catalytic process with a vast range of aldehydes and aldimines. Experimental as well as quantum mechanical calculations were done in order to understand the mechanism for the catalytic hydroboration.



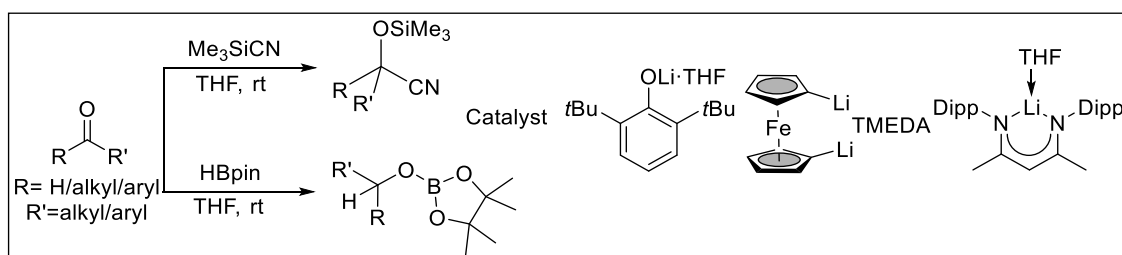
Scheme 4. Organosilicon compound for catalytic hydroboration of aldehydes and aldimines.

Chapter 4: Easily Accessible Lithium Compounds Catalyzed Hydroboration and Cyanosilylation of Aldehydes, Ketones, Esters, Amides and Carbodiimides

Driven by the demand for catalytic processes with reduced environmental impact and low cost, numerous groundbreaking results have been achieved in molecular catalysis using complexes of the heavier alkaline earth metals. Following the demonstration of the hydroboration of carbonyl

compounds using a magnesium alkyl complex, there has been a flurry of research activity on hydroboration reactions using compounds with alkaline earth metals as well as p-block elements. On the other hand, since the birth of lithium chemistry, the growth of s-block compounds is still in its early days, finding its feet slowly and gradually from curiosity driven explorations to important catalytic transformations. The advantages of using lithium compounds are (i) cheap, (ii) moderately abundant, (iii) readily accessible, and (iv) non-involvement in Schlenk equilibrium like group 2 elements. Moreover, as most of the main group catalysts are frequently prepared from the corresponding lithium reagents, taking advantage of the direct use of lithium compounds in catalysis would obviate the need for such additional transformations.

In light of our interests to develop the catalytic methods for the reduction of carbonyl compounds, we attempted to use three popular and readily accessible lithium compounds with different electronegative substituents, 2,6-ditert-butyl phenolate lithium, 1,1'-dilithioferrocene, and, [Dipp₂nacnac]Li for the reduction of aldehydes and ketones with HBpin under ambient conditions (Scheme 5). The reason behind this selection is to examine how the Lewis acidity of the Li center influences the catalytic activity due to the electronegativity of the attached substituents. In addition, all three lithium compounds have been utilized for the catalytic cyanosilylation of aldehyde and ketones as well; a transformation thus far not known to be catalyzed by group 1 complexes.



Scheme 5. Lithium compounds in catalytic hydroboration and cyanosilylation.

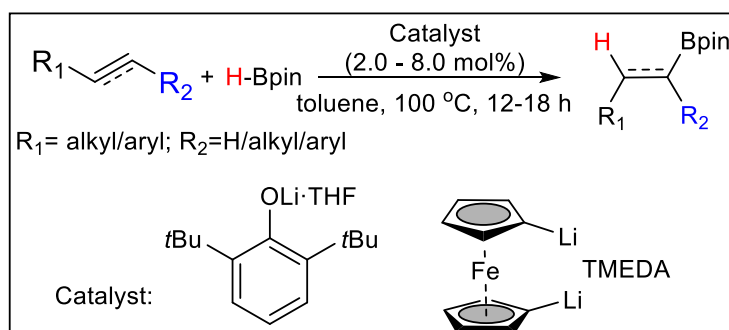
To broaden the horizons of lithium compounds in catalysis, we have successfully employed the same lithium compounds [2,6-ditert-butyl phenolate lithium, and 1,1'-dilithioferrocene] for the hydroboration of more challenging and less activated carbonyl compounds such as esters, amides or important unsaturated compounds like carbodiimides. Our result represented first lithium compound catalyzed reduction for esters, amides and carbodiimides.

The methodologies described have clearly opened new avenues for the catalytic application of lithium compounds, encouraged by the very economic and almost non-toxic nature of these reagents.

Chapter 5: Beyond Carbonyl Reduction: Lithium Compounds Catalyzed Hydroboration of Alkenes and Alkynes with Anti-Markovnikov Selectivity

Hydroboration using compounds with group 2 elements has been limited to the catalytic reduction of unsaturated polar bonds, such as aldehydes, ketones, imines, amides, esters etc. Although compounds with p-block elements are emerging as proficient catalysts for alkyne and alkene hydroboration, there are very limited reports on s-block metal catalyzed alkene or alkyne hydroboration. Herein, we report efficient hydroboration of more challenging substrates like alkenes and alkynes.

The catalytic hydroboration of alkenes and alkynes using very simple lithium compounds [2,6-di-tert-butyl phenolatelithium and 1,1'-dilithioferrocene] has been achieved with good yields, high functional group tolerance and excellent chemoselectivity. Deuterium labeling experiments confirm the cis addition of pinacolborane. The methodology has been further extended to myrcene, which undergoes selective 4,3-hydroboration. DFT calculations provide insights into the mechanism.



Scheme 6. Hydroboration of alkene and alkynes using easily accessible lithium compounds.

General Introduction

Abstract

This chapter presents an overview of the elementary interest and formidable synthetic challenges regarding the development of the chemistry of silylene and the application of the compounds with main group elements in small molecule activation and catalysis. A general introduction covering a brief description of important compounds in this research area is provided with the literature precedence. The objectives and the results presented in this thesis are outlined.

1. Introduction

1.1 A brief history of silylene: Divalent silicon compound

Since the commencement of organosilicon chemistry in late 19th century,¹ silicon has become a crucial element in research and has found several applications over the past few decades.² In this regard, the chemistry of divalent silicon compounds, namely silylenes, continues to be a thriving and rapidly developing area in synthetic chemistry, driven primarily by the fundamental studies of structure and bonding, but also encompassing more reactivity studies.³ Although silicon is the heavier congeners of carbon, their molecular and electronic features are entirely different. As a result, unlike the triplet state of methylene ($\text{H}_2\text{C}:$), silylene ($\text{H}_2\text{Si}:$) or other heavier metallylenes $\text{H}_2\text{M}:$ (where $\text{M} = \text{Ge}, \text{Sn}$ and Pb) show singlet ground state. This is because of the large energy gap and spatial difference between the s- and p- orbitals, which prevent to form a hybrid orbital.⁴ Silylenes represent ambiphilic nature due to the presence of a vacant $3p_z$ orbital and a lone pair of electrons (Figure 1.1).

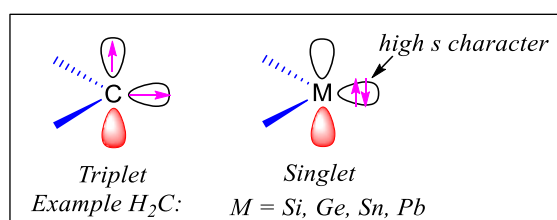


Figure 1.1. Differences between the ground states of carbenes and metallylenes.

The singlet-triplet energy gap ΔE_{ST} for $\text{H}_2\text{M}:$, [$\Delta E_{\text{ST}} = E_{(\text{triplet})} - E_{(\text{singlet})}$] as per the theoretical calculations are estimated to be 16.7 ($\text{M} = \text{Si}$), 21.8 ($\text{M} = \text{Ge}$), 24.8 ($\text{M} = \text{Sn}$), and 34.8 ($\text{M} = \text{Pb}$) Kcal/mol, whereas for $\text{H}_2\text{C}:$ it is -14.0 kcal/mol.⁵ Therefore, the relative stabilities of the singlet species of $\text{R}_2\text{M}:$ ($\text{M} = \text{C}, \text{Si}, \text{Ge}, \text{Sn}, \text{Pb}$; $\text{R} = \text{alkyl}$ or aryl) with respect to their corresponding dimers, $\text{R}_2\text{M}=\text{MR}_2$, are estimated to increase as we move down the group 14. In this regard, although divalent organolead compound namely, plumbylenes are expected to be stable and isolable, some of them are thermally unstable and undergo facile disproportionation reactions, if not stabilized electronically or sterically.⁶

Metallylenes are extremely reactive species due to their vacant p-orbitals. In fact, before 1980's, they could only be identified by the spectroscopic tools at low temperature in an argon matrix, or isolated as metallylene-metal complexes. Also, they are prone to dimerize or oligomerize, and shows high reactivity toward other molecules or solvent. As a result, metallylenes are usually difficult to stabilize or isolate under ambient condition without suitable thermodynamic and/or kinetic support.

In contrast to its lighter congener, the development of the chemistry of silylene is quite limited. It was first identified as a reactive and transient intermediate by Skell and Goldstein⁷ and subsequently low temperature matrix-isolation,⁸ gas phase kinetic studies⁹ and laser photolysis of silane¹⁰ became the primary modes of its characterization.

The breakthrough in the chemistry of stable Si(II) compounds came with the isolation of silicocene by Jutzi et al. in 1986,¹¹ and first N-heterocyclic silylene (NHSi) by Denk and coworkers in 1994.¹² These discoveries were followed by the isolation of several other stable silylenes with the delicate balance of suitable electronic and steric stabilization. For the electronic support, donor hetero atom of the associated ligand donates lone pair of electrons into a vacant coordination site of the central Si(II) atom to minimize the electrophilicity. On the other hand, the kinetic stabilization provides the shielding to the vacant orbital of Si(II) center from nucleophilic attack or solvent molecules with sufficient sterics of the attached bulky ligands (Figure 1.2). And therefore, it stabilizes the corresponding monomeric units and suppresses the possibility of dimerization or oligomerization.^{3,6}

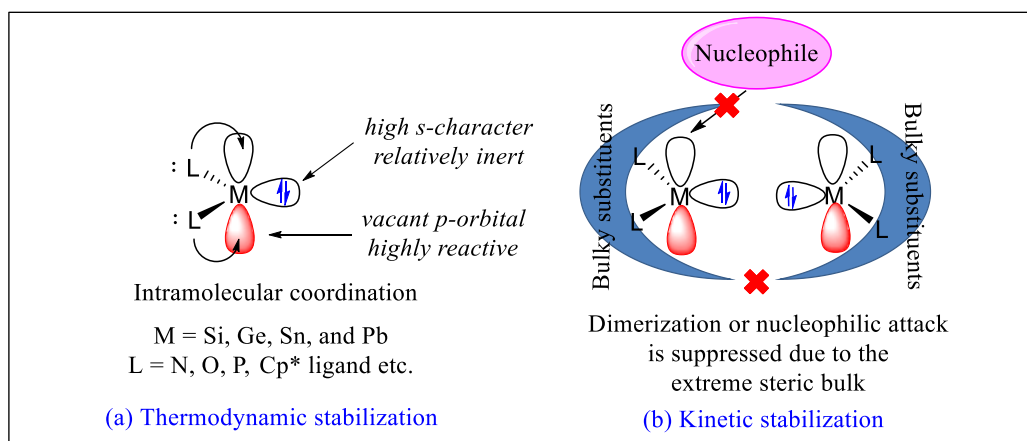
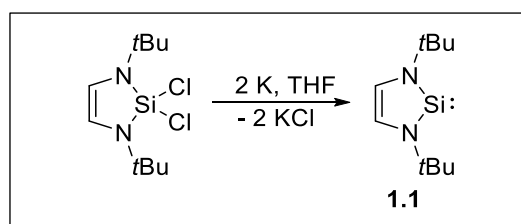


Figure 1.2. (a) Thermodynamic stabilization and (b) kinetic stabilization of metallylenes.

1.1.1 Two coordinate silylenes

1.1.1.1 N-Heterocyclic silylenes (NHSis)

The landmark discovery of N-heterocyclic carbene by Arduengo et al.¹³ encouraged the chemists to synthesize its next heavier analogue. In 1994, Denk and co-workers synthesized the first dicoordinate N-heterocyclic silylene by reduction of the corresponding dichlorosilane with elemental potassium in THF (Scheme 1.1).¹² The NHSi (**1.1**) is thermally stable (up to 150 °C) both in the solid state and in most of the aprotic organic solvents.



Scheme 1.1. Synthesis of the N-heterocyclic silylene **1.1**.

By tailor-made synthetic strategies, a fair number of stable unsaturated NHSis (**1.2** to **1.4**) have been reported in the following years.¹⁴ In continuation, N-heterocyclic silylenes with saturated backbones (**1.5-1.9**) have also been synthesized and structurally characterized via the reduction of the corresponding dibromosilane.¹⁵ Moreover, benzo- or pyrido-fused N-heterocyclic silylenes (**1.10**, **1.11** and **1.12**) have been reported by similar reduction methodology.¹⁶ Similarly in 2005, biphenyl scaffold based bis-silylene, **1.13** was also realized by Lappert et al (Chart 1.1).¹⁷

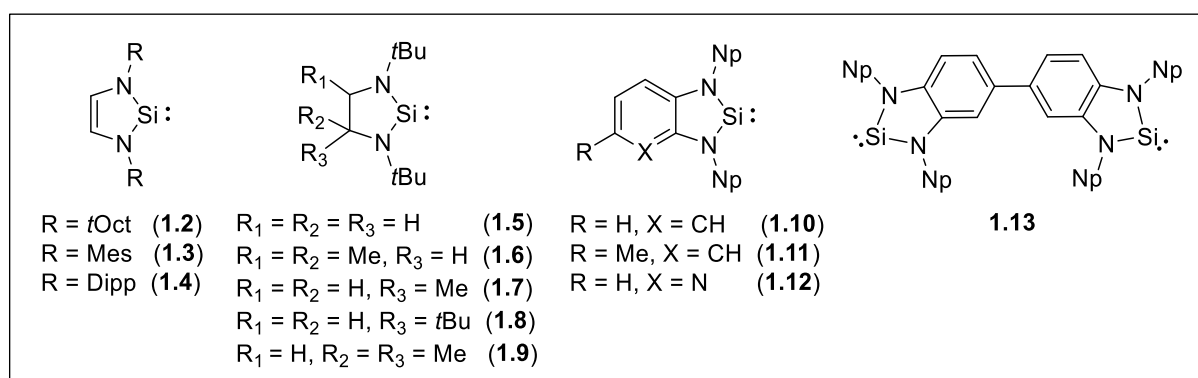
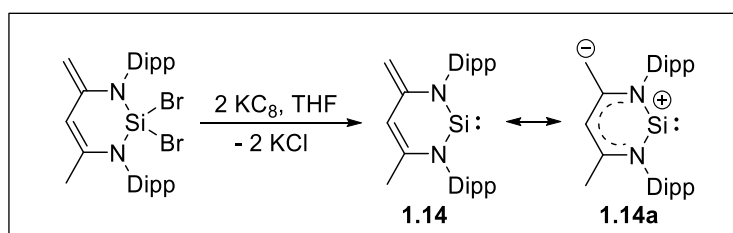


Chart 1.1. Selected examples of the N-heterocyclic silylenes.

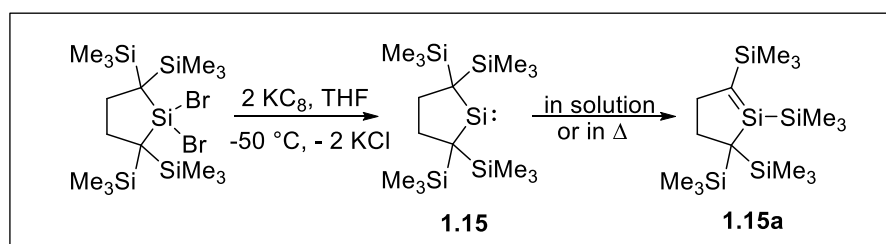
In 2006, Driess and co-workers have prepared a six membered NHSi stabilized by a β -diketiminato-like backbone (**1.14**).¹⁸ It was achieved by the reduction of corresponding dibromosilane precursor with KC_8 in THF. Surprisingly, the resonating structure indicated that NHSi (**1.14**) contains two nucleophilic centers, one at the central Si^{II} atom and the other at the CH_2 carbon atom of the β -diketiminato backbone (Scheme 1.2).



Scheme 1.2. Selected examples of the N-heterocyclic silylene.

1.1.1.2 Carbocyclic silylenes

In 1999, a carbocyclic silylene where the silicon center was kinetically protected by the bulky dialkyl substituents was reported by Kira and coworkers.¹⁹ Carbocyclic silylenes **1.15** was synthesized by the reduction of the precursor dibromosilane with KC_8 at low temperature. Interestingly, although **1.15** is stable in the solid state at 0 °C but easily isomerizes to the corresponding silaethene (**1.15a**) via 1,2-silyl migration in solution or if heated (Scheme 1.3).



Scheme 1.3. Synthesis and isomerization of carbocyclic silylene **1.15**.

In the following years few more analogues of silylene (**1.16-1.17**) have also been reported by other research groups.^{20,21} Surprisingly, instead of 1,2-silyl migration, **1.16** dimerize and equilibrate to the corresponding disilene (**1.16**)₂ in solution.²⁰ Furthermore, another carbocyclic silylenes (**1.18** and **1.19**) were obtained through the thermodynamic stabilization of phosphorous ylide substituents (Chart 1.2).²²

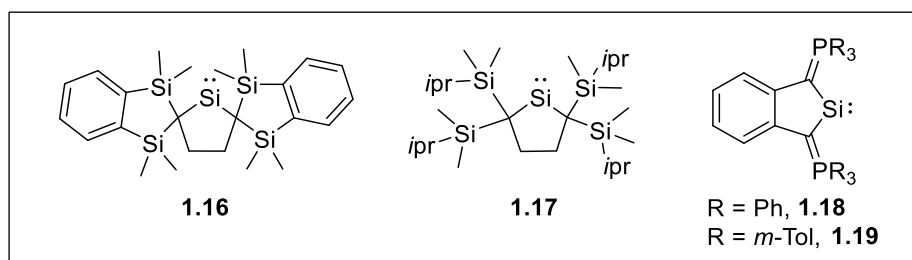


Chart 1.2. Selected examples of the cyclic dialkyl silylenes.

1.1.1.3 C,N- Stabilized cyclic silylenes

Cyclic two coordinated silylenes with both nitrogen and carbon substituents were also known in the literature. These include the cyclic amino(ylide)silylene and cyclic alkyl(amino)silylene (**1.20**²³ and **1.21**²⁴ respectively, Chart 1.3) reported by Kato and Baceiredo et al. and Iwamoto et al., respectively following the similar reduction methodology.

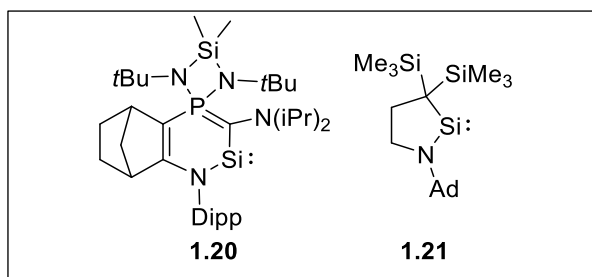


Chart 1.3. Selected examples of the C,N-stabilized cyclic silylenes.

1.1.1.4 Acyclic silylenes

The two-coordinate acyclic silylenes are one of the most wanted synthetic targets among the stable silylenes, due to their unusual reactivities. In 2003, for the first time West group reported the synthesis of acyclic silylene $[(\text{Me}_3\text{Si})_2\text{N}]_2\text{Si}$: (**1.22**) from the reduction of corresponding dibromo precursor with potassium graphite.²⁵ However, it was persistent only at low temperature ($-20\text{ }^\circ\text{C}$) and decomposed at ambient temperature, which was confirmed by solution phase spectroscopic methods.

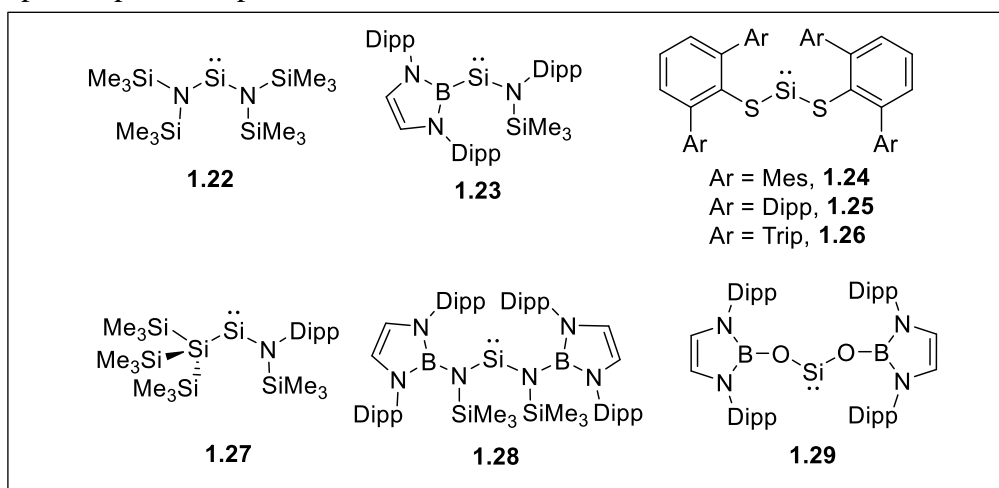


Chart 1.4. Selected examples of the two coordinated acyclic silylenes.

After introduction of bulky substituents, boryl substituted (**1.23**),^{26a} terphenyl thiolate substituted (**1.24-1.26**),^{26b} the hypersilyl substituted (**1.27**)^{26c} and amino substituted (**1.28**)^{26d} silylenes have been reported by various independent research group. Very recently, another two-coordinate acyclic dioxysilylene (**1.29**)^{26e} with strongly donating N-heterocyclic boryloxy ligand was reported by Aldridge's group by the reduction of diiodo precursor with $[(\text{Nacnac})\text{Mg}]_2$ at $80\text{ }^\circ\text{C}$ (Chart 1.4). Interestingly, among all acyclic silylenes, compounds **1.23** and **1.27** are known to activate molecular hydrogen at ambient temperature owing to the smaller HOMO-LUMO energy gaps.^{26a,26c}

1.1.2 Three coordinated silylenes

Compounds with three coordinated Si(II) atom could be considered as donor-stabilized silylenes. It has shown remarkable chemistry compared to its two-coordinate counterparts for its interesting electronic features. Three coordinated functionalized silylenes with halide substituent as an additional π -donor was found as the most developed class in the chemistry of silylene, as they can be considered as analogues of gaseous silicon dichloride.

In this regard, first three coordinated amidinato ligand based chloro-silylene (**1.30**) was reported in 2006 by Roesky and coworkers.²⁷ In the following years, a fair number of functionalized amidinato silylenes (**1.31-1.38**) through salt metathesis reaction were reported by various independent research groups (Chart 1.5).²⁸ In continuation, Tacke et al. have also synthesized functionalized silylenes (**1.3-1.40**) with the *N,N*-di(isopropyl)amidinato and guanidinato ligands.²⁹

Literature survey reveals that the ligands with nitrogen substituents have been studied extensively than other donor atoms such as carbon, oxygen, phosphorous, etc. Although the dihalo-derivatives of silicon are unstable and extremely reactive, and considered as indispensable building blocks in synthetic chemistry. In this regard, NHC-stabilized dihalosilylenes (**1.41-1.43**) were found to be reliable and synthesized by the groups of Roesky and Filippou.³⁰

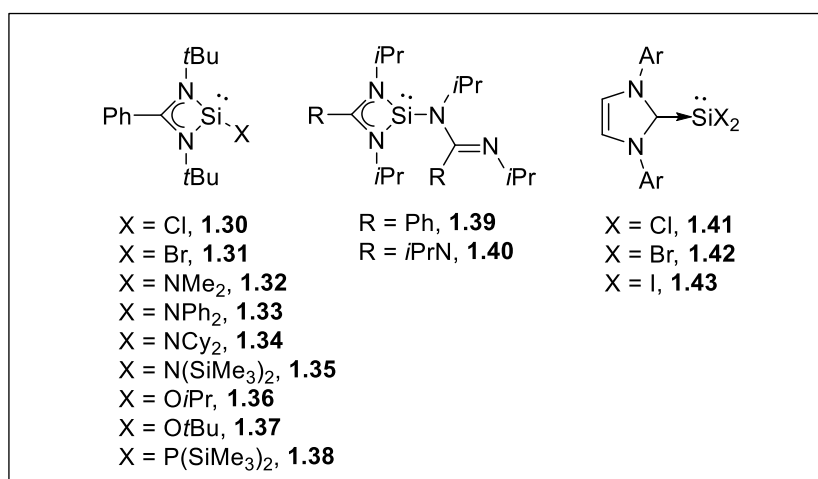


Chart 1.5. Selected examples of the three coordinated silylenes.

Ligands with phosphine-containing backbones have also been utilized as a donor ligand for the stabilization of two coordinated silylenes. In 2009, Kato and Baceiredo et al. have reported the first phosphine stabilized silylene (**1.44**) via reduction of dichlorophenylsilane precursor with

elemental magnesium.³¹ Subsequently, in 2011, other analogues silylene, **1.45** and **1.46** were reported by the same research group using similar synthetic protocol (Chart 1.6).³²

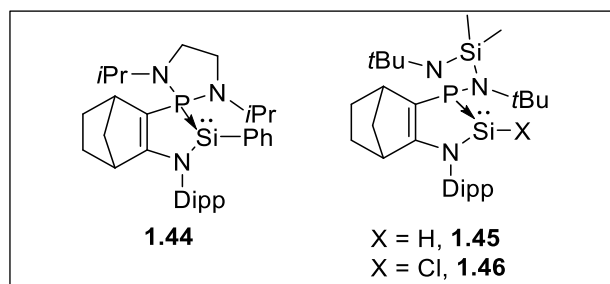


Chart 1.6. Selected examples of the three coordinated silylene.

1.2 Main group compounds as an alternative to the TM-complex

Over the past few decades, an array of compounds with low valent main group has been synthesized utilizing thermodynamic and /or kinetic support of numerous ligand systems. After successful isolation of such compounds, the obvious next attempt is their reactivity studies. For several decades, the catalytic reactions have been considered to be the exclusive domain of transition metals due to their variable oxidation state- changing ability. However, the escalating need for non-toxicity, environmentally benign and sustainability in chemical processes have led main group compounds as viable alternatives to the transition metal catalysts. Recent years' findings reveal that a considerable effort has been invested in main-group compounds to avoid the heavy, precious transition metals or the use of the conventional stoichiometric metal hydride in industrial catalysis. Impressive development is known in the field of low valent main-group compounds, such as B(I),³³ Al(I),³⁴ Si(0),^{35,36} and Ge(0)³⁷⁻³⁹ in the form of multiple bonded species, carbenoids, and donor stabilized (e.g. carbene, imine, phosphine) atoms.^{3a,40-43} These highly reactive species have shown common characteristic with the transition-metal complexes in the form of small energy separated frontier orbitals (Figure 1.3).⁴⁴

As a result, despite the enormous synthetic challenges, many of them display very interesting and unusual reactivity towards small molecules such as H₂, NH₃ etc. and in catalytic activity.

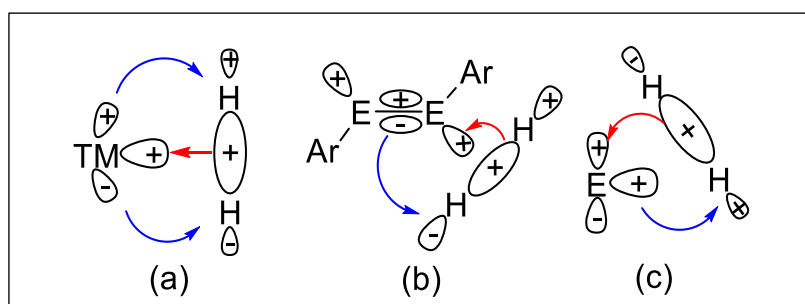


Figure 1.3. Frontier orbital interaction of dihydrogen with (a) transition metals, (b) main group multiple bonds, and (c) singlet main group species e.g. carbenes, tetrylenes.

1.2.1 Small molecule activation

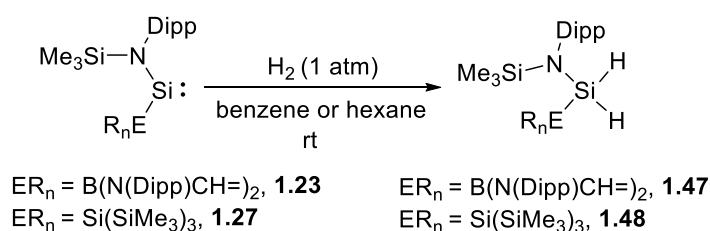
The small molecules such as H₂, NH₃, CO, CO₂ etc. are cheap, ubiquitous, prepared in large scales by many industrial processes and synthons for many targeting complex molecules. Oxidative addition and reductive elimination of a strong bond are the crucial steps for most of the transition metal based catalytic system. And this can also be achieved with the compounds with main group element and it is summarized by Nikonov and coworkers.^{45a} Moreover, many homogeneous and heterogeneous catalysis are based on these small molecules for the production of large varieties of important chemicals.^{45b}

The breakthrough in the activation of dihydrogen by compounds with low-valent main group elements was demonstrated first in 2005 by Power and coworkers. The heavier alkyne analogue of germanium [ArGe≡GeAr; Ar = 2,6-Trip₂C₆H₃ (Trip = 2,4,6-*i*Pr₃C₆H₂)] was utilized for the dihydrogen activation under mild conditions to yield a mixture of Ar(H)Ge=Ge(H)Ar, Ar(H)₂Ge–Ge(H)₂Ar and ArGeH₃.⁴⁶ Since then, a number of studies on the activation of small molecules, such as amines, silanes, and boranes, with carbenoids of Group 13 to 15 and related low valent compounds, heavy main-group analogues of alkene and alkynes have been realized.⁴⁷⁻⁴⁹

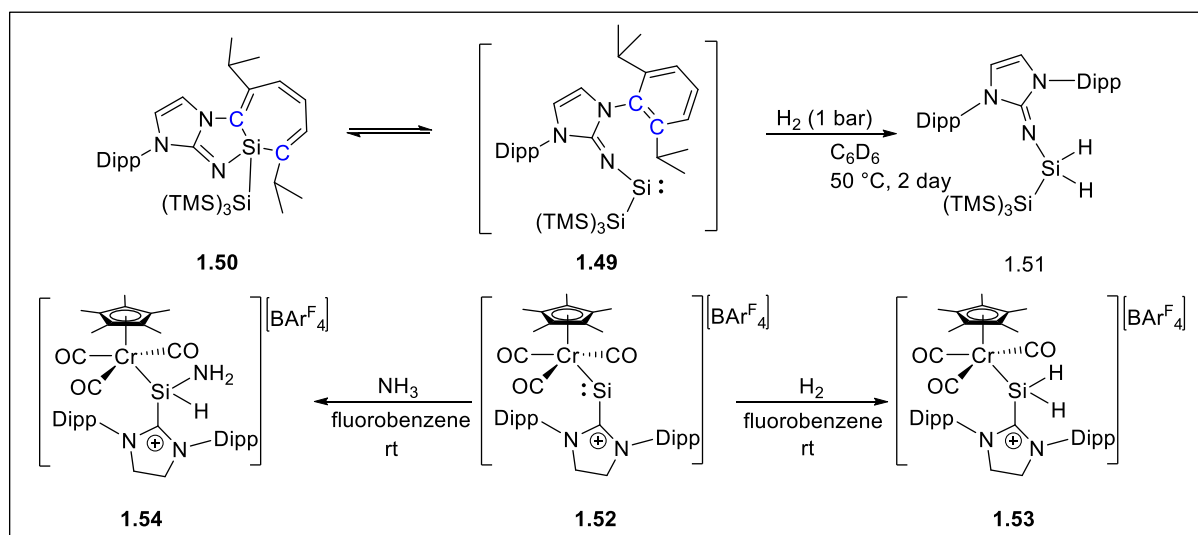
Bertrand and coworkers have reported successful activation of dihydrogen by both cyclic alkyl amino carbene and the acyclic alkyl amino carbene under mild condition to furnish the corresponding alkane products.⁵⁰ It is fair to mention here that, typical Arduengo-type saturated or unsaturated N-heterocyclic carbenes (NHC), are reported to be unreactive toward H₂. Detailed theoretical investigations by Bertrand and coworkers revealed that the activation of dihydrogen on the singlet carbene proceeded through heterolytic mechanism.⁵¹ In the initial step, the carbene donates lone pair of electrons to the antibonding σ* orbital of H₂, which helps to weaken the H–H bond in the transition state. In the next step, the hydridic end of the H₂ attacks the positively polarized carbocation center, leading to complete cleavage of the H–H bond to afford the alkane products. Later on, calculations by Ess et al. showed that the alkyl amino carbene behaves as an ambiphile for the activation, and not as a nucleophile.⁵²

Computational study by Wang and Ma suggest that, the activation of H₂ to a variety of cyclic and acyclic silylenes and germylenes proceeds through a typical concerted pathway.⁵³ The reactivity of metallylenes depends mainly on the singlet–triplet or HOMO–LUMO energy

gaps. As a matter of fact, NHSi and Power's bis(arylthio)-substituted acyclic silylenes do not activate dihydrogen because of their high HOMO–LUMO energy gaps;^{54,26a-b} Nevertheless, H₂ activation by Si(II) centers have been realized by two stable acyclic silylenes (i) a stable mixed (amido) boryl silylene (**1.23**), Si{B(NDippCH)₂}{N(SiMe₃)Dipp} and (ii) the bulky hypersilyl coordinated silylene (**1.27**), Si{Si(SiMe₃)₃}{N(SiMe₃)Dipp} to afford their corresponding dihydrosilanes.



Scheme 1.4. Activation of H₂ by acyclic silylenes **1.23** and **1.27**.



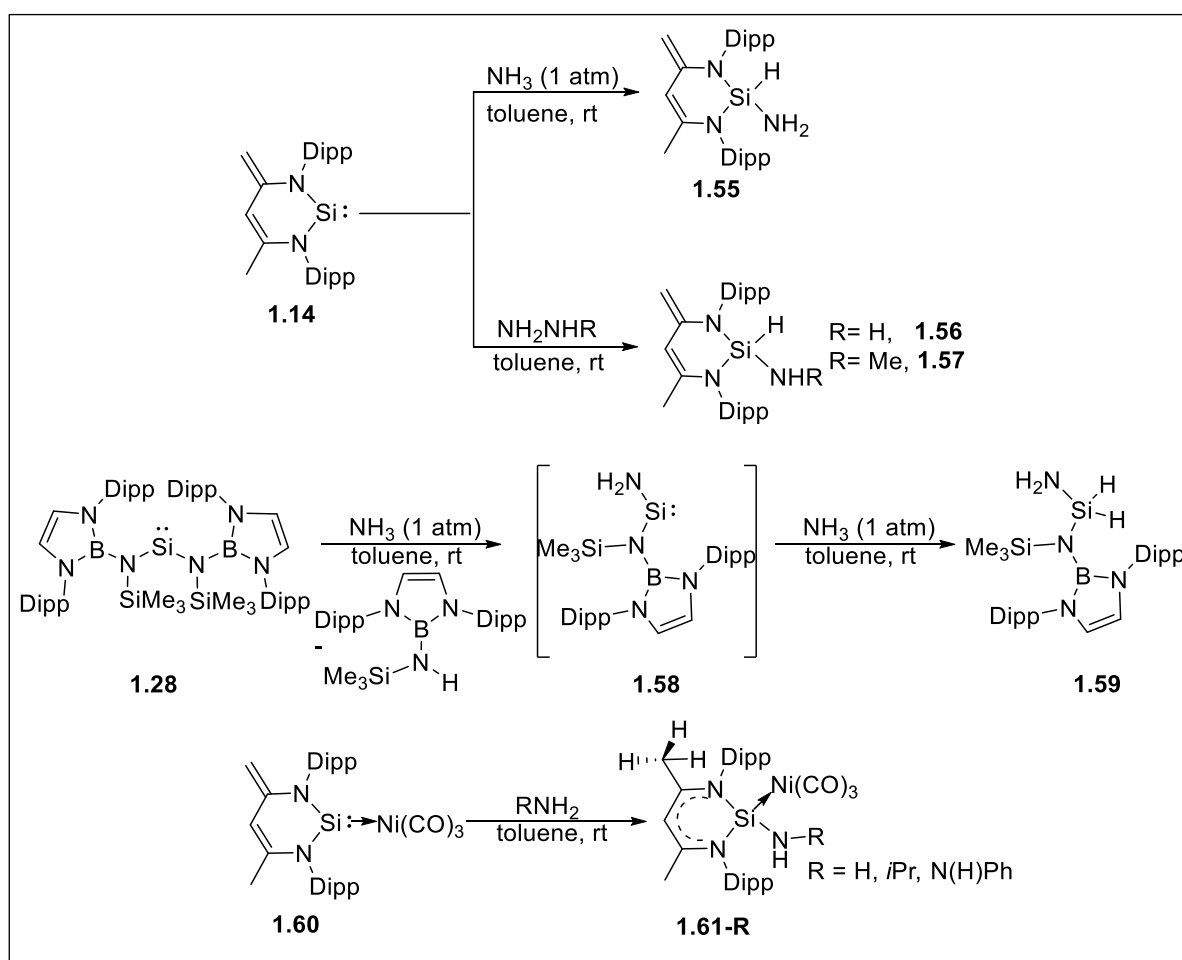
Scheme 1.5. Dihydrogen and ammonia activation by silylenes.

Very recently, an *in situ* generated N-heterocyclic imino-hypersilyl silylene (**1.49**) equilibrating with ‘silepin’ **1.50**, was also reported by the group of Inoue that is capable of activating dihydrogen.⁵⁵ Like acyclic silylene (**1.23** and **1.27**), **1.49** shows decreased HOMO–LUMO gap required for H₂ activation due to the presence of amido-type ligand and a σ-donating silyl substituent. Another dihydrogen activation is reported from Filippou et al. by using NHC-supported cationic metallasilylene (**1.52**), which can readily undergo hydrogenation to furnish corresponding silylium ion (**1.53**) (Scheme 1.5).⁵⁶

Likewise, dihydrogen activation, N–H bond activation is also a challenging task even for the transition-metal complexes.⁵⁷ Since the activation of the N–H bond of ammonia by

nucleophilic carbenes reported by Bertrand and coworkers in 2007,⁵⁰ a flurry of compounds with heavier low-valent main-group elements have been explored for such activation, as well as alkyl and aryl amines or substituted hydrazines.

Theoretical calculation by Sicilia et al. suggests that the formation of the 1,4-addition product is kinetically more feasible compared to the 1,1-addition product [26.6 kcal mol⁻¹ for 1,4-addition product vs 48.7 kcal mol⁻¹ for 1,1-addition product].⁵⁹ However, a drastic reduction in energy barrier to 15.3 kcal mol⁻¹ was observed for the 1,1-addition product when calculated with 2 equiv. of ammonia molecule. This observation clearly indicates the feasibility of the reaction in excess ammonia under ambient condition.



Scheme 1.6. Activation of ammonia and hydrazines with silylenes.

In a subsequent report, 1,1-addition of the N–H bond of the analogous hydrazine (**1.56**) and N-methyl hydrazine (**1.57**) on silylene **1.14** was also documented by Roesky and coworkers (Scheme 1.6).⁶⁰ Interestingly, NHC-supported cationic metallasilylene **1.52** is also able to activate ammonia under ambient condition as demonstrated by Filippou et al. (Scheme 1.5).⁵⁶ More recently, Aldridge and Jones have reported the N-H bond activation on a two-coordinate,

acyclic diaminosilylene, **1.28** when exposed to an excess dry NH_3 . This report shows anomalous reactivity of silylene, which led to a mixture of triaminosilane (**1.59**) and a secondary amine. The generation of a transient diaminosilylene intermediate (**1.58**) was proposed, which actually undergoes to σ -bond metathesis reaction to cleave ammonia N-H bond.^{26d}

Driess and coworkers also reported the activation of N-H bond of ammonia, isopropylamine, and phenylhydrazine on the $\text{Ni}(\text{CO})_3$ adduct of silylene **1.14** (**1.60**), in the 1,4-fashion to furnish corresponding β -diketiminate $\text{Si}(\text{II})\text{-Ni}(\text{CO})_3$ complex **1.61** (Scheme 1.6).⁶¹ Although the mechanism is not clear, the product formation was proposed by the intermolecular deprotonation of N-H bond by exocyclic methylene group of second molecule of silylene and followed by proton migration.

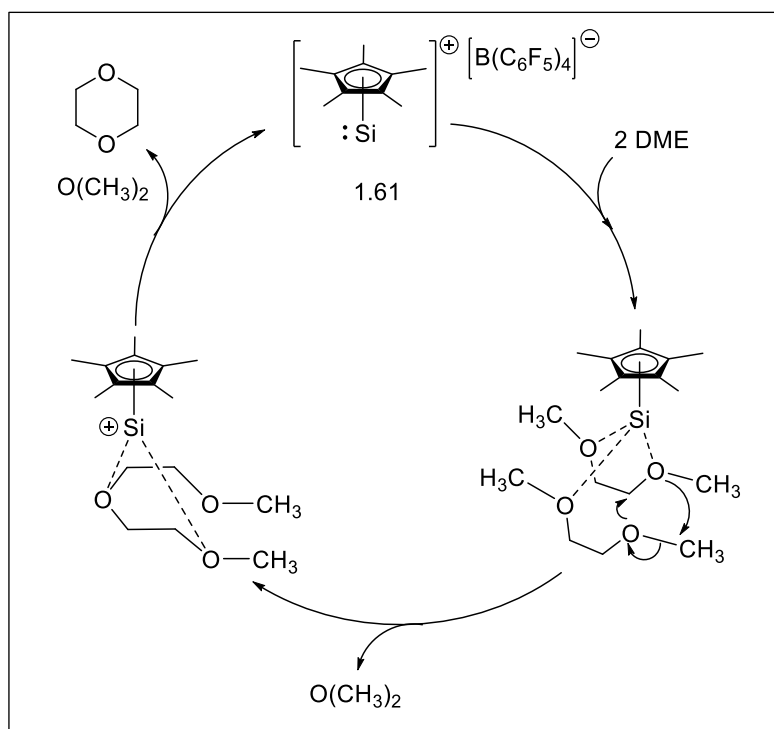
Similar to silylene, other heavier congeners such as germylene, stanaylene are also known for the activation of strong σ -bonds.

1.2.2 Main group compounds in homogeneous catalysis

Catalysis always remains as the center of interest to the world's chemical industry for the reduced energy demands. The importance of catalysis cannot be underrated, as its application are overstated with the industrial and academic settings. In this regard, TM-catalysts are very successful for the conversion of various organic substrates into value-added products with chemo-, regio- and stereoselectivity. However, the increasing cost, relatively low abundance and considerable toxicity of many noble TM-catalysts have spurred the development of alternative methods. Previously the application of the main group element was found to be restricted to some Lewis acid catalysis. The recent significant progress of the main group chemistry in oxidative cleavage of various strong σ -bonds and coordination of olefins,^{32a,43-44,62-63} unique reactivity patterns,⁶⁴ bring into the question: Can main group compounds mimic the traditional TM-complex in terms of the molecular catalysis? In response to this concern, the constant global effort has been applied to the s- and p-block elements of the periodic table for the identification of catalytic vectors. Since the Stephan's report on the heterolytic dihydrogen activation by the 'frustrated' Lewis pairs (FLPs) in 2007, these systems have shown remarkable progress in catalytic processes.⁶⁵ While FLP concept required specific synthetic strategies in designing and applications, many single component catalysts based on cheap and abundant s- and p- block elements have been emerging.

The study of compounds with low valent main group elements continues to be successful due to their anticipated application in stoichiometric reaction or in TM-metal free catalysis. In this light, the significant work by Roesky and Baceiredo on the stoichiometric conversion of CO₂ to methanol and hydrosilylation of olefins by Nacnac Ge(II)^{66a} and Si(II)^{66b} hydrides, respectively have opened up a new avenue for the study and application of the low valent main group compounds in molecular catalysis. Recently, a low valent Si(II) cation, **1.62** was reported to convert 1,2-dimethoxyethane (DME) into 1,4-dioxane and dimethyl ether catalytically (Scheme 1.7).^{66c} The proposed catalytic cycle of the DME conversion shows that two DME molecules coordinates weakly, with up to four contacts to the silicon atom of the cation. This activated state, undergoes a rearrangement in the ether frame diglyme, the latter remain coordinated to the Si(II) center. In the next step, the diglyme molecule is degraded to dimethyl ether and 1,4-dioxane in a similar fashion, and regenerated the catalyst.

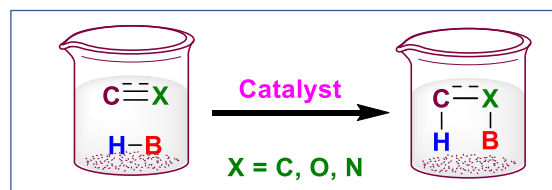
Also, the recent years findings demonstrated that in contrast to the use of the conventional stoichiometric metal hydride or hydrogenation process, the catalytic reduction of the unsaturated bonds with suitable hydride source has gained a significant interest across the globe.



Scheme 1.7 Si(II) cation catalyzed conversion of DME to 1,4-dioxane.

Herein for the current working interest, we discuss the recent progress and usual strategies in the catalytic reduction of unsaturated organic molecules by boranes, cyanating agent mediated by main group compounds in usual and low oxidation state.

1.2.2.1 Hydroboration



Scheme 1.8 Hydroboration of unsaturated compounds with HBpin.

The direct addition of a B–H bond across unsaturated bond such as $C\equiv C$, $C=C$, $C=O$, $C\equiv N$ and $C=N$ bonds- namely, hydroboration is a powerful tool for the bulk production of organoboron compounds (Scheme 1.8).⁶⁷ Catalytic hydroboration is one of the fundamental transformations with academic and industrial importance as these reactions are employed in the production of commodity and material synthesis and are also often encountered in chemical synthesis of complex molecules.⁶⁸

1.2.2.1.1 Hydroboration of carbonyl compounds

This reaction offers effective strategy for the reduction of carbonyl to alcohols and also, beneficial over the hydrogenation and other reduction process in the issue of selectivity and product yield. Precious transition metal compounds, mainly iridium, rhodium, and ruthenium complexes, Group 4 metallocenes and some Zn, Au, Cu complexes etc. are the most studied catalysts for hydroboration reactions.⁶⁷ In this scenario, Corey–Bakshi–Shibata (CBS) catalyst is one of the well-known metal-free catalysts used for the selective asymmetric reduction of ketones.⁶⁹⁻⁷⁰ Later on, Woodward et al. reported the chiral Ga-complex ($LiGa(MTB)_2$), by the combination of $LiGaH_4$ and 2-hydroxy-2'-mercapto-1,1'-binaphthyl, (R)-(-)-MTBH₂, catalyzed enantioselective reduction of prochiral ketones.⁷¹

Following the demonstration of the hydroboration of carbonyl compounds using a magnesium alkyl complex,⁷² a number of research groups have reported the hydroboration of carbonyl compounds with alkaline earth metal based catalysts (chart 1.7).⁷³⁻⁷⁷ In this regard, the growth of group 1 compounds is still at the beginning for the important catalytic transformations. The significant breakthroughs for lithium compounds to be used as single component catalysts came from the groups of Okuda⁷⁸⁻⁷⁹ and Mulvey⁸⁰ (Chart 1.7). Besides, a flurry of research activity has been reported on the carbonyl hydroboration reactions by compounds with p-block element (such as, P, Al, Ge, Sn, Pb etc.) as single site catalysts⁸¹⁻⁸⁶ (Chart 1.7).

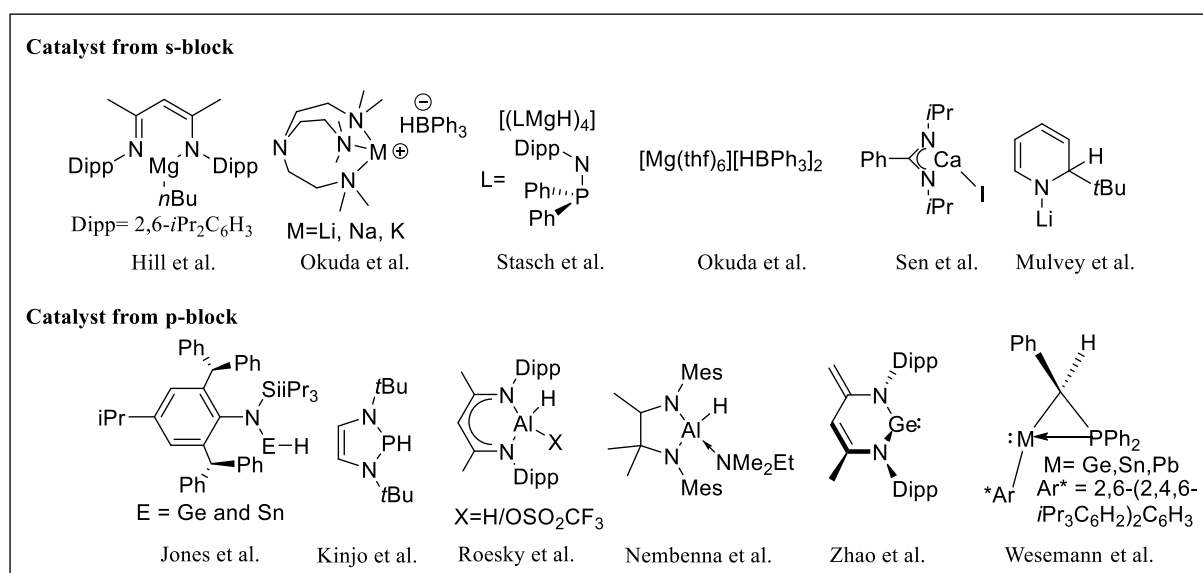


Chart 1.7. Selected examples of main group compounds for aldehyde and ketone hydroboration.

Unlike the hydro-functionalization of polar unsaturated compounds such as aldehydes, ketones, the hydroboration is quite challenging for the substrates like amides and esters. Amide or ester hydroboration represents one of the most straightforward method for bulk synthesis of amines or alcohols, respectively, since the starting materials are stable, inexpensive, stock feed in natural products or biologically important molecules and can be accessed by easy synthetic protocol.⁸⁷⁻⁹⁰ The successive catalytic reduction of amides by HBpin has reported independently from the group of Sadow and Panda by magnesium-complex (ToMMgMe)⁹¹ and aluminium complex⁹² respectively, but these methodologies are restricted for the reduction of tertiary and secondary amides. Recently a very interesting work from the group of Mandal and coworkers, showed that a combination of an abnormal NHC and potassium complex could serve as an efficient catalyst for the hydroboration of a broad ranges of primary amides with pinacolborane.⁹³ Likewise amides, esters are also inert towards mild reductant, and usually requires harsh reductants such as BH₃ and LiAlH₄, reagents⁹⁴ or metal-catalyzed hydrogenation, which needs very high temperature and pressure and capital-intensive setup and pose significant safety issues.⁹⁵ Only few magnesium-based catalysts are known from main group for the selective hydroboration of ester independently thanks to the pioneering works by Sadow,⁹⁶ Okuda,⁷⁶ Nebenna,⁹⁷ and Ma⁹⁸ group.

1.2.2.1.2 Hydroboration of imine, nitrile and carbodiimide

An important protocol for the high purity synthesis of amine is imine, nitrile or carbodiimide hydroboration which does not produce any kind of by product. Transition metal free imine

hydroboration was first reported by the group of Hill using a magnesium compound $[\text{CH}\{\text{C}(\text{Me})\text{NAr}\}_2\text{MgnBu}]$ ($\text{Ar} = 2,6\text{-}i\text{Pr}_2\text{C}_6\text{H}_3$)⁹⁹ and the group of Crudden using a Lewis adduct of DABCO and $\text{B}(\text{C}_6\text{F}_5)_3$ ¹⁰⁰.

Due to the extreme stability of the $\text{C}\equiv\text{N}$ bond in organonitrile, its hydroboration has become a topic of growing interest in recent years. Among the main group catalysts, few alkaline-earth metal^{85a}, Al-complexes¹⁰¹ are known to catalyze nitrile hydroboration. On the other hand, catalytic and selective single hydroboration of carbodiimides are quite rare and reported only with Mg,¹⁰² Al,¹⁰³ B,¹⁰⁴ and An¹⁰⁵ (Th or U) -based catalyst.

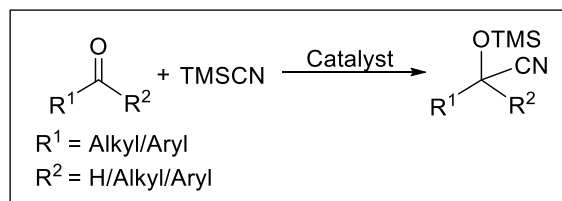
1.2.2.1.3 Hydroboration of alkene and alkyne

Alkenylboronic acid derivatives, including vinylboronates can be obtained via hydroboration of carbon-carbon double or triple bonds. They are widely useful in cross coupling reactions.¹⁰⁶ In this regard, it is worth to mention that the catalytic potential of the s- and p-block complexes are extensively studied for the reduction of unsaturated polar bonds ($\text{C}=\text{O}$, $\text{C}=\text{NR}$, etc.), but remains almost unexplored apart from group 13, for the non-polar unsaturated bond such as alkenes or alkynes. A series of main group compounds mainly based on B,¹⁰⁷ and Al¹⁰⁸ are known to reduce unsaturated non polar bond such as alkene or alkyne in presence of a suitable borane source. In this context, the utilization of s-block compounds in homogenous catalysis is limited, and known only for the hydrogenation¹⁰⁹ or hydrosilylation¹¹⁰ reaction. Development of catalytic hydroboration based on alkali or alkaline earth metal is known mostly for the polarized unsaturated functionalities such as aldehyde, ketone ester, nitrile etc. From the Group 2, few Mg-complexes are reported to catalyze alkyne hydroboration.^{102,111} Although LiAlH_4 catalyzed hydroboration of alkenes is known, a mechanistic investigation by Cowley and Thomas revealed that AlH_3 was the active catalyst.^{108c} This was further confirmed by using AlEt_3 (a surrogate of AlH_3) as a single site catalyst to accomplish the conversion. Recently, the group of Bao and Xue preliminarily showed that *n*-BuLi could also serve as an efficient catalyst for the hydroboration of alkynes with HBpin,¹¹² but they are limited in terms of substrate scope and mechanistic investigation was not disclosed.

1.2.2.2 Cyanosilylation

The cyanosilylation of carbonyl compounds is the formal addition of the cyano ($-\text{CN}$) and the silyl ($-\text{SiMe}_3$) group across the $\text{C}=\text{O}$ bond (Scheme 1.9). It represents one of the effective strategies for the versatile synthesis of the silylated cyanohydrin, an intermediate for the functionalized

compounds such as, esters, α -hydroxy acid, acyloins, and many other biologically active compounds.¹¹³



Scheme 1.9. Cyanosilylation of carbonyl compounds.

TMSCN is used as a safe cyanating source for this methodology to avoid toxic and hazardous HCN, NaCN or KCN. Several reagents including metal halides, metal alkoxides, Lewis acids, Lewis bases, inorganic salts, iodine, have been reported as an effective catalyst for the transfer the -CN group to carbonyl carbon from TMSCN.¹¹⁴ Some bifunctional catalysts,¹¹⁵ chiral Lewis acid–Lewis catalytic systems¹¹⁶ were also introduced for the asymmetric cyanosilylation of the aldehydes and ketones by groups of Shibasaki and Corey, independently. However, only a few well-defined neutral heavier main group compounds have been reported as single site catalysts to date thanks to pioneering works from the groups of Roesky, Zhi, Nagendran, and others (Chart 1.8).¹¹⁷⁻¹²⁵ The majority of them were known to catalyze aldehydes only.^{118,120-123} The use of alkaline earth metal complexes in catalytic cyanosilylation is very limited and recently reported independently from our group and Ma et al. with a monomeric calcium complex, $\text{PhC}(\text{NiPr})_2\text{CaI}^{119}$ and a magnesium(I) complex, $\{(\text{Xyl}(\text{nacnac}))\text{Mg}\}_2$ ($\text{Xyl} = 2,6\text{-Me}_2\text{-C}_6\text{H}_3$),¹²⁵ respectively (Chart 1.8).

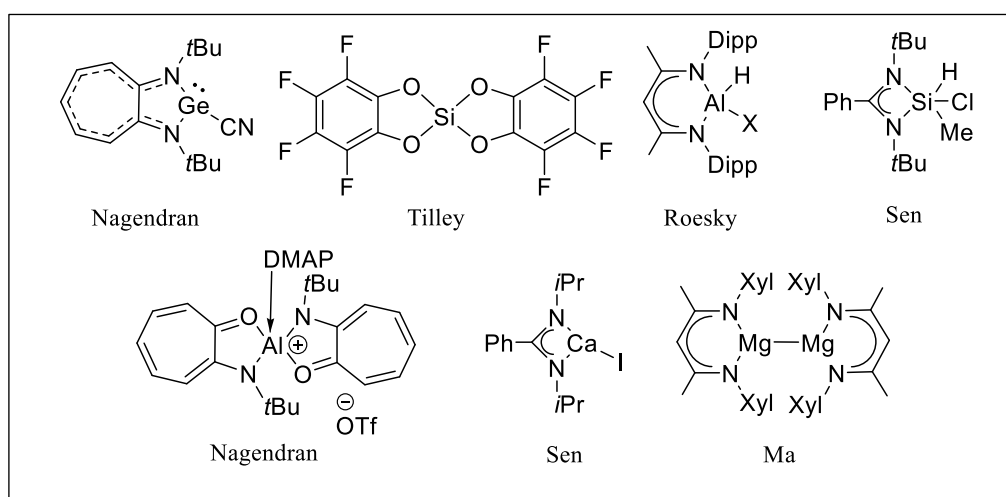


Chart 1.8. Examples of the main-group catalysts for the cyanosilylation of carbonyl compounds.

1.3 Aim and outline of the thesis

The introductory portion of the thesis has accounted that, with proper kinetic and/or thermodynamic support the synthetic chemists have overcome the challenges associated with the stabilization of silylene. A fair number of isolable silylenes have been reported and made the chemistry rich with their novel and unprecedented bonding and reactivity studies.

In this regard, three coordinated silylene represents a special class due to its interesting electronic feature and inherent stability. Literature survey revealed that, amidinate ligand system with its delicate kinetic and thermodynamic balance are quite pronounced for the isolation of low valent main group compounds. Benzamidinato-stabilized silylene with the composition of $LSiX$ [$L = PhC(NtBu)_2$] are well studied with electron-rich π -donating substituents ($X = Cl, Br, N(SiMe_3)_2, P(SiMe_3)_2$ etc.). While silylenes with π -donor substituents are unreactive for dihydrogen activation, the same lacking of π -donor ligands are known to split H-H bond. And this is due to the small HOMO-LUMO gap for the subsequent decrease in π donation from the ligand. Since the pioneering discovery of tetrakis(trimethylsilyl)silane by Benkeser, Gilman, and Smith, the use of tris(trimethylsilyl)silyl group in the development of low-valent main-group chemistry is increasing rapidly because of its pronounced steric effect and strong σ -donor strength. The utility of tris(trimethylsilyl)silyl group in silylene chemistry has been amply exemplified by Aldridge and co-workers with the isolation of $Si\{Si(SiMe_3)_3\}\{N(SiMe_3)Dipp\}$, a stable mixed (amido)-silylsilylene known to activate dihydrogen.¹⁷ This remarkable result led us to study the chemistry of three coordinated silylene with the combination of both benz-amidinate ligand and tris(trimethylsilyl)silyl group.

Having all the potentials to mimic the traditional TM-catalyst, there is an ongoing quest for improved small molecule activation to the catalysis by compounds with main group elements for academic and industrial importance. However, such studies are still at early days due to the paucity of well-defined main-group compounds.

The main aim of the thesis is to further extend our knowledge on the synthesis, and reactivity of a novel hypersilylsilylene. And also, the application of earth abundant, cheap or readily accessible main group compounds in homogeneous catalysis, mainly on hydroboration and cyanosilylation of unsaturated compounds. Both experimental and theoretical insights have been presented for the catalytic studies to understand the mechanism. All the compounds prepared were characterized by multinuclear NMR spectroscopy, single crystal X-ray diffraction, and HRMS spectrometry. The following chapters will cover all these aspects of the thesis.

Chapter 2 accounts the synthesis and characterization of a silylene with the combination of benzamidinate ligand $[\text{PhC}(\text{N}t\text{Bu})_2]$ and hypersilyl group under ambient condition in an excellent yield. Synthesized hypersilylsilylene was treated with various small molecules to study its reactivity. Similarly, reactivities with boranes have also been studied and summarized in this chapter. A versatile reactivity of hypersilylsilylene with aromatic and aliphatic disubstituted chlorophosphine is also presented in the same section.

Chapter 3 illustrates the catalytic application of previously known benz-amidinato silane, $[\text{PhC}(\text{N}t\text{Bu})_2\text{SiHCl}_2]$ on selective hydroboration of aldehydes and aldimines. This work represents the first example of a neutral penta-coordinated Si(IV) compound for the catalytic hydroboration. Complete stoichiometric reactions as well as theoretical calculations have been carried out thoroughly to identify a plausible mechanism.

Chapter 4 describes the utilization of readily accessible lithium compounds with different electronegative substituents for the catalytic reduction of various carbonyl compounds. Lithium compounds such as 2,6-ditert-butyl phenolate lithium (**4a**), 1, 1'-dilithioferrocene (**4b**) and nacnac lithium (**4c**) were used as single site catalyst for the hydroboration and cyanosilylation of aldehydes and ketones with HBpin and TMSCN respectively. Moreover, the catalytic hydroboration is extended for more challenging carbonyls such as esters and amides. For all the cases, mechanistic studies have been carried out to get the insight.

Chapter 5 represents the catalytic implementation of 2,6-ditert-butyl phenolate lithium (**4a**), 1,1'-dilithioferrocene (**4b**) on even more challenging unsaturated compounds having no such polarity difference-namely for alkene and alkyne. The reaction shows excellent chemo- and regioselective addition of HBpin across the unsaturated bond. Furthermore, this work represents the first utilization of main group catalysts on selective hydroboration of biologically important terpenes.

1.4 References

1. Friedel, C.; Crafts, J. M. *Liebigs Ann. Chem.* **1866**, *138*, 19.
2. Teichmann, J.; Wagner, M. *Chem. Commun.* **2018**, *54*, 1397–1412.
3. (a) Mizuhata, Y.; Sasamori, T.; Tokitoh, N. *Chem. Rev.* **2009**, *109*, 3479–3511. (b) Asay, M.; Jones, C.; Driess, M. *Chem. Rev.* **2011**, *111*, 354–396.
4. (a) Sasamori, T.; Tokitoh, N. *Encyclopedia of Inorganic Chemistry II*; King, R. B., Ed.; John Wiley & Sons: Chichester, U.K., 2005; pp 1698–1740. (b) *The Transition State: A*

- Theoretical Approach; Fueno, T.; Ed.; Gordon and Breach Science Publishers: Langhorne, PA, 1999; pp 147–161.
- Trinquier, G. *J. Am. Chem. Soc.* **1990**, *112*, 2130–2137.
 - (a) Weidenbruch, M. *J. Organomet. Chem.* **2002**, *646*, 39–52. (b) Weidenbruch, M. *Organometallics* **2003**, *22*, 4348–4360.
 - Skell, P. S.; Goldstein, E. J. *J. Am. Chem. Soc.* **1964**, *86*, 1442–1443.
 - (a) Gillette, G. R.; Noren, G. H.; West, R. *Organometallics* **1987**, *6*, 2617–2618. (b) Gillette, G. R.; Noren, G. H.; West, R. *Organometallics* **1989**, *8*, 487–491. (c) Ando, W.; Hagiwara, K.; Sekiguchi, A. *Organometallics* **1987**, *6*, 2270–2271. (d) Ando, W.; Sekiguchi, A.; Hagiwara, K.; Sakakibara, A.; Yoshida, H. *Organometallics* **1988**, *7*, 558–559.
 - (a) Becerra, R.; Cannady, J. P.; Walsh, R. *J. Phys. Chem. A* **2002**, *106*, 4922–4927. (b) Becerra, R.; Cannady, J. P.; Walsh, R. *J. Phys. Chem. A* **2003**, *107*, 9588–9593. (c) Becerra, R.; Cannady, J. P.; Walsh, R. *J. Phys. Chem. A* **2006**, *110*, 6680–6686.
 - (a) Leigh, W. J.; Moiseev, A. G.; Coulais, E.; Lollmahomed, F.; Askari, M. S. *Can. J. Chem.* **2008**, *86*, 1105–1117. (b) Steinmetz, M. G. *Chem. Rev.* **1995**, *95*, 1527–1588.
 - Jutzi, P.; Kanne, D.; Krüger, C. *Angew. Chem. Int. Ed.* **1986**, *25*, 164–164.
 - Denk, M.; Lennon, R.; Hayashi, R.; West, R.; Belyakov, A. V.; Verne, H. P.; Haaland, A.; Wagner, M.; Metzler, N. *J. Am. Chem. Soc.* **1994**, *116*, 2691–2692.
 - Arduengo, A. J.; Harlow, R. L.; Kline, M. *J. Am. Chem. Soc.* **1991**, *113*, 361–363.
 - (a) Zark, P.; Schäfer, A.; Mitra, A.; Haase, D.; Saak, W.; West, R.; Müller, T. *J. Organomet. Chem.* **2010**, *695*, 398–408. (b) Mitra, A.; Brodovitch, J.-C.; Krempner, C.; Percival, P. W.; Vyas, P.; West, R. *Angew. Chem. Int. Ed.* **2010**, *49*, 2893–2895. (c) Cui, H.; Shao, Y.; Li, X.; Kong, L.; Cui, C. *Organometallics* **2009**, *28*, 5191–5195.
 - (a) Tomasik, A. C.; Mitra, A.; West, R. *Organometallics* **2009**, *28*, 378–381. (b) Li, W.; Hill, N. J.; Tomasik, A. C.; Bikzhanova, G.; West, R. *Organometallics* **2006**, *25*, 3802–3805.
 - (a) Gehrhus, B.; Hitchcock, P. B.; Lappert, M. F.; Heinicke, J.; Boese, R.; Bläser, D. *J. Organomet. Chem.* **1996**, *521*, 211–220. (b) Gehrhus, B.; Lappert, M. F.; Heinicke, J.; Boese, R.; Bläser, D. *J. Chem. Soc., Chem. Commun.* **1995**, 1931–1932. (c) Denk, M.; Green, J. C.; Metzler, N.; Wagner, M. *J. Chem. Soc., Dalton Trans.* **1994**, 2405–2410.
 - Gehrhus, B.; Hitchcock, P. B.; Lappert, M. F. *Z. Anorg. Allg. Chem.* **2005**, *631*, 1383–1386.
 - Driess, M.; Yao, S.; Brym, M.; van Wüllen, C.; Lentz, D. *J. Am. Chem. Soc.* **2006**, *128*, 9628–9629.

19. Kira, M.; Ishida, S.; Iwamoto, T.; Kabuto, C. *J. Am. Chem. Soc.* **1999**, *121*, 9722–9723.
20. Abe, T.; Tanaka, R.; Ishida, S.; Kira, M.; Iwamoto, T. *J. Am. Chem. Soc.* **2012**, *134*, 20029–20032.
21. Ishida, S.; Abe, T.; Hirakawa, F.; Kosai, T.; Sato, K.; Kira, M.; Iwamoto, T. *Chem. - Eur. J.* **2015**, *21*, 15100–15103.
22. Asay, M.; Inoue, S.; Driess, M. *Angew. Chem. Int. Ed.* **2011**, *50*, 95890–9592.
23. Alvarado-Beltran, I.; Baceiredo, A.; Saffon-Merceron, N.; Branchadell, V.; Kato, T. *Angew. Chem. Int. Ed.* **2016**, *55*, 16141–16144.
24. Kosai, T.; Ishida, S.; Iwamoto, T. *Angew. Chem. Int. Ed.* **2016**, *55*, 15554–15558.
25. Lee, G.-H.; West, R.; Müller, T. *J. Am. Chem. Soc.* **2003**, *125*, 8114–8115.
26. (a) Protchenko, A. V.; Birjkumar, K. H.; Dange, D.; Schwarz, A. D.; Vidovic, D.; Jones, C.; Kaltsoyannis, N.; Mountford, P.; Aldridge, S. *J. Am. Chem. Soc.* **2012**, *134*, 6500–6503. (b) Rekken, B. D.; Brown, T. M.; Fettinger, J. C.; Tuononen, H. M.; Power, P. P. *J. Am. Chem. Soc.* **2012**, *134*, 6504–6507. (c) Protchenko, A. V.; Schwarz, A. D.; Blake, M. P.; Jones, C.; Kaltsoyannis, N.; Mountford, P.; Aldridge, S. *Angew. Chem. Int. Ed.* **2013**, *52*, 568–571. (d) Hadlington, T. J.; Abdalla, J. A. B.; Tirfoin, R.; Aldridge, S.; Jones, C. *Chem. Commun.* **2016**, *52*, 1717–1720. (e) Loh, Y. K.; Ying, L.; Ángeles Fuentes, M.; Do, D. C. H.; Aldridge, S. *Angew. Chem. Int. Ed.* **2019**, *58*, 4847–4851.
27. So, C.-W.; Roesky, H. W.; Magull, J.; Oswald, R. B. *Angew. Chem. Int. Ed.* **2006**, *45*, 3948–3950.
28. (a) Sen, S. S.; Roesky, H. W.; Stern, D.; Henn, J.; Stalke, D. *J. Am. Chem. Soc.* **2010**, *132*, 1123–1126. (b) Yeong, H.-X.; Lau, K.-C.; Xi, H.-W.; Lim, K. H.; So, C.-W. *Inorg. Chem.* **2010**, *49*, 371–373. (c) So, C.-W.; Roesky, H. W.; Gurubasavaraj, P. M.; Oswald, R. O.; Gamer, M. T.; Jones, P. G.; Blaurock, S. *J. Am. Chem. Soc.* **2007**, *129*, 12049–12054. (d) Azhakar, R.; Ghadwal, R. S.; Roesky, H. W.; Wolf, H.; Stalke, D. *Organometallics* **2012**, *31*, 4588–4592. (e) Sen, S. S.; Hey, J.; Herbst-Irmer, R.; Roesky, H. W.; Stalke, D. *J. Am. Chem. Soc.* **2011**, *133*, 12311–12316. (f) Inoue, S.; Wang, W.; Präsang, C.; Asay, M.; Irran, E.; Driess, M. *J. Am. Chem. Soc.* **2011**, *133*, 2868–2871.
29. (a) Junold, K.; Baus, J. A.; Burschka, C.; Tacke, R. *Angew. Chem. Int. Ed.* **2012**, *51*, 7020–7023. (b) Mück, F. M.; Junold, K.; Baus, J. A.; Burschka, C.; Tacke, R. *Eur. J. Inorg. Chem.* **2013**, 5821–5825. (c) Junold, K.; Nutz, M.; Baus, J. A.; Burschka, C.; Fonseca Guerra, C.; Bickelhaupt, F. M.; Tacke, R. *Chem. - Eur. J.* **2014**, *20*, 9319–9329.
30. (a) Ghadwal, R. S.; Roesky, H. W.; Merkel, S.; Henn, J.; Stalke, D. *Angew. Chem. Int. Ed.* **2009**, *48*, 5683–5686. (b) Ghadwal, R. S.; Azhakar, R.; Roesky, H. W. *Acc. Chem. Res.*

- 2013, 46, 444–456. (c) Filippou, A. C.; Chernov, O.; Schnakenburg, G. *Angew. Chem. Int. Ed.* **2009**, 48, 5687–5690. (d) Filippou, A. C.; Lebedev, Y. N.; Chernov, O.; Straßmann, M.; Schnakenburg, G. *Angew. Chem. Int. Ed.* **2013**, 52, 6974–6978.
31. Gau, D.; Kato, T.; Saffon-Merceron, N.; Cossío, F. P.; Baceiredo, A. *J. Am. Chem. Soc.* **2009**, 131, 8762–8763.
32. (a) Rodriguez, R.; Gau, D.; Contie, Y.; Kato, T.; Saffon-Merceron, N.; Baceiredo, A. *Angew. Chem. Int. Ed.* **2011**, 50, 11492–11495. (b) Gau, D.; Kato, T.; Saffon-Merceron, N.; De Cózar, A.; Cossío, F. P.; Baceiredo, A. *Angew. Chem. Int. Ed.* **2010**, 49, 6585–6588.
33. Kinjo, R.; Donnadiou, B.; Celik, M. A.; Frenking, G.; Bertrand, G. *Science* **2011**, 333, 610–613.
34. Cui, C.; Roesky, H. W.; Schmidt, H.-G.; Noltemeyer, M.; Hao, H.; Cimpoesu, F. *Angew. Chem. Int. Ed.* **2000**, 39, 4274–4276.
35. Mondal, K. C.; Roesky, H. W.; Schwarzer, M. C.; Frenking, G.; Niepötter, B.; Wolf, H.; Herbst-Irmer, R.; Stalke, D. *Angew. Chem. Int. Ed.* **2013**, 52, 2963–2967.
36. Xiong, Y.; Yao, S.; Inoue, S.; Epping, J. D.; Driess, M. *Angew. Chem. Int. Ed.* **2013**, 52, 7147–7150.
37. Xiong, Y.; Yao, S.; Tan, G.; Inoue, S.; Driess, M. *J. Am. Chem. Soc.* **2013**, 135, 5004–5007.
38. Li, Y.; Mondal, K. C.; Roesky, H. W.; Zhu, H.; Stollberg, P.; Herbst-Irmer, R.; Stalke, D.; Andrada, D. M. *J. Am. Chem. Soc.* **2013**, 135, 12422–12428.
39. Chu, T.; Belding, L.; van der Est, A.; Dudding, T.; Korobkov, I.; Nikonov, G. I. *Angew. Chem. Int. Ed.* **2014**, 53, 2711–2715.
40. Driess, M.; Grützmacher, H. *Angew. Chem. Int. Ed. Engl.* **1996**, 35, 828–856.
41. Fischer, R. C.; Power, P. P. *Chem. Rev.* **2010**, 110, 3877–3923.
42. Martin, D.; Soleilhavoup, M.; Bertrand, G. *Chem. Sci.* **2011**, 2, 389–399.
43. Power, P. P. *Acc. Chem. Res.* **2011**, 44, 627–637.
44. Power, P. P. *Nature* **2010**, 463, 171–177.
45. (a) Chu, T.; Nikonov, G. I. *Chem. Rev.* **2018**, 118, 3608–3680. (b) Wiberg, N.; Wiberg E. in *Lehrbuch der Anorganischen Chemie*, de Gruyter, 2007.
46. Spikes, G. H.; Fettingner, J. C.; Power, P. P. *J. Am. Chem. Soc.* **2005**, 127, 12232–12233.
47. Revunova, K.; Nikonov, G. I. *Dalton Trans.* **2015**, 44, 840–866.
48. Oestreich, M.; Hermeke, J.; Mohr, J. *Chem. Soc. Rev.* **2015**, 44, 2202–2220.
49. Hill, M. S.; Liptrot, D. J.; Weetman, C. *Chem. Soc. Rev.* **2016**, 45, 972–988.
50. Frey, G. D.; Lavallo, V.; Donnadiou, B.; Schoeller, W. W.; Bertrand, G. *Science* **2007**, 316, 439–441.

51. Denk, M. K.; Rodezno, J. M.; Gupta, S.; Lough, A. *J. Organomet. Chem.* **2001**, 617–618, 242–253.
52. Devarajan, D.; Doubleday, C. E.; Ess, D. H. *Inorg. Chem.* **2013**, 52, 8820–8833.
53. Wang, Y.; Ma, J. *J. Organomet. Chem.* **2009**, 694, 2567–2575.
54. Driess, M. *Nat. Chem.* **2012**, 4, 525–526.
55. Wendel, D.; Porzelt, A.; Herz, F. A. D.; Sarkar, D.; Jandl, C.; Inoue, S.; Rieger, B. *J. Am. Chem. Soc.* **2017**, 139, 8134–8137.
56. Filippou, A. C.; Baars, B.; Chernov, O.; Lebedev, Y. N.; Schnakenburg, G. *Angew. Chem. Int. Ed.* **2014**, 53, 565–570.
57. (a) Koelliker, R.; Milstein, D. *J. Am. Chem. Soc.* **1991**, 113, 8524–8525. (b) Zhao, J.; Goldman, A. S.; Hartwig, J. F. *Science* **2005**, 307, 1080–1082.
58. Jana, A.; Schulzke, C.; Roesky, H. W. *J. Am. Chem. Soc.* **2009**, 131, 4600–4601.
59. Alberto, M. E.; Russo, N.; Sicilia, E. *Chem. - Eur. J.* **2013**, 19, 7835–7846.
60. Jana, A.; Roesky, H. W.; Schulzke, C.; Samuel, P. P. *Organometallics* **2009**, 28, 6574–6577.
61. Meltzer, A.; Inoue, S.; Präsang, C.; Driess, M. *J. Am. Chem. Soc.* **2010**, 132, 3038–3046.
62. (a) Power, P. P. *Chem. Rec.* **2011**, 12, 238–255. (b) Chivers, T.; Konu, J. *Comments Inorg. Chem.* **2009**, 30, 131–176.
63. Yao, S.; Xiong, Y.; Driess, M. *Organometallics* **2011**, 30, 1748–1767.
64. Stephan, D. W. *Org. Biomol. Chem.* **2008**, 6, 1535–1539.
65. Stephan, D. W. *J. Am. Chem. Soc.* **2015**, 137, 10018–10032.
66. (a) Jana, A.; Tavcar, G.; Roesky, H. W.; John, M. *Dalton Trans.* **2010**, 39, 9487–9489. (b) Leszczyńska, K.; Mix, A.; Berger, R. J. F.; Rummel, B.; Neumann, B.; Stammler, H.-G.; Jutzi, P. *Angew. Chem. Int. Ed.* **2011**, 50, 6843–6846.
67. For selected reviews on main group compound catalyzed hydroboration, please see: (a) Chong, C. C.; Kinjo, R. *ACS Catal.* **2015**, 5, 3238–3259. (b) Nikonov, G. I. *ACS Catal.* **2017**, 7, 7257–7266. (c) Mukherjee, D.; Okuda, J. *Angew. Chem. Int. Ed.* **2018**, 57, 1458–1473.
68. Brown, H.C. *Tetrahedron* **1961**, 12, 117–138.
69. Corey, E. J.; Bakshi, R. K.; Shibata, S. *J. Am. Chem. Soc.* **1987**, 109, 5551–5553.
70. Corey, E. J.; Shibata, S.; Bakshi, R. K. *J. Org. Chem.* **1988**, 53, 2861–2863.
71. Blake, A. J.; Cunningham, A.; Ford, A.; Teat, S. J.; Woodward, S. *Chem. - Eur. J.* **2000**, 6, 3586–3594.

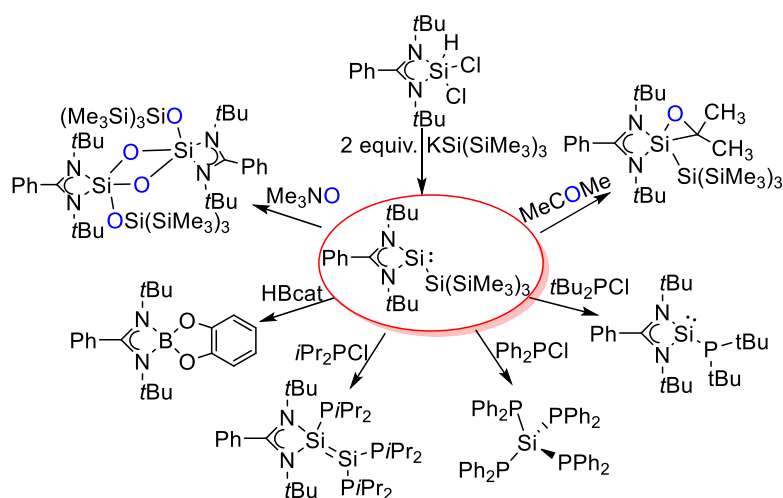
72. Arrowsmith, M.; Hadlington, T. J.; Hill, M. S.; Kociok-Köhn, G. *Chem. Commun.* **2012**, 48, 4567–4569.
73. Yadav, S.; Pahar, S.; Sen, S. S. *Chem. Commun.* **2017**, 53, 4562–4564.
74. Fohlmeister, L.; Stasch, A. *Chem. - Eur. J.* **2016**, 22, 10235–10246.
75. Mukherjee, D.; Shirase, S.; Spaniol, T. P.; Mashima, K.; Okuda, J. *Chem. Commun.* **2016**, 52, 13155–13158.
76. Mukherjee, D.; Ellern, A.; Sadow, A. D. *Chem. Sci.* **2014**, 5, 959–965.
77. Manna, K.; Ji, P.; Greene, F. X.; Lin, W. *J. Am. Chem. Soc.* **2016**, 138, 7488–7491.
78. Mukherjee, D.; Osseili, H.; Spaniol, T. P.; Okuda, J. *J. Am. Chem. Soc.* **2016**, 138, 10790–10793.
79. (a) Osseili, H.; Mukherjee, D.; Beckerle, K.; Spaniol, T. P.; Okuda, J. *Organometallics* **2017**, 36, 3029–3034. (b) Osseili, H.; Mukherjee, D.; Spaniol, T. P.; Okuda, J. *Chem. - Eur. J.* **2017**, 23, 14292–14298.
80. (a) McLellan, R.; Kennedy, A. R.; Mulvey, R. E.; Orr, S. A.; Robertson, S. D. *Chem. - Eur. J.* **2017**, 23, 16853–16861. (b) Pollard, V. A.; Orr, S. A.; McLellan, R.; Kennedy, A. R.; Hevia, E.; Mulvey, R. E. *Chem. Commun.* **2018**, 54, 1233–1236.
81. (a) Hadlington, T. J.; Hermann, M.; Frenking, G.; Jones, C. *J. Am. Chem. Soc.* **2014**, 136, 3028–3031. (b) Schneider, J.; Sindlinger, C. P.; Freitag, S. M.; Schubert, H.; Wesemann, L. *Angew. Chem. Int. Ed.*, **2017**, 56, 333–337. (c) Wu, Y.; Shan, C.; Sun, Y.; Chen, P.; Ying, J.; Zhu, J.; Liu, L(Leo); Zhao, Y. *Chem. Commun.* **2016**, 52, 13799–13802.
82. Chong, C.-C.; Hirao, H.; Kinjo, R. *Angew. Chem. Int. Ed.*, **2015**, 54, 190–194.
83. Yang, Z.; Zhong, M.; Ma, X.; De, S.; Anusha, C.; Parameswaran, P.; Roesky, H. W. *Angew. Chem. Int. Ed.*, **2015**, 54, 10225–10229.
84. (a) Jakhar, V. K.; Barman, M. K.; Nembenna, S. *Org. Lett.* **2016**, 18, 4710–4713. (b) Lawson, J. R.; Wilkins, L. C.; Melen, R. L. *Chem. - Eur. J.* **2017**, 23, 10997–11000.
85. (a) Weetman, C.; Anker, M. D.; Arrowsmith, M.; Hill, M. S.; Kociok-Köhn, G.; Liptrot, D. J.; Mahon, M. F. *Chem. Sci.* **2016**, 7, 628–641. (b) Weetman, C.; Hill, M. S.; Mahon, M. F. *Chem. Commun.* **2015**, 51, 14477–14480.
86. (a) Courtemanche, M.-A.; Légaré, M.-A.; Maron, L.; Fontaine, F.-G. *J. Am. Chem. Soc.* **2013**, 135, 9326–9329. (b) Franz, D.; Sirtl, L.; Pöthig, A.; Inoue, S. *Z. Anorg. Allg. Chem.* **2016**, 642, 1245–1250. (c) Lortie, J. L.; Dudding, T.; Gabidullin, B. M.; Nikonov, G. I. *ACS Catal.* **2017**, 7, 8454–8459.
87. Smith, A. M.; Whyman, R. *Chem. Rev.* **2014**, 114, 5477–5510.

88. Dodds, D. L.; Cole-Hamilton, D. J. *Catalytic Reduction of Amides Avoiding LiAlH₄ or B₂H₆. In Sustainable Catalysis: Challenges and Practices for the Pharmaceutical and Fine Chemical Industries*, ed. Dunn, P. J.; Hii, K. K.; Krische, M. J.; Williams, M. T. Wiley, Hoboken, NJ, **2013**, pp. 1–36.
89. Biermann, U.; Friedt, W.; Lang, S.; Luhs, W.; Machmuller, G.; Metzger, J. O.; Klaas, M. R.; Schafer, H. J.; Schneider, M. P. *Angew. Chem. Int. Ed.* **2000**, *39*, 2206–2224.
90. (a) Lohr, T. L.; Li, Z.; Marks, T. *J. Acc. Chem. Res.* **2016**, *49*, 824–834. (b) Wu, L.; Moteki, T.; Gokhale, A. A.; Flaherty, D. W.; Toste, F. D. *Chem* **2016**, *1*, 32–58. (c) Hu, C.; Creaser, D.; Siahrostami, S.; Grönbeck, H.; Ojagh, H.; Skoglundh, M. *Catal. Sci. Technol.* **2014**, *4*, 2427–2444. (d) Turek, T.; Trimm, D. L.; Cant, N. W. *Catal. Rev.: Sci. Eng.* **1994**, *36*, 645–683.
91. Lampland, N. L.; Hovey, M.; Mukherjee, D.; Sadow, A. D. *ACS Catal.* **2015**, *5*, 4219–4226.
92. Das, S.; karmakar, H.; Bhattacharjee, J.; Panda, T. K. *Dalton Trans.* **2019**, *48*, 11978–11984.
93. Bhunia, M.; Shaoo, S. R.; Das, A.; Ahmed, J.; Sreejyothi, P.; Mandal, S. K. *Chem. Sci.* **2020**, *11*, 1848–1854.
94. Ojima, I.; Nihonyanagi, M.; Kogure, T.; Kumagai, M.; Horiuchi, S.; Nakatsugawa, K. *J. Organomet. Chem.* **1975**, *94*, 449–461.
95. Selected references: (a) Dupau, P.; Tran Do, M.-L.; Gaillard, S.; Renaud, J.-L. *Angew. Chem. Int. Ed.* **2014**, *53*, 13004–13006. (b) Tan, X.; Wang, Y.; Liu, Y.; Wang, F.; Shi, L.; Lee, K.-H.; Lin, Z.; Lv, H.; Zhang, X. *Org. Lett.* **2015**, *17*, 454–457. (c) Pritchard, J.; Filonenko, G. A.; van Putten, R.; Hensen, E. J. M.; Pidko, E. A. *Chem. Soc. Rev.* **2015**, *44*, 3808–3833. (d) Tan, X.; Wang, Q.; Liu, Y.; Wang, F.; Lv, H.; Zhang, X. *Chem. Commun.* **2015**, *51*, 12193–12196. (e) Kim, D.; Le, L.; Drance, M. J.; Jensen, K. H.; Bogdanovski, K.; Cervarich, T. N.; Barnard, M. G.; Pudalov, N. J.; Knapp, S. M. M.; Chianese, A. R. *Organometallics* **2016**, *35*, 982–989.
96. Patnaik, S.; Sadow, A. D. *Angew. Chem. Int. Ed.* **2019**, *58*, 2505–2509.
97. Barman, M. K.; Baishya, A.; Nembenna, S. *Dalton Trans.* **2017**, *46*, 4152–4156.
98. Cao, X.; Wang, W.; Lu, K.; Yao, W.; Xue, F.; Ma, M. *Dalton Trans.* **2020**, *49*, 2776–2780.
99. Arrowsmith, M.; Hill, M. S.; Kociok-Köhn, G. *Chem. - Eur. J.*, **2013**, *19*, 2776–2783.
100. Eisenberger, P.; Bailey, A. M.; Crudden, C. M. *J. Am. Chem. Soc.*, **2012**, *134*, 17384–17387.

101. (a) Harinath, A.; Bhattacharjee, J.; Panda, T. K. *Adv. Synth. Catal.* **2019**, *361*, 850–857. (b) Liu, W.; Ding, Y.; Jin, D.; Shen, Q.; Yan, B.; Ma, X.; Yang, Z. *Green Chem.* **2019**, *21*, 3812–3815.
102. (a) Weetman, C.; Hill, M. S.; Mahon, M. F. *Chem. - Eur. J.* **2016**, *22*, 7158–7162. (b) Rauch, M.; Ruccolo, S.; Parkin, G. *J. Am. Chem. Soc.* **2017**, *139*, 13264–13267.
103. Ramos, A.; Antinolo, A.; Carrillo-Hermosilla, F.; Fernandez-Galan, R.; Garcia-Vivo, D.; *Chem. Commun.* **2019**, *55*, 3073–3076.
104. Ding, Y.; Ma, X.; Liu, Y.; Liu, W.; Yang, Z.; Roesky, H. W. *Organometallics* **2019**, *38*, 3092–3097.
105. Liu, H.; Kulbitski, K.; Tamm, M.; Eisen, M. S. *Chem. - Eur. J.* **2018**, *24*, 5738–5742.
106. (a) Miyaura, N.; Suzuki, A. *Chem. Rev.* **1995**, *95*, 2457–2483. (b) Tucker, C. E.; Davidson, J.; Knochel, P. *J. Org. Chem.* **1992**, *57*, 3482–3485. (c) Hall, D. G. *In Boronic Acids: Preparation, Applications in Organic Synthesis and Medicine*, Hall, D. G., Ed.; Wiley-VCH, Weinheim, Germany, 2011.
107. (a) Lawson, J. R.; Wilkins, L. C.; Melen, R. L. *Chem. - Eur. J.* **2017**, *23*, 10997–11000. (b) Carden, J. L.; Gierlichs, L. J.; Wass, D. F.; Browne, D. L.; Melen, R. L. *Chem. Commun.* **2019**, *55*, 318–321. (c) McGough, J. S.; Butler, S. M.; Cade, I. A.; Ingleson, M. J. *Chem. Sci.* **2016**, *7*, 3384–3389. (d) Fleige, M.; Möbus, J.; vom Stein, T.; Glorius, F.; Stephan, D. W. *Chem. Commun.* **2016**, *52*, 10830–10833. (e) Yin, Q.; Kemper, S.; Klare, H. F. T.; Oestreich, M. *Chem. - Eur. J.* **2016**, *22*, 13840–13844. (f) Prokofjevs, A.; Boussonihre, A.; Li, L.; Bonin, H.; Lacite, E.; Curran, D. P.; Vedejs, E. *J. Am. Chem. Soc.* **2012**, *134*, 12281–12288.
108. (a) Yang, Z.; Zhong, M.; Ma, X.; Nijesh, K.; De, S.; Parameswaran, P.; Roesky, H. W. *J. Am. Chem. Soc.* **2016**, *138*, 2548–2551. (b) Bismuto, A.; Thomas, S. P.; Cowley, M. J. *Angew. Chem. Int. Ed.* **2016**, *55*, 15356–15359. (c) Bismuto, A.; Cowley, M. J.; Thomas, S. P. *ACS Catal.* **2018**, *8*, 2001–2005.
109. Bauer, H.; Alonso, M.; Farber, C.; Elsen, H.; Pahl, J.; Causero, A.; Ballmann, G.; De Proft, F.; Harder, S. *Nature Catalysis* **2018**, *1*, 40–47.
110. (a) Buch, F.; Brettar, J.; Harder, S. *Angew. Chem. Int. Ed.* **2006**, *45*, 2741–2745. (b) Leich, V.; Spaniol, T. P.; Okuda, J. *Organometallics* **2016**, *35*, 1179–1182.
111. Magre, M.; Maity, B.; Falconnet, A.; Cavallo, L.; Rueping, M. *Angew. Chem. Int. Ed.* **2019**, *58*, 7025–7029.
112. Yan, D.; Wu, X.; Xiao, J.; Zhu, Z.; Xu, X.; Bao, X.; Yao, Y.; Shen, Q.; Xue, M. *Org. Chem. Front.* **2019**, *6*, 648–653.

113. (a) Gregory, R. J. H. *Chem. Rev.* **1999**, *99*, 3649–3682. (b) Special symposium for the synthesis of nonracemic cyanohydrins, see: *Tetrahedron* **2004**, *60*, 10371–10568. (c) Brunel, J. M.; Holmes, I. P. *Angew. Chem. Int. Ed.* **2004**, *43*, 2752–2778. (d) George, S. C.; Kim, S. S. *Bull. Korean Chem. Soc.* **2007**, *28*, 1167–1170. (e) Kanai, M.; Kato, N.; Ichikawa, E.; Shibasaki, M. *Synlett* **2005**, 1491–1508.
114. (a) Saravanan, P.; Anand, R. V.; Singh, V. K. *Tetrahedron Lett.* **1998**, *39*, 3823–3824. (b) Khan, N.; Agrawal, S.; Kureshy, R. I.; Sayed, H. R.; Singh, S. S.; Jasra, R. V. *J. Organomet. Chem.* **2007**, *692*, 4361–4366. (c) Karimi, B.; Ma'Man, L. *Org. Lett.* **2004**, *6*, 4813–4815. (d) Kantam, M. L.; Sreekanth, P.; Santhi, P. L. *Green. Chem.* **2000**, *2*, 47–48. (e) Iwanami, K.; Choi, J. C.; Sakakura, T.; Yasuda, H. *Chem Commun.* **2008**, 1002–1004. (f) Bandini, M.; Cozzi, P. G.; Garelli, A.; Melchiorre, P.; Unami-Ronchi, A. *Eur. J. Org. Chem.* **2002**, 3243–3249. (g) Suzuki, Y.; Abu Bakar, M. D.; Muramatsu, K.; Sato, M. *Tetrahedron* **2006**, *62*, 4227–4231. (h) Kadam, S. T.; Kim, S. S. *Appl. Organometal. Chem.* **2009**, *23*, 119–123.
115. Hamashima, Y.; Sawada, D.; Kanai, M.; Shibasaki, M. *J. Am. Chem. Soc.* **1999**, *121*, 2641–2642.
116. Ryu, D. H.; Corey, E. J. *J. Am. Chem. Soc.* **2004**, *126*, 8106–8107.
117. Yang, Z.; Zhong, M.; Ma, X.; De, S.; Anusha, C.; Parameswaran, P.; Roesky, H. W. *Angew. Chem. Int. Ed.* **2015**, *54*, 10225–10229.
118. Swamy, V. S. V. S. N.; Bisai, M. K.; Das, T.; Sen, S. S. *Chem. Commun.* **2017**, *53*, 6910–6913.
119. Yadav, S.; Dixit, R.; Vanka, K.; Sen, S. S. *Chem. - Eur. J.* **2018**, *24*, 1269–1273.
120. Li, Y.; Wang, J.; Wu, Y.; Zhu, H.; Samuel, P. P.; Roesky, H. W. *Dalton Trans.* **2013**, *42*, 13715–13722.
121. Sitwatch, R. K.; Nagendran, S. *Chem. - Eur. J.* **2014**, *20*, 13551–13556.
122. Liberman-Martin, A. L.; Bergman, R. G.; Tilley, T. D. *J. Am. Chem. Soc.* **2015**, *137*, 5328–5331.
123. Yang, Z.; Yi, Y.; Zhong, M.; De, S.; Mondal, T.; Koley, D.; Ma, X.; Zhang, D.; Roesky, H. W. *Chem. - Eur. J.* **2016**, *22*, 6932–6938.
124. Sharma, M. K.; Sinhababu, S.; Mukherjee, G.; Rajaraman, G.; Nagendran, S. *Dalton Trans.* **2017**, *46*, 7672–7676.
125. Wang, W.; Luo, M.; Li, J.; Pullarkat, S. A.; Ma, M. *Chem. Commun.* **2018**, *54*, 3042–3044.

Synthesis and Reactivity of a Hypersilylsilylene



Abstract

In this chapter, stabilization of an amidinosilylene with a bulky tris(trimethylsilyl)silyl substituent was realized with the preparation of $\text{PhC}(\text{N}t\text{Bu})_2\text{Si}\{\text{Si}(\text{SiMe}_3)_3\}$ from $\text{PhC}(\text{N}t\text{Bu})_2\text{SiHCl}_2$ with $\text{K}\{\text{Si}(\text{SiMe}_3)_3\}$. A series of reactions of hypersilylsilylene with Me_3NO , S, Se, and Te were performed. While siloxane derivatives are obtained from the reactions with Me_3NO , silachalcogenones are formed with other chalcogens. Silaoxirane formation is observed when silylene was treated with acetone, demonstrating the importance of the tris(trimethylsilyl)silyl group to kinetically and thermodynamically protect the silaoxirane derivative with less bulky substituents on the C atom. Conventional Lewis acid-base adducts are synthesized when hypersilylsilylene is treated with BH_3 and 9-BBN separately. Anomalous reactivity is observed for catecholborane, that led to the formation of an amidinato borane, $\text{PhC}(\text{N}t\text{Bu})_2\text{Bcat}$. Silaimines were formed when treated with trimethylsilyl azide and adamantyl azide, respectively. The versatile reactivity of hypersilylsilylene towards aromatic and aliphatic disubstituted chlorophosphine were also explored with the synthesis of novel tetraphosphinosilane, phosphinosilylene and disilene.

2.1 Introduction

The chemistry of stable silicon(II) compounds, namely silylene has seen tremendous development in fundamental studies of structure and bonding during the past decades. It possess an important area of research with their several applications as versatile ligand systems for transition-metal complexes and toward small molecule activation.¹ One of the most extensively studied silylenes is the benzamidinato-stabilized silylene of composition $LSiX$ [$L = PhC(NtBu)_2$]^{1e-i,2} presumably because of their ease of synthesis and thermal stability.³ However, a closer look would reveal that the majority of amidinatosilylenes contain an electron-rich π -donating functionalized group (X) such as Cl (**A**),³ Br (**B**),⁴ OiPr (**C**),⁵ NR₂ [R = Ph (**D**),⁶ Cy (**E**),⁶ *i*Pr (**F**),⁶ SiMe₃ (**G**)⁷], P(SiMe₃)₂ (**H**)],⁸ etc. Replacement of the π -donor ligand with a σ -donor group may reduce the HOMO–LUMO gap, but this would add more synthetic challenges. Nevertheless, the group of H. W. Roesky isolated the alkylfunctionalized amidinatosilylene $PhC(NtBu)_2SiR$ (**I**).⁹ Subsequently, the group of P. W. Roesky prepared the pentamethylcyclopentadienyl-functionalized amidinatosilylene $PhC(NtBu)_2SiCp^*$ (**J**).¹⁰ However, their reactivity studies are not well-documented, apart from the use of **J** as a ligand for zinc complexes.¹⁰ Parallel to this, Driess and co-workers prepared bis(silylenyl)ferrocene (**K**)¹¹ from the reaction of amidinatochlorosilylene (**A**) with dilithiated ferrocene. Very recently, Cui et al. reported a tethered amidinatosilylene, $PhC(NtBu)_2SiCH_2C(tBu)NDipp$ (**L**; Dipp = 2,6-*i*Pr₂-C₆H₃), where the Si^{II} unit is bound to the CH₂ moiety,¹² while Cabeza et al. prepared a mesityl-substituted amidinatosilylene, $PhC(NtBu)_2SiMes$ (**M**; Mes = 2,4,6-Me₃-C₆H₂).¹³ Silanides, being the heavier congeners to classical alkyl ligands, are of increasing importance because they have greater σ -donor strength than alkyl and π -donating ligands. However, access to silylsubstituted amidinato silylene has not been reported yet.

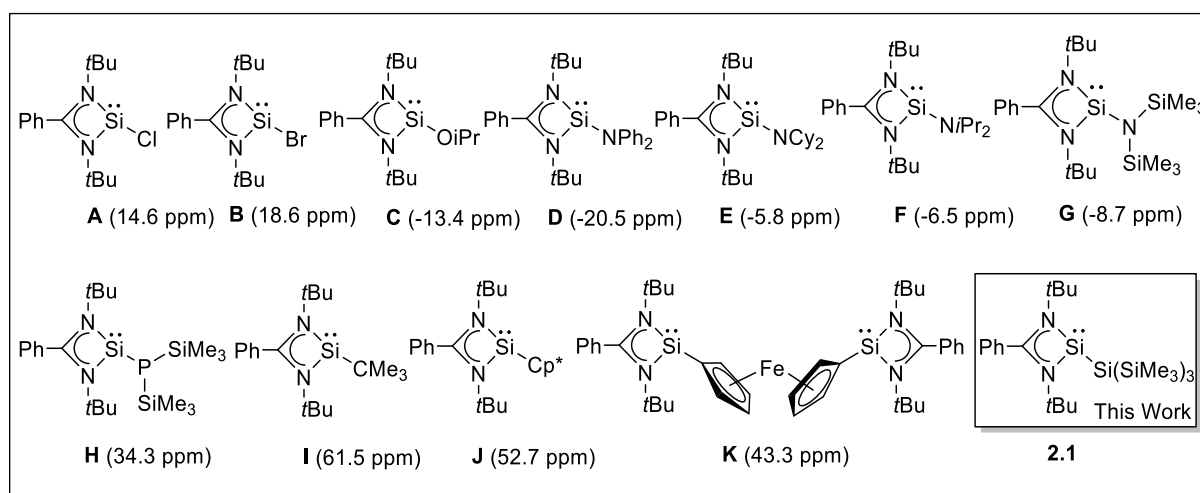


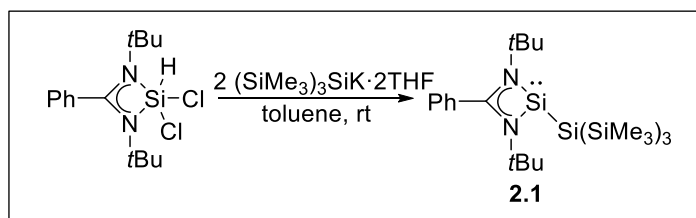
Chart 2.1. Selected example of amidinato silylenes.

Since the pioneering work by Benkeser, Gilman, and Smith on the synthesis of tetrakis(trimethylsilyl)silane,¹⁴ there is an increasing use of the tris(trimethylsilyl)silyl group in the synthesis of numerous organometallic compounds^{15,16} because it possesses a pronounced steric effect. Apart from the steric bulk, another major factor is the strong σ -donor strength of the silyl ligand. The delicate balance between these two factors— strong σ donation and kinetic protection— has orchestrated a rapid development in low-valent main-group chemistry. The usefulness of the tris(trimethylsilyl)silyl group in low-valent silicon chemistry has been amply exemplified by Aldridge and co-workers in the isolation of a stable mixed (amido)-silylsilylene, $\text{Si}\{\text{Si}(\text{SiMe}_3)_3\}\{\text{N}(\text{SiMe}_3)\text{Dipp}\}$.¹⁷ While silylenes with π -donating ligands have not been reported for dihydrogen activation, the silylenes lacking π -donor ligands are found to split dihydrogen in a facile manner,^{17,18} which can be attributed to a decrease of π donation, leading to a reduction in the HOMO–LUMO gap. This significant result led us to study the synthesis of tris(trimethylsilyl)silylamidinatosilylene (**2.1**). Subsequent to the synthesis of the silylene, we studied its reactivity toward S, Se, and Te, which led to silicon(IV) complexes (**2.4–2.6**) with Si=E bonds. The reaction of **2.1** with acetone affords the first structurally authenticated silaoxirane derivative (**2.7**). On the other hand, a versatile reactivity of organoboranes towards silylene were also developed. Synthesis of silaimines (**2.15–2.16**) were also successful when treated with organic azides. Interestingly, a tetradentate ligand namely tetraphosphosilane (**2.17**) was also realized by the reaction of **2.1** with chlorodiphenylphosphine. Synthesis of a phosphine substituted silylene (**2.18**), disilene (**2.19–2.21**) were also presented for the reaction of **2.1** with aliphatic disubstituted chlorophosphines.

2.2 Synthesis and characterization of hypersilylsilylene

The treatment of $\text{PhC}(\text{N}t\text{Bu})_2\text{SiHCl}_2$ with 2 equiv of $\text{KSi}(\text{SiMe}_3)_3$ in toluene at room temperature for 8 h afforded a new monomeric hypersilylsilane(II) compound (**2.1**) in more than 90% yield (Scheme 2.1). **2.1** is stable at room temperature and is the first example of a system having a $\text{Si}^{\text{II}}\text{–Si}^{\text{IV}}$ bond with an amidinate moiety. Hypersilylsilylene has been isolated as a pale-yellow crystalline solid with good solubility in toluene, tetrahydrofuran, diethyl ether, and *n*-hexane. Previously, Kira and coworkers reported the isomerization of dialkylsilylene to the corresponding silaethene via 1,2-trimethylsilyl migration.¹⁹ We have also warmed **2.1** up to 100 °C, but no migration of the trimethylsilyl group was observed. The ¹H NMR spectrum of **2.1** displays a resonance at 0.51 ppm for the three SiMe₃ groups. The resonance for the *t*Bu protons of the amidinate moiety appears at 1.21 ppm, integrating for 18 protons. The ²⁹Si NMR of **2.1** exhibit three resonances at 76.91 ppm for the Si^{II} center, –8.36 ppm for SiMe₃ moieties,

and -11.84 ppm for the silyl $\text{Si}(\text{SiMe}_3)_3$ moiety. The lack of π -donating substituents is reflected in the ^{29}Si NMR chemical shift of the Si^{II} center, which is significantly downfield with respect to those in **A–H**. The value is very close to that in $[\text{PhC}(\text{N}t\text{Bu})_2\text{Si}]_2$ (75.71 ppm).²⁰ In the high-resolution mass spectrometry spectrum, the molecular ion is observed as the most abundant peak, with the highest relative intensity at m/z 507.2883.



Scheme 2.1. Synthesis of Hypersilylsilylene **2.1**.

The molecular structure of **2.1** is shown in Figure 2.1, while the important bond lengths and angles are provided in the caption of Figure 2.1. Silylene **2.1** crystallizes in the monoclinic space group $P2_1/n$. The Si atom is three-coordinate and features a trigonal pyramidal geometry with a lone pair of electrons residing on the apex. The Si1–Si2 bond length in **2.1** is $2.433(13)$ Å, which is longer than the typical Si–Si single bond (2.35 Å), Aldridge’s $\text{Si}\{\text{Si}(\text{SiMe}_3)_3\}\{\text{N}(\text{SiMe}_3)\text{Dipp}\}$ [$2.386(1)$ Å],¹⁷ and the Si–Si bond length in interconnected amidinatobis-(silylene) $[\text{PhC}(\text{N}t\text{Bu})_2\text{Si}]_2$ [$2.413(2)$ Å].²⁰ The other Si–Si bond lengths vary from $2.3475(12)$ to $2.3740(13)$ Å, which are shorter than the Si1–Si2 bond.

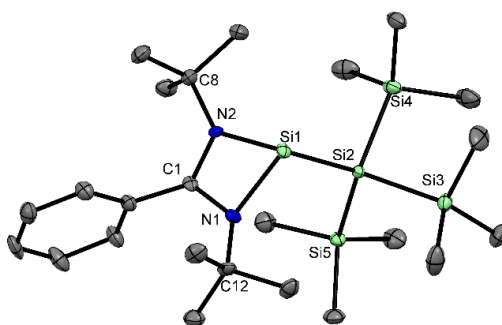


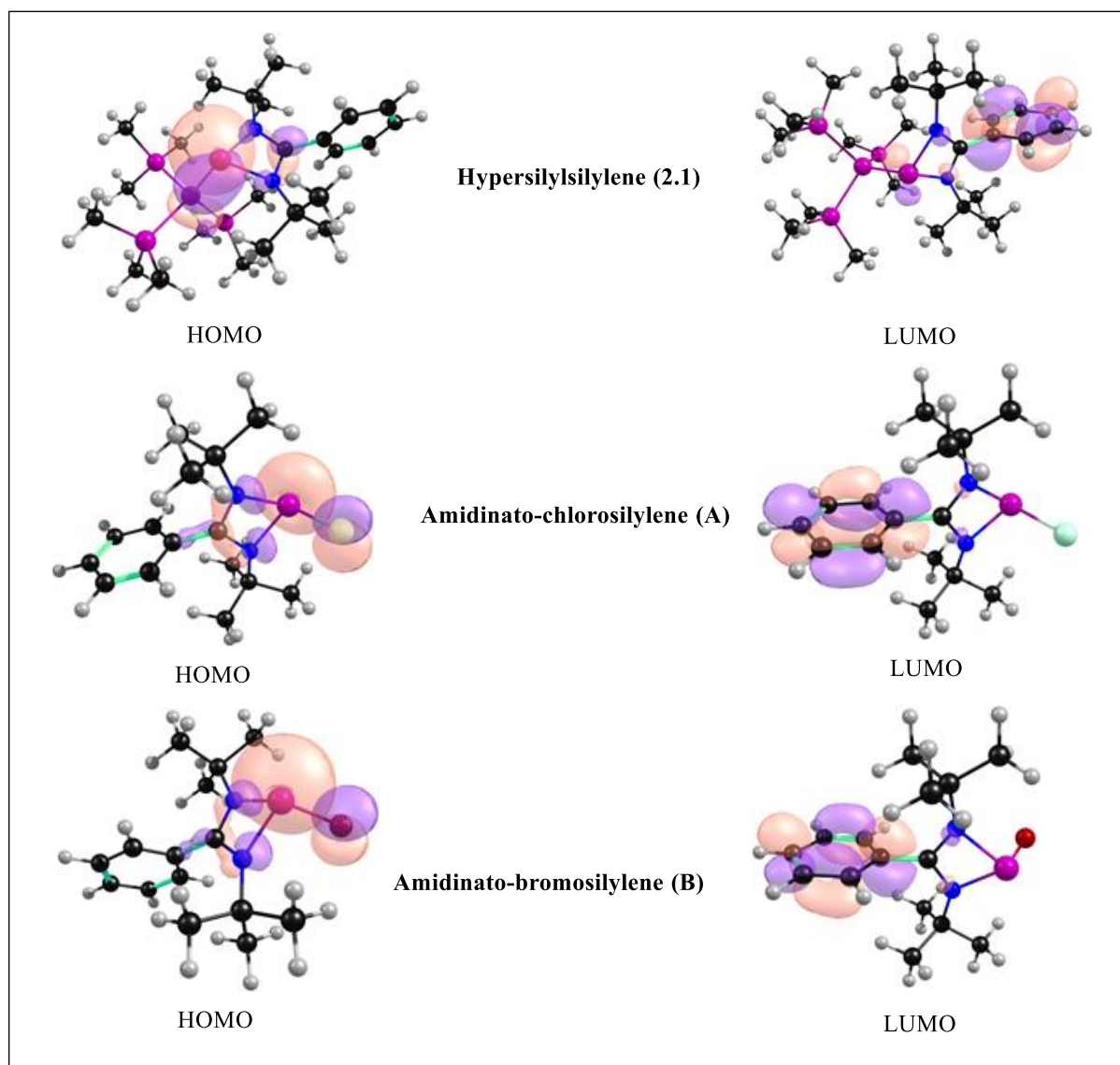
Figure 2.1. The molecular structure of **2.1**. Anisotropic displacement parameters are depicted at the 50% probability level. Selected bond lengths [Å] and angles [deg]: Si1–Si2 $2.4339(13)$, Si2–Si5 $2.3472(12)$, Si2–Si4 $2.3690(13)$, Si2–Si3 $2.3746(12)$, Si1–N1 $1.885(3)$, Si1–N2 $1.873(3)$; N1–Si1–N2 $69.27(11)$, N1–Si1–Si2 $103.14(9)$, N2–Si1–Si2 $105.49(9)$.

We have done geometry optimization of **2.1** for the ground-state singlet and triplet geometries using density functional theory (DFT) at the PBE/ TZVP level. The singlet geometry is found to be more stable than the triplet by 38.6 kcal mol⁻¹. The HOMO is located at the Si^{II} center of

2.1, and the LUMO is spread over the phenyl ring of the amidinate ligand. The HOMO–LUMO energy gap for the silylene has been determined to be 3.7 eV. We have also calculated the HOMO–LUMO energy gaps for the known amidinato silylenes using DFT studies, which reveal that the gaps are usually more than 4.00 eV [e.g., **A** (4.40 eV), **B** (4.35 eV), and **G** (4.13 eV)]. The decrease in the HOMO–LUMO gap for **2.1** results from the lack of π donation from the substituent bound to the Si^{II} center. Triplet silylene is 38.6 kcal/mol higher in energy than the singlet state.

Computational details of hypersilylsilylene (**2.1**) and other related amidinato-silylenes (**A**, **B** and **G**):

The HOMO-LUMO energy gap for **2.1**, **A**, **B**, and **G** are 3.7, 4.40, 4.35, and 4.13 eV respectively. The HOMO is located in the Si centre and LUMO is spread over the phenyl ring of amidinate ligand (Figure 2.2)



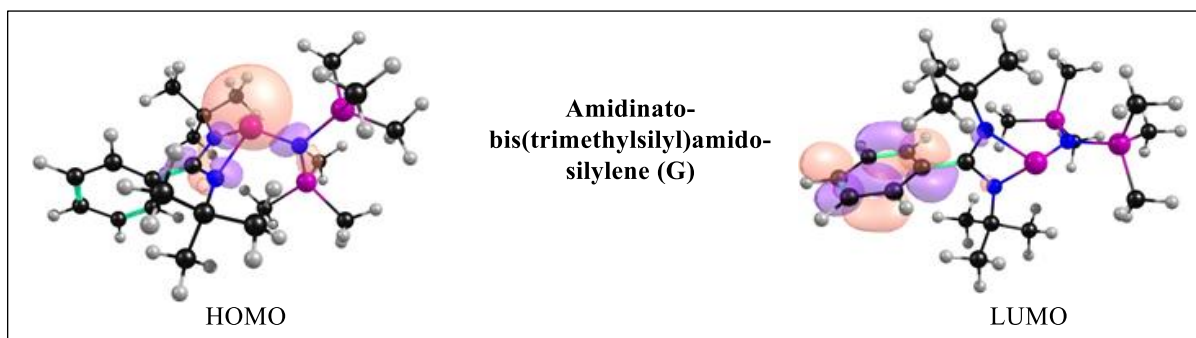
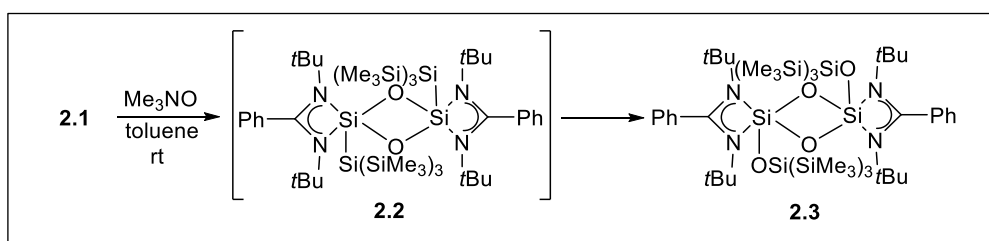


Figure 2.2. Computational details of silylenes.

2.3 Reaction with Me₃NO



Scheme 2.2. Reaction of **2.1** with trimethyl N-oxide and formation of **2.2** and **2.3**.

The reactions of silylene with oxygen-containing substrates are always interesting because they pave the way for siloxanes, which are used as precursors for siloxane-high polymers by the reactions of ring-opening living polymerization with anionic initiators.²¹ The reaction of **2.1** with Me₃NO led to stepwise oxygen insertion. In the first case, the oxygen atom attacks the Si^{II} center, which leads to a cyclodisiloxane derivative (**2.2**), presumably resulting from dimerization of the putative LSi(=O)Si(SiMe₃)₃.²² Subsequent insertion of oxygen takes place at the Si–Si bond, leading to **2.3** (Scheme 2.2). It is of note here that the formation of **2.2** was serendipitous, and we were fortunate to characterize it by single-crystal X-ray diffraction studies. **2.2** crystallizes in the monoclinic space group *P*2₁/*n*. The molecular structure of **2.2** is shown in Figure 2.3. The structure consists of a four-membered Si₂O₂ ring with a five-coordinate Si atom. The Si1–Si2 bond distance in **2.2** [2.5099(18) Å] is significantly elongated in comparison to that in **2.1**. This bond elongation is probably a consequence of the increased coordination number and enhanced steric bulk at the Si center.

A substantial increase in the Si1–Si2 bond length in the molecular structure of **2.2** might facilitate the further insertion of another O atom, which led to the formation of **2.3**. The ²⁹Si NMR spectrum of **2.3** features a sharp resonance at –116.06 ppm, which is consistent with the previously known five-coordinate Si atoms.^{1g} Molecular structure of **2.3** is shown in Figure 2.4. Like **2.2**, **2.3** also crystallizes in the monoclinic space group *P*2₁/*n* and possesses a Si₂O₂

ring with a five-coordinate Si atom with three Si–O and two Si–N bonds. Here it is worth mentioning that the Si···Si and O···O separations in the cyclodisiloxane moiety are 2.53 and 2.27 Å, respectively, for **2.2**. In the case of **2.3**, the Si···Si and O···O separations are 2.50 and 2.28 Å. From these data, it can be understood that there is no bond between the two Si atoms in the cyclodisiloxane rings and they are best described as containing four equivalent localized Si–O bonds with no appreciable σ bonding between the Si atoms.^{22,23} However, we were not able to prepare **2.2** on a reasonable scale that allows for full spectroscopic characterization. Nevertheless, a variable-temperature NMR experiment in toluene- d_8 shows the shift of the SiMe₃ protons from 0.54 to 0.51 ppm and finally to 0.49 ppm, indicating the formation of **2.3** from **2.1** via **2.2** (Figure 2.5).

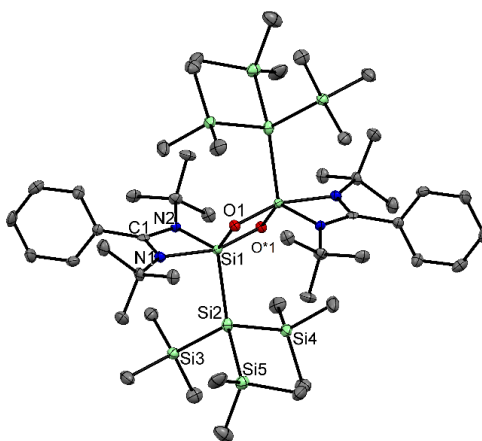


Figure 2.3. The molecular structure of **2.3**. Anisotropic displacement parameters are depicted at 50% probability level. Hydrogen atoms are omitted for clarity. Selected bond distances (Å) and bond angles (deg): Si1–N1 2.003(4), Si1–N2 1.849(4), Si1–O1 1.681(3), Si1–O1* 1.723(3), Si1–Si2 2.5099(18); N1–Si1–N2 67.56(17), N1–Si1–O1 91.43(16), N2–Si1–O1 122.58(16), O1–Si1–O1* 83.72(17).

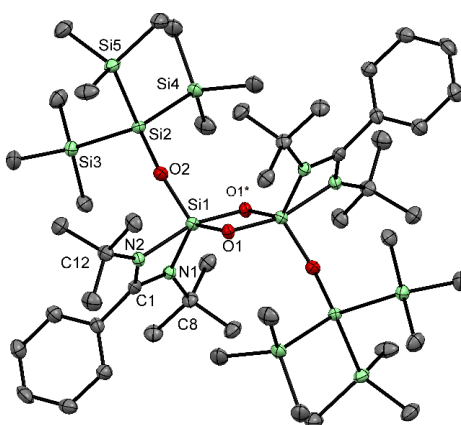


Figure 2.4. Molecular structure of **2.3**. Anisotropic displacement parameters are depicted at the 50% probability level. H atoms are omitted for clarity. Selected bond distances (Å) and angles (deg): Si1–N1 1.846(3), Si1–N2 1.965(3), Si1–O1 1.670(2), Si1–O1* 1.718(2), Si1–O2 1.646(2), Si2–O2 1.652(2); N1–Si1–N2 68.33(11), N1–Si1–O1 125.73(11), N2–Si1–O1 92.61(11), O1–Si1–O1* 84.79(11), O1–Si1–O2 119.41(11).

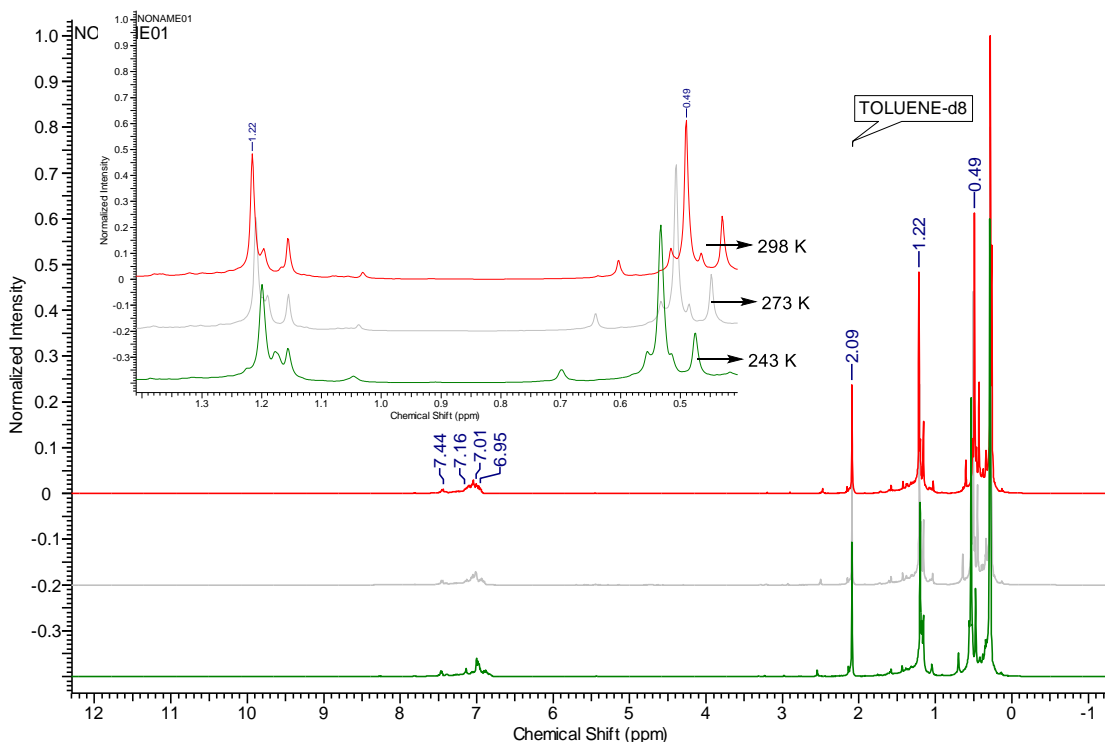
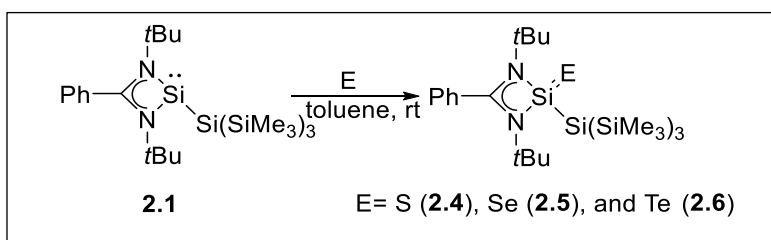


Figure 2.5. Variable temperature dependent ^1H NMR spectrum for the reaction of **2.1** with Me_3NO (toluene- d_8 , 400 MHz, 243 K to 298 K)

2.4 Reaction with heavier chalcogens (S, Se, Te)

Generation of silathiones has been shown to be possible from the reaction of silylene with elemental S.^{24–26} However, sometimes this leads to disilatene derivatives,²⁷ for which the steric factors have largely been held responsible as the bulky substituents can only be introduced at the Si center. We have studied the reactions of **2.1** with S, Se, and Te, which led to compounds with Si=S (**2.4**), Si=Se (**2.5**), and Si=Te (**2.6**) bonds (Scheme 2.3).



Scheme 2.3. Reactions of **2.1** with sulfur, selenium, and tellurium.

The ^{29}Si NMR spectra of **2.4–2.6** exhibit resonances at 27.50, 23.88, and 1.82 ppm, respectively, which are markedly deshielded from those in $\text{PhC}(\text{N}t\text{Bu})\text{Si}(=\text{E})\text{N}(\text{SiMe}_3)_2$ [-16.9 (S), -20 (Se), and -47.6 (Te) ppm],²⁶ reflecting the substitution of a π -donating NR_2 group with a σ -donating $\text{Si}(\text{SiMe}_3)_3$ moiety. The gradual upfield shift upon going from **2.4** to **2.6** is consistent with a decrease of the electronegativity from S to Te, and this trend was also observed for other silylenes.^{24,26} The $\text{Si}(\text{SiMe}_3)_3$ groups show high-field resonances at -123.13 (**2.4**), -119.99 (**2.5**), and -90.42 (**2.6**) ppm, which are in good agreement with that reported for the $\text{Si}(\text{SiMe}_3)_3$ group in Inoue's silepin (-138.2 ppm).²⁸ The molecular-ion peaks for **2.4–2.6** were detected at m/z 539.2630, 587.2041, and 637.1929, respectively, with the highest relative intensity. **2.4** crystallizes in the monoclinic space group $C2/c$. The molecular structure of **2.4** is shown in Figure 2.6. The $\text{Si}=\text{S}$ bond length in **2.4** is 1.9996(6) Å, which is consistent with a $\text{Si}=\text{S}$ bond and in good agreement with the $\text{Si}=\text{S}$ bond in $[\{\text{PhC}(\text{N}t\text{Bu})_2\}\text{Si}(\text{S})\text{N}(\text{SiMe}_3)_2]$ [1.987(8)Å], reported by Khan and co-workers.²⁵ However, the $\text{Si}=\text{S}$ bond length in **2.4** is longer than that in the silanethiones with three-coordinate Si atoms [1.948(4) and 1.9575(7) Å]^{24,29} but marginally shorter than the $\text{Si}=\text{S}$ bond with a five-coordinate Si atom [2.0193(9) Å].³⁰ Formation of the $\text{Si}=\text{S}$ bond is accompanied by a decrease in the $\text{Si1}-\text{Si2}$ bond length [2.3525(6) Å].

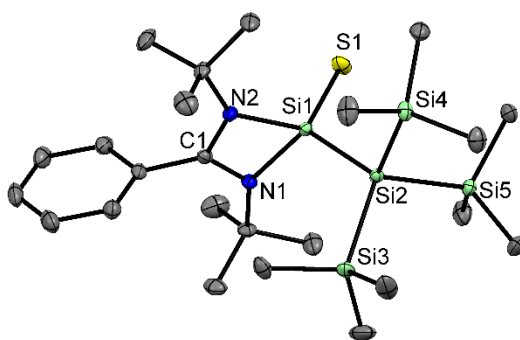


Figure 2.6. The molecular structure of **2.4**. Anisotropic displacement parameters are depicted at the 50% probability level. Selected bond lengths (Å) and angles (deg): $\text{Si1}-\text{N1}$ 1.8538(13), $\text{Si1}-\text{N2}$ 1.8578(14), $\text{Si1}-\text{S1}$ 1.9996(6), $\text{Si1}-\text{Si2}$ 2.3525(6); $\text{N1}-\text{Si1}-\text{N2}$ 70.66(6), $\text{S1}-\text{Si1}-\text{Si2}$ 113.82(2), $\text{N1}-\text{Si1}-\text{S1}$ 118.23(5), $\text{N2}-\text{Si1}-\text{S1}$ 117.29(5).

2.5 crystallizes in the monoclinic space group $P2_1$. Figure 2.7 depicts the molecular structure of **2.5**. The Si=Se bond length in **5** is 2.139(4) Å, which is consistent with the reported Si=Se bond length [2.136(9) Å] by Khan and co-workers,²⁵ and the Si=Se bond in [HC(CMeNAr){C(=CH₂)NAr}Si-(NHC)=Se] [2.1457(9) Å] reported by Driess and coworkers.³¹ The Si=Se bond length in **2.5** is considerably longer than the Si=Se bond reported by Kira's group [2.0963(5) Å],²⁴ where the Si atom is three-coordinate and somewhat shorter than Tacke's silaneselenone with a five-coordinate Si atom [2.1632(7) Å],³⁰ illustrating the dependence of the Si=Se bond length on the coordination number of Si.

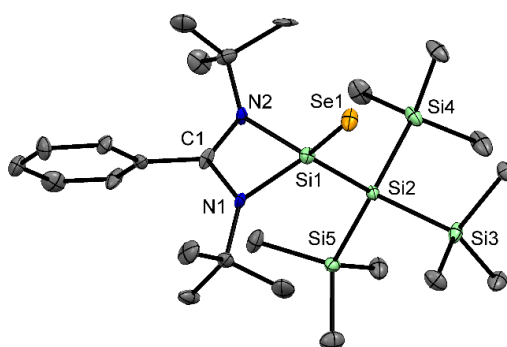


Figure 2.7. The molecular structure of **2.5**. Anisotropic displacement parameters are depicted at the 50% probability level. Selected bond lengths [Å] and angles [deg]: Si1–N1 1.873(13), Si1–N2 1.857(13), Si1–Se1 2.139(4), Si1–Si2 2.357(6), N1–Si1–N2 70.1(6), Se1–Si1–Si2 114.3(2), N1–Si1–Se1 117.6(5), N2–Si1–Se1 118.4(5).

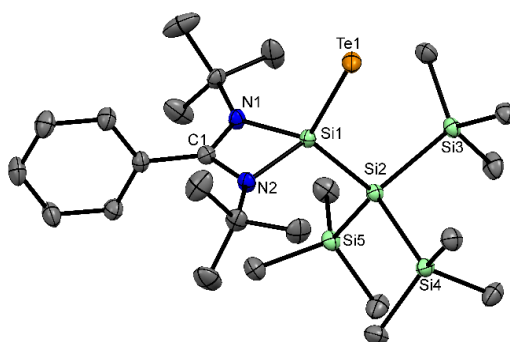


Figure 2.8. The molecular structure of **2.6**. Anisotropic displacement parameters are depicted at the 50% probability level. Selected bond lengths [Å] and angles [deg]: Si1–N1 1.849(3), Si1–N2 1.855(3), Si1–Te1 2.3723(8), Si1–Si2 2.3620(12), N1–Si1–N2 70.97(12), Te1–Si1–Si2 115.23(4), N1–Si1–Te1 116.33(9), N2–Si1–Te1 116.62(9).

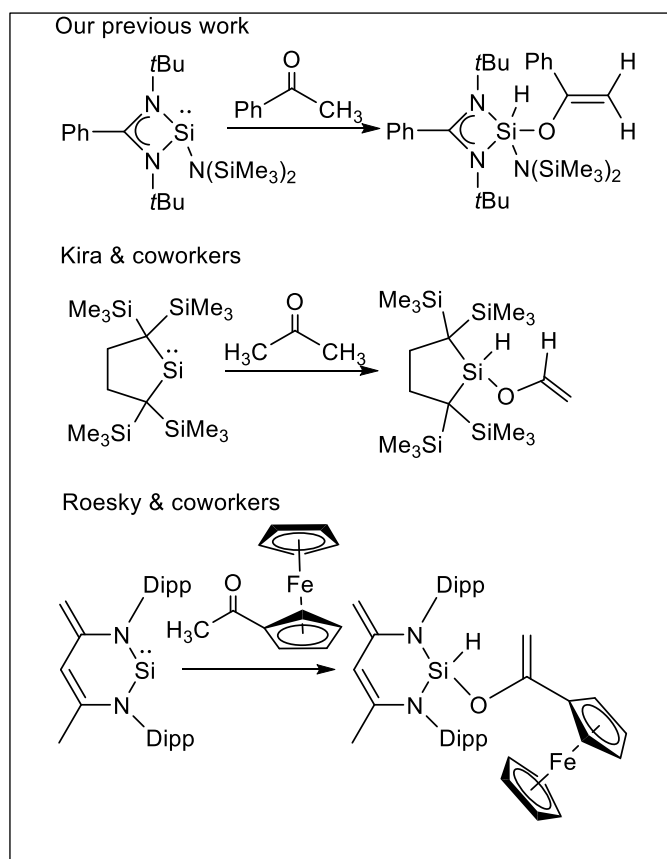
The molecular structure of **2.6**, which crystallizes in the orthorhombic space group $P2_12_12_1$ is shown in Figure 2.8. Consistent with this trend, the Si=Te bond length in **2.6** is 2.3723(8) Å,

matching well with the other Si=Te bonds with four coordinate Si atoms [HC(CMeNAr){C(=CH₂)NAr}Si-(NHC)=Te, 2.383(2) Å;³¹ PhC(NtBu)₂SiN{(SiMe₃)₂}=Te, 2.3720(15) Å²⁶], longer than Kira's three-coordinate Si=Te bonds [2.3210(6) Å],²⁴ but shorter than Tacke's five coordinate Si=Te bonds [2.4017(6) Å].³⁰ It is of note here that the presence of the double bond in **2.4–2.6** is deduced from geometrical features obtained from the structural studies. Topological analysis of the experimentally determined charge density of these bonds will be a more realistic tool for elucidating the nature of the bonding.³²

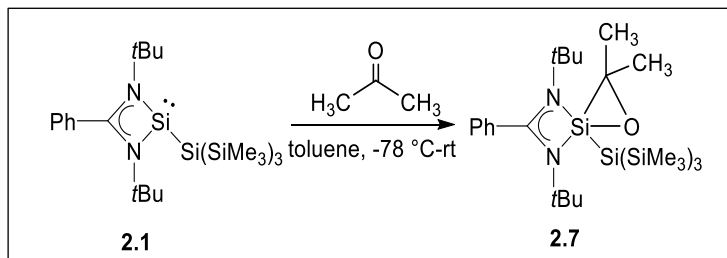
2.5 Reaction with acetone

Up to this point, the installed tris(trimethylsilyl)silyl group did not have much of a role to play in all of the reactions that we have described. We were, therefore, looking for a reaction that is not successful with other functionalized amidinosilylenes and may illustrate the importance of the tris- (trimethylsilyl)silyl group. One such reaction is formation of the silaoxirane derivative (**2.7**) with acetone. Silaoxirane, a heavier analogue of epoxides, has been prepared and studied recently because of its high reactivity. One protocol to access the silaoxiranes is the reaction of ketone with silylene. The methodology has been brought to the fore by Roesky and coworkers.³³ However, the formation of such silaoxiranes is feasible only when bulky ketones such as benzophenone and 2-adamantanone are employed.^{33,34} Interestingly, a ketone with a CH₃ unit has a propensity to undergo C–H activation with a silylene (Scheme 2.4). For example, the reaction of 2-acylferrocene with Driess' silylene [CH{(C=CH₂)(CMe)-(2,6-*i*Pr₂C₆H₃N)₂}Si],³⁴ the reaction of acetone with Kira's dialkylsilylene,³⁵ or the reaction of acetophenone with amidinosilylene PhC(NtBu)₂N(SiMe₃)₂ (**G**)³⁶ led to C–H bond activation of the CH₃ motif. In fact, in 1999, Walsh and co-workers studied the reaction of the parent silylene with acetone using Rice–Ramsperger–Kassel–Marcus (RRKM) modeling and ab initio studies and concluded that 2-siloxypropene formation is more favorable than silaoxirane formation.³⁷

Because there is no report of a reaction of any amidinosilylene with acetone, we thought about investigating this reaction with **2.1** to see if (a) silaoxirane is formed or (b) C–H bond activation occurs. The reaction indeed led to a silaoxirane (**2.7**) formation, benefiting from steric protection as well as thermodynamic stability from the –Si(SiMe₃)₃ substituent (Scheme 2.5). Although the mechanism for formation of **2.7** has not been definitively established, we presume that the attack at the Si electrophile by the O atom of acetone initiates the reaction with subsequent ring closure (Scheme 2.6).

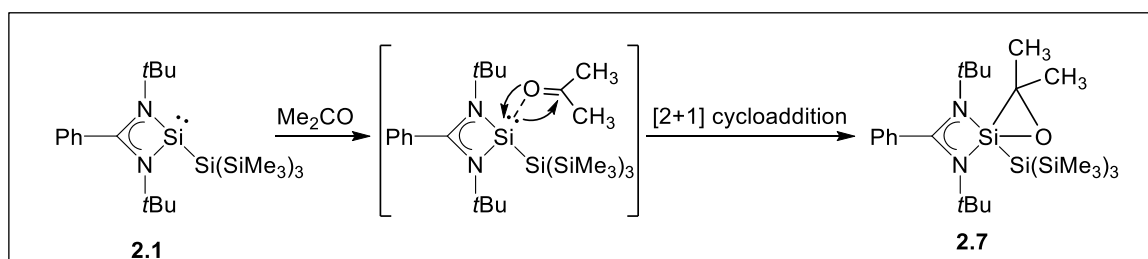


Scheme 2.4. Reactions of the reported silylenes with acetone.



Scheme 2.5. The reaction of **2.1** with acetone and the formation of silaoxirane **2.7**.

2.7 forms colorless crystals and shows durability in the solid state as well as in the solution state under an inert gas atmosphere with good benzene or toluene solubility. The ^{29}Si NMR spectrum of **2.7** shows a resonance at -96.42 ppm, consistent with a five-coordinate Si atom. **2.7** crystallizes in the monoclinic space group $P2_1/c$. The molecular structure of **2.7** is depicted in Figure 2.9. The Si atom in **2.7** is five-coordinate with distorted trigonal-bipyramidal geometry, with $148.0(3)^\circ$ the largest bond angle for O1–Si1–N2. N1, Si2, and C16 reside in the equatorial positions, whereas N2 and O1 occupy the axial positions. The Si–O bond distance in the ring is $1.729(5)$ Å, which is in good agreement with the Si–O single bonds observed for **2.2** and **2.3**. The Si–C bond length of $1.819(9)$ Å is typical for a Si–C single bond.³⁸



Scheme 2.6. Tentative mechanism for the formation of **2.7**.

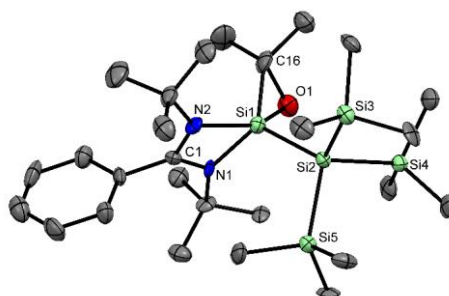


Figure 2.9. The molecular structure of **2.7**. Anisotropic displacement parameters are depicted at the 50% probability level. Selected bond lengths [Å] and angles [deg]: Si1–Si2 2.370(3), Si1–O1 1.729(5), Si1–C16 1.819(9), C16–O1 1.508(9), Si1–N1 1.843(6), Si1–N2 2.002(6); O1–Si1–C16 50.2(3), C16–O1–Si1 68.0(4), N1–Si1–N2 67.5(3), O1–Si1–Si2 104.5(2), O1–Si1–N2 148.0(3).

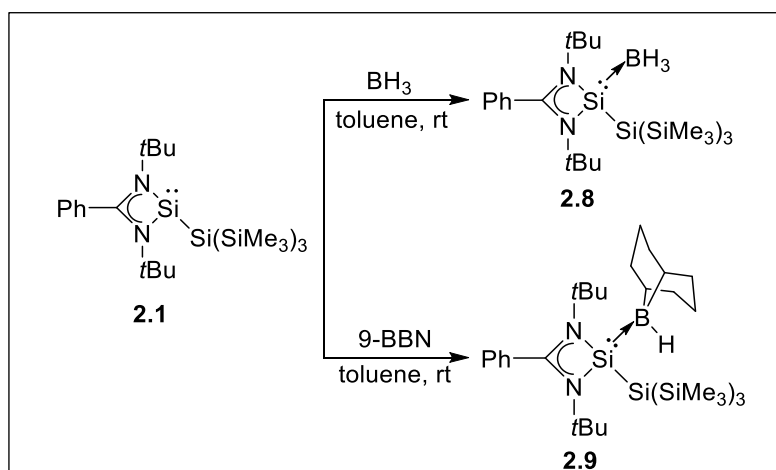
2.6 Diverse Reactivity of hypersilylsilylene towards boranes

Having vacant orbitals as well as reactive lone pairs of electrons at silicon, silylenes can mimic transition metals in many reactions such as activation of H_2 ,^{17,18,39} NH_3 ,⁴⁰ and P_4 ⁴¹ under mild reaction conditions. Silylenes are well known to form Lewis acid/base adducts, such as silylene–borane adducts when reacted with Lewis bases. The pioneering experimental studies by several groups involving West, Driess, Tacke, Roesky, Braun and their co-workers have significantly contributed to the initial advance of the silylene-borane chemistry.^{42,43} On the contrary, a recent result from our group have shown that the cooperative addition of HBpin to $\text{PhC}(\text{N}t\text{Bu})_2\text{SiN}(\text{SiMe}_3)_2$ (**G**)⁷ results in the cleavage of the B–H bond in a cooperative fashion across the Si and amidinate-C sites.^{44a} In the same line, So and coworkers reported the activation of B–H bond of BH_2OTf by $\text{PhC}(\text{N}t\text{Bu})_2\text{SiN}(\text{SiMe}_3)(\text{Dipp})$.^{44b} Furthermore, the reactivity of boron halides towards silylenes are relatively less explored, and only reported by Braunschweig,^{45,46} Iwamoto,⁴⁷ So,⁴⁸ Roesky⁴⁹ and their co-workers. It was observed that PhBCl_2 undergoes oxidative addition over the Si^{II} centre of NHSi or amidinatio

bis-silylene and followed by a ring expansion.^{45,48} Contrary to that, amidinato silylene with chloride or mesityl substituent are reported for the insertion of Si^{II} centre into B-Cl bond of PhBCl₂ and followed by migration of Cl and amidinate ligand.

Due to our current interest to explore the reactivity of hypersilylsilylene towards various small molecules, we were interested in studying the reactivity of silylene with several boranes with a focus on the comparison of the reactivities of boranes with the silylene. While BH₃, 9-BBN and PhBCl₂ form adducts with **2.1**, HBpin undergoes cooperative B-H bond activation, and HBcat led to amidinate boron.

The silylene–borane adducts **2.8** and **2.9** were prepared by treatment of **2.1** with BH₃ and 9-BBN in toluene at room temperature (Scheme 2.7). Their constitutions were established by multinuclear NMR spectroscopy and single-crystal X-ray diffraction studies. The ¹¹B chemical shifts of **2.8** and **2.9** appear at –35.9 and –10.5 ppm, respectively. The analogous ²⁹Si NMR shifts are observed at 96.1 and 77.8 ppm, respectively indicating the adduct formation. The molecular structures of **2.8** and **2.9** are depicted in Figures 2.10 and 2.11 with selected bond lengths and angles are given in the respective figure legends. The silicon and boron coordination polyhedra of **2.8** and **2.9** are best described as tetrahedral with Si–B bond lengths of 1.975(2) and 2.021(4) Å, which are shorter than the previously reported amidinato and guanidinato silylene borane adducts.^{42c,d,i} As a matter of fact, the Si–B bond length in **2.8** is one of the shortest Si→B dative bonds.



Scheme 2.7. Reactions of **2.1** with BH₃ and 9-BBN.

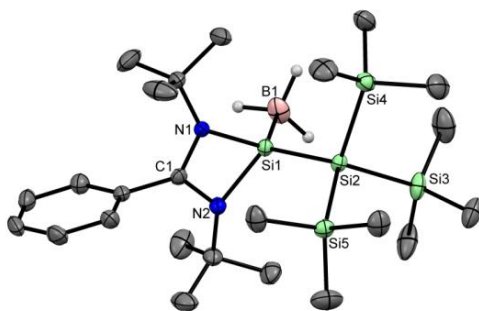


Figure 2.10. Molecular structure of **2.8**. Anisotropic displacement parameters are depicted at the 50% probability level. Hydrogen atoms (except the hydrogen atoms bonded to B) are omitted for clarity. Selected bond distances (Å) and bond angles (deg): Si1–B1 1.975(2), Si1–Si2 2.3742(8), Si1–N1 1.8433(13), Si1–N2 1.8462(15); N1–Si1–N2 70.75(6), N1–Si1–B1 116.39(9), N2–Si1–B1 116.28(9), B1–Si1–Si2 119.53(7).

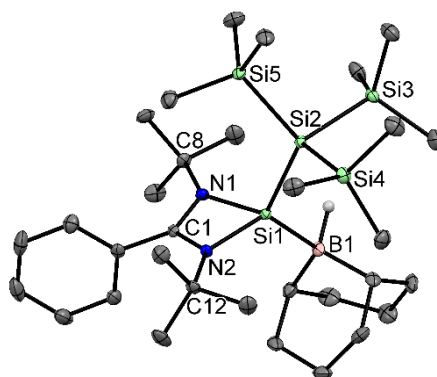
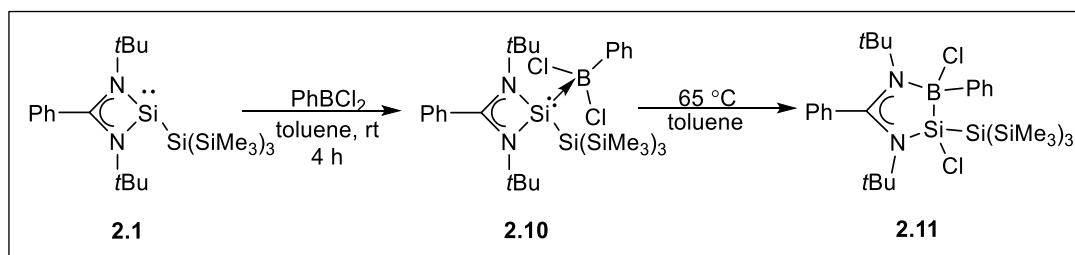


Figure 2.11. Molecular structure of **2.9**. Anisotropic displacement parameters are depicted at the 50% probability level. Hydrogen atoms (except the hydrogen atoms bonded to B) are omitted for clarity. Selected bond distances (Å) and bond angles (deg): Si1–B1 2.021(4), Si1–Si2 2.3895(12), Si1–N1 1.859(3), Si1–N2 1.869(2), B1–H1 1.17(4); N1–Si1–N2 70.19(11), N1–Si1–B1 110.05(14), N2–Si1–B1 123.42(14), B1–Si1–Si2 116.47(11).

Similarly, silylene-borane adduct **2.10** was accomplished by the reaction of **2.1** with PhBCl₂ in toluene at -78 °C to room temperature range (Scheme 2.8). Compound **2.10** was isolated as a colorless crystal from toluene solution in good yield and characterized by single-crystal X-ray diffraction studies and multinuclear NMR spectroscopy. The molecular structures of **2.10** is depicted in Figures 2.12 with selected bond lengths and angles. The four-coordinated B atom in **2.10** adopt distorted tetrahedral geometry with Si1–B1 bond length of 2.065(5) Å, typical for a coordinating bond. The ¹¹B NMR resonances of **2.10** observed at δ 3.13 ppm which is slightly down-fielded to those of L(Cl)Si→BPhCl₂ (δ -0.03 ppm).⁴⁹



Scheme 2.8. Reactions of **2.1** with PhBCl_2 .

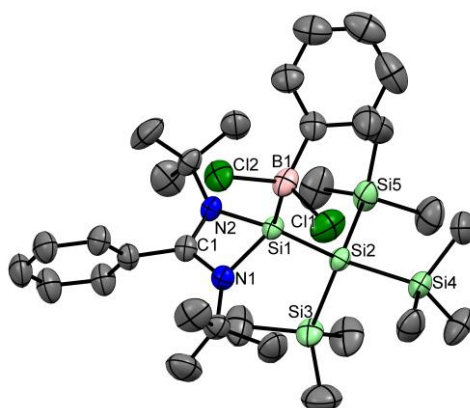
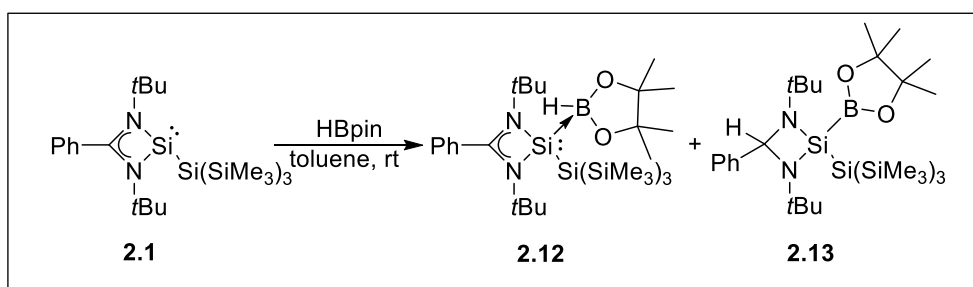


Figure 2.12. Molecular structure of **2.10**. Anisotropic displacement parameters are depicted at the 50% probability level. Hydrogen atoms are omitted for clarity. Selected bond distances (Å) and bond angles (deg): Si1–B1 2.065(5), Si1–Si2 2.4031(13), Si1–N1 1.836(3), Si1–N2 1.831(3), B1–Cl1 1.896(5), B1–Cl2 1.891(5); N1–Si1–N2 71.51(14), N1–Si1–B1 108.56(18), N2–Si1–B1 110.02(17), B1–Si1–Si2 125.70(14).

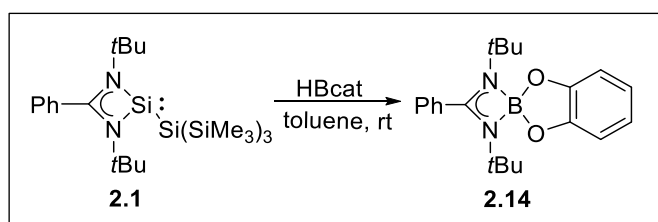
2.10 is not very stable and undergoes slow isomerization to the ring expansion product (**2.11**) via B–Cl bond activation at room temperature in longer duration. Interestingly, Compound **2.11** is stable and did not undergo any further isomerization by 1,2-migration of Cl substituent to obtain isomerization product, $\text{LB(Ph)SiCl}_2\text{Si(SiMe}_3)_3$ as reported for amidinate chloro or mesityl substituted silylene from Roesky and co-workers⁴⁹. Moreover, the complete conversion of **2.10** to **2.11** can be achieved by simply heating of toluene solution of **2.10** at 60 °C for 2 h (Scheme 2.8). **2.11** was obtained as a moisture and air-sensitive colorless crystal from toluene. Two different resonances in the ^1H NMR spectrum for the *t*Bu group (at δ 1.19 and 1.05 ppm) further confirms the formation of **2.11**. The ^{11}B NMR resonance (δ –0.45 ppm) is slightly downfield-shifted in comparison to that of **2.10**. The ^{29}Si NMR spectrum of **2.10** and **2.11** shows a broad resonance at δ 56.6 and 39.3 ppm respectively, for the silicon atom incorporated in the ring.

Next, we have reacted **2.1** with HBpin which shows a silylene–borane adduct (**2.12**) formation, which is reflected from the doublet resonance at δ 21.3 ppm in the ^{11}B NMR (Scheme 2.9). In addition, a new resonance at δ 5.81 ppm in the ^1H NMR spectrum with concomitant disappearance of HBpin resonances (q, BH, δ 2-3 ppm). The resonance at δ -59.9 ppm in the ^{29}Si NMR and 37.7 ppm in the ^{11}B NMR spectrum mirrors the four coordination at the silicon atom and suggest the formation of **2.13**. Unfortunately, we did not obtain suitable crystals for X-ray diffraction analysis. Nonetheless, all these data are in good agreement with our previously reported product obtained from the reaction between $\text{PhC}(\text{N}t\text{Bu})_2\text{SiN}(\text{SiMe}_3)_2$ and HBpin.^{44a}



Scheme 2.9. Reactions of **2.1** with HBpin.

The reaction of silylenes with HBcat is less known, presumably due to the lesser stability of the latter than HBpin. Recently, Hadlington et al. reported an unusual reaction of $[\text{bis}(\text{NHC})](\text{silylene})\text{Ni}^0$ complex with HBcat⁵⁰ which leads to the formation of an unprecedented hydroborylene coordinated (chloro)(silyl)nickel(II) complex through the cleavage of two B–O bonds and concomitant formation of two Si–O bonds.



Scheme 2.10. Reactions of **2.1** with HBcat.

The addition of HBcat to a toluene solution of **2.1** at low temperature and subsequent work up and storage afforded colorless single crystals. Their structural elucidation by an X-ray diffraction analysis revealed that an amidinato borane, $\text{PhC}(\text{N}t\text{Bu})_2\text{Bcat}$ (**2.14**) was formed (Scheme 2.10). The molecular structure of **2.14** is shown in Figure 2.13. The four coordinate B center in **2.14** sits in a tetrahedral environment, with a B–N distance of 1.58(3) Å. The ^{11}B NMR of **2.14** shows a resonance at 11.9 ppm. The fate of the silicon unit is not clear. We have performed an NMR tube reaction and after 6 h of reaction time, a possible mixture of three different types of compounds have been detected by ^1H , ^{11}B and ^{29}Si NMR spectroscopy. Which

suggest the formation of an adduct of HBcat with silylene cooperative 1,3-activation of B-H bond over Si-centre and boron inserted product (**2.14**) in 31%, 16% and 45% respectively, although we were not able to structurally characterize the compound.

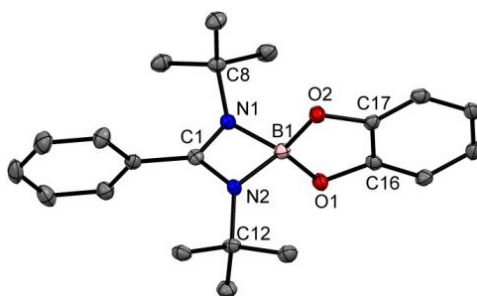


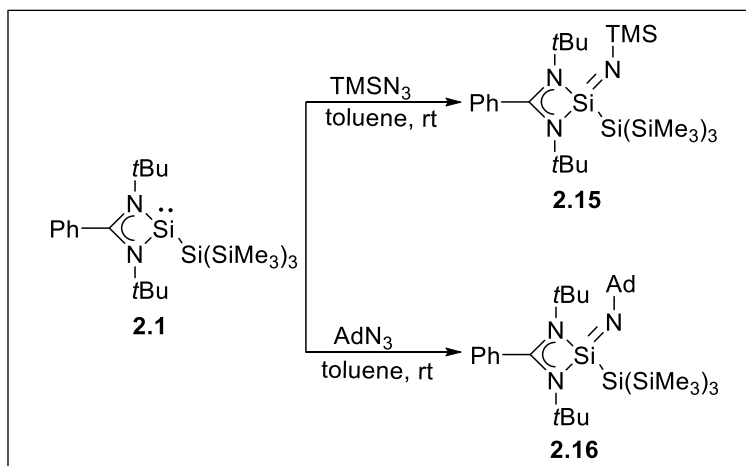
Figure 2.13. Molecular structure of **2.14**. Anisotropic displacement parameters are depicted at the 50% probability level. Hydrogen atoms (except the hydrogen atoms bonded to B) are omitted for clarity. Selected bond distances (Å) and bond angles (deg): B1–O1 1.455(3), B1–O2 1.459(3), B1–N1 1.589(3), B1–N2 1.583(3); O1–B1–O2 107.12(19), N1–B1–N2 81.74(16), O2–B1–N1 115.90(19), O1–B1–N2 116.86(19).

2.7 Reaction with organic azides: synthesis of silaimines

The synthesis of multiple bonded silicon compounds is challenging and it represents one of the most fascinating area of research for the silicon chemists over the last decades. In this regard, silaimines, ($R_2Si=NR'$, where R or R' is alkyl or aryl group) the silicon analogous of imines are key member of the silicon–heteroatom ($Si=X$, where X = O, P, S, Se, Te, N) multiply bonded compounds. In contrast to imines, silaimines shows remarkable reactivities towards unsaturated small molecules due to the polarizability of the Si=N double bond.⁵¹ Since the first isolation of silaimines in 1985 by Wiberg and coworkers⁵² a handful example of stable silaimines have been reported so far with suitable heteroatom donor substituents.^{51a,53-56} The role of hypersilyl ($-Si(SiMe_3)_3$) substituent for the stabilization of reactive species was noted from the above mentioned reactivities of the hypersilylsilylene. Herein, we have explored the reactivity of hypersilylsilylene with organic azides for the synthesis of silaimines which can be utilized further for the activation of small molecules.

The hypersilylsilaimine **2.15** and **2.16** were synthesized by the treatment of **2.1** with Me_3SiN_3 and AdN_3 , respectively in toluene (Scheme 2.11). Both the reactions proceeded smoothly at room temperature to afford the silaimines **2.15** and **2.16** in high yields. Their formation was confirmed by the multinuclear NMR spectroscopy and single-crystal X-ray diffraction analysis. The ^{29}Si NMR of **2.15** exhibit four resonances [δ -43.03 for

{Si(=NSiMe₃)Si(SiMe₃)₃}, -23.56 for {(Si(SiMe₃)₃}, -22.08 for {(=NSiMe₃)}, and -10.32 for {(Si(SiMe₃)₃]} for the four chemically different Si atoms. Similarly, compound **2.16** shows three different resonance [δ -50.72 (Si(=NAd)Si(SiMe₃)₃), -11.86 (Si(SiMe₃)₃), and 7.21 (Si(SiMe₃)₃)] in the ²⁹Si NMR spectrum.



Scheme 2.11. Reactions of **2.1** with TMSN₃ and AdN₃.

Figures 2.14 and 2.15 portray the molecular structures of **2.15** and **2.16**, respectively. Compound **2.15** and **2.16** crystallize in the orthorhombic space group *Pbca* and triclinic space group *P*-1 respectively. The central Si atoms are tetra-coordinated and displays a distorted tetrahedral geometry. The Si1–N3 bond lengths in **2.15** and **2.16** (1.609(8) and 1.608(6) Å) are consistent with the reported Si=N bond lengths [1.5936(14) and 1.5885(14) Å for trimethyl silyl and adamantyl substituent respectively] by Roesky and co-workers.^{53a}

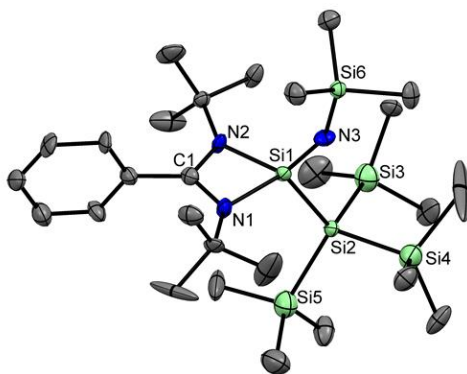


Figure 2.14. Molecular structure of **2.15**. Anisotropic displacement parameters are depicted at the 50% probability level. Hydrogen atoms are omitted for clarity. Selected bond distances (Å) and bond angles (deg): Si1–N3 1.609(8), Si1–Si2 2.350(3), Si1–N1 1.862(8), Si1–N2 1.863(7); N1–Si1–N2 70.6(3), N3–Si1–Si2 110.7(3), N2–Si1–N3 120.8(4), N1–Si1–Si2 114.0(3).

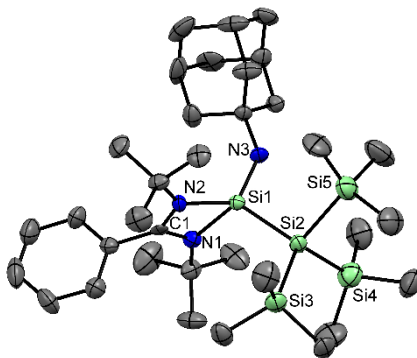
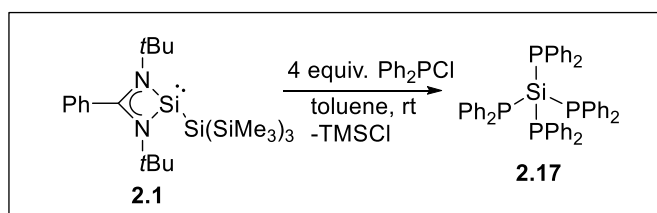


Figure 2.15. Molecular structure of **2.16**. Anisotropic displacement parameters are depicted at the 50% probability level. Hydrogen atoms are omitted for clarity. Selected bond distances (Å) and bond angles (deg): Si1–N3 1.608(6), Si1–Si2 2.322(3), Si1–N1 1.878(6), Si1–N2 1.864(6); N1–Si1–N2 69.6(3), N3–Si1–Si2 107.2(2), N2–Si1–N3 122.7(3), N1–Si1–Si2 116.0(2).

2.8 Reaction with disubstituted chlorophosphines

The usefulness of the tris(trimethylsilyl)silyl group for its substantial σ donation and delicate steric effect became popular with the isolation of various compounds with low valent main group elements. Nonetheless, further functionalization of the hypersilyl group is so far, not reported. The three trimethylsilyl substituents present in the hypersilyl moiety could be exploited for the synthesis of various silicon compounds through the removal of the SiMe_3 substituents using suitable reagents. After the successful synthesis of our hypersilylsilylene **2.1**, we have treated it with disubstituted chlorophosphines to functionalize hypersilyl substituent.



Scheme 2.12. Reactions of **2.1** with chlorodiphenylphosphine.

The synthesis of a new tetraphosphinosilane was realized by treating diphenylchlorophosphine with **2.1** in 4:1 molar ratio (Scheme 2.12). The reactions proceeded smoothly in toluene at room temperature to afford the tetraphosphinosilane, **2.17** in good yield. The structure of **2.17** was confirmed by multinuclear NMR spectroscopy and single-crystal X-ray diffraction analysis. The resonances at δ -115.4 ppm in ^{29}Si NMR of **2.17** reflects a tetra-coordinated silicon center. The molecular structure of **2.17** is depicted with selected bond length and bond angle in Figure 2.16. The Si center in **2.17** possesses a distorted tetrahedral environment with four phosphorous

substituents. The ^{31}P NMR of **2.17** shows a sharp singlet at δ -14.9 ppm. The fate of the amidinate moiety is still unclear as it decomposes to amidinate chloride salt as free ligand. To gain more insight, we have checked ^{29}Si NMR for an NMR tube reaction and which suggests the formation of amidinato trichlorosilane [LSiCl_3 , where $\text{L} = \text{PhC}(\text{N}t\text{Bu})_2$]. However, a stoichiometric reaction of Ph_2PCl and **2.1** at lower temperature resembles the formation of Roesky's silylene $\text{LSiP}(\text{Ph})_2$ with the successive cleavage of $\text{Si}^{\text{II}}\text{-Si}^{\text{IV}}$ bond. On the other hand, no product formation for the reaction of $\text{Si}(\text{SiMe}_3)_4$ and Ph_2PCl further implies the $\text{Si}^{\text{II}}\text{-Si}^{\text{IV}}$ bond cleavage for the formation of **2.17**.

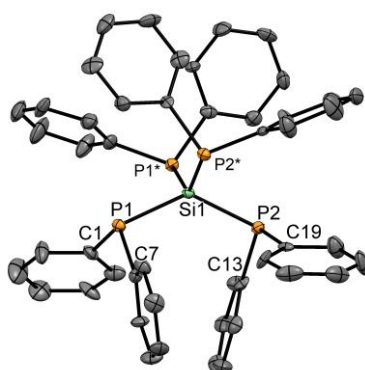
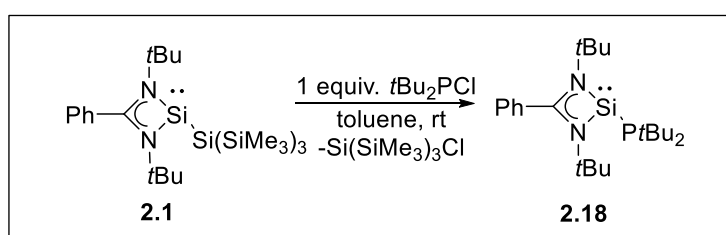


Figure 2.16. Molecular structure of **2.17**. Anisotropic displacement parameters are depicted at the 50% probability level. Hydrogen atoms are omitted for clarity. Selected bond distances (\AA) and bond angles (deg): Si1-P1 2.295(3), Si1-P2 2.286(3), P1-C1 1.869(8), P1-C7 1.847(7), P2-C13 1.830(7), P2-C19 1.802(7); P1-Si1-P2 95.54(3), P1-Si1-P1^* 104.51(16), P2-Si1-P2^* 105.10(16).



Scheme 2.13. Reactions of **2.1** with di-tert-butylchlorophosphine.

To explore the reactivity of hypersilylsilylene towards other chlorophosphines, next, we have treated **2.1** with di-tert-butylchlorophosphine in 1:1 molar ratio in toluene. An amidinate silylene with $-\text{PtBu}_2$ substituent (**2.18**) was isolated in good yield by the successive $\text{Si}^{\text{II}}\text{-Si}^{\text{IV}}$ bond cleavage. **2.18** was isolated as pale-yellow crystals from hexane, and it shows stability in the solid-state and in the solution state under an inert gas atmosphere. The constitutions of **2.18** were confirmed by the single-crystal X-ray diffraction studies and multinuclear NMR spectroscopy. The ^{31}P NMR of **2.18** shows a sharp singlet at δ 25.3 ppm. Compound **2.18**

exhibits a doublet (δ 48.2 ppm, $J_{\text{Si-P}} = 196.18$ Hz) resonance in the ^{29}Si NMR spectrum, which is upfield shifted as compared to that in **2.1**. **2.18** crystallizes in the monoclinic space group $P2_1/c$, and the molecular structure is depicted in Figure 2.17 with significant bond lengths and angles. The Si atom features a trigonal pyramidal geometry with three-coordination and a lone pair of electrons. The Si1–P1 bond length in **2.18** is 2.3087(3) Å, which is consistent with the reported Si–P bond length [2.307(8) Å] by Roesky and co-workers.⁵ However, the Si–P bond length in **2.18** is slightly longer than the Inoues’s silylene $\text{LSiP}(\text{SiMe}_3)_2$ [$\text{L} = \text{PhC}(\text{N}t\text{Bu})_2$] [2.2838(12) Å]⁸ but shorter than Roesky’s silylene $\text{LSiP}(\text{Ph})_2$ [2.3111(6) Å].⁶

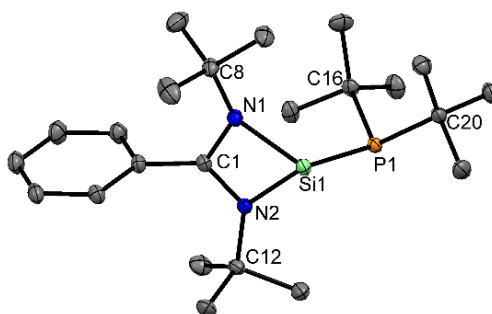


Figure 2.17. Molecular structure of **2.18**. Anisotropic displacement parameters are depicted at the 50% probability level. Hydrogen atoms are omitted for clarity. Selected bond distances (Å) and bond angles (deg): Si1–P1 2.3087(3), Si1–N1 1.8864(7), Si1–N2 1.8712(7); N1–Si1–N2 69.42(3), N1–Si1–P1 111.42(2), N2–Si1–P1 101.32(2).

We have carried out geometry optimization of **2.18**, using density functional theory (DFT) at the PBE/ TZVP level for the ground-state singlet and triplet geometries. The HOMO–LUMO energy gap for the silylene has been determined to be 5.62 eV. The HOMO is located over the Si–P bond of **2.18**, and the LUMO is spread over the phenyl ring of the amidinate ligand (Figure 2.18).

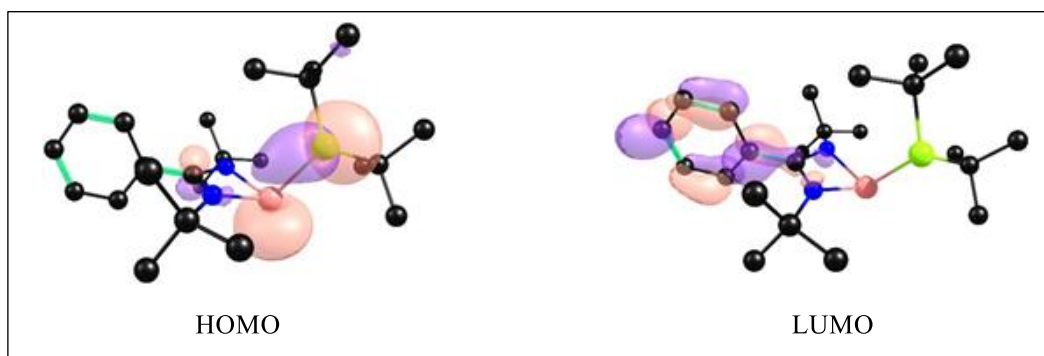
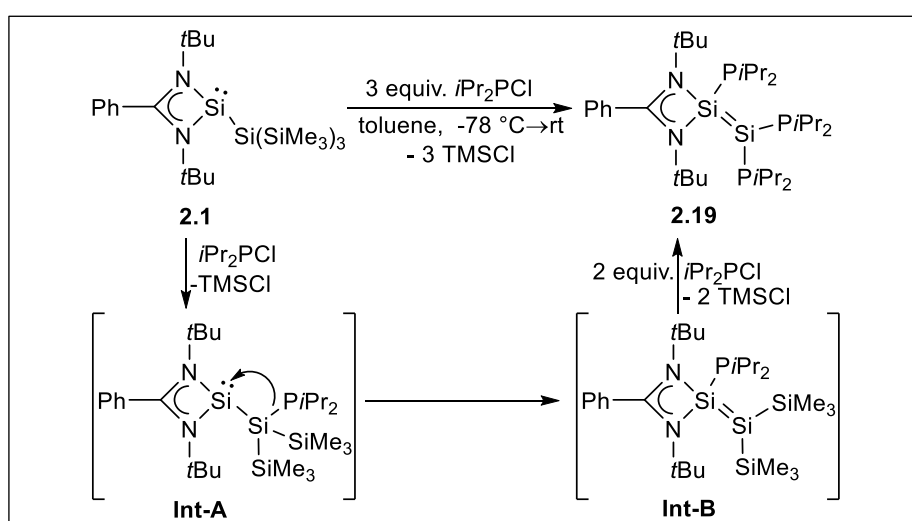


Figure 2.18. Computational details of **2.18**.

The anomalous reactivity of hypersilyl ($-\text{Si}(\text{SiMe}_3)_3$) substituent towards electronically different disubstituted chlorophosphine is noted from the isolation of tetraphosphinosilane and phosphinosilylene as mentioned above. Next, we were attentive to explore the reactivity of chlorodiisopropylphosphine with the hypersilylsilylene. Interestingly, a disilene, **2.19** is isolated via facile cleavage of $\text{Si}^{\text{IV}}-\text{Si}^{\text{IV}}$ bond of the $-\text{Si}(\text{SiMe}_3)_3$ substituent and followed by the isomerization of a silylene intermediate (**Int-A**) formed by the stoichiometric reaction of **2.1** with chlorodiisopropylphosphine. However, **Int-A** is not very stable and isomerizes to **Int-B** with the subsequent migration of a $-\text{P}i\text{Pr}_2$ substituent to the Si^{II} center. And finally with the removal of another two equivalent of trimethylsilyl chloride, **Int-B** converted to **2.19** (Scheme 2.14).



Scheme 2.14. Reactions of **2.1** with chlorodiisopropylphosphine.

The constitution of the **2.19** is confirmed by the multinuclear NMR spectroscopy and single-crystal X-ray diffraction studies. Two different set of resonance at δ -8.7 [$\text{LSi}(\text{P}i\text{Pr}_2)=\text{Si}(\text{P}i\text{Pr}_2)_2$] and -28.3 [$\text{LSi}(\text{P}i\text{Pr}_2)=\text{Si}(\text{P}i\text{Pr}_2)_2$] was observed in the ^{31}P NMR of **2.19**. Compound **2.19** crystallizes in the triclinic space group $P-1$, and its molecular structure is presented in Figure 2.19 with the important bond lengths and angles. The observed $\text{Si}=\text{Si}$ bond length in **2.19** is 2.2901(4) Å, which is in good agreement to the length of typical $\text{Si}=\text{Si}$ double bonds of the disilenes (2.14–2.29 Å).⁵⁷ To gain the further insights into the bonding characteristic of **2.19**, we have done a geometry optimization of **2.19** for the ground-state singlet and triplet geometries using density functional theory (DFT) at the PBE/ TZVP level. The HOMO–LUMO energy gap for the silylene has been determined to be 4.97 eV. The HOMO is located over the $\text{Si}-\text{Si}$ bond of **2.19**, and the LUMO is spread mostly over the phenyl ring of the amidinate ligand and some part on the Si atom (Figure 2.20).

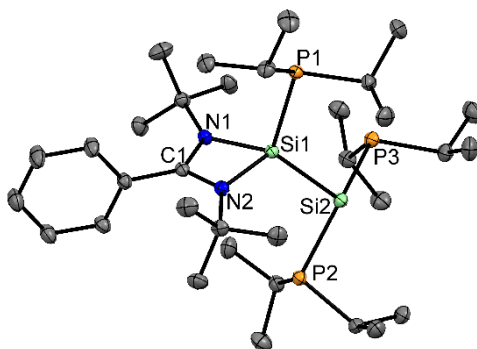


Figure 2.17. Molecular structure of **2.19**. Anisotropic displacement parameters are depicted at the 50% probability level. Hydrogen atoms are omitted for clarity. Selected bond distances (Å) and bond angles (deg): Si1–Si2 2.2901(4), Si1–P1 2.2853(4), Si2–P2 2.2817(5), Si2–P3 2.2708(4); P1–Si1–Si2 114.621(17), P2–Si2–Si1 98.692(17), N1–Si1–N2 70.83(4), P2–Si2–P3 125.906(19).

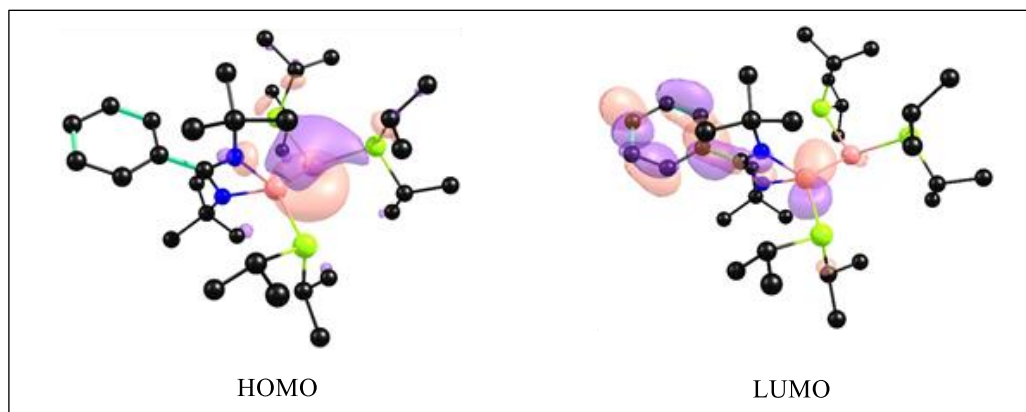
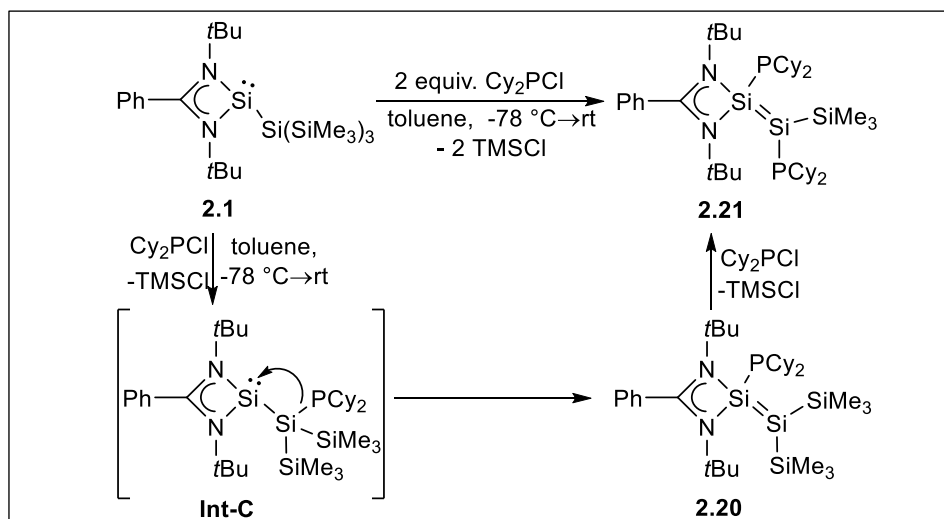


Figure 2.20. Computational details of **2.19**.

Similarly, other disilenes **2.20** and **2.21** were accomplished by the reaction of **2.1** with dicyclohexylchlorophosphine in toluene at $-78\text{ }^{\circ}\text{C}$ to room temperature range (Scheme 2.15). Herein, we have carried out two separate reaction of **2.1** with dicyclohexylchlorophosphine in 1:1 and 1:2 molar ratio. Compound **2.20** was isolated as orange-red color crystal from the hexane solution for the stoichiometric reaction and characterized through multinuclear NMR spectroscopy and single-crystal X-ray diffraction studies. The ^{31}P NMR of **2.20** shows a sharp resonances at δ -34.63 [$\text{LSi}(\text{PCy}_2)=\text{Si}(\text{SiMe}_3)_2$] ppm. Similarly, orange-red color crystal of the compound **2.21** was also isolated from the hexane solution for the 1:2 reaction. **2.21** was characterized through the single-crystal X-ray diffraction studies and multinuclear NMR spectroscopy. The ^{31}P NMR of **2.21** shows two sharp resonances for the two chemically

different phosphorus atom at δ -14.9 [LSi(PCy₂)=Si(PCy₂)(SiMe₃)] and -28.3 [LSi(PCy₂)=Si(PCy₂)(SiMe₃)] ppm.



Scheme 2.15. Reactions of **2.1** with dicyclohexylchlorophosphine.

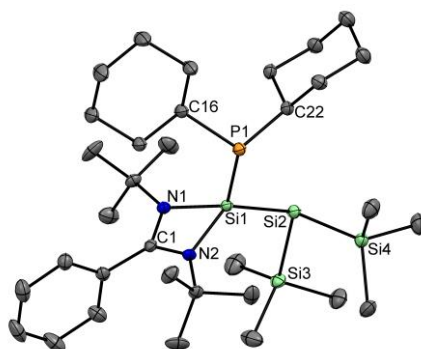


Figure 2.21. Molecular structure of **2.20**. Anisotropic displacement parameters are depicted at the 50% probability level. Hydrogen atoms are omitted for clarity. Selected bond distances (Å) and bond angles (deg): Si1–Si2 2.2860(9), Si1–P1 2.2729(9), Si2–Si3 2.3398(10), Si2–Si4 2.3686(10); P1–Si1–Si2 111.85(3), Si1–Si2–Si3 105.34(3), Si3–Si2–Si4 101.71(3), N1–Si1–N2 70.51(8), N1–Si1–P1 117.27(7).

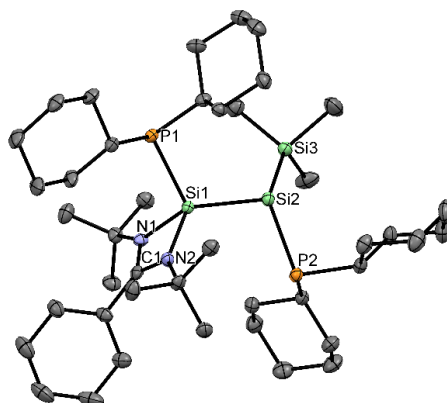


Figure 2.22. Molecular structure of **2.21**. Anisotropic displacement parameters are depicted at the 50% probability level. Hydrogen atoms are omitted for clarity. Selected bond distances (Å) and bond angles (deg): Si1–Si2 2.2720(8), Si1–P1 2.2808(7), Si2–P2 2.2707(8), Si2–Si3 2.3570(8); P1–Si1–Si2 111.69(3), P2–Si2–Si1 104.45(3), N1–Si1–N2 70.53(8), P2–Si2–Si3 117.91(3).

Compound **2.20** and **2.21** crystallizes in the monoclinic $P2_1/c$ and triclinic $P-1$ space group respectively. The molecular structure of **2.20** and **2.21** are depicted in Figure 2.21 and Figure 2.22 respectively with the important bond lengths and angles. The Si=Si bond length in **2.20** and **2.21** are 2.2860(9) Å and 2.2720(8) Å respectively, which are slightly shorter compared to that in **2.19** [2.2901(4) Å]. The constitution of **2.20** suggest the formation of **Int-C** via 1:1 reaction of **2.1** with dicyclohexylchlorophosphine. After the formation of **Int-C**, it isomerizes to **2.20** with the successive migration of $-PCy_2$ substituent to the Si^{II} -center. Then in the next step, trimethylsilyl group trans to the $-PCy_2$ substituents eliminates as trimethylsilyl chloride in presence of the second equivalent of dicyclohexylchlorophosphine and led to the formation of the compound **2.21**.

2.9 Conclusion

In summary, we have synthesized a new hypersilylsilylene (**2.1**) by using a bulky σ -donating $-Si(SiMe_3)_3$ substituent featuring the longest reported $Si^{II}-Si^{IV}$ bond. DFT studies revealed that the HOMO–LUMO energy gap is 3.7 eV. The reactivity of **2.1** with Me_3NO presented a stepwise O insertion to form dimeric products (**2.2** and **2.3**) containing a Si_2O_2 unit. Subsequently, silachalcogenones (**2.4–2.6**) were synthesized by the oxidative addition of **2.1** with S, Se, or Te. The reaction of acetone with **2.1** represents the first example of the formation of a silaoxirane derivative (**2.7**) from a methyl ketone, which was previously known to undergo C–H bond activation upon reaction with silylene. Anomalous reactivity of hypersilylsilylene towards boranes was observed. Silaimines **2.15** and **2.16** were synthesized by the treatment of **2.1** with organic azides. The formation of **2.7**, **2.15** and **2.16** can be attributed to the kinetic and thermodynamic protection provided by the bulky $-Si(SiMe_3)_3$ ligands. Also, the synthesis of a tetraphosphinosilane (**2.17**), phosphinosilylene (**2.18**) and disilene (**2.19–2.21**) were realized by the reaction of hypersilylsilylene with disubstituted chlorophosphines.

2.10 References

1. For recent reviews on silylene, see: (a) Haaf, M.; Schmedake, T. A.; West, R. *Acc. Chem. Res.* **2000**, *33*, 704–714. (b) Gehrhus, B.; Lappert, M. F. *J. Organomet. Chem.* **2001**,

- 617–618, 209–223. (c) Nagendran, S.; Roesky, H. W. *Organometallics* **2008**, *27*, 457–492. (d) Kira, M. *Chem. Commun.* **2010**, *46*, 2893–2903. (e) Yao, S.; Xiong, Y.; Driess, M. *Organometallics* **2011**, *30*, 1748–1767. (f) Asay, M.; Jones, C.; Driess, M. *Chem. Rev.* **2011**, *111*, 354–396. (g) Sen, S. S.; Khan, S.; Samuel, P. P.; Roesky, H. W. *Chem. Sci.* **2012**, *3*, 659–682. (h) Sen, S. S.; Khan, S.; Nagendran, S.; Roesky, H. W. *Acc. Chem. Res.* **2012**, *45*, 578–587. (i) Ghadwal, R. S.; Azhakar, R.; Roesky, H. W. *Acc. Chem. Res.* **2013**, *46*, 444–456. (j) Yadav, S.; Saha, S.; Sen, S. S. *ChemCatChem* **2016**, *8*, 486–501. (k) Teichmann, J.; Wagner, M. *Chem. Commun.* **2018**, *54*, 1397–1412. (l) Chu, T.; Nikonov, G. I. *Chem. Rev.* **2018**, *118*, 3608–3680.
- (a) Blom, B.; Driess, M. *In Functional Molecular Silicon Compounds II*; Scheschkewitz, D., Ed.; Springer, 2014. (b) Alvarez- Rodriguez, L.; Cabeza, J. A.; Garcia-Alvarez, P.; Polo, D. *Coord. Chem. Rev.* **2015**, *300*, 1–28. (c) Blom, D.; Gallego, D.; Driess, M. *Inorg. Chem. Front.* **2014**, *1*, 134–148. (d) Blom, D.; Stoelzel, M.; Driess, M. *Chem. - Eur. J.* **2013**, *19*, 40–62. (e) Zhou, Y.-P.; Driess, M. *Angew. Chem. Int. Ed.* **2019**, *58*, 3715–3728.
 - (a) Sen, S. S.; Roesky, H. W.; Stern, D.; Henn, J.; Stalke, D. *J. Am. Chem. Soc.* **2010**, *132*, 1123–1126. (b) So, C.-W.; Roesky, H. W.; Magull, J.; Oswald, R. B. *Angew. Chem. Int. Ed.* **2006**, *45*, 3948–3950.
 - Yeong, H.-X.; Lau, K.-C.; Xi, H.-W.; Hwa Lim, K.; So, C.-W. *Inorg. Chem.* **2010**, *49*, 371–373.
 - So, C.-W.; Roesky, H. W.; Gurubasavaraj, P. M.; Oswald, R. B.; Gamer, M. T.; Jones, P. G.; Blaurock, S. *J. Am. Chem. Soc.* **2007**, *129*, 12049–12054.
 - Azhakar, R.; Ghadwal, R. S.; Roesky, H. W.; Wolf, H.; Stalke, D. *Organometallics* **2012**, *31*, 4588–4592.
 - Sen, S. S.; Hey, J.; Herbst-Irmer, R.; Roesky, H. W.; Stalke, D. *J. Am. Chem. Soc.* **2011**, *133*, 12311–12316.
 - Inoue, S.; Wang, W.; Präsang, C.; Asay, M.; Irran, E.; Driess, M. *J. Am. Chem. Soc.* **2011**, *133*, 2868–2871.
 - Azhakar, R.; Ghadwal, R. S.; Roesky, H. W.; Wolf, H.; Stalke, D. *Chem. Commun.* **2012**, *48*, 4561–4563.
 - Schäfer, S.; Köppe, R.; Roesky, P. W. *Chem. - Eur. J.* **2016**, *22*, 7127–7133.
 - Wang, W.; Inoue, S.; Enthaler, S.; Driess, M. *Angew. Chem. Int. Ed.* **2012**, *51*, 6167–6171.
 - Bai, Y.; Zhang, Z.; Cui, C. *Chem. Commun.* **2018**, *54*, 8124–8127.
 - Cabeza, J. A.; García-Álvarez, P.; González-Álvarez, L. *Chem. Commun.* **2017**, *53*, 10275–10278.

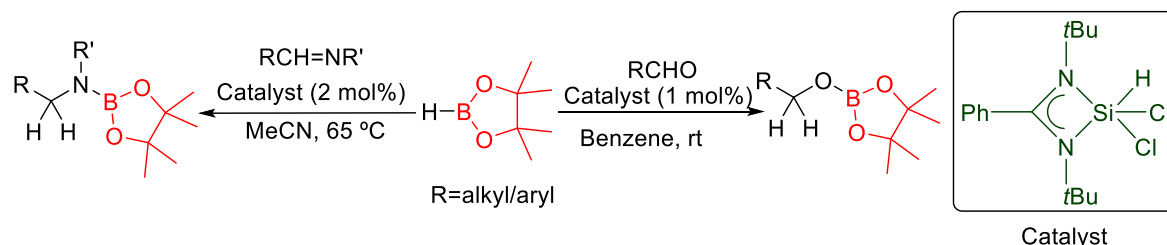
14. (a) Benkeser, R. A.; Severson, R. G. *J. Am. Chem. Soc.* **1951**, *73*, 1424–1427. (b) Gilman, H.; Wu, T. C. *J. Am. Chem. Soc.* **1951**, *73*, 4031–4033. (c) Gilman, H.; Smith, C. L. *J. Organomet. Chem.* **1967**, *8*, 245.
15. Roddick, D. M.; Tilley, T. D.; Rheingold, A. L.; Geib, S. J. *J. Am. Chem. Soc.* **1987**, *109*, 945–946.
16. (a) Kornev, A. N. *Russ. Chem. Rev.* **2004**, *73*, 1065–1089. (b) Klinkhammer, K. W. *Chem. - Eur. J.* **1997**, *3*, 1418–1431.
17. Protchenko, A. V.; Schwarz, A. D.; Blake, M. P.; Jones, C.; Kaltsoyannis, N.; Mountford, P.; Aldridge, S. *Angew. Chem. Int. Ed.* **2013**, *52*, 568–571.
18. Protchenko, A. V.; Birjkumar, K. H.; Dange, D.; Schwarz, A. D.; Vidovic, D.; Jones, C.; Kaltsoyannis, N.; Mountford, P.; Aldridge, S. *J. Am. Chem. Soc.* **2012**, *134*, 6500–6503.
19. Kira, M.; Ishida, S.; Iwamoto, T.; Kabuto, C. *J. Am. Chem. Soc.* **1999**, *121*, 9722–9723.
20. Sen, S. S.; Jana, A.; Roesky, H. W.; Schulzke, C. *Angew. Chem. Int. Ed.* **2009**, *48*, 8536–8538.
21. Unno, M.; Tanaka, R. *Silanols and Silsequioxanes in Efficient Methods for Preparing Silicon Compounds*; Roesky, H. W., Ed.; Academic Press/Elsevier, 2016.
22. (a) Sen, S. S.; Tavčar, G.; Roesky, H. W.; Kratzert, D.; Hey, J.; Stalke, D. *Organometallics* **2010**, *29*, 2343–2347. (b) Tavčar, G.; Sen, S. S.; Roesky, H. W.; Hey, J.; Kratzert, D.; Stalke, D. *Organometallics* **2010**, *29*, 3930–3935.
23. (a) Kudo, T.; Nagase, S. *J. Am. Chem. Soc.* **1985**, *107*, 2589–2595. (b) Bachrach, S. M.; Streitwieser, A. *J. Am. Chem. Soc.* **1985**, *107*, 1186–1190. (c) Michalczyk, M. J.; Fink, M. J.; Haller, K. J.; West, R.; Michl, J. *Organometallics* **1986**, *5*, 531–536.
24. Iwamoto, T.; Sato, K.; Ishida, S.; Kabuto, C.; Kira, M. *J. Am. Chem. Soc.* **2006**, *128*, 16914–16920.
25. Parvin, N.; Pal, S.; Khan, S.; Das, S.; Pati, S. K.; Roesky, H. W. *Inorg. Chem.* **2017**, *56*, 1706–1712.
26. Chan, Y.-C.; Li, Y.; Ganguly, R.; So, C.-W. *Eur. J. Inorg. Chem.* **2015**, 3821–3824.
27. Khan, S.; Michel, R.; Koley, D.; Roesky, H. W.; Stalke, S. *Inorg. Chem.* **2011**, *50*, 10878–10883.
28. Wendel, D.; Porzelt, A.; Herz, F. A. D.; Sarkar, D.; Jandl, C.; Inoue, S.; Rieger, B. *J. Am. Chem. Soc.* **2017**, *139*, 8134–8137.
29. Suzuki, H.; Tokitoh, N.; Nagase, S.; Okazaki, R. *J. Am. Chem. Soc.* **1994**, *116*, 11578–11579.

30. Junold, K.; Baus, J. A.; Burschka, C.; Auerhammer, D.; Tacke, R. *Chem. - Eur. J.* **2012**, *18*, 16288–16291.
31. Yao, S.; Xiong, Y.; Driess, M. *Chem. - Eur. J.* **2010**, *16*, 1281–1288.
32. Kocher, N.; Henn, J.; Gostevskii, B.; Kost, D.; Kalikhman, I.; Engels, B.; Stalke, D. *J. Am. Chem. Soc.* **2004**, *126*, 5563–5568.
33. Ghadwal, R. S.; Sen, S. S.; Roesky, H. W.; Granitzka, M.; Kratzert, D.; Merkel, S.; Stalke, D. *Angew. Chem. Int. Ed.* **2010**, *49*, 3952–3955.
34. Azhakar, R.; Ghadwal, R. S.; Roesky, H. W.; Hey, J.; Stalke, D. *Organometallics* **2011**, *30*, 3853–3858.
35. Ishida, S.; Iwamoto, T.; Kira, M. *Organometallics* **2010**, *29*, 5526–5534.
36. Swamy, V. S. V. S. N.; Parvin, N.; Vipin Raj, K.; Vanka, K.; Sen, S. S. *Chem. Commun.* **2017**, *53*, 9850–9853.
37. Becerra, R.; Cannady, J. P.; Walsh, R. *J. Phys. Chem. A* **1999**, *103*, 4457–4464.
38. Kaftory, M.; Kapon, M.; Botoshansky, M. *In The Chemistry of Organic Silicon Compounds*; Rappoport, Z., Apeloig, Y., Eds.; Wiley: Chichester, U.K., 1998; Vol. 2, Chapter 5.
39. Reiter, D.; Holzner, R.; Porzelt, A.; Altmann, P. J.; Frisch, P.; Inoue, S. *J. Am. Chem. Soc.* **2019**, *141*, 13536–13546.
40. (a) Hadlington, T. J.; Abdalla, J. A. B.; Tirfoin, R.; Aldridge, S.; Jones, C. *Chem. Commun.* **2016**, *52*, 1717–1720. (b) Jana, A.; Schulzke, C.; Roesky, H. W. *J. Am. Chem. Soc.* **2009**, *131*, 4600–4601.
41. For selected references, please see: (a) Sen, S. S.; Khan, S.; Roesky, H. W.; Kratzert, D.; Meindl, K.; Henn, J.; Stalke, D.; Demers, J.-P.; Lange, A. *Angew. Chem. Int. Ed.* **2011**, *50*, 2322–2325. (b) Khan, S.; Michel, R.; Sen, S. S.; Roesky, H. W.; Stalke, D. *Angew. Chem. Int. Ed.* **2011**, *50*, 11786–11789. (c) Xiong, Y.; Yao, S.; Brym, M.; Driess, M. *Angew. Chem. Int. Ed.* **2007**, *46*, 4511–4513.
42. (a) Metzler, N.; Denk, M. *Chem. Commun.* **1996**, 2657–2658. (b) Ghadwal, R. S.; Roesky, H. W.; Merkel, S.; Stalke, D. *Chem. - Eur. J.* **2010**, *16*, 85–88. (c) Azhakar, R.; Tavčar, G.; Roesky, H. W.; Hey, J.; Stalke, D. *Eur. J. Inorg. Chem.* **2011**, 475–477. (d) Jana, A.; Azhakar, R.; Sarish, S. P.; Samuel, P. P.; Roesky, H. W.; Schulzke, C.; Koley, D. *Eur. J. Inorg. Chem.* **2011**, 5006–5013. (e) Jana, A.; Leusser, D.; Objartel, I.; Roesky, H. W.; Stalke, D. *Dalton Trans.* **2011**, *40*, 5458–5463. (f) Al-Rafia, S. M. I.; Malcolm, A. C.; McDonald, R.; Ferguson, M. J.; Rivard, E. *Chem. Commun.* **2012**, *48*, 1308–1310. (g) Rodriguez, R.; Troadec, T.; Kato, T.; Saffon-Merceron, N.; Sotiropoulos, J.-M.; Baceiredo,

- A. *Angew. Chem. Int. Ed.* **2012**, *51*, 7158–7161. (h) Inoue, S.; Leszczyńska, K. *Angew. Chem. Int. Ed.* **2012**, *51*, 8589–8593. (i) Mück, F. M.; Baus, J. A.; Bertermann, R.; Burschka, C.; Tacke, R. *Organometallics* **2016**, *35*, 2583–2588. (j) Pahar, S.; Karak, S.; Pait, M.; Raj, K. V.; Vanka, K.; Sen, S. S. *Organometallics* **2018**, *37*, 1206–1213.
43. Tacke, R.; Ribbeck, T. *Dalton Trans.* **2017**, *46*, 13628–13659.
44. (a) Swamy, V. S. V. S. N.; Raj, K. V.; Vanka, K.; Sen, S. S.; Roesky, H. W. *Chem. Commun.* **2019**, *55*, 3536–3539. (b) Khoo, S., Shan, Y.-L.; Yang, M.-C.; Li, Y.; Su, M.-D.; So, C.-W. *Inorg. Chem.* **2018**, *57*, 5879–5887.
45. Gackstatter, A.; Braunschweig, H.; Kupfer, T.; Voigt, C.; Arnold, N. *Chem. - Eur. J.* **2016**, *22*, 16415–16419.
46. Braunschweig, H.; Bruckner, T.; Deißberger, A.; Dewhurst, R. D.; Gackstatter, A.; Gartner, A.; Hofmann, A.; Kupfer, T.; Prieschl, D.; Thiess, T.; Wang, S. R. *Chem. - Eur. J.* **2017**, *23*, 9491–9494.
47. Suzuki, Y.; Ishida, S.; Sato, S.; Isobe, H.; Iwamoto, T. *Angew. Chem. Int. Ed.* **2017**, *56*, 4593–4597.
48. Khoo, S.; Shan, Y.-L.; Yang, M.-C.; Li, Y.; Su, M.-D.; So, C.-W. *Inorg. Chem.* **2018**, *57*, 5879–5887.
49. Li, J.; Liu, Y.; Kundu, S.; Keil, H.; Zhu, H.; Herbst-Irmer, R.; Stalke, D.; Roesky, H. W. *Inorg. Chem.* **2020**, *59*, 12, 7910–7914.
50. Hadlington, T. J.; Szilvási, T.; Driess, M. *Angew. Chem. Int. Ed.* **2017**, *56*, 7470–7474.
51. (a) Kong, L.; Cui, C. *Organometallics* **2010**, *29*, 5738–5740. (b) Kocher, N.; Henn, J.; Gostevskii, B.; Kost, D.; Kalikhman, I.; Engels, B.; Stalke, D. *J. Am. Chem. Soc.* **2004**, *126*, 5563–5568. (c) Kocher, N.; Selinka, C.; Leusser, D.; Kost, D.; Kalikhman, I.; Stalke, D. *Z. Anorg. Allg. Chem.* **2004**, *630*, 1777–1793. (d) Niessmann, J.; Klingebiel, U.; Schäfer, M.; Boese, R. *Organometallics* **1998**, *17*, 947–953. (e) Stalke, D.; Klingebiel, U.; Sheldrick, G. M. *J. Organomet. Chem.* **1988**, *344*, 37–48. (f) Stalke, D.; Keweloh, N.; Klingebiel, U.; Noltemeyer, M.; Sheldrick, G. M. *Z. Naturforsch.* **1987**, *42b*, 1237–1244.
52. (a) Wiberg, N.; Schurz, K.; Fischer, G. *Angew. Chem.* **1985**, *97*, 1058–1059; *Angew. Chem. Int. Ed. Engl.* **1985**, *24*, 1053–1054. (b) Wiberg, N.; Schurz, K.; Reber, G.; Müller, G. *J. Chem. Soc., Chem. Commun.* **1986**, 591–592.
53. Examples of three-coordinate silaimines: (a) Samuel, P. P.; Azhakar, R.; Ghadwal, R. S.; Sen, S. S.; Roesky, H. W.; Granitzka, M.; Matussek, J.; Herbst-Irmer, R.; Stalke, D. *Inorg. Chem.* **2012**, *51*, 11049–11054. (b) Iwamoto, T.; Ohnishi, N.; Gui, Z.; Ishida, S.; Isobe, H.;

- Maeda, S.; Ohno, K.; Kira, M. *New J. Chem.* **2010**, *34*, 1637–1645. (c) Denk, M.; Hayashi, R. K.; West, R. *J. Am. Chem. Soc.* **1994**, *116*, 10813–10814.
54. Examples of amidinate and guanidinate coordinated silaimines: (a) Mück, F. M.; Förster, B.; Baus, J. A.; Nutz, M.; Burschka, C.; Bertermann, R.; Tacke, R. *Eur. J. Inorg. Chem.* **2016**, 3246–3252. (b) Mück, F. M.; Ulmer, A.; Baus, J. A.; Burschka, C.; Tacke, R. *Eur. J. Inorg. Chem.* **2015**, 1860–1864. (c) Khan, S.; Sen, S. S.; Kratzert, D.; Tavčar, G.; Roesky, H. W.; Stalke, D. *Chem. – Eur. J.* **2011**, *17*, 4283–4290.
55. Examples of N-heterocyclic carbene stabilized silaimines: (a) Cui, H.; Cui, C. *Dalton Trans.* **2015**, *44*, 20326–20329. (b) Cui, H.; Zhang, J.; Tao, Y.; Cui, C. *Inorg. Chem.* **2016**, *55*, 46–50.
56. An example of a silylenyl coordinated silaimine: Zhang, S.-H.; Xi, H.-W.; Lim, K. H.; Meng, Q.; Huang, M.-B.; So, C.-W. *Chem. - Eur. J.* **2012**, *18*, 4258–4263.
57. Recent reviews on disilene chemistry: (a) Präsang, C.; Scheschkewitz, D. Reactivity in the periphery of functionalized multiple bonds of heavier group 14 elements. *Chem. Soc. Rev.* **2016**, *45*, 900–921. (b) Iwamoto, T.; Ishida, S. In *Functional Molecular Silicon Compounds II: Low Oxidation States*, Scheschkewitz, D., Ed.; Springer International Publishing: Cham, 2014; pp 125–202.

Amidinato Silane for Catalytic Hydroboration of Aldehydes and Aldimines



Abstract

The transition metal free catalytic hydroboration of aldehydes and ketones is very limited and has not been reported with a well-defined silicon(IV) compound. Therefore, in this chapter, we chose to evaluate the potential of a previously reported silicon(IV) hydride $[\text{PhC}(\text{N}t\text{Bu})_2\text{SiHCl}_2]$, as a single component catalyst. Gratifyingly, it catalyzes the reductive hydroboration of a range of aldehydes with pinacolborane (HBpin) under ambient conditions. In addition, the same compound was utilized for the imine hydroboration in a slightly harsh condition. DFT calculation was carried out to understand the mechanism.

3.1 Introduction

The addition of a B–H bond to the C=C, C=O, and C=N bonds requires a catalyst. Group 4 metallocenes¹ and precious metal compounds, particularly the organometallic rhodium and iridium complexes² are the most studied catalysts for hydroboration reactions. Due to environmental concerns, limited terrestrial abundance, and the high cost of traditional transition metal catalysts, there is a recent surge in the exploration of compounds with main group elements as feasible alternatives to transition metal catalysts.^{3–6} Encouragingly, a number of research groups such as those of Hill, Roesky, Wesemann, Nembenna, Jones, Zhao, Kinjo, and others^{7–13} have started to use compounds with s- and p-block elements as single site catalysts for the catalytic hydroboration of aldehydes and ketones (Chart 3.1). However, when we look at the full gamut of single site neutral compounds reported for transition metal free hydroboration of aldehydes and ketones, there is one element missing that one might have expected to be there: silicon.

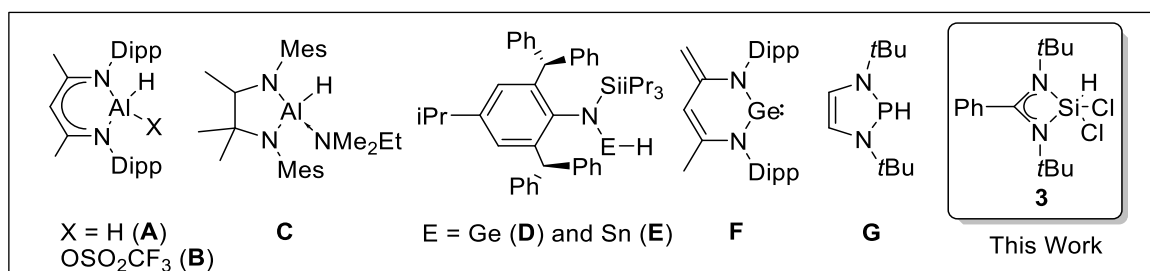
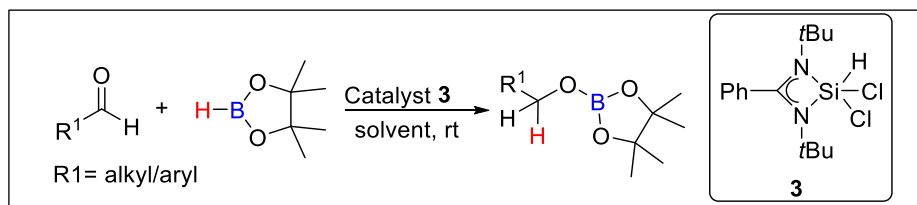


Chart 3.1. Single component compounds with heavier p-block elements that catalyze hydroboration of aldehydes (A–G); this work reports the first use of a neutral silicon(IV) compound (3) for aldehyde hydroboration.

Being isosteres of carbon and owing to their larger covalent radius, electropositive nature, low toxicity and relative abundance, silicon compounds are highly sought after as single component catalysts because a catalytic cycle based on silicon could be sustainable, economical, and green. Silylium ion promoted catalytic imine reduction and Diels–Alder reactions,^{14a,b,g} and bis(perfluorocatecholato)silane [Si(catF)₂] catalyzed aldehyde hydrosilylation^{14c} have been lately reported, illustrating the potential of silicon compounds as catalysts. Besides, there are recent theoretical and experimental reports on formylation of amines using a combination of CO₂ and a silane as the formylating reagent.^{14d,e} Cantat et al. very recently reported the hydroboration of CO₂ using a well-defined guanidine substituted hydrosilane.^{14f} Boosted by the success of alanes (A–C) and phosphane (G), we were interested in exploring the catalytic

potential of the previously reported benz-amidinato dichlorosilane [$\text{PhC}(\text{N}t\text{Bu})_2\text{SiHCl}_2$], (**3**),^{15a} for hydroboration reaction. Compound **3** was previously reported by Roesky et al. as a precursor for accessing silicon(II) chloride^{15a} and silicon(II) bis(trimethylsilyl) amide.^{15b}

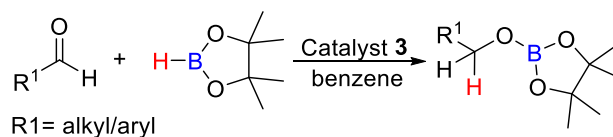
3.2 Hydroboration of aldehydes



Scheme 3.1. Silicon(IV) hydride (**3**) catalyzed hydroboration of aldehydes.

Direct addition of HBpin to benzaldehyde in the absence of the catalyst only afforded a trace amount of $\text{PhCH}_2\text{OBpin}$; an observation also noted by others.^{7a,8a,11,12} However, when the reaction was carried out in the presence of 1 mol% of **3**, it led to quantitative conversion to $\text{PhCH}_2\text{OBpin}$ at room temperature in an hour (Scheme 3.1). When the catalyst loading was reduced to 0.5 mol%, the conversion was still achieved albeit with a slightly lower yield (77%) (see Table 3.1). Therefore, each reaction was conducted at room temperature with 1 mol% of catalyst in an equimolar mixture of aldehyde and HBpin. We have also performed the reaction in the presence of only 1 mol% of HSiCl_3 as a catalyst, but only a trace amount of product formation was observed. We have explored the reactions in various solvents such as benzene, toluene, and dichloroethane and observed that the identity of the solvent had little effect on the yields. The products were identified by a combination of GC-MS, ^1H and ^{13}C NMR spectroscopy studies.

Table 3.1. Optimization table of hydroboration of benzaldehyde catalyzed by **3** in benzene.

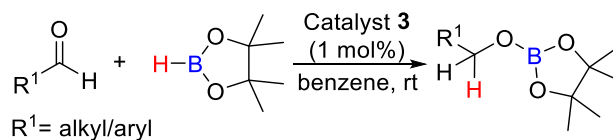


Entry	Catalyst (mol%)	Temperature	Time (h)	Conv. (%)
1	0.5	rt	1	77
2	0.5	50 °C	1	88

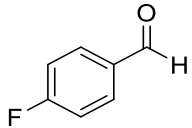
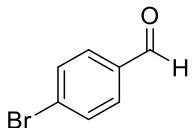
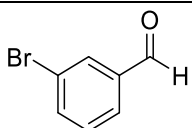
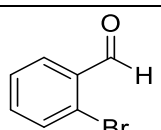
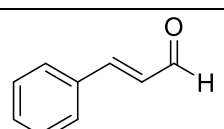
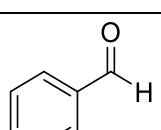
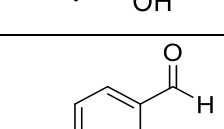
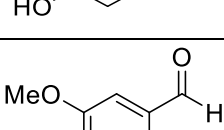
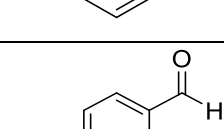
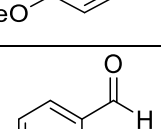
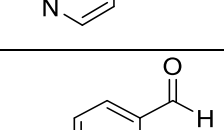
3	1.0	rt	1	96
4	1.5	rt	1	96

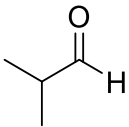
Subsequently, the scope of the catalytic reaction was examined with a range of aldehydes (Table 3.2). Reactions were monitored by ^1H NMR spectroscopy with the appearance of new upfield resonances corresponding to the α -protons of the boronate ester. Most of the aromatic aldehydes are converted to the corresponding boronate esters at room temperature in short reaction time in good yields (entries **3a–3n**). No inhibitory effect was observed for ortho substituents (entries **3f** and **3h**). The reaction showed tolerance towards fluoride groups, as demonstrated by the clean hydroboration of 4-fluorobenzaldehyde (entry **3d**). When salicylaldehyde or 4-hydroxybenzaldehyde was used, hydroboration occurred in the aldehyde functional group and double hydroboration occurred in the aldehyde and OH groups (minor products) (entries **3h** and **3i**). However, only the hydroxylborane dehydrocoupled product has not been formed. Hydroboration of cinnamaldehyde led to 1,2-adducts, keeping the olefinic functionality intact (entry **3g**). The reaction of 4-pyridine-carboxaldehyde with HBpin led to exclusive hydroboration of the carbonyl functionality instead of pyridine dearomatization (entry **3l**).

Table 3.2. Hydroboration of aldehydes catalyzed by **3**.^[a]



Entry	Substrate	Catalyst (mol%)	Time [h]	Yield [%] ^[b]
3a		-	0.5	trace
3b		1	1	96
3c		1	1	90

3d		1	1	90
3e		1	1	88
3e		1	1	85
3f		1	1	82
3g		1	1.5	95
3h		1	1	75
3i		1	1	72
3j		1	1	84
3k		1	1	70
3l		1	1	90
3m		1	1	52

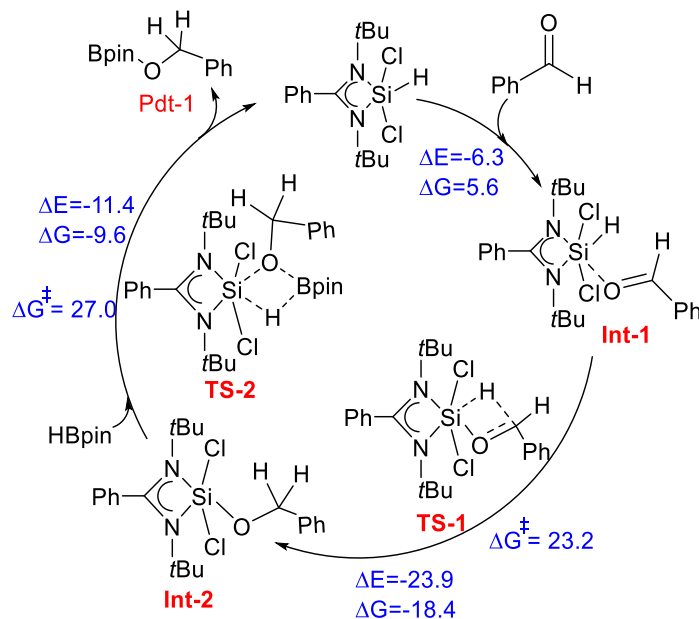
3n		1	5	95
----	---	---	---	----

^[a]All reactions carried out in benzene at room temperature using 1 equiv of HBpin. ^[b]Conversion was determined by NMR spectroscopy on the basis of the consumption of the aldehyde and the identity of the product was confirmed by RCH₂OBpin or resonances.

We further examined the scope of hydroboration for ketones. However, even after increasing the mol% of the catalyst, reaction temperature, time, and changing the solvent did not lead to the hydroboration of ketone. In fact, no reaction was observed between **3** and ketone, which can be attributed to the higher coordination and sterics around the silicon atom. Consistent with that, theoretical calculations also reveal that both barriers are substantially higher for ketones than for aldehydes.

3.3 Mechanistic investigations for the hydroboration of aldehydes

In order to understand the possible mechanistic pathway, simple NMR experiments were performed. As the silicon atom is in the +4 oxidation state, it is reasoned that the catalysis will occur via σ -bond metathesis, which has a modicum of precedence for non-metal p-block elements.¹⁶ When a 1:1 mixture of **3** and benzaldehyde in CDCl₃ was monitored by ¹H NMR, the development of a new singlet at δ 5.05 ppm was observed with a concomitant disappearance of the aldehyde proton (δ 9.95 ppm), as well as the Si–H proton (δ 6.26 ppm).^{15a} The ¹³C NMR spectrum was (in CDCl₃) also changed, with a new peak appearing at δ 66.00 ppm for a [–OCH₂–] substituent, which was further confirmed by Distortionless Enhancement by Polarization Transfer (DEPT) experiments. The ²⁹Si NMR spectrum showed a new resonance at δ –101.2 ppm, which is slightly upfield shifted compared with that in **3** (δ –96.6 ppm) but in good agreement with the previously reported penta-coordinate silicon compounds bearing a Si–O bond such as [PhC(N*t*Bu)₂SiCl₂OR, (R = *i*Pr and *t*Bu)].^{15c} Taken together, these data suggest the possible formation of an alkoxy compound [PhC(N*t*Bu)₂SiCl₂OCH₂Ph] (**Int-2**) as an intermediate. However, even after repeated attempts, we could not obtain single crystals of **Int-2**. In order to prove the formation of **Int-2** during the catalytic cycle, we performed a metathetical reaction between [PhC(N*t*Bu)₂SiCl₃]¹⁷ and potassium phenylmethanolate, which also led to **Int-2**. Comparison of spectra obtained from two different reactions unequivocally confirms that **Int-2** was being formed during the catalytic cycle. The formation of a strong Si–O bond can be presumed as the driving force for the metathesis reaction.



Scheme 3.2. The catalytic cycle and reaction mechanism for the benzaldehyde hydroboration by catalyst **3**. The relative free energy (ΔG) for each species is shown within parentheses in the catalytic cycle. ΔG^\ddagger represent the Gibbs free energy of activation respectively. All values are in kcal mol⁻¹.

Full quantum mechanical calculations were done with density functional theory (DFT) at the dispersion and solvent corrected PBE/TZVP level of theory in order to understand the mechanism (Scheme 3.2 and Fig. 3.1) of the aldehyde hydroboration reaction in the presence of catalyst **3**. In the first step of the reaction, a loosely bound complex (**Int-1**) is formed between catalyst **3** and benzaldehyde, with the benzaldehyde approaching the catalyst from the direction opposite the Si–N bond. The reaction energy (ΔE) and the Gibbs free energy (ΔG) for this step are -6.3 kcal mol⁻¹ and 5.6 kcal mol⁻¹, respectively. This is the prelude to the nucleophilic attack by the carbonyl oxygen of benzaldehyde on the silicon centre of the catalyst, with the hydride being transferred from the silicon centre to the electrophilic carbonyl carbon of the benzaldehyde. This occurs through a four-membered transition state (**TS-1**) and leads to the formation of **Int-2** (see Scheme 3.2). The ΔE (-23.9 kcal mol⁻¹) and ΔG (-18.4 kcal mol⁻¹) values for this step are highly negative and the activation energy (ΔG^\ddagger) barrier corresponding to the transition state is 28.8 kcal mol⁻¹, which is moderate and explains why the reaction can take place at room temperature. This is also the slowest step of the overall hydroboration reaction. The silicon centre of catalyst **3** therefore acts as the hydride donor to the electrophilic carbonyl carbon centre. In the next step, pinacolborane approaches the Si–O bond of **Int-2**, which then passes through a Si–O–B–H four membered cyclic transition state (**TS-2**), leading

to the formation of the hydroboration product (**Pdt-1**) along with the regeneration of the catalyst.

The regeneration of the catalyst has also been observed by ^1H NMR spectroscopy from the stoichiometric reaction between **Int-2** and HBpin with the reappearance of the Si–H resonance at δ 6.26 ppm in the reaction mixture and concomitant disappearance of the B–H protons. The four membered cyclic transition state (**TS-2**) involves a H-bonding interaction between the Si and B atoms and in this transition state a significant amount of B–H bond activation takes place (1.27 Å) in comparison with that in HBpin (1.19 Å). Such elongation allows hydride transfer from the boron to the silicon atom leading to simultaneous Si–O bond cleavage and B–O bond formation. The driving force of the reaction can be attributed to the oxophilicity of the boron atom.¹⁸ The ΔE (-11.4 kcal mol $^{-1}$) and ΔG (-9.6 kcal mol $^{-1}$) values for this step are highly negative and the barrier (ΔG^\ddagger) is 27.0 kcal mol $^{-1}$. To confirm the slowest step, we have employed energetic span model (ESM) calculations¹⁹ and found that the percentage contributions of the 1st and 2nd transition states are 95% and 5%, respectively. Hence the first step is seen to be the slowest step of the overall hydroboration process.

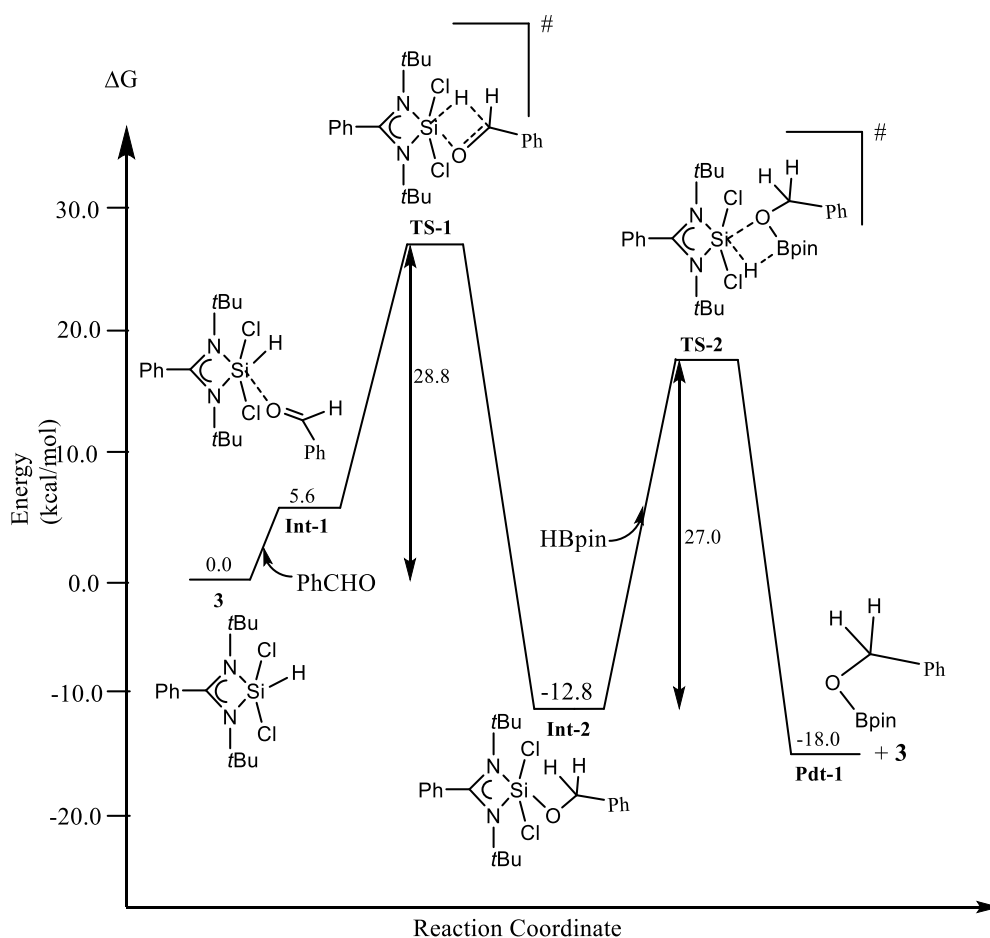
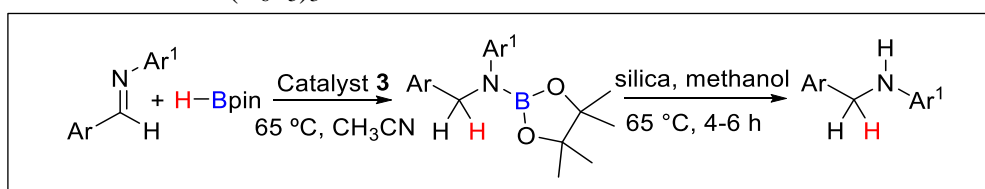


Figure 3.1. The reaction energy profile diagram for the catalytic hydroboration of benzaldehyde by catalyst **3**. The values (in kcal/mol) have been calculated at the PBE/TZVP level of theory with DFT.

3.4 Hydroboration of aldimines

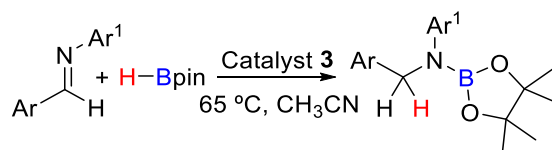
Silane catalyzed hydroboration has been extended to imines, which has been scarcely studied. The first transition metal-catalyzed imine hydroboration was reported by Baker and Westcott et al. using Au-complexes,²⁰ which were followed by few more reports.^{21–24} Transition metal free imine hydroboration was reported by the group of Hill using a magnesium compound [CH{C(Me)NAr}₂MgnBu] (Ar = 2,6-*i*Pr₂C₆H₃)²⁵ and the group of Crudden using a Lewis adduct of DABCO and B(C₆F₅)₃.²⁶



Scheme 3.3. Silicon(IV) hydride (**3**) catalyzed hydroboration of aldehydes.

It was observed that **3** catalyzes hydroboration of imines under slightly harsher conditions (Scheme 3.3). No product formation was observed at ambient temperature even after 24 h reaction. When the reaction was conducted at 65 °C in acetonitrile, the conversion was achieved in good yield (See optimization, Table 3.3). Purification of products by SiO₂ column chromatography led exclusively to the corresponding secondary amines (entry **3o–3v**, Table 3.4). The products were identified by ¹H and ¹³C NMR spectroscopies. Aromatic aldimines with electron donating or withdrawing substituents are converted to the corresponding secondary amines in moderate to good yields (entries **3o–3v**). The reaction showed tolerance towards fluoride groups, as demonstrated by the clean hydroboration of **3s** and **3t**. Slight steric influence of mesityl substituents is observed upon moderate product formation from **3v**.

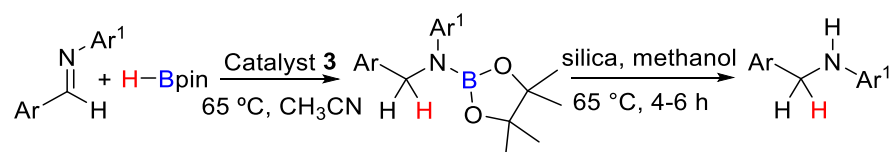
Table 3.3. Optimization table of hydroboration of diphenyl imines catalyzed by **3** in acetonitrile.



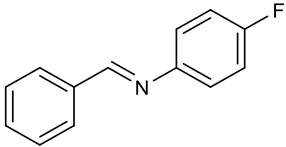
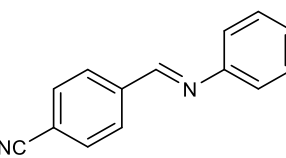
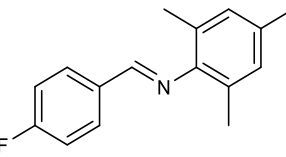
Entry	Catalyst	Temperature	Time	Conv.
-------	----------	-------------	------	-------

	(mol%)		(h)	(%)
1	1	rt	24	0
2	2	rt	24	Trace
3	2	65 °C	24	70
4	2	65 °C	48	95

Table 3.4. Hydroboration of imines Catalyzed by **3** and the conversion of amine boronates to secondary amines.^[a]



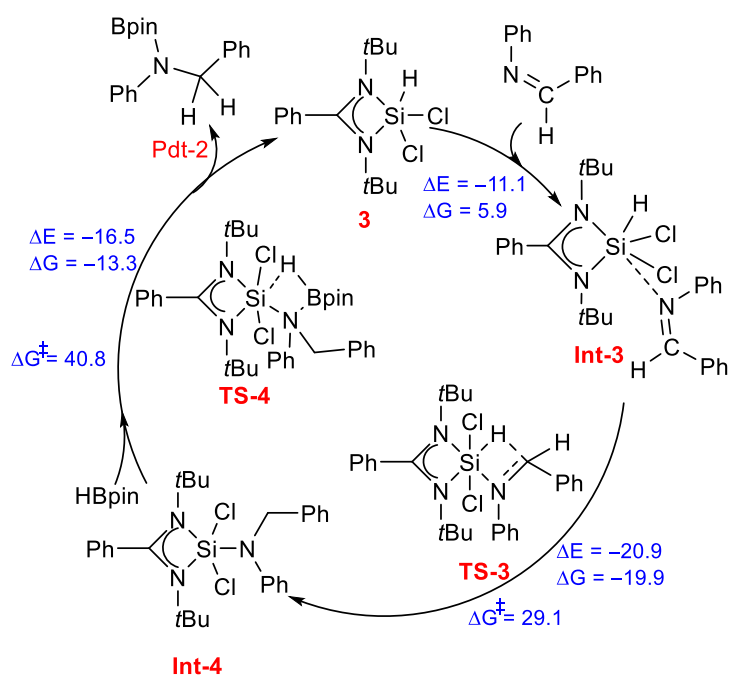
Entry	Substrate	Cat (mol%)	Time [h]	Yield [%] ^[b]
3o		2	48	86
3p		2	48	74
3q		2	48	87
3r		2	50	88
3s		2	72	76

3t		2	72	79
3u		2	72	88
3v		2	72	52

^[a]All reactions carried out in acetonitrile at 65 °C using 1 equiv of HBpin. ^[b] Yields are isolated yield of secondary amines.

3.5 Mechanistic investigations for the hydroboration of aldimines

We have carried out quantum mechanical calculations to explore the reaction mechanism at the same level of theory for imine hydroboration in the presence of a silane catalyst (Scheme 3.4 and Fig. 3.2). In the first step of the reaction, a loosely bound complex (**Int-3**) is formed between catalyst **3** and diphenyl aldimine, with the benzaldehyde approaching the catalyst from the direction opposite the Si–N bond. The reaction energy (ΔE) and the Gibbs free energy (ΔG) for this step are $-11.1 \text{ kcal mol}^{-1}$ and $5.9 \text{ kcal mol}^{-1}$, respectively. The nucleophilic attack occurs by the imine nitrogen on the silicon centre of the catalyst, with the hydride being transferred from the silicon centre to the electrophilic carbon of the aldimine. This happens via a four-membered transition state (**TS-3**) and leads to the formation of **Int-4** (see Scheme 3.4). The ΔE ($-20.9 \text{ kcal mol}^{-1}$) and ΔG ($-19.9 \text{ kcal mol}^{-1}$) values for this step are negative and the activation energy (ΔG^\ddagger) barrier corresponding to the transition state is $35.0 \text{ kcal mol}^{-1}$, which is slightly higher and explains why the reaction needs higher temperature compared to the aldehyde hydroboration. Bond making and breaking between the Si–N and B–H bonds are involved in the transition state (**TS-4**) with significant B–H bond activation (1.28 \AA), which led to the formation of product (**Pdt-2**) and regenerates the catalyst (**3**) back. The only differences between this case and aldehydes are the energy barriers, especially at the second transition state (**TS-4**), with the barrier being $40.8 \text{ kcal mol}^{-1}$. This higher barrier explains why the reaction requires heating to 65 °C.



Scheme 3.4. The catalytic cycle and reaction mechanism for the aldimine hydroboration by catalyst **3**. The relative free energy (ΔG) for each species is shown within parentheses in the catalytic cycle. ΔG^\ddagger represent the Gibbs free energy of activation respectively. All values are in kcal mol⁻¹.

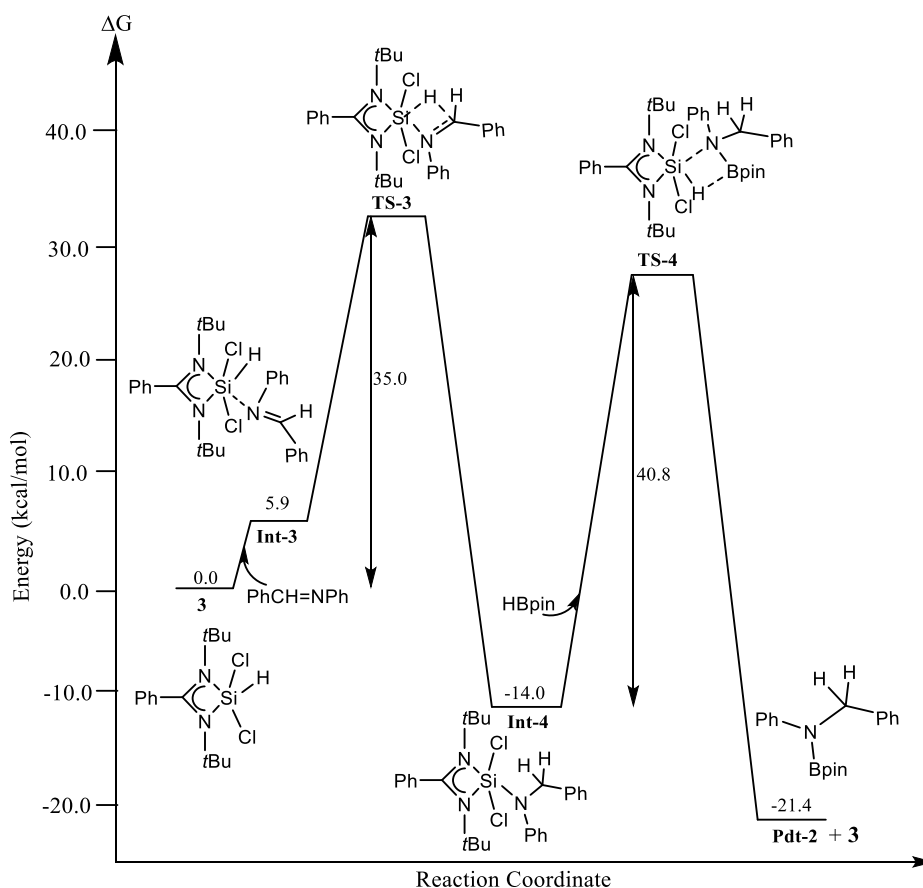


Figure 3.2. The reaction energy profile diagram for the catalytic imine hydroboration by catalyst **3**. Calculated at the PBE/TZVP level of theory with DFT. All values are in kcal mol⁻¹.

3.6 Conclusion

In summary, we have demonstrated the first use of a well-defined neutral silicon(IV) compound for catalytic hydroboration of aldehydes and aldimines. The initial step in the catalytic cycle is the facile addition of the Si–H bond to the C=O bond via a four-membered transition state. The second step involves the σ -bond metathesis between [PhC(N*t*Bu)₂SiCl₂OCH₂Ph] (**Int-2**) and HBpin, resulting in product formation along with the regeneration of the catalyst. The mechanism was further supported by DFT calculations.

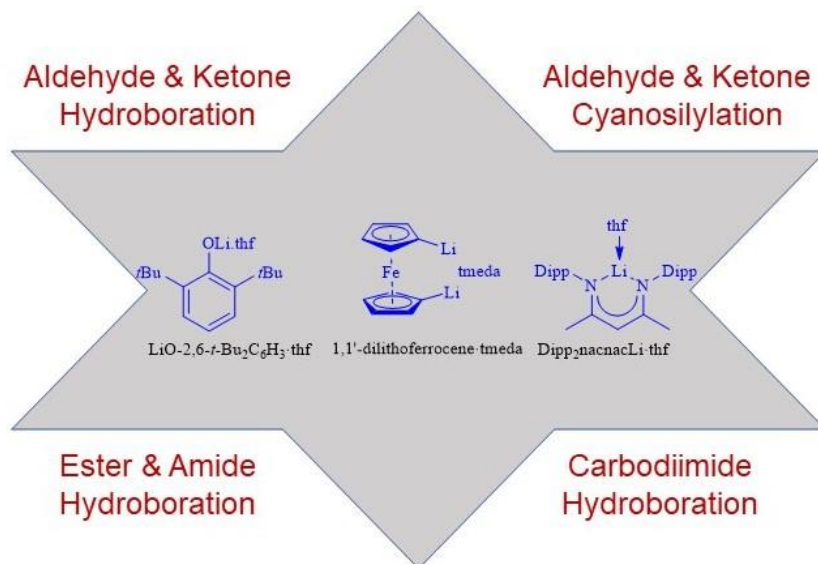
3.7 References

1. (a) He, X.; Hartwig, J. F. *J. Am. Chem. Soc.* **1996**, *118*, 1696–1702. (b) Hartwig, J. F.; Muhoro, C. N. *Organometallics* **2000**, *19*, 30–38.
2. (a) Oshima, K.; Ohmura, T.; Suginome, M. *J. Am. Chem. Soc.* **2012**, *134*, 3699–3702. (b) Cid, J.; Carbo, J. J.; Fernandez, E. *Chem. - Eur. J.* **2012**, *18*, 1512–1521. (c) Smith, S. M.; Takacs, J. M. *Org. Lett.* **2010**, *12*, 4612–4615. (d) Smith, S. M.; Takacs, J. M. *J. Am. Chem. Soc.* **2010**, *132*, 1740–1741. (e) Lata, C. J.; Crudden, C. M. *J. Am. Chem. Soc.* **2010**, *132*, 131–137. (f) Nguyen, B.; Brown, J. M. *Adv. Synth. Catal.* **2009**, *351*, 1333–1343.
3. Yadav, S.; Saha, S.; Sen, S. S. *ChemCatChem* **2016**, *7*, 486–501.
4. Chong, C. C.; Kinjo, R. *ACS Catal.* **2015**, *5*, 3238–3259.
5. For catalysis with alkaline earth metal, please see: (a) Stennett, T. E.; Harder, S. *Chem. Soc. Rev.* **2016**, *45*, 1112–1128. (b) Hill, M. S.; Liptrot, D. J.; Weetman, C. *Chem. Soc. Rev.* **2016**, *45*, 972–988. (c) Harder, S. *Chem. Rev.* **2010**, *110*, 3852–3876.
6. (a) Zhou, Q.-L. *Angew. Chem., Int. Ed.*, **2016**, *55*, 5352–5353. (b) Bagherzadeh, S.; Mankad, N. P. *Chem. Commun.* **2016**, *35*, 3844–3846. (c) Mukherjee, D.; Osseili, H.; Spaniol, T. P.; Okuda, J. *J. Am. Chem. Soc.* **2016**, *138*, 10790–10793. (d) Sau, S. C.; Bhattacharjee, R.; Vardhanapu, P. K.; Vijaykumar, G.; Datta, A.; Mandal, S. K. *Angew. Chem. Int. Ed.*, **2016**, *55*, 15147–15151.
7. (a) Arrowsmith, M.; Hadlington, T. J.; Hill, M. S.; Kociok-Köhn, G. *Chem. Commun.* **2012**, *48*, 4567–4569. (b) Weetman, C.; Anker, M. D.; Arrowsmith, M.; Hill, M. S.; Kociok-Köhn, G.; Liptrot, D. J.; Mahon, M. F. *Chem. Sci.* **2016**, *7*, 628–641. (c) Weetman, C.; Hill, M. S.; Mahon, M. F. *Chem. Commun.* **2015**, *51*, 14477–14480. (d) Manna, K.; Ji, P.;

- Greene, F. X.; Lin, W. *J. Am. Chem. Soc.* **2016**, *138*, 7488–7491. (e) Mukherjee, D.; Ellern, A.; Sadow, A. D. *Chem. Sci.* **2014**, *5*, 959–965. (f) Fohlmeister, L.; Stasch, A. *Chem. -Eur. J.* **2016**, *22*, 10235–10246. (g) Mukherjee, D.; Shirase, S.; Spaniol, T. P.; Mashima, K.; Okuda, J. *Chem. Commun.* **2016**, *52*, 13155–13158.
8. (a) Yang, Z.; Zhong, M.; Ma, X.; De, S.; Anusha, C.; Parameswaran, P.; Roesky, H. W. *Angew. Chem., Int. Ed.*, **2015**, *54*, 10225–10229. (b) Yang, Z.; Zhong, M.; Ma, X.; Nijesh, K.; De, S.; Parameswaran, P.; Roesky, H. W. *J. Am. Chem. Soc.* **2016**, *138*, 2548–2551.
9. Schneider, J.; Sindlinger, C. P.; Freitag, S. M.; Schubert, H.; Wesemann, L. *Angew. Chem., Int. Ed.*, **2017**, *56*, 333–337.
10. Jakhar, V. K.; Barman, M. K.; Nembenna, S. *Org. Lett.* **2016**, *18*, 4710–4713.
11. Hadlington, T. J.; Hermann, M.; Frenking, G.; Jones, C. *J. Am. Chem. Soc.* **2014**, *136*, 3028–3031.
12. Wu, Y.; Shan, C.; Sun, Y.; Chen, P.; Ying, J.; Zhu, J.; Liu, L(Leo); Zhao, Y. *Chem. Commun.* **2016**, *52*, 13799–13802.
13. Chong, C.-C.; Hirao, H.; Kinjo, R. *Angew. Chem., Int. Ed.*, **2015**, *54*, 190–194.
14. (a) Müther, K.; Mohr, J.; Oestreich, M. *Organometallics* **2013**, *32*, 6643–6646. (b) Nödling, A. R.; Müther, K.; Rohde, V. H. G.; Hilt, G.; Oestreich, M. *Organometallics* **2014**, *33*, 302–308. (c) Liberman-Martin, A. L.; Bergman, R. G.; Tilley, T. D. *J. Am. Chem. Soc.* **2015**, *137*, 5328–5331. (d) Hao, L.; Zhao, Y.; Yu, B.; Yang, Z.; Zhang, H.; Han, B.; Gao, X.; Liu, Z. *ACS Catal.* **2015**, *5*, 4989–4993. (e) Zhou, Q.; Li, Y. *J. Am. Chem. Soc.* **2015**, *137*, 10182–10189. (f) von Wolff, N.; Lefèvre, G.; Berthet, J.-C.; Thuéry, P.; Cantat, T. *ACS Catal.* **2016**, *6*, 4526–4535. (g) Müther, K.; Oestreich, M. *Chem. Commun.* **2011**, *47*, 334–336.
15. (a) Sen, S. S.; Roesky, H. W.; Stern, D.; Henn, J.; Stalke, D. *J. Am. Chem. Soc.* **2010**, *132*, 1123–1126. (b) Sen, S. S.; Hey, J.; Herbst-Irmer, R.; Roesky, H. W.; Stalke, D. *J. Am. Chem. Soc.* **2011**, *133*, 12311–12316. (c) So, C.-W.; Roesky, H. W.; Gurubasavaraj, P. M.; Oswald, R. B.; Gamer, M. T.; Jones, P. G.; Blaurock, S. *J. Am. Chem. Soc.* **2007**, *129*, 12049–12054.
16. (a) Wang, Y.; Chen, W.; Lu, Z.; Li, Z.-H.; Wang, H. *Angew. Chem., Int. Ed.*, **2013**, *52*, 7496–7499. (b) Chong, C.-C.; Hirao, H.; Kinjo, R. *Angew. Chem. Int. Ed.*, **2014**, *53*, 3342–3346. (c) Nikonov, G. I.; Vyboishchikov, S. F.; Shirobokov, O. G. *J. Am. Chem. Soc.* **2012**, *134*, 5488–5491.
17. So, C.-W.; Roesky, H. W.; Magull, J.; Oswald, R. B. *Angew. Chem. Int. Ed.*, **2006**, *45*, 3948–3951.

18. For comparison of oxophilicity, please see: Kepp, K. S. *Inorg. Chem.* **2016**, *55*, 9461–9470.
19. (a) Kozuch, S.; Shaik, S. *Acc. Chem. Res.* **2010**, *44*, 101–110. (b) Kozuch, S.; Martin, J. M. L. *ACS Catal.* **2011**, *1*, 246–253.
20. Baker, R. T.; Calabrese, J. C.; Westcott, S. A. *J. Organomet. Chem.* **1995**, *498*, 109–117.
21. Koren-Selfridge, L.; Londino, H. N.; Vellucci, J. K.; Simmons, B. J.; Casey, C. P.; Clark, T. B. *Organometallics* **2009**, *28*, 2085–2090.
22. King, A. E.; Stieber, S. C. E.; Henson, N. J.; Kozimor, S. A.; Scott, B. L.; Smythe, N. C.; Sutton, A. D.; Gordon, J. C. *Eur. J. Inorg. Chem.* **2016**, 1635–1640.
23. Vogels, C. M.; O'Connor, P. O.; Phillips, T. E.; Watson, K. J.; Shaver, M. P.; Hayes, P. J.; Westcott, S. A. *Can. J. Chem.* **2001**, *79*, 1898–1905.
24. Kaithal, A.; Chatterjee, B.; Gunanathan, C. *J. Org. Chem.* **2016**, *81*, 11153–11161.
25. Arrowsmith, M.; Hill, M. S.; Kociok-Köhn, G. *Chem. - Eur. J.* **2013**, *19*, 2776–2783.
26. Eisenberger, P.; Bailey, A. M.; Crudden, C. M. *J. Am. Chem. Soc.* **2012**, *134*, 17384–17387.

Easily Accessible Lithium Compounds Catalyzed Hydroboration and Cyanosilylation of Aldehydes, Ketones, Esters, Amides and Carbodiimides



Abstract

Simple and readily accessible lithium compounds such as 2,6-ditert-butyl phenolate lithium, 1,1' dilithioferrocene, and nacnac lithium are found to be efficient single site catalysts for hydroboration of a range of aldehydes and ketones with HBpin at room temperature. The former two lithium derivatives have been further utilized for the hydroboration of more challenging and less activated carbonyl compounds such as esters, amides or important unsaturated compounds like carbodiimides. The efficacy of catalysts is extended to the cyanosilylation of aldehydes and ketones with Me_3SiCN . We have divided the chapter into two sub-chapters. The first sub-chapter deals with hydroboration and cyanosilylation of aldehydes and ketones with lithium compounds, while the second sub-chapter comprises of hydroboration of amides, esters, and carbodiimides.

4.1 Easily accessible lithium compound catalyzed mild and facile hydroboration and cyanosilylation of aldehydes and ketones

4.1.1 Introduction

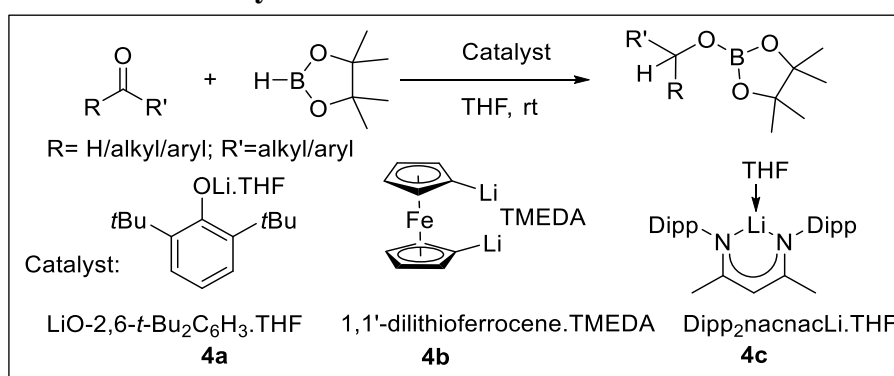
While the birth of lithium chemistry occurred one hundred years ago,¹ the growth of s-block compounds is still in its early days, finding its feet slowly and gradually from the curiosity driven research to important catalytic transformations. Driven by the demand for catalytic processes with reduced environmental impact and low cost, numerous groundbreaking results have been achieved in molecular catalysis using complexes of the heavier alkaline earth metals.² Following the demonstration of the hydroboration of carbonyl compounds using a magnesium alkyl complex,³ there has been a flurry of research activity on hydroboration reactions using compounds with alkaline earth metals⁴⁻⁸ as well as p-block elements.⁹⁻¹⁶ For the heavier alkaline earth metal catalysts, Schlenk equilibrium is an issue, which is likely to impose a severe limitation on the preparation as well as the activity of the catalyst. In this context, group 1 complexes are advantageous over their adjacent neighbours as they are not involved in Schlenk-type equilibria.

Moreover, as catalysts involving group 2 and p-block elements are usually prepared from the corresponding lithium compounds, the direct use of lithium compounds in catalysis would obviate the need for such additional transformations. In fact, group 1 complexes have been sporadically reported for hydrosilylation of alkenes¹⁷ or hydrogenation of aldimines,¹⁸ but they were not very efficient compared to their corresponding group 2 complexes in terms of reactivity or selectivity or both. Hence, group 1 based complexes have remained largely unexplored in molecular catalysis. The paradigm has shifted with the two significant breakthroughs that recently came from the groups of Okuda^{19,20} and Mulvey.²¹ These breakthroughs have created a new avenue for lithium compounds to be used as single component catalysts for important organic transformations.

Okuda and co-workers noted that the success of lithium catalysts relies on the combination of the Lewis acidity of the Li atom and the hydricity of the borate anions. A Li catalyst with a [HB(C₆F₅)₃] anion was reported to be inert, which was attributed to the diminished hydricity of the borate anion.¹⁹ Thus, there remains a scope for the study of the catalytic properties of lithium compounds with no hydridic hydrogen present in the counter anion. In light of our interests in developing catalytic methods for the reduction of carbonyl compounds,^{4,12,22,23} we attempted to use three popular and readily accessible lithium compounds with different electronegative substituents, 2,6-di-*tert*-butyl phenolate lithium (**4a**), nacnac lithium (**4c**) and

1,1'-dilithioferrocene (**4b**) (Scheme 4.1.1), for the reduction of aldehydes and ketones with HBpin under ambient conditions. The reason behind this selection is to examine how the Lewis acidity of the Li center influences the catalytic activity. For example, the Li atom in **4c** is purportedly more Lewis acidic than that in **4a**, as the Li atom in **4c** is bound to two nitrogen atoms, while the Li atom in **4a** is bound to only one oxygen atom. It is also interesting to compare the catalytic competence of **4b** with that of the other catalysts, as it possesses two active Li centres, although they are bound to less electronegative carbon atoms. Consistently with our hypothesis, the catalytic activity (TOF) of **4c** is found to be better than that of **4a** or **4b**.

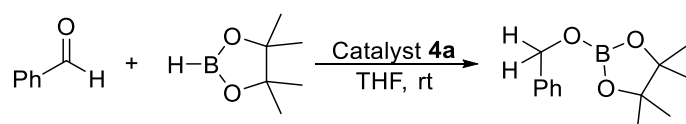
4.1.2 Hydroboration of aldehydes and ketones



Scheme 4.1.1. Hydroboration of aldehydes and ketones using **4a-4c** as catalysts.

The hydroboration reactions for a variety of aldehydes (Table 4.1.3, **5a-5p**) and ketones (Table 4.1.4, **6a-6m**) have been evaluated using **4a/4b/4c** as the catalyst (for optimization, please see the Tables 4.1.1a-c and 4.1.2a-c). Both aliphatic and aromatic aldehydes underwent hydroboration within an hour with excellent TOFs (Table 4.1.3), which reflects the high efficiency of the catalysts. Similarly, a wide range of aromatic and aliphatic ketones were converted to the corresponding boronate esters within 2-3 hours, keeping the mol% constant. For all the cases, yields are calculated based on the integration area of the product and starting material signals in the ¹H spectra using mesitylene as an internal standard.

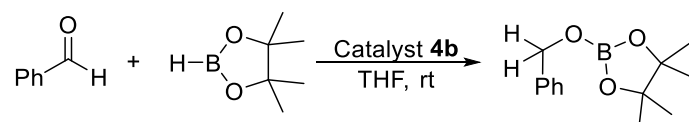
Table 4.1.1a Optimization table of hydroboration of benzaldehyde catalyzed by **4a**.



Entry	Catalyst (mol%)	Time (min)	Solvent	NMR yield (%)
1.	0.5	60	THF	98

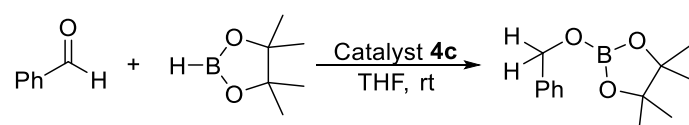
2.	0.5	15	THF	97
3.	0.2	60	THF	94
4.	0.1	60	THF	91
5.	0.1	30	THF	71
6.	0.05	120	THF	76

Table 4.1.1b Optimization table of hydroboration of benzaldehyde catalyzed by **4b**.

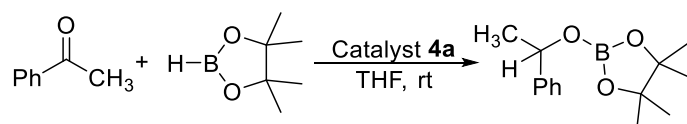


Entry	Catalyst (mol%)	Time (min)	Solvent	NMR yield (%)
1	0.5	30	THF	>99
2	0.5	10	THF	99
3	0.1	60	THF	>99
4	0.1	40	THF	94
5	0.1	30	THF	90
6	0.05	120	THF	84

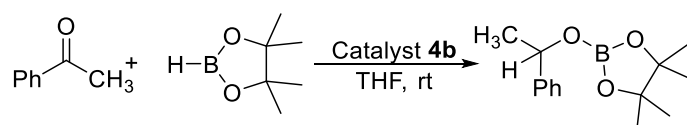
Table 4.1.1c Optimization table of hydroboration of benzaldehyde catalyzed by **4c**.



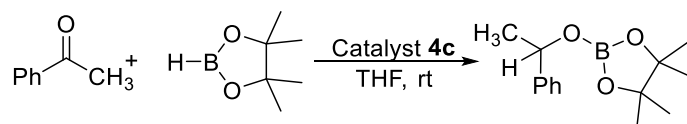
Entry	Catalyst (mol%)	Time (min)	Solvent	NMR yield (%)
1	0.5	30	THF	>99
2	0.5	15	THF	96
3	0.1	60	THF	96
4	0.1	50	THF	90
5	0.1	40	THF	82
6	0.05	120	THF	81

Table 4.1.2a Optimization table of hydroboration of acetophenone catalyzed by **4a**.

Entry	Catalyst (mol%)	Time (h)	Solvent	NMR yield (%)
1	0.5	3	THF	99
2	0.4	2	THF	99
3	0.3	2	THF	98
4	0.2	3	THF	99
5	0.1	3	THF	94
6	0.1	2.5	THF	71

Table 4.1.2b Optimization table of hydroboration of acetophenone catalyzed by **4b**.

Entry	Catalyst (mol%)	Time (h)	Solvent	NMR yield (%)
1	0.5	3	THF	>99
2	0.4	2	THF	>99
3	0.2	2	THF	98
4	0.1	2.25	THF	96
5	0.1	2	THF	95
6	0.1	1.5	THF	73

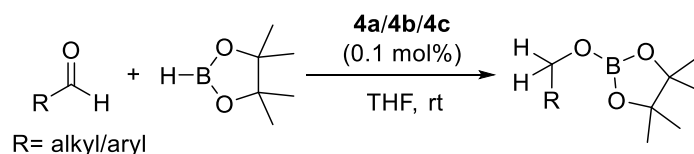
Table 4.1.2c Optimization table of hydroboration of acetophenone catalyzed by **4c**.

Entry	Catalyst (mol%)	Time (h)	Solvent	NMR yield (%)
1	0.5	3	THF	>99
2	0.4	2	THF	>99
3	0.2	2	THF	>99
4	0.1	2.25	THF	98

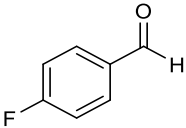
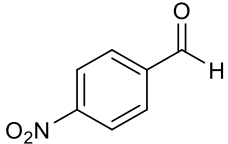
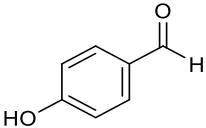
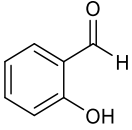
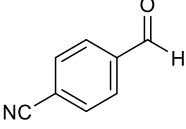
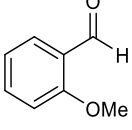
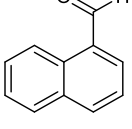
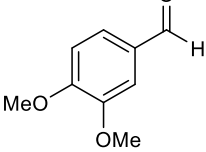
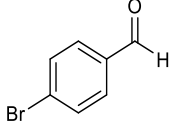
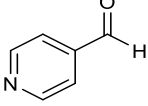
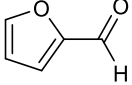
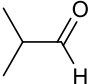
5	0.1	2	THF	98
6	0.1	1.5	THF	69

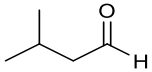
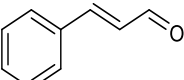
Both aromatic and aliphatic aldehydes (Table 4.1.3, entry **5a–5p**) were screened under optimized condition with all three catalyst. Benzaldehyde derivatives having different other functional groups also shows excellent chemoselectivity. Similarly, acetophenone derivatives bearing both electron-withdrawing and electron-donating functionalities (Table 4.1.4, entry **6a–6h**) gave good yields, demonstrating a negligible electronic effect. Increasing the steric demands also has little effect on the yield, as seen in the case of hydroboration of benzophenone (Table 4.1.4, entry **6i**). All of the catalysts show good functional group tolerance. The nitrile (Table 4.1.3, entry **5g**), hydroxy (Table 4.1.3, entry **5e–5f** and Table 4.1.4, entry **6l**), heterocycle (Table 4.1.3, entry **5l** and **5m**), and amino (Table 4.1.4, entry **6g**) containing substrates yielded the desired boronate esters. Furthermore, the bromo functionality (Table 4.1.3, entry **5k** and Table 4.1.4, entry **6e**) does not suffer from the lithium–bromide exchange. Interestingly, trans-cinnamaldehyde (Table 4.1.3, entry **5p**) undergoes reduction for aldehyde group keeping the olefine functionality intact. In some cases, the catalytic efficiencies vary, as **4c** gives the lowest yield for **5b** and **5c**. **4b** gives a quantitative yield in the most cases, presumably due to the presence of two Li centres, except for with **5i** and **6l**.

Table 4.1.3 Substrate scope for the hydroboration of aldehydes. Reaction conditions: 0.1 mol% catalyst and room temperature in THF. Reaction time (except trans-cinnamaldehyde): **4a**, 60 min; **4b**, 40 min; **4c**, 50 min.



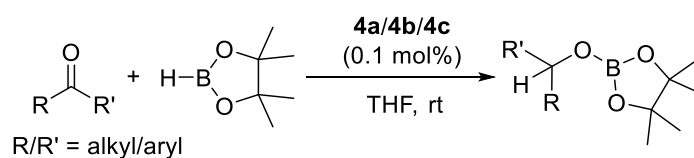
Entry	Substrate	NMR yield (%)	TOF (h ⁻¹)
5a		91 ^a /94 ^b /90 ^c	910 ^a /705 ^b /1080 ^c
5b		80 ^a /98 ^b /52 ^c	800 ^a /735 ^b /624 ^c

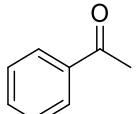
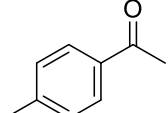
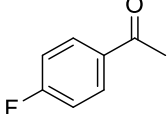
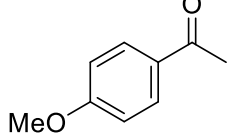
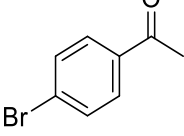
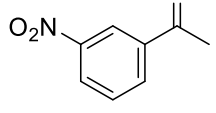
5c		78 ^a /99 ^b /60 ^c	780 ^a /743 ^b /720 ^c
5d		96 ^a /99 ^b /97 ^c	960 ^a /743 ^b /1164 ^c
5e		74 ^a /80 ^b /83 ^c	740 ^a /600 ^b /996 ^c
5f		71 ^a /71 ^b /73 ^c	710 ^a /533 ^b /876 ^c
5g		99 ^a / $>$ 99 ^b / $>$ 99 ^c	990 ^a / $>$ 743 ^b / $>$ 1188 ^c
5h		98 ^a / $>$ 99 ^b / $>$ 99 ^c	980 ^a / $>$ 743 ^b / $>$ 1188 ^c
5i		82 ^a /67 ^b /85 ^c	820 ^a /503 ^b /1020 ^c
5j		$>$ 99 ^a /99 ^b / $>$ 99 ^c	$>$ 990 ^a /743 ^b / $>$ 1188 ^c
5k		97 ^a /98 ^b /99 ^c	910 ^a /735 ^b /1188 ^c
5l		92 ^a /94 ^b /92 ^c	920 ^a /705 ^b /1104 ^c
5m		95 ^a /98 ^b /99 ^c	950 ^a /735 ^b /1188 ^c
5n		94 ^a /96 ^b /96 ^c	940 ^a /720 ^b /1152 ^c

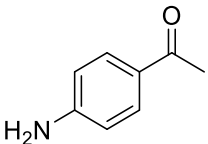
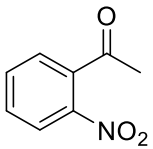
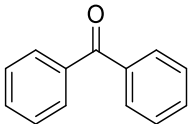
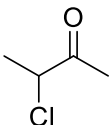
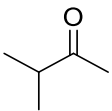
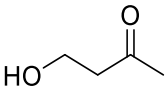
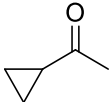
5o		92 ^a /82 ^b /92 ^c	920 ^a /615 ^b /1104 ^c
5p ^d		64 ^a /90 ^b /65 ^c	128 ^a /90 ^b /130 ^c

Superscripts a, b and c stand for the catalyst **4a**, **4b** and **4c**, respectively; ^dthe reaction time for trans-cinnamaldehyde reduction was 5 h.

Table 4.1.4 Substrate scope for the hydroboration of ketones. Reaction conditions: 0.1 mol% catalyst and room temperature in THF. Reaction time: **4a**, 3 h; **4b**, 2 h; **4c**, 2 h. Yields are calculated w.r.t. mesitylene as an internal standard.



Entry	Substrate	NMR yield (%)	TOF (h ⁻¹)
6a		94 ^a /95 ^b /98 ^c	313 ^a /237 ^b /490 ^c
6b		99 ^a /94 ^b / $>99^c$	330 ^a /235 ^b / $>495^c$
6c		99 ^a /99 ^b /97 ^c	330 ^a /247 ^b /485 ^c
6d		$>99^a$ / $>99^b$ / $>99^c$	$>330^a$ / $>247^b$ / $>495^c$
6e		98 ^a /99 ^b /99 ^c	326 ^a /247 ^b /495 ^c
6f		$>99^a$ /93 ^b / $>99^c$	$>330^a$ /232 ^b / $>495^c$

6g		98 ^a / ^{>} 99 ^b /99 ^c	326 ^a / ^{>} 247 ^b /495 ^c
6h		98 ^a /95 ^b /97 ^c	326 ^a /237 ^b /485 ^c
6i		99 ^a / ^{>} 99 ^b / ^{>} 99 ^c	330 ^a / ^{>} 247 ^b / ^{>} 495 ^c
6j		99 ^a / ^{>} 99 ^b /95 ^c	330 ^a / ^{>} 247 ^b /475 ^c
6k		99 ^a /78 ^b /95 ^c	330 ^a /195 ^b /475 ^c
6l		86 ^a /65 ^b /84 ^c	286 ^a /162 ^b /420 ^c
6m		94 ^a /98 ^b /98 ^c	313 ^a /245 ^b /490 ^c

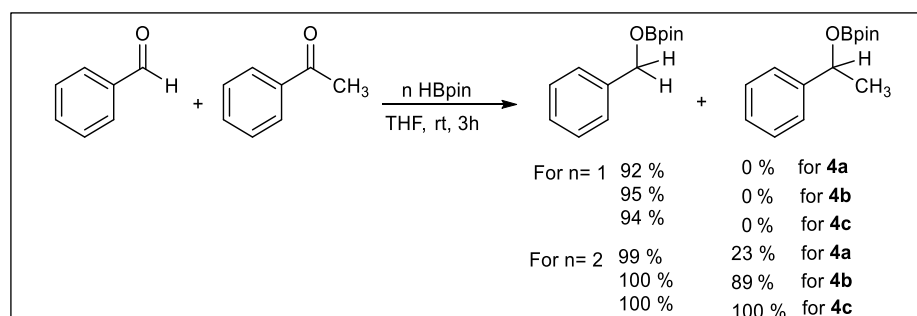
We compared the catalytic activities of **4a–4c** for benzophenone and trans-cinnamaldehyde with those of some known catalysts (Table 4.1.5). The most active one is the lithium hydridotriphenylborate, which showed a remarkable TOF of 66600 h⁻¹ for benzophenone.¹⁹ Among rare earth catalysts, Marks' La^{NTMS} has the highest TOF of >40 000 h⁻¹,^{24a} while among transition metal catalysts, Mankad's copper carbene was reported to be the most active (TOF of 1000 h⁻¹).^{24b} Hill's magnesium alkyl complex was reported with a TOF of 500 h⁻¹ for benzophenone,³ while Stasch's magnesium catalyst [(L)MgH]₄ (L = Ph₂PNDipp; Dipp = 2,6-*i*Pr₂C₆H₃) was recorded with a TOF of 1760 h⁻¹.⁵ We have found that **4c** shows very good efficiency with a TOF of 495 h⁻¹. Although **4b** gives the best yield, the activities of **4a** and **4b** are slightly poorer (TOF: 330 h⁻¹ and 247 h⁻¹, respectively) than that of **4c**. The TOF for the trans-cinnamaldehyde was calculated to be 130 h⁻¹ for **4c**, which is second only to Okuda's lithium hydridotriphenylborate (210 h⁻¹).¹⁹ In comparison, **4a** and **4b** were recorded with TOFs of 128 and 90 h⁻¹, respectively, but their superiority was marked over the other reported main

group catalysts for trans-cinnamaldehyde reduction (e.g. $[\text{Mg}(\text{thf})_6][\text{HBPh}_3]_2$: 11.2 h^{-1} ,⁵ $\text{nacnacAl}(\text{H})\text{OTf}$: 16.5 h^{-1} ,¹⁴ $\text{PhC}(\text{N}t\text{Bu})_2\text{SiHCl}_2$: 63.3 h^{-1} ,¹² and $\text{PhC}(\text{N}i\text{Pr})_2\text{CaI}$: 69 h^{-1}).⁴

Table 4.1.5 Hydroboration of trans-cinnamaldehyde: A comparison of TOF (h^{-1})

Catalyst	TOF (h^{-1})
$[\text{Mg}(\text{thf})_6][\text{HBPh}_3]_2$	11.2
$\text{nacnacAl}(\text{H})\text{OTf}$	16.5
$\text{PhC}(\text{N}t\text{Bu})_2\text{SiHCl}_2$	63.5
$\text{PhC}(\text{N}i\text{Pr})_2\text{CaI}$	69
lithium hydridotriphenylborate	210 (100 °C, 48 h)
2,6-di- <i>tert</i> -butyl phenolate lithium (4a)	128
nacnac lithium (4c)	130
1,1'-dilithioferrocene (4b)	200 (60 °C, 5 h)

4.1.3 Competitive experiment for aldehyde/ketone hydroboration—a selectivity study



Scheme 4.1.2. Competitive aldehyde/ketone hydroboration selectivity study.

Excellent chemoselectivity was observed in a competitive experiment with all three catalysts (Scheme 4.1.2). Three different reaction with 1 equiv. benzaldehyde (0.5 mmol), 1 equiv. acetophenone (0.5 mmol), 1 equiv. pinacolborane (0.5 mmol), 0.5 mL stock solution of **4a**, **4b** and **4c** catalyst (0.1 mol%) in THF were charged in a Schlenk tube with a magnetic bead inside the glove box. The reaction mixture was allowed to stir at room temperature for 3 h.

Another three reaction with 1 equiv. benzaldehyde (0.5 mmol), 1 equiv. acetophenone (0.5 mmol), 2 equiv. pinacolborane (0.5 mmol), 0.5 mL stock solution of **4a**, **4b** and **4c** catalyst (0.1 mol%) in THF were charged in a Schlenk tube with a magnetic bead inside the glove box. The reaction mixture was allowed to stir at room temperature for 3 h. Upon completion of reaction, the solvent was removed using high vacuum in Schlenk line and mesitylene (0.5 mmol) as

internal standard, was added while making the NMR in CDCl₃. The progress of the reaction was monitored by ¹H NMR, which indicated the completion of the reaction by the disappearance of aldehyde (RCHO) proton and appearance of a new OCH₂ resonance.

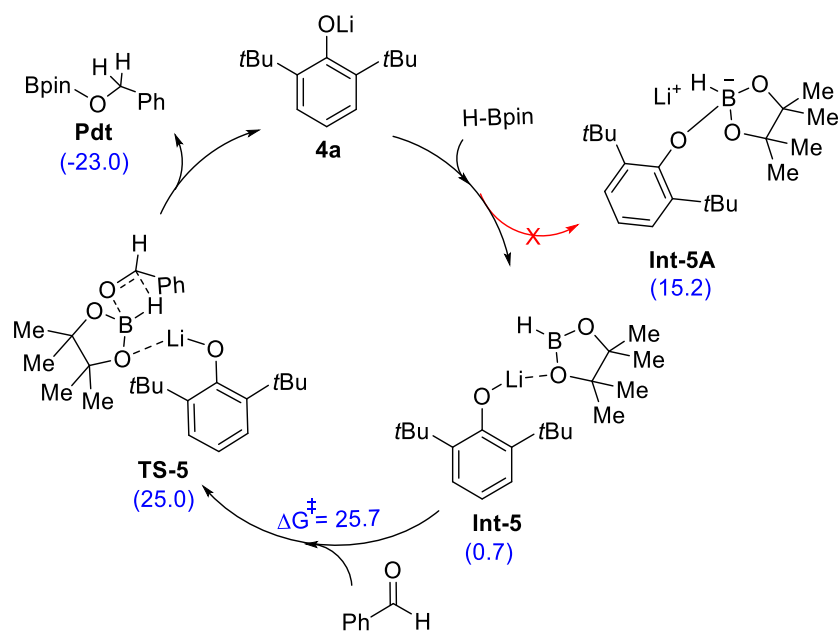
4.1.4 Mechanistic investigations

We have investigated the hydroboration mechanism for **4a** and **4c**. We found that **4a** reacts with HBpin but no change in the ¹H NMR spectrum was detected in the reaction of **4a** with an aldehyde. However, the NMR experiments indicate that no reaction takes place between **4c** and HBpin. Therefore, the catalytic pathways for **4a** and **4c** appear to be different. The reaction between **4a** and HBpin in toluene-d₈ shows a resonance at δ 4.7 ppm in the ¹¹B NMR spectrum, indicating a fourcoordinated sp³ boron atom.^{25a} However, the prolonged time led to formation of trialkoxyborane [2,6-*t*Bu₂-C₆H₃-OBpin] and a BH₄⁻ anion, as a singlet and a quintet started to appear at δ 21.62 and 39.83 ppm after 2–3 h, respectively.^{25b}

To obtain mechanistic insights, full quantum chemical calculations were performed with density functional theory (DFT) at the dispersion and solvent corrected PBE/TZVP level of theory. The pathway is initiated with O-coordination of HBpin to the lithium atom of **4a**, resulting in the exergonic ($\Delta E = -11.5$ kcal mol⁻¹ and $\Delta G = -0.7$ kcal mol⁻¹) formation of **Int-5**, which has an O⋯Li bond length of 1.92 Å (See scheme 4.1.3). This binding mode is in agreement with the crystal structure of [DippnacnacCa(H₂Bpin)]₃ where primary bonding between the anion and the metal cation proceeds through an O⋯Ca interaction.²⁶

The other possibility of coordinating the phenolate oxygen to the boron atom of HBpin leading to a four-coordinate boron complex (**Int-5A**) was found to be thermodynamically unfavorable as the ΔG of the reaction was 15.2 kcal mol⁻¹. In the next step, the carbonyl oxygen atom of benzaldehyde attacks the boron centre of HBpin, with the hydride being transferred from the boron centre to the carbonyl carbon. This occurs through a four-membered transition state (**TS-5**), where a significant amount of the B–H bond activation (1.29 Å) takes place, which leads to the formation of the hydroboration product (**Pdt**) along with the regeneration of **4a** (Scheme 4.1.3 and Figure 4.1.1).

The ΔE (–27.2 kcal mol⁻¹) and ΔG (–22.3 kcal mol⁻¹) values for this step are highly negative and the activation energy (ΔG^\ddagger) barrier corresponding to the transition state is calculated to be 25.7 kcal mol⁻¹.



Scheme 4.1.3. The catalytic cycle and reaction mechanism for the aldehyde hydroboration by catalyst **4a**. ΔG and ΔG^\ddagger represent the Gibbs free energy of reaction and the Gibbs free energy of activation respectively. All values are in kcal/mol.

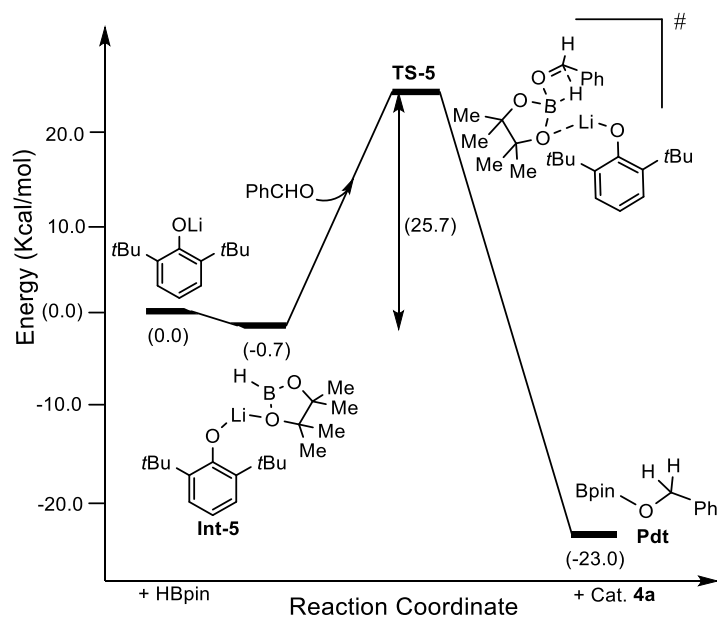
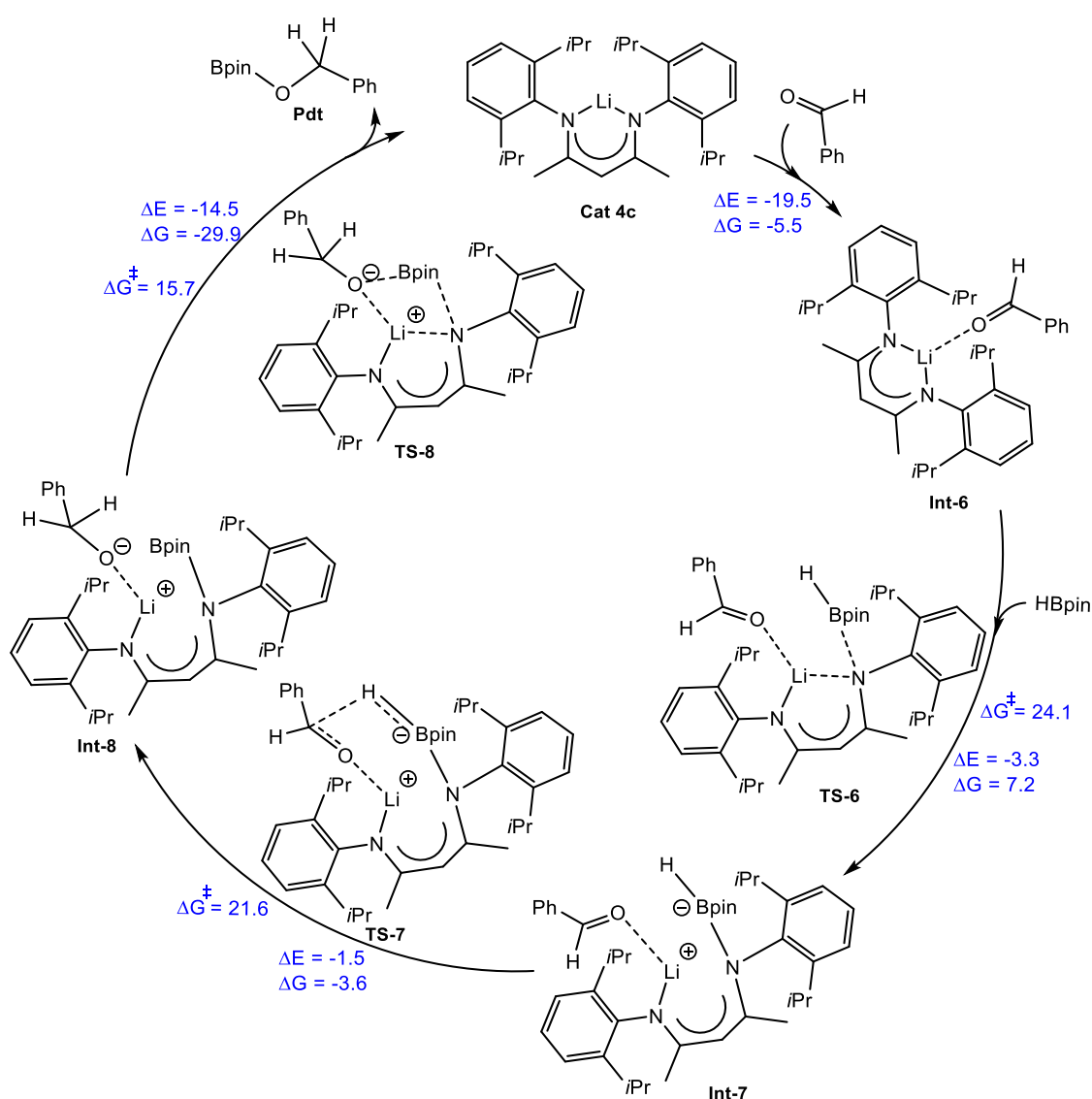


Figure 4.1.1. The reaction energy profile diagram for the catalytic aldehyde hydroboration by catalyst **4a**. The values (in kcal/mol) have been calculated at the PBE/TZVP level of theory with DFT.

In the case of **4c**, a weakly bound complex (**Int-6**) is formed between **4c** and benzaldehyde, with the oxygen atom of benzaldehyde approaching the lithium atom of **4c** (Scheme 4.1.4). The ΔE and ΔG for this step are -19.5 and -5.5 kcal mol⁻¹, respectively. Subsequently, nucleophilic attack by the lone pair of the N atom of **4c** in **Int-6** to the vacant p-orbital of the boron centre of HBpin takes place. A four-coordinated B centre is thus generated (**Int-7**). The ΔE and ΔG for this step are -3.3 kcal mol⁻¹ and 7.2 kcal mol⁻¹, respectively. The activation free energy for the N \cdots B bond formation is 24.1 kcal mol⁻¹.



Scheme 4.1.4. The catalytic cycle and the reaction mechanism for the aldehyde hydroboration by catalyst **4c**, calculated at the PBE/TZVP level of theory with DFT. ΔG and ΔG^\ddagger represent the Gibbs free energy of reaction and the Gibbs free energy of activation respectively. All values are in kcal/mol.

In the next step, the hydride is transferred from the boron centre to the electrophilic carbonyl carbon of the benzaldehyde through a three-membered transition state (**TS-7**), with a barrier of 21.6 kcal mol⁻¹. In this transition state, there is a significant amount of B–H bond activation (1.33 Å vs. 1.19 Å in the intermediate complex), which allows the hydride to transfer from the boron to the carbonyl carbon centre. In the last step, the oxygen centre of the aldehyde attacks the boron centre of pinacolborane and simultaneously, B··N bond cleavage occurs along with N··Li bond formation. This takes place through a four-membered transition state (**TS-8**) and leads to the formation of the hydroboration product (**Pdt**) along with the regeneration of the catalyst. The ΔE (−14.5 kcal mol⁻¹) and ΔG (−29.9 kcal mol⁻¹) values for this step are very favourable and the barrier (ΔG^\ddagger) corresponding to the transition state is 15.7 kcal mol⁻¹.

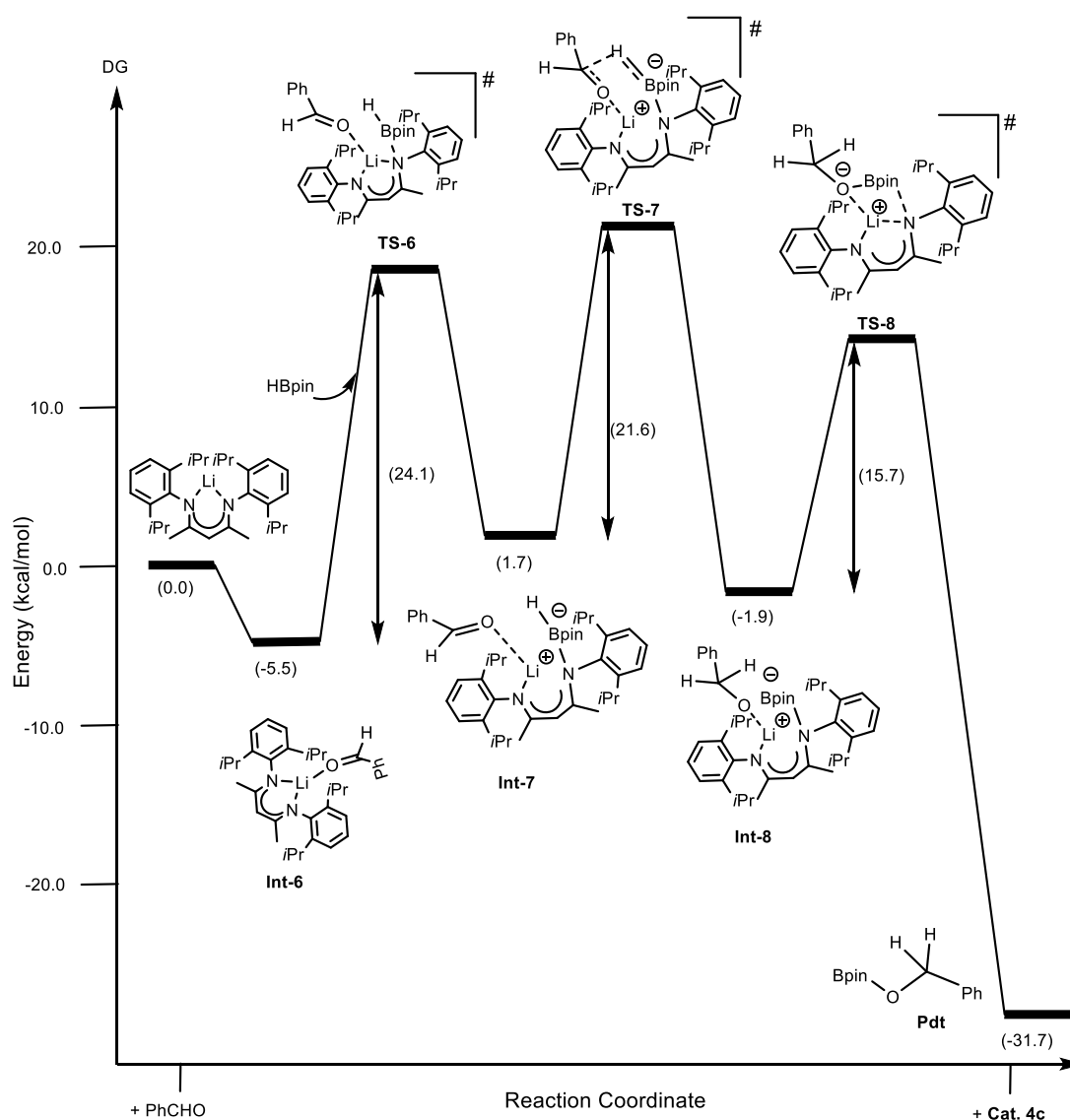
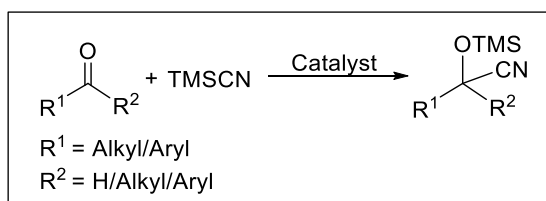


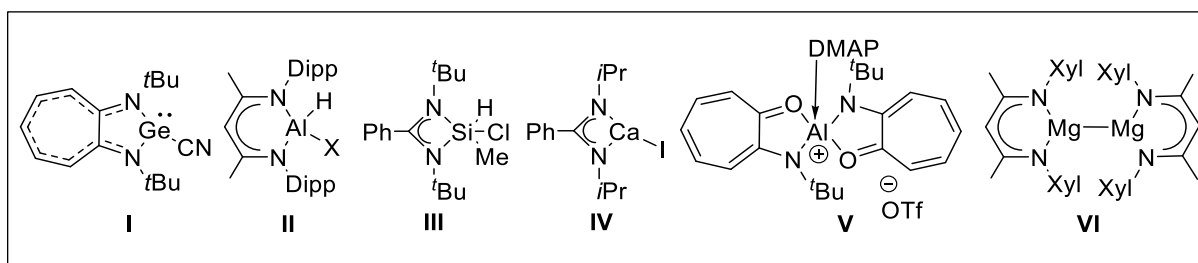
Figure 4.1.2. The reaction energy profile diagram for the catalytic aldehyde hydroboration by catalyst **4c**. The values (in kcal/mol) have been calculated at the PBE/TZVP level of theory with DFT.

4.1.5 Cyanosilylation of aldehydes and ketones



Scheme 4.1.5. Cyanosilylation of aldehydes and ketones

To broaden the horizons of lithium compounds in catalysis, we have employed **4a–4c** for the cyanosilylation of carbonyl compounds (Scheme 4.1.5); a transformation thus far not known to be catalyzed by group 1 complexes. In contrast to the large number of publications on main group compound catalyzed hydroboration, only a few studies on main group compound catalyzed cyanosilylation have been reported (Scheme 4.1.6).^{12,22,23,27–32} The majority of them were reported to only catalyze aldehydes.^{22,27–30} The use of alkaline earth metal complexes in catalytic cyanosilylation is an emerging area. Recently, our group and Ma et al. independently reported the cyanosilylation of aldehydes and ketones with a calcium complex, $\text{PhC}(\text{N}i\text{Pr})_2\text{CaI}^{23}$ and a magnesium(I) complex, $\{(\text{Xyl}n\text{acnac})\text{Mg}\}_2$ ($\text{Xyl} = 2,6\text{-Me}_2\text{-C}_6\text{H}_3$),³² respectively. However, the use of lithium compounds as catalysts in cyanosilylation has not been reported so far.

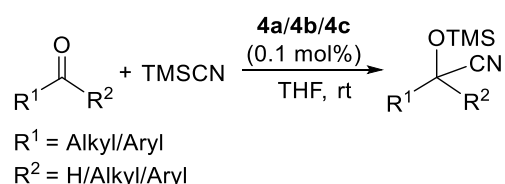


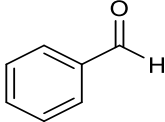
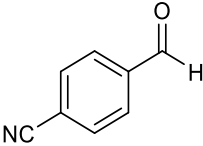
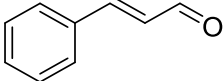
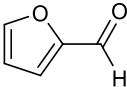
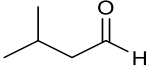
Scheme 4.1.6. Selected examples of the reported main-group catalysts for the cyanosilylation of carbonyl compounds.

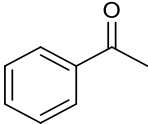
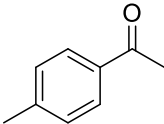
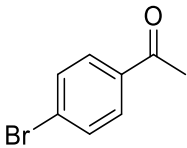
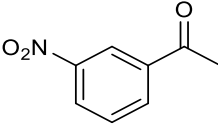
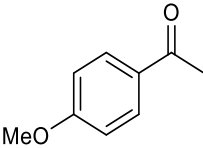
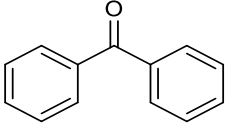
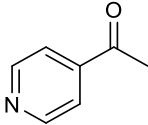
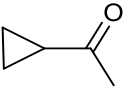
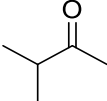
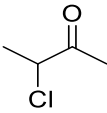
An initial screening of the catalytic effect of **4a–4c** revealed good conversion in most cases at room temperature in a reasonable amount of time (for aldehydes: 1 h & for ketones: 2 h) with 0.1 mol% catalyst loading. The catalytic efficiencies and selectivity of **4a–4c** were found to be very similar. Benzaldehyde, acetophenone, and benzophenone (Table 4.1.6, entries **7a**, **7f** and **7k**) were smoothly converted into the corresponding cyanohydrins. For the reduction of benzophenone, these lithium catalysts are superior to **IV** (3 mol%, 2 h, 82% yield). No other main group catalyst has been reported for cyanosilylation of benzophenone so far. In the case of α,β -unsaturated cinnamaldehyde, the 1,2 addition of Me_3SiCN took place selectively, and

no Michael addition product was formed (Table 4.1.6, entry **7c**). Cyanation of aliphatic aldehydes and ketones (Table 4.1.6, entries **7e**, **7m**, **7n** and **7o**) was found to proceed efficiently. Unlike other main group catalysts, which were reported to catalyze acetophenone substrates with either electron-withdrawing (**IV**²³ and **V**³¹) or electron-donating groups (**II**¹² and **VI**³²), it was observed that **4a–4c** can tolerate both electron-withdrawing as well as electron-donating substituents (Table 4.1.6, **4g–4j**) for cyanosilylation. Heteroarenes (Table 4.1.5, **7d** and **7l**) were tolerated under the reaction conditions to other substituents. ~30% chloride to cyanide exchange product, along with the formation of the desired cyanohydrin, was observed for **7o**.

Table 4.1.6. The scope of cyanosilylation with aldehyde and ketone substrates. Reaction conditions: 0.1 mol% catalyst and room temperature in THF. Reaction time for aldehydes: 1 h and for ketones: 2 h. Yields are calculated w.r.t. mesitylene as an internal standard.



Entry	Substrate	NMR yield (%)	TOF(h ⁻¹)
7a		87 ^a /84 ^b /86 ^c	870 ^a /840 ^b /860 ^c
7b		83 ^a /87 ^b /86 ^c	415 ^a /435 ^b /860 ^c
7c		91 ^a /92 ^b /90 ^c	910 ^a /920 ^b /900 ^c
4d		83 ^a /88 ^b /80 ^c	830 ^a /880 ^b /800 ^c
7e		92 ^a /87 ^b /87 ^c	920 ^a /870 ^b /870 ^c

7f		93 ^a /96 ^b /98 ^c	465 ^a /480 ^b /490 ^c
7g		93 ^a /95 ^b /98 ^c	465 ^a /475 ^b /490 ^c
7h		98 ^a /99 ^b /99 ^c	490 ^a /495 ^b /495 ^c
7i		93 ^a /87 ^b /98 ^c	465 ^a /435 ^b /490 ^c
7j		99 ^a /99 ^b /99 ^c	495 ^a /495 ^b /495 ^c
7k		99 ^a /99 ^b /99 ^c	495 ^a /495 ^b /495 ^c
7l		89 ^a /89 ^b /85 ^c	445 ^a /445 ^b /425 ^c
7m		97 ^a /90 ^b /80 ^c	485 ^a /450 ^b /400 ^c
7n		90 ^a /91 ^b /80 ^c	450 ^a /455 ^b /400 ^c
7o		56 ^a /51 ^b /45 ^c	280 ^a /255 ^b /225 ^c

4.1.6 Conclusion

Herein, we have demonstrated that the reduction of a variety of carbonyl compounds with HBpin and Me₃SiCN can be catalyzed rapidly by very simple lithium compounds (**4a–4c**) under mild and facile conditions with excellent functional group tolerance and TOFs. We have investigated the hydroboration mechanism for **4a** and **4c**. The methodologies described have clearly opened up new avenues for the catalytic application of lithium compounds, encouraged by the very economic and almost non-toxic nature of these reagents.

4.2 Lithium compounds as swiss-army-knife hydroboration catalysts: Reduction of amides, esters and carbodiimides

4.2.1 Introduction

Catalytic hydroboration using main group compounds for the synthesis of organoboranes has gained considerable attention to supplant the pitfall of transition metal catalysts.³³⁻³⁴ The increasing demand on the production of commodity and fine chemical, drugs, agrochemicals, materials synthesis has led to develop various strategies from chemists.³⁵⁻³⁶ Unlike the hydrofunctionalization of polar unsaturated compounds such as aldehydes, ketones, imines, the hydroboration of more challenging substrates like esters, amide, and carbodiimides are still in infancy. Amide or ester hydroboration represents one of the most straightforward method for the bulk synthesis of amine or alcohol respectively, since the starting materials are stable, inexpensive, stock feed in natural products or biologically important molecules and can be accessed by easy synthetic protocol.³⁷⁻⁴⁰ Selective reduction of such unsaturated compounds is quite challenging from thermodynamic and kinetic aspects and usually requires harsh reductants such as LiAlH₄, NaBH₄, or B₂H₆ or BH₃, reagents.⁴¹ But avoiding stoichiometric metal hydride or harsh reducing agents for amide reduction were identified as key challenging conversions by the ACS Green Chemistry Institute Pharmaceutical Roundtable,⁴² due to poor functional group tolerance and environmental concern.⁴³⁻⁴⁴ In contrast, catalytic hydrogenation pathway is appealing for its atom economy, although it needs very high temperature and pressure and capital-intensive setup and pose significant safety issue.⁴⁵ And to date there are no report on catalytic hydrogenation of primary amides.⁴⁶ Also, it would not be unfair to comment that the reduction of primary amides to primary amines are more demanding compared to the secondary and tertiary amide.⁴⁷

Sadow and coworkers reported the catalytic reduction of amides by HBpin using a magnesium compound via deoxygenative pathway.⁴⁸ Panda and coworkers have prepared an aluminium complex, which also exhibits amide hydroboration in ambient condition.⁴⁹ However, these methodologies are somewhat restricted for the reduction of tertiary and secondary amides with limited substrate scope while incompetent for the reduction of primary amides. Recently, Lohr and Marks reported La[N(SiMe₃)₂] catalyzed deoxygenative reduction of secondary and tertiary amides with HBpin,⁵⁰ but reduction does not occur with the acetamide and benzamide. On the other hand, Mandal and coworkers have shown that the combination of an abnormal NHC and potassium complex could serve as an efficient cooperative catalyst for the hydroboration of a broad ranges of primary amides with HBpin.⁵¹ However, neither aNHC nor potassium complex can alone perform the reduction. For hydroboration of esters, only few magnesium-based catalysts are known, independently by the group of Sadow,⁵² Okuda,⁶ Nebennna,⁵³ and others.⁵⁴

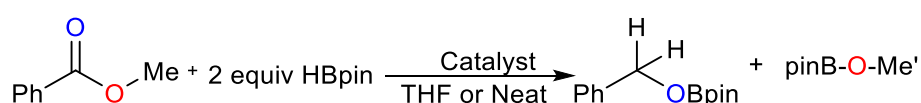
Another important protocol for high purity synthesis of amine is carbodiimide hydroboration which does not produce any kind of byproduct. Catalytic and selective single hydroboration of carbodiimides are quite rare and reported only with Mg,⁵⁵ Al,⁵⁶ B,⁵⁷ and An⁵⁸ (Th or U) -based catalyst.

Lithium compounds are emerging as molecular catalysis, thanks to two significant breakthroughs that recently came from the groups of Okuda^{20a,59} and Mulvey^{21a} for the hydroboration of aldehydes and ketones. Earlier, we have demonstrated the use of readily accessible lithium compounds [2,6-di-tert-butyl phenolate lithium (**4a**), 1,1'-dilithioferrocene (**4b**), and [Dipp₂nacnac]Li·THF (**4c**)] as catalysts for the reduction of aldehydes, ketones, alkenes, and alkynes.⁶⁰ Herein, we report the first single-site chemoselective hydroboration for the reduction of tertiary, secondary, and primary amides using HBpin in presence of catalyst **4a**. This methodology offers a selective deoxygenative strategy for the synthesis of a large number of corresponding alkyl and aryl amines from all three amide categories. Instead, we propose the suitable mechanistic pathway based on experimental and theoretical studies. Also, the catalytic activity of lithium compounds (**4a** and **4b**) have been extended further for the chemoselective hydroboration of esters and carbodiimides. However, low and non-selective conversion was observed when **4b** was used as the catalyst for amide hydroboration.

4.2.2 Hydroboration of esters

For hydroboration of esters, methyl benzoate was selected as a model substrate, catalyst loadings are typically 3.0-6.0 mol % (6.0 mol% for **4a** and 3.0 % for **4b**) and the reactions were over by 8-10 h when heated at 45-80 °C (See optimization, Table 4.2.1, entry 5 and 12). Product yields were calculated based on the integration area of the product boronate ester in the ^1H spectra using mesitylene as an internal standard.

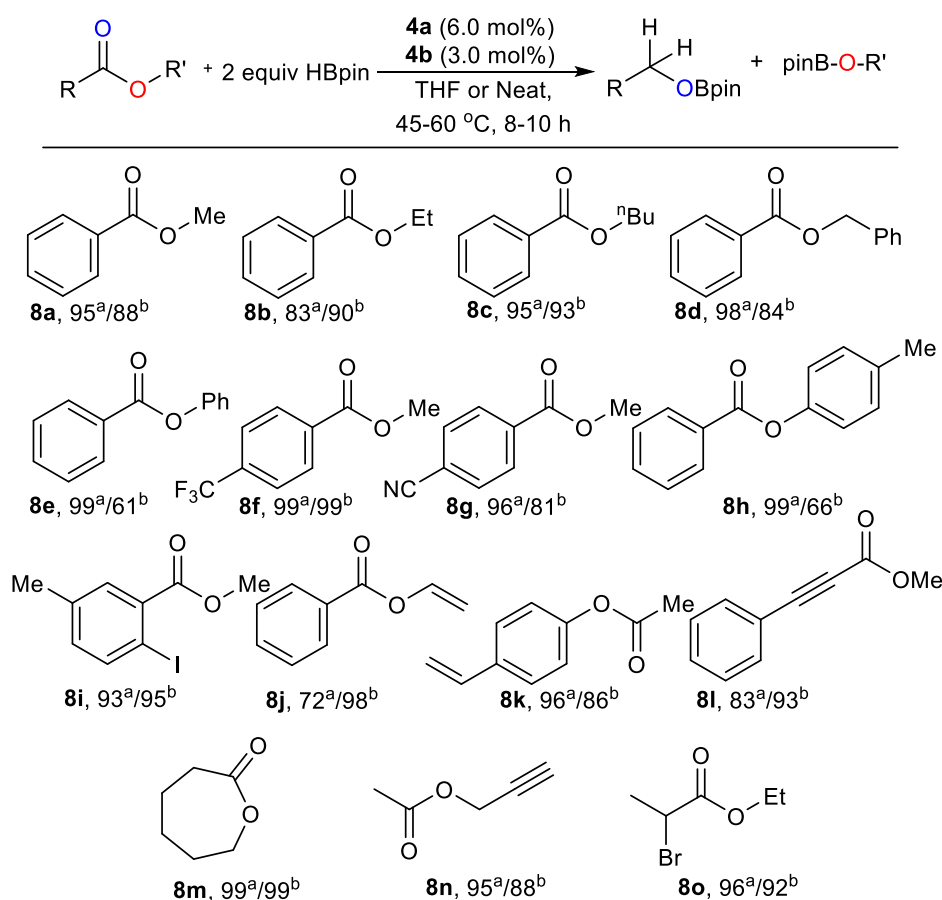
Table 4.2.1. Optimization table for the hydroboration of methylbenzoate catalyzed by **4a** and **4b**.



Entry	Catalyst	Catalyst (mol%)	Solvent	Temperature (°C)	Time (h)	NMR yield (%)
1.	4a	6.0	Neat	rt	12	35
2.	4a	6.0	Neat	60	10	44
3.	4a	6.0	THF	60	10	44.5
4.	4a	6.0	Neat	80	12	96.5
5.	1a	6.0	Neat	80	10	95
6.	4a	5.0	Neat	80	10	81
7.	4a	6.0	Neat	80	8	73
8.	4b	6.0	THF	rt	12	98
9.	4b	4.0	THF	rt	12	83
10.	4b	4.0	THF	45	10	>99
11.	4b	3.0	THF	45	10	97
12.	4b	3.0	THF	45	8	88
13.	4b	3.0	THF	45	6	82
14.	4b	2.0	THF	45	8	75

Both aliphatic and aromatic esters underwent hydroboration to form corresponding boronate esters in good to excellent yield. Aromatic esters with short to long alkyl chain show negligible steric influence and provide desired products in quantitative yields (**8a-8d**). Also, aromatic esters with electron withdrawing or donating substituents at *o/m/p* positions react with HBpin

and shows complete conversion (Scheme 4.2.1, **8f-8i**) to the product. Similarly, the aliphatic esters underwent smooth reduction when treated with HBpin (**8m-8o**). Quantitative conversion was documented for the reaction of ϵ -caprolactone (**8m**) under similar reaction condition. Chemoselective reduction of esters is very important and quite challenging in presence of other reducible functional groups. In this regard, we have demonstrated the hydroboration of esters in the presence of other functional groups such as, conjugated or non-conjugated C=C double bonds (**8j**, and **8k**) and C \equiv C triple bonds (**8l**, and **8n**). Esters with halide substituents (**8i** and **8o**) are also tolerated well and show selective reduction of ester without any lithium halide exchange.



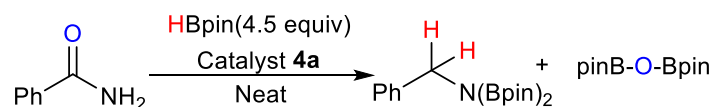
Scheme 4.2.1. Scope of hydroboration with esters substrates. Reaction conditions: 3.0-6.0 mol% catalyst, 8-10 h reaction at 45-80 °C temperature in neat or in THF. Yields were determined by ¹H NMR integration relative to mesitylene. Superscripts a and b stand for the catalysts **4a** and **4b** respectively.

4.2.3 Hydroboration of amides

A systematic study was carried out to establish the optimization condition for the catalytic reduction of benzamide as a model substrate for the primary amides with HBpin (See

optimization, Table 4.2.2). In the absence of any solvent, the reaction of benzamide (1 equiv, 0.25 mmol) and HBPin (4.5 equiv, 1.12 mmol) at 60 °C for 18 h in the presence of catalyst **4a** (5 mol%) afforded 87% of corresponding borylamine (see entry 9, Table 4.2.2). Although, quantitative conversion of benzamide to corresponding borylamine is achievable in presence of 5 equiv. HBpin (Entry 10), we have chosen entry 9 as optimized condition to observe the electronic influence of the substituents. Note that, same reaction, under catalyst free condition produces only 55% yield in 20 h reaction time (Table 4.2.2, entry 12). For comparison purpose, KOtBu (5.0 mol%) was also employed as the catalyst, which afforded 73% yield under the same reaction conditions for the hydroboration of benzamide in 20 h (Table 4.2.2, entry 11).

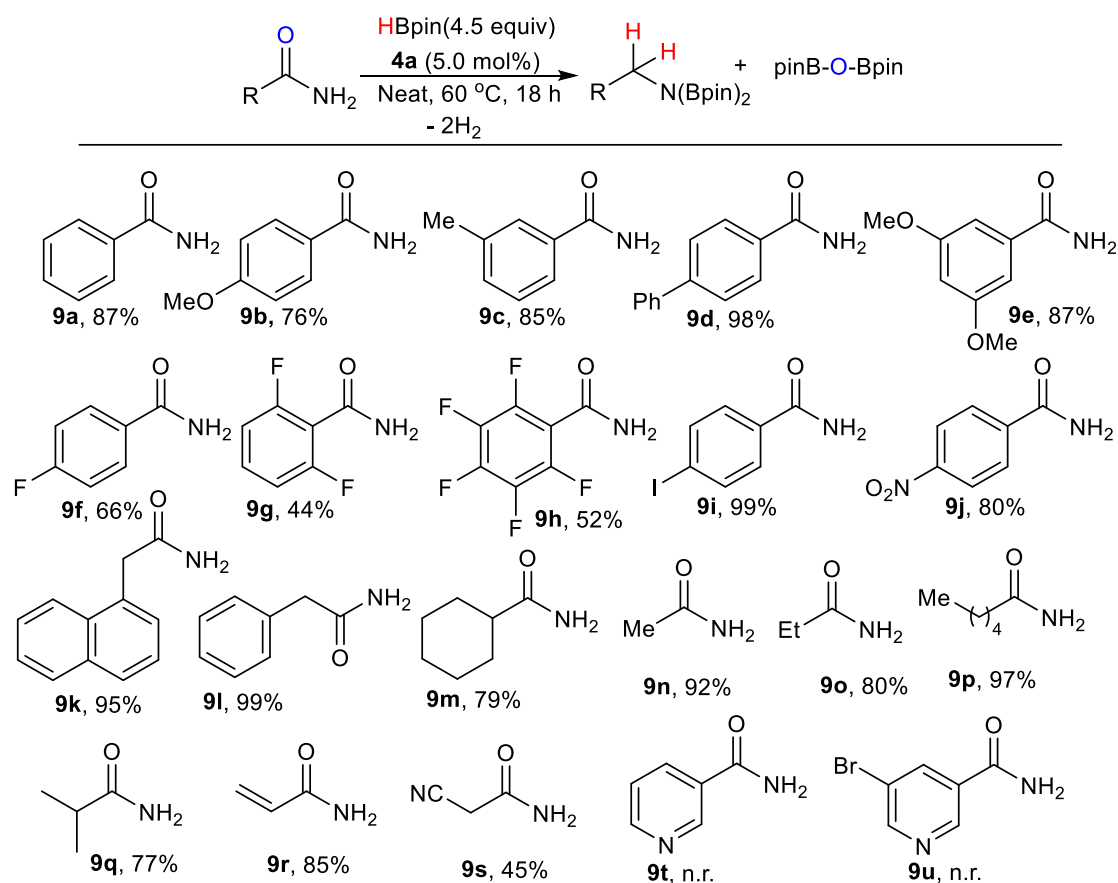
Table 4.2.2. Optimization table of hydroboration of benzamide catalyzed by **4a**.



Entry	Catalyst	Catalyst (mol%)	Equiv. of HBpin	Solvent	Temperature (°C)	Time (h)	NMR yield (%)
1.	4a	5.0	4.0	THF	25	18	0
2.	4a	5.0	4.0	Toluene	25	18	0
3.	4a	5.0	4.0	C ₆ D ₆	25	18	0
4.	4a	5.0	4.0	Toluene	50	18	16.5
5.	4a	5.0	4.0	Neat	50	18	76
6.	4a	5.0	4.0	Neat	60	18	83
7.	4a	5.0	4.0	Neat	60	15	67
8.	4a	3.0	4.0	Neat	60	18	60
9.	4a	5.0	4.5	Neat	60	18	87
10.	4a	5.0	5.0	Neat	60	18	99
11.	KOtBu	5.0	4.5	Neat	60	20	73
12.	---	---	4.5	Neat	60	20	55

Subsequently, the scope of the reaction was tested with a range of aromatic and aliphatic primary amides, and the corresponding borylated products were obtained in good to excellent yield (Scheme 4.2.2). Some of the corresponding borylated amines were successively converted to the corresponding primary amines and isolated as their hydrochloride salts upon

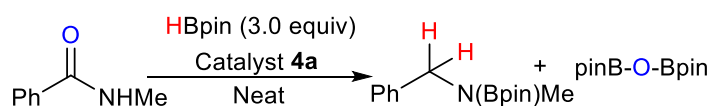
hydrolysis and acidification. Smooth hydroboration was observed for the different aromatic amides with electron donating or withdrawing substituents at *o/m/p* position (**9a-9j**). Under the optimized conditions, aromatic amides bearing electron-donating functional group (Me, OMe, Ph, and I) provides better conversion when compared with electron-withdrawing groups (F and NO₂). The catalyst shows very good tolerance towards the functional groups such as halogens (**9f-9i**), alkoxy (**9b** and **9e**) and nitro (**9j**) containing substrates. Both electronic and steric influence was reflected on the moderate conversion of 2,6-difluorobenzamide (**9g**), and perfluorobenzamide (**9h**). On the other hand, no product formation was observed for the pyridine containing substrate such as nicotinamide (**9t**) and 3-bromo nicotinamide (**9u**) probably due to the coordination of pyridine lone pair with HBpin.



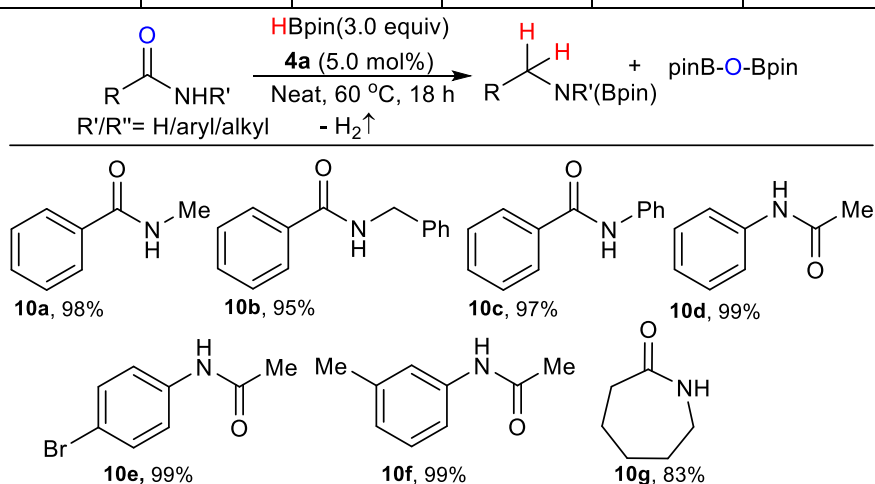
Scheme 4.2.2. Lithium compound catalyzed hydroboration primary amides. Reaction conditions: Amide (0.25 mmol), HBpin (1.12 mmol, 4.5 equiv), 5.0 mol% catalyst, 18 h reaction at 60 °C temperature in neat. Yields were determined by the ¹H NMR integration relative to mesitylene as an internal standard.

It is of note here that the hydroboration of the aliphatic amides is also very important as the aliphatic amines represent a privilege class in drug molecules. Herein, we employed the standard reaction condition for the aliphatic amides bearing aromatic moiety such as 2-(naphthalen-1-yl) acetamide (**9k**) and 2-phenylacetamide (**9l**), and for both the cases almost quantitative conversion of their corresponding borylated amines was observed. Furthermore, the cyclic amide (**9m**), short to long chain aliphatic amides (**9n-9q**) were also tested and all of them afford the desired products good to excellent yields. Conjugated amide, such as acrylamide (**9r**) undergoes hydroboration in both the functional group and form the same product as obtained from **9o**. However, in addition to amide hydroboration (45% yield), reduction of both cyano and amide functionality was also observed for **9s** in 22% yield.

Table 4.2.3. Optimization table of hydroboration of *N*-methylbenzamide catalyzed by **4a**.



Entry	Catalyst	Catalyst (mol%)	Solvent	HBpin equiv	Temp (°C)	Time (h)	NMR yield (%)
1.	4a	5.0	Neat	2.0	100	12	69
2.	4a	5.0	Neat	2.0	80	18	66
3.	4a	5.0	Neat	2.0	80	24	81
4.	4a	8.0	Neat	2.0	80	18	74
5.	4a	5.0	Neat	2.0	60	18	65
6.	4a	5.0	Neat	3.0	60	18	96
7.	4a	5.0	Neat	3.0	50	12	83

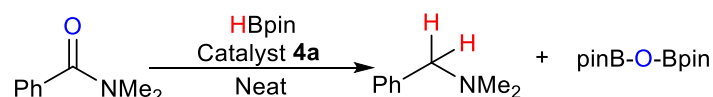


Scheme 4.2.3. Scope of hydroboration with secondary amides.

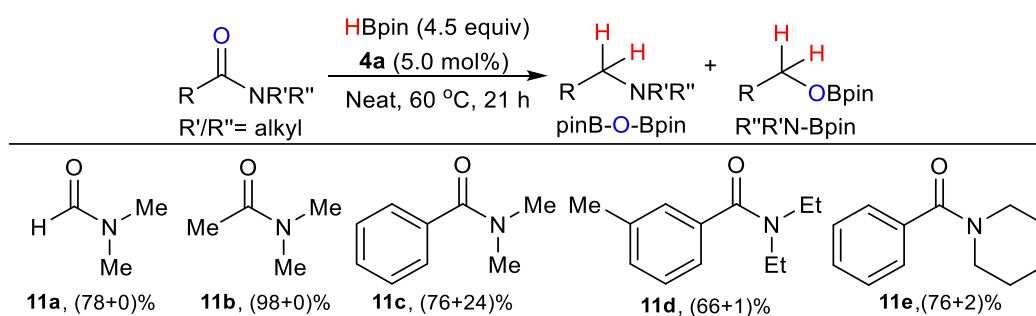
With good results in hand for the reduction of primary amides, the reactivity of secondary and tertiary amides was studied in the presence of **4a** under the optimized reaction conditions (Scheme 4.2.3, and Scheme 4.2.4). Here, *N*-methylbenzamide and *N,N*-dimethyl benzamide were used as substrates for the optimization of secondary and tertiary amide hydroboration, respectively (See optimization table 4.2.3, entry 6, and table 4.2.4, entry 6 respectively).

Similar to primary amide hydroboration, secondary amides also deoxygenate to secondary amines with subsequent release of dihydrogen in presence of three equivalent HBpin. Both aromatic and aliphatic *N*-alkyl or *N*-aryl substituted secondary amide (**10a-10g**) underwent hydroboration smoothly and form corresponding borylated secondary amines in good to excellent yield. Cyclic secondary amide, such as ϵ -caprolactam (**10g**) provides corresponding borylated amine in good yield without suffering any polymerization.

Table 4.2.4. Optimization table of hydroboration of *N,N*-dimethylbenzamide catalyzed by **4a**.



Entry	Catalyst	Catalyst (mol%)	Solvent	HBpin equiv	Temp (°C)	Time (h)	NMR yield of RCH ₂ NR' ₂ (%)	NMR yield of RCH ₂ OBpin (%)
1.	4a	5.0	Neat	2.0	60	18	32	8.5
2.	4a	8.0	Neat	2.0	60	18	33	8
3.	4a	5.0	Neat	3.0	60	18	51	15
4.	4a	5.0	Neat	3.0	60	24	52	15
5.	4a	5.0	Neat	3.5	60	21	65	19
6.	4a	5.0	Neat	4.5	60	21	76	24
7.	4a	3.0	Neat	4.5	60	21	73	23
8.	4a	5.0	Neat	4.5	60	18	70.5	23

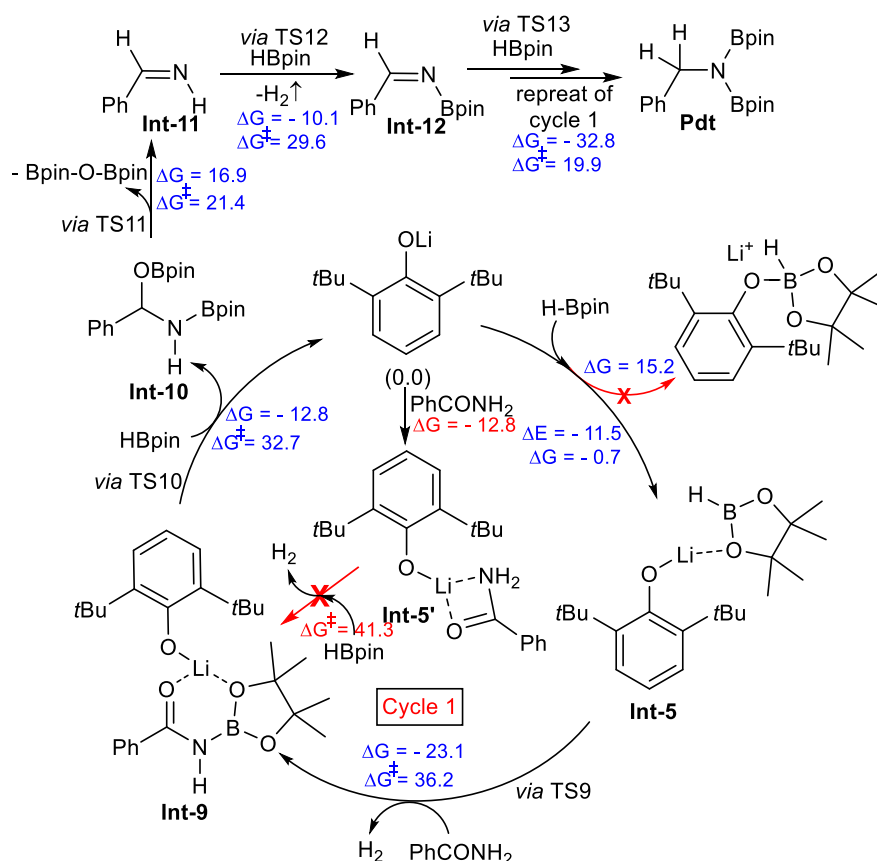


Scheme 4.2.4. Scope of hydroboration with tertiary amides.

The methodology works smoothly for the hydroboration of tertiary amides substrates as well. The slight excess of HBpin (4.5 equiv.) and longer reaction time (21 h) was found necessary to obtain good conversion over the selected temperature range and this was also noted by the groups by Lohr and Marks.⁵⁰ In comparison to primary or secondary amides, moderate to good conversion were achieved for all three tertiary amides (**11a-11e**) probably due to the more steric around the nitrogen center. It is fair to mention here that, selective formation of corresponding amine product was observed for all the substrates except *N,N*-dimethyl benzamide (**11c**), which produces both C-O and C-N bond cleavage product in 76% and 24% respectively.

4.2.4 Mechanistic investigations

We have performed a series of stoichiometric reaction to gain the mechanistic insight for the primary amide hydroboration with **4a**. In the stoichiometric reaction of **4a** with benzamide in THF or CDCl_3 , a possible formation of **Int-5'** at room temperature was indicated by ^1H NMR spectroscopy. However, a new set of resonance in the ^{11}B NMR at δ 4.7 ppm for the reaction between **4a** and HBpin in toluene- d_8 indicates the formation of an intermediate (**Int-5**)⁶⁰ as mentioned in the aldehydes and ketones hydroboration section of this chapter. Also, to identify whether BH_3 is involved in hidden catalysis as it may form by the decomposition of HBpin for the amide hydroboration or not,⁶¹ we have carried out the same reaction in presence of 10 mol% TMEDA. Formation of corresponding borylated amine with 73% yield for the benzamide substrate suggest for the negligible or low influence of BH_3 in catalysis. Notably, although the evolution of molecular dihydrogen was observed for the non-catalytic reaction of benzamide and HBpin, the evolution accelerated in the presence of catalyst and it was monitored by ^1H NMR resonance at δ 4.48 ppm.⁵¹ Furthermore, the formation of N-borylated imine (**Int-12**) was detected with a sharp resonance in the ^1H NMR at δ 10.20 ppm, when hydroboration was carried out at room temperature in toluene or by ceasing the standard heating reaction after 1h.



Scheme 4.2.5. Mechanism for the hydroboration of benzamide.

Based on these experiments stated above and DFT calculation, a plausible mechanism is outlined for the hydroboration of primary amides in Scheme 4.2.5. Full quantum chemical calculations were done with density functional theory (DFT) with the dispersion and solvent corrected PBE/TZVP level of theory in order to understand the mechanism (Scheme 4.2.5 and Figure 4.2.1) of the primary amide hydroboration reaction in the presence of catalyst **4a**. In the first step of the reaction, a weakly bound complex (**Int-5**) is formed between catalyst **4a** and pinacolborane, with one of the oxygen atoms of pinacolborane approaching towards the lithium atom of **4a** and making a weak coordinate bond. The reaction energy (ΔE) and the Gibbs free energy (ΔG) for this step are -11.5 kcal/mol and -0.7 kcal/mol respectively. We cannot ignore the possibility of the binding of amide oxygen with the lithium atom of **4a**, which would lead to the formation of **Int-5'**. The corresponding reaction free energy for this step is favorable by 12.8 kcal/mol. Now, in the next step, either benzamide approaches towards the B-H bond of **Int-5** and makes a four membered transition state **TS-9** involving N \cdots H \cdots H \cdots B atoms where H₂ evolution takes place leading to the formation of **Int-9** with the free energy of activation barrier 36.2 kcal/mol or pinacolborane approaches towards the N-H bond of **Int-5'** and similarly makes a four membered transition state **TS-9'** involving N \cdots H \cdots H \cdots B atoms where

H₂ extrusion occurs leading towards **Int-9**. The barrier for this step was calculated to be 41.3 kcal/mol (Shown in red in Scheme 4.2.5). During the experiments, we have observed the evolution of H₂ gas in the initial phase of the reaction. Therefore, from the DFT calculations, we have excluded the H₂ evolution pathway via **TS-9'** due to the high energy barrier, which cannot be achievable under the reaction conditions. As the reaction proceeds through the **TS-9** pathway, in the next step, another molecule of pinacolborane comes towards the carbonyl group of **Int-9**. This is the prelude to the nucleophilic attack by the oxygen atom of carbonyl group to the boron atom of pinacolborane, with the hydride being transferred to the carbonyl carbon atom of **Int-9**. This occurs through a four-membered transition state (**TS-10**) and leads to the formation of **Int-10**. This step is thermodynamically favorable and Gibbs free energy is -12.8 kcal/mol. The activation free energy (ΔG^\ddagger) barrier corresponding to the transition state is 32.7 kcal/mol. Furthermore, the elimination of Bpin-O-Bpin from **Int-10** leads to the formation of the important intermediate imine (**Int-11**) via a four membered transition state (**TS-11**) involving O···C···N···B atoms. The reaction free energy (ΔG) and the barrier (ΔG^\ddagger) for this step are 16.9 kcal/mol and 21.4 kcal/mol respectively. In the next step, the imine (**Int-11**) reacts with a third molecule of pinacolborane, where the B-H bond of pinacolborane approaches towards the N-H bond of the imine (**Int-11**), thereby making a four membered transition state (**TS-12**) and leading to the formation of **Int-12** by evolution of one equivalent of H₂ gas. The reaction free energy (ΔG) and the barrier (ΔG^\ddagger) for this step are -10.1 kcal/mol and 29.6 kcal/mol. In the last step of the reaction, **Int-12** reacts with a fourth molecule of pinacolborane, where the B-H bond of pinacolborane approaches towards the imine double bond of **Int-12**, making a four membered transition state (**TS-13**) involving C···H···B···N atoms, which leads to the formation of Bpin substituted amine. In this case, both the B-H bond and the imine double bond activation takes place. The reaction free energy (ΔG) and the barrier (ΔG^\ddagger) for this step are -32.8 kcal/mol and 19.9 kcal/mol respectively. The ΔG (-23.1 kcal/mol) value for the slowest step is significantly negative and the barrier corresponding to the transition state is 36.2 kcal/mol, which is moderate and explains why the reaction can take place at the employed reaction temperature (60 °C).

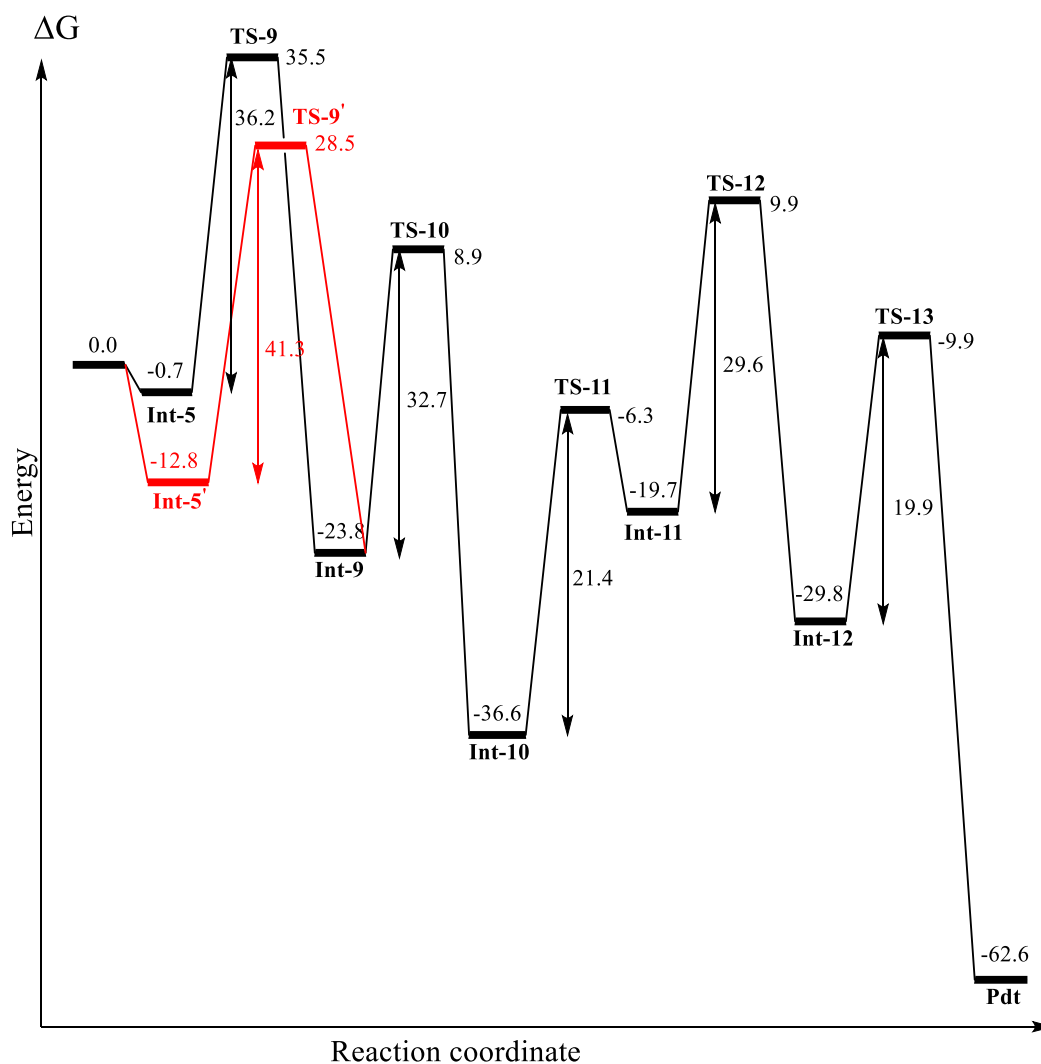


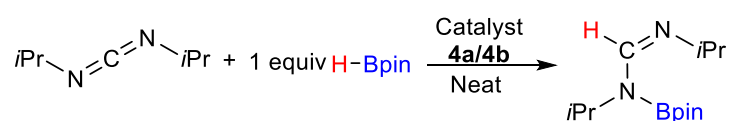
Figure 4.2.1. The reaction energy profile diagram for the catalytic benzamide hydroboration by catalyst **4a**. The values (in kcal/mol) have been calculated at the PBE/TZVP level of theory with density functional theory (DFT).

4.2.5 Hydroboration of carbodiimides

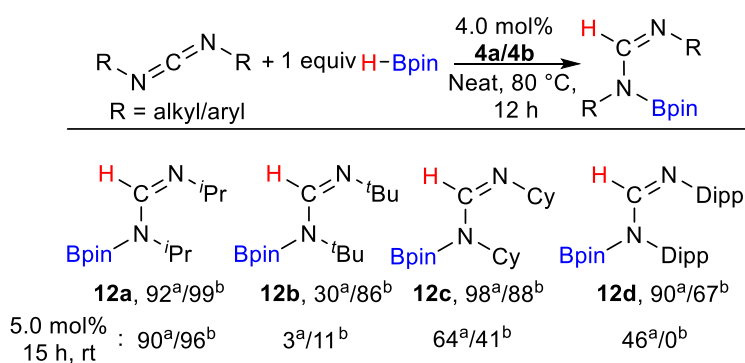
We started our investigation with *N,N'*-diisopropylcarbodiimide in presence of equimolar equivalent of HBpin at 80°C, which afforded the desired singly reduced *N*-boryl formamidine (**12a**) product in excellent yield within 12 h (entry 6 and entry 13, Table 4.2.5). It is of note here that, although *N,N'*-diisopropylcarbodiimide undergoes hydroboration at room temperature with both the catalyst, rest of the substrates shows poor conversion under same reaction condition (See Table 4.2.5, entry 4 and entry 10, and Scheme 4.2.6). Therefore, maintaining the optimized reaction condition at 80 °C, the scope of the reaction was

investigated and product *N*-borylformamidine [R¹NCHN(Bpin)R¹] was identified through ¹H NMR spectrum with a singlet resonance at δ = 7.90 ppm. Other substrate such as *N,N'*-di-tert-butylcarbodiimide (**12b**), *N,N'*-dicyclohexylcarbodiimide (**12c**), and bis-(2,6-diisopropylphenyl)carbodiimide (**12d**) provides moderate to good yields of desired mono hydroboration product under standard reaction condition (Scheme 4.2.6). It is noteworthy that an attempted reaction of *i*PrN=C=N*i*Pr and two equivalents of HBpin afforded 52% mono hydroboration and 24% double hydroboration product under same reaction condition.

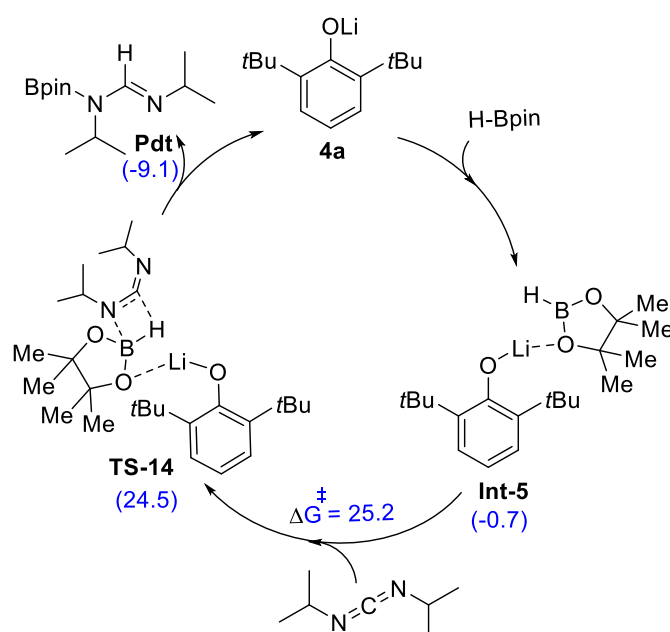
Table 4.2.5. Optimization table for the hydroboration of *N,N*-diisopropylcarbodiimide by **4a** and **4b**.



Entry	Catalyst	Catalyst (mol%)	Solvent	Temperature (°C)	Time (h)	NMR yield (%)
1.	1a	3.0	Neat	rt	1	20
2.	1a	3.0	Neat	rt	15	53
3.	1a	5.0	Neat	rt	13	84
4.	1a	5.0	Neat	rt	15	90
5.	1a	3.0	Neat	60	15	66
6.	1a	4.0	Neat	80	15	92
7.	1a	4.0	Neat	80	18	>99
8.	1b	3.0	Neat	rt	1	54
9.	1b	5.0	Neat	rt	13	87
10.	1b	5.0	Neat	rt	15	96
11.	1b	2.0	Neat	80	12	92
12.	1b	3.0	Neat	80	12	95
13.	1b	4.0	Neat	80	12	99
14.	1b	4.0	Neat	60	12	86



Scheme 4.2.6. Scope of hydroboration with carbodiimide substrates. Reaction conditions: 4.0 mol% catalyst, 12 h reaction at 80 °C in neat condition.



Scheme 4.2.7. The catalytic cycle for the carbodiimide hydroboration by catalyst **4a**. ΔG and ΔG^\ddagger represent the Gibbs free energy of reaction and the barrier, respectively. All values are in kcal/mol.

Full quantum chemical calculations were carried out with density functional theory (DFT) with the dispersion and solvent corrected PBE/TZVP level of theory in order to understand the mechanism (Scheme 4.2.7 and Figure 4.2.2) of the carbodiimide hydroboration reaction in the presence of catalyst **4a**. In the first step of the reaction in the presence of catalyst **4a**, a weakly bound complex (**Int-5**) is formed between catalyst **4a** and pinacolborane as stated earlier for the hydroboration of aldehydes, ketones and amides. Now the carbodiimide approaches towards the B-H bond of the **Int-5**. This is the prelude to the nucleophilic attack by the imide nitrogen of carbodiimide to the boron center of the pinacolborane, with the hydride being

transferred from the boron center to the electrophilic sp-hybridized carbon of the imide. This occurs through a four-membered transition state (**TS-14**) and leads to the formation of hydroboration product (**Pdt**) along with the regeneration of the catalyst **4a** (see Scheme 4.2.7 and Figure 4.2.2). The ΔE (-12.1 kcal/mol) and ΔG (-8.4 kcal/mol) values for this step are significantly negative and the activation energy (ΔG^\ddagger) barrier corresponding to the transition state is 25.2 kcal/mol. This is also the slowest step of the overall hydroboration reaction. In this transition state there is a significant amount of B-H bond activation (the B-H bond distance increases to 1.91 Å), which allows the hydride transfer from the boron to the sp-hybridized imide carbon center along with the simultaneous C=N bond cleavage and B-N bond formation.

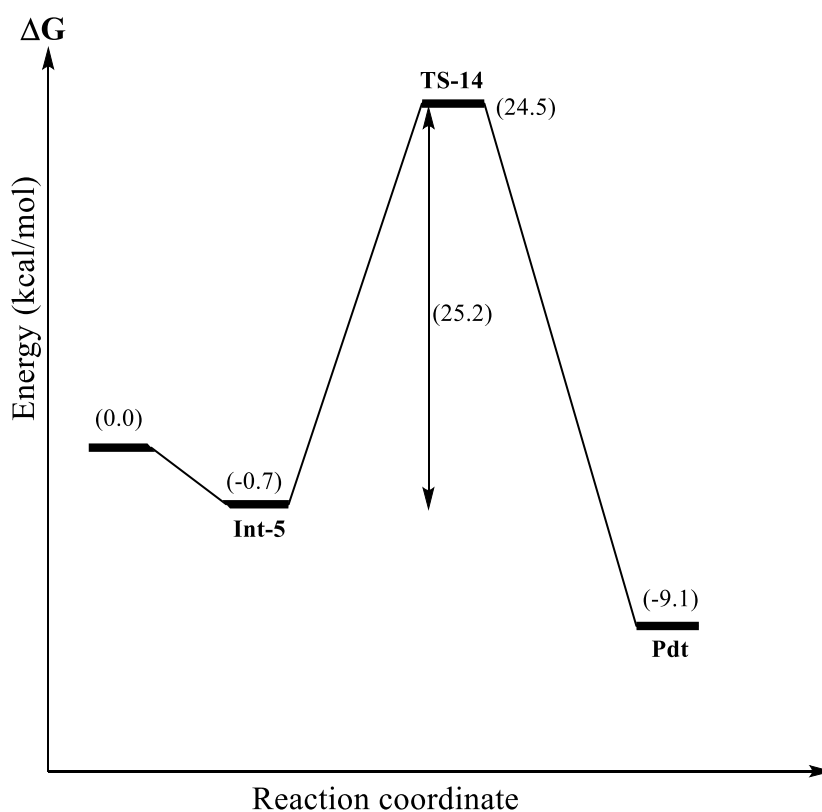


Figure 4.2.2. The reaction energy profile diagram for the catalytic hydroboration of carbodiimide by catalyst **4a**. The values (in kcal/mol) have been calculated at the PBE/TZVP level of theory with density functional theory (DFT).

4.2.6 Conclusion

In summary, due to its importance in asymmetric synthesis, the hydroboration of amides demands for the development of new catalysts and processes that are environmentally sustainable and efficient. Here, for the first time, we have demonstrated the utility of easily

accessible, cost effective and almost non-toxic lithium compound for the catalytic hydroboration for a wide range of primary, secondary, and tertiary amides. Furthermore, with the combined experimental and theoretical studies, we propose a mechanistic pathway which reveal that the role of the lithium compounds could be interpreted in the binding of sterically demanding Lewis acids to one of the Lewis basic O atoms of HBpin, and thereby setting up a platform for the HBpin to offer its B–H bond to the unsaturated amide functionality. In addition, this reduction methodology is further extended for other challenging substrates such as esters and carbodiimides.

4.3 References

1. Schlenk, W.; Holtz, J. *Ber. Dtsch. Chem. Ges.* **1917**, *50*, 262–274.
2. (a) Harder, S. *Chem. Rev.* **2010**, *110*, 3852–3876. (b) Stennett, T. E.; Harder, S. *Chem. Soc. Rev.* **2016**, *45*, 1112–1128. (c) Hill, M. S.; Liptrot, D. J.; Weetman, C. *Chem. Soc. Rev.* **2016**, *45*, 972–988. (d) Revunova, K.; Nikonov, G. I. *Dalton Trans.* **2015**, *44*, 840–866.
3. Arrowsmith, M.; Hadlington, T. J.; Hill, M. S.; Kociok-Köhn, G. *Chem. Commun.* **2012**, *48*, 4567–4569.
4. Yadav, S.; Pahar, S.; Sen, S. S. *Chem. Commun.* **2017**, *53*, 4562–4564.
5. Fohlmeister, L.; Stasch, A. *Chem. – Eur. J.* **2016**, *22*, 10235–10246.
6. Mukherjee, D.; Shirase, S.; Spaniol, T. P.; Mashima, K.; Okuda, J. *Chem. Commun.* **2016**, *52*, 13155–13158.
7. Mukherjee, D.; Ellern, A.; Sadow, A. D. *Chem. Sci.* **2014**, *5*, 959–964.
8. Manna, K.; Ji, P.; Greene, F. X.; Lin, W. *J. Am. Chem. Soc.* **2016**, *138*, 7488–7491.
9. (a) Hadlington, T. J.; Hermann, M.; Frenking, G.; Jones, C. *J. Am. Chem. Soc.* **2014**, *136*, 3028–3031. (b) Schneider, J.; Sindlinger, C. P.; Freitag, S. M.; Schubert, H.; Wesemann, L. *Angew. Chem. Int. Ed.*, **2017**, *56*, 333–337. (c) Wu, Y.; Shan, C.; Sun, Y.; Chen, P.; Ying, J.; Zhu, J.; Liu, L(Leo); Zhao, Y. *Chem. Commun.* **2016**, *52*, 13799–13802.
10. Chong, C.-C.; Hirao, H.; Kinjo, R. *Angew. Chem. Int. Ed.*, **2015**, *54*, 190–194.
11. Bisai, M. K.; Pahar, S.; Das, T.; Vanka, K.; Sen, S. S. *Dalton Trans.* **2017**, *46*, 2420–2424.
12. Yang, Z.; Zhong, M.; Ma, X.; De, S.; Anusha, C.; Parameswaran, P.; Roesky, H. W. *Angew. Chem. Int. Ed.* **2015**, *54*, 10225–10229.
13. (a) Jakhar, V. K.; Barman, M. K.; Nembenna, S. *Org. Lett.* **2016**, *18*, 4710–4713. (b) Lawson, J. R.; Wilkins, L. C.; Melen, R. L. *Chem. - Eur. J.* **2017**, *23*, 10997–11000.

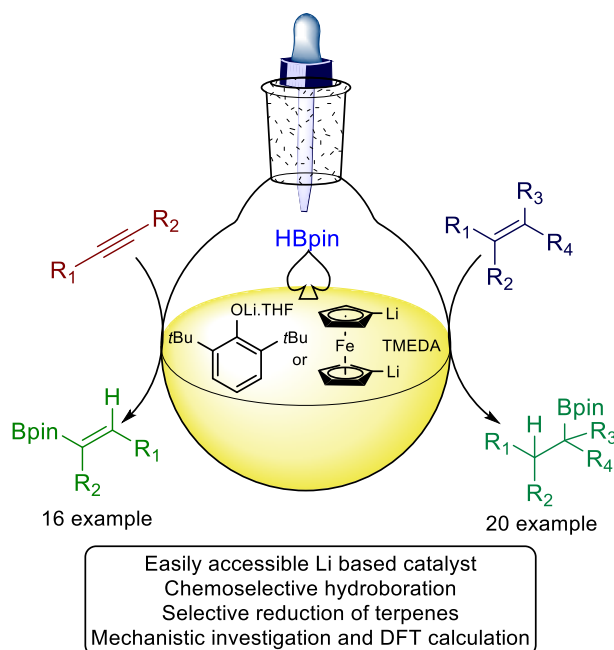
14. (a) Weetman, C.; Anker, M. D.; Arrowsmith, M.; Hill, M. S.; Kociok-Köhn, G.; Liptrot, D. J.; Mahon, M. F. *Chem. Sci.* **2016**, *7*, 628–641. (b) Weetman, C.; Hill, M. S.; Mahon, M. F. *Chem. Commun.* **2015**, *51*, 14477–14480.
15. (a) Courtemanche, M.-A.; Légaré, M.-A.; Maron, L.; Fontaine, F.-G. *J. Am. Chem. Soc.* **2013**, *135*, 9326–9329. (b) Franz, D.; Sirtl, L.; Pöthig, A.; Inoue, S. *Z. Anorg. Allg. Chem.* **2016**, *642*, 1245–1250. (c) Lortie, J. L.; Dudding, T.; Gabidullin, B. M.; Nikonov, G. I. *ACS Catal.* **2017**, *7*, 8454–8459.
16. For selected reviews on main group compound catalyzed hydroboration, please see: (a) Chong, C. C.; Kinjo, R. *ACS Catal.* **2015**, *5*, 3238–3259. (b) Nikonov, G. I. *ACS Catal.* **2017**, *7*, 7257–7266. (c) Mukherjee, D.; Okuda, J. *Angew. Chem. Int. Ed.* **2018**, *57*, 1458–1473. (d) Dagorne, S.; Wehmschulte, R. *ChemCatChem* **2018**, *10*, 2509 – 2520
17. (a) Buch, F.; Brettar, J.; Harder, S. *Angew. Chem. Int. Ed.* **2006**, *45*, 2741–2745. (b) Leich, V.; Spaniol, T. P.; Okuda, J. *Organometallics* **2016**, *35*, 1179–1182.
18. Bauer, H.; Alonso, M.; Färber, C.; Elsen, H.; Pahl, J.; Causero, A.; Ballmann, G.; De Proft, F.; Harder, S. *Nat. Catal.* **2018**, *1*, 40–47.
19. Mukherjee, D.; Osseili, H.; Spaniol, T. P.; Okuda, J. *J. Am. Chem. Soc.* **2016**, *138*, 10790–10793.
20. (a) Osseili, H.; Mukherjee, D.; Beckerle, K.; Spaniol, T. P.; Okuda, J. *Organometallics* **2017**, *36*, 3029–3034. (b) Osseili, H.; Mukherjee, D.; Spaniol, T. P.; Okuda, J. *Chem. – Eur. J.* **2017**, *23*, 14292–14298.
21. (a) McLellan, R.; Kennedy, A. R.; Mulvey, R. E.; Orr, S. A.; Robertson, S. D. *Chem. – Eur. J.* **2017**, *23*, 16853–16861. (b) Pollard, V. A.; Orr, S. A.; McLellan, R.; Kennedy, A. R.; Hevia, E.; Mulvey, R. E. *Chem. Commun.* **2018**, *54*, 1233–1236.
22. Swamy, V. S. V. S. N.; Bisai, M. K.; Das, T.; Sen, S. S. *Chem. Commun.* **2017**, *53*, 6910–6913.
23. Yadav, S.; Dixit, R.; Vanka, K.; Sen, S. S. *Chem. - Eur. J.* **2018**, *24*, 1269–1273.
24. (a) Weidner, V. L.; Barger, C. J.; Delferro, M.; Lohr, T. L.; Marks, T. J. *ACS Catal.* **2017**, *7*, 1244–1247. (b) Bagherzadeh, S.; Mankad, N. P. *Chem. Commun.* **2016**, *52*, 3844–3846.
25. (a) Bonet, A.; Gulyás, H.; Fernández, E. *Angew. Chem. Int. Ed.*, **2010**, *49*, 5130–5134. (b) Query, I. P.; Squier, P. A.; Larson, E. M.; Isley, N. A.; Clark, T. B. *J. Org. Chem.* **2011**, *76*, 6452–6456.
26. Harder, S.; Spielmann, J. *J. Organomet. Chem.* **2012**, *698*, 7–14.
27. Li, Y.; Wang, J.; Wu, Y.; Zhu, H.; Samuel, P. P.; Roesky, H. W. *Dalton Trans.* **2013**, *42*, 13715–13722.

28. Sitwatch, R. K.; Nagendran, S. *Chem. - Eur. J.* **2014**, *20*, 13551–13556.
29. Liberman-Martin, A. L.; Bergman, R. G.; Tilley, T. D. *J. Am. Chem. Soc.* **2015**, *137*, 5328–5331.
30. Yang, Z.; Yi, Y.; Zhong, M.; De, S.; Mondal, T.; Koley, D.; Ma, X.; Zhang, D.; Roesky, H. W. *Chem. – Eur. J.* **2016**, *22*, 6932–6938.
31. Sharma, M. K.; Sinhababu, S.; Mukherjee, G.; Rajaraman, G.; Nagendran, S. *Dalton Trans.* **2017**, *46*, 7672–7676.
32. Wang, W.; Luo, M.; Li, J.; Pullarkat, S. A.; Ma, M. *Chem. Commun.* **2018**, *54*, 3042–3044.
33. For reviews on transition metal catalyzed hydroboration: (a) Beletskaya, I.; Pelter, A. *Tetrahedron* **1997**, *53*, 4957–5026. (b) Miyaura, N., in *Catalytic Heterofunctionalization*, ed. A. Togni and H. Grützmacher, Wiley-VCH, Weinheim, 2001, pp. 1–46. (c) Vogels, C. M.; Westcott, S. W. *Curr. Org. Chem.* **2005**, *9*, 687–699.
34. For selected reviews on main group compound catalysed hydroboration, please see: (a) Chong, C. C.; Kinjo, R. *ACS Catal.* **2015**, *5*, 3238–3259. (b) Nikonov, G. I. *ACS Catal.* **2017**, *7*, 7257–7266. (c) Mukherjee, D.; Okuda, J. *Angew. Chem. Int. Ed.* **2018**, *57*, 1458–1473. (d) Dagorne, S.; Wehmschulte, R. *ChemCatChem* **2018**, *10*, 2509 – 2520.
35. (a) Andersson, P. G.; Munslow, I. J. *Modern reduction methods*, Wiley, New York, 2008, pp. 1–522; (b) Ricci, A. *Modern Amination Method*, Wiley, New York, 2000, pp. 1–258; (c) Weissmehl, K.; Arpe, H. J. *Industrial Organic Chemistry*, Wiley VCH, Weinheim, 4th edn, 1997.
36. Lawrence, S. A. *Amines: Synthesis Properties and Applications*, Cambridge University Press, Cambridge, 2004.
37. Smith, A. M.; Whyman, R. *Chem. Rev.* **2014**, *114*, 5477–5510.
38. Dodds, D. L.; Cole-Hamilton, D. J. *Catalytic Reduction of Amides Avoiding LiAlH₄ or B₂H₆*. In *Sustainable Catalysis: Challenges and Practices for the Pharmaceutical and Fine Chemical Industries*, ed. P. J. Dunn, K. K. Hii, M. J. Krische and M. T. Williams, Wiley, Hoboken, NJ, 2013, pp. 1–36.
39. Biermann, U.; Friedt, W.; Lang, S.; Luhs, W.; Machmuller, G.; Metzger, J. O.; Klaas, M. R.; Schafer, H. J.; Schneider, M. P. *Angew. Chem. Int. Ed.* **2000**, *39*, 2206–2224.
40. (a) Lohr, T. L.; Li, Z.; Marks, T. J. *Acc. Chem. Res.* **2016**, *49*, 824–834. (b) Wu, L.; Moteki, T.; Gokhale, A. A.; Flaherty, D. W.; Toste, F. D. *Chem* **2016**, *1*, 32–58. (c) Hu, C.; Creaser, D.; Siahrostami, S.; Grönbeck, H.; Ojagh, H.; Skoglundh, M. *Catal. Sci. Technol.* **2014**, *4*, 2427–2444. (d) Turek, T.; Trimm, D. L.; Cant, N. W. *Catal. Rev.: Sci. Eng.* **1994**, *36*, 645–683.

41. Ojima, I.; Nihonyanagi, M.; Kogure, T.; Kumagai, M.; Horiuchi, S.; Nakatsugawa, K. *J. Organomet. Chem.* **1975**, *94*, 449–461.
42. Gaylord, N. G. *Reduction with Complex Metal Hydrides*, Interscience, New York, 1956.
43. Constable, D. J. C.; Dunn, P. J.; Hayler, J. D.; Humphrey, G. R.; Leazer, J. L. Jr.; Linderman, R. J.; Lorenz, K.; Manley, J.; Pearlman, B. A.; Wells, A.; Zaks, A.; Zhang, T. Y. *Green Chem.* **2007**, *9*, 411–420.
44. (a) Brown, H. C. *Hydroboration*. W. A. Benjamin: New York, 1962. (b) Seyden-Penne, J. *Reductions by the Alumino- and Boro-hydrides in Organic Synthesis*, John Wiley & Sons, Inc, New York, 1997.
45. Selected references: (a) Dupau, P.; Tran Do, M.-L.; Gaillard, S.; Renaud, J.-L. *Angew. Chem. Int. Ed.* **2014**, *53*, 13004–13006. (b) Tan, X.; Wang, Y.; Liu, Y.; Wang, F.; Shi, L.; Lee, K.-H.; Lin, Z.; Lv, H.; Zhang, X. *Org. Lett.* **2015**, *17*, 454–457. (c) Pritchard, J.; Filonenko, G. A.; van Putten, R.; Hensen, E. J. M.; Pidko, E. A. *Chem. Soc. Rev.* **2015**, *44*, 3808–3833. (d) Tan, X.; Wang, Q.; Liu, Y.; Wang, F.; Lv, H.; Zhang, X. *Chem. Commun.* **2015**, *51*, 12193–12196. (e) Kim, D.; Le, L.; Drance, M. J.; Jensen, K. H.; Bogdanovski, K.; Cervarich, T. N.; Barnard, M. G.; Pudalov, N. J.; Knapp, S. M. M.; Chianese, A. R. *Organometallics* **2016**, *35*, 982–989.
46. Núñez Magro, A. A.; Eastham, G. R.; Cole-Hamilton, D. J. *Chem. Commun.* **2007**, 3154–3156.
47. Hie, L.; Nathel, N. F. F.; Shah, T. K.; Baker, E. L.; Hong, X.; Yang, Y. F.; Liu, P.; Houk, K. N.; Garg, N. K. *Nature* **2015**, *524*, 79–83.
48. Lampland, N. L.; Hovey, M.; Mukherjee, D.; Sadow, A. D. *ACS Catal.* **2015**, *5*, 4219–4226.
49. Das, S.; karmakar, H.; Bhattacharjee, J.; Panda, T. K. *Dalton Trans.* **2019**, *48*, 11978–11984.
50. Barger, C. J.; Dicken, R. D.; Weidner, V. L.; Motta, A.; Lohr, T. L.; Marks, T. J. *J. Am. Chem. Soc.* **2020**, *142*, 8019–8028.
51. Bhunia, M.; Shaoo, S. R.; Das, A.; Ahmed, J.; Sreejyothi, P.; Mandal, S. K. *Chem. Sci.* **2020**, *11*, 1848–1854.
52. (a) Mukherjee, D.; Ellern, A.; Sadow, A. D. *Chem. Sci.* **2014**, *5*, 959–964. (b) Patnaik, S.; Sadow, A. D. *Angew. Chem. Int. Ed.* **2019**, *58*, 2505–2509.
53. Barman, M. K.; Baishya, A.; Nembenna, S. *Dalton Trans.* **2017**, *46*, 4152–4156.

54. (a) Cao, X.; Wang, W.; Lu, K.; Yao, W.; Xue, F.; Ma, M. *Dalton Trans.* **2020**, 49, 2776-2780. (b) Barger, C. J.; Motta, A.; Weidner, V. L.; Lohr, T. L.; Marks, T. J. *ACS Catal.* **2019**, 9, 9015–9024.
55. (a) Weetman, C.; Hill, M. S.; Mahon, M. F. *Chem.-Eur. J.* **2016**, 22, 7158–7162. (b) Rauch, M.; Ruccolo, S.; Parkin, G. *J. Am. Chem. Soc.* **2017**, 139, 13264–13267.
56. Ramos, A.; Antinolo, A.; Carrillo-Hermosilla, F.; Fernandez- Galan, R.; Garcia-Vivo, D. *Chem. Commun.* **2019**, 55, 3073–3076.
57. Ding, Y.; Ma, X.; Liu, Y.; Liu, W.; Yang, Z.; Roesky, H. W. *Organometallics* **2019**, 38, 3092–3097.
58. Liu, H.; Kulbitski, K.; Tamm, M.; Eisen, M. S. *Chem. - Eur. J.* **2018**, 24, 5738–5742.
59. Mukherjee, D.; Osseili, H.; Spaniol, T. P.; Okuda, J. *J. Am. Chem. Soc.* **2016**, 138, 10790–10793.
60. (a) Bisai, M. K.; Das, T.; Vanka, K.; Sen, S. S. *Chem. Commun.* **2018**, 54, 6843–6846. (b) Bisai, M. K.; Yadav, S.; Das, T.; Vanka, K.; Sen, S. S. *Chem. Commun.* **2019**, 55, 11711–11714.
61. Bage, A. D.; Hunt, T. A.; Thomas, S. P. *Org. Lett.* **2020**, 22, 4107–4112.

Beyond Carbonyl Reduction: Lithium Compounds Catalyzed Hydroboration of Alkenes and Alkynes with Anti-Markovnikov Selectivity



Abstract:

The hydroboration of alkenes and alkynes using easily accessible lithium compounds [2,6-di-tert-butyl phenolate lithium and 1,1'-dilithioferrocene] has been achieved with good yields, high functional group tolerance and excellent chemoselectivity. Deuterium labeling experiments confirm the cis-addition of pinacolborane. The methodology has been further extended to myrcene, which undergoes selective 4,3-hydroboration. DFT calculations provide insights into the mechanism.

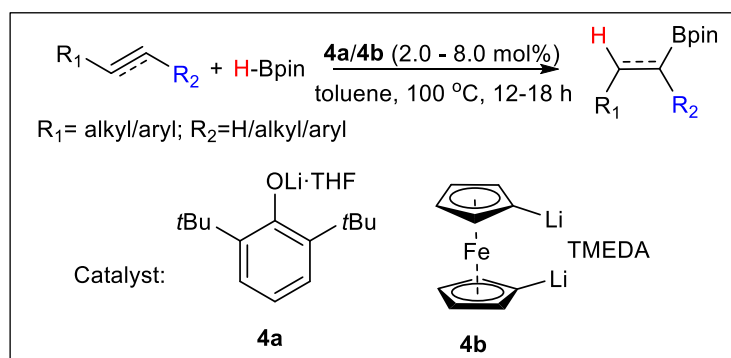
5.1 Introduction

Hydroboration of functionalized alkynes and alkenes using excess pinacolborane (HBpin) is known,¹ but their catalytic conversion usually requires a late transition metal catalyst.² Recently, the demand for supplanting the transition metal catalysts by more earth abundant and less toxic main group surrogates is ever increasing. Hydroboration using compounds with group 2 elements has been limited to the catalytic reduction of unsaturated polar bonds, such as aldehydes, ketones, imines, amides, esters etc.³⁻¹⁴ Although compounds with p-block elements are emerging as proficient catalysts for alkyne¹⁵⁻²⁰ and alkene²¹⁻²³ hydroboration, there are very limited reports on s-block metal catalyzed alkene or alkyne hydroboration. While Rueping and coworkers reported the first magnesium catalyzed hydroboration of terminal and internal alkynes,²⁴ the group of Parkin demonstrated styrene hydroboration by a terminal magnesium hydride.²⁵ Besides, Zhao and co-workers reported the hydroboration of carbonyl groups and styrene substrates using NaOH powder, although the scope of styrene substrates was somewhat limited.²⁶

The advantages of using lithium compounds are (i) cheap, (ii) moderately abundant (65 ppm in the Earth's crust), (iii) readily accessible, and (iv) they do not involve in Schlenk equilibrium like group 2 elements. Insofar, we have discussed the hydroboration of aldehydes, ketones, esters, amides, and carbodiimides. Hence, we wished to probe whether our systems, 2,6-*tert*-butyl phenolatelithium (**4a**), 1,1'-dilithioferrocene (**4b**), and [Dipp₂nacnac]Li·THF (**4c**), are capable of reducing non-polar substrates like alkenes or alkynes.

A further impetus comes from a result that described the use of *n*-BuLi as an efficient catalyst for the hydroboration of alkynes with HBpin.²⁷ Herein, we report efficient hydroboration of more challenging alkenes and alkynes by **4a** and **4b** (Scheme 5.1). Only a trace amount of conversion was observed when **4c** was used as the catalyst.

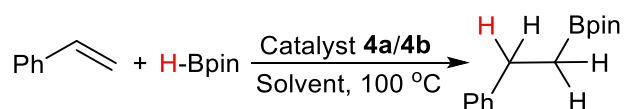
5.2 Hydroboration of alkene and alkyne



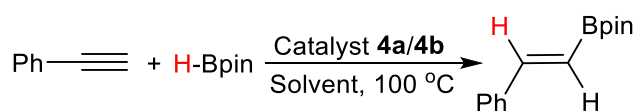
Scheme 5.1. Lithium compound catalyzed hydroboration of alkenes and alkynes.

A brief screening of catalyst loading, temperature and time has been carried out for the hydroboration of styrene or phenylacetylene with 1.1 equivalent of HBpin (see Tables 5.1 and 5.2) to achieve the best conversion. For hydroboration of alkynes, the catalyst loadings were 2.0 mol% and the reactions were over around 12 h when heated at 100 °C. Note that, the catalyst loading is substantially lesser than that for *n*BuLi (10 mol%) catalyzed alkyne hydroboration.³⁵ For comparison purpose, cyclopentadienyllithium (CpLi) was employed as the catalyst. With 2.0 mol% catalyst loading CpLi afforded 65% yield under the same reaction conditions for the hydroboration of phenylacetylene (see Table 5.2, entry 6). Slightly higher catalyst loadings (4.0 mol% for **4b** and 8.0 mol% for **4a**) and time (18 h) are required for alkenes.

Table 5.1. Optimization table of hydroboration of styrene catalyzed by **4a** and **4b**.



Entry	Catalyst	Catalyst (mol%)	Solvent	Temperature (°C)	Time (h)	NMR yield (%)
1.	4b	2.0	Toluene	100	24	84
2.	4b	3.0	Toluene	100	24	93
3.	4b	4.0	Toluene	100	24	96
4.	4b	3.0	Toluene	100	20	79
5.	4b	3.0	Toluene	100	18	75
6.	4b	4.0	Toluene	100	18	89
7.	4b	4.0	Toluene	100	15	84
8.	4b	5.0	Toluene	100	12	76
9.	4a	5.0	Acetonitrile	100	24	10
10.	4a	5.0	DMF	100	24	<5
11.	4a	5.0	DMSO	100	24	<5
12.	4a	5.0	1,4-Dioxane	100	24	46
13.	4a	5.0	Toluene	100	18	45
14.	4a	5.0	Neat	100	24	56
15.	4a	8.0	Neat	100	18	92
16.	4a	8.0	Neat	100	12	75

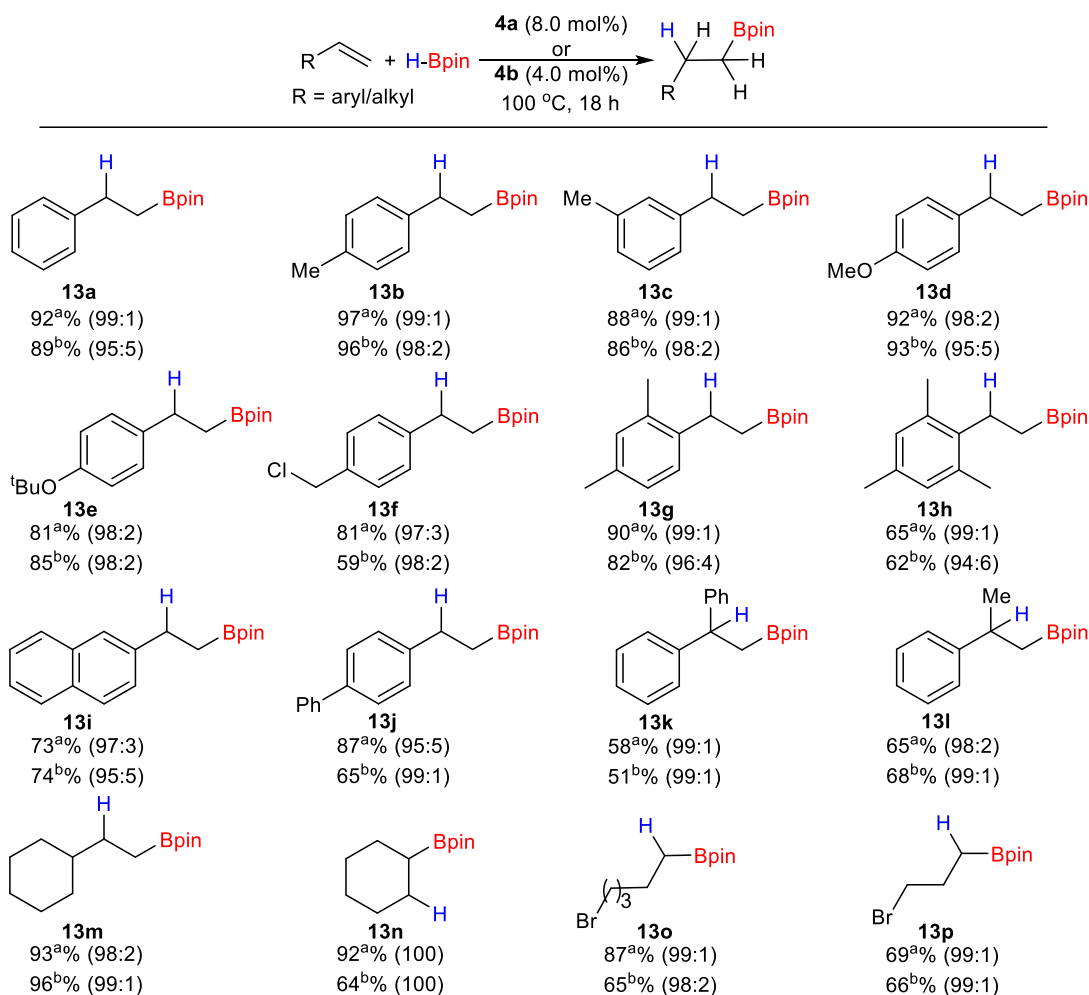
Table 5.2. Optimization table of hydroboration of phenylacetylene catalyzed by **4a** and **4b**.

Entry	Catalyst	Catalyst (mol%)	Solvent	Temperature (°C)	Time (h)	NMR yield (%)
1.	4a	0.5	Toluene	100	18	35
2.	4a	1.0	Toluene	100	18	64
3.	4a	2.0	Toluene	100	12	92
4.	4a	3.0	Toluene	100	12	94
5.	4a	2.0	Toluene	100	10	85
6.	CpLi	2.0	Toluene	100	12	65
7.	4b	0.5	Toluene	100	18	55
8.	4b	1.0	Toluene	100	18	76
9.	4b	2.0	Toluene	100	12	90
10.	4b	3.0	Toluene	100	12	93
11.	4b	3.0	Toluene	80	16	72
12.	4b	2.0	Toluene	100	10	80

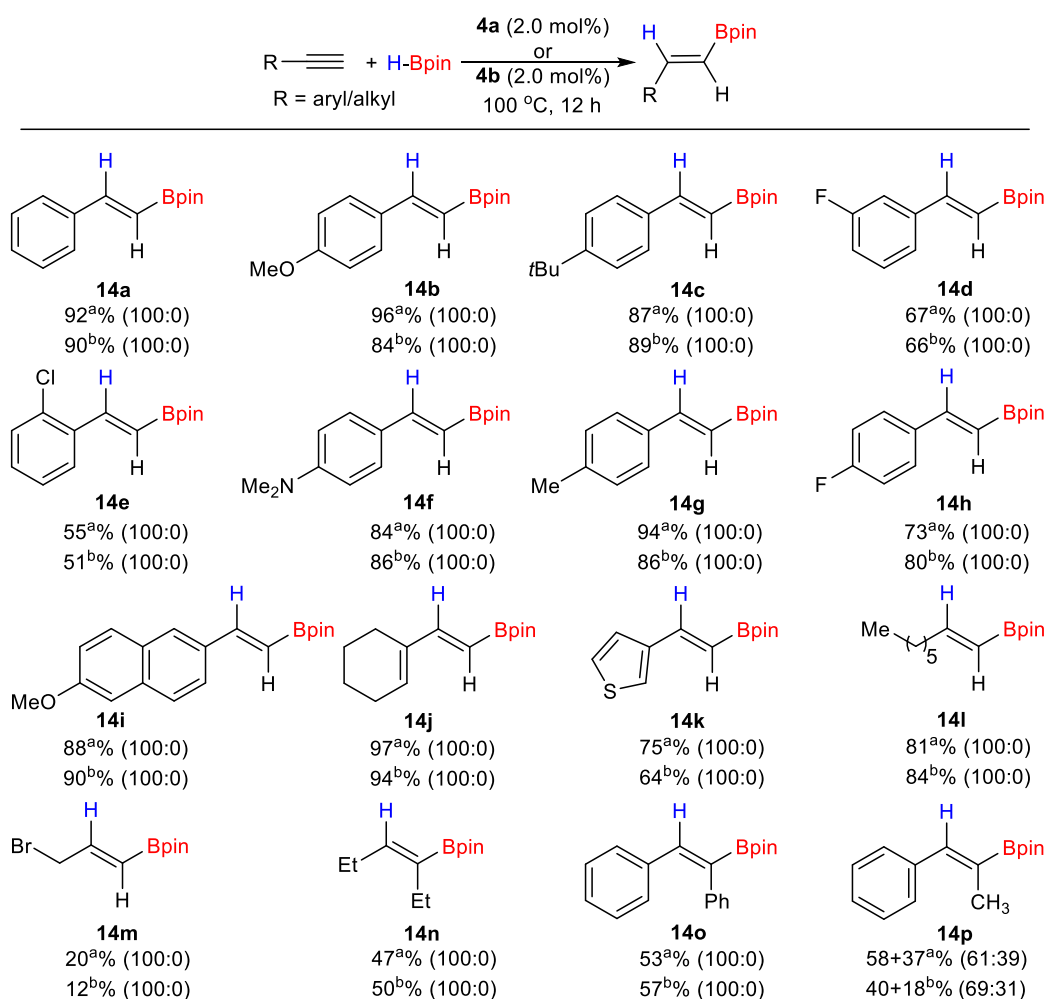
Both aliphatic and aromatic alkenes/alkynes underwent hydroboration to form the corresponding alkyl or vinyl-boronates in good to excellent yields (Schemes 5.2 and 5.3), reflecting the high efficiency of the catalysts. Smooth hydroboration of different aromatic alkenes or alkynes with electron donating or withdrawing substituents at *o*/*m*/*p* positions was observed. Both catalysts tolerate functional groups such as halogens (**13f**, **13o**, **13p**, **14d**, and **14h**), alkoxy (**13d**, **13e**, **14b**, and **14i**), heterocycle (**14k**), and amino (**14f**) containing substrates. However, in addition to alkyne hydroboration, lithium halide exchange was also observed for **3e** in 29% yield. The lithium halide exchange was more pronounced for **14m** as the metathesis product was obtained in more than 70% yield. Intramolecular chemoselective hydroboration of alkynes over alkenes was observed for **14j**.

In contrast to terminal alkynes, internal alkynes (**14n**, **14o**, and **14p**) form their corresponding boronates in moderate yields under the optimization conditions. However, similar to Rueping's magnesium catalyst, by increasing the catalyst loading (5 mol%) and reaction time (36 h), good yields are achieved for **14o** (80%). We have also tested an unsymmetrical alkyne, phenylpropyne, for hydroboration which afforded a mixture of α - and β -vinyl boronates (**14p**)

in 2:3 and 3:7 ratios for **4a** and **4b**, respectively. Aliphatic alkenes (**13m–13p**) or alkynes (**14l–14n**) were effectively converted to their corresponding products. Increase of the sterics has little effect on the yield as seen in the cases of hydroboration of **13h**, **13k**, **14n**, and **14o**.

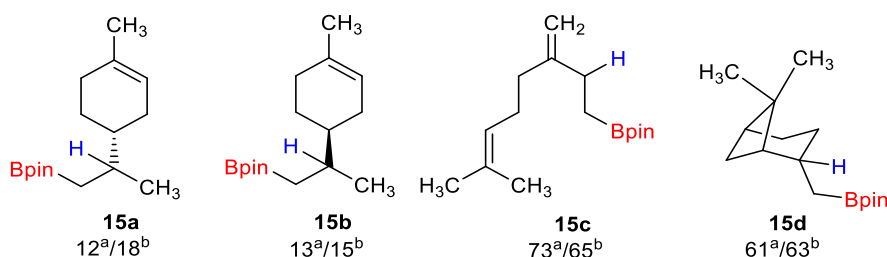


Scheme 5.2. Hydroboration scope with alkene substrates. Reaction conditions: Alkene (0.50 mmol), HBpin (0.55 mmol, 1.1 equiv) in neat or in toluene. Yields were determined by the ¹H NMR integration relative to mesitylene. Henceforth superscripts a and b stand for the catalysts **4a** and **4b** respectively. Ratios in parentheses report the distribution of regioisomers (linear vs branched).



Scheme 5.3. Scope of hydroboration with alkyne substrates. Reaction conditions: Alkyne (0.50 mmol), HBpin (0.55 mmol, 1.1 equiv), 2.0 mol% catalyst, 12 h reaction at 100 °C in toluene. Yields were determined by the ¹H NMR integration relative to mesitylene. Superscripts a and b stand for the catalysts **4a** and **4b** respectively. Ratios in parentheses report the distribution of regioisomers (anti-Markovnikov vs Markovnikov).

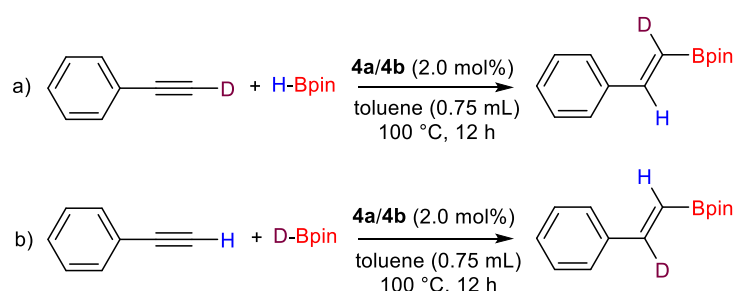
5.3 Hydroboration of terpenes



Scheme 5.4. Selective hydroboration of terpenes.

To further explore the catalytic potential of **4a** and **4b**, naturally occurring terpenes have been chosen for the selective hydroboration of the olefinic bond. Although poor yields were obtained for R- or S-limonene (**15a** and **15b**), myrcene (**15c**) and β -pinene (**15d**) were converted to the corresponding alkyl boronate ester in good yield with excellent selectivity (Scheme 5.4). Interestingly, 4,3-selective hydroboration of 2-substituted 1,3-diene (**15c**) was observed for both the catalysts. Note that, hydroboration of dienes to access allylboranes is less-established, and only known with transition metals such as Fe,²⁸ Co,²⁹ Ni,³⁰ Ir,³¹ etc. This is the first report of a main group element catalyzed selective hydroboration of myrcene.

5.4 Regio- and chemo-selective study

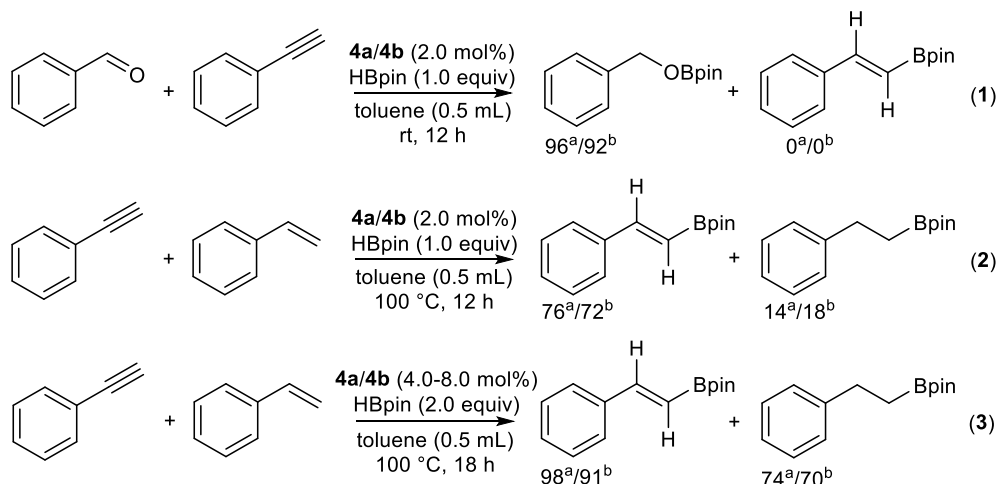


Scheme 5.5. Deuterium labelling experiment: (a) Hydroboration of phenylacetylene-D with HBpin. (b) Hydroboration of phenylacetylene with DBpin.

Deuterium labelling experiments were carried out for the catalytic hydroboration of alkynes to understand the stereoselectivity. A sharp resonance at δ 6.18 ppm in the ^2H NMR for the catalytic reduction of $\text{PhC}\equiv\text{CD}$ with HBpin designates a cis configuration of the deuterium and phenyl ring [(a), Scheme 5.5]. Similarly, the cis arrangement of deuterium and the Bpin moiety was confirmed from the resonance at δ 7.28 ppm in the ^2H NMR spectrum for the catalytic reaction of $\text{PhC}\equiv\text{CH}$ and DBpin [(b), Scheme 5.5]. This experiment attests a cis stereoselectivity, which is in good agreement with ScOTf mediated alkyne hydroboration, reported by Geetharani and coworkers.³²

Intermolecular chemoselective hydroboration of aldehydes, alkenes and alkynes was also studied in three different sets of reactions and the results are summarized in Scheme 5.6. The equimolar mixture of benzaldehyde, phenylacetylene and HBpin were charged with catalyst **4a/4b**, which produced corresponding boronate ester of the aldehyde over alkyne in more than 92% yield at rt or at heating condition (eqⁿ 1). The competing experiment involving a mixture of phenylacetylene, styrene and HBpin in 1:1:1 molar ratio led to 76% and 14% product yield for alkyne and alkene hydroboration respectively (eqⁿ 2). On the other hand, almost quantitative

hydroboration of phenylacetylene and around 70% conversion of styrene were obtained in subsequent addition of a second equivalent of HBpin (eqⁿ 3). This experiment shows a good catalytic chemoselectivity of alkynes even in presence of olefinic bond under same reaction condition.



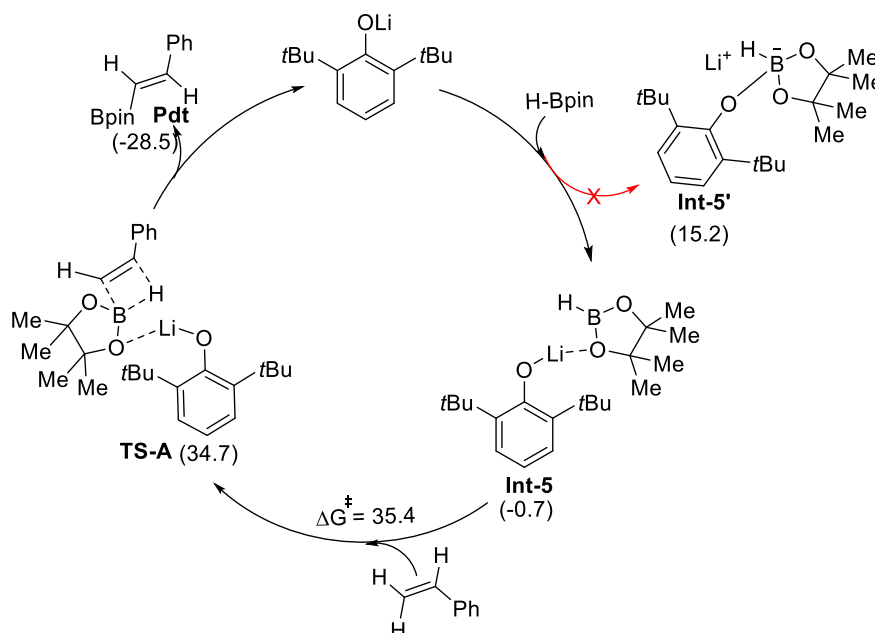
Scheme 5.6. Competitive experiment for chemoselective hydroboration.

5.5 Mechanistic investigations

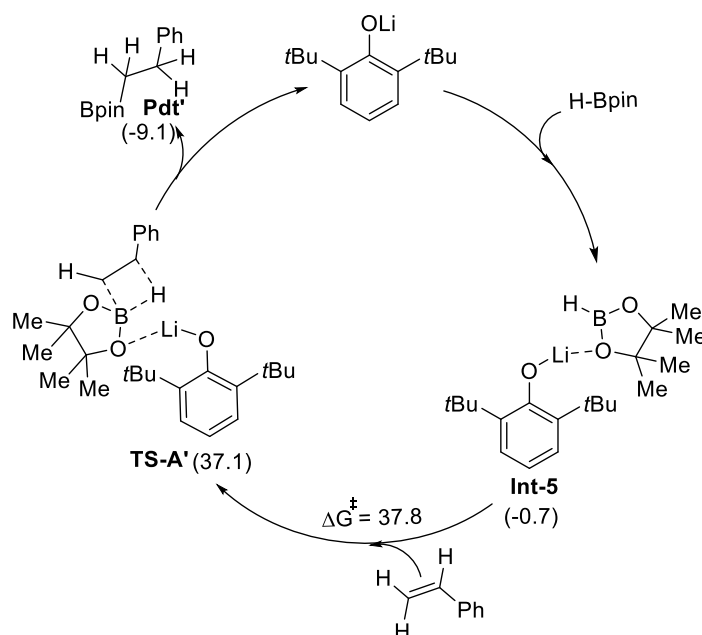
No appreciable changes in the ¹H NMR was observed from the stoichiometric reaction of **4a** with styrene or phenylacetylene, even after heating at 100 °C overnight. However, the reaction between **4a** and HBpin in toluene-d₈ shows a new set of resonance in the ¹¹B NMR at δ 4.7 ppm, indicating the formation of an intermediate (**Int-5**)³³⁻³⁴ along with a singlet at δ 21.6 and a quintet at -39.8 ppm for the formation of a trialkoxyborane [2,6-*t*Bu₂-C₆H₃-OBpin] and BH₄⁻ anion, respectively. In addition, a singlet at δ 86.9 and a quartet at δ -25.4 ppm were also observed, probably due to the decomposition of HBpin and the Lewis base·BH₃ adduct.³⁵ A white precipitate is formed in the NMR tube after 3–4 h and the filtrate part shows only three peaks at δ 4.7, 21.6 and -39.8 ppm in the ¹¹B NMR spectrum. No conclusive NMR spectra were obtained from the stoichiometric reactions between **4b** and HBpin and peak broadening was always observed.

Full quantum chemical calculations were done with density functional theory (DFT) at the dispersion and solvent corrected PBE/TZVP level of theory in order to understand the mechanism of the alkene and alkyne hydroboration reactions in the presence of **4a** (Schemes 5.7 and 5.8). In the first step of the reaction, a weakly coordinating complex (**Int-5**) is formed between catalyst **4a** and HBpin, with one of the oxygen atoms of pinacolborane approaching towards the lithium atom of **4a**. The reaction energy (Δ*E*) and the Gibbs free energy (Δ*G*) for this step are -11.5 kcal mol⁻¹ and -0.7 kcal mol⁻¹ respectively. Another possibility of

coordinating phenolate oxygen to the boron atom of pinacolborane leading to a four-coordinate boron complex (**Int-5'**) was found to be thermodynamically unfavorable due to the high ΔG (15.2 kcal mol⁻¹) of the reaction. Following this, the alkene or alkyne substrate approaches towards the B–H bond of **Int-5**. This is the overture to the nucleophilic attack by the C–C double or triple bond of the alkene or alkyne to the boron centre of the HBpin, with the hydride being transferred from the boron centre to the alkene or alkyne carbon centre having minimum hydrogen. This occurs through a four-membered transition state (**TS-A**)/(**TS-A'**) and leads to the respective hydroboration product along with the regeneration of the catalyst. The ΔE (-32.8 kcal mol⁻¹ and -11.9 kcal mol⁻¹) and ΔG (-28.5 kcal mol⁻¹ and -9.1 kcal mol⁻¹) values for these steps are highly negative and the barriers (ΔG^\ddagger s) corresponding to the transition states are moderate: 35.4 kcal mol⁻¹ and 37.8 kcal mol⁻¹ for the alkyne and alkene respectively. The moderate barriers explain the delicate feasibility of the reaction at 100 °C. In the transition states, there is a significant amount of B–H bond activation (1.27 Å vs. 1.19 Å in the intermediate complex), which allows the hydride transfer from the boron to the alkene or alkyne carbon centre, along with the simultaneous C–C double and triple bond cleavage and B–O bond formation.



Scheme 5.7. The catalytic cycle and reaction mechanism for the alkyne hydroboration by catalyst **4a**. The relative free energy (ΔG) for each species are shown within the parenthesis of the catalytic cycle. ΔG^\ddagger represent the Gibbs free energy of activation respectively. The values (in kcal/mol) have been calculated at the PBE/TZVP level of theory with DFT.



Scheme 5.8. The catalytic cycle and reaction mechanism for the alkene hydroboration by **4a**. The relative free energy (ΔG) for each species are shown within the parenthesis of the catalytic cycle. ΔG^\ddagger represent the Gibbs free energy of activation respectively. The values (in kcal/mol) have been calculated at the PBE/TZVP level of theory with DFT.

5.6 Conclusion

In summary, we are unwavering the utility of very simple, cost effective and almost non-toxic lithium compounds (**4a** and **4b**) for the catalytic hydroboration of a range of alkenes and alkynes including conjugated terpenes. The chemoselectivity and regioselectivity for the described catalytic process have been investigated. DFT calculations reveal that the role of the Li compounds could be interpreted in the binding of sterically demanding Lewis acids to one of the Lewis basic O atoms of HBpin, and thereby setting up a platform for the HBpin to offer its B–H bond to the unsaturated alkene and alkyne.

5.7 References

1. Tucker, C. E.; Davidson, J.; Knochel, P. *J. Org. Chem.* **1992**, *57*, 3483–3485.
2. For reviews on transition metal catalyzed hydroboration: (a) Beletskaya, I.; Pelter, A. *Tetrahedron* **1997**, *53*, 4957–5026. (b) Miyaura, N. in *Catalytic Heterofunctionalization*, ed. Togni, A.; Grützmacher, H. *Wiley-VCH, Weinheim*, 2001, pp. 1–46. (c) Vogels, C.M.; Westcott, S. W. *Curr. Org. Chem.* **2005**, *9*, 687–699.
3. Arrowsmith, M.; Hadlington, T. J.; Hill, M. S.; Kociok-Köhn, G. *Chem. Commun.* **2012**, *48*, 4567–4569.

- Arrowsmith, M.; Hill, M. S.; Kociok-Köhn, G. *Chem. – Eur. J.* **2013**, *19*, 2776–2783.
- Weetman, C.; Hill, M. S.; Mahon, M. F. *Chem. Commun.* **2015**, *51*, 14477–14480.
- Manna, K.; Ji, P.; Greene, F. X.; Lin, W. *J. Am. Chem. Soc.* **2016**, *138*, 7488–7491.
- Mukherjee, D.; Shirase, S.; Spaniol, T. P.; Mashima, K.; Okuda, J. *Chem. Commun.* **2016**, *52*, 13155–13158.
- Fohlmeister, L.; Stasch, A. *Chem. - Eur. J.* **2016**, *22*, 10235–10246.
- Weetman, C.; Anker, M. D.; Arrowsmith, M.; Hill, M. S.; Kociok-Köhn, G.; Liptrot, D. J.; Mahon, M. F. *Chem. Sci.* **2016**, *7*, 628–641.
- Yadav, S.; Pahar, S.; Sen, S. S. *Chem. Commun.* **2017**, *53*, 4562–4564.
- Yadav, S.; Dixit, R.; Bisai, M. K.; Vanka, K.; Sen, S. S. *Organometallics* **2018**, *37*, 4576–4584.
- Mukherjee, D.; Ellern, A.; Sadow, A. D. *Chem. Sci.* **2014**, *5*, 959–964.
- Lampland, N. L.; Hovey, M.; Mukherjee, D.; Sadow, A. D. *ACS Catal.* **2015**, *5*, 4219–4226.
- For reviews on main group compound carbonyl hydroboration, see: (a) Shegavi, M. L.; Bose, S. K. *Catal. Sci. Technol.* **2019**, *9*, 3307–3336. (b) Chong, C. C.; Kinjo, R. *ACS Catal.* **2015**, *5*, 3238–3259.
- Yang, Z.; Zhong, M.; Ma, X.; Nijesh, K.; De, S.; Parameswaran, P.; Roesky, H. W. *J. Am. Chem. Soc.* **2016**, *138*, 2548–2551.
- Bismuto, A.; Thomas, S. P.; Cowley, M. J. *Angew. Chem. Int. Ed.* **2016**, *55*, 15356–15359.
- McGough, J. S.; Butler, S. M.; Cade, I. A.; Ingleson, M. J. *Chem. Sci.* **2016**, *7*, 3384–3389.
- Fleige, M.; Möbus, J.; Stein, T. V.; Glorius, F.; Stephan, D. W. *Chem. Commun.* **2016**, *52*, 10830–10833.
- (a) Lawson, J. R.; Wilkins, L. C.; Melen, R. L. *Chem. - Eur. J.* **2017**, *23*, 10997–11000. (b) Carden, J. L.; Gierlich, L. J.; Wass, D. F.; Browne, D. L.; Melen, R. L. *Chem. Commun.* **2019**, *55*, 318–321.
- Franz, D.; Sirtl, L.; Pöthig, A.; Inoue, S. *Z. Anorg. Allg. Chem.* **2016**, *642*, 1245–1250.
- Yin, Q.; Kemper, S.; Klare, H. F. T.; Oestreich, M. *Chem. - Eur. J.* **2016**, *22*, 13840–13844.
- Prokofjevs, A.; Boussonihre, A.; Li, L.; Bonin, H.; Lacite, E.; Curran, D. P.; Vedejs, E. *J. Am. Chem. Soc.* **2012**, *134*, 12281–12288.
- Bismuto, A.; Cowley, M. J.; Thomas, S. P. *ACS Catal.* **2018**, *8*, 2001–2005.
- Magre, M.; Maity, B.; Falconnet, A.; Cavallo, L.; Rueping, M. *Angew. Chem. Int. Ed.* **2019**, *58*, 7025–7029.
- Rauch, M.; Rucolo, S.; Parkin, G.; *J. Am. Chem. Soc.* **2017**, *139*, 13264–13267.

26. Wu, Y.; Shan, C.; Ying, J.; Su, J.; Zhu, J.; Liu, L. L.; Zhao, Y. *Green Chem.* **2017**, *19*, 4169–4175.
27. Yan, D.; Wu, X.; Xiao, J.; Zhu, Z.; Xu, X.; Bao, X.; Yao, Y.; Shen, Q.; Xue, M. *Org. Chem. Front.* **2019**, *6*, 648–653.
28. Yu, J. Y.; Moreau, B.; Ritter, T. *J. Am. Chem. Soc.* **2009**, *131*, 12915–12917.
29. Ely, R. J.; Morken, J. P. *J. Am. Chem. Soc.* **2010**, *132*, 2534–2535.
30. Obligacion, J. V.; Chirik, P. J. *J. Am. Chem. Soc.* **2013**, *135*, 19107–19110.
31. Fiorito, D.; Mazet, C. *ACS Catal.* **2018**, *8*, 9382–9387.
32. Mandal, S.; Verma, P. K.; Geetharani, K. *Chem. Commun.* **2018**, *54*, 13690–13693.
33. Bisai, M. K.; Das, T.; Vanka, K.; Sen, S. S. *Chem. Commun.* **2018**, *54*, 6843–6846.
34. (a) Bonet, A.; Gulyás, H.; Fernández, E. *Angew. Chem., Int. Ed.* **2010**, *49*, 5130–5134. (b) Dasgupta, R.; Das, S.; Hiwase, S.; Pati, S.; Khan, S. *Organometallics* **2019**, *38*, 1429–1435.
35. Burgess, K.; vander Donk, W. A.; Westcott, S. A.; Marder, T. B.; Baker, R. T.; Calabrese, J. C. *J. Am. Chem. Soc.* **1992**, *114*, 9350–9359.

Appendix: Experimental and spectral details

6.1: Chapter 2 experimental details

6.1.1. Synthesis and experimental details of complex **2.1, 2.3-2.21**

6.1.2. Crystal structure details of complex **2.1-2.10** and **2.14-2.21**

6.2. Chapter 3 experimental details

6.2.1. General procedure for the catalytic hydroboration of aldehydes

6.2.2. Spectroscopic data for the hydroboration product of aldehydes

6.2.3. General procedure for the catalytic hydroboration of aldimines

6.2.4. Spectroscopic data for the hydroboration product of aldimines

6.2.5. Isolation and characterization of the intermediate

6.2.6. Details of DFT calculations

6.3. Chapter 4 experimental details

6.3.1. General procedure for the catalytic hydroboration of aldehydes

6.3.2. Spectroscopic data for the hydroboration product of aldehydes

6.3.3. General procedure for the catalytic hydroboration of ketones

6.3.4. Spectroscopic data for the hydroboration product of ketones

6.3.5. Isolation and characterization of the intermediate

6.3.6. General procedure for the catalytic cyanosilylation of aldehydes and ketones

6.3.7. Spectroscopic data for the cyanosilylation product of aldehydes and ketones

6.3.8. General procedure for the catalytic hydroboration of ester

6.3.9. Spectroscopic data for the hydroboration product of ester

6.3.10. General procedure for the catalytic hydroboration of primary amides

6.3.11. Spectroscopic data for the hydroboration product of primary amides

6.3.12. Control experiments for the mechanistic investigation of primary amide

6.3.13. General procedure for the catalytic hydroboration of secondary amides

6.3.14. Spectroscopic data for the hydroboration product of secondary amides

6.3.15. General procedure for the catalytic hydroboration of tertiary amides

6.3.16. Spectroscopic data for the hydroboration product of tertiary amides

6.3.17. General procedure for the catalytic hydroboration of carbodiimides

6.3.18. Spectroscopic data for the hydroboration product of carbodiimides

6.3.19. Details of DFT calculations

6.4: Chapter 5 experimental details

6.4.1. General procedure for the catalytic hydroboration of alkenes

6.4.2. Spectroscopic data for the hydroboration product of alkenes

6.4.3. General procedure for the catalytic hydroboration of alkynes

6.4.4. Spectroscopic data for the hydroboration product of alkynes

6.4.5. General catalytic procedure for the hydroboration of terpenes

6.4.6. Spectroscopic data for the hydroboration product of terpenes

6.4.7. Competitive experiment for aldehyde/alkyne/alkene hydroboration-selectivity study

6.4.8. Deuterium labeling experiments

6.4.9. Isolation and characterization of the intermediate

6.1: Chapter 2 experimental details

6.1.1. Synthesis and experimental details of complex 2.1-2.21

Synthesis of Hypersilylsilylene (2.1)

To the 30 mL toluene solution of $\text{PhC}(\text{N}t\text{Bu})_2\text{SiHCl}_2$ (1.000 g, 3.03 mmol) 10 mL toluene solution of potassium tris(trimethylsilyl)silane (2.600 g, 6.03 mmol) was added drop by drop at room temperature. Immediately, the solution was turned to a deep brown-red color with the formation of KCl. The resulting suspension was stirred for 8 h. The solvent was then removed in vacuo, dried for 2-3 h and the residue was extracted with toluene (30 mL). The filtrate was concentrated to afford pale yellow crystals of **2.1**. Yield: 1.410 g (92.1%). Mp 99-100 °C. ^1H NMR (400 MHz, C_6D_6 , 298 K): δ 7.15-6.88 (m, 5H, *Ph*), 1.21 (s, 18H, *tBu*), 0.51 (s, 27H, *SiMe*₃) ppm; $^{13}\text{C}\{^1\text{H}\}$ NMR (100.6 MHz, C_6D_6 , 298 K): δ 153.5 (NCN), 135.2 (*Ph*), 130.8-130.6 (*Ph*), 129.9 (*Ph*), 129.6 (*Ph*), 128.9 (*Ph*), 127.7 (*Ph*), 126.0 (*Ph*), 53.9 (*CMe*₃), 32.3 (*CMe*₃), 5.0 (*Si(SiMe*₃)₃) ppm; $^{29}\text{Si}\{^1\text{H}\}$ NMR (79.5 MHz, C_6D_6 , 298 K): δ 76.91 (*SiSi(SiMe*₃)₃), -8.36 (*SiSi(SiMe*₃)₃), -11.84 (*SiSi(SiMe*₃)₃) ppm. ESI-HRMS calcd. for $\text{C}_{24}\text{H}_{51}\text{N}_2\text{Si}_5$ $[\text{M}+\text{H}]^+ = 507.2893$, found 507.2883.

Synthesis of $[[\text{PhC}(\text{N}t\text{Bu})_2]\text{Si}\{\text{OSi}(\text{Si}(\text{CH}_3)_3)_3\text{O}\}_2$ (2.3)

To the mixture of **2.1** (0.400 g, 0.78 mmol) and Me_3NO (0.060 g, 0.79 mmol), 10 mL toluene was added at -30 °C and stirred for 15 min. After additional stirring for 12 h at room temperature, the reaction mixture was dried in vacuo. The residue was extracted in 5 mL toluene, concentrated and kept at -4 °C for 2 days to yield colorless crystals of **2.3**. Yield: 0.156 g (38.7%). ^1H NMR (400 MHz, C_6D_6 , 298 K): δ 6.96-6.86 (m, 10H, *Ph*), 1.37 (s, 36H, *tBu*), 0.44 (br, 54H, *SiMe*₃) ppm; $^{13}\text{C}\{^1\text{H}\}$ NMR (50.3 MHz, C_6D_6 , 298 K): δ 153.2 (NCN), 141.2 (*Ph*), 131.2 (*Ph*), 130.3 (*Ph*), 129.9 (*Ph*), 127.6 (*Ph*), 127.5 (*Ph*), 54.6 (*CMe*₃), 32.7 (*CMe*₃), 3.3 (*Si(SiMe*₃)₃) ppm; $^{29}\text{Si}\{^1\text{H}\}$ NMR (79.5 MHz, C_6D_6 , 298 K): δ -10.13 (*SiSi(SiMe*₃)₃), -22.01 (*SiSi(SiMe*₃)₃), -116.06 (*SiSi(SiMe*₃)₃) ppm.

Synthesis of $[[\text{PhC}(\text{N}t\text{Bu})_2]\text{SiSi}(\text{Si}(\text{CH}_3)_3)_3\text{S}$ (2.4)

To the mixture of **2.1** (0.300 g, 0.59 mmol) and 1/8 equivalent of S_8 (0.019 g, 0.59 mmol) in a 100 mL Schlenk flask, 15 mL toluene was added slowly at room temperature. Immediately, the solution was turned to pale yellow. After stirring for 6 h at room temperature, the solution was filtered

through cannula. The filtrate part was concentrated to 2 mL and kept at -4 °C overnight to get colorless crystal of **2.4** suitable for single crystal X-ray analysis. Yield: 0.263 g (82.7%). Mp 154-155 °C. ^1H NMR (200 MHz, C_6D_6 , 298 K): δ 7.31-6.84 (m, 5H, *Ph*), 1.25 (s, 18H, *tBu*), 0.54 (s, 27H, *SiMe*₃) ppm; $^{13}\text{C}\{^1\text{H}\}$ NMR (100.6 MHz, C_6D_6 , 298 K): δ 174.1 (NCN), 131.6 (*Ph*), 130.8 (*Ph*), 129.6 (*Ph*), 128.7 (*Ph*), 128.1 (*Ph*), 55.5 (*CMe*₃), 32.6 (*CMe*₃), 4.0 (*Si(SiMe*₃)₃) ppm; $^{29}\text{Si}\{^1\text{H}\}$ NMR (79.5 MHz, C_6D_6 , 298 K): δ 27.50 (*Si(=S)Si(SiMe*₃)₃), -10.17 (*-Si(SiMe*₃)₃), -123.13 (*SiSi(SiMe*₃)₃) ppm. ESI-HRMS calcd. for $\text{C}_{24}\text{H}_{51}\text{N}_2\text{Si}_5\text{S}$ $[\text{M}+\text{H}]^+ = 539.2614$, found 539.2630.

Synthesis of **[PhC(*NtBu*)₂]SiSi(Si(CH₃)₃)₃Se (2.5)**

A mixture of **2.1** (0.245 g, 0.48 mmol) and Se (0.039 g, 0.49 mmol) was taken in a 100 mL Schlenk flask and toluene (10 mL) was added to the mixture. Immediately, after addition of solvent, the solution was turned to pale green. After stirring for 12 h at room temperature, the solution was filtered through cannula. The filtrate was concentrated to 2 mL and kept at -4 °C overnight to get colorless crystal of **2.5** suitable for single crystal X-ray analysis. Yield: 0.210 g (74.2%). Mp 221-222 °C. ^1H NMR (200 MHz, C_6D_6 , 298 K): δ 7.30 (d, $^3J_{\text{H-H}} = 6.69$ Hz, 1H, *Ph*), 7.02 (s, 1H, *Ph*), 7.05-6.84 (m, 3H, *Ph*), 1.26 (s, 18H, *tBu*), 0.54 (s, 27H, *SiMe*₃) ppm; $^{13}\text{C}\{^1\text{H}\}$ NMR (100.6 MHz, C_6D_6 , 298 K): δ 173.7 (NCN), 131.7 (*Ph*), 130.9 (*Ph*), 129.5 (*Ph*), 128.6 (*Ph*), 128.2 (*Ph*), 55.8 (*CMe*₃), 32.5 (*CMe*₃), 3.9 (*Si(SiMe*₃)₃) ppm; $^{29}\text{Si}\{^1\text{H}\}$ NMR (79.5 MHz, C_6D_6 , 298 K): δ 23.88 (*Si(=Se)Si(SiMe*₃)₃), -10.05 (*SiSi(SiMe*₃)₃), -119.99 (*SiSi(SiMe*₃)₃) ppm. ESI-HRMS calcd. for $\text{C}_{24}\text{H}_{51}\text{N}_2\text{Si}_5\text{Se}$ $[\text{M}+\text{H}]^+ = 587.2058$, found 587.2041.

Synthesis of **[PhC(*NtBu*)₂]SiSi(Si(CH₃)₃)₃Te (2.6)**

THF (10 mL) was added slowly to the mixture of **2.1** (0.200 g, 0.39 mmol) and Te (0.051 g, 0.49 mmol), taken in a 100 mL Schlenk flask. The suspension was stirred at room temperature for 36 h to form a greenish yellow mixture with a black precipitate. The volatiles were removed under reduced pressure, and the residue was extracted with toluene (10 mL). After filtration through cannula, the filtrate part was concentrated to 2 mL and kept at -4 °C overnight to get pale yellow crystal of **2.6** suitable for single crystal X-ray analysis. Yield: 0.123 g (49.0 %). Mp. 225-226 °C. ^1H NMR (200 MHz, C_6D_6 , 298 K): δ 7.31-6.94 (m, 5H, *Ph*), 1.27 (s, 18H, *tBu*), 0.50 (s, 27H, *SiMe*₃) ppm; $^{13}\text{C}\{^1\text{H}\}$ NMR (50.2 MHz, C_6D_6 , 298 K): δ 172.7 (NCN), 132.1 (*Ph*), 131.0 (*Ph*), 130.3 (*Ph*), 129.5 (*Ph*), 129.0 (*Ph*), 128.2 (*Ph*), 56.3 (*CMe*₃), 32.5 (*CMe*₃), 3.8 (*Si(SiMe*₃)₃) ppm;

$^{29}\text{Si}\{^1\text{H}\}$ NMR (79.5 MHz, C_6D_6 , 298 K): δ 1.82 ($\text{Si}(=\text{Te})\text{Si}(\text{SiMe}_3)_3$), -15.89 ($-\text{Si}(\text{SiMe}_3)_3$), -90.42 ($\text{SiSi}(\text{SiMe}_3)_3$) ppm. ESI-HRMS calcd. for $\text{C}_{24}\text{H}_{51}\text{N}_2\text{Si}_5\text{Te}$ $[\text{M}+\text{H}]^+ = 637.1955$, found 637.1929.

Synthesis of $[\text{PhC}(\text{N}t\text{Bu})_2]\text{SiSi}(\text{Si}(\text{CH}_3)_3)_3 \cdot \text{CH}_3\text{COCH}_3$ (**2.7**)

CH_3COCH_3 (35 μL , 0.60 mmol) was added to the 10 mL toluene solution of **2.1** (0.200 g, 0.59 mmol) at -78 $^\circ\text{C}$. The reaction mixture was allowed to warm to room temperature and stirred further for 6 h. After that all the volatiles were removed in vacuum and dissolved again in toluene (10 mL), and the solution was filtered through cannula. The resulting filtrate was supersaturated to get colorless crystals of **2.7** suitable for single crystal X-ray analysis. Yield: 0.227 g (67.9% yield). Mp. 139-140 $^\circ\text{C}$. ^1H NMR (200 MHz, C_6D_6 , 298 K): δ 7.28-7.00 (m, 5H, *Ph*), 1.83 (s, 3H, *CH*₃), 1.79 (s, 3H, *CH*₃), 1.36 (s, 9H, *tBu*), 1.21 (s, 9H, *tBu*), 0.65 (s, 27H, *SiMe*₃) ppm; $^{13}\text{C}\{^1\text{H}\}$ NMR (50.2 MHz, C_6D_6 , 298 K): δ 173.6 (NCN), 134.1 (*Ph*), 130.3 (*Ph*), 130.1 (*Ph*), 129.6 (*Ph*), 128.6 (*Ph*), 128.0 (*Ph*), 126.0 (*Ph*), 61.8 (*C(CH*₃)₂), 53.9 (*CMe*₃), 53.7 (*CMe*₃), 32.5 (*CMe*₃), 32.2 (*CMe*₃), 29.8 (*CH*₃), 28.4 (*CH*₃), 4.7 (*Si(SiMe*₃)₃) ppm; $^{29}\text{Si}\{^1\text{H}\}$ NMR (79.5 MHz, C_6D_6 , 298 K): δ -9.63 (*SiSi(SiMe*₃)₃), -96.42 (*SiSi(SiMe*₃)₃), -116.60 (*SiSi(SiMe*₃)₃) ppm.

Synthesis of $[\text{PhC}(\text{N}t\text{Bu})_2]\text{SiSi}(\text{Si}(\text{CH}_3)_3)_3 \cdot \text{BH}_3$ (**2.8**)

$\text{BH}_3 \cdot \text{SMe}_2$ (200 μL , 2 M, 0.39 mmol) was added to the 10 mL toluene solution of **2.1** (0.200 g, 0.39 mmol) at -35 $^\circ\text{C}$. The reaction mixture was allowed to warm to room temperature slowly and stirred further for 12 h. After that all the volatiles were removed in vacuum and dissolved again in toluene (10 mL), and the solution was filtered through canula. The resulting filtrate was concentrated (to about 3 mL), and was stored overnight in a freezer at -4 $^\circ\text{C}$ to afford colorless crystals of **2.8** suitable for single crystal X-ray analysis. Yield: 0.172 g (84.0%). Mp 200-201 $^\circ\text{C}$. ^1H NMR (200 MHz, C_6D_6 , 298 K): δ 7.32-7.28 (m, 1H, *Ph*), 7.14-7.08 (m, 1H, *Ph*), 7.00-6.87 (m, 3H, *Ph*), 1.17 (s, 18H, *tBu*), 0.49 (s, 27H, *SiMe*₃) ppm; $^{13}\text{C}\{^1\text{H}\}$ NMR (50.2 MHz, C_6D_6 , 298 K): δ 168.27 (NCN), 132.21 (*Ph*), 130.95 (*Ph*), 130.26 (*Ph*), 129.09 (*Ph*), 55.0 (*CMe*₃), 32.2 (*CMe*₃), 4.3 (*Si(SiMe*₃)₃) ppm; ^{11}B NMR (128.4 MHz, C_6D_6 , 298 K): δ -35.92 ppm; $^{29}\text{Si}\{^1\text{H}\}$ NMR (79.5 MHz, C_6D_6 , 298 K): δ 96.14 (*Si(BH*₃)*Si(SiMe*₃)₃), -8.21 (*SiSi(SiMe*₃)₃), -128.13 (*SiSi(SiMe*₃)₃) ppm. ESI-HRMS calcd. for $\text{C}_{24}\text{H}_{54}\text{N}_2\text{Si}_5\text{B}$ $[\text{M}+\text{H}]^+ = 521.3221$, found 521.3036.

Synthesis of [PhC(NtBu)₂]SiSi(Si(CH₃)₃)₃·9-BBN (2.9)

Toluene (5 mL) and THF (3 mL) was added to the mixture of **2.1** (0.100 g, 0.19 mmol) and 9-BBN (0.048 g, 0.19 mmol), taken in a 50 mL Schlenk flask at room temperature and stirred for 12 h. The solution was filtered through cannula and filtrate part was supersaturated to get colorless crystal of **2.9** suitable for single crystal X-ray analysis. (0.118 g, 80.0% yield). Mp 221-223 °C. ¹H NMR (200 MHz, C₆D₆, 298 K): δ 7.16-6.89 (m, 5H, *Ph*), 1.87-1.41 (br., 14H, CH), 1.16 (s, 18H, *t*Bu), 0.49 (s, 27H, SiMe₃) ppm; ¹³C{¹H} NMR (50.2 MHz, C₆D₆, 298 K): δ 167.5 (NCN), 141.2 (*Ph*), 138.1 (*Ph*), 131.3 (*Ph*), 130.3 (*Ph*), 129.6 (*Ph*), 126.0 (*Ph*), 54.7 (CMe₃), 38.1, 34.0 (CMe₃), 33.3, 32.3, 29.5, 28.2, 27.3, 24.0, 23.4, 22.9, 4.7 (Si(SiMe₃)₃) ppm; ¹¹B NMR (C₆D₆, 128.4 MHz): δ -10.5 ppm; ²⁹Si{¹H} NMR (79.5 MHz, C₆D₆, 298 K): δ 77.81 (Si(9-BBN)Si(SiMe₃)₃), -3.26 (SiSi(SiMe₃)₃), -123.79 (SiSi(SiMe₃)₃) ppm. ESI-HRMS calcd. for C₃₂H₆₆N₂Si₅B [M+H]⁺ = 629.4160, found 629.4686.

Synthesis of [PhC(NtBu)₂]SiSi(Si(CH₃)₃)₃·PhBCl₂ (2.10)

A solution of PhBCl₂ (0.097 g, 0.59 mmol) in toluene (10 mL) was added drop by drop to a solution of **2.1** (0.300 g, 0.59 mmol) in toluene at -78 °C, via cannula. The reaction mixture was allowed to warm to room temperature slowly and stirred further for 4 h. After that all the volatiles were removed in vacuum and dissolved again in toluene (10 mL), and the solution was filtered through canula. The resulting filtrate was concentrated in vacuo to about 3 mL and stored at -4°C in a freezer for overnight to obtain colorless crystals of compound **2.10**. (0.283 g, 72% yield). Mp: 156-157 °C. ¹H NMR (400 MHz, CDCl₃, 298 K): δ 7.89-7.91 (d, ³J_{H-H} = 8.13 Hz, 2H, *Ph*), 7.52-7.56 (m, 2H, *Ph*), 7.41-7.48 (m, 4H, *Ph*), 7.29 (m, 1H, *Ph*), 7.17 (t, 1H, *Ph*), 1.16 (s, 18H, *t*Bu), 0.40 (s, 27H, SiMe₃) ppm; ¹³C NMR (100.67 MHz, CDCl₃, 298 K): δ 172.2 (NCN), 133.6 (*Ph*), 131.9 (*Ph*), 131.0 (*Ph*), 130.8 (*Ph*), 129.3 (*Ph*), 128.2 (*Ph*), 127.9 (*Ph*), 127.7 (*Ph*), 126.9 (*Ph*), 120.0 (*Ph*), 54.7 (CMe₃), 31.6 (CMe₃), 30.9 (CMe₃), 4.09 (SiMe₃) ppm; ¹¹B NMR (160.4 MHz, CDCl₃, 298 K): δ 3.13 ppm; ²⁹Si{¹H} NMR (99.3 MHz, CDCl₃, 298 K): δ 55.62 (Si(PhBCl₂)Si(SiMe₃)₃), -7.91 (SiSi(SiMe₃)₃), -126.76 (SiSi(SiMe₃)₃) ppm.

Synthesis of [PhC(NtBu)₂]SiB(Ph)(Cl)SiCl(Si(CH₃)₃)₃ (2.11)

The solution of **2.10** (200 mg, 0.30 mmol) in 10 mL toluene was heated to 60 °C for 2 h with vigorous stirring. After that, the solution was filtered through canula and resulting filtrate was

dried in vacuo to obtain colorless powder of compound **2.11**. (0.150 g, 75% yield). Mp: 126-127 °C. ^1H NMR (200 MHz, C_6D_6 , 298 K): δ 8.26-8.28 (m, 1H, *Ph*), 7.45-7.49 (t, 2H, *Ph*), 7.21-7.24 (t, 3H, *Ph*), 6.91-6.95 (t, 2H, *Ph*), 6.78-6.82 (t, 2H, *Ph*), 1.19 (s, 9H, *tBu*), 1.05 (s, 9H, *tBu*), 0.48 (s, 27H, *SiMe*₃) ppm; ^{13}C NMR (100.6 MHz, CDCl_3 , 298 K): δ 178.2 (NCN), 135.4 (*Ph*), 134.5 (*Ph*), 133.4 (*Ph*), 131.9 (*Ph*), 130.7 (*Ph*), 129.8 (*Ph*), 129.6 (*Ph*), 128.9 (*Ph*), 126.8 (*Ph*), 126.0 (*Ph*), 125.8 (*Ph*), 65.8 (*CMe*₃), 59.5 (*CMe*₃), 35.5 (*CMe*₃), 34.9 (*CMe*₃), 4.6 (*SiMe*₃) ppm; ^{11}B NMR (160.4 MHz, CDCl_3 , 298 K): δ -0.45 ppm; ^{29}Si NMR (99.36 MHz, C_6D_6 , 298 K): δ 39.00 (*SiB(Ph)(Cl)SiCl(SiMe*₃)₃), -9.00 (*SiSi(SiMe*₃)₃), -103.74 (*SiSi(SiMe*₃)₃) ppm.

Synthesis of [**PhC(N*t*Bu)**]₂**SiSi(Si(CH₃)₃)₃·HBPin (2.12 and 2.13)**

To the 10 mL toluene solution of **2.1** (0.200 g, 0.39 mmol), 5 mL toluene solution of HBpin (0.051 g, 0.39 mmol) was added dropwise at room temperature and stirred for 12 h. After that all the volatiles were removed in vacuum to get sticky reaction mixture of **2.12** (54% yield) and **2.13** (31% yield).

Spectral details for **2.12**: ^1H NMR (200 MHz, C_6D_6 , 298 K): δ 7.12-7.00 (m, 5H, *Ph*), 1.24 (s, 18H, *tBu*), 1.01 (s, 12H, *Bpin*), 0.46 (s, 27H, *SiMe*₃) ppm; ^{11}B NMR (C_6D_6 , 128.4 MHz): δ 21.7 ppm; $^{29}\text{Si}\{^1\text{H}\}$ NMR (79.5 MHz, C_6D_6 , 298 K): δ 76.87 (*SiSi(SiMe*₃)₃), -9.10 (*SiSi(SiMe*₃)₃), -115.97 (*SiSi(SiMe*₃)₃) ppm.

Spectral details for **2.13**: ^1H NMR (200 MHz, C_6D_6 , 298 K): δ 7.84-7.83 (d, $J = 7.93$ Hz, 1H, *Ph*), 7.27-7.25 (m, 2H, *Ph*), 7.15-7.13 (m, 2H, *Ph*), 5.81 (s, 1H, NCHN), 1.32 (s, 12H, *Bpin*), 1.20 (s, 18H, *tBu*), 0.48 (s, 27H, *SiMe*₃) ppm; ^{11}B NMR (C_6D_6 , 128.4 MHz): δ 37.7 ppm; $^{29}\text{Si}\{^1\text{H}\}$ NMR (79.5 MHz, C_6D_6 , 298 K): δ -0.01 (*Si(SiMe*₃)₃), -59.97 (*Si(Bpin)(SiMe*₃)₃), -96.03 (*SiSi(SiMe*₃)₃) ppm.

Synthesis of compound [**PhC(N*t*Bu)**]₂**Bcat (2.14)**

To the 10 mL toluene solution of **2.1** (0.200 g, 0.39 mmol), 8 mL toluene solution of HBcat (0.048 g, 0.39 mmol) was added dropwise at -78 °C. The reaction mixture was allowed to warm to room temperature slowly and stirred further for 12 h. After that all the volatiles were removed in vacuum and dissolved again in toluene (10 mL), and the solution was filtered through canula. The resulting filtrate was supersaturated to get the colorless crystal of **2.14** (0.065 g, 47% yield). Mp: 117-118

°C. ^1H NMR (200 MHz, CDCl_3 , 298 K): δ 7.63 (t, 1H, *Ph*), 7.51 (t, 2H, *Ph*), 7.30 (d, $^3J_{\text{H-H}} = 8.38$ Hz, 2H, *Ph*), 6.80-6.75 (m, 2H, catechol-*Ph*), 6.73-6.69 (m, 2H, catechol-*Ph*), 0.98 (s, 18H, *t*Bu) ppm; $^{13}\text{C}\{^1\text{H}\}$ NMR (100.6 MHz, CDCl_3 , 298 K): δ 166.8 (NCN), 150.6 (*Ph*), 132.3 (*Ph*), 129.7 (*Ph*), 128.2 (*Ph*), 126.9 (*Ph*), 118.6 (*Ph*), 109.1 (*Ph*), 56.3 (CMe_3), 30.5 (CMe_3) ppm; ^{11}B NMR (CDCl_3 , 160.4 MHz, 298K): δ 14.1 ppm.

Synthesis of compound $[\text{PhC}(\text{N}t\text{Bu})_2]\text{Si}(=\text{NSiMe}_3)\text{Si}(\text{SiMe}_3)_3$ (**2.15**)

Trimethylsilyl azide (125 mg, 1.08 mmol) was added to the toluene (25 mL) solution of **2.1** (0.500 g, 0.98 mmol) at -35 °C. The reaction mixture was allowed to warm to room temperature slowly and stirred further for 6 h. After that all the volatiles were removed in vacuum and dried for 2 h. Compound was dissolved again in toluene (3 mL), and was stored overnight in a freezer at -4 °C to afford colorless crystals of **2.15** suitable for single crystal X-ray analysis (0.483 g, 82.5% yield). Mp: 159-160 °C. ^1H NMR (200 MHz, C_6D_6 , 298 K): δ 7.34-7.24 (m, 1H, *Ph*), 7.21-7.12 (m, 1H, *Ph*), 6.97-6.80 (m, 3H, *Ph*), 1.18 (s, 18H, *t*Bu), 0.54 (s, 9H, NSiMe_3), 0.51 (s, 27H, $\text{Si}(\text{SiMe}_3)_3$) ppm; $^{13}\text{C}\{^1\text{H}\}$ NMR (100.6 MHz, C_6D_6 , 298 K): δ 174.4 (NCN), 131.7 (*Ph*), 130.6 (*Ph*), 129.6 (*Ph*), 128.3 (*Ph*), 128.2 (*Ph*), 54.5 (CMe_3), 32.6 (CMe_3), 6.5 (SiMe_3), 4.1 (NSiMe_3) ppm; $^{29}\text{Si}\{^1\text{H}\}$ NMR (99.3 MHz, C_6D_6 , 298 K): δ -10.32 ($\text{Si}(\text{SiMe}_3)_3$), -22.08 ($=\text{NSiMe}_3$), -23.56 ($\text{Si}(\text{SiMe}_3)_3$), -43.03 ($\text{Si}(=\text{NSiMe}_3)\text{Si}(\text{SiMe}_3)_3$) ppm.

Synthesis of compound $[\text{PhC}(\text{N}t\text{Bu})_2]\text{Si}(=\text{NAd})\text{Si}(\text{SiMe}_3)_3$ (**2.16**)

15 mL toluene was added to the mixture of **2.1** (0.400 g, 0.78 mmol) and adamantly azide (140 mg, 0.78 mmol) at -35 °C. The reaction mixture was allowed to warm to room temperature slowly and stirred further for 12 h. After that all the volatiles were removed in vacuum and dried for 2-3 h and the residue was extracted with toluene (5 mL). The resulting filtrate was supersaturated to get pale-yellow crystals of **2.16** suitable for single crystal X-ray analysis. However, crude product was used for spectroscopic characterization. ^1H NMR (200 MHz, C_6D_6 , 298 K): δ 7.34-7.32 (d, $^3J_{\text{H-H}} = 7.25$ Hz, 1H, *Ph*), 7.13-6.88 (m, 4H, *Ph*), 2.29-2.24 (br, 6H, *Ad*), 1.92-1.70 (m, 9H, *Ad*), 1.24 (s, 18 H, *t*Bu), 0.57 (s, 27H, $\text{Si}(\text{SiMe}_3)_3$) ppm; $^{13}\text{C}\{^1\text{H}\}$ NMR (100.6 MHz, C_6D_6 , 298 K): δ 173.3 (NCN), 132.0 (*Ph*), 130.3 (*Ph*), 129.6 (*Ph*), 128.9 (*Ph*), 128.0 (*Ph*), 126.0 (*Ph*), 54.1 (CMe_3), 52.4 (*Ad*), 47.6 (*Ad*), 38.2 (*Ad*), 32.9 (*Ad*), 32.0 (CMe_3), 30.9 (*Ad*), 29.5 (*Ad*), 4.1 ($\text{Si}(\text{SiMe}_3)_3$) ppm; $^{29}\text{Si}\{^1\text{H}\}$ NMR (79.5 MHz, C_6D_6 , 298 K): δ 7.21 ($\text{Si}(\text{SiMe}_3)_3$), -11.86 ($\text{Si}(\text{SiMe}_3)_3$), -50.72 ($\text{Si}(=\text{NAd})\text{Si}(\text{SiMe}_3)_3$) ppm.

Synthesis of compound Si(PPh₂)₄ (2.17)

To the 20 mL toluene solution of **2.18** (0.500 g, 0.98 mmol), 10 mL toluene solution of Ph₂PCl (0.870 g, 3.94 mmol) was added dropwise at room temperature. Upon addition, the reaction mixture turned colorless and was stirred for 12 h. After that all the volatiles were removed in *vacuo* and washed with 10 mL n-hexane. Precipitate part was re-dissolved in toluene (10 mL), and the solution was filtered through canula. The resulting filtrate was concentrated to ~4 mL and stored at -4°C in a freezer for overnight to get colorless crystals of compound **2.17** (0.363 g, 48% yield). ¹H NMR (200 MHz, C₆D₆, 298 K): δ 7.56-7.52 (m, 16H, *Ph*), 6.97-6.94 (m, 24H, *Ph*) ppm; ¹³C{¹H} NMR (100.6 MHz, C₆D₆, 298 K): δ 135.1 (t, *Ph*), 129.2 (s, *Ph*), 128.9 (t, *Ph*) ppm; ³¹P NMR (C₆D₆, 161.9 MHz, 298 K): δ -14.9 ppm; ²⁹Si{¹H} NMR (99.3 MHz, C₆D₆, 298 K): δ -115.4 ppm. *Please note: Compound 2.17 always crystallizes along with benz-amidinate·HCl salt from this reaction.*

Synthesis of compound [PhC(N*t*Bu)₂]SiPtBu₂ (2.18)

10 mL toluene solution of *t*Bu₂PCl (0.241 g, 1.28 mmol) was added dropwise to the 20 mL toluene solution of **2.1** (0.650 g, 1.28 mmol) taken in a 50 mL Schlenk flask at -78 °C and stirred for 1 h. The reddish-yellow reaction mixture was allowed to warm to room temperature and stirred for additional 12 h. After that all the volatiles were removed under reduced pressure, dried for 2 h and the residue was extracted with *n*-hexane (10 mL). The solution was filtered through canula and resulting filtrate was concentrated to ~3 mL and stored at -4 °C for overnight to get the yellow crystal of **2.18** (0.225 g, 80.5% yield) Mp: 126-127 °C. ¹H NMR (500 MHz, C₆D₆, 298 K): δ 7.20-7.19 (d, ³J_{H-H} = 7.25 Hz, 1H, *Ph*), 7.05-7.04 (d, ³J_{H-H} = 7.63 Hz, 1H, *Ph*), 7.00-6.93 (m, 2H, *Ph*), 6.91-6.87 (t, 1H, *Ph*), 1.76-1.74 (d, ³J_{P-H} = 10.68 Hz, 9H, *PtBu*), 1.58-1.56 (d, 9H, ³J_{P-H} = 10.68 Hz, *PtBu*), 1.27 (s, 18H, C(CH₃)₃) ppm; ¹³C{¹H} NMR (100.6 MHz, C₆D₆, 298 K): δ 156.2 (d, NCN), 135.2 (d, *Ph*), 130.6 (d, *Ph*), 129.9 (*Ph*), 127.8 (*Ph*), 54.5 (CMe₃), 34.8 (*PtBu*), 33.7 (*PtBu*), 32.5 (d, CMe₃) ppm; ³¹P NMR (C₆D₆, 202.4 MHz, 298K): δ 25.3 ppm; ²⁹Si{¹H} NMR (99.3 MHz, C₆D₆, 298 K): δ 48.2 (d, J_{Si-P} = 196.18 Hz) ppm.

Synthesis of compound [PhC(N*t*Bu)₂]Si(=Si(P*i*Pr₂)₂)P*i*Pr₂ (2.19)

To the 15 mL toluene solution of **2.1** (0.300 g, 0.59 mmol), 10 mL toluene solution of *i*Pr₂PCl (0.271 g, 1.77 mmol) was added dropwise at -78 °C. The reaction mixture turned dark orange-red

upon addition of chlorodiisopropylphosphine. The reaction mixture was allowed to warm to room temperature slowly and stirred further for 6 h. After that all the volatiles were removed under reduced pressure, dried for 2 h and the residue was extracted with *n*-hexane (10 mL). The solution was filtered through canula and the resulting filtrate was supersaturated and stored at -35°C in a freezer for more than 30 days to get red crystals of **2.19** (0.320 g, 85% crude yield and $< 5\%$ crystal yield). ^1H NMR (200 MHz, C_6D_6 , 298 K): δ 7.04-7.03 (m, 3H, *Ph*), 6.96-6.92 (m, 2H, *Ph*), 2.42-2.34 (doublet of septet, 2H, $\text{CH}(\text{CH}_3)_2$), 1.83-1.74 (doublet of septet, 4H, $\text{CH}(\text{CH}_3)_2$), 1.30 (s, 18H, *t*Bu), 1.19-1.17 (m, 12H, $\text{CH}(\text{CH}_3)_2$), 1.07-0.99 (m, 24H, $\text{CH}(\text{CH}_3)_2$) ppm; $^{13}\text{C}\{^1\text{H}\}$ NMR (100.6 MHz, CDCl_3 , 298 K): δ 171.0 (NCN), 132.2 (*Ph*), 131.6 (*Ph*), 130.0 (d, *Ph*), 127.8 (d, *Ph*), 55.5 (CMe_3), 32.3(CMe_3), 29.5, 29.2, 24.9-24.6, 24.4-24.1, 23.8-23.7, 23.3-23.2, 17.4 ppm; ^{31}P NMR (C_6D_6 , 202.4 MHz, 298K): δ -8.80 { $\text{LSi}(\text{P}i\text{Pr}_2)=\text{Si}(\text{P}i\text{Pr}_2)_2$ }, -28.43 $\text{LSi}(\text{P}i\text{Pr}_2)=\text{Si}(\text{P}i\text{Pr}_2)_2$ } ppm; $^{29}\text{Si}\{^1\text{H}\}$ NMR (99.3 MHz, C_6D_6 , 298 K): δ 68.9–66.7 {m, $\text{LSi}(\text{P}i\text{Pr}_2)=\text{Si}(\text{P}i\text{Pr}_2)_2$ }, -94.5 $\text{LSi}(\text{P}i\text{Pr}_2)=\text{Si}(\text{P}i\text{Pr}_2)_2$ } ppm.

Synthesis of compound [$\text{PhC}(\text{N}t\text{Bu})_2$] $\text{Si}(=\text{Si}(\text{TMS})_2)$ PCy_2 (**2.20**)

To the 10 mL toluene solution of **2.1** (0.250 g, 0.49 mmol), 5 mL toluene solution of $\text{Cy}_2\text{P}i\text{Cl}$ (0.110 g, 0.44 mmol, 0.95 equiv. wrt **2.1**) was added dropwise at -78°C . The reaction mixture immediately turned dark orange-red upon addition of chlorodicyclohexylphosphine. The reaction mixture was allowed to stir for 1 h at -78°C and then additional 1 h at room temperature. After that all the volatiles were removed under reduced pressure, dried for 30 min and the residue was extracted with *n*-hexane (10 mL). The solution was filtered through canula and the resulting filtrate concentrated to ~ 2 mL and stored at -4°C in a freezer for overnight to get orange-red crystals of **2.20** (0.226 g, 72.6% yield). Mp: $143-145^{\circ}\text{C}$. ^1H NMR (200 MHz, C_6D_6 , 298 K): 7.49-7.47 (d, $^3J_{\text{H-H}} = 7.63$ Hz, 1H, *Ph*), 6.99-6.88 (m, 4H, *Ph*), 2.53-2.46 (br, 4H, *Cy*), 2.32-2.29 (br, 4H, *Cy*), 1.81-1.78 (br, 4H, *Cy*), 1.46 (br, 2H, *Cy*), 1.23 (s, 6H, *Cy*), 1.26 (s, 18H, *t*Bu), 0.74 (s, 18H, SiMe_3) ppm; $^{13}\text{C}\{^1\text{H}\}$ NMR (100.5 MHz, CDCl_3 , 298 K): δ 171.4 (NCN), 136.2 (*Ph*), 130.2 (*Ph*), 130.0 (*Ph*), 127.8 (*Ph*), 57.0 (CMe_3), 56.0 (CMe_3), 35.2, 34.8, 34.5, 34.2, 34.0, 33.8, 33.4, 33.0, 32.8 (CMe_3), 32.7 (CMe_3), 31.9, 31.7, 31.6, 30.5, 28.9, 28.2, 28.1, 27.7, 27.3, 27.2, 26.9, 26.7 (*Cy*), 3.2 (SiMe_3) ppm; ^{31}P NMR (C_6D_6 , 202.4 MHz, 298K): δ -14.77 { $\text{LSi}(\text{PCy}_2)=\text{Si}(\text{SiMe}_3)_2$ } ppm; $^{29}\text{Si}\{^1\text{H}\}$ NMR (99.3 MHz, C_6D_6 , 298 K): δ 73.12–71.99 {d, $J_{\text{Si-P}} = 112.62$ Hz,

LSi(PCy₂)=Si(SiMe₃)₂}, -7.61 {LSi(PCy₂)=Si(SiMe₃)₂}, -128.67– -128.91 {d, $J_{\text{Si-P}} = 123.52$ Hz, LSi(PCy₂)=Si(PCy₂)(SiMe₃)} ppm.

Synthesis of compound [PhC(N*t*Bu)₂]Si(=Si(PCy₂)(SiMe₃))PCy₂ (2.21)

To the 10 mL toluene solution of **2.1** (0.200 g, 0.39 mmol), 5 mL toluene solution of Cy₂PCl (0.183 g, 0.78 mmol) was added dropwise at -78 °C. The reaction mixture immediately turned dark orange-red upon addition of chlorodicyclohexylphosphine. The reaction mixture was allowed to stir for 1 h at -78 °C and then additional 3 h at room temperature. After that all the volatiles were removed under reduced pressure, dried for 2 h and the residue was extracted with *n*-hexane (10 mL). The solution was filtered through canula and the resulting filtrate concentrated to ~4 mL and stored at -4°C in a freezer for overnight to get orange-red crystals of **2.21** (0.235 g, 79% yield). Mp: 166-167 °C. ¹H NMR (200 MHz, C₆D₆, 298 K): δ 7.74-7.73 (d, $^3J_{\text{H-H}} = 6.87$ Hz, 1H, *Ph*), 7.02-7.01 (m, 1H, *Ph*), 6.94-6.90 (m, 3H, *Ph*), 2.51-2.45 (br, 5H, *Cy*), 2.38-2.35 (br, 5H, *Cy*), 2.28-2.23 ((br, 6H, *Cy*), 1.80-1.74 (m, 14H, *Cy*), 1.69-1.61 (m, 14H, *Cy*), 1.39 (s, 18H, *t*Bu), 0.76 (s, 9H, *SiMe*₃) ppm; ¹³C{¹H} NMR (125.7 MHz, CDCl₃, 298 K): δ 170.6 (NCN), 132.5 (*Ph*), 131.3 (*Ph*), 130.8 (*Ph*), 55.6 (CMe₃), 35.1, 34.8, 34.6, 34.4, 34.3, 33.8, 33.3, 33.0, 32.9 (*Cy*), 32.5 (CMe₃), 30.5, 29.5, 28.7, 28.5, 27.7, 27.6, 26.9 (*Cy*), 7.0 (*SiMe*₃) ppm; ³¹P NMR (C₆D₆, 202.4 MHz, 298K): δ -26.88 {LSi(PCy₂)=Si(PCy₂)(SiMe₃)}, -37.46 {LSi(PCy₂)=Si(PCy₂)(SiMe₃)} ppm; ²⁹Si{¹H} NMR (99.3 MHz, C₆D₆, 298 K): δ 73.67–72.15 {dd, $J_{\text{Si-P}} = 41.78$ Hz, LSi(PCy₂)=Si(PCy₂)(SiMe₃)}, -0.01 {LSi(PCy₂)=Si(PCy₂)(SiMe₃)}, -127.74– -129.02 {d, $J_{\text{Si-P}} = 127.16$ Hz, LSi(PCy₂)=Si(PCy₂)(SiMe₃)} ppm.

6.1.2. Crystal structure details of complex 2.1-2.10 and 2.13-2.21

Crystal Data for compound 2.1. CCDC 1895596. C₂₄H₅₀N₂Si₅, M = 507.11, pale yellow, 0.32 x 0.05 x 0.04 mm³, monoclinic, space group *P*2₁/*n*, *a* = 9.4918(9) Å, *b* = 35.546(3) Å, *c* = 9.7769(7) Å, $\alpha = \gamma = 90^\circ$, $\beta = 104.472(3)^\circ$, *V* = 3194.0(5) Å³, *Z* = 4, *T* = 100(2) K, $2\theta_{\text{max}} = 57.422^\circ$, *D*_{calc} (g.cm⁻³) = 1.055, *F*(000) = 1112.0, μ (mm⁻¹) = 0.237, 31467 reflections collected, 8253 unique reflections (*R*_{int} = 0.1015), 5748 observed (*I* > 2σ(*I*)) reflections, multi-scan absorption correction, *T*_{min} = 0.927, *T*_{max} = 0.991, 295 refined parameters, *S* = 1.123, *R*1 = 0.0825, *wR*2 = 0.1433 (all data *R* = 0.1289, *wR*2 = 0.1433), maximum and minimum residual electron densities; $\Delta\rho_{\text{max}} = 0.485$, $\Delta\rho_{\text{min}} = -0.383$ (eÅ³).

Crystal Data for compound 2.2. CCDC 1895537. $C_{48}H_{100}N_4Si_{10}O_2$, $M = 1046.21$, colorless, $0.13 \times 0.11 \times 0.04 \text{ mm}^3$, monoclinic, space group $P2_1/n$, $a = 12.6495(11) \text{ \AA}$, $b = 13.8221(14) \text{ \AA}$, $c = 17.5749(16) \text{ \AA}$, $\alpha = \gamma = 90^\circ$, $\beta = 103.549(3)^\circ$, $V = 2987.3(5) \text{ \AA}^3$, $Z = 2$, $T = 100(2) \text{ K}$, $2\theta_{\max} = 49.998^\circ$, $D_{\text{calc}} (\text{g.cm}^{-3}) = 1.163$, $F(000) = 1144.0$, $\mu (\text{mm}^{-1}) = 0.258$, 32784 reflections collected, 5252 unique reflections ($R_{\text{int}} = 0.1330$), 3691 observed ($I > 2\sigma(I)$) reflections, multi-scan absorption correction, $T_{\min} = 0.967$, $T_{\max} = 0.990$, 305 refined parameters, $S = 1.130$, $R1 = 0.0784$, $wR2 = 0.1743$ (all data $R = 0.1189$, $wR2 = 0.1743$), maximum and minimum residual electron densities; $\Delta\rho_{\max} = 0.898$, $\Delta\rho_{\min} = -0.401 (\text{e}\text{\AA}^{-3})$.

Crystal Data for compound 2.3. CCDC 1895535. $C_{48}H_{100}N_4Si_{10}O_4$, $M = 1078.21$, pale yellow, $0.14 \times 0.13 \times 0.12 \text{ mm}^3$, monoclinic, space group $P2_1/n$, $a = 12.8822(4) \text{ \AA}$, $b = 13.9371(4) \text{ \AA}$, $c = 18.0181(6) \text{ \AA}$, $\alpha = \gamma = 90^\circ$, $\beta = 106.435(2)^\circ$, $V = 3102.80(17) \text{ \AA}^3$, $Z = 2$, $T = 100(2) \text{ K}$, $2\theta_{\max} = 56.872^\circ$, $D_{\text{calc}} (\text{g.cm}^{-3}) = 1.154$, $F(000) = 1176.0$, $\mu (\text{mm}^{-1}) = 0.253$, 61812 reflections collected, 7797 unique reflections ($R_{\text{int}} = 0.1741$), 5044 observed ($I > 2\sigma(I)$) reflections, multi-scan absorption correction, $T_{\min} = 0.965$, $T_{\max} = 0.970$, 313 refined parameters, $S = 1.062$, $R1 = 0.0736$, $wR2 = 0.1476$ (all data $R = 0.1277$, $wR2 = 0.1476$), maximum and minimum residual electron densities; $\Delta\rho_{\max} = 0.465$, $\Delta\rho_{\min} = -0.373 (\text{e}\text{\AA}^{-3})$.

Crystal Data for compound 2.4. CCDC 1895536. $C_{24}H_{50}N_2Si_5S$, $M = 539.17$, colorless, $0.25 \times 0.22 \times 0.12 \text{ mm}^3$, monoclinic, space group $C2/c$, $a = 43.9485(16) \text{ \AA}$, $b = 9.3573(3) \text{ \AA}$, $c = 16.5044(6) \text{ \AA}$, $\alpha = \gamma = 90^\circ$, $\beta = 105.528(2)^\circ$, $V = 6539.5(4) \text{ \AA}^3$, $Z = 8$, $T = 100(2) \text{ K}$, $2\theta_{\max} = 55.000^\circ$, $D_{\text{calc}} (\text{g.cm}^{-3}) = 1.095$, $F(000) = 2352.0$, $\mu (\text{mm}^{-1}) = 0.297$, 62042 reflections collected, 7520 unique reflections ($R_{\text{int}} = 0.0440$), 6446 observed ($I > 2\sigma(I)$) reflections, multi-scan absorption correction, $T_{\min} = 0.928$, $T_{\max} = 0.965$, 304 refined parameters, $S = 1.054$, $R1 = 0.0374$, $wR2 = 0.0863$ (all data $R = 0.0480$, $wR2 = 0.0863$), maximum and minimum residual electron densities; $\Delta\rho_{\max} = 0.398$, $\Delta\rho_{\min} = -0.277 (\text{e}\text{\AA}^{-3})$.

Crystal Data for compound 2.5. CCDC 1895606. $C_{24}H_{50}N_2Si_5Se$, $M = 586.07$, colorless, $0.37 \times 0.29 \times 0.13 \text{ mm}^3$, monoclinic, space group $P2_1$, $a = 16.2732(10) \text{ \AA}$, $b = 9.6437(6) \text{ \AA}$, $c = 21.0296(11) \text{ \AA}$, $\alpha = \gamma = 90^\circ$, $\beta = 96.349(3)^\circ$, $V = 3280.0(3) \text{ \AA}^3$, $Z = 4$, $T = 100(2) \text{ K}$, $2\theta_{\max} = 51.996^\circ$, $D_{\text{calc}} (\text{g.cm}^{-3}) = 1.187$, $F(000) = 1248.0$, $\mu (\text{mm}^{-1}) = 1.342$, 52788 reflections collected, 12370 unique reflections ($R_{\text{int}} = 0.0935$), 11079 observed ($I > 2\sigma(I)$) reflections, multi-scan absorption

correction, $T_{\min} = 0.603$, $T_{\max} = 0.840$, 608 refined parameters, $S = 1.073$, $R1 = 0.0872$, $wR2 = 0.2251$ (all data $R = 0.1023$, $wR2 = 0.2251$), maximum and minimum residual electron densities; $\Delta\rho_{\max} = 3.207$, $\Delta\rho_{\min} = -0.918$ ($e\text{\AA}^3$).

Crystal Data for compound 2.6. CCDC 1895590. $C_{24}H_{50}N_2Si_5Te$, $M = 634.71$, yellow, $0.28 \times 0.22 \times 0.12$ mm³, orthorhombic, space group $P2_12_12_1$, $a = 9.5611(5)$ Å, $b = 16.4263(11)$ Å, $c = 21.3294(14)$ Å, $\alpha = \beta = \gamma = 90^\circ$, $V = 3349.9(4)$ Å³, $Z = 4$, $T = 100(2)$ K, $2\theta_{\max} = 69.336^\circ$, D_{calc} ($\text{g}\cdot\text{cm}^{-3}$) = 1.258, $F(000) = 1320.0$, μ (mm^{-1}) = 1.081, 135345 reflections collected, 13356 unique reflections ($R_{\text{int}} = 0.0488$), 11312 observed ($I > 2\sigma(I)$) reflections, multi-scan absorption correction, $T_{\min} = 0.752$, $T_{\max} = 0.878$, 304 refined parameters, $S = 0.917$, $R1 = 0.0358$, $wR2 = 0.1211$ (all data $R = 0.0553$, $wR2 = 0.1211$), maximum and minimum residual electron densities; $\Delta\rho_{\max} = 0.685$, $\Delta\rho_{\min} = -2.185$ ($e\text{\AA}^3$).

Crystal Data for compound 2.7. CCDC 1895534. $C_{27}H_{56}N_2OSi_5$, $M = 565.18$, colorless, $0.18 \times 0.12 \times 0.04$ mm³, monoclinic, space group $P2_1/c$, $a = 9.652(5)$ Å, $b = 16.504(8)$ Å, $c = 21.958(11)$ Å, $\alpha = \gamma = 90^\circ$, $\beta = 98.308(11)^\circ$, $V = 3461(3)\text{\AA}^3$, $Z = 4$, $T = 296(2)\text{K}$, $2\theta_{\max} = 52.488^\circ$, D_{calc} ($\text{g}\cdot\text{cm}^{-3}$) = 1.085, $F(000) = 1240.0$, μ (mm^{-1}) = 0.227, 11635 reflections collected, 6703 unique reflections ($R_{\text{int}} = 0.1855$), 2347 observed ($I > 2\sigma(I)$) reflections, multi-scan absorption correction, $T_{\min} = 0.960$, $T_{\max} = 0.991$, 334 refined parameters, $S = 0.937$, $R1 = 0.0948$, $wR2 = 0.2063$ (all data $R = 0.2664$, $wR2 = 0.2063$), maximum and minimum residual electron densities; $\Delta\rho_{\max} = 0.507$, $\Delta\rho_{\min} = -0.495$ ($e\text{\AA}^3$).

Crystal Data for compound 2.8. CCDC 1895595. $C_{24}H_{53}BN_2Si_5$, $M = 520.94$, colorless, $0.21 \times 0.17 \times 0.06$ mm³, triclinic, space group $P-1$, $a = 9.107(3)$ Å, $b = 9.783(3)$ Å, $c = 19.471(6)$ Å, $\alpha = 96.995(7)^\circ$, $\beta = 90.177(7)^\circ$, $\gamma = 106.574(7)^\circ$, $V = 1649.0(8)$ Å³, $Z = 2$, $T = 296(2)$ K, $2\theta_{\max} = 57.15^\circ$, D_{calc} ($\text{g}\cdot\text{cm}^{-3}$) = 1.049, $F(000) = 572.0$, μ (mm^{-1}) = 0.231, 74149 reflections collected, 8275 unique reflections ($R_{\text{int}} = 0.0920$), 5893 observed ($I > 2\sigma(I)$) reflections, multi-scan absorption correction, $T_{\min} = 0.954$, $T_{\max} = 0.986$, 316 refined parameters, $S = 1.281$, $R1 = 0.0420$, $wR2 = 0.1029$ (all data $R = 0.0766$, $wR2 = 0.1029$), maximum and minimum residual electron densities; $\Delta\rho_{\max} = 0.349$, $\Delta\rho_{\min} = -0.280$ ($e\text{\AA}^3$).

Crystal Data for compound 2.9. CCDC 1895594. $C_{32}H_{65}BN_2Si_5$, $M = 629.12$, colorless, $0.24 \times 0.19 \times 0.05 \text{ mm}^3$, orthorhombic, space group $Pbca$, $a = 19.5064(18) \text{ \AA}$, $b = 18.6573(15) \text{ \AA}$, $c = 20.996(2) \text{ \AA}$, $\alpha = \beta = \gamma = 90^\circ$, $V = 7641.4(12) \text{ \AA}^3$, $Z = 8$, $T = 100(2) \text{ K}$, $2\theta_{\text{max}} = 52.0^\circ$, $D_{\text{calc}} (\text{g}\cdot\text{cm}^{-3}) = 1.094$, $F(000) = 2768.0$, $\mu (\text{mm}^{-1}) = 0.210$, 132793 reflections collected, 7502 unique reflections ($R_{\text{int}} = 0.1749$), 5809 observed ($I > 2\sigma(I)$) reflections, multi-scan absorption correction, $T_{\text{min}} = 0.951$, $T_{\text{max}} = 0.990$, 380 refined parameters, $S = 1.109$, $R1 = 0.0669$, $wR2 = 0.0944$ (all data $R = 0.0944$, $wR2 = 0.0944$), maximum and minimum residual electron densities; $\Delta\rho_{\text{max}} = 0.346$, $\Delta\rho_{\text{min}} = -0.365 (\text{e}\text{\AA}^3)$.

Crystal data for compound 2.10. CCDC 2039629. $C_{30}H_{55}BCl_2N_2Si_5$, $M = 665.92$, colorless, $0.18 \times 0.11 \times 0.07 \text{ mm}^3$, monoclinic, space group $P2_1yb$, $a = 9.6721(5) \text{ \AA}$, $b = 18.2279(7) \text{ \AA}$, $c = 11.4391(5) \text{ \AA}$, $\alpha = \gamma = 90^\circ$, $\beta = 105.099(2)^\circ$, $V = 1947.11(15) \text{ \AA}^3$, $Z = 2$, $T = 301(2) \text{ K}$, $2\theta_{\text{max}} = 56.75^\circ$, $D_{\text{calc}} (\text{g cm}^{-3}) = 1.136$, $F(000) = 716.0$, $\mu (\text{mm}^{-1}) = 0.342$, 33122 reflections collected, 9698 unique reflections ($R_{\text{int}} = 0.0584$), 7559 observed ($I > 2\sigma(I)$) reflections, multi-scan absorption correction, $T_{\text{min}} = 0.940$, $T_{\text{max}} = 0.976$, 376 refined parameters, $S = 0.807$, $R1 = 0.0415$, $wR2 = 0.1340$ (all data $R = 0.0634$, $wR2 = 0.1340$), maximum and minimum residual electron densities; $\Delta\rho_{\text{max}} = 0.176$, $\Delta\rho_{\text{min}} = -0.225 (\text{e}\text{\AA}^3)$.

Crystal data for compound 2.14: CCDC 1993346. $C_{21}H_{27}BN_2O_2$, $M = 350.25$, colorless, $0.21 \times 0.18 \times 0.08 \text{ mm}^3$, orthorhombic, space group $P2_1ac2_1ab$, $a = 8.8777(10) \text{ \AA}$, $b = 11.0310(13) \text{ \AA}$, $c = 19.949(2) \text{ \AA}$, $\alpha = \beta = \gamma = 90^\circ$, $V = 1953.6(4) \text{ \AA}^3$, $Z = 4$, $T = 100 \text{ K}$, $2\theta_{\text{max}} = 56.644^\circ$, $D_{\text{calc}} (\text{g cm}^{-3}) = 1.191$, $F(000) = 752.0$, $\mu (\text{mm}^{-1}) = 0.076$, 58998 reflections collected, 4861 unique reflections ($R_{\text{int}} = 0.0901$), 4395 observed ($I > 2\sigma(I)$) reflections, multi-scan absorption correction, $T_{\text{min}} = 0.984$, $T_{\text{max}} = 0.994$, 242 refined parameters, $S = 1.128$, $R1 = 0.0493$, $wR2 = 0.0916$ (all data $R = 0.0573$, $wR2 = 0.0916$), maximum and minimum residual electron densities; $\Delta\rho_{\text{max}} = 0.260$, $\Delta\rho_{\text{min}} = -0.177 (\text{e}\text{\AA}^3)$.

Crystal data for compound 2.16: $C_{34}H_{65}N_3Si_5$, $M = 656.34$, pale yellow, $0.25 \times 0.14 \times 0.12 \text{ mm}^3$, triclinic, space group $P-1$, $a = 10.232(4) \text{ \AA}$, $b = 11.462(4) \text{ \AA}$, $c = 18.283(7) \text{ \AA}$, $\alpha = 73.178(9)^\circ$, $\beta = 77.265(9)^\circ$, $\gamma = 87.278(9)^\circ$, $V = 2001.6(13) \text{ \AA}^3$, $Z = 2$, $T = 296(2) \text{ K}$, $2\theta_{\text{max}} = 48.998^\circ$, $D_{\text{calc}} (\text{g cm}^{-3}) = 1.089$, $F(000) = 720.0$, $\mu (\text{mm}^{-1}) = 0.204$, 31747 reflections collected, 6665 unique reflections ($R_{\text{int}} = 0.1896$), 3104 observed ($I > 2\sigma(I)$) reflections, multi-scan absorption correction,

$T_{\min} = 0.950$, $T_{\max} = 0.976$, 394 refined parameters, $S = 1.023$, $R1 = 0.1056$, $wR2 = 0.2874$ (all data $R = 0.2249$, $wR2 = 0.2874$), maximum and minimum residual electron densities; $\Delta\rho_{\max} = 1.492$, $\Delta\rho_{\min} = -0.639$ ($\text{e}\text{\AA}^3$).

Crystal data for compound 2.17: $\text{C}_{48}\text{H}_{40}\text{P}_4\text{Si}$, $2(\text{C}_7\text{H}_8)$, $M = 924.99$, colorless, $0.22 \times 0.12 \times 0.08$ mm^3 , orthorhombic, space group $Fddd$, $a = 16.9651(8)$ \AA , $b = 17.8178(8)$ \AA , $c = 33.5851(15)$ \AA , $\alpha = \beta = \gamma = 90^\circ$, $V = 10152.1(8)$ \AA^3 , $Z = 8$, $T = 296(2)$ K, $2\theta_{\max} = 55.5^\circ$, D_{calc} (g cm^{-3}) = 1.210, $F(000) = 4016$, μ (mm^{-1}) = 0.211, 42647 reflections collected, 3188 unique reflections ($R_{\text{int}} = 0.0710$), 2533 observed ($I > 2\sigma(I)$) reflections, multi-scan absorption correction, $T_{\min} = 0.912$, $T_{\max} = 0.967$, 149 refined parameters, $S = 1.369$, $R1 = 0.0531$, $wR2 = 0.1363$ (all data $R = 0.0825$, $wR2 = 0.1363$), maximum and minimum residual electron densities; $\Delta\rho_{\max} = 0.707$, $\Delta\rho_{\min} = -0.460$ ($\text{e}\text{\AA}^3$).

Crystal data for compound 2.18: $\text{C}_{23}\text{H}_{41}\text{N}_2\text{PSi}$, $M = 404.64$, yellow, $0.21 \times 0.15 \times 0.11$ mm^3 , monoclinic, space group $P2_1/c$, $a = 14.8313(4)$ \AA , $b = 10.7456(3)$ \AA , $c = 16.0057(5)$ \AA , $\alpha = \gamma = 90^\circ$, $\beta = 106.7500(10)^\circ$, $V = 2442.62(12)$ \AA^3 , $Z = 4$, $T = 100(2)$ K, $2\theta_{\max} = 84.74^\circ$, D_{calc} ($\text{g}\cdot\text{cm}^{-3}$) = 1.100, $F(000) = 888.0$, μ (mm^{-1}) = 0.172, 112509 reflections collected, 22039 unique reflections ($R_{\text{int}} = 0.0797$), 13785 observed ($I > 2\sigma(I)$) reflections, multi-scan absorption correction, $T_{\min} = 0.965$, $T_{\max} = 0.981$, 256 refined parameters, $S = 0.931$, $R1 = 0.0518$, $wR2 = 0.1858$ (all data $R = 0.1044$, $wR2 = 0.1858$), maximum and minimum residual electron densities; $\Delta\rho_{\max} = 2.023$, $\Delta\rho_{\min} = -0.791$ ($\text{e}\text{\AA}^3$).

Crystal data for compound 2.19: $\text{C}_{33}\text{H}_{65}\text{N}_2\text{P}_3\text{Si}_2$, $M = 638.96$, orange, $0.28 \times 0.15 \times 0.02$ mm^3 , triclinic, space group $P-1$, $a = 11.8079(5)$ \AA , $b = 11.9281(5)$ \AA , $c = 14.7611(6)$ \AA , $\alpha = 111.9750(10)^\circ$, $\beta = 90.2060(10)^\circ$, $\gamma = 92.7860(10)^\circ$, $V = 1925.18(14)$ \AA^3 , $Z = 2$, $T = 100(2)$ K, $2\theta_{\max} = 82.04^\circ$, D_{calc} ($\text{g}\cdot\text{cm}^{-3}$) = 1.102, $F(000) = 700.0$, μ (mm^{-1}) = 0.240, 227326 reflections collected, 25235 unique reflections ($R_{\text{int}} = 0.0804$), 17485 observed ($I > 2\sigma(I)$) reflections, multi-scan absorption correction, $T_{\min} = 0.958$, $T_{\max} = 0.995$, 379 refined parameters, $S = 1.228$, $R1 = 0.0543$, $wR2 = 0.2065$ (all data $R = 0.0999$, $wR2 = 0.2065$), maximum and minimum residual electron densities; $\Delta\rho_{\max} = 0.771$, $\Delta\rho_{\min} = -0.884$ ($\text{e}\text{\AA}^3$).

Crystal data for compound 2.20: C₃₃H₆₃N₂PSi₄, M = 631.18, orange, 0.21 x 0.14 x 0.06 mm³, monoclinic, space group *P2₁/c*, *a* = 10.8454(18) Å, *b* = 18.482(3) Å, *c* = 19.518(4) Å, $\alpha = \gamma = 90^\circ$, $\beta = 104.318(5)^\circ$, *V* = 3790.6(12) Å³, *Z* = 4, *T* = 100(2) K, $2\theta_{\max} = 55.60^\circ$, *D*_{calc} (g.cm⁻³) = 1.106, *F*(000) = 1384.0, μ (mm⁻¹) = 0.222, 161072 reflections collected, 9452 unique reflections (*R*_{int} = 0.1107), 7471 observed (*I* > 2σ(*I*)) reflections, multi-scan absorption correction, *T*_{min} = 0.955, *T*_{max} = 0.987, 373 refined parameters, *S* = 1.192, *R*1 = 0.0544, *wR*2 = 0.1726 (all data *R* = 0.0748, *wR*2 = 0.1726), maximum and minimum residual electron densities; $\Delta\rho_{\max} = 0.637$, $\Delta\rho_{\min} = -0.526$ (eÅ⁻³).

Crystal data for compound 2.21: C₄₂H₇₆N₂P₂Si₃, M = 755.25, orange, 0.15 x 0.09 x 0.05 mm³, triclinic, space group *P*-1, *a* = 12.7206(6) Å, *b* = 13.1115(6) Å, *c* = 15.2568(6) Å, $\alpha = 65.3310(10)^\circ$, $\beta = 82.3740(10)^\circ$, $\gamma = 76.975(2)^\circ$, *V* = 2250.75(17) Å³, *Z* = 2, *T* = 100(2) K, $2\theta_{\max} = 56.61^\circ$, *D*_{calc} (g.cm⁻³) = 1.114, *F*(000) = 828.0, μ (mm⁻¹) = 0.206, 63818 reflections collected, 11089 unique reflections (*R*_{int} = 0.0835), 8142 observed (*I* > 2σ(*I*)) reflections, multi-scan absorption correction, *T*_{min} = 0.970, *T*_{max} = 0.990, 451 refined parameters, *S* = 0.978, *R*1 = 0.0508, *wR*2 = 0.1571 (all data *R* = 0.0835, *wR*2 = 0.1571), maximum and minimum residual electron densities; $\Delta\rho_{\max} = 0.619$, $\Delta\rho_{\min} = -0.619$ (eÅ⁻³).

6.2: Chapter 3 experimental details

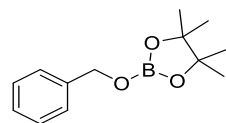
6.2.1. General procedure for the catalytic hydroboration of aldehydes:

Aldehyde (0.5 mmol), pinacolborane (0.5 mmol), catalyst **3** (1 mol%), benzene (1 mL) were charged in a Schlenk tube with a magnetic bead inside the glove box. The reaction mixture was allowed to stir at room temperature. The progress of the reaction was monitored by ¹H NMR, which indicated the completion of the reaction by the disappearance of aldehyde (RCHO) proton and appearance of a new OCH₂ resonance.

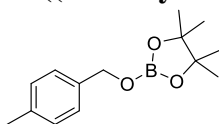
For isolation of corresponding primary alcohol of some aldehydes, reactions were scaled up and carried out at same reaction condition as mentioned. Upon completion of the reaction, resulted boronate ester residue were hydrolyzed by silica gel with methanol at 60 °C for 4–6 hrs. The completion of hydrolysis was checked by TLC. Upon completion, the reaction mixture was filtered and washed three times with dichloromethane. The combined organic layers were dried, evaporated and the residue was purified by column chromatography over silica gel (100–200 mesh) with pet ether/ethyl acetate (20:1) mixture as eluent, which provided the pure primary alcohols.

6.2.2. Spectroscopic data for the hydroboration product of aldehydes

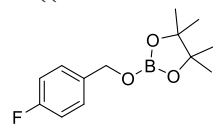
2-(benzyloxy)-pinacolborane (3a): ^1H NMR (CDCl_3 , 200 MHz, 298 K): δ 7.28-7.18 (m, 5H, ArH), 4.85 (s, 2H, OCH_2), 1.18 (s, 12H, CH_3) ppm; $^{13}\text{C}\{^1\text{H}\}$ NMR (CDCl_3 , 50.2 MHz, 298 K): δ 139.1 (Ph), 128.2 (Ph), 127.2 (Ph), 126.6 (Ph), 82.9 ($\text{C}(\text{CH}_3)_2$), 66.5 (CH_2), 24.4 (CH_3) ppm.



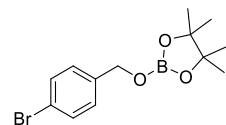
2-((4-methylbenzyl)oxy)-pinacolborane (3b): ^1H NMR (CDCl_3 , 200 MHz, 298 K): δ 7.18-7.14 (d, $^3J_{\text{H-H}} = 8.0$ Hz, 2H, ArH), 7.07-7.03 (d, $^3J_{\text{H-H}} = 7.9$ Hz, 2H, ArH), 4.80 (s, 2H, CH_2), 2.25 (s, 3H, Ar CH_3), 1.18 (s, 12H, CH_3) ppm; $^{13}\text{C}\{^1\text{H}\}$ NMR (CDCl_3 , 50.2 MHz, 298 K): δ 139.9 (Ph), 136.2 (Ph), 126.8 (Ph), 126.7 (Ph), 82.8 ($\text{C}(\text{CH}_3)_2$), 66.5 (CH_2), 24.5 (CH_3), 21.0 (Ar- CH_3) ppm.



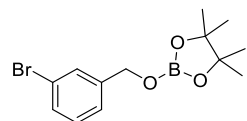
2-((4-fluorobenzyl)oxy)-pinacolborane (3c): ^1H NMR (CDCl_3 , 200 MHz, 298 K): δ 7.30-6.85 (m, 4H, ArH), 4.80 (s, 2H, CH_2), 1.19 (s, 12H, CH_3) ppm; $^{13}\text{C}\{^1\text{H}\}$ NMR (CDCl_3 , 50.2 MHz, 298 K): δ 162.1 (d, $J_{\text{C-F}} = 245.17$ Hz, Ph), 134.8 (Ph), 128.5 (d, $J_{\text{C-F}} = 8.05$ Hz, Ph), 115.0 (d, $J_{\text{C-F}} = 21.22$ Hz, Ph), 83.0 ($\text{C}(\text{CH}_3)_2$), 65.9 (CH_2), 24.5 (CH_3) ppm.



2-((4-bromobenzyl)oxy)-pinacolborane (3d): ^1H NMR (CDCl_3 , 200 MHz, 298 K): δ 7.36 (d, 2H, ArH), 7.12 (d, 2H, ArH), 4.78 (s, 2H, CH_2), 1.18 (s, 12H, CH_3) ppm.

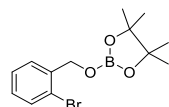


2-((3-bromobenzyl)oxy)-pinacolborane (3e): ^1H NMR (CDCl_3 , 200 MHz, 298 K): δ 7.49-7.06



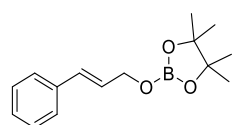
(m, 4H, ArH), 4.81 (s, 2H, CH_2), 1.19 (s, 12H, CH_3) ppm; $^{13}\text{C}\{^1\text{H}\}$ NMR (CDCl_3 , 50.2 MHz, 298 K): δ 141.45 (Ph), 137. (Ph), 130.3 (Ph), 129.8 (Ph), 129.6 (Ph), 125.0 (Ph), 83.1 ($\text{C}(\text{CH}_3)_2$), 65.7 (CH_2), 24.5 (CH_3) ppm.

2-((2-bromobenzyl)oxy)-pinacolborane (3f): ^1H NMR (CDCl_3 , 200 MHz, 298 K): δ 7.47-



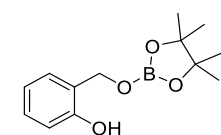
6.97(m, 4H, ArH), 4.90(s, 2H, CH_2), 1.19 (s, 12H, CH_3) ppm; $^{13}\text{C}\{^1\text{H}\}$ NMR (CDCl_3 , 50.2 MHz, 298 K): δ 138.2 (Ph), 132.1 (Ph), 128.5 (Ph), 127.7 (Ph), 127.2 (Ph), 121.4 (Ph), 83.0 ($\text{C}(\text{CH}_3)_2$), 66.2 (CH_2), 24.5 (CH_3) ppm.

2-(cinnamyloxy)-pinacolborane (3g): ^1H NMR (CDCl_3 , 200 MHz, 298 K): δ 7.32-7.09 (m, 5H,



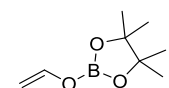
ArH), 6.61-6.49 (d, 1H, $^3J_{\text{H-H}} = 15.7$ Hz, 1H ArCH), 6.29-6.13 (m, 1H, CHCH), 4.48-4.45 (d, 2H, $^3J_{\text{H-H}} = 5.3$ Hz, CH_2), 1.18 (s, 12H, CH_3) ppm; $^{13}\text{C}\{^1\text{H}\}$ NMR (CDCl_3 , 50.2 MHz, 298 K): δ 136.7 (Ph), 130.5 (Ar-CHCH), 128.4 (Ar-CH), 127.4 (Ph), 126.6 (Ph), 126.3 (Ph), 82.8 ($\text{C}(\text{CH}_3)_2$), 65.1 (CH_2), 24.5 (CH_3) ppm.

2-(2-hydroxybenzyloxy)-pinacolborane (3h): ^1H NMR (CDCl_3 , 200 MHz, 298 K): δ 17.11-7.07



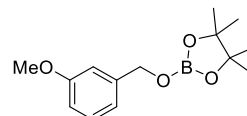
(d, $^3J_{\text{H-H}} = 7.58$ Hz, 2H, ArH), 6.84-6.79 (m, 2H, ArH), 4.90 (s, 2H, CH_2), 1.19 (s, 12H, CH_3) ppm; $^{13}\text{C}\{^1\text{H}\}$ NMR (CDCl_3 , 50.2 MHz, 298 K): δ 152.0 (ArC-OH), 129.5 (Ph), 129.2 (Ph), 128.2 (Ph), 124.1 (Ph), 116.8 (Ph), 83.5 ($\text{C}(\text{CH}_3)_2$), 64.5 (CH_2), 24.4 (CH_3) ppm.

2-(4-hydroxybenzyloxy)-pinacolborane (3i): ^1H NMR (CDCl_3 , 200 MHz, 298 K): δ 7.19-6.90



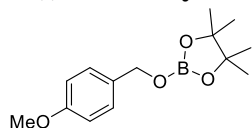
(m, 4H, ArH), 4.76 (s, 2H, CH_2), 1.18 (s, 12H, CH_3) ppm; $^{13}\text{C}\{^1\text{H}\}$ NMR (CDCl_3 , 50.2 MHz, 298 K): δ 155.5 (ArC-OH), 132.4 (Ph), 128.1 (Ph), 124.1 (Ph), 116.0 (Ph), 83.0 ($\text{C}(\text{CH}_3)_2$), 66.5 (CH_2), 24.4 (CH_3) ppm.

2-((3-methoxybenzyl)oxy)-pinacolborane (3j): ^1H NMR (CDCl_3 , 200 MHz, 298 K): δ 7.20-6.67



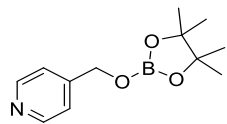
(m, 4H, ArH), 4.83 (s, 2H, CH_2), 3.71 (s, 3H, OCH_3), 1.18 (s, 12H, CH_3) ppm; $^{13}\text{C}\{^1\text{H}\}$ NMR (CDCl_3 , 50.2 MHz, 298 K): δ 159.5 (ArC-OMe), 140.7 (Ph), 129.2 (Ph), 118.7 (Ph), 113.0 (Ph), 111.7 (Ph), 82.9 ($\text{C}(\text{CH}_3)_2$), 66.4 (CH_2), 55.0 (OCH_3), 24.5 (CH_3) ppm.

2-(((4-methoxybenzyl)oxy)-pinacolborane (3k): $^1\text{H NMR}$ (CDCl_3 , 200 MHz, 298 K): δ 7.22-7.17



(d, $^3J_{\text{H-H}} = 8.84$ Hz, 2H, ArH), 6.80-6.76 (d, $^3J_{\text{H-H}} = 8.72$ Hz, 2H, ArH), 4.77 (s, 2H, CH_2), 3.70 (s, 3H, OCH_3), 1.18 (s, 12H, CH_3) ppm.

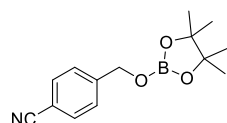
4-(((4,4,5,5-tetramethyl-1,3,2-dioxaborolan-2-yl)oxy)methyl)pyridine (3l): $^1\text{H NMR}$ (CDCl_3 ,



200 MHz, 298 K): δ 8.51-8.48 (d, $^3J_{\text{H-H}} = 6.06$ Hz, 2H, ArH), 7.21-7.18 (d, $^3J_{\text{H-H}} = 5.81$ Hz, 2H, ArH), 4.87 (s, 2H, CH_2), 1.19 (s, 12H, CH_3) ppm; $^{13}\text{C}\{^1\text{H}\}$ NMR (CDCl_3 , 50.2 MHz, 298 K): δ 149.3 (Ar), 128.2 (Ar), 120.8 (Ar), 83.2

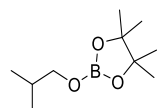
($\text{C}(\text{CH}_3)_2$), 64.8 (CH_2), 24.4 (CH_3) ppm.

4-(((4,4,5,5-tetramethyl-1,3,2-dioxaborolan-2-yl)oxy)methyl)benzotrile (3m): $^1\text{H NMR}$



(CDCl_3 , 200 MHz, 298 K): δ 7.56-7.52 (d, $^3J_{\text{H-H}} = 8.46$ Hz, 2H, ArH), 7.38-7.33 (d, $^3J_{\text{H-H}} = 7.83$ Hz, 2H, ArH), 4.89 (s, 2H, CH_2), 1.19 (s, 12H, CH_3) ppm.

2-isobutoxy-4,4,5,5-tetramethyl-1,3,2-dioxaborolane (3n): $^1\text{H NMR}$ (CDCl_3 , 200 MHz, 298 K):

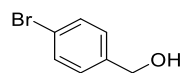


δ 3.60 (d, $^3J_{\text{H-H}} = 6.57$ Hz, 2H, CH_2), 1.81 (sept, 1H, $\text{CH}(\text{CH}_3)_2$), 1.25 (s, 12H, CH_3), 0.88 (d, $^3J_{\text{H-H}} = 6.69$ Hz, 6H, $\text{CH}(\text{CH}_3)_2$) ppm; $^{13}\text{C}\{^1\text{H}\}$ NMR (CDCl_3 , 50.2 MHz,

298 K): δ 82.42 ($\text{C}(\text{CH}_3)_2$), 71.21 (CH_2), 29.68 ($\text{CH}(\text{CH}_3)_2$), 24.43 (CH_3), 18.61 (CH_3) ppm.

Isolation of primary alcohols

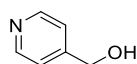
4-bromo benzyl alcohol (3d'): Yield: 146.5 mg (78.3%); $^1\text{H NMR}$ (CDCl_3 , 200 MHz, 298 K): δ



7.42-7.37 (d, $^3J_{\text{H-H}} = 8.46$ Hz, 2H, ArH), 7.17-7.13 (d, $^3J_{\text{H-H}} = 7.83$ Hz, 2H, ArH), 4.55 (s, 2H, CH_2), 1.61 (s, 1H, OH) ppm; $^{13}\text{C}\{^1\text{H}\}$ NMR (CDCl_3 , 50.2 MHz, 298

K): δ 139.7 (Ph), 128.5 (Ph), 128.3 (Ph), 64.5 (CH_2) ppm.

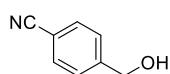
(Pyridine-4-yl)methanol (3l'): Yield: 89.5 mg (83%); $^1\text{H NMR}$ (CDCl_3 , 200 MHz, 298 K): δ 8.48-



8.45 (d, $^3J_{\text{H-H}} = 5.94$ Hz, 2H, ArH), 7.31-7.28 (d, $^3J_{\text{H-H}} = 6.06$ Hz, 2H, ArH), 4.74 (s, 2H, CH_2), 3.99 (s, 1H, OH) ppm; $^{13}\text{C}\{^1\text{H}\}$ NMR (CDCl_3 , 50.2 MHz, 298 K): δ 151.0

(Ph), 149.2 (Ph), 121.2 (Ph), 62.9 (CH_2) ppm.

4-cyano benzylalcohol (3m'): Yield: 53 mg (40%); $^1\text{H NMR}$ (CDCl_3 , 200 MHz, 298 K): δ 7.67-



7.63 (d, $^3J_{\text{H-H}} = 8.34$ Hz, 2H, ArH), 7.50-7.46 (d, $^3J_{\text{H-H}} = 8.59$ Hz, 2H, ArH), 4.79 (s, 2H, CH_2), 2.05 (s, 1H, OH) ppm; $^{13}\text{C}\{^1\text{H}\}$ NMR (CDCl_3 , 50.2 MHz, 298 K): δ

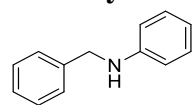
146.2 (ArC-CN), 132.2 (Ph), 126.9 (Ph), 118.8 (CN), 111.1 (C-CN), 64.1 (CH_2), 24.7 (CH_3) ppm.

6.2.3. General catalytic procedure for the hydroboration of aldimines

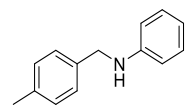
Imine (1 mmol), pinacolborane (1 mmol), catalyst **3** (2 mol %), acetonitrile (1 mL) were charged in a Schlenk tube with a magnetic bead inside the glove box. The reaction mixture was allowed to stir at room temperature and then slowly heated at 65 °C for 48-72 h. The progress of the reaction was monitored by ¹H NMR, which indicated the completion of the reaction by the disappearance of Imine (RCHNR') proton and appearance of a new CH₂ resonance. Upon completion of the reaction, resulted boronate ester residues were hydrolyzed with silica gel and methanol at 65 °C for 4-6 h. The completion of hydrolysis was checked by TLC. Upon completion, the reaction mixture was filtered and washed three times with dichloromethane. The combined organic layers were dried, evaporated and the residue was purified by column chromatography over silica gel (100–200 mesh) with pet ether/ethyl acetate (1:5) mixture as eluent, which provided the pure secondary amines.

6.2.4. Spectroscopic data for the hydroboration product of aldimines

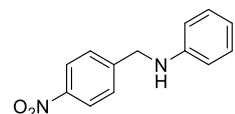
N-benzylaniline (3o): Isolated Yield: 157.5 mg (86%); ¹H NMR (CDCl₃, 200 MHz, 298 K): δ 7.36-7.13 (m, 7H, ArH), 6.74-6.61 (m, 3H, ArH), 4.32 (s, 2H, CH₂), 4.01 (s, 1H, NH) ppm; ¹³C{¹H} NMR (CDCl₃, 50.2 MHz, 298 K): δ 148.1 (Ph), 139.4 (Ph), 129.2 (Ph), 128.6 (Ph), 127.4 (Ph), 127.2 (Ph), 117.5 (Ph), 112.8 (Ph), 48.3 (CH₂) ppm.



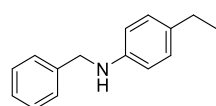
N-(4-methylbenzyl)aniline (3p): Isolated Yield: 146 mg (74%); ¹H NMR (CDCl₃, 200 MHz, 298 K): δ 7.20-7.05 (m, 6H, ArH), 6.67-6.53 (m, 3H, ArH), 4.20 (s, 2H, CH₂), 3.89 (s, 1H, NH), 2.26 (s, 3H, CH₃) ppm; ¹³C{¹H} NMR (CDCl₃, 50.2 MHz, 298 K): δ 148.2 (Ph), 136.8 (Ph), 136.3 (Ph), 129.2 (Ph), 129.2 (Ph), 127.5 (Ph), 117.4 (Ph), 112.8 (Ph), 48.0 (CH₂), 21.0 (CH₃) ppm.



N-(4-nitrobenzyl)aniline (3q): Isolated Yield: 198.5 mg (87%); ¹H NMR (CDCl₃, 200 MHz, 298 K): δ 8.20-8.16 (d, ³J_{H-H} = 8.84 Hz, 2H, ArH), 7.55-7.51 (d, ³J_{H-H} = 8.84 Hz, 2H, ArH), 7.22-7.12 (m, 2H, ArH), 6.78-6.71 (t, ³J_{H-H} = 7.0 Hz, 1H, ArH), 6.60-6.56 (d, ³J_{H-H} = 7.58 Hz, 2H, ArH), 4.47 (s, 2H, CH₂), 4.25 (s, 1H, NH) ppm; ¹³C{¹H} NMR (CDCl₃, 50.2 MHz, 298 K): δ 147.4 (Ph), 147.3 (Ph), 147.1 (Ph), 129.3 (Ph), 127.6 (Ph), 123.8 (Ph), 118.1 (Ph), 112.8 (Ph), 47.5 (CH₂) ppm.

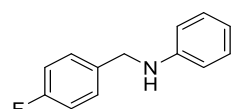


N-benzyl-4-ethylaniline (3r): Isolated Yield: 186 mg (88%); ^1H NMR (CDCl_3 , 200 MHz, 298 K):



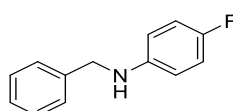
δ 7.31-7.11 (m, 5H, ArH), 6.95-6.90 (d, $^3J_{\text{H-H}} = 8.46$ Hz, 2H, ArH), 6.51-6.47 (d, $^3J_{\text{H-H}} = 6.46$ Hz, 2H, ArH), 4.21 (s, 2H, CH_2), 3.81 (s, 1H, NH), 2.51-2.39 (q, $^3J_{\text{H-H}} = 22.74$ Hz, 2H, CH_2CH_3), 1.14-1.06 (t, $^3J_{\text{H-H}} = 15.16$ Hz, 3H, CH_2CH_3) ppm; $^{13}\text{C}\{^1\text{H}\}$ NMR (CDCl_3 , 50.2 MHz, 298 K): δ 146.0 (Ph), 139.6 (Ph), 133.4 (Ph), 128.5 (Ph), 127.5 (Ph), 127.1 (Ph), 112.9 (Ph), 48.6 (CH_2NH), 27.9 (CH_2CH_3), 15.9 (CH_2CH_3) ppm.

N-(4-fluorobenzyl)aniline (3s): Isolated Yield: 152.9 mg (76%); ^1H NMR (CDCl_3 , 200 MHz, 298



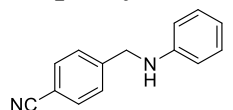
K): δ 7.28-7.21 (m, 2H, ArH), 7.15-7.05 (m, 2H, ArH), 6.98-6.89 (m, 2H, ArH), 6.68-6.51 (m, 3H, ArH), 4.21 (s, 2H, CH_2), 3.92 (s, 1H, NH) ppm; $^{13}\text{C}\{^1\text{H}\}$ NMR (CDCl_3 , 50.2 MHz, 298 K): δ 162.0 (d, $J_{\text{C-F}} = 245.17$ Hz, ArC-F), 147.9 (Ph), 135.1 (Ph), 129.2 (Ph), 128.9 (d, $J_{\text{C-F}} = 8.05$ Hz, Ph), 117.7, (Ph), 115.4 (d, $J_{\text{C-F}} = 21.22$ Hz, Ar-C), 112.8 (Ph), 47.5 (CH_2) ppm.

N-benzyl-4-fluoroaniline (3t): Isolated Yield: 158.9 mg (79%); ^1H NMR (CDCl_3 , 200 MHz, 298



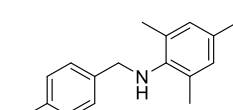
K): δ 7.36-7.23 (m, 5H, ArH), 6.91-6.82 (m, 2H, ArH), 6.58-6.51 (m, 2H, ArH), 4.27 (s, 2H, CH_2), 3.92 (s, 1H, NH) ppm; $^{13}\text{C}\{^1\text{H}\}$ NMR (CDCl_3 , 50.2 MHz, 298 K): δ 155.8 (d, $J_{\text{C-F}} = 234.9$ Hz, ArC-F), 144.4 (Ph), 139.2 (Ph), 128.6 (Ph), 127.4 (Ph), 127.2 (Ph), 115.6 (d, $J_{\text{C-F}} = 22.32$ Hz, Ph), 113.6 (d, $J_{\text{C-F}} = 7.32$ Hz, Ph), 48.9 (CH_2) ppm.

4-((phenylamino)methyl)benzonitrile (3u): ^1H NMR (CDCl_3 , 200 MHz, 298 K): δ 7.55-7.51 (d,



$^3J_{\text{H-H}} = 8.46$ Hz, 2H, ArH), 7.41-7.37 (d, $^3J_{\text{H-H}} = 8.08$ Hz, 2H, ArH), 7.17-7.05 (q, $^3J_{\text{H-H}} = 6.46$ Hz, 2H, ArH), 6.69-6.62 (t, $^3J_{\text{H-H}} = 14.65$ Hz, 1H, ArH), 6.52-6.47 (d, $^3J_{\text{H-H}} = 7.71$ Hz, 2H, ArH), 4.34 (s, 2H, CH_2), 4.14 (s, 1H, NH) ppm; $^{13}\text{C}\{^1\text{H}\}$ NMR (CDCl_3 , 50.2 MHz, 298 K): δ 147.3 (CN), 145.3 (Ph), 132.3 (Ph), 129.3 (Ph), 127.6 (Ph), 118.8 (Ph), 118.0 (Ph), 112.8 (Ph), 110.8 (Ph), 47.7 (CH_2) ppm.

N-(4-fluorobenzyl)-2,4,6-trimethylaniline (3v): Isolated Yield: 126.5 mg (52%); ^1H NMR



(CDCl_3 , 200 MHz, 298 K): δ 7.29-7.18 (m, 2H, ArH), 6.99-6.90 (m, 2H, ArH), 6.76 (s, 2H, CH_2), 3.94 (s, 2H, NH), 2.95 (s, 1H, CH_3) ppm.

6.2.5. Isolation and characterization of the intermediate

Stoichiometric reaction of catalyst **3 and benzaldehyde:** A solution of benzaldehyde (0.1 g, 1 mmol) in toluene (5 mL) was added dropwise to the toluene solution (15 mL) of **3** (0.3 g, 1 mmol) at $-60\text{ }^{\circ}\text{C}$. The reaction mixture was stirred at room temperature overnight. Volatiles of the mixture were removed under reduced pressure. The residue was extracted with toluene and concentration of the solution led to colorless solid of **Int-2**. Yield: 0.40 g (49%). ^1H NMR (CDCl_3 , 500 MHz, 298 K): δ 7.80-7.28 (m, 10H, *ArH*), 5.05 (s, 2H, *OCH*₂), 1.17 (s, 18H, *CH*₃) ppm; $^{13}\text{C}\{^1\text{H}\}$ NMR (CDCl_3 , 125.7 MHz, 298 K): δ 155.1 (NCN), 66.0 (*OCH*₂), 55.4 (*C(CH*₃)₃), 31.5 (*CH*₃) ppm; $^{29}\text{Si}\{^1\text{H}\}$ NMR (CDCl_3 , 79.5 MHz, 298 K): δ -101.28 ppm.

Note: The formation of Int-2 was always accompanied with the formation of free amidinate ligand! As a result, designation of phenyl carbons in Int-2 from the ^{13}C NMR spectrum was difficult.

Alternative Preparation of Int-2: To the solution of KOBn (0.2 g, 1.36 mmol) in 10 mL toluene, toluene solution (20 mL) of $\text{PhC}(\text{N}t\text{Bu})_2\text{SiCl}_3$ (0.5 g, 1.36 mmol) was added drop by drop at $-78\text{ }^{\circ}\text{C}$. The reaction mixture was stirred for 30 min at $-78\text{ }^{\circ}\text{C}$ and then slowly allowed to room temperature and stirred overnight. The filtrate was collected by filtration through celite pad glass frit, concentrated under vacuum and kept for crystallization. Yield: 52%.

6.2.6. Details of DFT calculations

All the calculations in this study have been performed with density functional theory (DFT), with the aid of the Turbomole 6.4 suite of programs, using the PBE functional. The TZVP basis set has been employed. The resolution of identity (RI), along with the multiple accelerated resolution of identity (marij) approximations have been employed for an accurate and efficient treatment of the electronic Coulomb term in the DFT calculations. Dispersion correction (disp3) and solvent correction were incorporated with optimization calculations using the COSMO model, with dichloroethane ($\epsilon = 10.36$) as the solvent. The values reported are ΔG values, with zero-point energy corrections, internal energy and entropic contributions included through frequency calculations on the optimized minima with the temperature taken to be 298.15 K. Harmonic frequency calculations were performed for all stationary points to confirm them as a local minima or transition state structures. The efficiency of a catalytic cycle, as well as the relative prominence of transition states, can be estimated using the *AUTOF* program, which is based on the energetic

span model (ESM) defined by Shaik and co-workers. According to this model, the TOF-determining transition state (TDTS) and intermediate (TDI) can be located from a catalytic cycle by the evaluation of the degree of TOF control (X_{TOF}). TOF can be calculated by the following equation:

$$\text{TOF} = \frac{K_B T}{h} e^{-\delta E/RT}$$

Where δE , the energetic span, can be defined as,

$$\delta E = T_{\text{TDTS}} - T_{\text{TDI}} \quad \text{If TDTS appears after TDI}$$

$$\delta E = T_{\text{TDTS}} - T_{\text{TDI}} + \Delta G_r \quad \text{If TDTS appears before TDI}$$

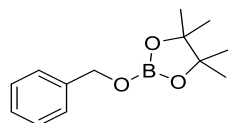
6.3: Chapter 4 experimental details

6.3.1. General catalytic procedure for the hydroboration of aldehydes

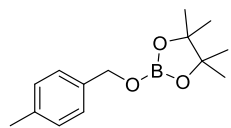
Aldehyde (0.5 mmol), pinacolborane (0.5 mmol), 0.5 mL stock solution of catalyst (0.1 mol%) in THF were charged in a Schlenk tube with a magnetic bead inside the glove box. The reaction mixture was allowed to stir at room temperature for 60 min for **4a**, 40 min for **4b** and 50 min for **4c** respectively. Upon completion of reaction, the solvent was removed using high vacuum in Schlenk line and mesitylene (0.5 mmol) as internal standard, was added while making the NMR in CDCl_3 . The progress of the reaction was monitored by ^1H NMR, which indicated the completion of the reaction by the disappearance of aldehyde (RCHO) proton and appearance of a new OCH_2 resonance.

6.3.2. Spectroscopic data for the hydroboration product of aldehydes

2-(benzyloxy)-pinacolborane (5a): ^1H NMR (CDCl_3 , 200 MHz, 298 K): δ 7.28-7.18 (m, 5H, *Ph*), 4.84 (s, 2H, CH_2), 1.16 (s, 12H, CH_3) ppm; $^{13}\text{C}\{^1\text{H}\}$ NMR (CDCl_3 , 50.2 MHz, 298 K): δ 139.1 (ArC-R), 128.1 (*Ph*), 127.2 (*Ph*), 126.5 (*Ph*), 82.7 ($\text{C}(\text{CH}_3)_2$), 66.5 (CH_2), 24.4 (CH_3) ppm.

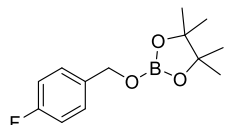


2-((4-methylbenzyl)oxy)-pinacolborane (5b): ^1H NMR (CDCl_3 , 200 MHz, 298 K): δ 7.17-7.13



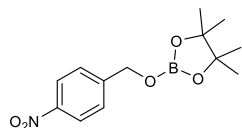
(d, $^3J_{\text{H-H}} = 8.08$ Hz, 2H, ArH), 7.05-7.01 (d, $^3J_{\text{H-H}} = 7.96$ Hz, 2H, ArH), 4.80 (s, 2H, CH_2), 2.23 (s, 3H, Ar CH_3), 1.16 (s, 12H, CH_3) ppm; $^{13}\text{C}\{^1\text{H}\}$ NMR (CDCl_3 , 50.2 MHz, 298 K): δ 136.8 (Ph), 136.2 (Ph), 129.6 (Ph), 129.5 (Ph), 128.8 (Ph), 82.7 ($\text{C}(\text{CH}_3)_2$), 66.4 (CH_2), 24.4 (CH_3), 20.9 (Ar- CH_3) ppm.

2-((4-fluorobenzyl)oxy)-pinacolborane (5c): ^1H NMR (CDCl_3 , 200 MHz, 298 K): δ 7.25-7.18



(t, 2H, ArH), 6.95-6.86 (t, 2H, ArH), 4.78 (s, 2H, CH_2), 1.17 (s, 12H, CH_3) ppm; $^{13}\text{C}\{^1\text{H}\}$ NMR (CDCl_3 , 50.2 MHz, 298 K): δ 162.1 (d, $J_{\text{C-F}} = 245.17$ Hz, ArC-F), 134.88 (Ar-C), 128.5 (d, $J_{\text{C-F}} = 8.05$ Hz, Ar-C), 114.9 (d, $J_{\text{C-F}} = 21.22$ Hz, Ar-C), 82.8 ($\text{C}(\text{CH}_3)_2$), 65.9 (CH_2), 24.4 (CH_3) ppm.

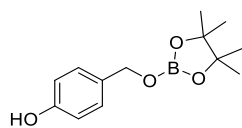
2-(4-nitrobenzyloxy)-pinacolborane (5d): ^1H NMR (CDCl_3 , 200 MHz, 298 K): δ 8.09 (d, $^3J_{\text{H-H}}$



= 8.59 Hz, 2H, ArH), 7.40 (d, $^3J_{\text{H-H}} = 8.46$ Hz, 2H, ArH), 4.93 (s, 2H, CH_2), 1.20 (s, 12H, CH_3) ppm; $^{13}\text{C}\{^1\text{H}\}$ NMR (CDCl_3 , 50.2 MHz, 298 K): δ 147.0 (ArC- NO_2), 146.4 (Ph), 123.3 (Ph), 83.1 ($\text{C}(\text{CH}_3)_2$), 65.3 (CH_2), 24.3 (CH_3)

ppm.

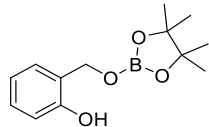
2-(4-hydroxybenzyloxy)-pinacolborane (5e): ^1H NMR (CDCl_3 , 200 MHz, 298 K): δ 7.09 (d, $^3J_{\text{H-H}}$



$_{\text{H}} = 8.59$ Hz, 2H, ArH), 7.74-6.71 (m, 2H, ArH), 4.75 (s, 2H, CH_2), 1.17 (s, 12H, CH_3) ppm; $^{13}\text{C}\{^1\text{H}\}$ NMR (CDCl_3 , 50.2 MHz, 298 K): δ 155.5 (ArC-OH), 132.4 (Ph), 130.6 (Ph), 128.6 (Ph), 115.2 (Ph), 83.0 ($\text{C}(\text{CH}_3)_2$), 66.5

(CH_2), 24.3 (CH_3) ppm.

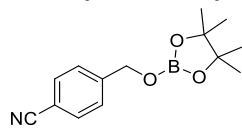
2-(2-hydroxybenzyloxy)-pinacolborane (5f): ^1H NMR (CDCl_3 , 200 MHz, 298 K): δ 7.14-7.04



(m, 2H, ArH), 6.79 (d, $^3J_{\text{H-H}} = 8.59$ Hz, 2H, ArH), 4.89 (s, 2H, CH_2), 1.17 (s, 12H, CH_3) ppm; $^{13}\text{C}\{^1\text{H}\}$ NMR (CDCl_3 , 50.2 MHz, 298 K): δ 154.8 (ArC-OH), 129.4 (Ph), 124.2 (Ph), 120.1 (Ph), 116.7 (Ph), 83.4 ($\text{C}(\text{CH}_3)_2$), 64.3 (CH_2), 24.3

(CH_3) ppm.

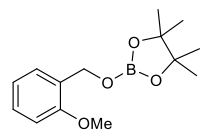
2-(4-cyanobenzyloxy)-pinacolborane (5g): ^1H NMR (CDCl_3 , 200 MHz, 298 K): δ 7.51 (d, $^3J_{\text{H-H}}$



= 7.71 Hz, 2H, ArH), 7.33 (d, $^3J_{\text{H-H}} = 7.58$ Hz, 2H, ArH), 4.88 (s, 2H, CH_2), 1.18 (s, 12H, CH_3) ppm; $^{13}\text{C}\{^1\text{H}\}$ NMR (CDCl_3 , 50.2 MHz, 298 K): δ 144.3

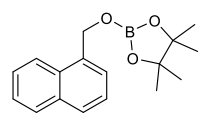
(Ph), 131.8 (Ph), 126.6 (Ph), 118.5 (Ar-CN), 110.8 (ArC-CN), 83.0 (C(CH₃)₂), 65.5 (CH₂), 24.3 (CH₃) ppm; ¹¹B NMR (C₆D₆, 128 MHz, 298 K): δ 22.78 ppm.

2-((2-methoxybenzyl)oxy)-pinacolborane (5h): ¹H NMR (CDCl₃, 200 MHz, 298 K): δ 7.33 (d,



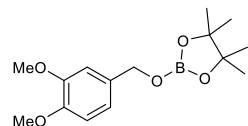
³J_{H-H} = 7.45 Hz, 1H, ArH), 7.13 (t, 1H, ArH), 6.85 (t, 1H, ArH), 6.73 (s, 1H, ArH), 4.91 (s, 2H, CH₂), 3.67 (s, 3H, OCH₃), 1.17 (s, 12H, CH₃) ppm; ¹³C{¹H} NMR (CDCl₃, 50.2 MHz, 298 K): δ 156.3 (ArC-OMe), 128.0 (Ph), 127.5 (Ph), 127.1 (Ph), 120.1 (Ph), 109.6 (Ph), 82.6 (C(CH₃)₂), 62.0 (CH₂), 54.8 (Ar-OCH₃), 24.4 (CH₃) ppm.

2-(naphthalen-1-ylmethoxy)-pinacolborane (5i): ¹H NMR (CDCl₃, 200 MHz, 298 K): δ 7.97-



7.92 (m, 1H, ArH), 7.75-7.68 (m, 2H, ArH), 7.53-7.49 (m, 1H, ArH), 7.40-7.33 (m, 2H, ArH), 5.33 (s, 2H, CH₂), 1.17 (s, 12H, CH₃) ppm; ¹³C{¹H} NMR (CDCl₃, 50.2 MHz, 298 K): δ 136.3 (Ph), 134.9 (Ph), 130.8 (Ph), 128.3 (Ph), 128.0 (Ph), 125.9 (Ph), 125.4 (Ph), 125.1 (Ph), 124.7 (Ph), 123.2 (Ph), 82.7 (C(CH₃)₂), 64.8 (CH₂), 24.4 (CH₃) ppm.

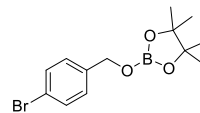
2-(((3,4-dimethoxybenzyl)oxy)-pinacolborane (5j): ¹H NMR (CDCl₃, 200 MHz, 298 K): δ 6.85-



6.77 (m, 2H, ArH), 6.72 (s, 1H, ArH), 4.77 (s, 2H, CH₂), 3.77 (s, 3H, OCH₃), 3.74 (s, 3H, OCH₃), 1.17 (s, 12H, CH₃) ppm; ¹³C{¹H} NMR (CDCl₃, 50.2

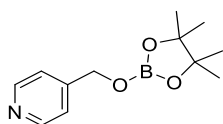
MHz, 298 K): δ 148.7 (ArC-OMe), 148.2 (ArC-OMe), 131.7 (Ph), 119.1 (Ph), 110.7 (Ph), 110.2 (Ph), 82.6 (C(CH₃)₂), 66.4 (CH₂), 55.6 (-OCH₃), 55.4 (-OCH₃), 24.3 (CH₃) ppm; ¹¹B NMR (C₆D₆, 128 MHz, 298 K): δ 22.90 ppm.

2-((4-bromobenzyl)oxy)-pinacolborane (5k): ¹H NMR (CDCl₃, 200MHz, 298 K): δ 7.34 (d, ³J_{H-}



H = 8.34 Hz, 2H, ArH), 7.11 (d, ³J_{H-H} = 8.34 Hz, 2H, ArH), 4.77 (s, 2H, CH₂), 1.16 (s, 12H, CH₃) ppm; ¹³C{¹H} NMR (CDCl₃, 50.2 MHz, 298 K): δ 138.0 (Ph), 131.2 (Ph), 128.2 (Ph), 121.0 (Ar-Br), 82.9 (C(CH₃)₂), 65.8 (CH₂), 24.4 (CH₃) ppm.

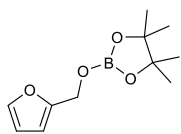
4-(((4,4,5,5-tetramethyl-1,3,2-dioxaborolan-2-yl)oxy)methyl)pyridine (5l): ¹H NMR (CDCl₃,



200 MHz, 298 K): δ 8.48 (d, ³J_{H-H} = 5.81 Hz, 2H, ArH), 7.16 (d, ³J_{H-H} = 5.43 Hz, 2H, ArH), 4.84 (s, 2H, CH₂), 1.18 (s, 12H, CH₃) ppm; ¹³C{¹H} NMR (CDCl₃, 50.2 MHz, 298 K): δ 149.0 (Ar), 148.1 (Ar), 120.5 (Ar), 82.7

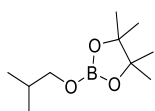
(C(CH₃)₂), 64.4 (CH₂), 24.1 (CH₃) ppm.

2-(furan-2-ylmethoxy)-pinacolborane (5m): ^1H NMR (CDCl_3 , 200 MHz, 298 K): δ 7.25 (t, $^3J_{\text{H-H}}$



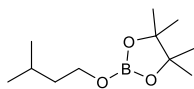
$\text{H} = 2.65$ Hz, 1H, ArH), 6.70 (s, 2H, ArH), 4.73 (s, 2H, CH_2), 1.16 (s, 12H, CH_3) ppm; $^{13}\text{C}\{^1\text{H}\}$ NMR (CDCl_3 , 50.2 MHz, 298 K): δ 152.3 (Ar), 142.1 (Ar), 110.0 (Ar), 108.0 (Ar), 82.7 ($\text{C}(\text{CH}_3)_2$), 58.9 (CH_2), 24.3 (CH_3) ppm.

2-isobutoxy-pinacolborane (5n): ^1H NMR (CDCl_3 , 200 MHz, 298 K): δ 3.53 (d, $^3J_{\text{H-H}} = 6.44$ Hz,



2H, CH_2), 1.73 (sept, 1H, $\text{CH}(\text{CH}_3)_2$), 1.16 (s, 12H, CH_3), 0.81 (d, $^3J_{\text{H-H}} = 6.69$ Hz, 6H, $\text{CH}(\text{CH}_3)_2$) ppm; $^{13}\text{C}\{^1\text{H}\}$ NMR (CDCl_3 , 50.2 MHz, 298 K): δ 82.4 ($\text{C}(\text{CH}_3)_2$), 71.2 (CH_2), 29.7 ($\text{CH}(\text{CH}_3)_2$), 24.4 (CH_3), 21.0 (CH_3), 18.6 (CH_3) ppm.

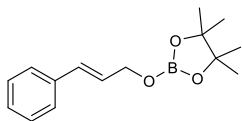
2-(isopentyloxy)-pinacolborane (5o): ^1H NMR (CDCl_3 , 200 MHz, 298 K): δ 3.79 (t, $^3J_{\text{H-H}} = 13.14$



Hz, 2H, CH_2), 1.74-1.51 (m, 1H, $\text{CH}_2\text{CH}(\text{CH}_3)_2$), 1.37 (q, 2H, CH_2), 1.16 (s, 12H, CH_3), 0.82 (d, $^3J_{\text{H-H}} = 7.51$ Hz, 6H, $\text{CH}(\text{CH}_3)_2$) ppm; $^{13}\text{C}\{^1\text{H}\}$ NMR (CDCl_3 , 50.2

MHz, 298 K): δ 82.4 ($\text{C}(\text{CH}_3)_2$), 63.2 (CH_2), 40.2 (CH_2), 24.4 ($\text{CH}(\text{CH}_3)_2$), 24.4 (CH_3), 21.0 (CH_3) ppm.

2-(cinnamyloxy)-pinacolborane (5p): ^1H NMR (CDCl_3 , 200 MHz, 298 K): δ 7.29-7.14 (m, 5H,



ArH), 6.57-6.50 (d, 1H, $^3J_{\text{H-H}} = 15.79$ Hz, 1H, ArCH), 6.25-6.12 (m, 1H, CHCH), 4.46-4.43 (d, 2H, $^3J_{\text{H-H}} = 6.1$ Hz, CH_2), 1.17 (s, 12H, CH_3) ppm;

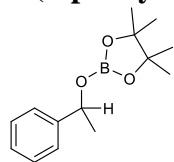
$^{13}\text{C}\{^1\text{H}\}$ NMR (CDCl_3 , 50.2 MHz, 298 K): δ 136.6 (ArC-R), 130.4 (Ar-CHCH), 128.3 (Ar-CH), 127.3 (Ph), 126.6 (Ph), 126.2 (Ph), 82.6 ($\text{C}(\text{CH}_3)_2$), 65.0 (CH_2), 24.3 (CH_3) ppm.

6.3.3. General catalytic procedure for the hydroboration of ketones

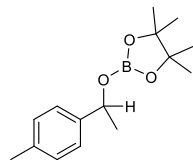
Ketones (0.5 mmol), pinacolborane (0.5 mmol), 0.5 mL stock solution of catalyst (0.1 mol%) in THF were charged in a Schlenk tube with a magnetic bead inside the glove box. The reaction mixture was allowed to stir at room temperature for 3h for **4a** and 2h for **4b** and **4c**. Upon completion of reaction, the solvent was removed using high vacuum in Schlenk line and mesitylene (0.5 mmol) as internal standard, was added while making the NMR in CDCl_3 . The progress of the reaction was monitored by ^1H NMR, which indicated the completion of the reaction by appearance of a new CH resonance.

6.3.4. Spectroscopic data for the hydroboration product of ketones

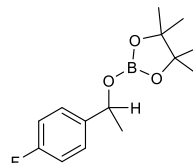
2-(1-phenylethoxy)-pinacolborane (6a): ^1H NMR (CDCl_3 , 200 MHz, 298 K): δ 7.31-7.12 (m, 5H, ArH), 5.17 (q, 1H, BpinOCH), 1.41 (d, $^3J_{\text{H-H}} = 6.44$ Hz, 3H, OCHCH₃), 1.14 (s, 6H, C(CH₃)₂), 1.11 (s, 6H, C(CH₃)₂) ppm; $^{13}\text{C}\{^1\text{H}\}$ NMR (CDCl_3 , 50.2 MHz, 298 K): δ 144.4 (ArC-R), 128.0 (Ph), 126.9 (Ph), 125.1 (Ph), 82.4 (C(CH₃)₂), 72.4 (OCHCH₃), 25.2 (OCHCH₃), 24.3 (C(CH₃)₂) ppm.



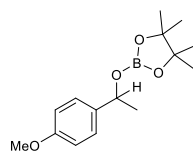
2-(1-(p-tolyl)ethoxy)-pinacolborane (6b): ^1H NMR (CDCl_3 , 200 MHz, 298 K): δ 7.17 (d, $^3J_{\text{H-H}} = 8.08$ Hz, 2H, ArH), 7.02 (d, $^3J_{\text{H-H}} = 7.96$ Hz, 2H, ArH), 5.15 (q, 1H, BpinOCH), 2.22 (s, 3H, Ar-CH₃), 1.40 (d, $^3J_{\text{H-H}} = 6.44$ Hz, 3H, OCHCH₃), 1.14 (s, 6H, C(CH₃)₂), 1.11 (s, 6H, C(CH₃)₂) ppm; $^{13}\text{C}\{^1\text{H}\}$ NMR (CDCl_3 , 50.2 MHz, 298 K): δ 141.5 (ArC-R), 136.5 (Ph), 128.5 (Ph), 125.2 (Ph), 82.5 (C(CH₃)₂), 72.3 (OCHCH₃), 25.3 (OCHCH₃), 24.4 (C(CH₃)₂), 21.0 (Ar-CH₃) ppm.



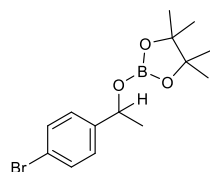
2-(1-(4-fluorophenyl)ethoxy)-pinacolborane (6c): ^1H NMR (CDCl_3 , 200 MHz, 298 K): δ 7.27-7.20 (m, 2H, ArH), 6.93-6.85 (m, 2H, ArH), 5.14 (q, 1H, BpinOCH), 1.38 (d, $^3J_{\text{H-H}} = 6.44$ Hz, 3H, OCHCH₃), 1.14 (s, 6H, C(CH₃)₂), 1.12 (s, 6H, C(CH₃)₂) ppm; $^{13}\text{C}\{^1\text{H}\}$ NMR (CDCl_3 , 50.2 MHz, 298 K): δ 161.8 (d, $J_{\text{C-F}} = 244.4$ Hz, ArC-F), 140.3 (Ph), 127.0 (Ph), 114.8 (d, $J_{\text{C-F}} = 21.2$ Hz, Ar-C), 82.6 (C(CH₃)₂), 71.9 (OCHCH₃), 25.3 (OCHCH₃), 24.4 (C(CH₃)₂), 24.3 (C(CH₃)₂) ppm.



2-(1-(4-methoxyphenyl)ethoxy)-pinacolborane (6d): ^1H NMR (CDCl_3 , 200 MHz, 298 K): δ 7.20 (d, $^3J_{\text{H-H}} = 8.59$ Hz, 2H, ArH), 6.75 (d, $^3J_{\text{H-H}} = 8.72$ Hz, 2H, ArH), 5.14 (q, 1H, BpinOCH), 3.66 (s, 3H, -OCH₃), 1.39 (d, $^3J_{\text{H-H}} = 6.44$ Hz, 3H, OCHCH₃), 1.14 (s, 6H, C(CH₃)₂), 1.12 (s, 6H, C(CH₃)₂) ppm; $^{13}\text{C}\{^1\text{H}\}$ NMR (CDCl_3 , 50.2 MHz, 298 K): δ 158.6 (ArC-OMe), 136.6 (Ph), 126.4 (Ph), 113.3 (Ph), 82.4 (C(CH₃)₂), 72.0 (OCHCH₃), 54.9 (Ar-OCH₃), 25.1 (OCHCH₃), 24.3 (C(CH₃)₂), 24.3 (C(CH₃)₂) ppm.

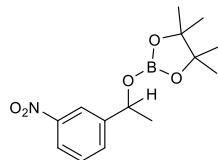


2-(1-(4-bromophenyl)ethoxy)-pinacolborane (6e): ^1H NMR (CDCl_3 , 200 MHz, 298 K): δ 7.33 (d, $^3J_{\text{H-H}} = 8.46$ Hz, 2H, ArH), 7.13 (d, $^3J_{\text{H-H}} = 8.46$ Hz, 2H, ArH), 5.12 (q, 1H, BpinOCH), 1.37 (d, $^3J_{\text{H-H}} = 6.44$ Hz, 3H, OCHCH₃), 1.14 (s, 6H, C(CH₃)₂), 1.11 (s, 6H, C(CH₃)₂) ppm; $^{13}\text{C}\{^1\text{H}\}$ NMR (CDCl_3 , 50.2 MHz, 298 K): δ 143.4 (ArC-R), 131.0 (Ph), 126.9 (Ph), 120.6 (ArC-Br), 82.5 (C(CH₃)₂), 71.7 (OCHCH₃),



54.9 (Ar-OCH₃), 25.0 (OCHCH₃), 24.2 (C(CH₃)₂) ppm; ¹¹B NMR (C₆D₆, 128 MHz, 298 K): δ 22.57 ppm.

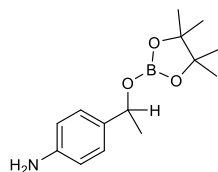
2-(1-(3-nitrophenyl)ethoxy)-pinacolborane (6f): ¹H NMR (CDCl₃, 200 MHz, 298 K): δ 8.16 (s,



1H, ArH), 7.99 (d, ³J_{H-H} = 8.08 Hz, 1H, ArH), 7.60 (d, ³J_{H-H} = 7.71 Hz, 1H, ArH), 7.38 (t, 1H, ArH), 5.25 (q, 1H, BpinOCH), 1.44 (d, ³J_{H-H} = 6.44 Hz, 3H, OCHCH₃), 1.18 (s, 6H, C(CH₃)₂), 1.15 (s, 6H, C(CH₃)₂) ppm; ¹³C{¹H} NMR

(CDCl₃, 50.2 MHz, 298 K): δ 148.0 (ArC-NO₂), 146.4 (ArC-R), 131.3 (Ph), 129.0 (Ph), 121.9 (Ph), 120.2 (Ph), 82.8 (C(CH₃)₂), 71.4 (OCHCH₃), 24.9 (OCHCH₃), 24.2 (C(CH₃)₂) ppm.

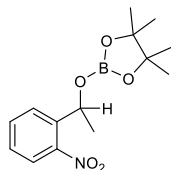
2-(1-(4-aminophenyl)ethoxy)-pinacolborane (6g): ¹H NMR (CDCl₃, 200 MHz, 298 K): δ 7.03



(s, 2H, ArH), 6.48 (s, 2H, ArH), 5.08 (q, 1H, BpinOCH), 3.50 (s, 2H, Ar-NH₂), 1.38 (d, ³J_{H-H} = 6.44 Hz, 3H, OCHCH₃), 1.12 (s, 12H, C(CH₃)₂) ppm; ¹³C{¹H} NMR (CDCl₃, 50.2 MHz, 298 K): δ 145.4 (ArC-NH₂), 134.2 (ArC-R), 126.3

(Ph), 114.6 (Ph), 82.3 (C(CH₃)₂), 72.2 (OCHCH₃), 24.9 (OCHCH₃), 24.3 (C(CH₃)₂), 24.2 (C(CH₃)₂) ppm.

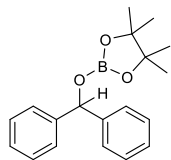
2-(1-(2-nitrophenyl)ethoxy)-pinacolborane (6h): ¹H NMR (CDCl₃, 200 MHz, 298 K): δ 7.79 (d,



³J_{H-H} = 8.21 Hz, 2H, ArH), 7.51 (t, 1H, ArH), 7.27 (t, 1H, ArH), 5.73 (q, 1H, BpinOCH), 1.50 (d, ³J_{H-H} = 6.32 Hz, 3H, OCHCH₃), 1.12 (s, 6H, C(CH₃)₂), 1.08 (s, 6H, C(CH₃)₂) ppm; ¹³C{¹H} NMR (CDCl₃, 50.2 MHz, 298 K): δ 147.1 (ArC-NO₂), 140.2 (ArC-R), 133.2 (Ph), 127.6 (Ph), 127.4 (Ph), 123.7 (Ph), 82.7 (C(CH₃)₂),

68.0 (OCHCH₃), 24.5 (OCHCH₃), 24.4 (C(CH₃)₂), 24.4 (C(CH₃)₂) ppm.

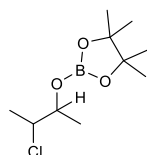
2-(benzhydryloxy)-pinacolborane (6i): ¹H NMR (CDCl₃, 200 MHz, 298 K): δ 7.33-7.29 (m, 4H,



ArH), 7.22-7.10 (m, 6H, ArH), 6.13 (s, 1H, BpinOCH), 1.09 (s, 12H, C(CH₃)₂) ppm; ¹³C{¹H} NMR (CDCl₃, 50.2 MHz, 298 K): δ 142.9 (ArC-R), 128.1 (Ph), 128.0 (Ph), 127.1 (Ph), 126.3 (Ph), 82.7 (C(CH₃)₂), 77.7 (OCHPh), 24.2 (C(CH₃)₂)

ppm; ¹¹B NMR (C₆D₆, 128 MHz, 298 K): δ 22.86 ppm.

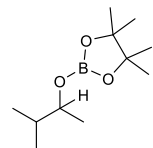
2-((3-chlorobutan-2-yl)oxy)-pinacolborane (6j): ¹H NMR (CDCl₃, 200 MHz, 298 K): δ 4.19 (q,



1H, OCHCH₃), 3.86 (q, 1H, -CHClCH₃), 1.37 (dd, 3H, CHClCH₃), 1.22-1.18 (dd, 3H, OCHCH₃), 1.17 (s, 12H, C(CH₃)₂) ppm; ¹³C{¹H} NMR (CDCl₃, 50.2 MHz, 298

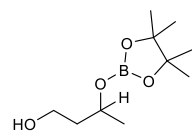
K): δ 82.5 ($C(CH_3)_2$), 73.7 (d, $OCHCHClCH_3$), 60.4 (d, $OCHCHClCH_3$), 24.2 ($C(CH_3)_2$), 24.1 ($C(CH_3)_2$), 19.6 (d, $O(CHClCH_3)CHCH_3$), 18.3 (d, $CHClCH_3$) ppm.

2-((3-methylbutan-2-yl)oxy)-pinacolborane (6k): 1H NMR ($CDCl_3$, 200 MHz, 298 K): δ 3.87



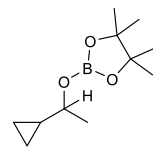
(q, 1H, $OCHCH_3$), 1.66-1.47 (m, 1H, $CH(CH_3)$), 1.16 (s, 12H, $C(CH_3)_2$), 1.06 (d, $^3J_{H-H}$ = 6.32 Hz, 3H, $OCHCH_3$), 0.82 (d, $^3J_{H-H}$ = 3.03 Hz, 3H, $CH(CH_3)$), 0.79 (d, $^3J_{H-H}$ = 3.03 Hz, 3H, $CH(CH_3)$) ppm; $^{13}C\{^1H\}$ NMR ($CDCl_3$, 50.2 MHz, 298 K): δ 82.1 ($C(CH_3)_2$), 75.2 ($OCHCH_3$), 34.1 ($OCHC(CH_3)_2$), 24.3 ($C(CH_3)_2$), 24.2 ($C(CH_3)_2$), 19.1 ($OCHCH_3$), 17.9 ($CH(CH_3)_2$), 17.5 ($CH(CH_3)_2$) ppm.

3-((4,4,5,5-tetramethyl-1,3,2-dioxaborolan-2-yl)oxy)butan-1-ol (6l): 1H NMR ($CDCl_3$, 200



MHz, 298 K): δ 4.25 (s, 1H, OH), 4.05-3.98 (m, 1H, $OCHCH_3$), 3.91-3.72 (m, 3H, CH_2OH), 1.75-1.52 (m, 2H, CH_2CH_2OH), 1.15 (s, 12H, $C(CH_3)_2$), 1.15 (d, $^3J_{H-H}$ = 7.33 Hz, 3H, $OCHCH_3$) ppm; $^{13}C\{^1H\}$ NMR ($CDCl_3$, 50.2 MHz, 298 K): δ 82.3 ($C(CH_3)_2$), 68.3 (CH_2OH), 61.6 ($OCHCH_3$), 39.5 (CH_2CH_2OH), 24.5 ($OCHCH_3$), 24.3 ($C(CH_3)_2$) ppm.

2-(1-cyclopropylethoxy)-pinacolborane (6m): 1H NMR ($CDCl_3$, 200 MHz, 298 K): δ 3.48 (q,



1H, $OCHCH_3$), 1.20 (d, $^3J_{H-H}$ = 6.32 Hz, 3H, $OCHCH_3$), 1.15 (s, 12H, $C(CH_3)_2$), 0.92-0.77 (m, 2H, $CyCH_2$), 0.37-0.30 (m, 2H, $CyCH_2$), 0.12-0.04 (m, 1H, $CyCH$) ppm; $^{13}C\{^1H\}$ NMR ($CDCl_3$, 50.2 MHz, 298 K): δ 82.2 ($C(CH_3)_2$), 74.7 ($OCHCH_3$), 24.3 ($C(CH_3)_2$), 24.2 ($C(CH_3)_2$), 22.1 ($OCHCH_3$), 18.1 ($CyCH$), 2.7 ($CyCH_2$), 1.9 ($CyCH_2$) ppm.

6.3.5. Isolation and characterization of the intermediate

Stoichiometric reaction of catalyst 4a and HBpin: A solution of HBpin (0.09 g, 0.70 mmol) in THF (2 mL) was added dropwise to the THF solution (8 mL) of **4a** (0.2 g, 0.70 mmol) at -78 °C. The reaction mixture was stirred at -78 °C for 15 min then at room temperature for overnight. After addition of HBpin, solution was clear up to 3-4 h and after that white ppt started forming slowly. The solution was filtered and then filtrate was dried for characterization. Yield (0.207 g, 88.8%), 1H NMR ($CDCl_3$, 200 MHz, 298 K): δ 7.26 (d, $^3J_{H-H}$ = 7.58 Hz, 2H, ArH), 7.00 (t, 1H, ArH), 1.45 (s, 18H, $C(CH_3)_3$), 1.31 (s, 12H, $C(CH_3)_2$) ppm; $^{13}C\{^1H\}$ NMR ($CDCl_3$, 50.2 MHz,

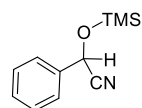
298 K): δ 151.2 (*Ph*), 140.9 (*Ph*), 125.5 (*Ph*), 122.9 (*Ph*), 83.5 ($C(CH_3)_2$), 35.2 ($C(CH_3)_2$), 31.5 ($C(CH_3)_2$) ppm; ^{11}B NMR (toluene-*d*8, 128 MHz, 298 K): δ 21.62, 4.66, -39.83 (quintet) ppm.

6.3.6. General catalytic procedure for the cyanosilylation of aldehydes and ketones

Aldehyde or ketones (0.5 mmol), TMSCN (0.5 mmol), 0.5 mL stock solution of catalyst (0.1 mol%) in THF were charged in a Schlenk tube with a magnetic bead inside the glove box. The reaction mixture was allowed to stir at room temperature for 1h for aldehydes and 2 h for ketones for **4a**, **4b** and **4c** respectively. Upon completion of reaction, the solvent was removed using high vacuum in Schlenk line and mesitylene (0.5 mmol) as internal standard, was added while making the NMR in $CDCl_3$. The progress of the reaction was monitored by 1H and ^{13}C NMR spectroscopy.

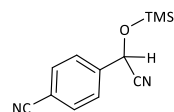
6.3.7. Spectroscopic data for the cyanosilylation product of aldehydes and ketones

2-phenyl-2-((trimethylsilyl)oxy)acetonitrile (7a): 1H NMR ($CDCl_3$, 200 MHz, 298 K): δ 7.25-

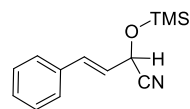


7.20 (m, 5H, *ArH*), 5.37 (s, 1H, $CHOSi(CH_3)_3$), 0.14 (s, 9H, $Si(CH_3)_3$) ppm; $^{13}C\{^1H\}$ NMR ($CDCl_3$, 50.2 MHz, 298 K): δ 136.2 (*ArC-R*), 129.1 (*Ph*), 128.7 (*Ph*), 126.2 (*Ph*), 119.0 (*CN*), 63.5 ($CHOSi(CH_3)_3$), -0.4 ($Si(CH_3)_3$) ppm.

4-(cyano((trimethylsilyl)oxy)methyl)benzonitrile (7b): 1H NMR ($CDCl_3$, 200 MHz, 298 K): δ

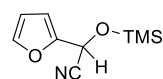


7.60-7.46 (m, 5H, *ArH*), 5.45 (s, 1H, $CHOSi(CH_3)_3$), 0.19 (s, 9H, $Si(CH_3)_3$) ppm; $^{13}C\{^1H\}$ NMR ($CDCl_3$, 50.2 MHz, 298 K): δ 140.9 (*Ph*), 132.4 (*Ph*), 126.6 (*Ph*), 118.0 (*Ar-CN*), 117.8 (*Ph*), 122.9 (*CN*), 62.5 ($CHOSi(CH_3)_3$), -0.6 ($Si(CH_3)_3$) ppm.



(E)-4-phenyl-2-((trimethylsilyl)oxy)but-3-enitrile (7c): 1H NMR ($CDCl_3$, 200 MHz, 298 K): δ 7.29-7.17 (m, 5H, *ArH*), 6.70 (d, $^3J_{H-H} = 16.2$ Hz, 1H, *PhCHCH*), 6.06 (dd, 1H, $^3J_{H,H} = 16.08$ Hz, *PhCHCH*), 4.96 (d, $^3J_{H,H} = 5.93$ Hz, 1H, $CHOSi(CH_3)_3$), 0.16 (s, 9H, $CHCHOSi(CH_3)_3$) ppm; $^{13}C\{^1H\}$ NMR ($CDCl_3$, 50.2 MHz, 298 K): δ 134.9 (*ArC-R*), 133.7 (*Ph*), 128.6 (*ArCH=CHCH(OTMS)(CN)*), 123.4 (*ArCH=CHCH(OTMS)(CN)*), 118.2 (*CN*), 62.0 ($CHOSi(CH_3)_3$), -0.3 ($Si(CH_3)_3$) ppm.

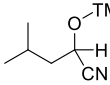
2-(furan-2-yl)-2-((trimethylsilyl)oxy)acetonitrile (7d): 1H NMR ($CDCl_3$, 200 MHz, 298 K): δ



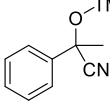
7.32 (s, 1H, *ArH*), 6.42 (d, $^3J_{H-H} = 3.28$ Hz, 1H, *ArH*), 6.27 (dd, $^3J_{H-H} = 3.59$ Hz, 1H, *ArH*), 5.40 (s, 1H, $CHOSi(CH_3)_3$), 0.10 (s, 9H, $Si(CH_3)_3$) ppm; $^{13}C\{^1H\}$ NMR

(CDCl₃, 50.2 MHz, 298 K): δ 148.2 (Ar), 143.6 (Ar), 117.0 (CN), 110.6 (Ar), 109.5 (Ar), 57.2 (CHOSi(CH₃)₃), -0.6 (Si(CH₃)₃) ppm.

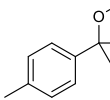
4-methyl-2-((trimethylsilyl)oxy)pentanenitrile (7e): ¹H NMR (CDCl₃, 200 MHz, 298 K): δ 4.33

 (t, 1H, CHOSi(CH₃)₃), 1.82-1.52 (m, 2H, CH₂CH(CH₃)₂), 1.82-1.52 (m, 1H, CH₂CH(CH₃)₂), 0.87 (d, ³J_{H-H} = 4.67 Hz, 3H, CH(CH₃)₂), 0.84 (d, ³J_{H-H} = 6.44 Hz, 3H, CH(CH₃)₂), 0.13 (s, 9H, Si(CH₃)₃) ppm; ¹³C{¹H} NMR (CDCl₃, 50.2 MHz, 298 K): δ 120.0 (CN), 59.7 (CHOSi(CH₃)₃), 44.8 (CH₂CH(CH₃)₂), 23.6 (CH₂CH(CH₃)₂), 22.3 (CH₂CH(CH₃)₂), 21.7 (CH₂CH(CH₃)₂), -0.6 (Si(CH₃)₃) ppm.

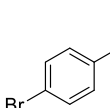
2-phenyl-2-((trimethylsilyl)oxy)propanenitrile (7f): ¹H NMR (CDCl₃, 200 MHz, 298 K): δ 7.46

 (dd, ³J_{H-H} = 8.31 Hz, 2H, ArH), 7.32-7.21 (m, 3H, ArH), 1.75 (s, 3H, CCH₃OTMS), 0.10 (s, 9H, Si(CH₃)₃) ppm; ¹³C{¹H} NMR (CDCl₃, 50.2 MHz, 298 K): δ 141.9 (ArC-R), 128.4 (Ph), 124.4 (Ph), 121.4 (CN), 71.4 (CHOSi(CH₃)₃), 33.3 (CHCH₃), 0.8 (Si(CH₃)₃) ppm.

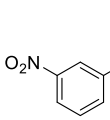
2-(p-tolyl)-2-((trimethylsilyl)oxy)propanenitrile (7g): ¹H NMR (CDCl₃, 200 MHz, 298 K): δ

 7.36-7.32 (d, ³J_{H-H} = 8.21 Hz, 2H, ArH), 7.10-7.06 (d, ³J_{H-H} = 8.34 Hz, 2H, ArH), 2.25 (s, 3H, Ar-CH₃), 1.74 (s, 3H, CCH₃OTMS), 0.08 (s, 9H, Si(CH₃)₃) ppm; ¹³C{¹H} NMR (CDCl₃, 50.2 MHz, 298 K): δ 139.0 (Ph), 138.3 (Ph), 129.1 (Ph), 124.4 (Ph), 121.6 (CN), 71.4 (CHOSi(CH₃)₃), 33.3 (CHCH₃), 20.8 (Ar-CH₃), 0.9 (Si(CH₃)₃) ppm.

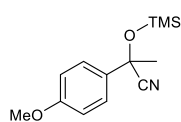
2-(4-bromophenyl)-2-((trimethylsilyl)oxy)propanenitrile (7h): ¹H NMR (CDCl₃, 200 MHz,

 298 K): δ 7.43-7.29 (m, 4H, ArH), 1.72 (s, 3H, CCH₃OTMS), 0.11 (s, 9H, Si(CH₃)₃) ppm.

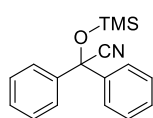
2-(4-aminophenyl)-2-((trimethylsilyl)oxy)propanenitrile (7i): ¹H NMR (CDCl₃, 200 MHz, 298

 K): δ 8.35-8.33 (m, 1H, ArH), 8.13-8.09 (d, ³J_{H-H} = 8.08 Hz, 1H, ArH), 7.83-7.79 (d, ³J_{H-H} = 7.83 Hz, 1H, ArH), 7.49 (t, 1H, ArH), 1.81 (s, 3H, CCH₃OTMS), 0.19 (s, 9H, Si(CH₃)₃) ppm; ¹³C{¹H} NMR (CDCl₃, 50.2 MHz, 298 K): δ 148.2 (ArC-NO₂), 148.2 (ArC-R), 130.4 (Ph), 129.7 (Ph), 123.4 (Ph), 120.5 (Ph), 119.5 (CN), 70.5 (CHOSi(CH₃)₃), 33.0 (CHCH₃), 0.7 (Si(CH₃)₃) ppm.

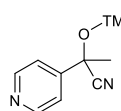
2-(4-methoxyphenyl)-2-((trimethylsilyl)oxy)propanenitrile (7j): ^1H NMR (CDCl_3 , 200 MHz, 298 K): δ 7.39-7.35 (d, $^3J_{\text{H-H}} = 8.72$ Hz, 2H, ArH), 6.82-6.78 (d, $^3J_{\text{H-H}} = 8.72$ Hz, 2H, ArH), 3.68 (s, 3H, OCH_3), 1.74 (s, 3H, CCH_3OTMS), 0.08 (s, 9H, $\text{Si}(\text{CH}_3)_3$) ppm; $^{13}\text{C}\{^1\text{H}\}$ NMR (CDCl_3 , 50.2 MHz, 298 K): δ 159.6 (ArC-OMe), 133.8 (Ph), 125.8 (Ph), 121.5 (Ph), 113.7 (CN), 71.7 ($\text{CHOSi}(\text{CH}_3)_3$), 54.9 (OCH_3), 33.2 (CHCH_3), 0.8 ($\text{Si}(\text{CH}_3)_3$) ppm.



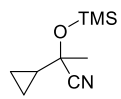
2,2-diphenyl-2-((trimethylsilyl)oxy)acetonitrile (7k): ^1H NMR (CDCl_3 , 200 MHz, 298 K): δ 7.46-7.41 (m, 4H, ArH), 7.27-7.16 (m, 6H, ArH), 0.08 (s, 9H, $\text{Si}(\text{CH}_3)_3$) ppm; $^{13}\text{C}\{^1\text{H}\}$ NMR (CDCl_3 , 50.2 MHz, 298 K): δ 141.8 (ArC-R), 128.5 (Ph), 128.4 (Ph), 125.7 (Ph), 120.5 (CN), 76.2 ($\text{CHOSi}(\text{CH}_3)_3$), 0.7 ($\text{Si}(\text{CH}_3)_3$) ppm.



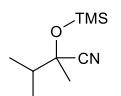
2-(pyridin-4-yl)-2-((trimethylsilyl)oxy)propanenitrile (7l): ^1H NMR (CDCl_3 , 200 MHz, 298 K): δ 8.59-8.56 (d, $^3J_{\text{H-H}} = 5.94$ Hz, 2H, ArH), 7.37-7.34 (d, $^3J_{\text{H-H}} = 6.06$ Hz, 2H, ArH), 1.73 (s, 3H, CCH_3OTMS), 0.15 (s, 9H, $\text{Si}(\text{CH}_3)_3$) ppm; $^{13}\text{C}\{^1\text{H}\}$ NMR (CDCl_3 , 50.2 MHz, 298 K): δ 150.6 (Ar), 150.6 (Ar), 150.1 (Ar), 120.9 (Ar), 120.2 (Ar), 119.0 (CN), 70.3 ($\text{CHOSi}(\text{CH}_3)_3$), 32.7 (CHCH_3), 0.7 ($\text{Si}(\text{CH}_3)_3$) ppm.



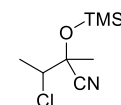
2-cyclopropyl-2-((trimethylsilyl)oxy)propanenitrile (7m): ^1H NMR (CDCl_3 , 200 MHz, 298 K): δ 1.53 (s, 3H, CCH_3OTMS), 1.06 (q, 1H, $\text{CHC}(\text{CH}_3)(\text{CN})\text{OTMS}$), 0.56-0.39 (m, 4H, CH_2), 0.15 (s, 9H, $\text{Si}(\text{CH}_3)_3$) ppm; $^{13}\text{C}\{^1\text{H}\}$ NMR (CDCl_3 , 50.2 MHz, 298 K): δ 120.8 (CN), 70.4 ($\text{CHOSi}(\text{CH}_3)_3$), 29.3 (CCH_3OTMS), 21.4 ($\text{CHC}(\text{CH}_3)(\text{CN})\text{OTMS}$), 2.3 (CH_2), 1.8 (CH_2), 1.1 ($\text{Si}(\text{CH}_3)_3$) ppm.



2,3-dimethyl-2-((trimethylsilyl)oxy)butanenitrile (7n): ^1H NMR (CDCl_3 , 200 MHz, 298 K): δ 1.75 (sept, 1H, $\text{CHC}(\text{CH}_3)(\text{CN})\text{OTMS}$), 1.41 (s, 3H, CCH_3OTMS), 0.96-0.92 (m, 6H, $\text{C}(\text{CH}_3)_2$), 0.16 (s, 9H, $\text{Si}(\text{CH}_3)_3$) ppm; $^{13}\text{C}\{^1\text{H}\}$ NMR (CDCl_3 , 50.28 MHz, 298 K): δ 121.3 (CN), 73.3 ($\text{CHOSi}(\text{CH}_3)_3$), 38.9 ($\text{OCHC}(\text{CH}_3)_2$), 25.8 (CCH_3OTMS), 17.0 ($\text{CH}(\text{CH}_3)_2$), 16.7 ($\text{CH}(\text{CH}_3)_2$), 1.0 ($\text{Si}(\text{CH}_3)_3$) ppm.



3-chloro-2-methyl-2-((trimethylsilyl)oxy)butanenitrile (7o): ^1H NMR (CDCl_3 , 200 MHz, 298 K): δ 3.94 (quat, 1H, $\text{CHC}(\text{CH}_3)(\text{CN})\text{OTMS}$), 1.54 (s, 3H, CCH_3OTMS), 1.47-1.44 (d, $^3J_{\text{H-H}} = 6.69$ Hz, 3H, $\text{CH}(\text{CH}_3)\text{Cl}$), 0.19 (s, 9H, $\text{Si}(\text{CH}_3)_3$) ppm.

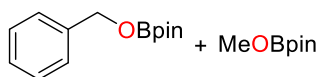


6.3.8. General catalytic procedure for the hydroboration of esters

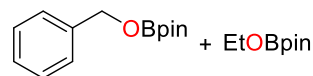
Ester (0.25 mmol), pinacolborane (0.50 mmol), catalyst (6.0 mol% for **4a** or, 3.0 mol% for **4b**) were mixed together in a Schlenk tube or in a screw cap NMR tube inside the glove box. The reaction mixture was allowed to heat at 80 °C for 10 h in neat condition (for **4a**) or at 45 °C for 8 h in 0.5 mL THF solvent (for **4b**). After reaction, mesitylene (0.25 mmol) as an internal standard, was added while making the NMR in appropriate deuterated solvent. The progress of the reaction was monitored by ¹H NMR, which indicated the completion of the reaction by the appearance of a new Bpin-OCH₂R resonance.

6.3.9. Spectroscopic data of the boronate esters of corresponding esters

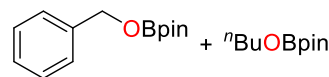
Entry 8a: ¹H NMR (CDCl₃, 200 MHz, 298 K): δ 7.48-7.22 (m, 5H, PhCH₂OBpin), 4.87 (s, 2H, PhCH₂OBpin), 3.54 (s, 3H, MeOBpin), 1.20 (s, 12H, MeOBpin), 1.19 (s, 12H, PhCH₂OBpin) ppm; ¹³C{¹H} NMR (CDCl₃, 100.53 MHz, 298 K): δ 139.0 (ArC-R), 128.0 (Ph), 127.1 (Ph), 126.5 (Ph), 82.7 (PhCH₂OBpin), 82.5 (MeOBpin), 66.4 (PhCH₂OBpin), 52.3 (MeOBpin), 24.4 (PhCH₂OBpin & MeOBpin) ppm.



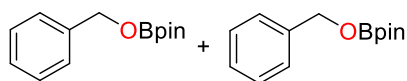
Entry 8b: ¹H NMR (CDCl₃, 200 MHz, 298 K): δ 7.40-7.23 (m, 5H, PhCH₂OBpin), 4.88 (s, 2H, PhCH₂OBpin), 3.85 (q, 2H, CH₃CH₂OBpin), 1.21 (s, 12H, EtOBpin), 1.19 (s, 12H, PhCH₂OBpin), 1.12 (t, 3H, CH₃CH₂OBpin) ppm; ¹³C{¹H} NMR (CDCl₃, 50.3 MHz, 298 K): δ 139.1 (ArC-R), 128.1 (Ph), 127.2 (Ph), 126.6 (Ph), 82.7 (PhCH₂OBpin), 82.4 (EtOBpin), 66.5 (PhCH₂OBpin), 60.5 (CH₃CH₂OBpin), 24.4 (PhCH₂OBpin & EtOBpin), 17.0 (CH₃CH₂OBpin) ppm.



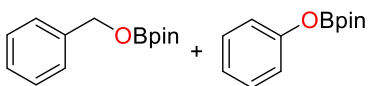
Entry 8c: ¹H NMR (CDCl₃, 200 MHz, 298 K): δ 7.34-7.15 (m, 5H, PhCH₂OBpin), 4.87 (s, 2H, PhCH₂OBpin), 3.79 (t, 2H, CH₃CH₂CH₂CH₂OBpin), 1.46 (t, 2H, CH₃CH₂CH₂CH₂OBpin), 1.30 (m, 2H, CH₃CH₂CH₂CH₂OBpin), 1.19 (s, 12H, ⁿBuOBpin), 1.18 (s, 12H, PhCH₂OBpin), 0.86 (t, 3H, CH₃CH₂CH₂CH₂OBpin) ppm; ¹³C{¹H} NMR (CDCl₃, 50.32 MHz, 298 K): δ 139.0 (ArC-R), 128.1 (Ph), 127.1 (Ph), 126.5 (Ph), 82.7 (PhCH₂OBpin), 82.3 (ⁿBuOBpin), 66.5 (PhCH₂OBpin), 64.4 (CH₃CH₂CH₂CH₂OBpin), 33.3 (CH₃CH₂CH₂CH₂OBpin), 24.4 (PhCH₂OBpin & ⁿBuOBpin), 18.6 (CH₃CH₂CH₂CH₂OBpin), 13.5 (CH₃CH₂CH₂CH₂OBpin) ppm.



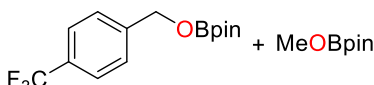
Entry 8d: ^1H NMR (CDCl_3 , 200 MHz, 298 K): δ 7.36-7.18 (m, 10H, $\text{PhCH}_2\text{OBpin}$), 4.87 (s, 4H, $\text{PhCH}_2\text{OBpin}$), 1.20 (s, 12H, $\text{PhCH}_2\text{OBpin}$) ppm; $^{13}\text{C}\{^1\text{H}\}$ NMR (CDCl_3 , 50.32 MHz, 298 K): δ 139.0 (ArC-R), 128.0 (Ph), 127.1 (Ph), 126.4 (Ph), 82.6 ($\text{PhCH}_2\text{OBpin}$), 66.4 ($\text{PhCH}_2\text{OBpin}$), 24.3 ($\text{PhCH}_2\text{OBpin}$) ppm.



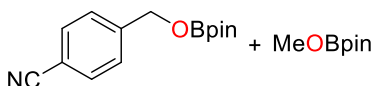
Entry 8e: ^1H NMR (CDCl_3 , 200 MHz, 298 K): δ 7.32-6.93 (m, 10H, $\text{PhCH}_2\text{OBpin}$), 4.86 (s, 4H, $\text{PhCH}_2\text{OBpin}$), 1.23 (s, 12H, PhOBpin), 1.18 (s, 12H, $\text{PhCH}_2\text{OBpin}$) ppm; $^{13}\text{C}\{^1\text{H}\}$ NMR (CDCl_3 , 100.53 MHz, 298 K): δ 153.2 (PhOBpin), 139.0 ($\text{PhCH}_2\text{OBpin}$), 129.0 (PhOBpin), 128.0 ($\text{PhCH}_2\text{OBpin}$), 127.1 ($\text{PhCH}_2\text{OBpin}$), 126.5 ($\text{PhCH}_2\text{OBpin}$), 122.8 ($\text{PhCH}_2\text{OBpin}$), 119.3 ($\text{PhCH}_2\text{OBpin}$), 83.2 (PhOBpin), 82.7 ($\text{PhCH}_2\text{OBpin}$), 66.4 ($\text{PhCH}_2\text{OBpin}$), 24.3 ($\text{PhCH}_2\text{OBpin}$ & PhOBpin) ppm.



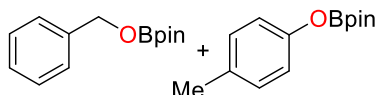
Entry 8f: ^1H NMR (CDCl_3 , 200 MHz, 298 K): δ 7.52 (d, 2H, $^3J_{\text{H-H}} = 8.27$ Hz, $\text{Ph}(\text{CF}_3)\text{CH}_2\text{OBpin}$), 7.39 (d, 2H, $^3J_{\text{H-H}} = 8.03$ Hz, $\text{Ph}(\text{CF}_3)\text{CH}_2\text{OBpin}$), 4.92 (s, 2H, $\text{Ph}(\text{CN})\text{CH}_2\text{OBpin}$), 3.54 (s, 3H, MeOBpin), 1.21 (s, 12H, $\text{PhCH}_2\text{OBpin}$), 1.19 (s, 12H, MeOBpin) ppm; $^{13}\text{C}\{^1\text{H}\}$ NMR (CDCl_3 , 100.53 MHz, 298 K): δ 143.1 ($\text{CF}_3\text{PhCH}_2\text{OBpin}$), 129.3 (q, $\text{CF}_3\text{PhCH}_2\text{OBpin}$), 126.5 ($\text{CF}_3\text{PhCH}_2\text{OBpin}$), 125.1 ($\text{CF}_3\text{PhCH}_2\text{OBpin}$), 125.0 ($\text{CF}_3\text{PhCH}_2\text{OBpin}$), 83.0 ($\text{CF}_3\text{PhCH}_2\text{OBpin}$), 82.6 (MeOBpin), 65.7 ($\text{CF}_3\text{PhCH}_2\text{OBpin}$), 52.3 (MeOBpin), 24.3 ($\text{CF}_3\text{PhCH}_2\text{OBpin}$ & MeOBpin) ppm.



Entry 8g: ^1H NMR (CDCl_3 , 200 MHz, 298 K): δ 7.57 (d, 2H, $^3J_{\text{H-H}} = 7.94$ Hz, $\text{Ph}(\text{CN})\text{CH}_2\text{OBpin}$), 7.39 (d, 2H, $^3J_{\text{H-H}} = 7.72$ Hz, $\text{Ph}(\text{CN})\text{CH}_2\text{OBpin}$), 4.93 (s, 2H, $\text{Ph}(\text{CN})\text{CH}_2\text{OBpin}$), 3.56 (s, 3H, MeOBpin), 1.23 (s, 12H, MeOBpin), 1.21 (s, 12H, $\text{PhCH}_2\text{OBpin}$) ppm; $^{13}\text{C}\{^1\text{H}\}$ NMR (CDCl_3 , 100.53 MHz, 298 K): δ 144.3 ($\text{CNPhCH}_2\text{OBpin}$), 131.7 ($\text{CNPhCH}_2\text{OBpin}$), 126.5 ($\text{CNPhCH}_2\text{OBpin}$), 118.4 ($\text{CNPhCH}_2\text{OBpin}$), 110.7 ($\text{CNPhCH}_2\text{OBpin}$), 82.8 ($\text{CNPhCH}_2\text{OBpin}$), 82.3 (MeOBpin), 65.3 ($\text{CNPhCH}_2\text{OBpin}$), 52.1 (MeOBpin), 24.2 ($\text{PhCH}_2\text{OBpin}$ & MeOBpin) ppm.



Entry 8h: ^1H NMR (CDCl_3 , 200 MHz, 298 K): δ 7.31-7.16 (m, 5H, $\text{PhCH}_2\text{OBpin}$ & MePhOBpin), 7.02-6.86 (m, 4H, $\text{PhCH}_2\text{OBpin}$ & MePhOBpin), 4.88 (s, 4H, $\text{PhCH}_2\text{OBpin}$), 2.22 (s, 3H, MePhOBpin), 1.24 (s, 12H, $\text{PhCH}_2\text{OBpin}$) ppm.



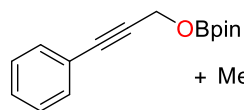
MePhOBpin), 1.20 (s, 12H, PhCH₂OBpin) ppm; ¹³C{¹H} NMR (CDCl₃, 100.53 MHz, 298 K): δ 151.0 (MePhOBpin), 139.0 (PhCH₂OBpin), 132.1 (MePhOBpin), 129.6 (MePhOBpin), 129.5 (MePhOBpin), 128.0 (PhCH₂OBpin), 127.1 (PhCH₂OBpin), 126.5 (PhCH₂OBpin), 119.0 (PhCH₂OBpin), 115.0 (MePhOBpin), 83.2 (MePhOBpin), 82.7 (PhCH₂OBpin), 66.4 (PhCH₂OBpin), 24.3 (PhCH₂OBpin & MePhOBpin), 20.4 (MePhOBpin) ppm.

Entry 8i: ¹H NMR (CDCl₃, 200 MHz, 298 K): δ 7.57 (d, 1H, ³J_{H-H} = 7.94 Hz, MePh(I)CH₂OBpin), 7.25 (s, 1H, MePh(I)CH₂OBpin), 6.77 (m, 1H, MePh(I)CH₂OBpin), 4.79 (s, 2H, MePh(I)CH₂OBpin), 3.55 (s, 3H, MeOBpin), 2.24 (s, 3H, MePh(I)CH₂OBpin), 1.22 (s, 12H, MeOBpin), 1.19 (s, 12H, PhCH₂OBpin) ppm; ¹³C{¹H} NMR (CDCl₃, 100.53 MHz, 298 K): δ 140.4 (MePh(I)CH₂OBpin), 138.3 (MePh(I)CH₂OBpin), 129.5 (MePh(I)CH₂OBpin), 128.2 (MePh(I)CH₂OBpin), 91.8 (MePh(I)CH₂OBpin), 82.8 (MePh(I)CH₂OBpin), 82.5 (MeOBpin), 70.3 (MePh(I)CH₂OBpin), 52.3 (MeOBpin), 24.3 (MePh(I)CH₂OBpin), 24.2 (MeOBpin), 20.7 (MePh(I)CH₂OBpin) ppm.

Entry 8j: ¹H NMR (CDCl₃, 200 MHz, 298 K): δ 7.29-7.18 (m, 5H, PhCH₂OBpin), 5.35-4.96 (m, 1H, CH₂=CHOBpin), 4.87 (s, 2H, PhCH₂OBpin), 4.68-4.21 (CH₂=CHOBpin), 4.01-3.63 (CH₂=CHOBpin), 1.21 (s, 12H, PhCH₂OBpin), 1.20 (s, 12H, MeOBpin) ppm; ¹³C{¹H} NMR (CDCl₃, 100.53 MHz, 298 K): δ 144.7 (H₂C=CHOBpin), 139.1 (ArC-R), 128.1 (Ph), 127.2 (Ph), 126.5 (Ph), 97.9 (H₂C=CHOBpin), 96.1 (H₂C=CHOBpin), 83.3 (H₂C=CHOBpin), 82.7 (PhCH₂OBpin), 66.5 (PhCH₂OBpin), 24.4 (PhCH₂OBpin & H₂C=CHOBpin) ppm.

Entry 8k: ¹H NMR (CDCl₃, 200 MHz, 298 K): δ 7.27 (d, 2H, ³J_{H-H} = 8.49 Hz, H₂C=CHPhOBpin), 7.00 (d, 2H, ³J_{H-H} = 8.60 Hz, H₂C=CHPhOBpin), 6.61 (q, 1H, H₂C=CHPhOBpin), 5.57 (d, 1H, ³J_{H-H} = 17.64 Hz, H₂C=CHPhOBpin), 5.10 (d, 1H, ³J_{H-H} = 10.91 Hz, H₂C=CHPhOBpin), 3.85 (q, 2H, CH₃CH₂OBpin), 1.21 (s, 12H, H₂C=CHPhOBpin), 1.20 (s, 12H, EtOBpin), 1.14 (q, 2H, CH₃CH₂OBpin) ppm; ¹³C{¹H} NMR (CDCl₃, 100.53 MHz, 298 K): δ 156.0 (H₂C=CHPhOBpin), 136.2 (H₂C=CHPhOBpin), 129.7 (H₂C=CHPhOBpin), 127.2 (H₂C=CHPhOBpin), 115.3 (H₂C=CHPhOBpin), 110.8 (H₂C=CHPhOBpin), 83.0 (H₂C=CHPhOBpin), 82.6 (EtOBpin), 60.5 (CH₃CH₂OBpin), 24.3 (CF₃PhCH₂OBpin), 24.2 (EtOBpin), 17.0 (CH₃CH₂OBpin) ppm.

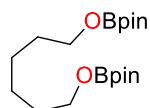
Entry 8l: ^1H NMR (CDCl_3 , 200 MHz, 298 K): δ 7.36 (br, 2H, $\text{PhCH}_2\text{OBpin}$), 7.23 (br, 3H, $\text{PhCH}_2\text{OBpin}$), 4.64 (s, 2H, $\text{PhCH}_2\text{OBpin}$), 3.54 (s, 3H, MeOBpin),



+ MeOBpin

1.19 (s, 24H, MeOBpin & $\text{PhCH}_2\text{OBpin}$) ppm; $^{13}\text{C}\{^1\text{H}\}$ NMR (CDCl_3 , 100.53 MHz, 298 K): δ 131.4 (Ph), 128.1 (Ph), 128.0 (Ph), 122.5 (Ph), 85.6 ($\text{PhC}\equiv\text{CCH}_2\text{OBpin}$), 85.1 ($\text{PhC}\equiv\text{CCH}_2\text{OBpin}$), 83.0 ($\text{PhC}\equiv\text{CCH}_2\text{OBpin}$), 82.5 (MeOBpin), 53.3 ($\text{PhC}\equiv\text{CCH}_2\text{OBpin}$), 52.2 (MeOBpin), 24.3 ($\text{PhC}\equiv\text{CCH}_2\text{OBpin}$ & MeOBpin) ppm.

Entry 8m: ^1H NMR (CDCl_3 , 200 MHz, 298 K): δ 3.78 (t, 4H,



pinBOCH₂CH₂CH₂CH₂CH₂CH₂OBpin),

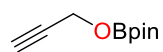
1.58-1.44 (m, 4H,

pinBOCH₂CH₂CH₂CH₂CH₂CH₂OBpin),

1.37-1.31 (m, 4H,

pinBOCH₂CH₂CH₂CH₂CH₂CH₂OBpin), 1.19 (s, 24H, $\text{pinBO}(\text{CH}_2)_6\text{OBpin}$) ppm; $^{13}\text{C}\{^1\text{H}\}$ NMR (CDCl_3 , 100.61 MHz, 298 K): δ 82.4 ($\text{pinBO}(\text{CH}_2)_6\text{OBpin}$), 65.0 ($\text{pinBOCH}_2\text{CH}_2\text{CH}_2\text{CH}_2\text{CH}_2\text{CH}_2\text{OBpin}$), 32.0 ($\text{pinBOCH}_2\text{CH}_2\text{CH}_2\text{CH}_2\text{CH}_2\text{CH}_2\text{OBpin}$), 25.7 ($\text{pinBOCH}_2\text{CH}_2\text{CH}_2\text{CH}_2\text{CH}_2\text{CH}_2\text{OBpin}$), 24.8 ($\text{pinBO}(\text{CH}_2)_6\text{OBpin}$) ppm.

Entry 8n: ^1H NMR (CDCl_3 , 200 MHz, 298 K): δ 4.41 (d, 2H, $^3J_{\text{H-H}} = 2.32$ Hz, $\text{HC}\equiv\text{CCH}_2\text{OBpin}$),



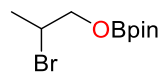
+ EtOBpin

3.85 (q, 2H, $\text{CH}_3\text{CH}_2\text{OBpin}$), 2.37 (t, 1H, $\text{HC}\equiv\text{CCH}_2\text{OBpin}$), 1.21 (s, 12H,

EtOBpin), 1.20 (s, 12H, $\text{HC}\equiv\text{CCH}_2\text{OBpin}$), 1.13 (t, 3H, $\text{CH}_3\text{CH}_2\text{OBpin}$)

ppm; $^{13}\text{C}\{^1\text{H}\}$ NMR (CDCl_3 , 100.53 MHz, 298 K): δ 83.0 ($\text{HC}\equiv\text{CCH}_2\text{OBpin}$), 82.3 (EtOBpin), 73.4 ($\text{HC}\equiv\text{CCH}_2\text{OBpin}$), 60.3 ($\text{CH}_3\text{CH}_2\text{OBpin}$), 52.6 ($\text{HC}\equiv\text{CCH}_2\text{OBpin}$), 24.2 ($\text{HC}\equiv\text{CCH}_2\text{OBpin}$ & $\text{CH}_3\text{CH}_2\text{OBpin}$), 16.9 ($\text{CH}_3\text{CH}_2\text{OBpin}$) ppm.

Entry 8o: ^1H NMR (CDCl_3 , 200 MHz, 298 K): δ 4.11-3.79 (m, 5H, $\text{CH}_3\text{CH}(\text{Br})\text{CH}_2\text{OBpin}$ &



+ EtOBpin

$\text{CH}_3\text{CH}_2\text{OBpin}$), 1.62 (d, 3H, $^3J_{\text{H-H}} = 6.50$ Hz, $\text{CH}_3\text{CH}(\text{Br})\text{CH}_2\text{OBpin}$),

1.21 (s, 12H, EtOBpin), 1.19 (s, 12H, $\text{CH}_3\text{CH}(\text{Br})\text{CH}_2\text{OBpin}$), 1.13 (t, 3H,

$\text{CH}_3\text{CH}_2\text{OBpin}$) ppm; $^{13}\text{C}\{^1\text{H}\}$ NMR (CDCl_3 , 100.53 MHz, 298 K): δ 82.8 ($\text{CH}_3\text{CH}(\text{Br})\text{CH}_2\text{OBpin}$), 82.2 (EtOBpin), 69.7 ($\text{CH}_3\text{CH}(\text{Br})\text{CH}_2\text{OBpin}$), 60.3 ($\text{CH}_3\text{CH}_2\text{OBpin}$), 47.5 ($\text{CH}_3\text{CH}(\text{Br})\text{CH}_2\text{OBpin}$), 24.2 ($\text{CH}_3\text{CH}(\text{Br})\text{CH}_2\text{OBpin}$ & $\text{CH}_3\text{CH}_2\text{OBpin}$), 21.7 ($\text{CH}_3\text{CH}(\text{Br})\text{CH}_2\text{OBpin}$), 16.9 ($\text{CH}_3\text{CH}_2\text{OBpin}$) ppm.

6.3.10. General catalytic procedure for the hydroboration of primary amides

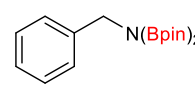
Primary amide (0.25 mmol), pinacolborane (4.5 equiv, 1.125 mmol), catalyst (5.0 mol% **4a**) were mixed together in a Schlenk tube or in a screw cap NMR tube inside the glove box. The reaction mixture was allowed to heat at 60 °C for 18 h without adding any solvent. After reaction, mesitylene (0.25 mmol) as an internal standard, was added while making the NMR in appropriate deuterated solvent. The progress of the reaction was monitored by ¹H NMR, which indicated the completion of the reaction by the appearance of a new R-CH₂-N(Bpin)₂ resonance. Upon completion, the reaction mixture was stirred with 1.0 mL 2.0 (M) NaOH solutions and 1.0 mL Et₂O for 1 h to complete the hydrolysis. Next, the reaction mixture was worked up with Et₂O:H₂O mixture (1:1) and the Et₂O part were concentrated in vacuum to get corresponding reduced amines. Consequently, 1.0 mL 1.0 (M) methanolic HCl solution was added to the concentrated amines followed by addition of 1.0 mL Et₂O and the corresponding amine hydrochloride salt was purified by washing with Et₂O. Isolated amine hydrochlorides were characterized through NMR spectroscopy in DMSO-d₆.

Hydroboration product of primary amides, namely **9a**, **9e**, **9f**, **9h**, **9j**, **9k**, **9l** and **9m** were isolated and in all the cases little discrepancy was observed with the NMR yield.

6.3.11. Analytical data of the borylated amines of corresponding primary amides

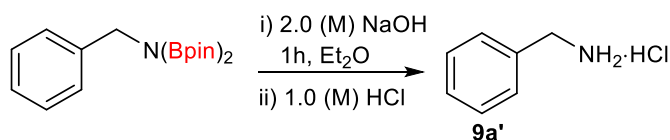
For every reaction, along with the *N*-borylated amine Bpin-O-Bpin formed as second product which show a singlet at δ 1.17-1.18 ppm in ¹H NMR and peak at δ 24.1-24.4 and 82.4-82.9 ppm in ¹³C NMR.

Entry 9a: ¹H NMR (CDCl₃, 200 MHz, 298 K): δ 7.31-7.29 (m, 2H, *Ph*), 7.24-7.20 (t, 2H, *Ph*),

 7.16-7.12 (t, 1H, *Ph*), 4.23 (s, 2H, PhCH₂N(Bpin)₂), 1.18 (s, 24H, N(Bpin)₂) ppm; ¹³C{¹H} NMR (CDCl₃, 100.6 MHz, 298 K): δ 142.9 (*Ph*), 127.6 (*Ph*), 127.3 (*Ph*), 125.9 (*Ph*), 82.2 (PhCH₂N(Bpin)₂), 47.1 (PhCH₂N(Bpin)₂), 24.4 (PhCH₂N(Bpin)₂) ppm.

Phenylmethanamine hydrochloride (**9a'**).

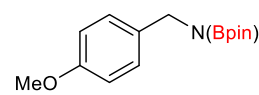
The general procedure was followed for the isolation of phenylmethanamine hydrochloride salt, **9a'** (29 mg, 80.8% yield) as a colorless solid.



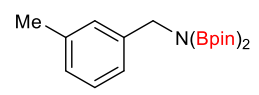
^1H NMR (200 MHz, DMSO- d_6): δ 8.54 (br, 3H, $\text{NH}_2\cdot\text{HCl}$), 7.51-7.50 (d, $^3J_{\text{H-H}} = 6.50$ Hz, 2H, *Ph*), 7.43-7.35 (m, 3H, *Ph*), 3.99 (br, 2H, CH_2) ppm.

$^{13}\text{C}\{^1\text{H}\}$ (100.6 MHz, DMSO- d_6): δ 134.1 (*Ph*), 129.0 (*Ph*), 128.6 (*Ph*), 128.4 (*Ph*), 42.1 (CH_2) ppm.

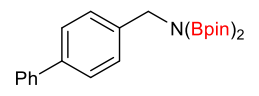
Entry 9b: ^1H NMR (CDCl_3 , 200 MHz, 298 K): δ 7.27-7.24 (m, 2H, *Ph*), 6.78-6.77 (m, 2H, *Ph*),

 4.16 (s, 2H, $\text{PhCH}_2\text{N}(\text{Bpin})_2$), 3.75 (s, 3H, OCH_3), 1.20 (s, 24H, $\text{N}(\text{Bpin})_2$) ppm; $^{13}\text{C}\{^1\text{H}\}$ NMR (CDCl_3 , 100.6 MHz, 298 K): δ 157.9 (*ArC-OMe*), 133.7 (*Ph*), 128.6 (*Ph*), 112.9 (*Ph*), 81.6 ($\text{PhCH}_2\text{N}(\text{Bpin})_2$), 54.8 (*-OMe*), 46.3 ($\text{PhCH}_2\text{N}(\text{Bpin})_2$), 24.3 ($\text{PhCH}_2\text{N}(\text{Bpin})_2$) ppm.

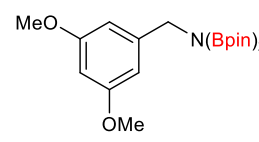
Entry 9c: ^1H NMR (CDCl_3 , 200 MHz, 298 K): δ 7.29-7.10 (m, 5H, *Ph*), 3.96 (s, 2H,

 $\text{PhCH}_2\text{N}(\text{Bpin})_2$), 2.34 (s, 3H, CH_3), 1.20 (s, 24H, $\text{N}(\text{Bpin})_2$) ppm; $^{13}\text{C}\{^1\text{H}\}$ NMR (CDCl_3 , 100.6 MHz, 298 K): δ 142.5 (*ArC-Me*), 137.6 (*Ph*), 128.0 (*Ph*), 127.6 (*Ph*), 123.6 (*Ph*), 81.9 ($\text{PhCH}_2\text{N}(\text{Bpin})_2$), 46.9 ($\text{PhCH}_2\text{N}(\text{Bpin})_2$), 24.3 ($\text{PhCH}_2\text{N}(\text{Bpin})_2$), 21.2 (*Ar-CH3*) ppm.

Entry 9d: ^1H NMR (CDCl_3 , 200 MHz, 298 K): δ 7.63-7.60 (m, 2H, *Ph*), 7.53-7.51 (d, $^3J_{\text{H-H}} = 8.13$

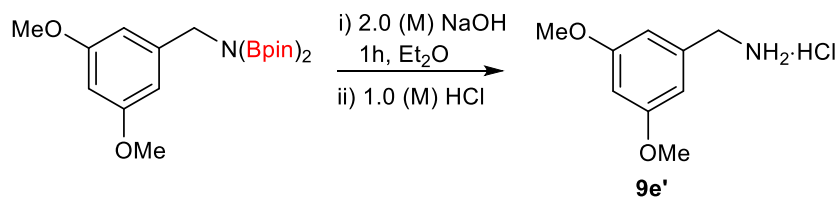
 Hz, 2H, *Ph*), 7.46-7.40 (m, 4H, *Ph*), 7.36-7.32 (m, 1H, *Ph*), 4.30 (s, 2H, $\text{PhCH}_2\text{N}(\text{Bpin})_2$), 1.24 (s, 24H, $\text{N}(\text{Bpin})_2$) ppm; $^{13}\text{C}\{^1\text{H}\}$ NMR (CDCl_3 , 100.6 MHz, 298 K): δ 142.0 ($\text{CH}_2\text{ArC-Ph}$), 141.0 ($\text{CH}_2\text{Ar-CAr}$), 128.4 (*Ph*), 127.7 (*Ph*), 126.7 (*Ph*), 126.3 (*Ph*), 82.8 ($\text{PhPhCH}_2\text{N}(\text{Bpin})_2$), 46.9 ($\text{PhPhCH}_2\text{N}(\text{Bpin})_2$), 24.3 ($\text{PhCH}_2\text{N}(\text{Bpin})_2$) ppm.

Entry 9e: ^1H NMR (CDCl_3 , 200 MHz, 298 K): δ 6.52 (m, 2H, *Ph*), 6.30 (s, 1H, *Ph*), 7.46-7.40

 (m, 4H, *Ph*), 7.36-7.32 (m, 1H, *Ph*), 4.18 (s, 2H, $\text{PhCH}_2\text{N}(\text{Bpin})_2$), 3.76 (s, 3H, OCH_3), 1.22 (s, 24H, $\text{N}(\text{Bpin})_2$) ppm; $^{13}\text{C}\{^1\text{H}\}$ NMR (CDCl_3 , 100.6 MHz, 298 K): δ 160.7 (*ArC-OMe*), 160.2 (*ArC-OMe*), 145.2 (*Ph*), 105.1 (*Ph*), 98.6 (*Ph*), 81.6 ($\text{PhCH}_2\text{N}(\text{Bpin})_2$), 54.8 (*-OMe*), 47.2 ($\text{PhCH}_2\text{N}(\text{Bpin})_2$), 24.3 ($\text{PhCH}_2\text{N}(\text{Bpin})_2$) ppm.

(3,5-dimethoxyphenyl)methanamine hydrochloride (**9e'**).

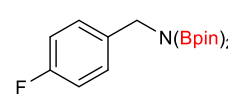
The general procedure was followed for the isolation of (3,5-dimethoxyphenyl)methanamine hydrochloride salt, **9e'** (39.7 mg, 78% yield) as a colorless solid.



^1H NMR (200 MHz, DMSO- d_6): δ 8.61 (br, 3H, $\text{NH}_2\cdot\text{HCl}$), 6.75-6.74 (d, $^3J_{\text{H-H}} = 2.25$ Hz, 2H, *Ph*), 6.48-6.47 (t, 1H, *Ph*), 3.94-3.90 (q, 2H, CH_2), 3.74 (s, 6H, *OMe*) ppm.

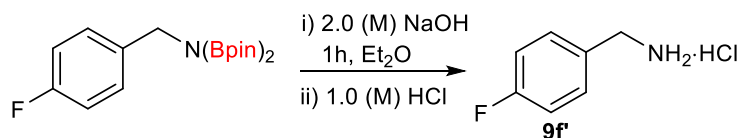
$^{13}\text{C}\{^1\text{H}\}$ (100.6 MHz, DMSO- d_6): δ 160.5 (*Ph*), 136.2 (*Ph*), 106.8 (*Ph*), 99.9 (*Ph*), 55.3 (*OMe*), 42.1 (CH_2) ppm.

Entry 9f: ^1H NMR (CDCl_3 , 200 MHz, 298 K): δ 7.31-7.26 (m, 2H, *Ph*), 6.95-6.90 (t, 2H, *Ph*),

 4.19 (s, 2H, $\text{PhCH}_2\text{N}(\text{Bpin})_2$), 1.18 (s, 24H, $\text{N}(\text{Bpin})_2$) ppm; $^{13}\text{C}\{^1\text{H}\}$ NMR (CDCl_3 , 100.5 MHz, 298 K): δ 162.5-160.1 (ArC-F), 138.6-138.3 (*Ph*), 129.0 (*Ph*), 114.4-114.2 (*Ph*), 81.7 ($\text{PhCH}_2\text{N}(\text{Bpin})_2$), 46.3 ($\text{PhCH}_2\text{N}(\text{Bpin})_2$), 24.3 ($\text{PhCH}_2\text{N}(\text{Bpin})_2$) ppm.

(4-fluorophenyl)methanamine hydrochloride (**9f'**).

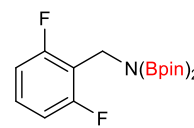
The general procedure was followed for the isolation of (4-fluorophenyl)methanamine hydrochloride salt, **9f'** (23 mg, 57% yield) as a colorless solid.



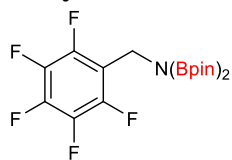
^1H NMR (200 MHz, DMSO- d_6): δ 8.61 (br, 3H, $\text{NH}_2\cdot\text{HCl}$), 7.59-7.58 (m, 2H, *Ph*), 7.26-7.21 (m, 2H, *Ph*), 3.99 (q, 2H, CH_2) ppm.

$^{13}\text{C}\{^1\text{H}\}$ (100.6 MHz, DMSO- d_6): δ 163.3-160.8 (*Ph*), 131.5-131.4 (*Ph*), 130.4 (*Ph*), 115.4-115.2 (*Ph*), 41.3 (CH_2) ppm.

Entry 9g: ^1H NMR (CDCl_3 , 200 MHz, 298 K): δ 7.05-7.00 (m, 1H, *Ph*), 6.75-6.71 (t, 2H, *Ph*),

 4.32 (s, 2H, $\text{PhCH}_2\text{N}(\text{Bpin})_2$), 1.16 (s, 24H, $\text{N}(\text{Bpin})_2$) ppm; $^{13}\text{C}\{^1\text{H}\}$ NMR (CDCl_3 , 100.5 MHz, 298 K): δ 163.0 (ArC-F), 160.6-160.5 (ArC-F), 128.0-127.9 (*Ph*), 112.3-112.0 (*Ph*), 110.8-112.5 (*Ph*), 81.5 ($\text{PhCH}_2\text{N}(\text{Bpin})_2$), 35.7 ($\text{PhCH}_2\text{N}(\text{Bpin})_2$), 24.1 ($\text{PhCH}_2\text{N}(\text{Bpin})_2$) ppm.

Entry 9h: ^1H NMR (CDCl_3 , 200 MHz, 298 K): δ 4.33 (s, 2H, $\text{PhCH}_2\text{N}(\text{Bpin})_2$), 1.18 (s, 24H, $\text{N}(\text{Bpin})_2$) ppm.



(Perfluorophenyl)methanamine hydrochloride (9h').

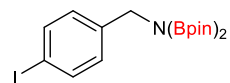
The general procedure was followed for the isolation of (perfluorophenyl)methanamine hydrochloride salt, **9h'** (23 mg, 57% yield) as a colorless solid.



^1H NMR (200 MHz, DMSO-d_6): δ 8.86 (bs, 3H, $\text{NH}_2\cdot\text{HCl}$), 4.12 (br, 2H, CH_2) ppm.

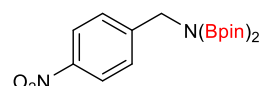
$^{13}\text{C}\{^1\text{H}\}$ (100.6 MHz, DMSO-d_6): δ 146.4-144.0 (*Ar*), 142.2-139.7 (*Ar*), 138.1-135.6 (*Ar*), 108.3 (*Ar*), 29.6 (CH_2) ppm.

Entry 9i: ^1H NMR (CDCl_3 , 200 MHz, 298 K): δ 7.59-7.56 (d, $^3J_{\text{H-H}} = 8.25$ Hz, 2H, *Ph*), 7.08-7.06 (d, $^3J_{\text{H-H}} = 8.25$ Hz, 2H, *Ph*), 4.17 (s, 2H, $\text{PhCH}_2\text{N}(\text{Bpin})_2$), 1.20 (s, 24H, $\text{N}(\text{Bpin})_2$) ppm; $^{13}\text{C}\{^1\text{H}\}$ NMR (CDCl_3 , 100.5 MHz, 298 K): δ 142.4 (*ArC-I*),



137.1 (*Ph*), 129.3 (*Ph*), 91.0 (*Ph*), 82.0 ($\text{PhCH}_2\text{N}(\text{Bpin})_2$), 46.4 ($\text{PhCH}_2\text{N}(\text{Bpin})_2$), 24.2 ($\text{PhCH}_2\text{N}(\text{Bpin})_2$) ppm.

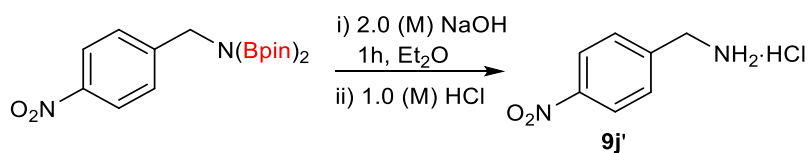
Entry 9j: ^1H NMR (CDCl_3 , 200 MHz, 298 K): δ 8.11-7.56 (m, 2H, *Ph*), 7.46-7.43 (m, 2H, *Ph*),



4.31 (s, 2H, $\text{PhCH}_2\text{N}(\text{Bpin})_2$), 1.18 (s, 24H, $\text{N}(\text{Bpin})_2$) ppm; $^{13}\text{C}\{^1\text{H}\}$ NMR (CDCl_3 , 100.5 MHz, 298 K): δ 150.3 (*ArC-NO*₂), 146.2 (*Ph*), 127.7 (*Ph*), 122.8 (*Ph*), 81.5 ($\text{NO}_2\text{PhCH}_2\text{N}(\text{Bpin})_2$), 46.6 ($\text{NO}_2\text{PhCH}_2\text{N}(\text{Bpin})_2$), 24.2 ($\text{NO}_2\text{PhCH}_2\text{N}(\text{Bpin})_2$) ppm.

(4-nitrophenyl)methanamine hydrochloride (9j').

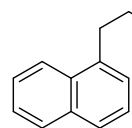
The general procedure was followed for the isolation of (4-nitrophenyl)methanamine hydrochloride salt, **9j'** (34 mg, 72% yield) as a white solid.



^1H NMR (200 MHz, DMSO- d_6): δ 8.80 (br, 3H, $\text{NH}_2\cdot\text{HCl}$), 8.27-8.25 (d, $^3J_{\text{H-H}} = 8.88$ Hz, 2H, *Ph*), 7.82-7.79 (d, $^3J_{\text{H-H}} = 8.88$ Hz, 2H, *Ph*), 4.18 (q, 2H, CH_2) ppm.

$^{13}\text{C}\{^1\text{H}\}$ (100.6 MHz, DMSO- d_6): δ 147.3 (*Ph*), 141.7 (*Ph*), 130.2 (*Ph*), 123.5 (*Ph*), 41.3 (CH_2) ppm.

Entry 9k: ^1H NMR (CDCl_3 , 200 MHz, 298 K): δ 8.38-8.36 (d, $^3J_{\text{H-H}} = 8.38$ Hz, 1H, *Ar*), 7.79-8.77

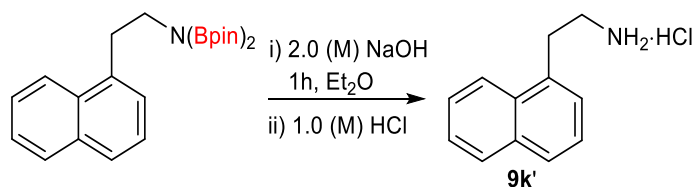


(d, $^3J_{\text{H-H}} = 7.63$ Hz, 1H, *Ar*), 7.67-7.65 (d, $^3J_{\text{H-H}} = 7.75$ Hz, 1H, *Ar*), 7.49-7.40 (m, 2H, *Ar*), 7.36-7.29 (m, 2H, *Ar*), 3.42-3.38 (t, 2H, $\text{ArCH}_2\text{CH}_2\text{N}(\text{Bpin})_2$), 3.19-3.15 (t, 2H, $\text{ArCH}_2\text{CH}_2\text{N}(\text{Bpin})_2$), 1.18 (s, 24H, $\text{N}(\text{Bpin})_2$) ppm; $^{13}\text{C}\{^1\text{H}\}$

NMR (CDCl_3 , 100.5 MHz, 298 K): δ 136.2 (*Ar*), 133.6 (*Ar*), 132.3 (*Ar*), 128.2 (*Ar*), 126.8 (*Ar*), 126.4 (*Ar*), 125.2 (*Ar*), 125.1 (*Ar*), 125.0 (*Ar*), 124.4 (*Ar*), 81.8 ($\text{ArCH}_2\text{CH}_2\text{N}(\text{Bpin})_2$), 44.7 ($\text{ArCH}_2\text{CH}_2\text{N}(\text{Bpin})_2$), 37.0 ($\text{ArCH}_2\text{CH}_2\text{N}(\text{Bpin})_2$), 24.2 ($\text{ArCH}_2\text{CH}_2\text{N}(\text{Bpin})_2$) ppm.

Naphthalen-1-ylmethanamine hydrochloride (**9k'**).

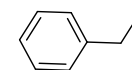
The general procedure was followed for the isolation of Naphthalen-1-ylmethanamine hydrochloride salt, **9k'** (46.5 mg, 89.5% yield) as a colorless solid.



^1H NMR (200 MHz, DMSO- d_6): δ 8.43 (br, 3H, $\text{NH}_2\cdot\text{HCl}$), 8.22-8.20 (d, $^3J_{\text{H-H}} = 8.26$ Hz, 1H, *Ph*), 7.95-7.93 (d, $^3J_{\text{H-H}} = 7.75$ Hz, 1H, *Ph*), 7.84-7.82 (d, $^3J_{\text{H-H}} = 7.25$ Hz, 1H, *Ph*), 7.59-7.51 (m, 2H, *Ph*), 7.47-7.42 (m, 2H, *Ph*), 3.43 (t, 2H, CH_2), 3.07 (sept, 2H, CH_2) ppm.

$^{13}\text{C}\{^1\text{H}\}$ (100.6 MHz, DMSO- d_6): δ 133.5 (*Ar*), 131.3 (*Ar*), 128.7 (*Ar*), 127.4 (*Ar*), 126.9 (*Ar*), 126.3 (*Ar*), 125.8 (*Ar*), 125.6 (*Ar*), 123.5 (*Ar*), 30.1 (CH_2) ppm.

Entry 9l: ^1H NMR (CDCl_3 , 200 MHz, 298 K): δ 7.25-7.23 (m, 2H, *Ph*), 7.20-7.14 (m, 3H, *Ph*),

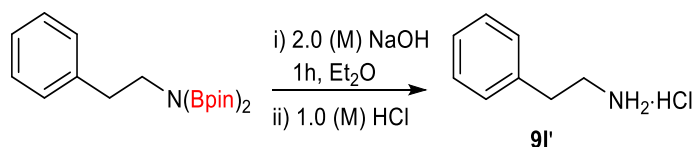


3.35-3.31 (t, 2H, $\text{PhCH}_2\text{CH}_2\text{N}(\text{Bpin})_2$), 2.75-2.72 (t, 2H, $\text{PhCH}_2\text{CH}_2\text{N}(\text{Bpin})_2$), 1.19 (s, 24H, $\text{N}(\text{Bpin})_2$) ppm; $^{13}\text{C}\{^1\text{H}\}$ NMR (CDCl_3 ,

100.53 MHz, 298 K): δ 140.2 (ArC-R), 129.0 (*Ph*), 127.8 (*Ph*), 125.4 (*Ph*), 81.8 ($\text{PhCH}_2\text{CH}_2\text{N}(\text{Bpin})_2$), 44.9 ($\text{PhCH}_2\text{CH}_2\text{N}(\text{Bpin})_2$), 39.2 ($\text{PhCH}_2\text{CH}_2\text{N}(\text{Bpin})_2$), 24.3 ($\text{PhCH}_2\text{CH}_2\text{N}(\text{Bpin})_2$) ppm.

2-phenylethanamine hydrochloride (**9l'**).

The general procedure was followed for the isolation of 2-phenylethanamine hydrochloride salt, **9l'** (37 mg, 94% yield) as a colorless solid.



^1H NMR (200 MHz, DMSO- d_6): δ 8.28 (br, 3H, $\text{NH}_2\cdot\text{HCl}$), 7.33-7.30 (m, 2H, *Ph*), 7.26-7.21 (m, 3H, *Ph*), 2.99 (sept, 2H, CH_2), 2.93-2.89 (m, 2H, CH_2) ppm.

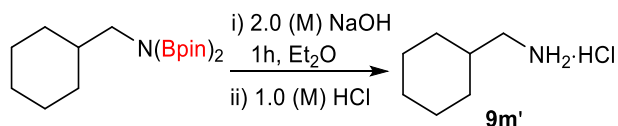
$^{13}\text{C}\{^1\text{H}\}$ (100.6 MHz, DMSO- d_6): δ 137.5 (*Ph*), 128.6 (*Ph*), 128.6 (*Ph*), 126.7 (*Ph*), 39.9 (CH_2), 32.9 (CH_2) ppm.

Entry 9m: ^1H NMR (CDCl_3 , 200 MHz, 298 K): δ 2.87-2.86 (m, 2H, *Cy*), 1.67-1.65 (m, 4H, *Cy*),

1.60 (br, 1H, *Cy*), 1.19 (s, 24H, $\text{N}(\text{Bpin})_2$), 1.14-1.08 (m, 4H, *Cy*), 0.89-0.83 (m, 2H, *Cy*) ppm; $^{13}\text{C}\{^1\text{H}\}$ NMR (CDCl_3 , 100.5 MHz, 298 K): δ 81.7 ($\text{CyCH}_2\text{N}(\text{Bpin})_2$), 49.4 ($\text{CyCH}_2\text{N}(\text{Bpin})_2$), 47.6 ($\text{CyCH}_2\text{N}(\text{Bpin})_2$), 40.2 ($\text{CyCH}_2\text{N}(\text{Bpin})_2$), 30.3 ($\text{CyCH}_2\text{N}(\text{Bpin})_2$), 26.5 ($\text{CyCH}_2\text{N}(\text{Bpin})_2$), 25.9 ($\text{CyCH}_2\text{N}(\text{Bpin})_2$), 24.3 ($\text{PhCH}_2\text{CH}_2\text{N}(\text{Bpin})_2$) ppm.

Cyclohexylmethanamine hydrochloride (**9m'**).

The general procedure was followed for the isolation of 2-phenylethanamine hydrochloride salt, **9m'** (28mg, 74.8% yield) as a colorless solid.



^1H NMR (200 MHz, DMSO- d_6): δ 6.19 (br, 3H, $\text{NH}_2\cdot\text{HCl}$), 2.58-2.56 (d, $^3J_{\text{H-H}} = 6.57$ Hz, 2H, CH_2), 1.75-1.52 (m, 6H, *Cy*), 1.22-1.09 (m, 3H, *Cy*), 0.93-0.84 (m, 2H, *Cy*) ppm.

$^{13}\text{C}\{^1\text{H}\}$ (100.6 MHz, DMSO- d_6): δ 44.6 (ipso-C, *Cy*), 35.7 (CH_2), 29.8 (CH_2 , *Cy*), 25.7 (CH_2 , *Cy*), 25.1 (CH_2 , *Cy*) ppm.

Entry 9n: ^1H NMR (CDCl_3 , 200 MHz, 298 K): δ 3.09-3.04 (q, 2H, CH_2), 1.22 (s, 24H, $\text{N}(\text{Bpin})_2$), $\text{H}_3\text{C}-\text{CH}_2-\text{N}(\text{Bpin})_2$ 1.05-1.01 (t, 3H, CH_3) ppm; $^{13}\text{C}\{^1\text{H}\}$ NMR (CDCl_3 , 100.5 MHz, 298 K): δ 81.4 ($\text{CyCH}_2\text{N}(\text{Bpin})_2$), 38.0 ($\text{CH}_3\text{CH}_2\text{N}(\text{Bpin})_2$), 24.1 ($\text{CH}_3\text{CH}_2\text{N}(\text{Bpin})_2$), 18.8 ($\text{CH}_3\text{CH}_2\text{N}(\text{Bpin})_2$) ppm.

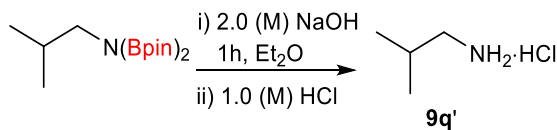
Entry 9o: ^1H NMR (CDCl_3 , 200 MHz, 298 K): δ 3.02-2.98 (t, 2H, CH_2), 1.42-1.40 (m, 2H, CH_2), $\text{Et}-\text{CH}_2-\text{N}(\text{Bpin})_2$ 1.21 (s, 24H, $\text{N}(\text{Bpin})_2$), 0.86-0.82 (t, 3H, CH_3) ppm; $^{13}\text{C}\{^1\text{H}\}$ NMR (CDCl_3 , 100.5 MHz, 298 K): δ 81.5 ($\text{CH}_3\text{CH}_2\text{CH}_2\text{N}(\text{Bpin})_2$), 44.9 ($\text{CH}_3\text{CH}_2\text{CH}_2\text{N}(\text{Bpin})_2$), 26.3 ($\text{CH}_3\text{CH}_2\text{CH}_2\text{N}(\text{Bpin})_2$), 24.1 ($\text{CH}_3\text{CH}_2\text{CH}_2\text{N}(\text{Bpin})_2$), 10.7 ($\text{CH}_3\text{CH}_2\text{CH}_2\text{N}(\text{Bpin})_2$) ppm.

Entry 9p: ^1H NMR (CDCl_3 , 200 MHz, 298 K): δ 3.04-3.01 (t, 2H, $\text{CH}_3(\text{CH}_2)_4\text{CH}_2\text{N}(\text{Bpin})_2$), 1.29-1.27 (m, 4H, $\text{CH}_3(\text{CH}_2)_2(\text{CH}_2)_2\text{CH}_2\text{N}(\text{Bpin})_2$), 1.21 (s, 24H, $\text{N}(\text{Bpin})_2$), 1.17-1.05 (m, 4H, $\text{CH}_3(\text{CH}_2)_2(\text{CH}_2)_2\text{CH}_2\text{N}(\text{Bpin})_2$), 0.89-0.86 (t, 3H, CH_3) ppm; $^{13}\text{C}\{^1\text{H}\}$ NMR (CDCl_3 , 100.5 MHz, 298 K): δ 81.8 ($\text{CH}_3(\text{CH}_2)_4\text{CH}_2\text{N}(\text{Bpin})_2$), 40.1 ($\text{CH}_3(\text{CH}_2)_4\text{CH}_2\text{N}(\text{Bpin})_2$), 30.9 ($\text{CH}_3(\text{CH}_2)_3\text{CH}_2\text{CH}_2\text{N}(\text{Bpin})_2$), 29.9 ($\text{CH}_3(\text{CH}_2)_2\text{CH}_2\text{CH}_2\text{CH}_2\text{N}(\text{Bpin})_2$), 28.7 ($\text{CH}_3\text{CH}_2\text{CH}_2(\text{CH}_2)_3\text{N}(\text{Bpin})_2$), 26.1 ($\text{CH}_3\text{CH}_2\text{CH}_2(\text{CH}_2)_3\text{N}(\text{Bpin})_2$), 24.1 ($\text{CH}_3(\text{CH}_2)_4\text{CH}_2\text{N}(\text{Bpin})_2$), 13.6 ($\text{CH}_3\text{CH}_2\text{CH}_2(\text{CH}_2)_3\text{N}(\text{Bpin})_2$) ppm.

Entry 9q: ^1H NMR (CDCl_3 , 200 MHz, 298 K): δ 2.85-2.83 (d, $^3J_{\text{H-H}} = 7.00$ Hz, 2H, CH_2), 1.68-1.58 (m, 1H, CH), 1.19 (s, 24H, $\text{N}(\text{Bpin})_2$), 0.82-0.80 (d, $^3J_{\text{H-H}} = 6.63$ Hz, 6H, CH_3) ppm; $^{13}\text{C}\{^1\text{H}\}$ NMR (CDCl_3 , 100.5 MHz, 298 K): δ 81.5 ($(\text{CH}_3)_2\text{CHCH}_2\text{N}(\text{Bpin})_2$), 50.6 ($(\text{CH}_3)_2\text{CHCH}_2\text{N}(\text{Bpin})_2$), 30.3 ($(\text{CH}_3)_2\text{CHCH}_2\text{N}(\text{Bpin})_2$), 24.1 ($(\text{CH}_3)_2\text{CHCH}_2\text{N}(\text{Bpin})_2$), 19.5 ($(\text{CH}_3)_2\text{CHCH}_2\text{N}(\text{Bpin})_2$) ppm.

2-methylpropan-1-amine hydrochloride (9q').

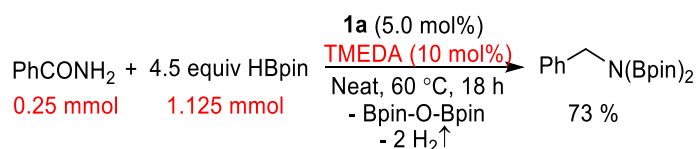
The general procedure was followed for the isolation of 2-phenylethanamine hydrochloride salt, **9q'** (19 mg, 69.8% yield) as a colorless solid.



^1H NMR (200 MHz, $\text{DMSO}-d_6$): δ 7.87 (br, 3H, $\text{NH}_2 \cdot \text{HCl}$), 2.62-2.0 (d, $^3J_{\text{H-H}} = 7.00$ Hz, 2H, CH_2), 1.85 (sept, 1H, $\text{CH}(\text{CH}_3)_2$), 0.92-0.91 (d, $^3J_{\text{H-H}} = 6.63$ Hz, 2H, $\text{CH}(\text{CH}_3)_2$) ppm.

A Schlenk tube was charged with benzamide (30.2 mg, 0.1 mmol), HBpin (144 mg, 1.12 mmol), **4a** (3.5 mg, 0.005 mmol, 5 mol%) and toluene (1 mL) in an argon filled glovebox and the reaction mixture was stirred for 16 h, at room temperature. Next, volatiles were removed using high vacuum and ^1H NMR spectroscopy of the reaction mixture was recorded in CDCl_3 . A sharp resonance at δ 10.20 ppm was observed in ^1H NMR spectrum for benzamide substrate, which clearly indicates the formation of an imine intermediate.

❖ Reaction in presence of TMEDA.



To identify whether the BH_3 (decomposition product of HBpin in presence of nucleophilic lithium catalyst) is behaving as hidden catalyst in the hydroboration of benzamide or not, we performed the reaction in presence of *N,N,N',N'*-Tetramethylethylenediamine (TMEDA) as a BH_3 scavenger. An oven dried 20 mL Schlenk tube was charged with **4a** (3.5 mg, 5.0 mol%) and HBpin (144 mg, 1.12 mmol, 4.5 equiv), and TEMDA (2.9 mg, 10 mol%) inside the Argon-filled glovebox. Subsequently benzamide (30.2 mg, 0.25 mmol, 1.0 equiv), was added to the reaction mixture and heated at 60°C for 18h in an oil bath. After completion of the reaction 0.25 mmol mesitylene was added as an internal standard prior to the NMR measurement in CDCl_3 solvent. For the mentioned reaction, 73% NMR yield (87% for without TMEDA) for the corresponding N-borylated product was observed (Scheme S4). Which clearly suggest for the non-involvement or very less influence of BH_3 as an active catalyst for the hydroboration of benzamide.

❖ Stoichiometric reaction of **4a** and benzamide.

10 mL toluene was added to the mixture of **4a** (200 mg, 0.70 mmol) and benzamide (86 mg, 0.70 mmol) at room temperature. The reaction mixture was stirred for 12 h at room temperature. Upon completion, the reaction mixture was dried in vacuum and subjected for characterization. The ^1H NMR spectrum shows no peak for the THF molecules and suggest possible coordination of benzamide to the catalyst. Yield: 0.214 g, 91%. ^1H NMR (C_6D_6 , 200 MHz, 298 K): δ 7.84-7.82 (d, $^3J_{\text{H-H}} = 7.25$ Hz, 2H, *Ph*), 7.57-7.53 (t, 1H, *Ph*), 7.48-7.44 (t, 2H, *Ph*), 7.20-7.18 (d, $^3J_{\text{H-H}} = 7.88$ Hz, 2H, *Ph*), 6.85-6.82 (t, 1H, *Ph*), 1.46 (s, 18H, $\text{C}(\text{CH}_3)_3$) ppm.

❖ Stoichiometric reaction of catalyst 4a and HBpin.

A solution of HBpin (135 mg, 1.05 mmol) in toluene (3 mL) was added dropwise to the toluene solution (10 mL) of **4a** (300 mg, 1.05 mmol) at room temperature. The reaction mixture was stirred for 12 h at room temperature. After addition of HBpin, solution was clear up to 3-4 h and after that white ppt started forming slowly. The reaction mixture was subjected for characterization. Yield: 0.192 g, 55 %. ^1H NMR (C_6D_6 , 200 MHz, 298 K): δ 7.22 (d, $^3J_{\text{H-H}} = 7.83$ Hz, 2H, *Ph*), 6.92 (t, 1H, *Ph*), 1.52 (s, 18H, $\text{C}(\text{CH}_3)_3$), 1.06 (s, 12H, CH_3) ppm; $^{13}\text{C}\{^1\text{H}\}$ NMR (toluene- d_8 , 100.5 MHz, 298 K): δ 152.1 (*Ph*), 141.1 (*Ph*), 125.9 (*Ph*), 123.2 (*Ph*), 83.3 ($\text{C}(\text{CH}_3)_2$), 35.4 ($\text{C}(\text{CH}_3)_3$), 31.8 ($\text{C}(\text{CH}_3)_3$), 31.6 (CH_3) ppm; ^{11}B NMR (toluene- d_8 , 128 MHz, 298 K): δ 86.9 (s), 21.7 (s), 4.6 (s), -25.7 (quadruplet), -39.9 (quintet), 29.1-27.8 (d, for unreacted HBpin) ppm.

Upon filtration and evaporation of solvent, the filtrate part shows only three peaks at δ 4.6 (s), 21.7 (s), and -39.9 (quintet) in the ^{11}B NMR spectrum.

6.3.14. General catalytic procedure for the hydroboration of secondary amides.

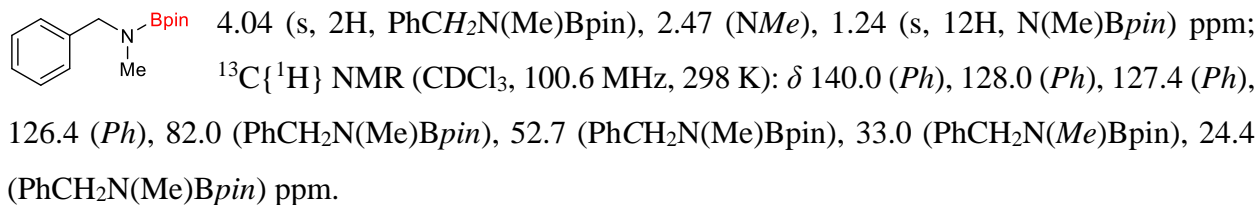
Primary amide (0.25 mmol), pinacolborane (3.0 equiv, 0.75 mmol), catalyst (5.0 mol% **4a**) were mixed together in a Schlenk tube or in a screw cap NMR tube inside the glove box. The reaction mixture was allowed to heat at 60 °C for 18 h without adding any solvent. After reaction, mesitylene (0.25 mmol) as an internal standard, was added while making the NMR in appropriate deuterated solvent. The progress of the reaction was monitored by ^1H NMR, which indicated the completion of the reaction by the appearance of a new $\text{R-CH}_2\text{-NR}'(\text{Bpin})$ resonance.

Upon completion, the reaction mixture was stirred with 1.0 mL 2.0 (M) NaOH solutions and 1.0 mL Et_2O for 1 h to complete the hydrolysis. Next, the reaction mixture was worked up with $\text{Et}_2\text{O}:\text{H}_2\text{O}$ mixture (1:1) and the Et_2O part were concentrated in vacuum to get corresponding reduced amines. Consequently, 1.0 mL 1.0 (M) methanolic HCl solution was added to the concentrated amines followed by addition of 1.0 mL Et_2O and the corresponding amine hydrochloride salt was purified by washing with Et_2O . Isolated amine hydrochlorides were characterized through NMR spectroscopy in $\text{DMSO-}d_6$.

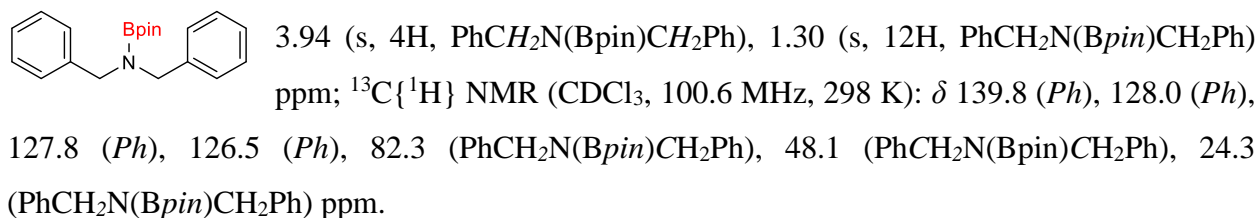
Hydroboration product of secondary amides, namely **10b** were isolated and little discrepancy was observed with the NMR yield.

6.3.14. Analytical data of the borylated amines of corresponding secondary amides.

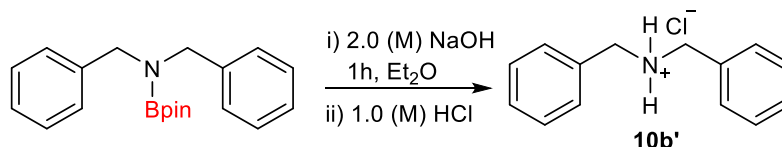
Entry 10a: ^1H NMR (CDCl_3 , 200 MHz, 298 K): δ 7.33-7.27 (m, 2H, *Ph*), 7.22-7.20 (m, 3H, *Ph*),



Entry 10b: ^1H NMR (CDCl_3 , 200 MHz, 298 K): δ 7.31-7.27 (m, 4H, *Ph*), 7.23-7.19 (m, 6H, *Ph*),

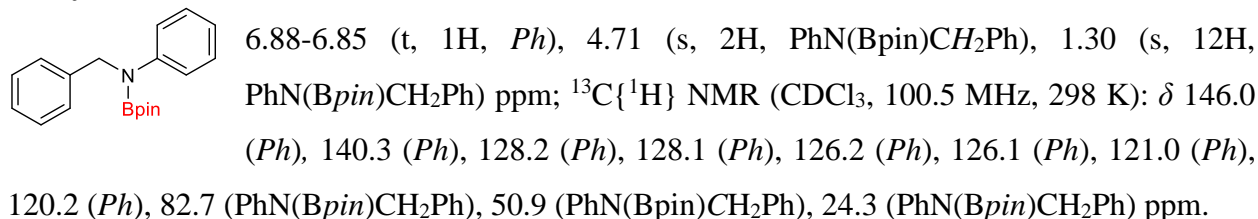
**Dibenzylamine hydrochloride (10b').**

The general procedure was followed for the isolation of phenylmethanamine hydrochloride salt, **10b'** (51 mg, 87% yield) as a colorless solid.

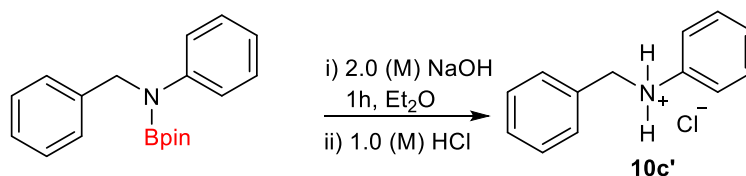


^1H NMR (200 MHz, $\text{DMSO}-d_6$): δ 10.04 (br, 2H, $\text{NH}\cdot\text{HCl}$), 7.61-7.59 (m, 4H, *Ph*), 7.44-7.40 (m, 6H, *Ph*), 4.11 (s, 4H, CH_2) ppm.

Entry 10c: ^1H NMR (CDCl_3 , 200 MHz, 298 K): δ 7.29-7.22 (m, 6H, *Ph*), 7.18-7.12 (m, 3H, *Ph*),

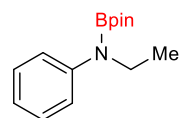
**Dibenzylamine hydrochloride (10c').**

The general procedure was followed for the isolation of phenylmethanamine hydrochloride salt, **10c'** (50 mg, 91 % yield) as a colorless solid.

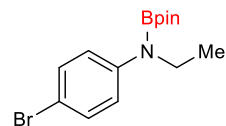


^1H NMR (200 MHz, DMSO- d_6): δ 7.51-7.49 (m, 1H, Ph), 7.38-7.2 (m, H, Ph), 4.48 (s, 4H, CH_2) ppm; $^{13}\text{C}\{^1\text{H}\}$ (100.6 MHz, DMSO- d_6): δ 138.0(Ph), 133.1 (Ph), 129.8 (Ph), 129.4 (Ph), 128.4 (Ph), 128.3 (Ph), 126.3 (Ph), 121.5 (Ph), 52.3 (CH_2) ppm.

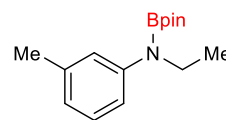
Entry 10d: ^1H NMR (CDCl_3 , 200 MHz, 298 K): δ 7.27-7.23 (m, 4H, Ph), 6.94-6.90 (m, 1H, Ph), 3.57-3.51 (q, 2H, CH_2), 1.28 (s, 12H, $\text{PhN(Bpin)CH}_2\text{CH}_3$), 1.16-1.12 (t, 3H, $\text{PhN(Bpin)CH}_2\text{CH}_3$) ppm; $^{13}\text{C}\{^1\text{H}\}$ NMR (CDCl_3 , 100.6 MHz, 298 K): δ 145.8 (Ph), 128.3 (Ph), 121.0 (Ph), 120.7 (Ph), 82.2 ($\text{PhN(Bpin)CH}_2\text{Me}$), 41.5 ($\text{PhN(Bpin)CH}_2\text{Me}$), 24.3 ($\text{PhN(Bpin)CH}_2\text{Ph}$), 15.2 ($\text{PhN(Bpin)CH}_2\text{Me}$) ppm.



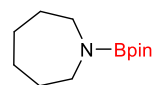
Entry 10e: ^1H NMR (CDCl_3 , 200 MHz, 298 K): δ 7.39-7.34 (d, $^3J_{\text{H-H}} = 9.04$ Hz, 2H, Ph), 7.20-7.15 (d, $^3J_{\text{H-H}} = 9.04$ Hz, 2H, Ph), 3.60-3.50 (q, 2H, CH_2), 1.32 (s, 12H, $\text{PhN(Bpin)CH}_2\text{CH}_3$), 1.20-1.13 (t, 3H, $\text{PhN(Bpin)CH}_2\text{CH}_3$) ppm; $^{13}\text{C}\{^1\text{H}\}$ NMR (CDCl_3 , 100.6 MHz, 298 K): δ 144.9 (Ar), 131.2 (Ar), 122.2 (Ar), 114.0 (Ar), 113.4 (Ar), 82.5 ($\text{ArN(Bpin)CH}_2\text{Me}$), 41.4 ($\text{ArN(Bpin)CH}_2\text{Me}$), 24.3 ($\text{ArN(Bpin)CH}_2\text{Ph}$), 14.9 ($\text{ArN(Bpin)CH}_2\text{Me}$) ppm.



Entry 10f: ^1H NMR (CDCl_3 , 200 MHz, 298 K): δ 7.22-7.15 (m, 3H, Ph), 6.83 (s, 1H, Ph), 3.68-3.58 (q, 2H, CH_2), 2.42 (s, 3H, Me), 1.37 (s, 12H, $\text{PhN(Bpin)CH}_2\text{CH}_3$), 1.27-1.21 (t, 3H, $\text{PhN(Bpin)CH}_2\text{CH}_3$) ppm; $^{13}\text{C}\{^1\text{H}\}$ NMR (CDCl_3 , 100.5 MHz, 298 K): δ 145.7 (Ar), 137.7 (Ar), 128.1 (Ar), 122.0 (Ar), 121.5 (Ar), 118.3 (Ar), 82.1 ($\text{PhN(Bpin)CH}_2\text{Me}$), 41.7 ($\text{ArN(Bpin)CH}_2\text{Me}$), 24.3 ($\text{ArN(Bpin)CH}_2\text{Ph}$), 21.5 (Ar-Me), 15.2 ($\text{ArN(Bpin)CH}_2\text{Me}$) ppm.



Entry 10g: ^1H NMR (CDCl_3 , 200 MHz, 298 K): δ 3.06-3.03 (t, 4H, $\text{RCH}_2\text{N(Bpin)CH}_2\text{R}$), 1.73 (br, 4H, $\text{RCH}_2\text{CH}_2\text{N(Bpin)CH}_2\text{CH}_2\text{R}$), 1.60 (br, 4H, $\text{CH}_2\text{CH}_2\text{CH}_2\text{N(Bpin)CH}_2\text{CH}_2\text{CH}_2$), 1.18 (s, 12H, $\text{CH}_2\text{CH}_2\text{CH}_2\text{N(Bpin)CH}_2\text{CH}_2\text{CH}_2$) ppm; $^{13}\text{C}\{^1\text{H}\}$ NMR (CDCl_3 , 100.6 MHz, 298 K): δ 81.4 ($\text{PhCH}_2\text{N(Me)Bpin}$), 46.7 ($-\text{CH}_2\text{CH}_2\text{CH}_2\text{N(Bpin)CH}_2\text{CH}_2\text{CH}_2-$), 30.9 (-



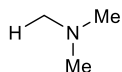
$\text{CH}_2\text{CH}_2\text{CH}_2\text{N}(\text{Bpin})\text{CH}_2\text{CH}_2\text{CH}_2-$), 27.0 ($-\text{CH}_2\text{CH}_2\text{CH}_2\text{N}(\text{Bpin})\text{CH}_2\text{CH}_2\text{CH}_2-$), 24.3 ($-\text{CH}_2\text{CH}_2\text{CH}_2\text{N}(\text{Bpin})\text{CH}_2\text{CH}_2\text{CH}_2-$) ppm.

6.3.15. General catalytic procedure for the hydroboration of tertiary amides.

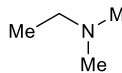
N,N-dimethyl benzaide (37.5 mg, 0.25 mmol), pinacolborane (144 mg, 4.5 equiv, 1.125 mmol), catalyst (3.58 mg, 5.0 mol% of **4a**) were mixed together in a Schlenk tube or in a screw cap NMR tube inside the glove box. The reaction mixture was allowed to heat at 60 °C for 21 h without adding any solvent. Upon completion, mesitylene (0.25 mmol) as an internal standard, was added while making the NMR in appropriate deuterated solvent. The progress of the reaction was monitored by ^1H NMR, which indicated the completion of the reaction by the appearance of a new $\text{R}-\text{CH}_2-\text{NR}'\text{R}''$ resonance.

6.3.16. Analytical data of the amines of corresponding tertiary amides

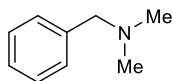
Entry 11a: ^1H NMR (CDCl_3 , 200 MHz, 298 K): δ 2.46 (NMe_3) ppm; $^{13}\text{C}\{^1\text{H}\}$ NMR (CDCl_3 , 100.6 MHz, 298 K): δ 48.2 (NMe_3) ppm.



Entry 11b: ^1H NMR (CDCl_3 , 200 MHz, 298 K): δ 2.85-2.74 (q, 2H, CH_2CH_3), 2.48 (NMe_2), 1.16 (t, 3H, CH_3CH_2) ppm; $^{13}\text{C}\{^1\text{H}\}$ NMR (CDCl_3 , 100.6 MHz, 298 K): δ 48.2 (NMe_3) ppm.

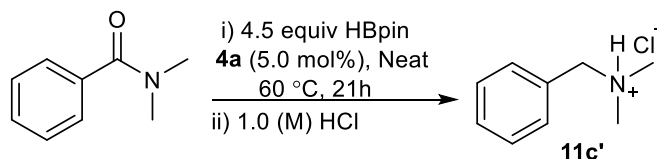


Entry 11c: ^1H NMR (CDCl_3 , 200 MHz, 298 K): δ 7.40-7.30 (m, 5H, *Ph*), 3.96 (s, 2H, $\text{PhCH}_2\text{N}(\text{Me})_2$), 2.48 (NMe_2), 1.26 (s, 24H, *BpinOBpin*) ppm; $^{13}\text{C}\{^1\text{H}\}$ NMR (CDCl_3 , 100.6 MHz, 298 K): δ 131.9 (*Ph*), 128.7 (*Ph*), 128.1 (*Ph*), 126.4 (*Ph*), 67.1 ($\text{PhCH}_2\text{N}(\text{Me})_2$), 49.3 ($\text{PhCH}_2\text{N}(\text{Me})_2$) ppm.



N,N-dimethyl-1-phenylmethanamine hydrochloride (**11c'**).

The general procedure was followed for the isolation of phenylmethanamine hydrochloride salt, **11c'** (28 mg, 65.4% yield) as a colorless solid.



^1H NMR (200 MHz, DMSO- d_6): δ 7.56 (br, 2H, *Ph*), 7.44-7.43 (m, 3H, *Ph*), 4.26-4.25 (d, $^3J_{\text{H-H}} = 4.13$ Hz, 2H, CH_2), 2.67-2.66 (d, $^3J_{\text{H-H}} = 3.50$ Hz, 6H, CH_3) ppm.

$^{13}\text{C}\{^1\text{H}\}$ (100.6 MHz, DMSO- d_6): δ 131.1, 130.5, 129.6, 128.9, 59.6, 41.6 ppm.

Entry 11d: ^1H NMR (CDCl_3 , 200 MHz, 298 K): δ 7.19-7.11 (m, 4H, *Ph*), 3.86 (s, 2H, $\text{PhCH}_2\text{N}(\text{Me})_2$), 2.71-2.66 (N(CH_2CH_3) $_2$), 2.34 (s, 3H, *Me*), 1.27-1.26 (d, $^3J_{\text{H-H}} = 7.38$ Hz, 6H, (N(CH_2CH_3) $_2$) ppm; $^{13}\text{C}\{^1\text{H}\}$ NMR (CDCl_3 , 100.6 MHz, 298 K): δ 136.9 (*Ar*), 132.5 (*Ar*), 131.0 (*Ar*), 128.9-128.8 (*Ar*), 127.7-127.5 (*Ar*), 61.8 ($\text{ArCH}_2\text{N}(\text{Et})_2$), 52.1 ($\text{PhCH}_2\text{N}(\text{CH}_2\text{CH}_3)_2$), 8.7 ($\text{PhCH}_2\text{N}(\text{CH}_2\text{CH}_3)_2$) ppm.

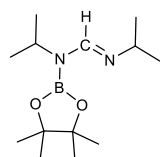
Entry 11e: ^1H NMR (CDCl_3 , 200 MHz, 298 K): δ 7.40-7.30 (m, 5H, *Ph*), 3.98 (s, 2H, PhCH_2NCy), 2.92-2.87 (m, 2H, PhCH_2NPip), 2.65-2.59 (m, 2H, PhCH_2NPip), 2.21-2.11 (m, 2H, PhCH_2NPip), 1.62-1.52 (m, 4H, PhCH_2NPip) ppm; $^{13}\text{C}\{^1\text{H}\}$ NMR (CDCl_3 , 100.6 MHz, 298 K): δ 132.6 (*Ph*), 130.5 (*Ph*), 128.3 (*Ph*), 127.5 (*Ph*), 66.9 (PhCH_2NPip), 56.4 (PhCH_2NPip), 22.2 (PhCH_2NPip), 20.5 (PhCH_2NPip) ppm.

6.3.17. General catalytic procedure for the hydroboration of carbodiimide

Carbodiimide (0.25 mmol), pinacolborane (0.28 mmol, 1.1 equiv), catalyst (4.0 mol% for **4a** or, 4.0 mol% for **4b**) were mixed together in a Schlenk tube or in a screw cap NMR tube inside the glove box. The reaction mixture was allowed to heat at 80 °C for 12 h (for **4a**) and 15 h (for **4b**) in neat condition without any solvent. After reaction, mesitylene (0.25 mmol) as an internal standard, was added while making the NMR in appropriate deuterated solvent. The progress of the reaction was monitored by ^1H NMR, which indicated the completion of the reaction by the appearance of a new Bpin-NRCHR resonance.

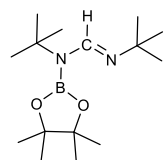
6.3.18. Spectroscopic data of the borylated amines of corresponding carbodiimides

Entry 12a: ^1H NMR (CDCl_3 , 200 MHz, 298 K): δ 7.90 (s, 1H, (*i*Pr)NCHN(*i*Pr)Bpin), 4.53 (septet, 1H, $\text{CH}(\text{CH}_3)_2$), 3.38 (septet, 1H, $\text{CH}(\text{CH}_3)_2$), 1.30 (s, 12H, (*i*Pr)NCHN(*i*Pr)Bpin), 1.26 (d, 6H, $J_{\text{H-H}} = 4.1$ Hz, $\text{CH}(\text{CH}_3)_2$), 1.18 (d, 6H, $J_{\text{H-H}} = 6.3$ Hz, $\text{CH}(\text{CH}_3)_2$) ppm;

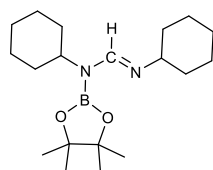


$^{13}\text{C}\{^1\text{H}\}$ NMR (CDCl_3 , 100.6 MHz, 298 K): δ 152.0 (NCHN), 81.4 (Bpin-*ipso*), 57.3 (BNCH(CH_3) $_2$), 45.5 (NCH(CH_3) $_2$), 25.2 (BNCH(CH_3) $_2$), 24.5(*Bpin*), 23.6 (NCH(CH_3) $_2$) ppm.

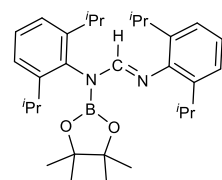
Entry 12b: ^1H NMR (CDCl_3 , 200 MHz, 298 K): δ 7.92 (s, 1H, (*t*Bu)NCHN(*t*Bu)Bpin), 1.39 (s, 18H, C(CH_3) $_3$), 1.29 (s, 12H, (*t*Bu)NCHN(*t*Bu)Bpin) ppm; $^{13}\text{C}\{^1\text{H}\}$ NMR (CDCl_3 , 100.6 MHz, 298 K): δ 147.3 (NCHN), 82.4 (Bpin-*ipso*), 54.2 (C(CH_3) $_3$), 30.5 (C(CH_3) $_3$), 24.3(*Bpin*) ppm.



Entry 12c: ^1H NMR (CDCl_3 , 200 MHz, 298 K): δ 7.80 (s, 1H, (Cy)NCHN(Cy)Bpin), 4.00 (hept, 2H, BNCH(CH_2) $_2$), 2.89 (hept, 2H, NCH(CH_2) $_2$), 1.78-1.56 (m, 14 H, Cy), 1.30-1.21 (m, 6 H, Cy), 1.17 (s, 12H, *Bpin*) ppm; $^{13}\text{C}\{^1\text{H}\}$ NMR (CDCl_3 , 100.5 MHz, 298 K): δ 150.4 (NCHN), 82.4 (Bpin-*ipso*), 64.9 (BNCH(CH_3) $_2$), 50.8 (NCH(CH_3) $_2$), 35.3 (BNCH(CH_2) $_2$ (CH_2) $_2$ CH $_2$), 34.7 (BNCH(CH_2) $_2$ (CH_2) $_2$ CH $_2$), 31.7 (NCH(CH_2) $_2$ (CH_2) $_2$ CH $_2$), 31.4 (NCH(CH_2) $_2$ (CH_2) $_2$ CH $_2$), 26.4 (BNCH(CH_2) $_2$ (CH_2) $_2$ CH $_2$), 25.9 (BNCH(CH_2) $_2$ (CH_2) $_2$ CH $_2$), 25.3 (BNCH(CH_2) $_2$ (CH_2) $_2$ CH $_2$), 24.6 (*Bpin*) ppm.



Entry 12d: ^1H NMR (CDCl_3 , 200 MHz, 298 K): δ 8.11 (s, 1H, (Dipp)NCHN(Dipp)Bpin), 7.37-7.33 (m, 1H, *Ph*), 7.25 (s, 1H, *Ph*), 7.14-7.12 (m, 1H, *Ph*), 7.09-7.07 (m, 2H, *Ph*), 7.03-6.99 (m, 1H, *Ph*), 3.18 (hept, 2H, BNCH(CH_3) $_2$), 3.08 (hept, 2H, NCH(CH_3) $_2$), 1.38-1.37 (d, 6H, $J_{\text{H-H}} = 6.87$ Hz, CH(CH_3) $_2$), 1.31-1.30 (d, 6H, $J_{\text{H-H}} = 6.87$ Hz, CH(CH_3) $_2$), 1.24 (s, 12H, *Bpin*), 1.20-1.18 (d, 12H, CH(CH_3) $_2$) ppm; $^{13}\text{C}\{^1\text{H}\}$ NMR (CDCl_3 , 100.5 MHz, 298 K): δ 152.7 (NCH), 147.7 (*Ph*), 145.5 (*Ph*), 142.5 (*Ph*), 139.4 (*Ph*), 133.1 (*Ph*), 128.1 (*Ph*), 123.4 (*Ph*), 123.0 (*Ph*), 122.4 (*Ph*), 83.8 (Bpin-*ipso*), 28.4 (CH(CH_3) $_2$), 27.2 (CH(CH_3) $_2$), 24.9 (CH(CH_3) $_2$), 24.4 (CH(CH_3) $_2$), 24.3 (*Bpin*), 23.1 (CH(CH_3) $_2$), 23.0 (CH(CH_3) $_2$) ppm.



6.3.19. Details of DFT calculations

All the calculations in this study have been performed with density functional theory (DFT), with the aid of the Turbomole 6.4 suite of programs, using the PBE functional. The TZVP basis set has been employed. The resolution of identity (RI), along with the multiple accelerated resolution of identity (marij) approximations have been employed for an accurate and efficient treatment of the electronic Coulomb term in the DFT calculations. Dispersion correction (disp3) and solvent

correction were incorporated with optimization calculations using the COSMO model, with dichloroethane ($\epsilon = 10.36$) as the solvent. The values reported are ΔG values, with zero-point energy corrections, internal energy and entropic contributions included through frequency calculations on the optimized minima with the temperature taken to be 298.15 K. Harmonic frequency calculations were performed for all stationary points to confirm them as a local minima or transition state structures.

6.4: Chapter 5 experimental details

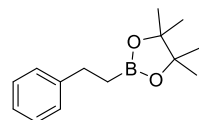
6.4.1. General catalytic procedure for the hydroboration of alkenes

Alkene (0.50 mmol), pinacolborane (1.1 equiv, 0.55 mmol), catalyst (8.0 mol% for **4a**, and 4.0 mol% for **4b**) were mixed together in a Schlenk tube with a magnetic bead inside the glove box. The reaction mixture was allowed to stir at 100 °C for 18 h in neat condition or in 0.5 mL toluene solvent for **4a** and **4b** respectively. Volatiles of the mixture were removed under reduced pressure and mesitylene (0.5 mmol) as an internal standard, was added while making the NMR in appropriate deuterated solvent. The progress of the reaction was monitored by ^1H NMR, which indicated the completion of the reaction by the disappearance of alkene ($\text{RCH}=\text{CH}_2$) proton and appearance of a new $\text{RCH}_2\text{CH}_2\text{Bpin}$ resonance.

Upon completion, the reaction mixture was eluted with Et_2O :hexane (2:8) mixture through a short plug of silica and the product was purified by silica gel column chromatography eluted with mostly EtOAc :hexane (02:98) mixture. Hydroboration product of four alkene namely **13e**, **13f**, **13g** and **13m** was isolated and in all the cases little discrepancy was observed with the NMR yield.

6.4.2. Spectroscopic data for the hydroboration product of alkene

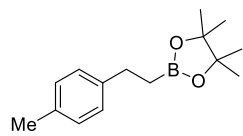
4,4,5,5-tetramethyl-2-phenethyl-1,3,2-dioxaborolane (13a): ^1H NMR (CDCl_3 , 200 MHz, 298



K): δ 7.29-7.11 (m, 5H, ArH), 2.74 (t, 2H, ArCH₂CH₂), 1.19 (s, 12H, CH₃), 1.14 (t, 2H, ArCH₂CH₂) ppm; $^{13}\text{C}\{^1\text{H}\}$ NMR (CDCl_3 , 50.2 MHz, 298 K): δ 144.3 (Ph), 128.2 (Ph), 128.1 (Ph), 127.9 (Ph), 127.7 (Ph), 125.4 (Ph), 82.9 (C(CH₃)₂), 29.9

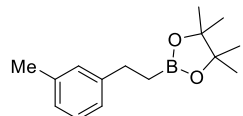
(CH₂), 24.7 (Bpin) ppm.

4,4,5,5-tetramethyl-2-(4-methylphenethyl)-1,3,2-dioxaborolane (13b): ^1H NMR (CDCl_3 , 200



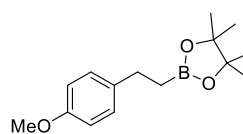
MHz, 298 K): δ 7.08-6.80 (m, 4H, ArH), 2.66 (t, 2H, ArCH₂CH₂), 2.21 (s, 3H, ArCH₃), 1.17-1.12 (s, 14H, CH₃ & ArCH₂CH₂) ppm; $^{13}\text{C}\{^1\text{H}\}$ NMR (CDCl_3 , 50.2 MHz, 298 K): δ 141.2 (Ph), 134.6 (Ph), 128.7 (Ph), 127.7 (Ph), 82.9 (C(CH₃)₂), 29.4 (CH₂), 24.6 (Bpin), 20.8 (CH₃) ppm.

4,4,5,5-tetramethyl-2-(3-methylphenethyl)-1,3,2-dioxaborolane (13c): ^1H NMR (CDCl_3 , 200



MHz, 298 K): δ 7.17-6.81 (m, 4H, ArH), 2.66 (t, 2H, ArCH₂CH₂), 2.23 (s, 3H, ArCH₃), 1.19-1.13 (s, 14H, CH₃ & ArCH₂CH₂) ppm; $^{13}\text{C}\{^1\text{H}\}$ NMR (CDCl_3 , 50.28 MHz, 298 K): δ 144.2 (Ph), 128.7 (Ph), 128.0 (Ph), 126.1 (Ph), 124.9 (Ph), 82.9 (C(CH₃)₂), 29.8 (CH₂), 24.7 (Bpin), 21.2 (CH₃) ppm.

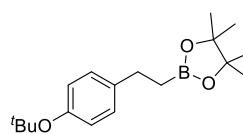
2-(4-methoxyphenethyl)-4,4,5,5-tetramethyl-1,3,2-dioxaborolane (13d): ^1H NMR (C_6D_6 , 200



MHz, 298 K): δ 7.25-7.02 (m, 2H, ArH), 6.91-6.77 (m, 2H, ArH), 3.44 (s, 3H, -OMe), 2.86 (t, 2H, ArCH₂CH₂), 1.25 (t, 2H, ArCH₂CH₂), 1.11 (s, 12H, CH₃) ppm; $^{13}\text{C}\{^1\text{H}\}$ NMR (C_6D_6 , 50.2 MHz, 298 K): δ 158.5 (Ph), 137.0

(Ph), 130.6 (Ph), 129.5 (Ph), 114.3 (Ph), 83.2 (C(CH₃)₂), 55.0 (OMe), 29.9 (CH₂), 25.2 (Bpin) ppm.

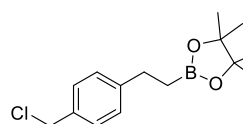
2-(4-(tert-butoxy)phenethyl)-4,4,5,5-tetramethyl-1,3,2-dioxaborolane (13e): According to



general procedure, 4-*tert*-Butoxystyrene (0.77 mmol, 137 mg), HBpin (0.78 mmol, 100 mg), **4b** (4.0 mol%, 9.0 mg) were reacted. The product was purified by silica gel column chromatography eluted with EtOAc:hexane

(02:98) mixture to get the boronate ester **13e** (181 mg, 76.5%) as a colorless oil. ^1H NMR (CDCl_3 , 200 MHz, 298 K): δ 7.17-7.01 (m, 2H, ArH), 6.82-6.79 (m, 2H, ArH), 2.66 (t, 2H, ArCH₂CH₂), 1.24 (s, 12H, CH₃), 1.18 (t, 2H, ArCH₂CH₂), 1.10 (s, 9H, -*O*tBu) ppm; $^{13}\text{C}\{^1\text{H}\}$ NMR (C_6D_6 , 50.2 MHz, 298 K): δ 154.2 (Ph), 139.8 (Ph), 129.1 (Ph), 124.8 (Ph), 124.6 (Ph), 83.2 (C(CH₃)₂), 77.7 (OC(CH₃)₃), 30.1 (OC(CH₃)₃), 29.3 (CH₂), 25.3 (Bpin) ppm.

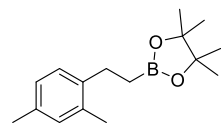
2-(4-(chloromethyl)phenethyl)-4,4,5,5-tetramethyl-1,3,2-dioxaborolane (13f): According to



general procedure, 4-Vinylbenzyl chloride (0.65 mmol, 100 mg), HBpin (0.65 mmol, 84 mg), **4a** (8.0 mol%, 14.9 mg) were reacted. The product was purified by silica gel column chromatography eluted with EtOAc:hexane

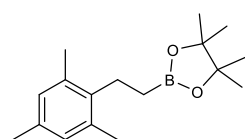
(01:99) mixture to get the boronate ester **13f** (132 mg, 72.1%) as a colorless oil. ^1H NMR (CDCl_3 , 200 MHz, 298 K): δ 7.19-7.01 (m, 4H, ArH), 4.41 (s, 2H, ArCH₂Cl), 2.68 (t, 2H, ArCH₂CH₂), 1.17-1.13 (s, 14H, CH₃ & ArCH₂CH₂) ppm; $^{13}\text{C}\{^1\text{H}\}$ NMR (CDCl_3 , 50.2 MHz, 298 K): δ 144.5 (Ph), 134.5 (Ph), 128.2 (Ph), 128.1 (Ph), 82.8 (C(CH₃)₂), 45.9 (ClCH₂), 29.5 (CH₂), 24.5 (Bpin) ppm; ^{11}B NMR (CDCl_3 , 128 MHz, 298 K): δ 34.0 ppm; LC-MS: m/z (%) = 245.2 [$\text{M}^+ - \text{Cl}$].

2-(2,4-dimethylphenethyl)-4,4,5,5-tetramethyl-1,3,2-dioxaborolane (13g): According to



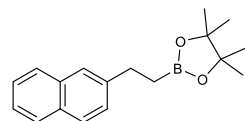
general procedure, 2,4-Dimethylstyrene (0.78 mmol, 103 mg), HBpin (0.78 mmol, 100 mg), **4a** (8.0 mol%, 17 mg) were reacted. The product was purified by silica gel column chromatography eluted with EtOAc:hexane (01:99) mixture to get the boronate ester **13g** (168 mg, 83.1%) as a colorless solid. ^1H NMR (CDCl_3 , 200 MHz, 298 K): δ 7.04-7.00 (d, $^3J_{\text{H-H}} = 8.27$ Hz, 1H, ArH), 6.87 (s, 2H, ArH), 2.63 (t, 2H, ArCH₂CH₂), 2.21 (s, 6H, ArCH₃), 1.16 (s, 12H, CH₃), 1.03 (t, 2H, ArCH₂CH₂) ppm; $^{13}\text{C}\{^1\text{H}\}$ NMR (CDCl_3 , 100.5 MHz, 298 K): δ 139.2 (Ph), 135.2 (Ph), 134.6 (Ph), 130.6 (Ph), 127.8 (Ph), 126.2 (Ph), 82.7 (C(CH₃)₂), 26.6 (CH₂), 24.6 (Bpin), 20.6 (CH₃), 19.0 (CH₃) ppm.

4,4,5,5-tetramethyl-2-(2,4,6-trimethylphenethyl)-1,3,2-dioxaborolane (13h) : ^1H NMR



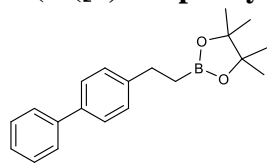
(CDCl_3 , 200 MHz, 298 K): δ 6.82 (s, 2H, ArH), 2.71 (t, 2H, ArCH₂CH₂), 2.32 (s, 6H, ArCH₃), 2.29 (s, 3H, ArCH₃), 1.28 (s, 12H, CH₃), 0.99 (t, 2H, ArCH₂CH₂) ppm; $^{13}\text{C}\{^1\text{H}\}$ NMR (CDCl_3 , 100.5 MHz, 298 K): δ 138.3 (Ph), 135.3 (Ph), 135.3 (Ph), 128.7 (Ph), 128.4 (Ph), 82.8 (C(CH₃)₂), 24.6 (CH₂), 24.6 (Bpin), 20.6 (CH₃), 19.4 (CH₃) ppm.

4,4,5,5-tetramethyl-2-(2-(naphthalen-2-yl)ethyl)-1,3,2-dioxaborolane (13i): ^1H NMR (CDCl_3 ,



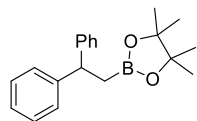
500 MHz, 298 K): δ 7.90-7.84 (m, 3H, ArH), 7.77 (s, 1H, ArH), 7.55-7.48 (m, 3H, ArH), 3.05 (t, 2H, ArCH₂CH₂), 1.36(t, 2H, ArCH₂CH₂), 1.32 (s, 12H, CH₃) ppm; $^{13}\text{C}\{^1\text{H}\}$ NMR (CDCl_3 , 125.7 MHz, 298 K): δ 141.8 (Ar), 133.6 (Ar), 131.8 (Ar), 127.6 (Ar), 127.5 (Ar), 127.3 (Ar), 127.2 (Ar), 125.6 (Ar), 124.8 (Ar), 83.0 (C(CH₃)₂), 30.0 (CH₂), 24.7 (Bpin) ppm.

2-(2-([1,1'-biphenyl]-4-yl)ethyl)-4,4,5,5-tetramethyl-1,3,2-dioxaborolane (13j): ^1H NMR



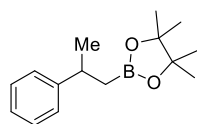
(C_6D_6 , 200 MHz, 298 K): δ 7.53-7.43 (m, 4H, ArH), 7.30-7.16 (m, 5H, ArH), 2.90 (t, 2H, ArCH₂CH₂), 1.08 (s, 12H, CH₃), 1.04 (t, 2H, ArCH₂CH₂) ppm; $^{13}\text{C}\{^1\text{H}\}$ NMR (C_6D_6 , 100.5 MHz, 298 K): δ 137.8 (Ph), 129.3 (Ph), 129.2 (Ph), 127.7 (Ph), 127.6 (Ph), 83.3 (C(CH₃)₂), 30.5 (CH₂), 25.3 (Bpin) ppm.

2-(2,2-diphenylethyl)-4,4,5,5-tetramethyl-1,3,2-dioxaborolane (13k): ^1H NMR (CDCl_3 , 200



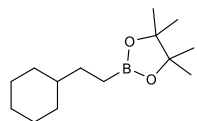
MHz, 298 K): δ 7.32-6.94 (m, 10H, ArH), 4.33 (t, 1H, ArCHPh), 1.25 (s, 12H, CH₃), 1.06 (d, 2H, ArCH(Me)CH₂) ppm; $^{13}\text{C}\{^1\text{H}\}$ NMR (CDCl_3 , 50.2 MHz, 298 K): δ 150.0 (Ph), 146.7 (Ph), 141.3 (Ph), 128.3 (Ph), 128.1 (Ph), 125.7 (Ph), 82.8 (C(CH₃)₂), 46.4 (CHPh₂), 31.5 (CH₂), 24.4 (Bpin) ppm.

4,4,5,5-tetramethyl-2-(2-phenylpropyl)-1,3,2-dioxaborolane (13l): ^1H NMR (CDCl_3 , 200



MHz, 298 K): δ 7.23-7.02 (m, 5H, ArH), 3.10-2.93 (sextet, 1H, ArCHMe), 1.25 (d, 2H, ArCH(Me)CH₂), 1.20-1.08 (br, 14H, CH₃) ppm; $^{13}\text{C}\{^1\text{H}\}$ NMR (CDCl_3 , 50.2 MHz, 298 K): δ 149.0 (Ph), 128.0 (Ph), 126.5 (Ph), 126.5 (Ph), 82.7 (C(CH₃)₂), 35.7 (CHMePh), 24.7 (CH₂), 24.6 (CH₃), 24.5 (Bpin) ppm.

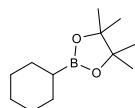
2-(2-cyclohexylethyl)-4,4,5,5-tetramethyl-1,3,2-dioxaborolane (13m): According to general



procedure, Vinylcyclohexane (0.78 mmol, 86 mg), HBpin (0.78 mmol, 100 mg), **4b** (4.0 mol%, 9 mg) were reacted. The product was purified by silica gel column chromatography eluted with EtOAc:hexane (02:98) mixture to get the boronate ester **13m** (165 mg, 88.7%) as a colorless liquid.

^1H NMR (CDCl_3 , 200 MHz, 298 K): δ 1.69-1.58 (m, 4H), 1.26-1.14 (m, 17H), 1.14-1.07 (m, 2H), 0.83-0.85 (m, 4H) ppm; $^{13}\text{C}\{^1\text{H}\}$ NMR (CDCl_3 , 125.7 MHz, 298 K): δ 82.5 (C(CH₃)₂), 39.8 (CH), 32.9 (CH₂), 31.2 (CH₂), 26.6 (CH₂), 26.3 (CH₂), 24.6 (Bpin) ppm.

2-cyclohexyl-4,4,5,5-tetramethyl-1,3,2-dioxaborolane (13n): ^1H NMR (CDCl_3 , 200 MHz, 298



K): δ 1.72-1.50 (m, 5H), 1.30-1.19 (m, 17H), 0.93-0.90 (m, 1H) ppm; $^{13}\text{C}\{^1\text{H}\}$ NMR (CDCl_3 , 125.7 MHz, 298 K): δ 82.6 (C(CH₃)₂), 27.9 (CH), 27.2 (CH₂), 26.4 (CH₂), 24.6 (Bpin) ppm.

2-(5-bromopentyl)-4,4,5,5-tetramethyl-1,3,2-dioxaborolane (13o): ^1H NMR (CDCl_3 , 200 MHz, 298 K): δ 3.30 (t, 2H, CH_2Br), 1.80 (q, 2H, CH_2), 1.37 (br, 4H, CH_2), 1.17 (s, 12H, CH_3), 0.74 (t, 2H, CH_2) ppm; $^{13}\text{C}\{^1\text{H}\}$ NMR (CDCl_3 , 50.2 MHz, 298 K): δ 82.6 ($\text{C}(\text{CH}_3)_2$), 33.4 (CH_2), 32.4 (CH_2), 30.5 (CH_2), 24.5 (CH_2), 23.0 (*Bpin*) ppm.

2-(3-bromopropyl)-4,4,5,5-tetramethyl-1,3,2-dioxaborolane (13p): ^1H NMR (CDCl_3 , 200 MHz, 298 K): δ 3.33 (t, 2H, CH_2Br), 1.90 (q, 2H, CH_2), 1.17 (s, 12H, CH_3), 0.92-0.82 (m, 2H, CH_2) ppm; $^{13}\text{C}\{^1\text{H}\}$ NMR (CDCl_3 , 50.2 MHz, 298 K): δ 82.9 ($\text{C}(\text{CH}_3)_2$), 35.7 (CH_2), 27.3 (CH_2), 24.5 (*Bpin*) ppm.

6.4.3. General catalytic procedure for the hydroboration of alkynes

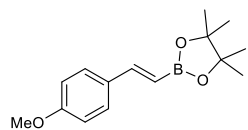
Alkyne (0.50 mmol), pinacolborane (1.1 equiv., 0.55 mmol), catalyst (**4a**, 2.0 mol% or **4b**, 2.0 mol%) were charged in a Schlenk tube with a magnetic bead inside the glove box. The reaction mixture was allowed to stir at 100 °C for 12 h after adding 0.5 mL of toluene for **4a** and **4b**. Upon completion of the reaction, the solvent was removed using vacuum in a Schlenk line and mesitylene (0.5 mmol) was added as the internal standard, while making the NMR in appropriate deuterated solvent. The progress of the reaction was monitored by the ^1H NMR spectroscopy, which indicated the completion of the reaction by the disappearance of alkyne ($\text{RC}\equiv\text{CH}$) proton and the appearance of a new $\text{CH}=\text{CH}$ resonance.

Upon completion, the reaction mixture was eluted with Et_2O :hexane (2:8) mixture through a short plug of silica and the product was purified by silica gel column chromatography eluted with mostly EtOAc :hexane (02:98) mixture. Hydroboration product of four alkynes namely **14b**, **14c**, **14j** and **14l** was isolated and in all the cases little discrepancy was observed with the NMR yield.

6.4.4. Spectroscopic data for the hydroboration product of alkyne

(E)-4,4,5,5-tetramethyl-2-styryl-1,3,2-dioxaborolane (14a): ^1H NMR (CDCl_3 , 200 MHz, 298 K): δ 7.44-7.32 (m, 2H, *ArH*), 7.31-7.22 (m, 4H, *ArH* and *ArCH*), 6.17-6.07 (d, 1H, $^3J_{\text{H-H}} = 18.44$ Hz, *ArCHCH*), 1.24 (s, 12H, CH_3) ppm; $^{13}\text{C}\{^1\text{H}\}$ NMR (CDCl_3 , 50.2 MHz, 298 K): δ 149.4 ($\text{ArC}=\text{CBpin}$), 137.4 (*Ph*), 128.7 (*Ph*), 128.4 (*Ph*), 126.9 (*Ph*), 83.2 ($\text{C}(\text{CH}_3)_2$), 24.7 (*Bpin*) ppm; ^{11}B NMR (C_6D_6 , 128 MHz, 298 K): δ 30.5 ppm.

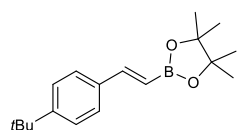
(E)-2-(4-methoxystyryl)-4,4,5,5-tetramethyl-1,3,2-dioxaborolane (14b): According to general



procedure, 4-Ethynylanisole (0.75 mmol, 100 mg), HBpin (0.76 mmol, 97 mg), **4a** (4.0 mol%, 4.3 mg) were reacted. The product was purified by silica gel column chromatography eluted with EtOAc:hexane (02:98) mixture to get

the boronate ester **14b** (170 mg, 86.7%) as a colorless liquid. ^1H NMR (CDCl_3 , 200 MHz, 298 K): δ 7.38-7.26 (m, 3H, ArH), 6.80 (m, 2H, ArH and ArCH), 6.02-5.92 (d, 1H, $^3J_{\text{H-H}} = 18.32$ Hz, ArCHCH), 3.70 (s, 3H, OCH₃), 1.24 (s, 12H, CH₃) ppm; $^{13}\text{C}\{^1\text{H}\}$ NMR (CDCl_3 , 50.2 MHz, 298 K): δ 160.2 (ArC=CBpin), 149.0 (ArC-OMe), 130.3 (Ph), 128.4 (Ph), 113.9 (Ph), 83.1 (C(CH₃)₂), 55.1 (OMe), 24.7 (Bpin) ppm; ^{11}B NMR (C_6D_6 , 128 MHz, 298 K): δ 30.7 ppm.

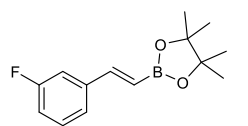
(E)-2-(4-(tert-butyl)styryl)-4,4,5,5-tetramethyl-1,3,2-dioxaborolane (14c): According to



general procedure, 4-*tert*-Butylphenylacetylene (0.77 mmol, 123 mg), HBpin (0.78 mmol, 100 mg), **4a** (4.0 mol%, 4.3 mg) were reacted. The product was purified by silica gel column chromatography eluted with EtOAc:hexane

(02:98) mixture to get the boronate ester **14c** (201 mg, 90.3%) as a pale yellow solid. ^1H NMR (CDCl_3 , 200 MHz, 298 K): δ 7.40-7.25 (m, 5H, ArH and ArCH), 6.14-6.05 (d, 1H, $^3J_{\text{H-H}} = 18.44$ Hz, ArCHCH), 1.25 (s, 9H, C(CH₃)₃), 1.22 (s, 12H, CH₃) ppm; $^{13}\text{C}\{^1\text{H}\}$ NMR (CDCl_3 , 50.2 MHz, 298 K): δ 151.9 (ArC=CBpin), 149.3 (Ph), 134.7 (Ph), 131.8 (Ph), 125.3 (Ph), 125.1 (Ph), 83.1 (C(CH₃)₂), 34.5 (CMe₃), 31.1 (CMe₃), 24.7 (Bpin) ppm.

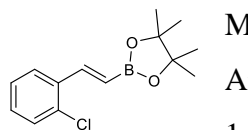
(E)-2-(3-fluorostyryl)-4,4,5,5-tetramethyl-1,3,2-dioxaborolane (14d): ^1H NMR (CDCl_3 , 200



MHz, 298 K): δ 7.36-7.27 (d, 1H, $^3J_{\text{H-H}} = 18.32$ Hz, ArCH), 7.21-7.10 (m, 3H, ArH), 6.97-6.87 (m, 1H, ArH), 6.18-6.09 (d, 1H, $^3J_{\text{H-H}} = 18.32$ Hz, ArCHCH), 1.27 (s, 12H, CH₃) ppm; $^{13}\text{C}\{^1\text{H}\}$ NMR (CDCl_3 , 50.2 MHz, 298 K): δ 165.4

(ArC=CBpin), 160.5 (Ph), 148.0-147.9 (Ph), 139.9-139.7 (Ph), 129.9-129.8 (Ph), 122.9-122.8 (Ph), 115.7-115.3 (Ph), 113.4-113.0 (Ph), 83.3 (C(CH₃)₂), 24.6 (Bpin) ppm.

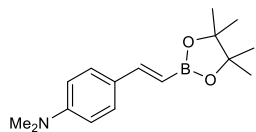
(E)-2-(2-chlorostyryl)-4,4,5,5-tetramethyl-1,3,2-dioxaborolane (14e): ^1H NMR (CDCl_3 , 200



MHz, 298 K): δ 7.80-7.71 (d, 1H, $^3J_{\text{H-H}} = 18.30$ Hz, ArCHCH), 7.55-7.50 (m, 1H, ArH), 7.40-7.02 (m, 3H, ArH), 6.15-6.05 (d, 1H, $^3J_{\text{H-H}} = 18.32$ Hz, ArCHCH), 1.21 (s, 12H, CH₃) ppm; $^{13}\text{C}\{^1\text{H}\}$ NMR (CDCl_3 , 50.2 MHz, 298 K): δ 144.7

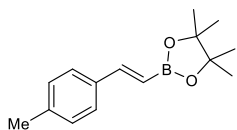
(ArC=CBpin), 133.7 (Ph), 133.6 (Ph), 129.5 (Ph), 129.4 (Ph), 129.0 (Ph), 126.6 (Ph), 126.1 (Ph), 83.1 (C(CH₃)₂), 24.5 (Bpin) ppm.

(E)-N,N-dimethyl-4-(2-(4,4,5,5-tetramethyl-1,3,2-dioxaborolan-2-yl)vinyl)aniline (14f): ^1H



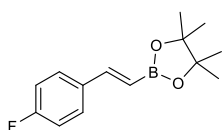
NMR (CDCl_3 , 200 MHz, 298 K): δ 7.36-7.32 (m, 3H, ArH and ArCH), 6.60-6.56 (d, 2H, $^3J_{\text{H-H}} = 8.27$ Hz, ArH), 5.94-5.85 (d, 1H, $^3J_{\text{H-H}} = 18.30$ Hz, ArCHCH), 2.87 (s, 6H, -NMe₂), 1.25 (s, 12H, CH₃) ppm; $^{13}\text{C}\{^1\text{H}\}$ NMR (CDCl_3 , 50.2 MHz, 298 K): δ 150.8 (ArC=CBpin), 149.7 (Ph), 128.9 (Ph), 128.3 (Ph), 125.8 (Ph), 111.8 (Ph), 82.8 (C(CH₃)₂), 40.0 (NMe₂), 24.7 (Bpin) ppm.

(E)-4,4,5,5-tetramethyl-2-(4-methylstyryl)-1,3,2-dioxaborolane (14g): ^1H NMR (CDCl_3 , 200



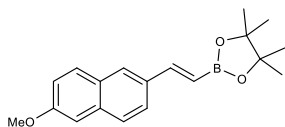
MHz, 298 K): δ 7.37-7.27 (m, 3H, ArH and ArCH), 7.05-7.01 (d, 2H, $^3J_{\text{H-H}} = 7.96$ Hz, ArH), 6.09-6.00 (d, 1H, $^3J_{\text{H-H}} = 18.44$ Hz, ArCHCH), 2.23 (s, 3H, ArCH₃), 1.21 (s, 12H, CH₃) ppm; $^{13}\text{C}\{^1\text{H}\}$ NMR (CDCl_3 , 50.2 MHz, 298 K): δ 149.4 (ArC=CBpin), 138.8 (Ph), 134.8 (Ph), 129.2 (Ph), 126.9 (Ph), 83.2 (C(CH₃)₂), 24.7 (Bpin), 21.2 (Me) ppm; ^{11}B NMR (C_6D_6 , 128 MHz, 298 K): δ 30.73 ppm.

(E)-2-(4-fluorostyryl)-4,4,5,5-tetramethyl-1,3,2-dioxaborolane (14h): ^1H NMR (CDCl_3 , 200



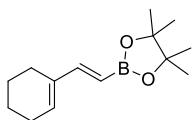
MHz, 298 K): δ 7.42-7.29 (m, 3H, ArH and ArCH), 6.99-6.90 (m, 2H, ArH), 6.08-5.99 (d, 1H, $^3J_{\text{H-H}} = 18.44$ Hz, ArCHCH), 1.26 (s, 12H, CH₃) ppm; $^{13}\text{C}\{^1\text{H}\}$ NMR (CDCl_3 , 50.2 MHz, 298 K): δ 165.5 (ArC=CBpin), 160.5 (Ph), 133.6 (Ph), 128.6-128.5 (Ph), 115.6-115.2 (Ph), 83.2 (C(CH₃)₂), 24.6 (Bpin) ppm.

2-(6-methoxynaphthalen-2-yl)-4,4,5,5-tetramethyl-1,3,2-dioxaborolane (14i): ^1H NMR



(CDCl_3 , 200 MHz, 298 K): δ 7.79-7.54 (m, 5H, ArH and ArCH), 7.16-7.10 (m, 2H, ArH), 6.32-6.23 (d, 1H, $^3J_{\text{H-H}} = 18.32$ Hz, ArCHCH), 3.90 (s, 3H, OCH₃), 1.35 (s, 12H, CH₃) ppm; $^{13}\text{C}\{^1\text{H}\}$ NMR (CDCl_3 , 50.2 MHz, 298 K): δ 158.1 (ArC=CBpin), 149.6 (Ph), 134.9 (Ph), 132.9 (Ph), 129.8 (Ph), 128.7 (Ph), 127.7 (Ph), 127.0 (Ph), 123.9 (Ph), 118.9 (Ph), 105.8 (Ph), 83.2 (C(CH₃)₂), 55.1 (OMe), 24.7 (Bpin) ppm.

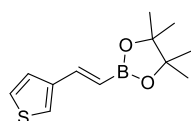
(E)-2-(2-(cyclohex-1-en-1-yl)vinyl)-4,4,5,5-tetramethyl-1,3,2-dioxaborolane (14j): According



to general procedure, 1-Ethynylcyclohexene (0.77 mmol, 82 mg), HBpin (0.78 mmol, 100 mg), **4a** (4.0 mol%, 4.3 mg) were reacted. The product was purified by silica gel column chromatography eluted with EtOAc:hexane (03:97) mixture to get the boronate ester **14j** (170 mg, 94.0%) as a colorless liquid. ^1H NMR (CDCl_3 , 200 MHz,

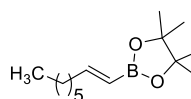
298 K): δ 7.22-7.13 (d, 1H, $^3J_{\text{H-H}} = 18.30$ Hz, RCHCH), 6.05 (s, 1H, Internal-CH), 5.62-5.52 (d, 1H, $^3J_{\text{H-H}} = 18.19$ Hz, RCHCH), 2.27 (br, 4H, -CH₂), 1.74 (br, 4H, -CH₂), 1.38 (s, 12H, CH₃) ppm; $^{13}\text{C}\{^1\text{H}\}$ NMR (CDCl₃, 50.2 MHz, 298 K): δ 152.8 (RC=CBpin), 136.8 (C=C), 133.4 (C=C), 82.4 (C(CH₃)₂), 25.8 (CH₂), 24.3 (Bpin), 23.4 (CH₂), 22.1 (CH₂), 22.0 (CH₂), 20.8 (CH₂) ppm.

(E)-4,4,5,5-tetramethyl-2-(2-(thiophen-3-yl)vinyl)-1,3,2-dioxaborolane (14k): ^1H NMR



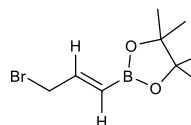
(CDCl₃, 200 MHz, 298 K): δ 7.38-7.29 (d, 1H, $^3J_{\text{H-H}} = 18.30$ Hz, ArCHCH), 7.21-7.17 (m, 2H, ArCH), 7.13-7.11 (m, 1H, ArCH), 5.94-5.85 (d, 1H, $^3J_{\text{H-H}} = 18.30$ Hz, RCHCH), 1.21 (s, 12H, CH₃) ppm; $^{13}\text{C}\{^1\text{H}\}$ NMR (CDCl₃, 50.2 MHz, 298 K): δ 143.0 (ArC=CBpin), 141.1 (Ar), 129.8 (Ar), 125.9 (Ar), 124.8 (Ar), 124.6 (Ar), 82.9 (C(CH₃)₂), 24.6 (Bpin) ppm.

(E)-4,4,5,5-tetramethyl-2-(2-(thiophen-3-yl)vinyl)-1,3,2-dioxaborolane (14l): According to



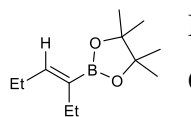
general procedure, 1-octyne (0.78 mmol, 86 mg), HBpin (0.78 mmol, 100 mg), **4a** (4.0 mol%, 4.3 mg) were reacted. The product was purified by silica gel column chromatography eluted with EtOAc:hexane (03:97) mixture to get the boronate ester **14l** (87 mg, 73.0%) as a colorless liquid. ^1H NMR (CDCl₃, 200 MHz, 298 K): δ 7.80-7.71(dt, 1H, $^3J_{\text{H-H}} = 17.86$ Hz, RCHCH), 5.59-5.50 (d, 1H, $^3J_{\text{H-H}} = 18.30$ Hz, RCHCH), 2.30-2.20 (quat, 2H, -CH₂), 1.53 (br, 8H, -CH₂), 1.36 (s, 12H, CH₃), 0.99 (s, 3H, CH₃) ppm; $^{13}\text{C}\{^1\text{H}\}$ NMR (CDCl₃, 50.2 MHz, 298 K): δ 154.5 (RC=CBpin), 82.7 (C(CH₃)₂), 35.7 (CH₂), 31.6 (CH₂), 28.8 (CH₂), 28.1 (CH₂), 24.6 (Bpin), 13.9 (CH₃) ppm.

(E)-2-(3-bromoprop-1-en-1-yl)-4,4,5,5-tetramethyl-1,3,2-dioxaborolane (14m): ^1H NMR



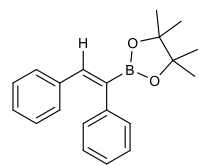
(C₆D₆, 200 MHz, 298 K): δ 5.88-5.82 (m, 1H, CH=CHBpin), 5.64-5.55 (d, 1H, $^3J_{\text{H-H}} = 17.53$ Hz, CH=CHBpin), 3.85-3.82 (d, 2H, $^3J_{\text{H-H}} = 8.49$ Hz, BrCH₂-), 1.19 (s, 12H, CH₃) ppm.

(Z)-2-(hex-3-en-3-yl)-4,4,5,5-tetramethyl-1,3,2-dioxaborolane (14n): ^1H NMR (C₆D₆, 200



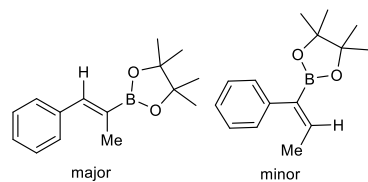
MHz, 298 K): δ 6.64-6.57 (t, 1H, EtCH), 2.38-2.28 (m, 4H, CH₂CH₃), 1.12 (s, 12H, CH₃), 1.05 (m, 6H, CH₂CH₃) ppm; $^{13}\text{C}\{^1\text{H}\}$ NMR (C₆D₆, 50.2 MHz, 298 K): δ 147.8 (RC=CBpin), 83.3 (C(CH₃)₂), 25.2 (Bpin), 22.4 (CH₂), 22.1 (CH₂), 15.6(CH₂), 14.4 (CH₂) ppm.

(Z)-2-(1,2-diphenylvinyl)-4,4,5,5-tetramethyl-1,3,2-dioxaborolane (14o): ^1H NMR (C_6D_6 , 200



MHz, 298 K): δ 7.54 (s, 1H), 7.42-7.31(m, 4H), 7.25-7.19 (m, 5H), 1.45 (s, 12H) ppm; $^{13}\text{C}\{^1\text{H}\}$ NMR (C_6D_6 , 50.2 MHz, 298 K): δ 143.1 (ArC=CBpin), 140.3 (Ph), 136.8 (Ph), 131.4 (Ph), 128.7 (Ph), 128.1 (Ph), 128.0 (Ph), 127.7 (Ph), 126.1 (Ph), 83.5 ($\text{C}(\text{CH}_3)_2$), 24.7 (Bpin) ppm.

(Z)-4,4,5,5-tetramethyl-2-(1-phenylprop-1-en-2-yl)-1,3,2-dioxaborolane and (Z)-4,4,5,5-



tetramethyl-2-(1-phenylprop-1-en-1-yl)-1,3,2-dioxaborolane (14p): Major isomer: ^1H NMR (CDCl_3 , 200 MHz, 298 K): δ 7.64-

7.40 (m, 6H, ArCH), 2.28 (s, 3H, CH_2CH_3), 1.53 (s, 12H, CH_3) ppm; $^{13}\text{C}\{^1\text{H}\}$ NMR (CDCl_3 , 50.28 MHz, 298 K): δ 142.3, 137.7, 131.3,

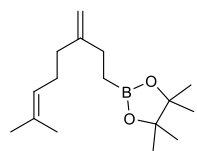
129.2, 127.8, 126.9, 83.2, 24.6, 22.4, 15.6 ppm. Minor isomer: ^1H NMR (C_6D_6 , 200 MHz, 298 K): δ 7.64-7.40 (m, 6H, ArCH), 2.03-1.99 (d, 3H, $^3J_{\text{H-H}} = 6.95$ Hz, CHCH_3), 1.49 (s, 12H, CH_3) ppm; $^{13}\text{C}\{^1\text{H}\}$ NMR (CDCl_3 , 50.2 MHz, 298 K): δ 142.4 (ArC=CBpin), 139.6 (Ph), 128.9 (Ph), 127.5 (Ph), 125.6 (Ph), 83.1 ($\text{C}(\text{CH}_3)_2$), 24.5 (Bpin), 15.7 (CH_3) ppm.

6.4.5. General catalytic procedure for the hydroboration of terpenes

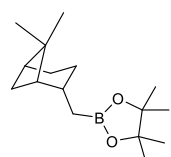
Terpene (0.50 mmol), pinacolborane (1.1 equiv., 0.55 mmol), catalyst (8.0 mol% for **4a**, and 4.0 mol% for **4b**) were mixed together in a Schlenk tube with a magnetic bead inside the glove box. The reaction mixture was allowed to stir at 100 °C for 18 h in neat condition or in 0.5 mL toluene for **4a** and **4b** respectively. Volatiles of the mixture were removed under reduced pressure and mesitylene (0.5 mmol) was added while making the NMR in appropriate deuterated solvent. The progress of the reaction was monitored by the ^1H NMR spectroscopy, which indicated the completion of the reaction by the disappearance of alkene ($\text{RCH}=\text{CH}_2$) proton and the appearance of a new $\text{RCH}_2\text{CH}_2\text{Bpin}$ resonance.

6.4.6. Spectroscopic data for the hydroboration product of terpenes

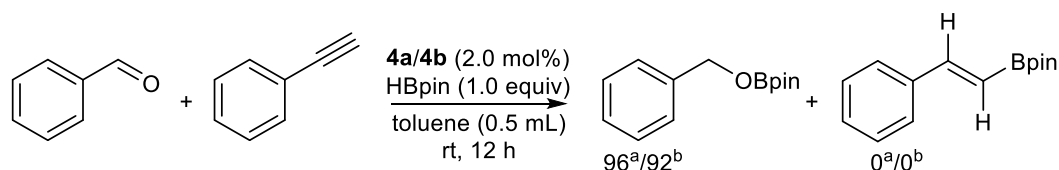
Conversion of R-(+)-Limonene and S-(-)-Limonene to their corresponding hydroboration products was identified by the ^1H NMR spectroscopy using mesitylene as the internal standard. However, their spectra were not assigned because of the overlapping of the peak with the unreacted starting materials.

4,4,5,5-tetramethyl-2-(7-methyl-3-methyleneoct-6-en-1-yl)-1,3,2-dioxaborolane (15c): ^1H 

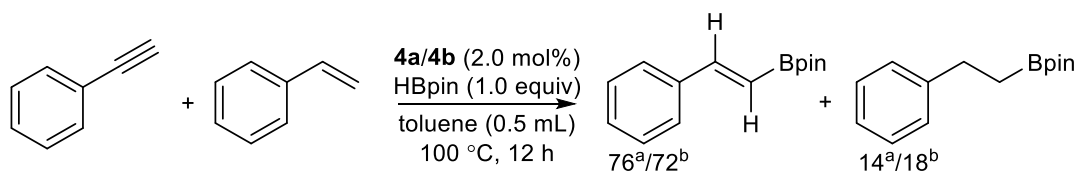
NMR (C_6D_6 , 200 MHz, 298 K): δ 5.24-5.01 (m, 1H), 4.94 (s, 2H), 2.16-1.94 (m, 6H), 1.63 (s, 3H), 1.55 (s, 3H), 1.16 (s, 12H), 0.88 (t, 2H) ppm; $^{13}\text{C}\{^1\text{H}\}$ NMR (C_6D_6 , 50.2 MHz, 298 K): δ 151.2 ($\text{R}_2\text{C}=\text{CH}_2$), 131.3 ($\text{Me}_2\text{C}=\text{CHR}$), 124.0 ($\text{Me}_2\text{C}=\text{CHR}$), 107.5 ($\text{R}_2\text{C}=\text{CH}_2$), 82.4 ($\text{C}(\text{CH}_3)_2$), 36.0 (CH_2), 29.9 (CH_2), 26.6 (CH_2), 25.5 (CH_2), 24.6 (*Bpin*), 17.4 (CH_3) ppm.

2-(((1S,2S,5S)-6,6-dimethylbicyclo[3.1.1]heptan-2-yl)methyl)-4,4,5,5-tetramethyl-1,3,2-

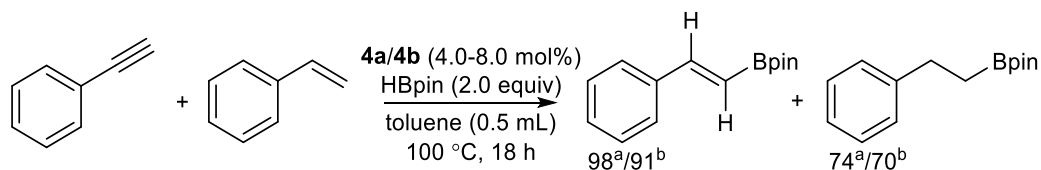
dioxaborolane (15d): The ^1H NMR spectrum was not assigned since the proton resonances of **15d** overlap with the other diastereomer and unreacted starting materials. $^{13}\text{C}\{^1\text{H}\}$ NMR (C_6D_6 , 50.2 MHz, 298 K): δ 82.6 ($\text{C}(\text{CH}_3)_2$), 48.7 (CMe_2), 40.5 (CH), 40.3 (CH), 38.7 (CH), 31.5 (CH_2), 26.8 (CH_2), 26.0 (CH_2), 24.7 (CH_2), 24.7 (CH_2), 23.4 (*Bpin*), 20.1 (CH_3) ppm.

6.4.7. Competitive experiment for aldehyde/alkyne/alkene hydroboration-selectivity study**Selective hydroboration of benzaldehyde over phenylacetylene in presence of 1 equiv.****HBpin:**

Benzaldehyde (53 mg, 0.50 mmol), Phenylacetylene (51 mg, 0.50 mmol), pinacolborane (64 mg, 0.50 mmol), catalyst (2.0 mol% for **4a** or 2.0 mol% for **4b**) were charged in a Schlenk tube inside the glove box. The reaction mixture was stirred for 12 hat room temperature after the addition of 0.50 mL toluene. Upon completion of the reaction, volatiles of the mixture were removed under reduced pressure. The progress of the reaction was monitored by ^1H NMR after addition of mesitylene (0.50 mmol) as an internal standard in CDCl_3 . A sharp resonance at $\delta = 4.84$ ppm indicates for the formation of hydroboration product from benzaldehyde.

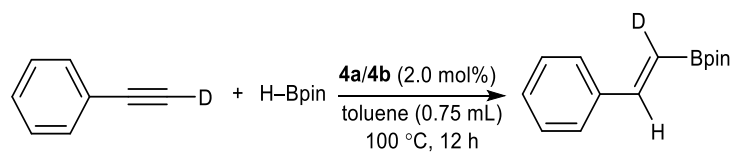
Selective hydroboration of phenylacetylene over styrene in presence of 1 equiv. HBpin:

Phenylacetylene (51 mg, 0.50 mmol), styrene (52 mg, 0.50 mmol), pinacolborane (64 mg, 0.50 mmol), catalyst (2.0 mol% for **4a** or 2.0 mol% for **4b**) were charged in a Schlenk tube inside the glove box. The reaction mixture was stirred for 12 h at 100 °C after addition of 0.50 mL toluene. Upon completion of the reaction, volatiles of the mixture were removed under reduced pressure. The progress of the reaction was monitored by ¹H NMR after addition of mesitylene (0.50 mmol) as an internal standard in CDCl₃. Formation of the hydroboration product was identified from the doublet resonance at $\delta = 6.14$ ppm for alkyne and triplet resonance at $\delta = 2.70$ ppm for alkene.

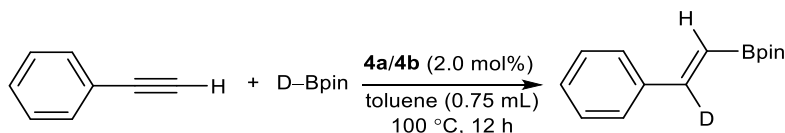
Hydroboration of phenylacetylene and styrene in presence of 2 equiv. HBpin:

Phenylacetylene (51 mg, 0.50 mmol), styrene (52 mg, 0.50 mmol), pinacolborane (128 mg, 1.00 mmol), catalyst (8.0 mol% for **4a** or 4.0 mol% for **4b**) were mixed together in a Schlenk tube inside the glove box. The reaction mixture was heated at 100 °C for 18 h after addition of 0.50 mL toluene. Upon completion of the reaction, volatiles of the mixture were removed under reduced pressure. The progress of the reaction was monitored by ¹H NMR after addition of mesitylene (0.5 mmol) as an internal standard in CDCl₃. Formation of the hydroboration product was identified from the doublet resonance at $\delta = 6.14$ ppm for alkyne and triplet resonance at $\delta = 2.70$ ppm for alkene.

6.4.8. Deuterium labeling experiments



Phenylacetylene- d_1 (51.5 mg, 0.50 mmol), pinacolborane (75 mg, 0.59 mmol), catalyst (2.0 mol% for **4a** or 2.0 mol% for **4b**) and 0.75 mL toluene were charged in a screw cap NMR tube inside the glove box. The reaction mixture was heated at 100 °C for 12 h before the volatiles of the mixture were removed under reduced pressure. The progress of the reaction was monitored by ^2H NMR after dissolving in CDCl_3 , shows a peak at $\delta = 6.18$ ppm, which indicates a *cis* orientation of deuterium and phenyl group.



Phenylacetylene (31 mg, 0.30 mmol), pinacolborane- d_1 (42 mg, 0.32 mmol in 0.75 mL toluene), catalyst (2.0 mol% for **4a** or 2.0 mol% for **4b**) were charged in a screw cap NMR tube inside the glove box. The reaction mixture was heated at 100 °C for 12 h before the volatiles of the mixture were removed under reduced pressure. The progress of the reaction was monitored by ^2H NMR after dissolving in CD_3CN , which indicated the peak at $\delta = 7.28$ ppm, due to the *cis* orientation of deuterium and Bpin unit.

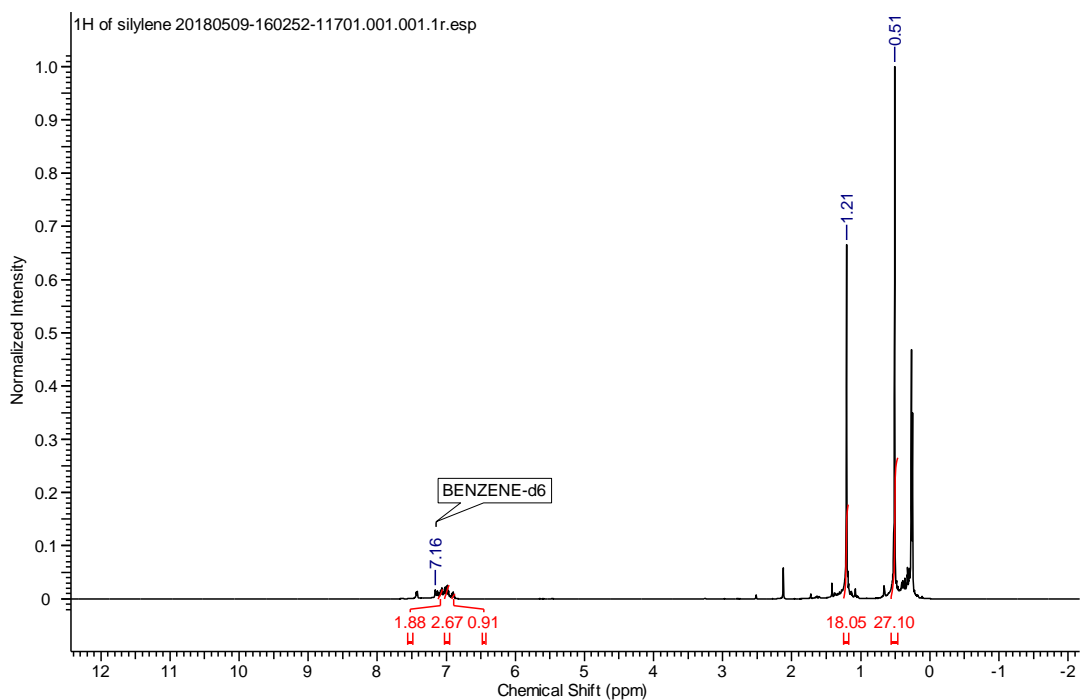
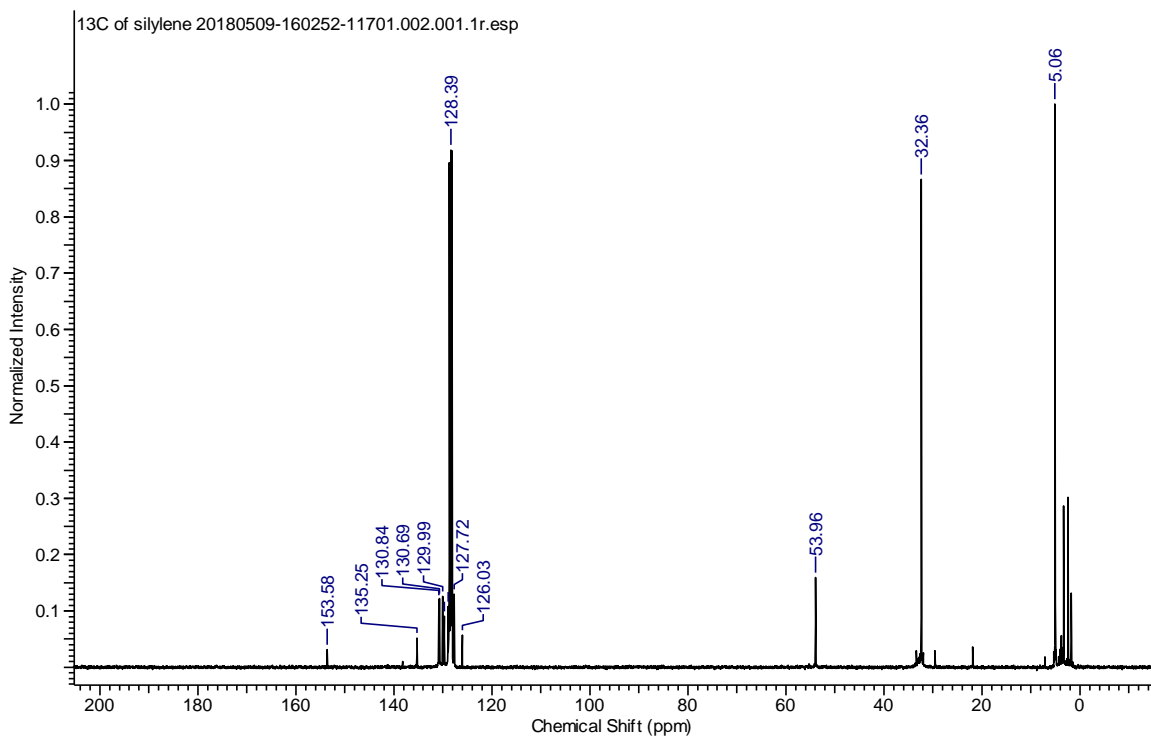
6.4.9. Isolation and characterization of the intermediate

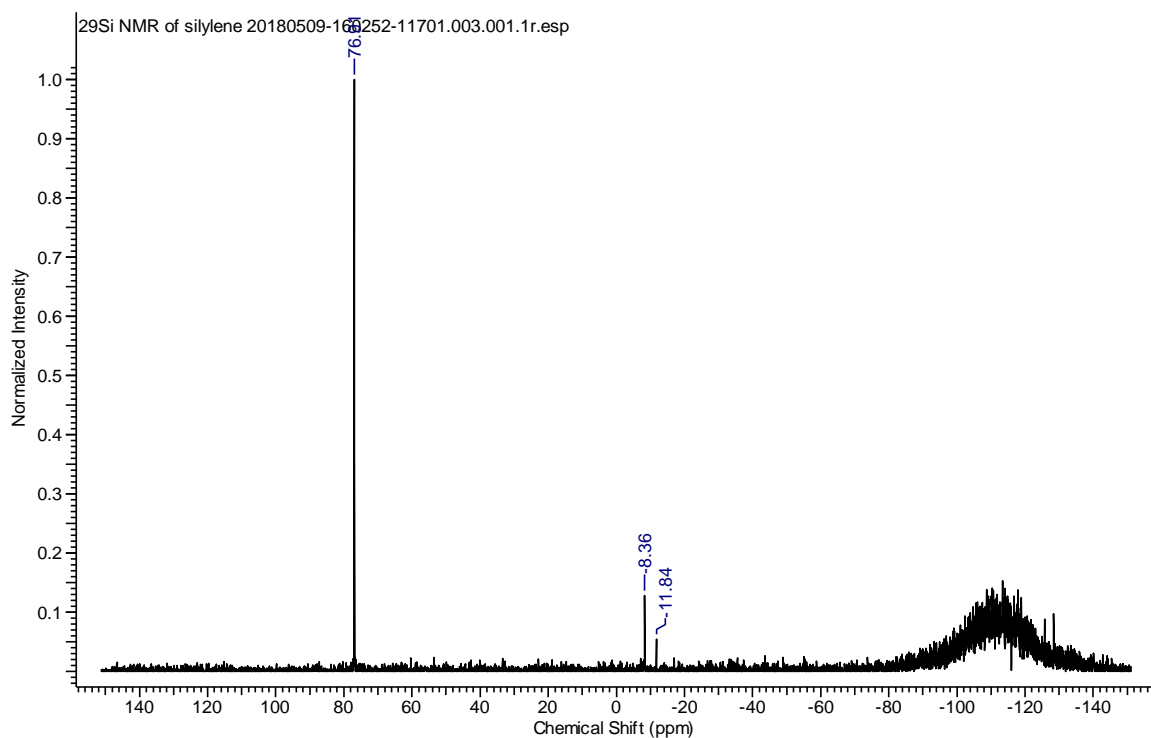
Stoichiometric reaction of catalyst 4a and HBpin: A solution of HBpin (135 mg, 1.05 mmol) in toluene (5 mL) was added drop by drop to the toluene solution (10 mL) of **4a** (300 mg, 1.05 mmol) at room temperature. The reaction mixture was stirred for overnight. After addition of HBpin, solution was clear up to 3-4 h and after that white ppt started forming slowly. The reaction mixture was subjected for characterization. Yield (0.192 g, 55 %), ^1H NMR (C_6D_6 , 200 MHz, 298 K): δ 7.22 (d, $^3J_{\text{H-H}} = 7.83$ Hz, 2H, ArH), 6.92 (t, 1H, ArH), 1.52 (s, 18H, $\text{C}(\text{CH}_3)_3$), 1.06 (s, 12H, CH_3) ppm; $^{13}\text{C}\{^1\text{H}\}$ NMR (toluene- d_8 , 100.5 MHz, 298 K): δ 152.1 (*Ph*), 141.1 (*Ph*), 125.9 (*Ph*), 123.2 (*Ph*), 83.3 ($\text{C}(\text{CH}_3)_2$), 35.4 ($\text{C}(\text{CH}_3)_3$), 31.8 ($\text{C}(\text{CH}_3)_3$), 31.6 (CH_3) ppm; ^{11}B NMR (toluene- d_8 , 128 MHz, 298 K): δ 86.9 (s), 21.7 (s), 4.6 (s), -25.7 (quatrate), -39.9 (quintet), 29.1-27.8 (d, for

unreacted HBpin) ppm. Upon filtration and evaporation of solvent, the filtrate part shows only three peaks at δ 4.6 (s), 21.7 (s), and -39.9 (quintet) in the ^{11}B NMR spectrum.

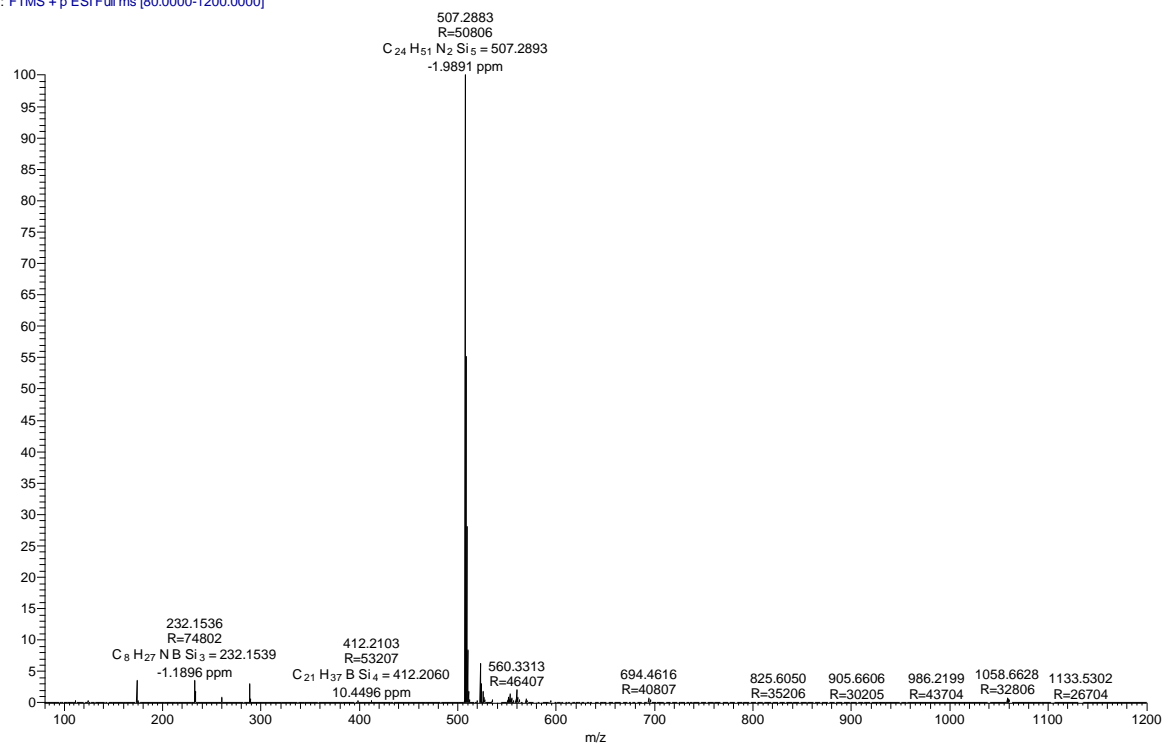
Stoichiometric reaction of 4a with phenylacetylene or styrene: No reaction was observed when an equimolar amount of **4a** was treated separately with phenylacetylene or styrene in toluene or benzene solvent at room temperature. Further heating at 100 °C overnight does not indicate any appreciable changes in the ^1H NMR spectra.

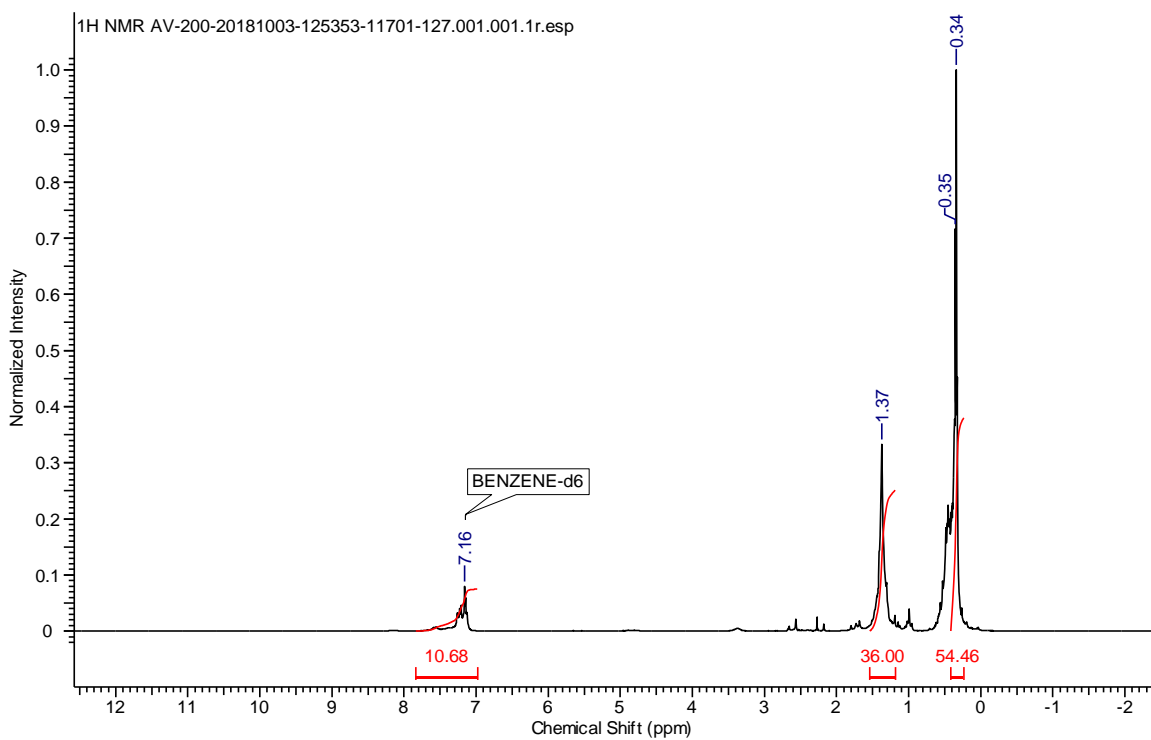
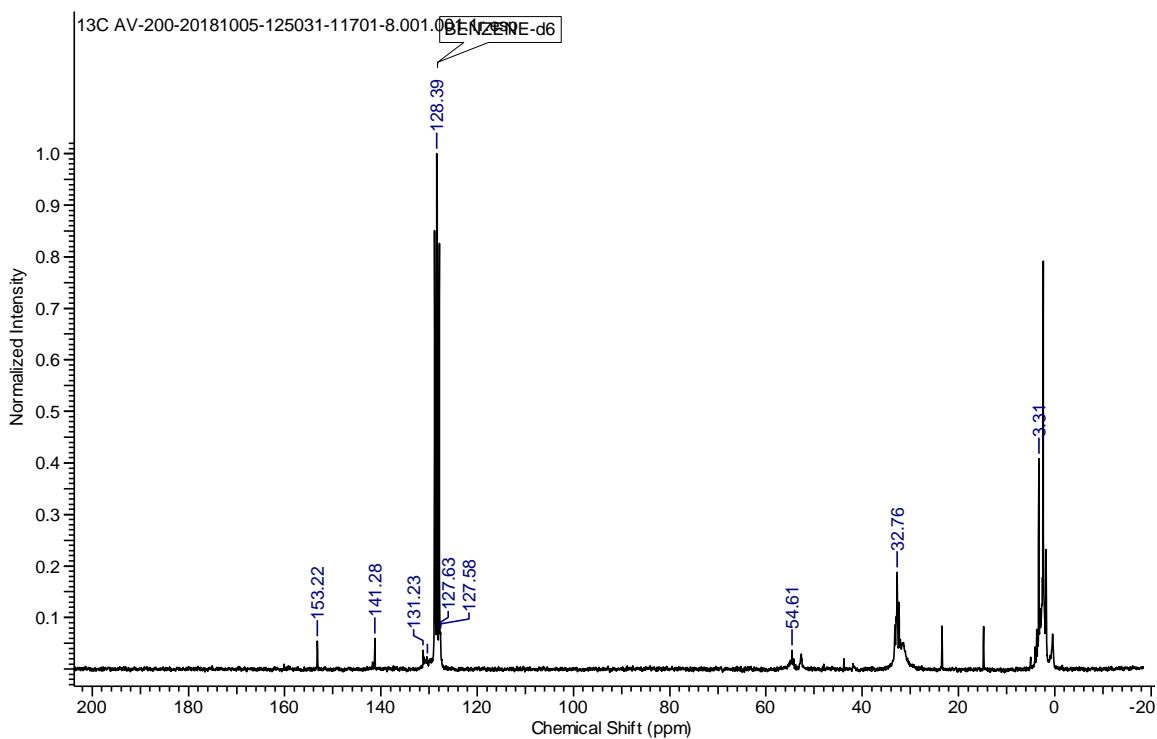
Representative NMR spectra of 2.1–2.21

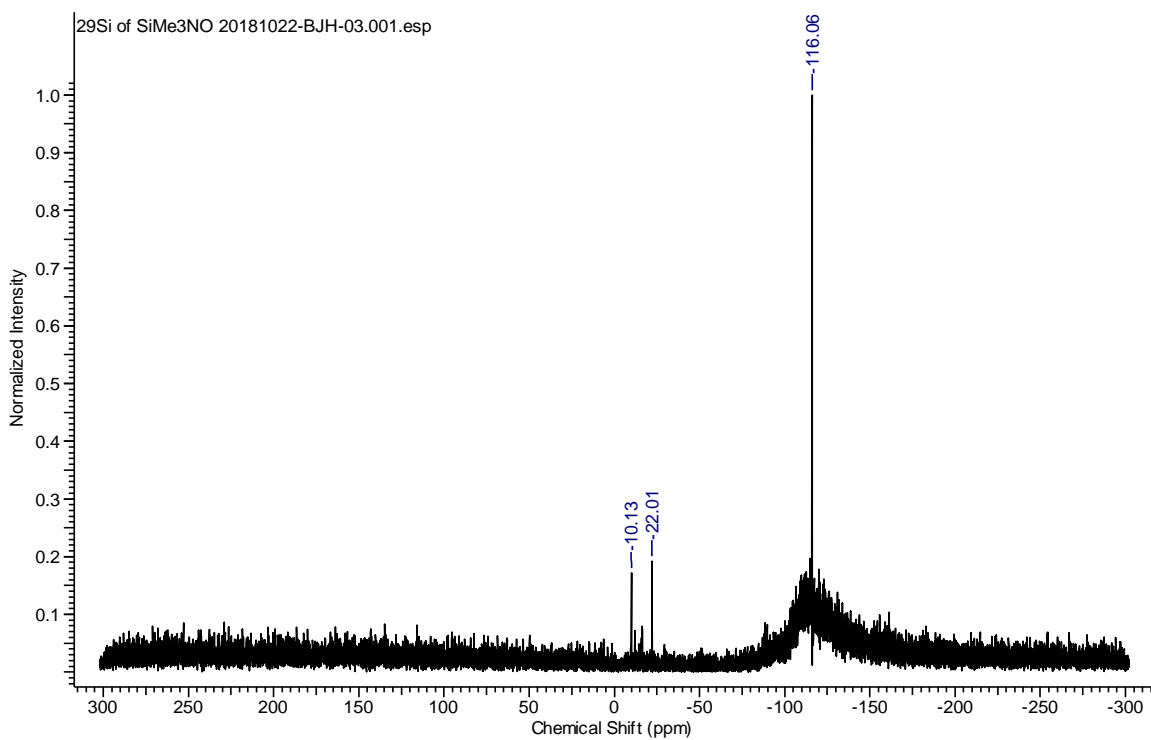
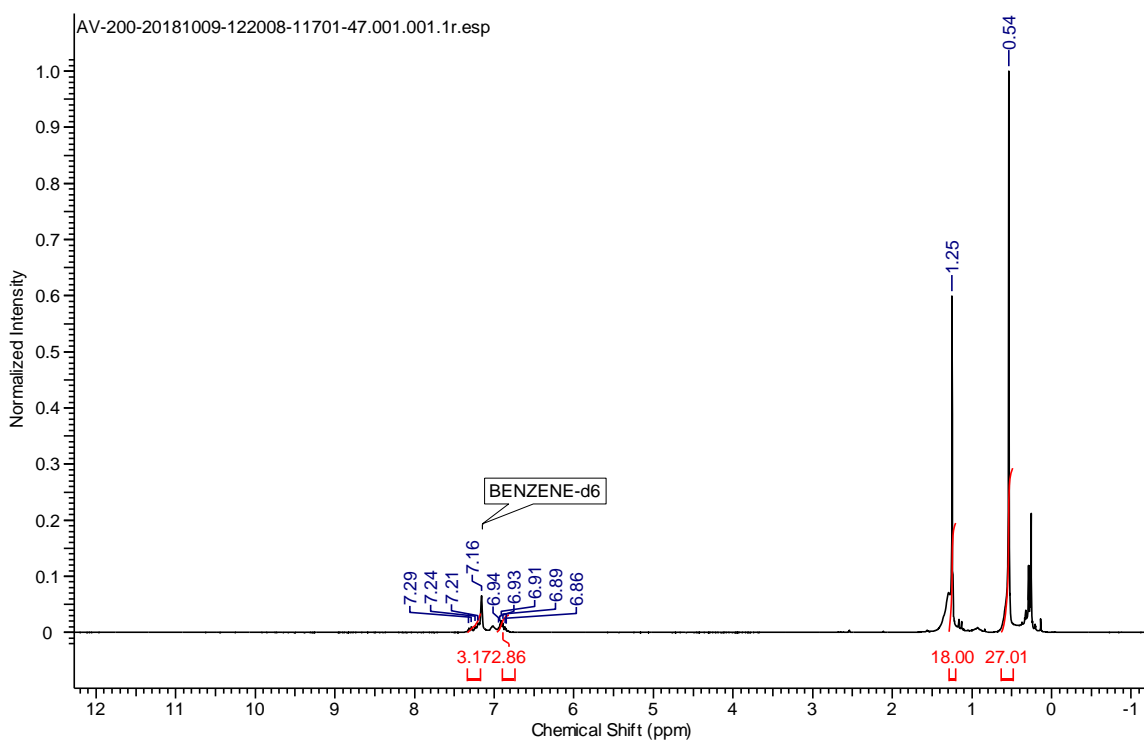
Figure S1. ¹H NMR Spectrum of 2.1 (C₆D₆, 400 MHz, 298 K)Figure S2. ¹³C NMR Spectrum of 2.1 (C₆D₆, 100.6 MHz, 298 K)

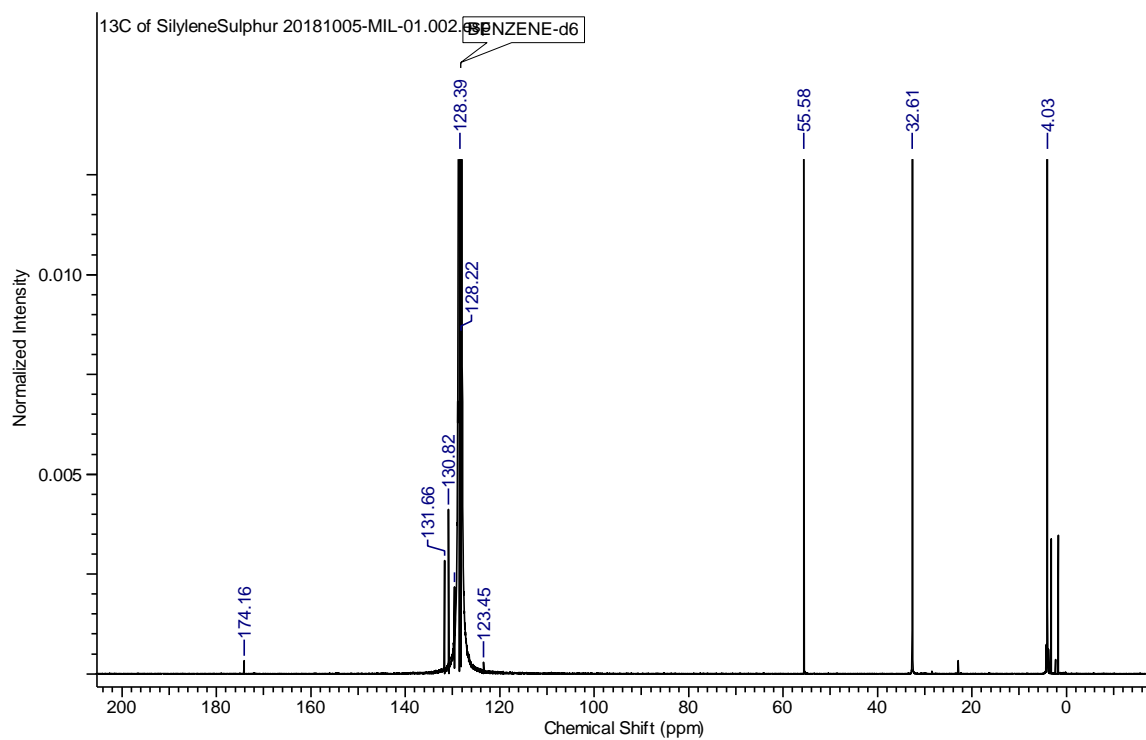
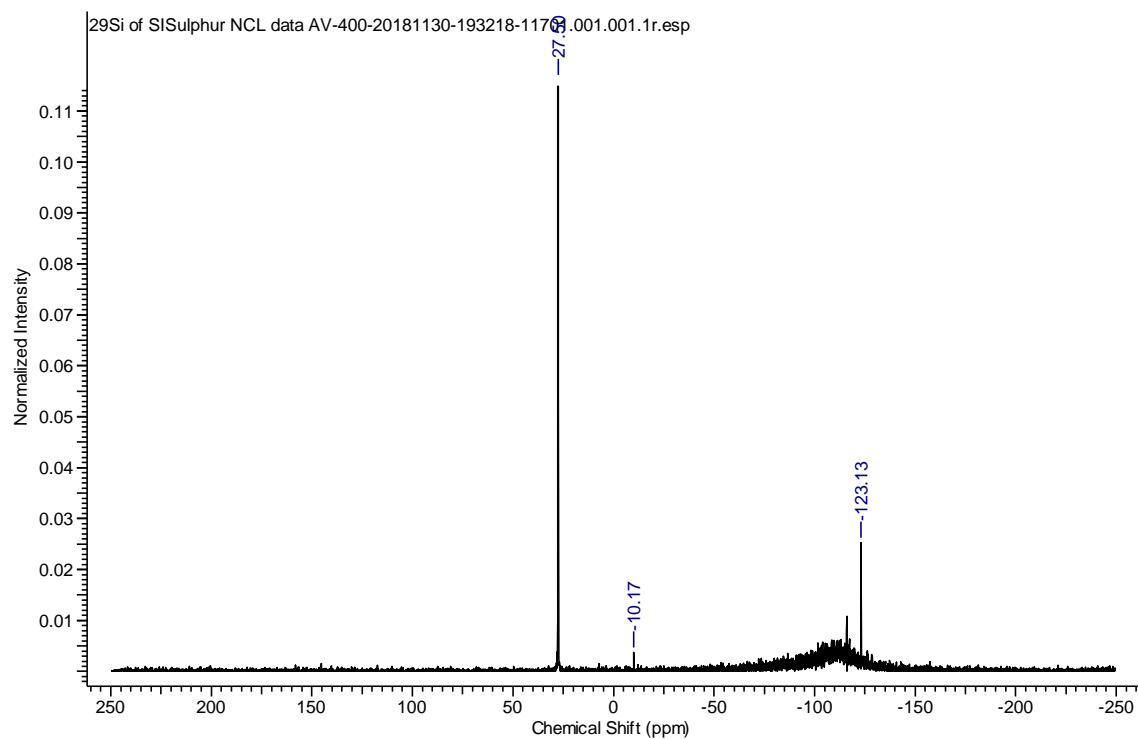
Figure S3. ^{29}Si NMR Spectrum of **2.1** (C_6D_6 , 79.5 MHz, 298 K)

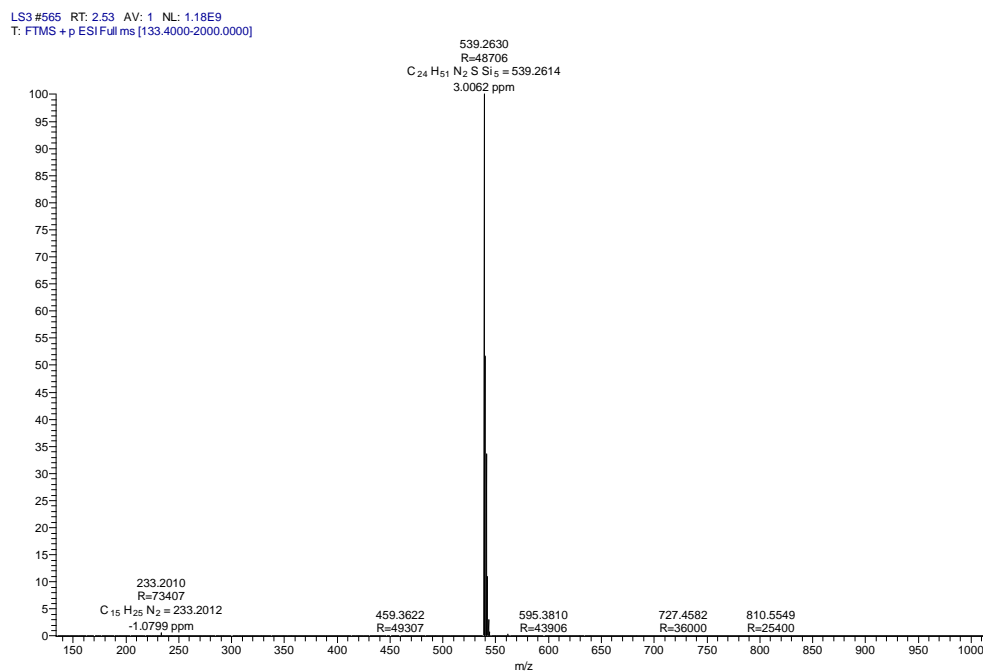
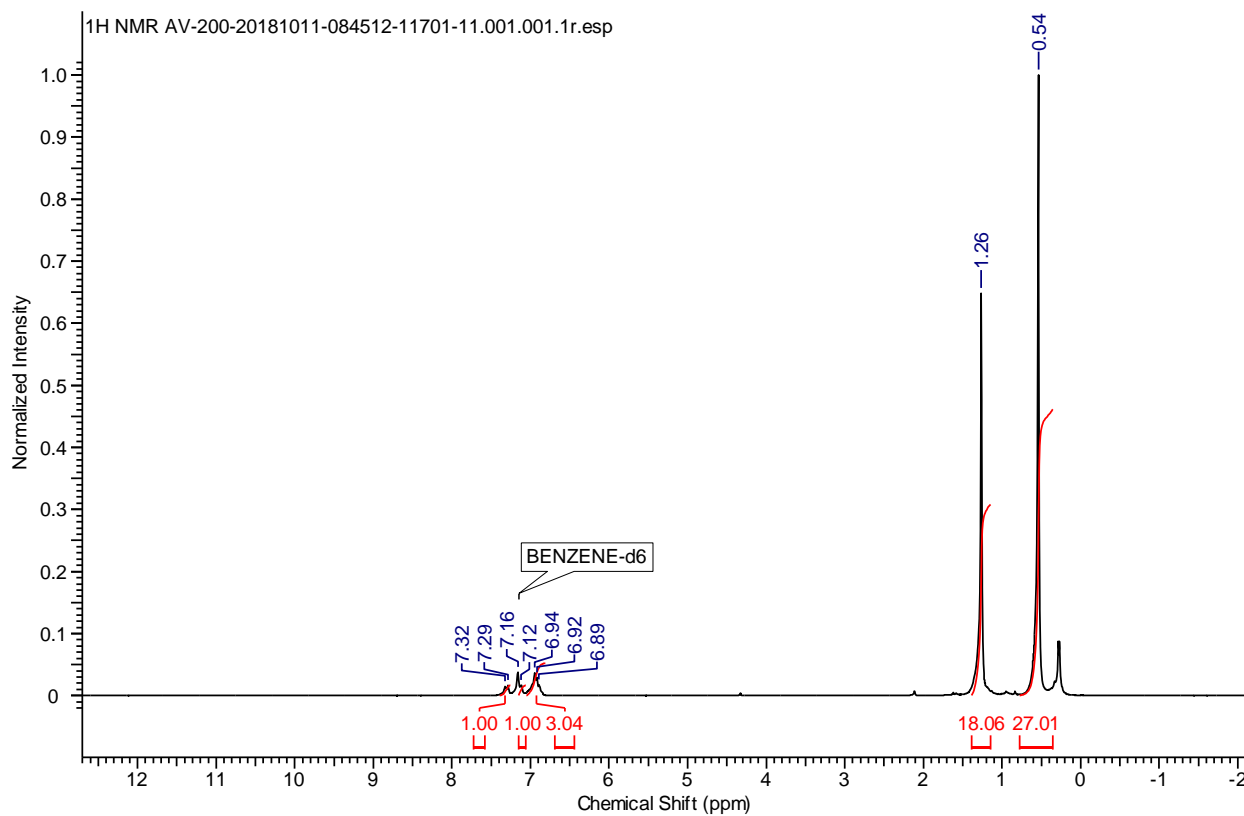
MB-01 #468 RT: 2.08 AV: 1 NL: 2.26E9
T: FTMS + p ESI Full ms [80.0000-1200.0000]

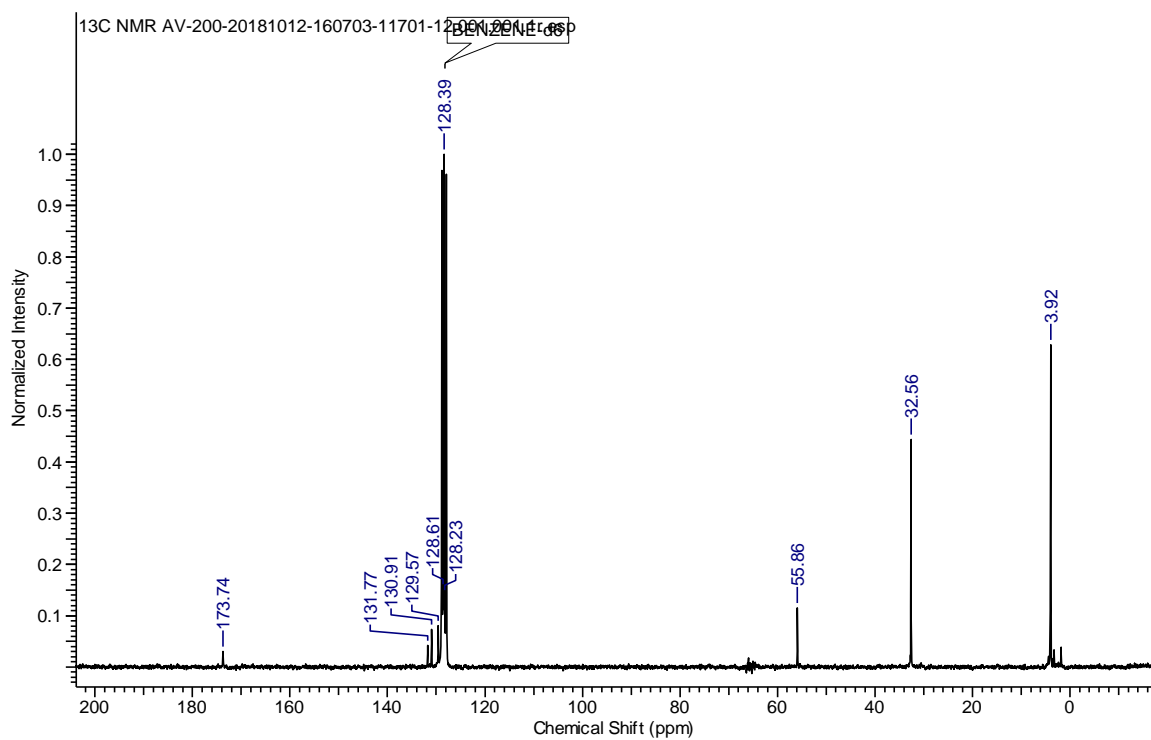
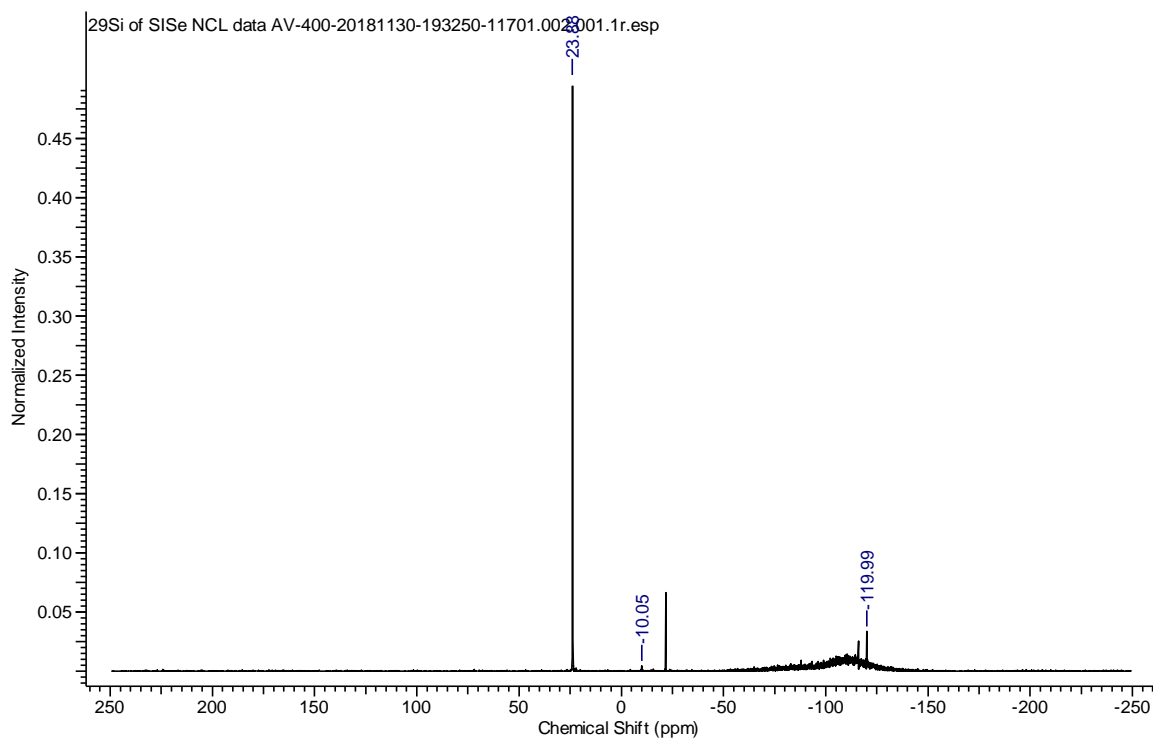
Figure S4. HRMS of **2.1**.

Figure S5. ¹H NMR Spectrum of **2.3** (C₆D₆, 200 MHz, 298 K)Figure S6. ¹³C NMR Spectrum of **2.3** (C₆D₆, 100.6 MHz, 298 K)

Figure S7. ^{29}Si NMR Spectrum of **2.3** (C_6D_6 , 79.5 MHz, 298 K)Figure S8. ^1H NMR Spectrum of **2.4** (C_6D_6 , 200 MHz, 298 K)

Figure S9. ¹³C NMR Spectrum of **2.4** (C₆D₆, 100.6 MHz, 298 K)Figure S10. ²⁹Si NMR Spectrum of **2.4** (C₆D₆, 79.5 MHz, 298 K)

Figure S11. HRMS of **2.4**.Figure S12. ¹H NMR Spectrum of **2.5** (C₆D₆, 200 MHz, 298 K)

Figure S13. ¹³C NMR Spectrum of **2.5** (C₆D₆, 50.3 MHz, 298 K)Figure S14. ²⁹Si NMR Spectrum of **2.5** (C₆D₆, 79.5 MHz, 298 K)

MBSI #807 RT: 3.63 AV: 1 NL: 2.07E5
T: FTMS + p ESI Full ms [133.4000-2000.0000]

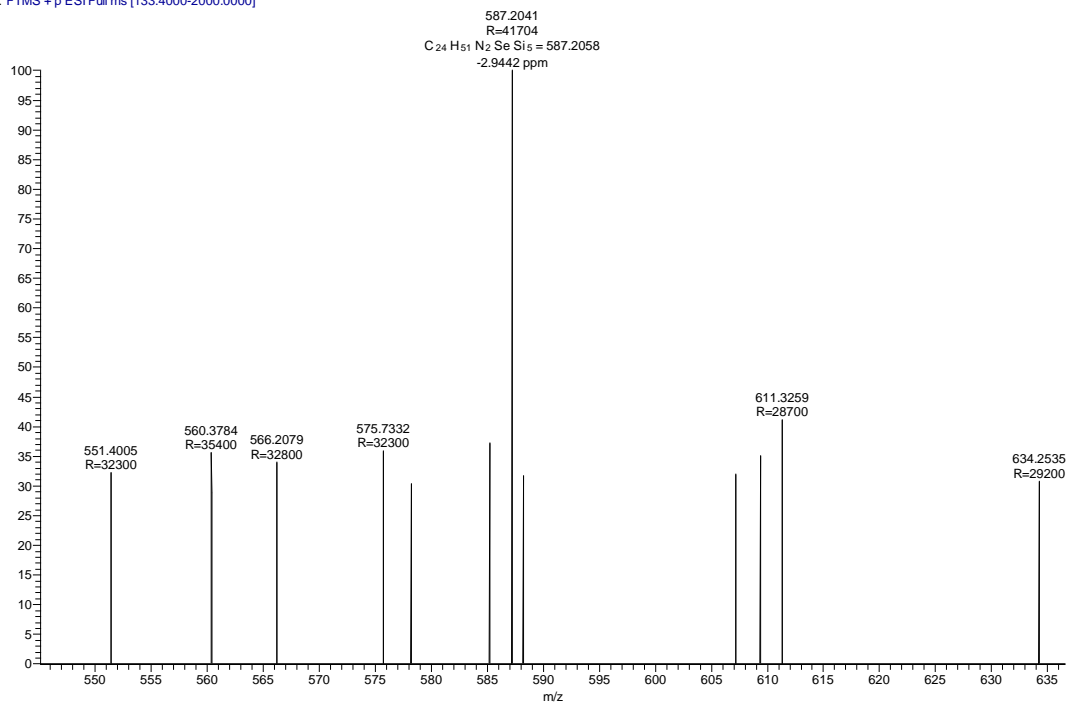
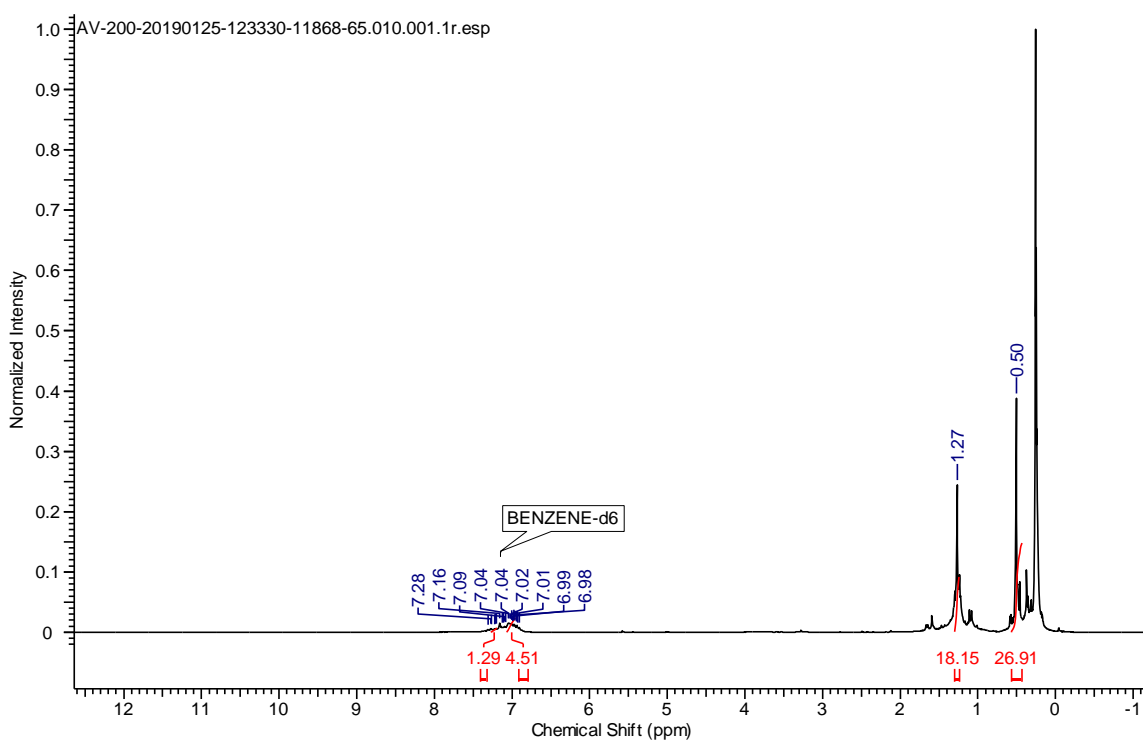
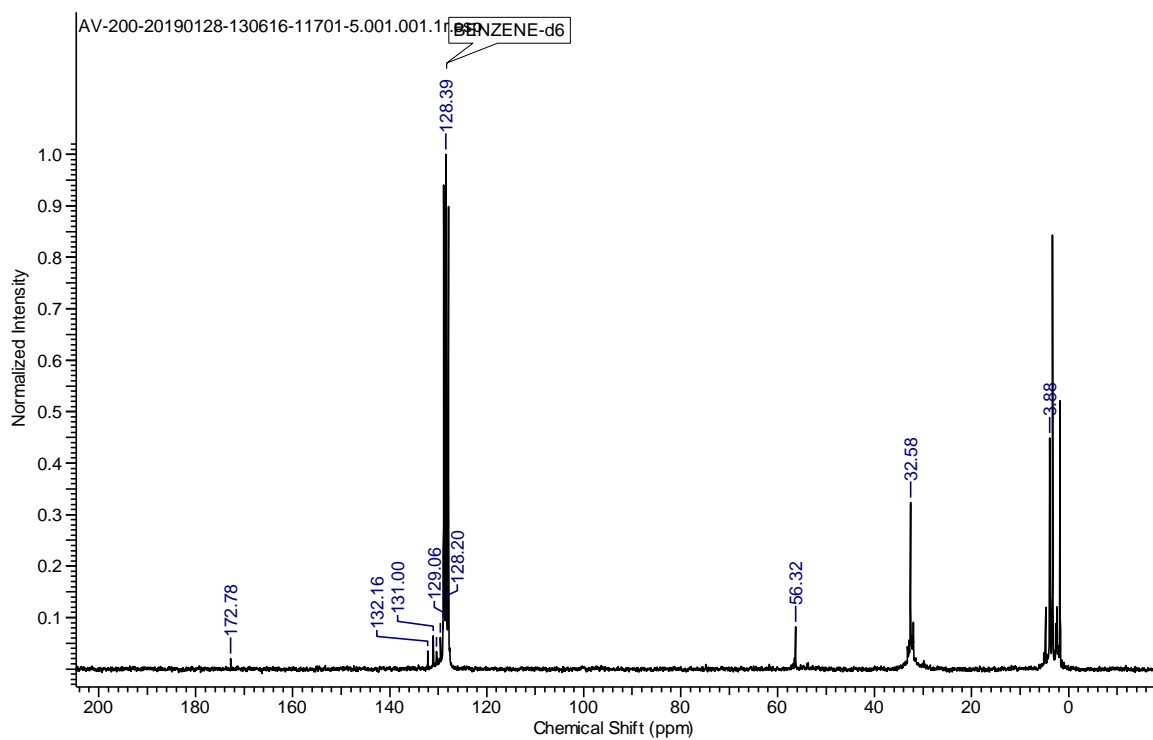
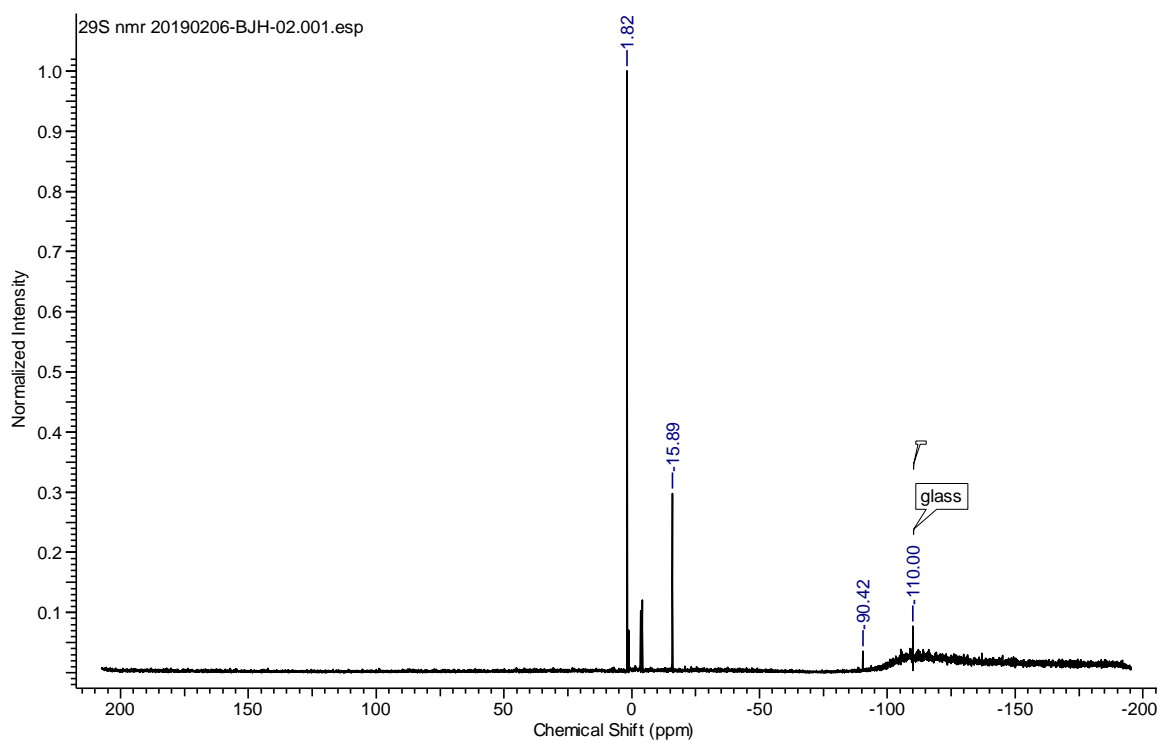


Figure S15. HRMS of 2.5.

Figure S16. 1H NMR Spectrum of 2.6 (C_6D_6 , 200 MHz, 298 K)

Figure S17. ¹³C NMR Spectrum of **2.6** (C₆D₆, 50.3 MHz, 298 K)Figure S18. ²⁹Si NMR Spectrum of **2.6** (C₆D₆, 79.5 MHz, 298 K)

MB-06 #451 RT: 2.01 AV: 1 NL: 9.58E7
T: FTMS + p ESI Full ms [80.0000-1200.0000]

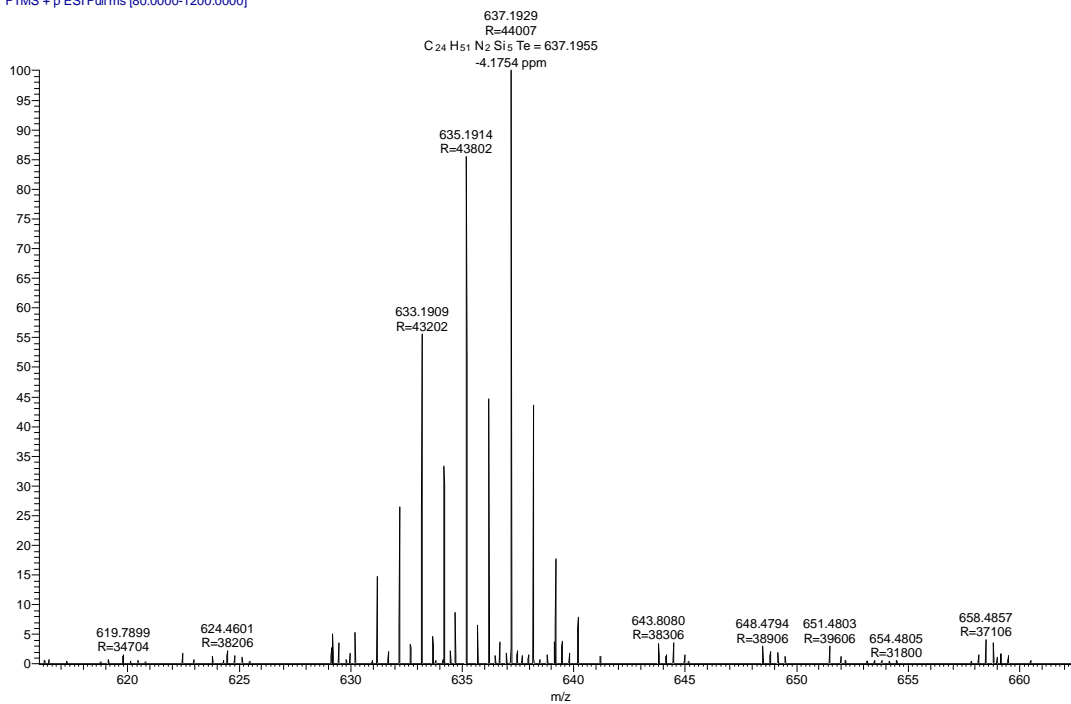


Figure S19. HRMS of 2.6.

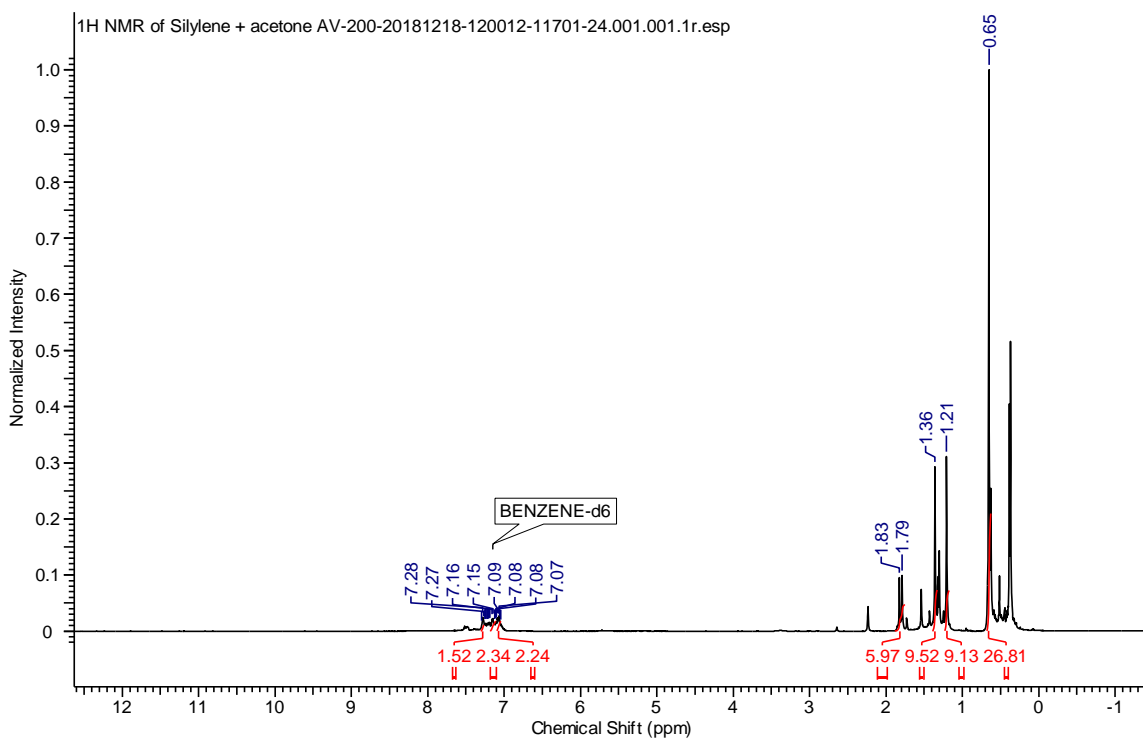
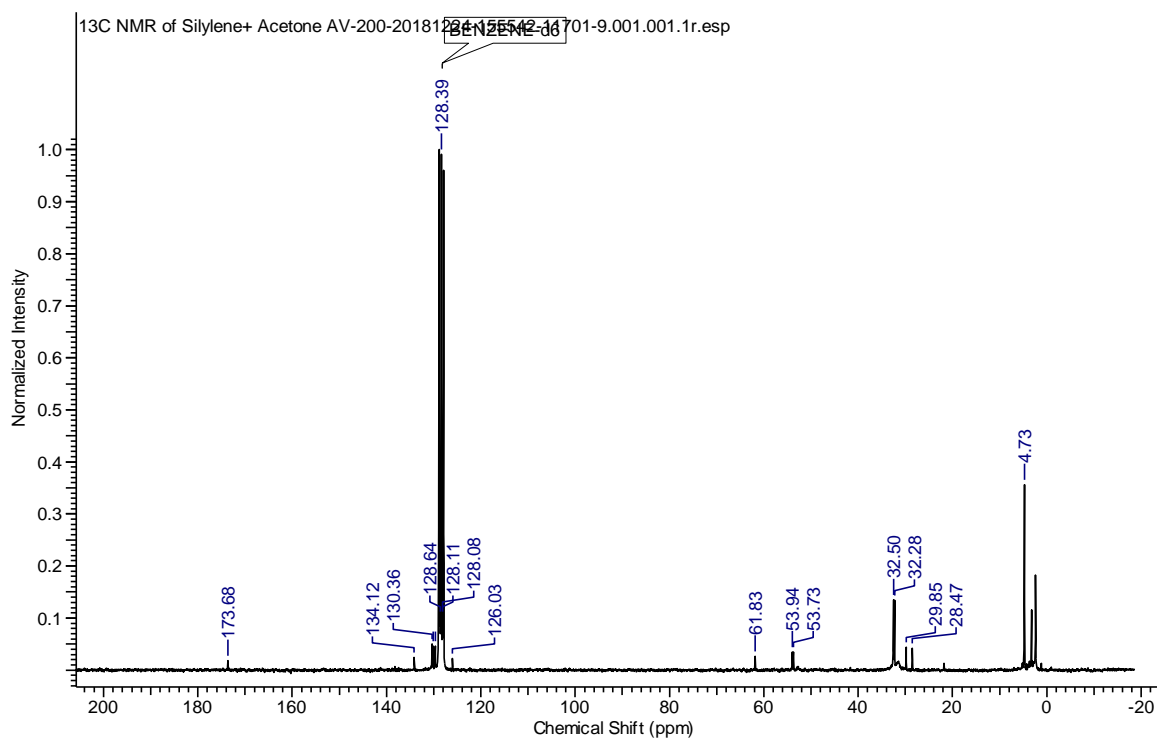
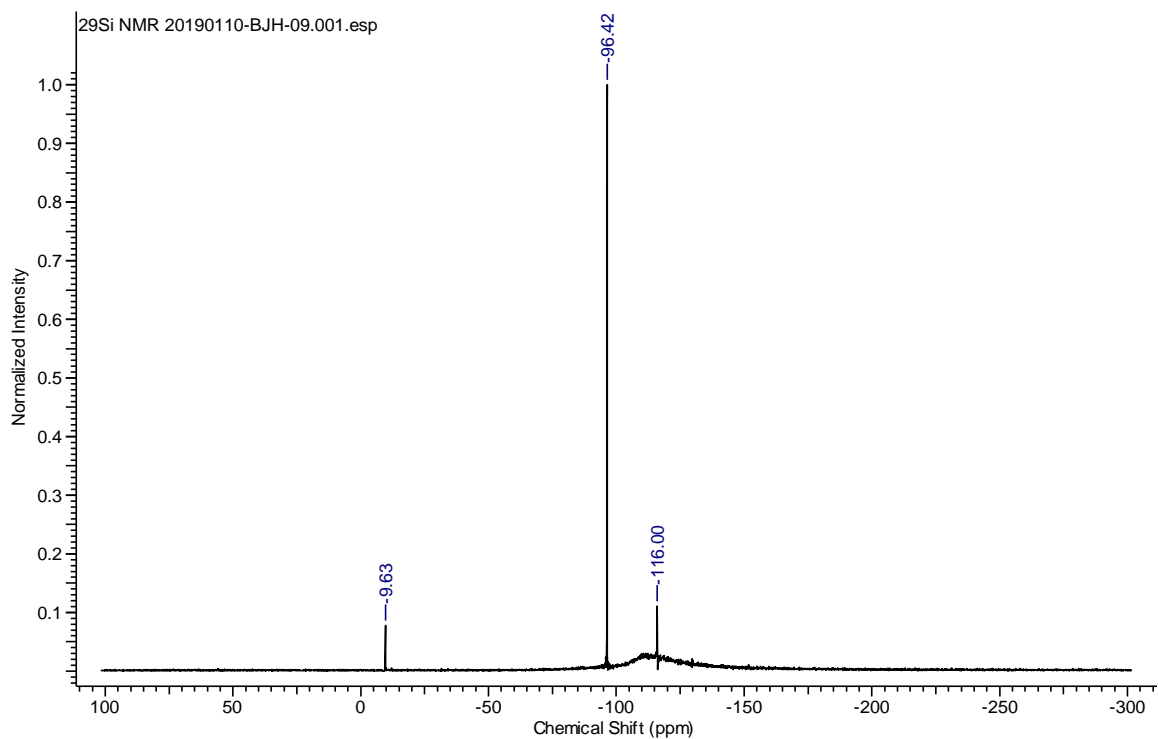
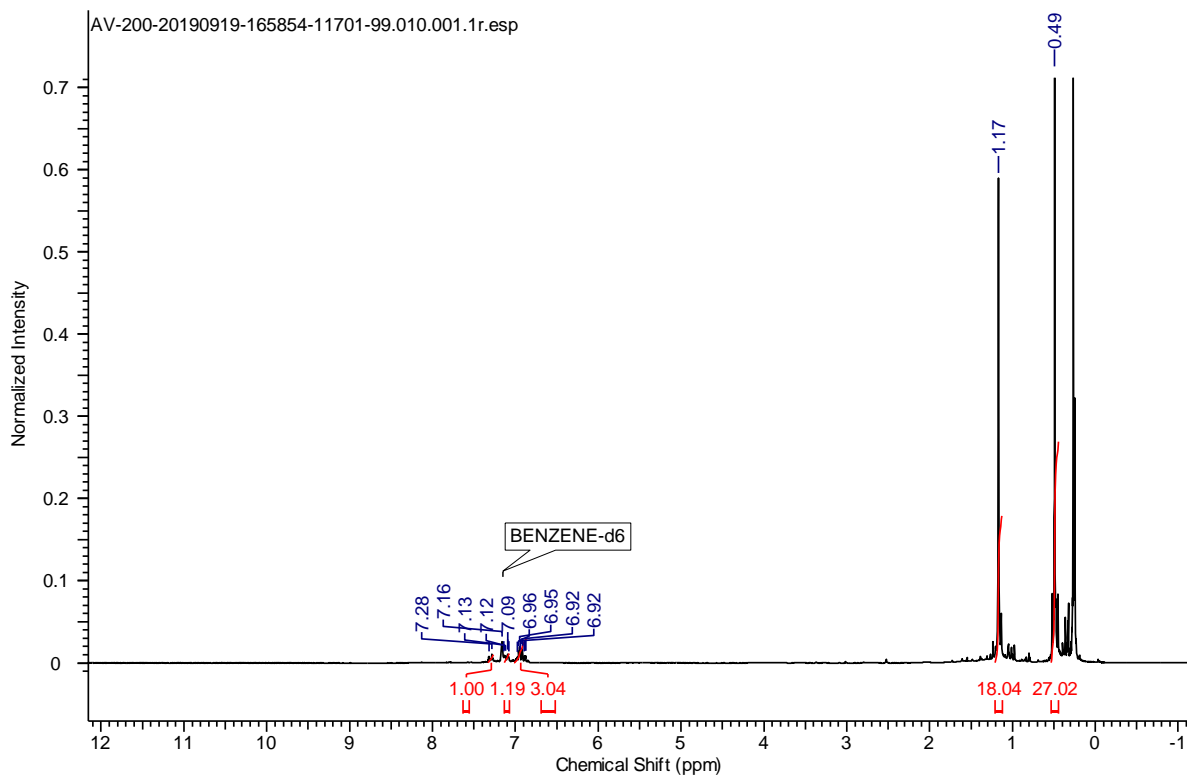
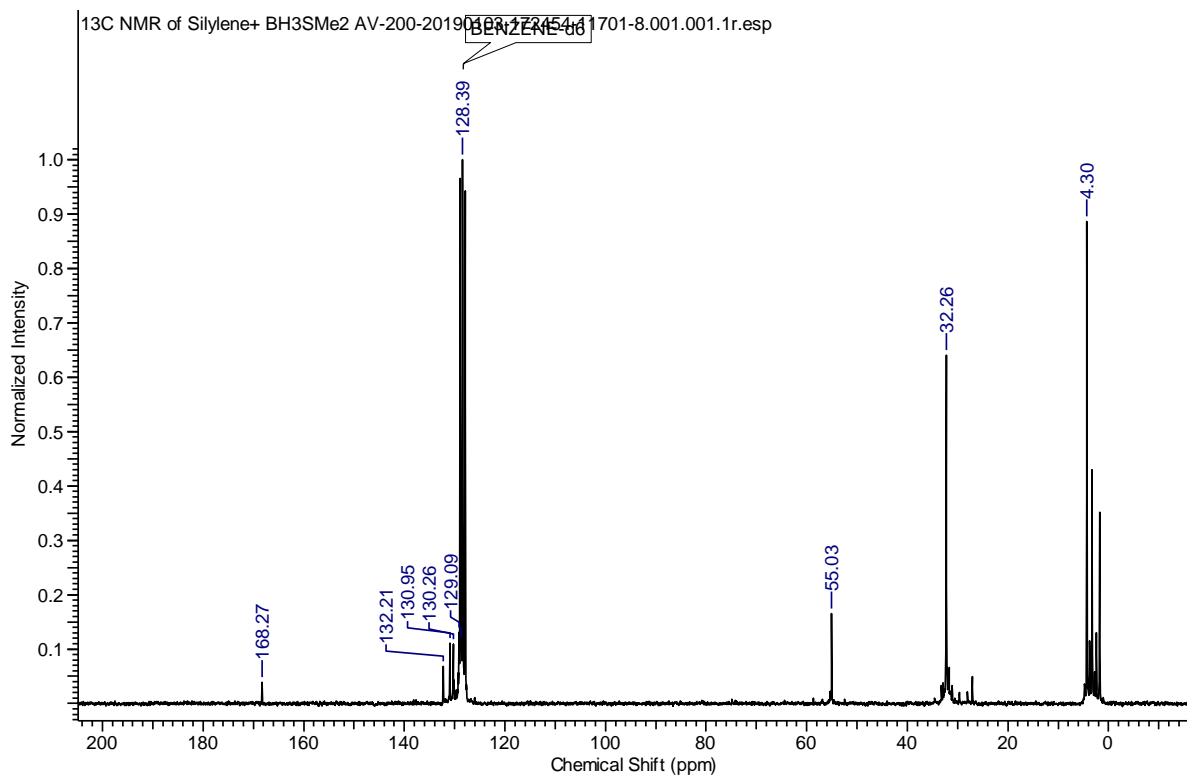
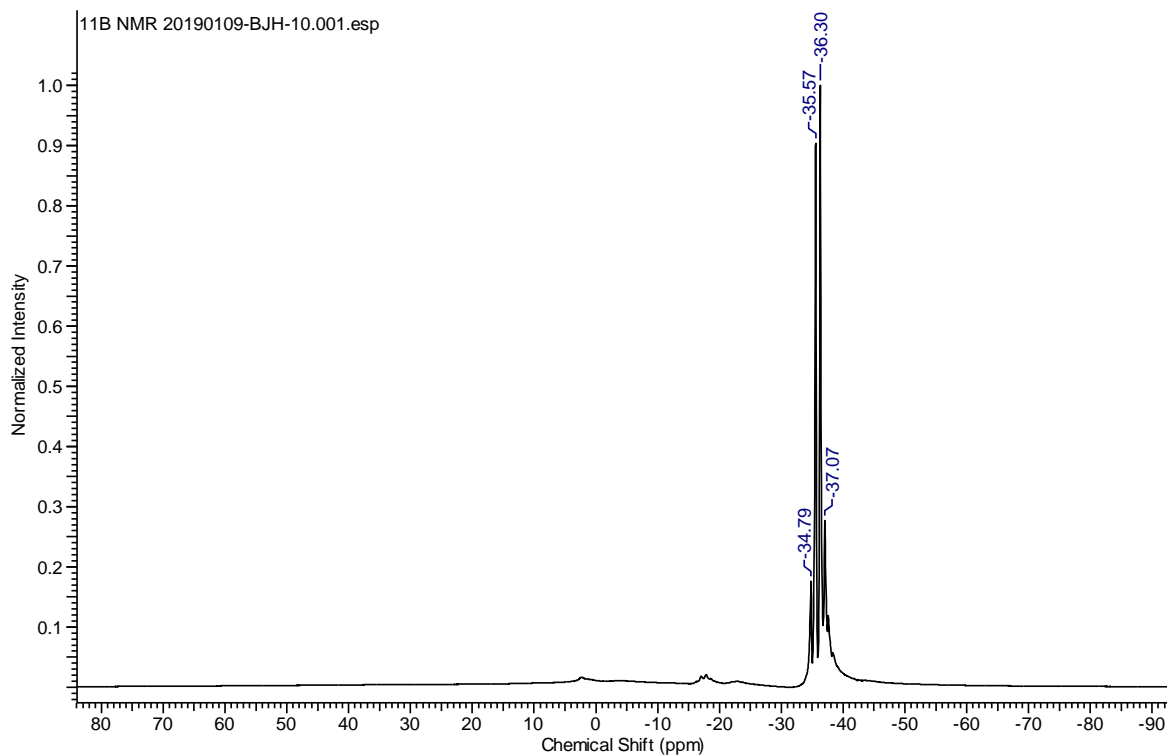
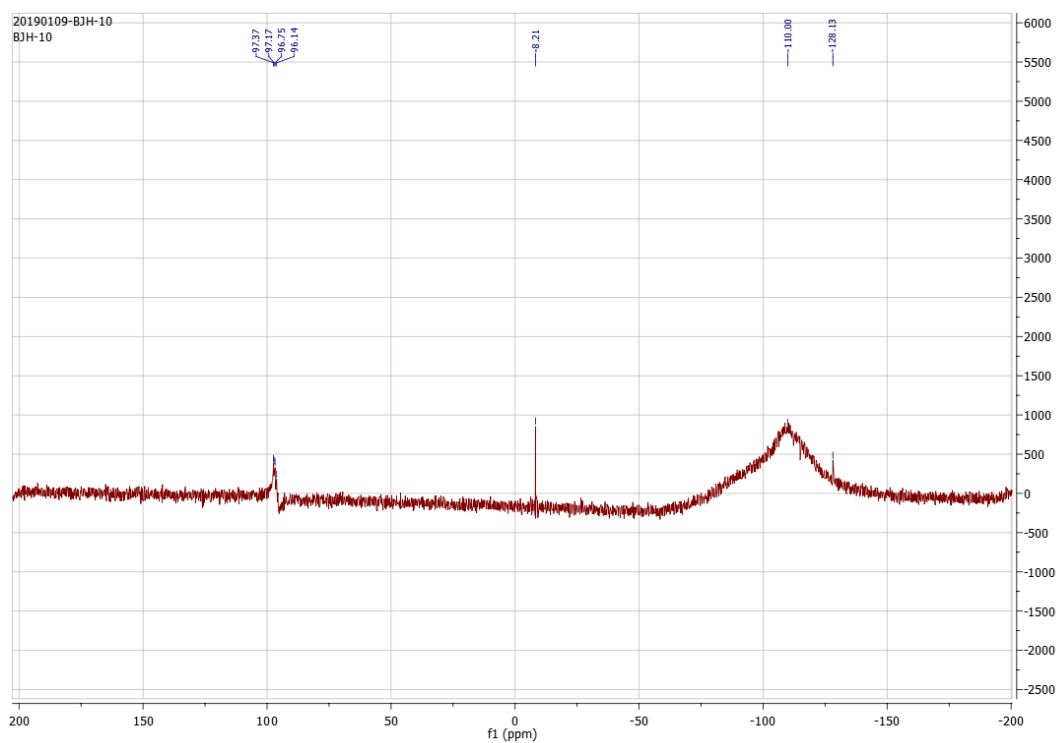


Figure S20. ¹H NMR Spectrum of 2.7 (C₆D₆, 200 MHz, 298 K)

Figure S21. ¹³C NMR Spectrum of **2.7** (C₆D₆, 50.3 MHz, 298 K)Figure S22. ²⁹Si NMR Spectrum of **2.7** (C₆D₆, 79.5 MHz, 298 K)

Figure S23. ^1H NMR Spectrum of **2.8** (C_6D_6 , 200 MHz, 298 K)Figure S24. ^{13}C NMR Spectrum of **2.8** (C_6D_6 , 50.3 MHz, 298 K)

Figure S25. ^{11}B NMR Spectrum of **2.8** (C_6D_6 , 128.4 MHz, 298 K)Figure S26. ^{29}Si NMR Spectrum of **2.8** (C_6D_6 , 79.5 MHz, 298 K)

MB-01 #467 RT: 2.08 AV: 1 NL: 5.12E6
T: FTMS + p ESI Full ms [80.0000-1200.0000]

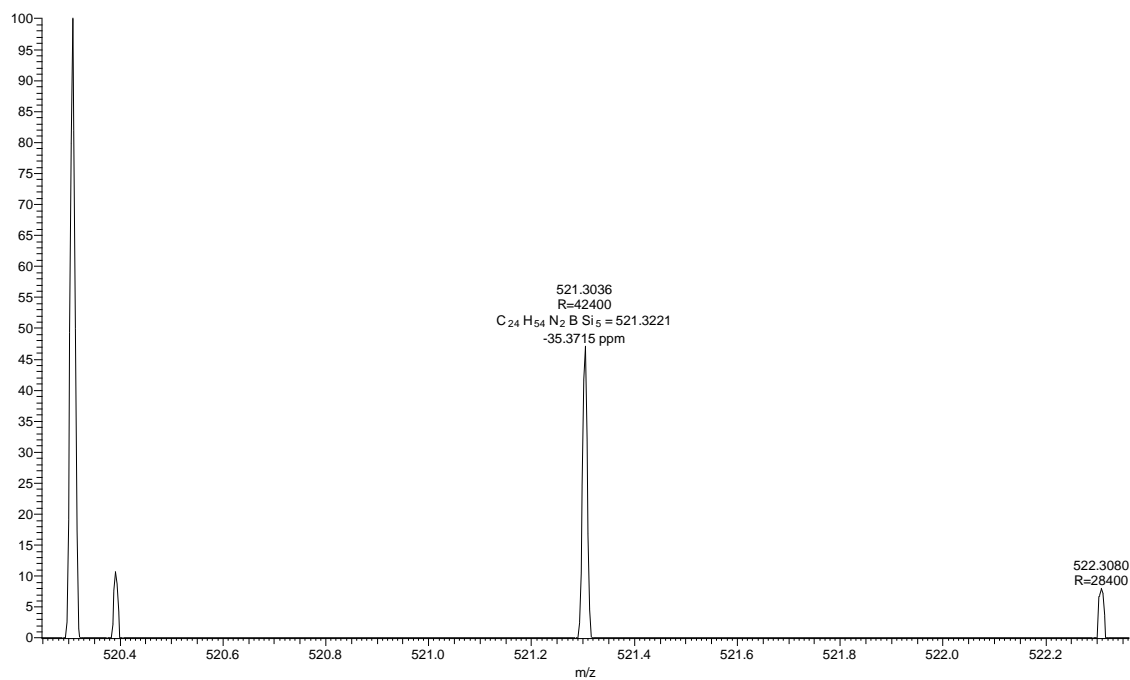


Figure S27. HRMS of **2.8**.

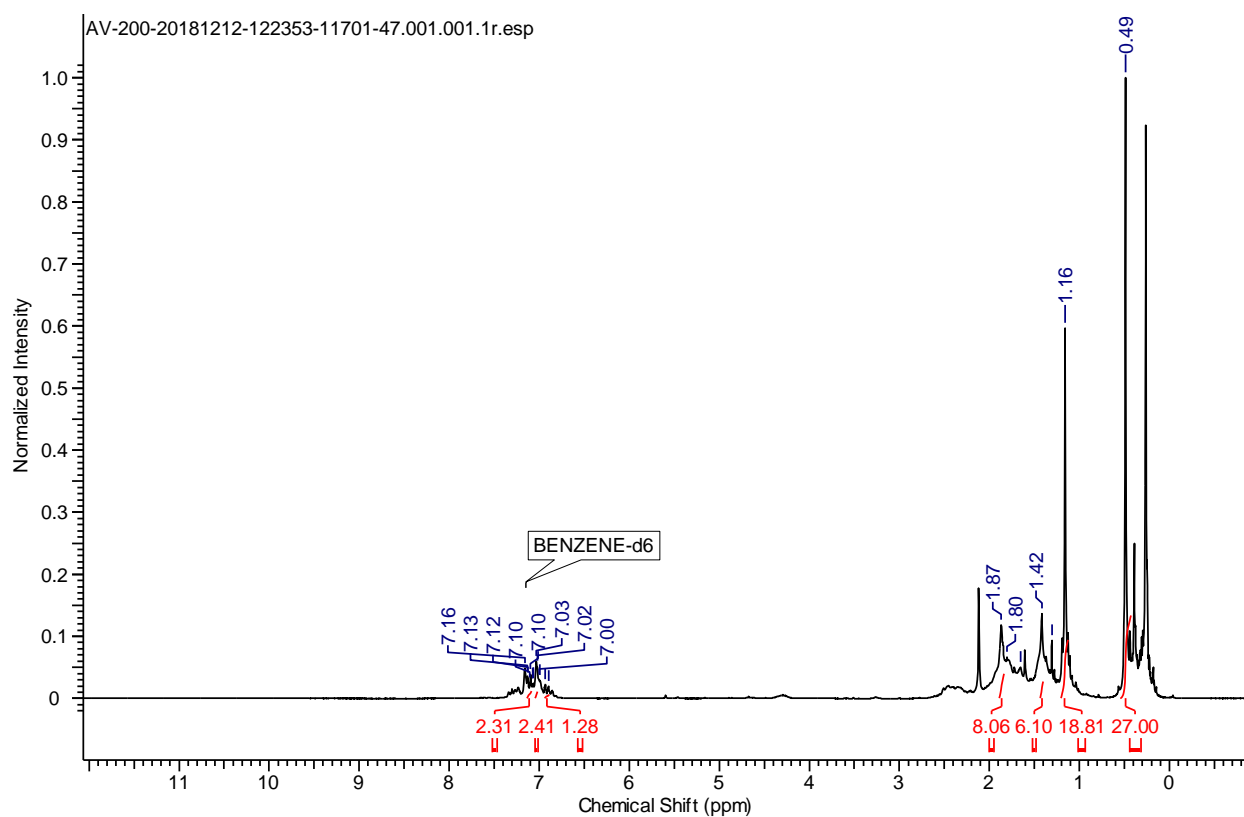
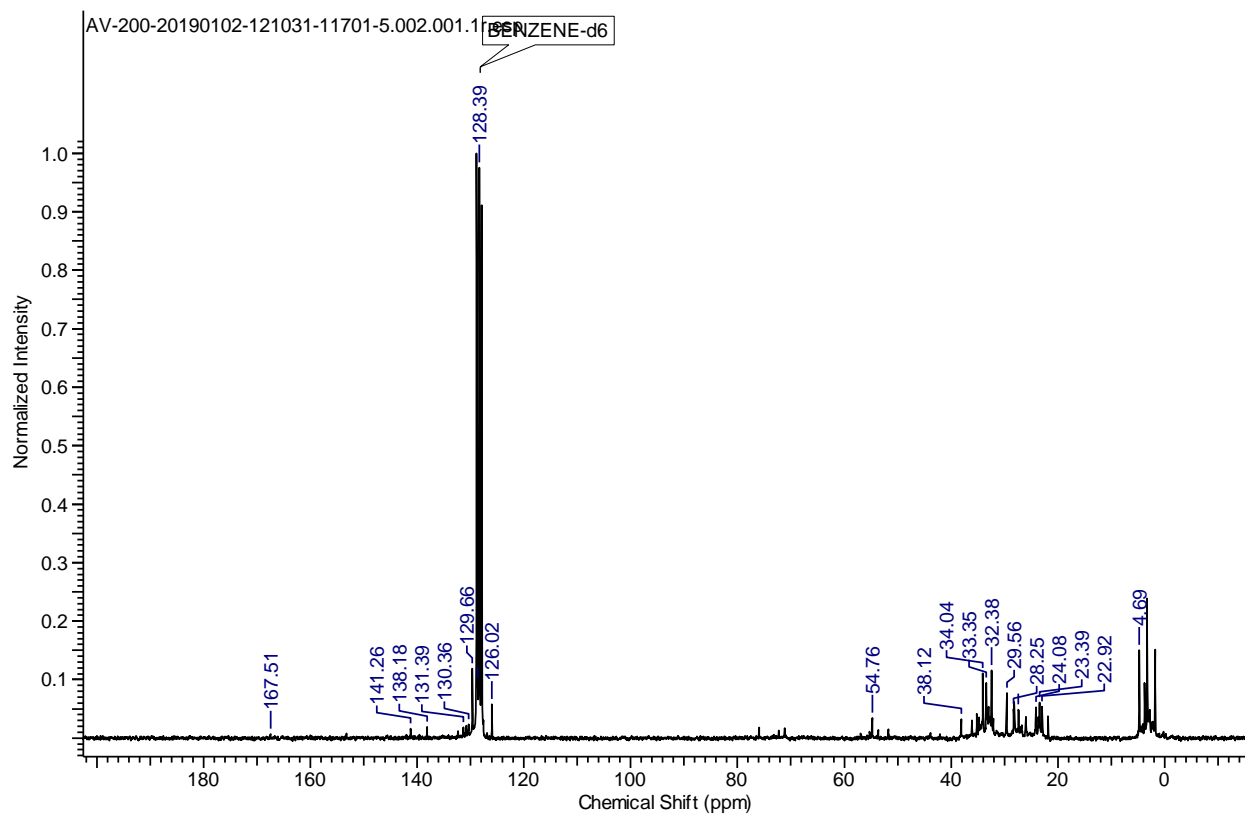
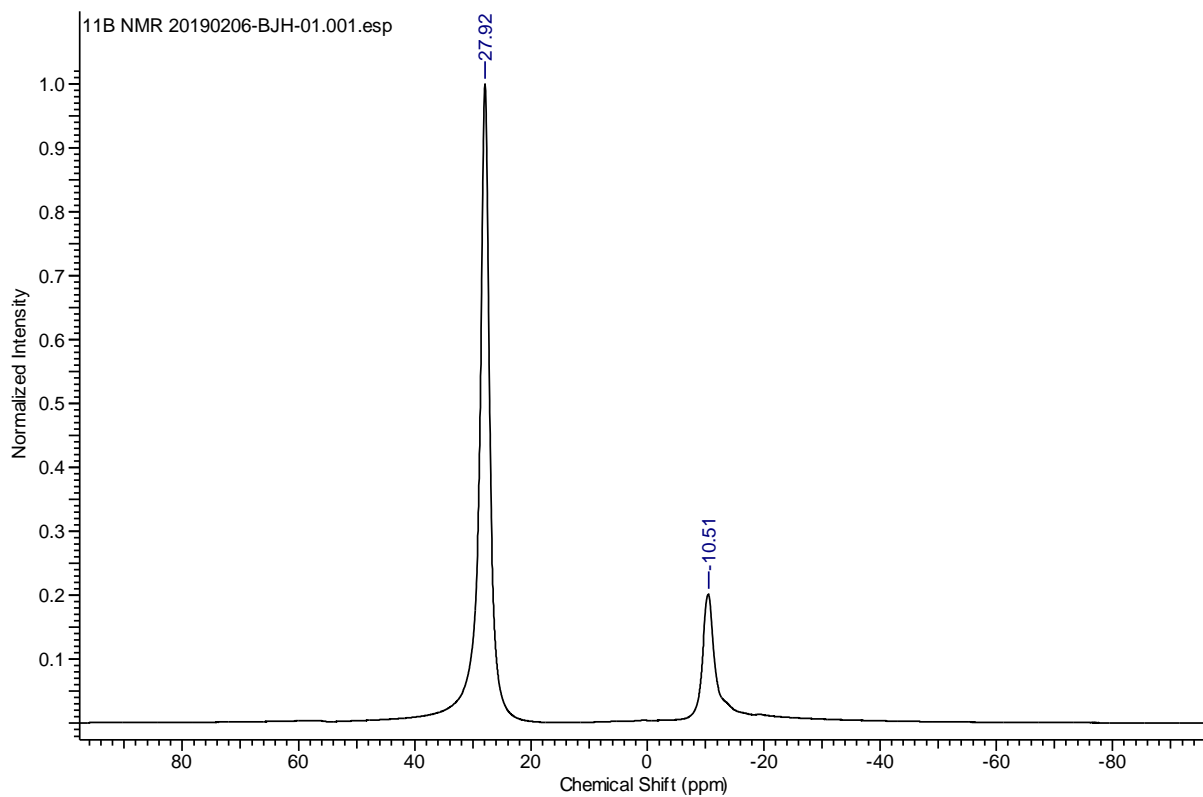
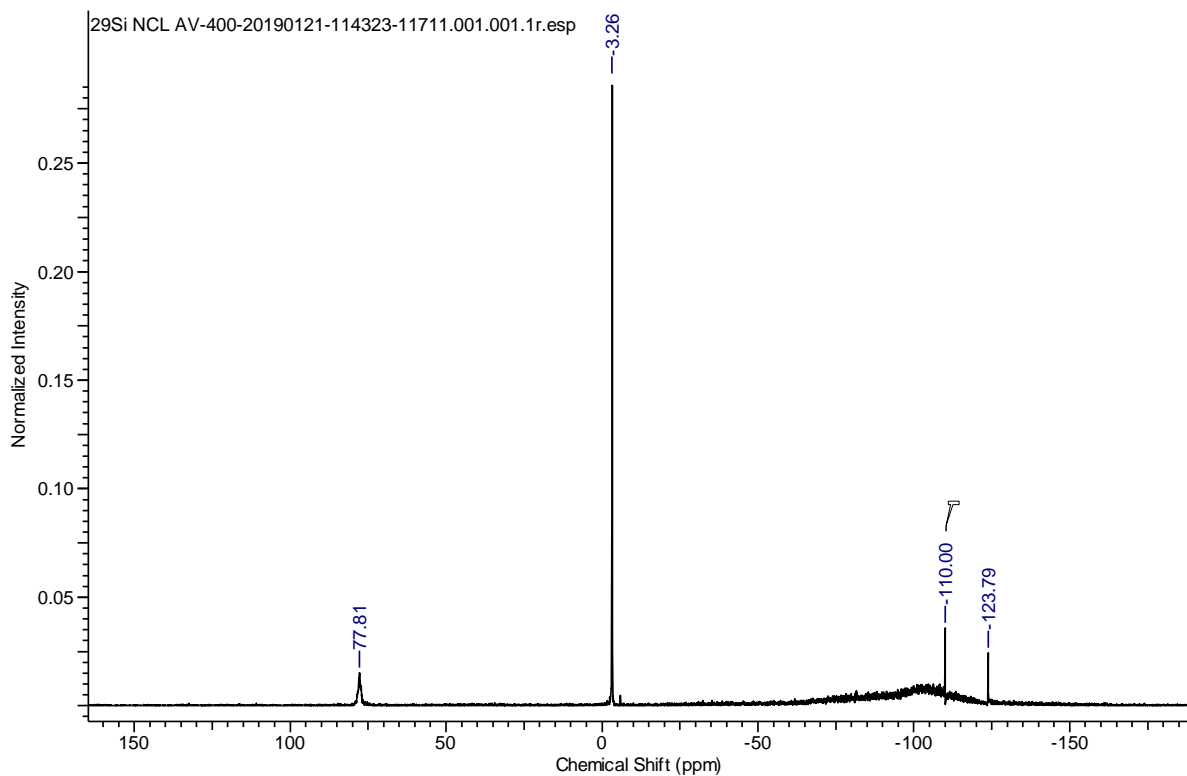
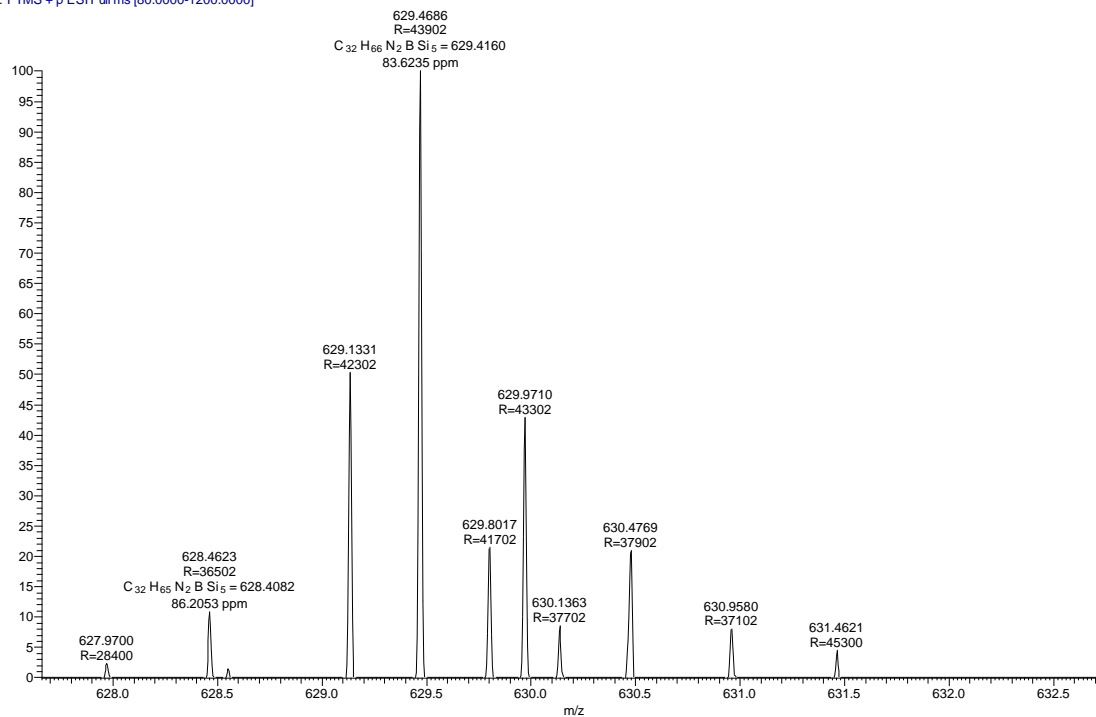


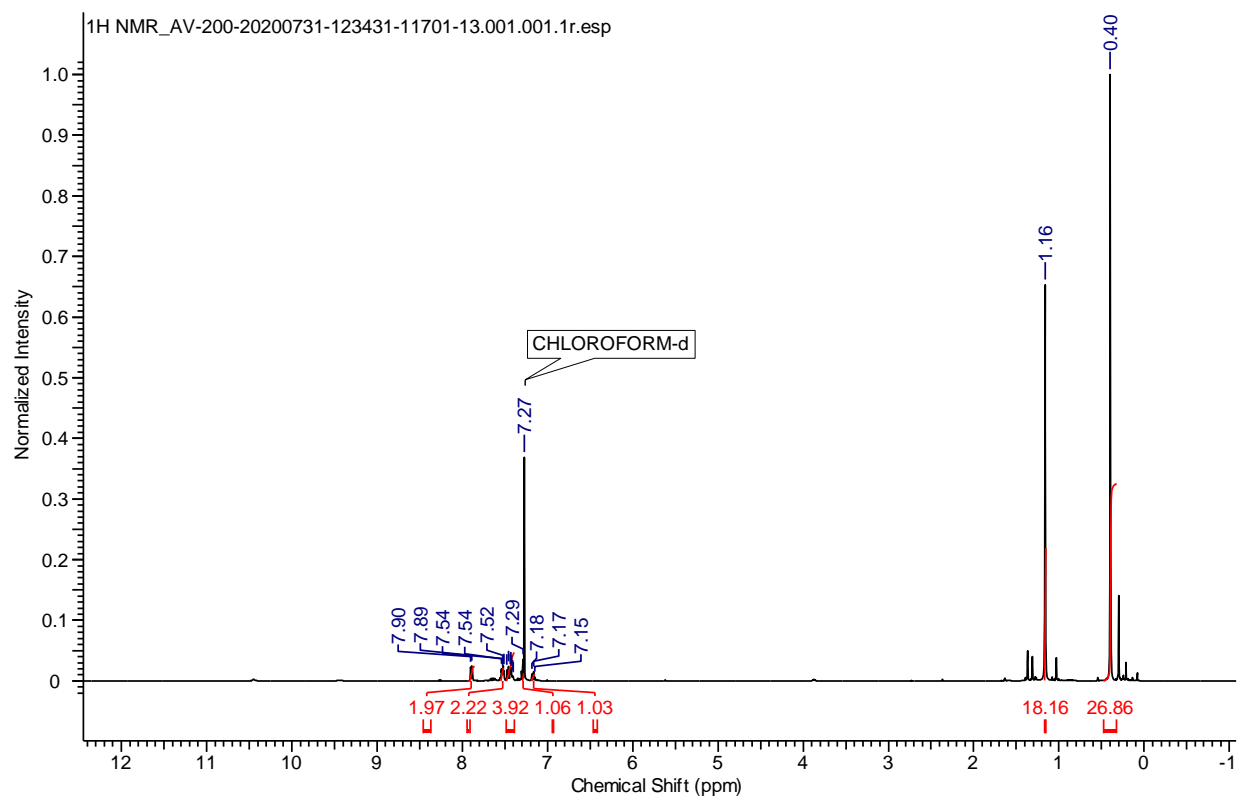
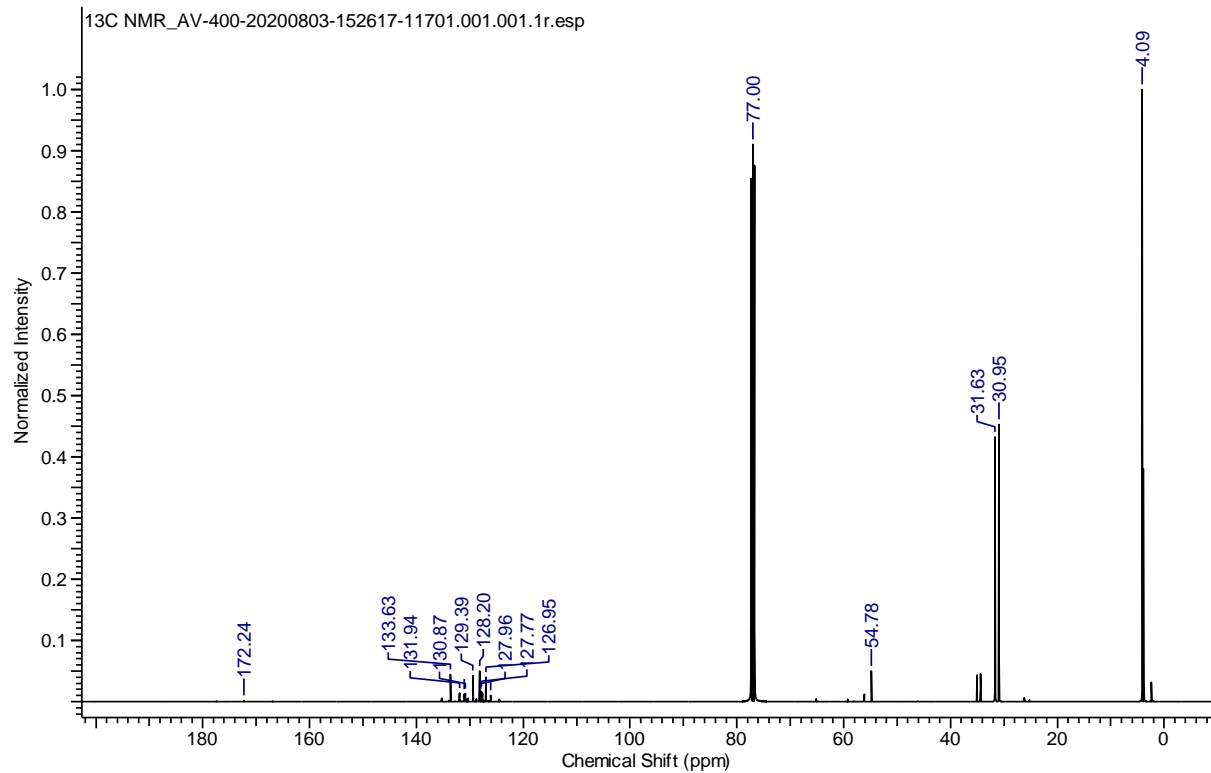
Figure S28. ¹H NMR Spectrum of **2.9** (C₆D₆, 200 MHz, 298 K)

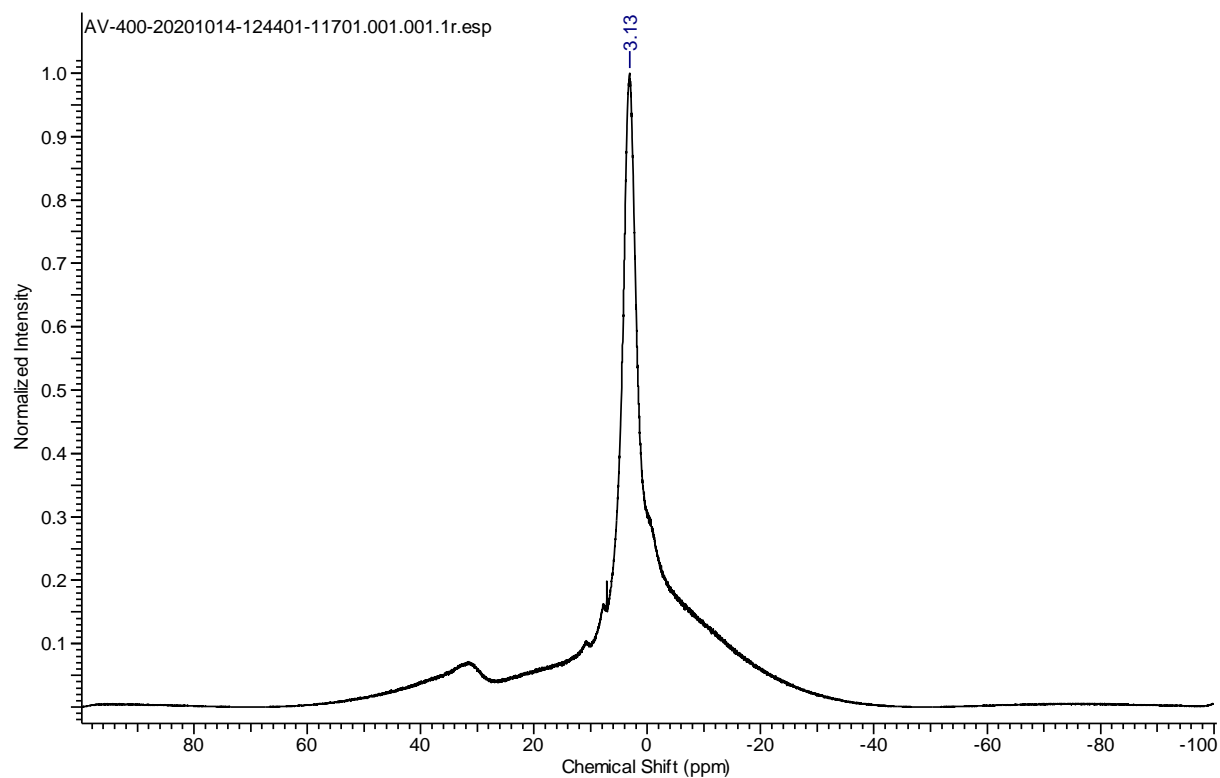
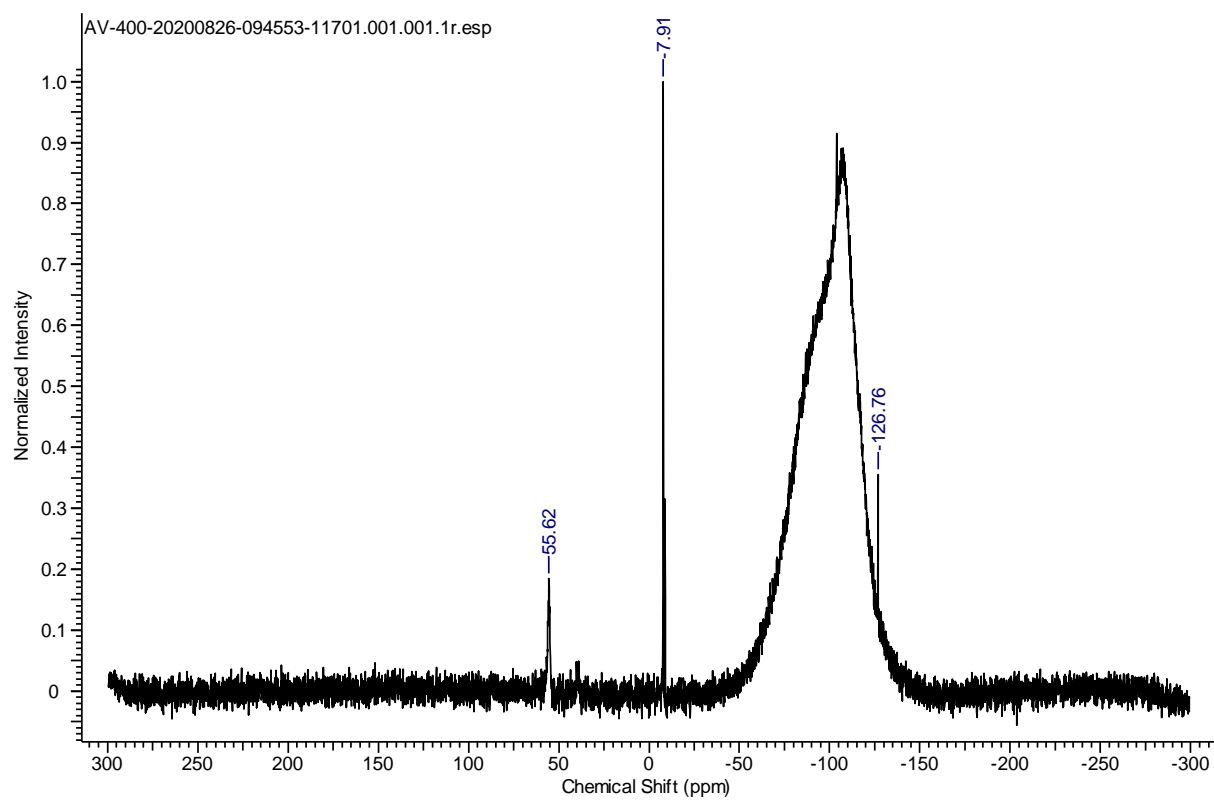
Figure S29. ^{13}C NMR Spectrum of **2.9** (C_6D_6 , 50.3 MHz, 298 K)Figure S30. ^{11}B NMR Spectrum of **2.9** (C_6D_6 , 128.4 MHz, 298 K)

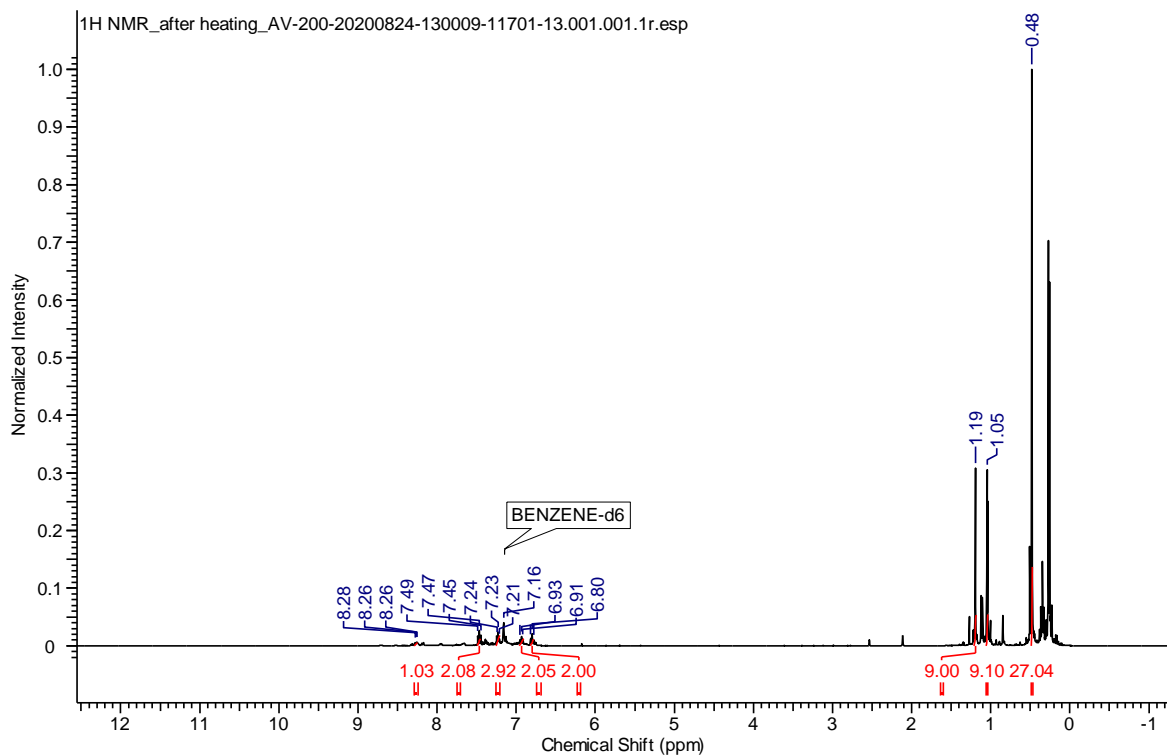
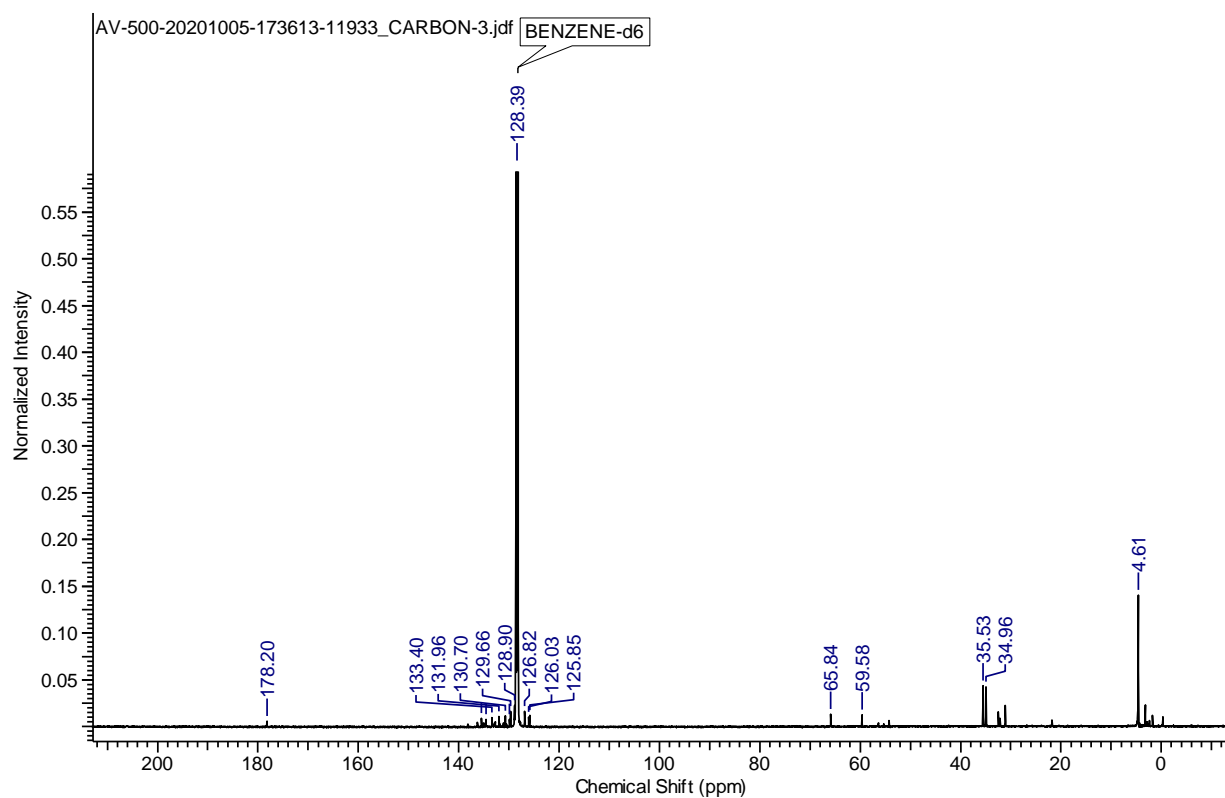
Figure S31. ^{29}Si NMR Spectrum of **2.9** (C_6D_6 , 79.5 MHz, 298 K)

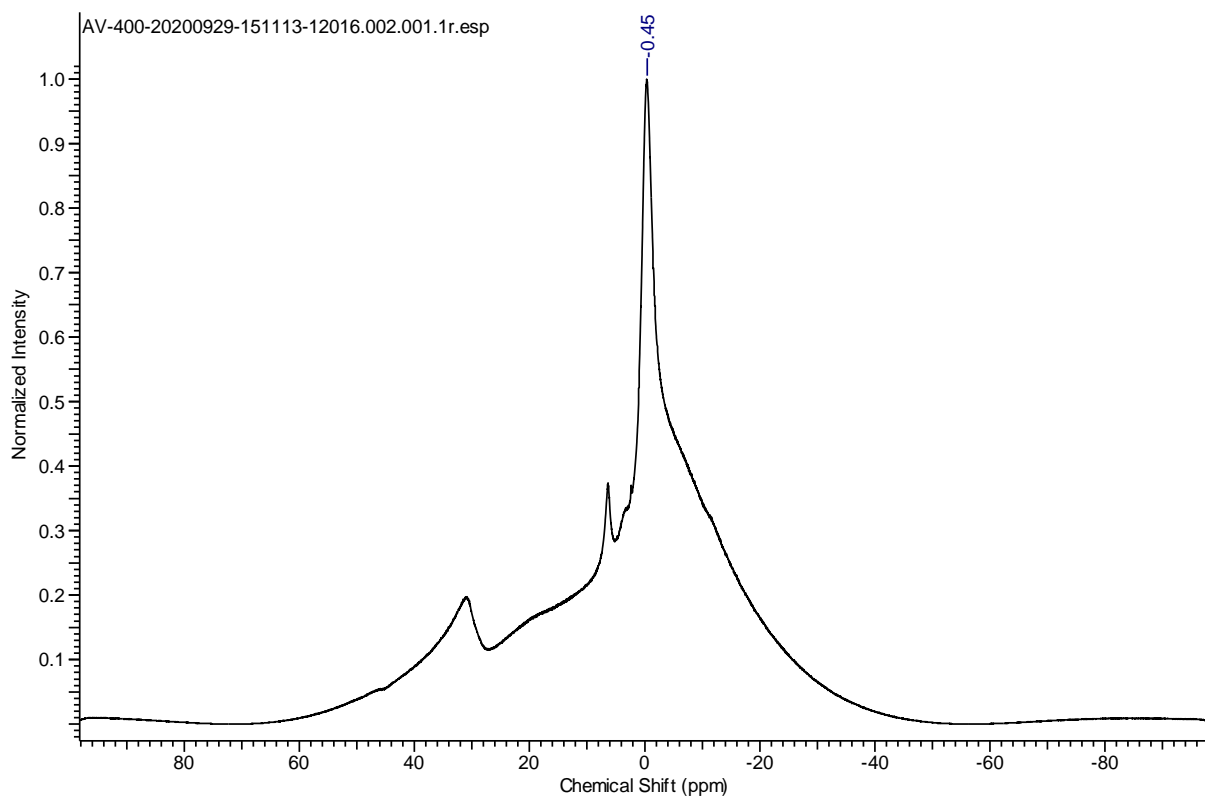
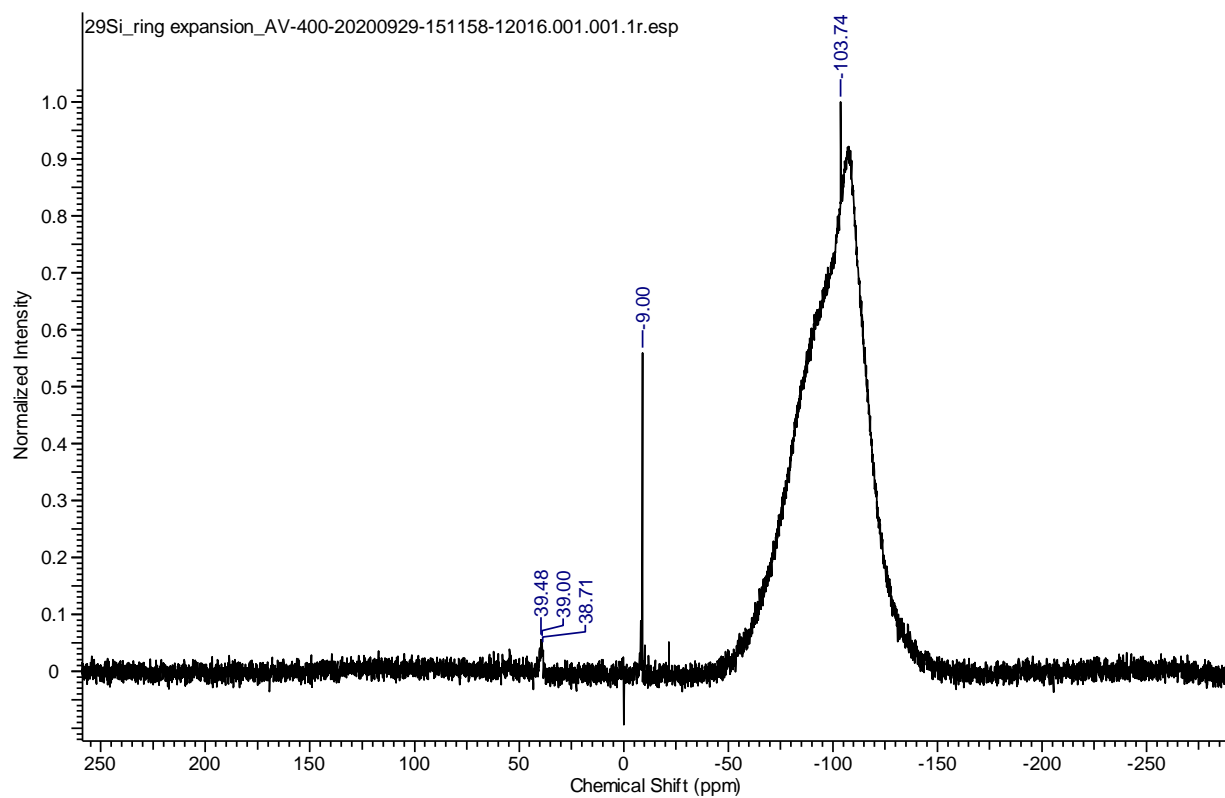
MB-02 #346 RT: 1.54 AV: 1 NL: 7.61E6
T: FTMS + p ESI Full ms [80.0000-1200.0000]

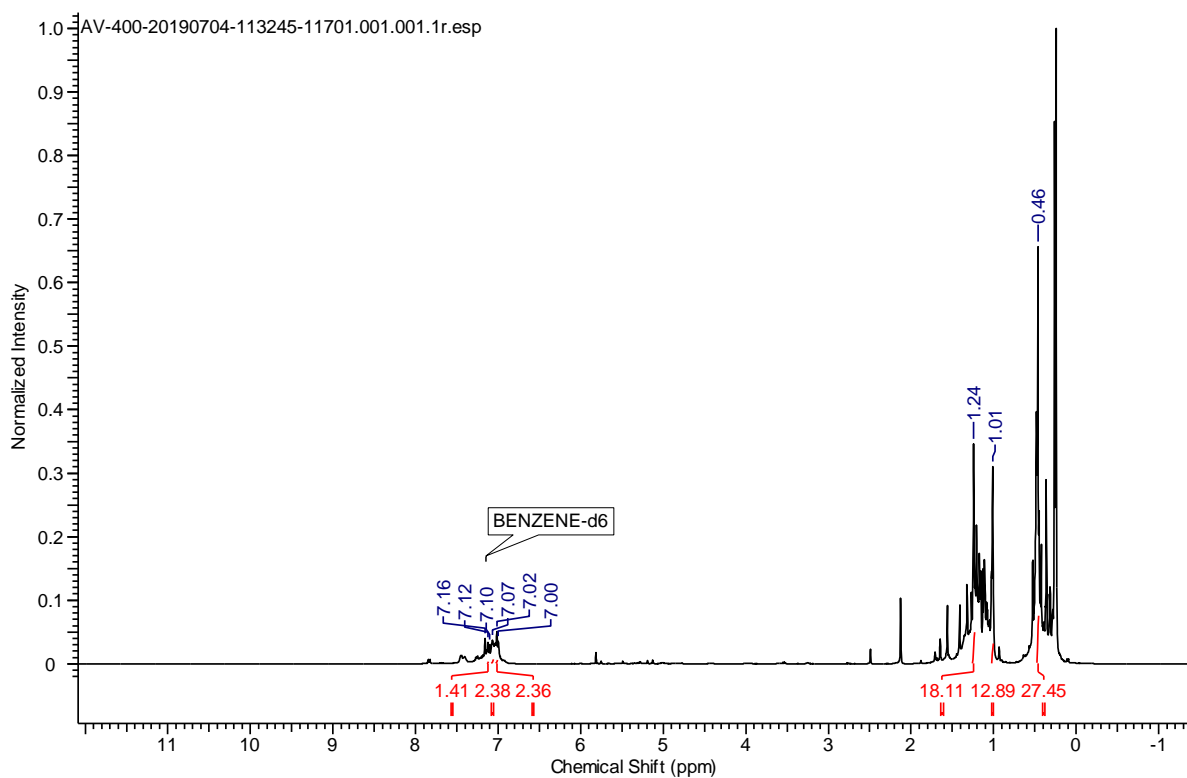
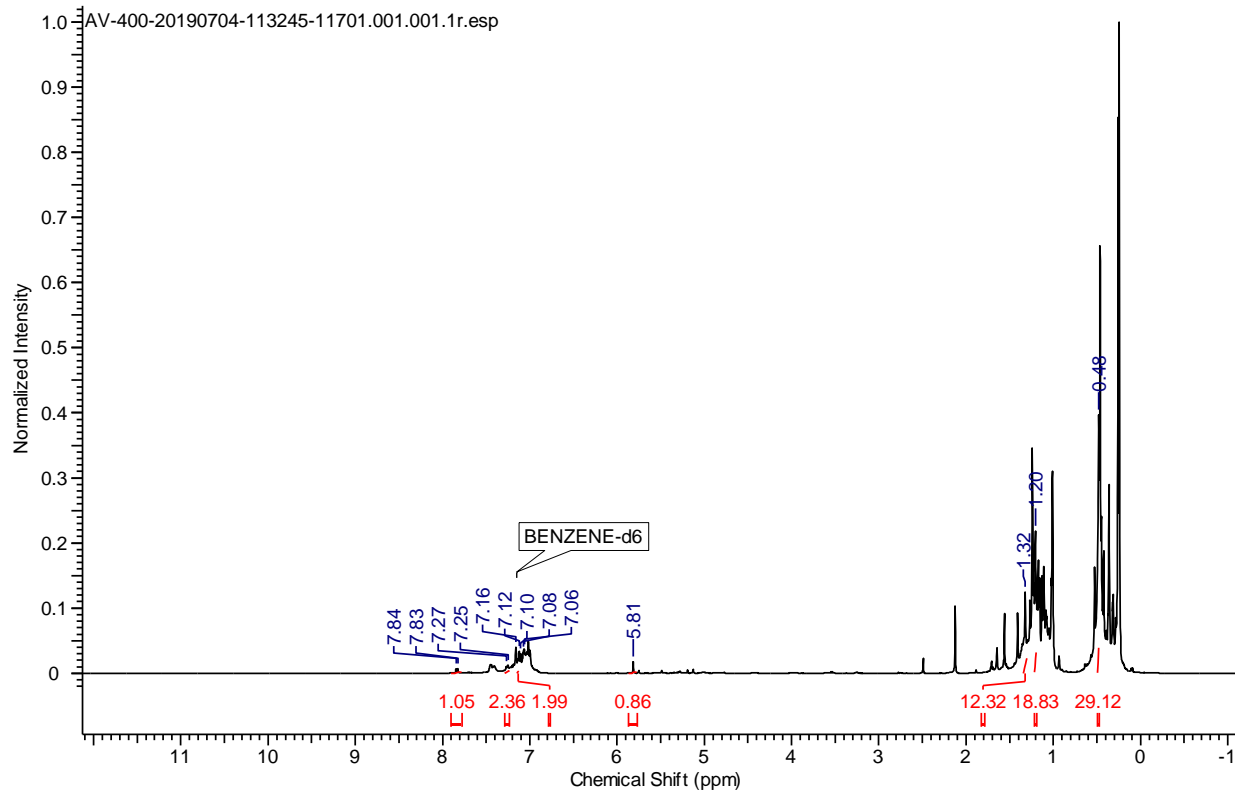
Figure S32. HRMS of **2.9**.

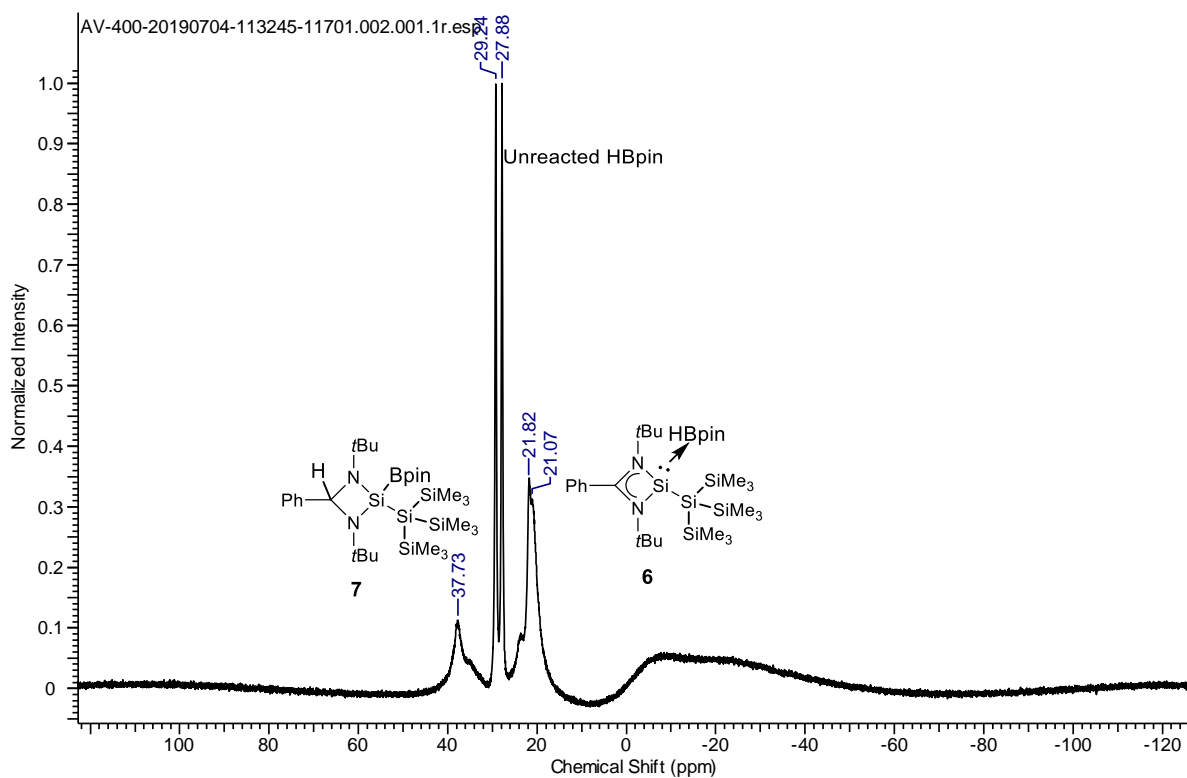
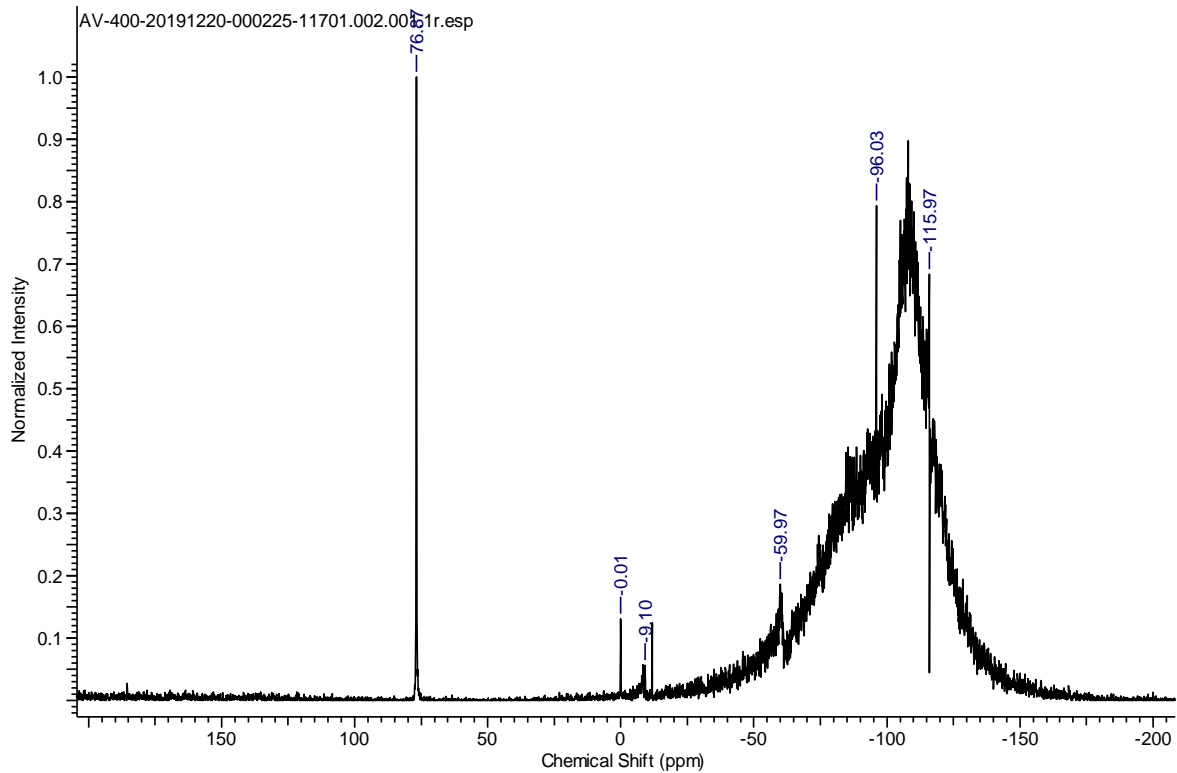
Figure S33. ¹H NMR of **2.10** (C₆D₆, 400 MHz, 298 K)Figure S34. ¹³C NMR of **2.10** (CDCl₃, 100.6 MHz, 298 K)

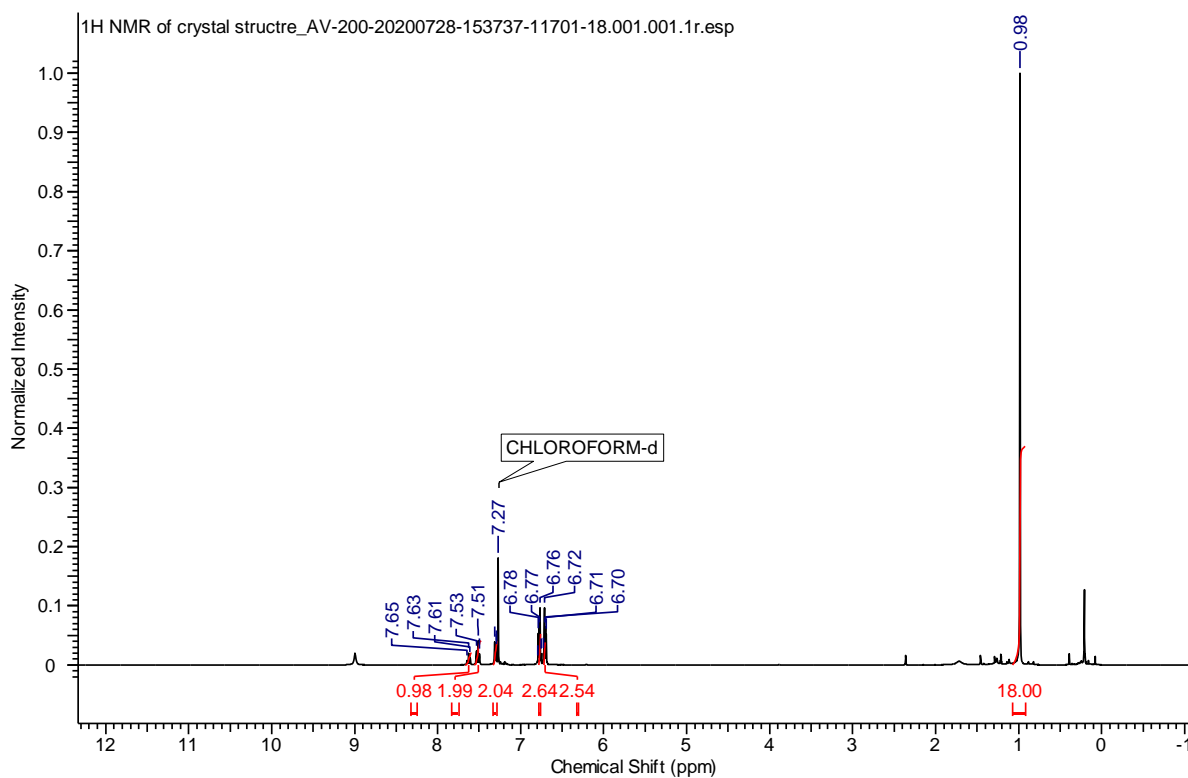
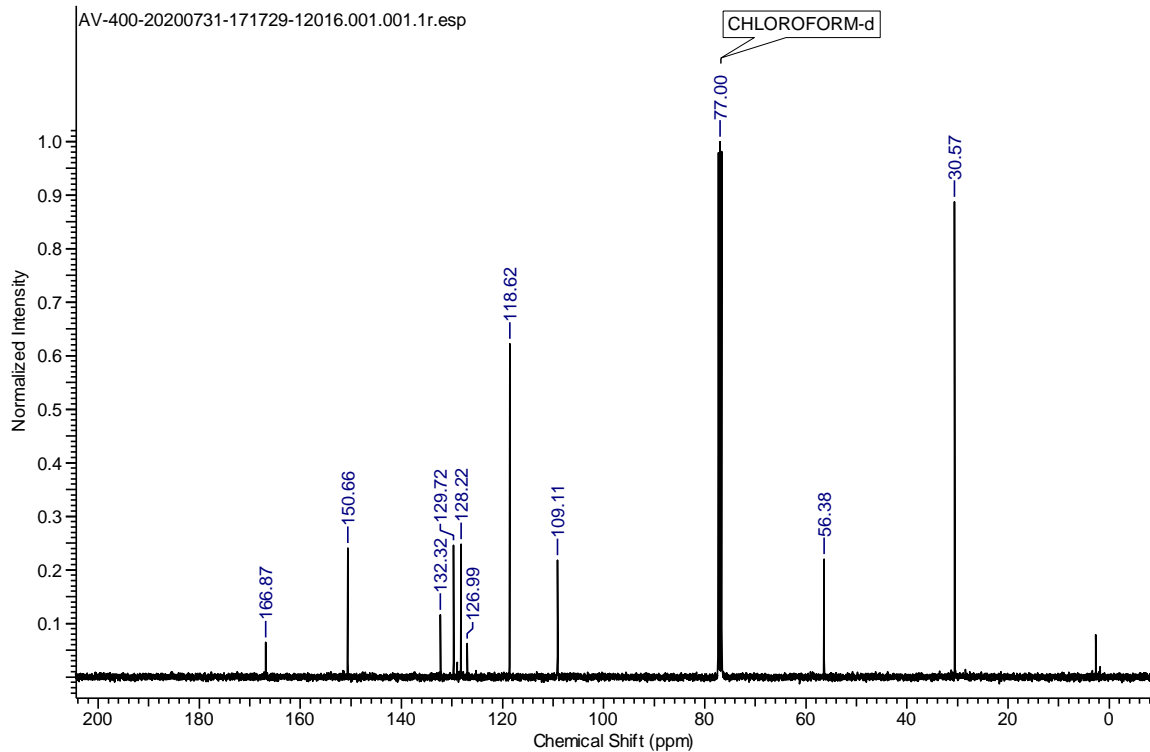
Figure S35. ^{11}B NMR of **2.10** (C_6D_6 , 160.4 MHz, 298 K)Figure S36. ^{29}Si NMR of **2.10** (CDCl_3 , 99.3 MHz, 298 K)

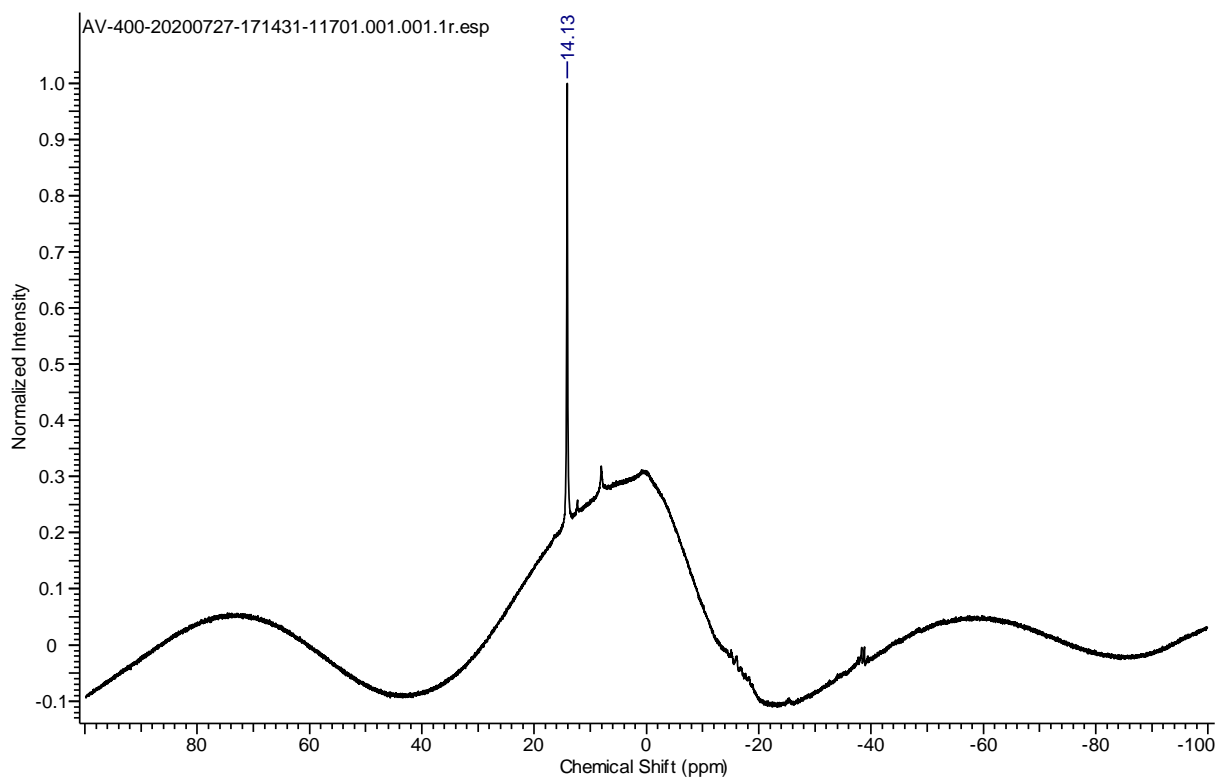
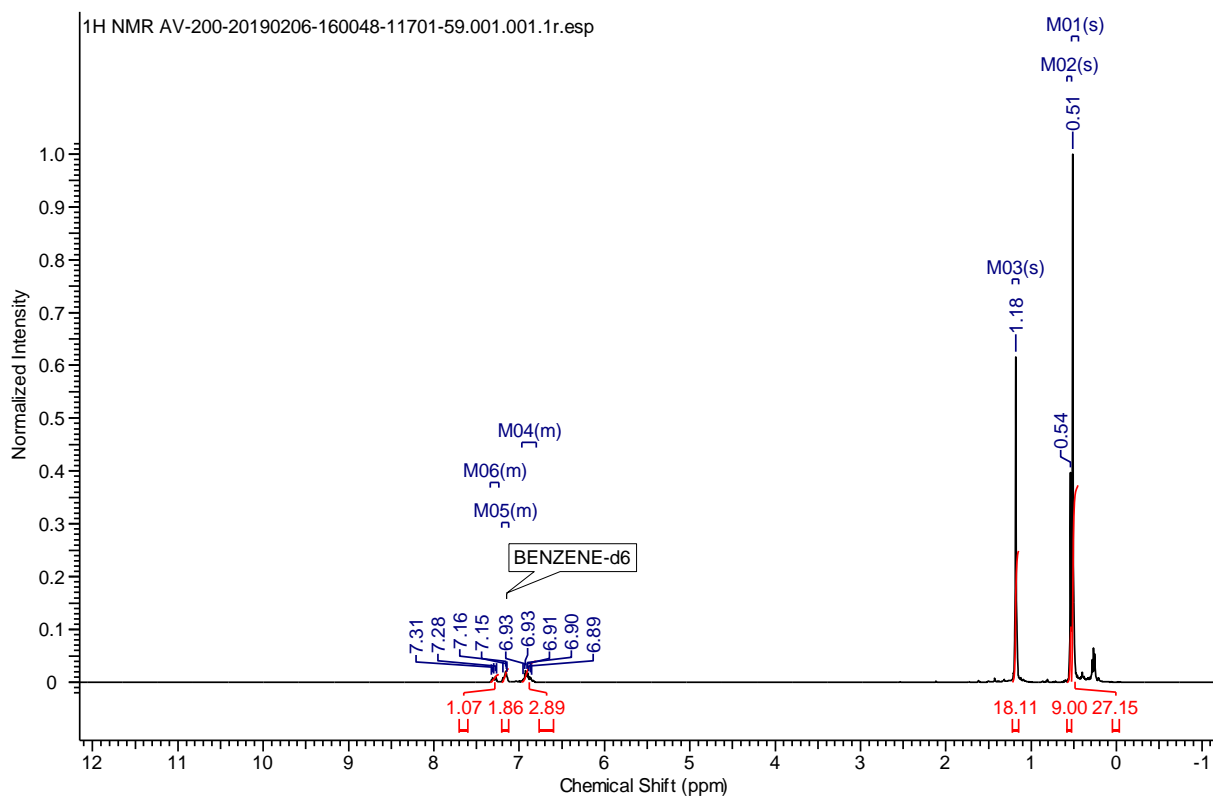
Figure S37. ^1H NMR Spectrum of **2.11** (C_6D_6 , 400 MHz, 298 K)Figure S38. ^{13}C NMR of **2.11** (C_6D_6 , 100.5 MHz, 298 K)

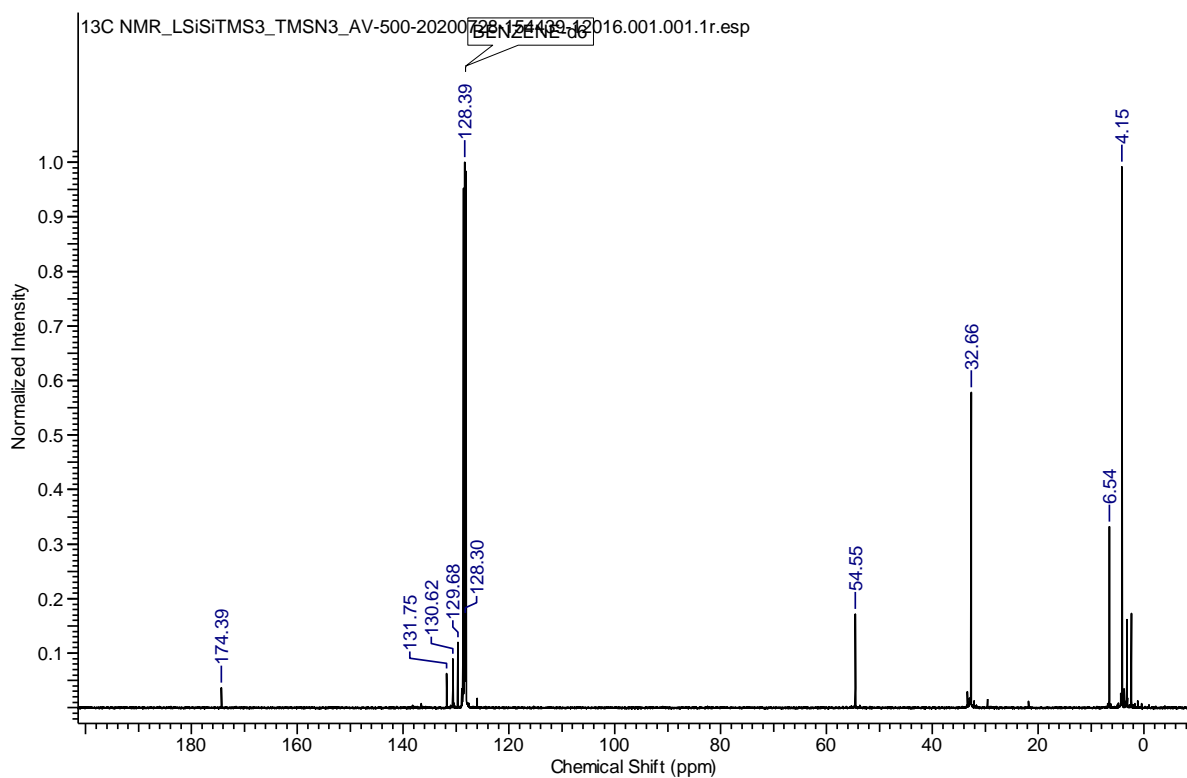
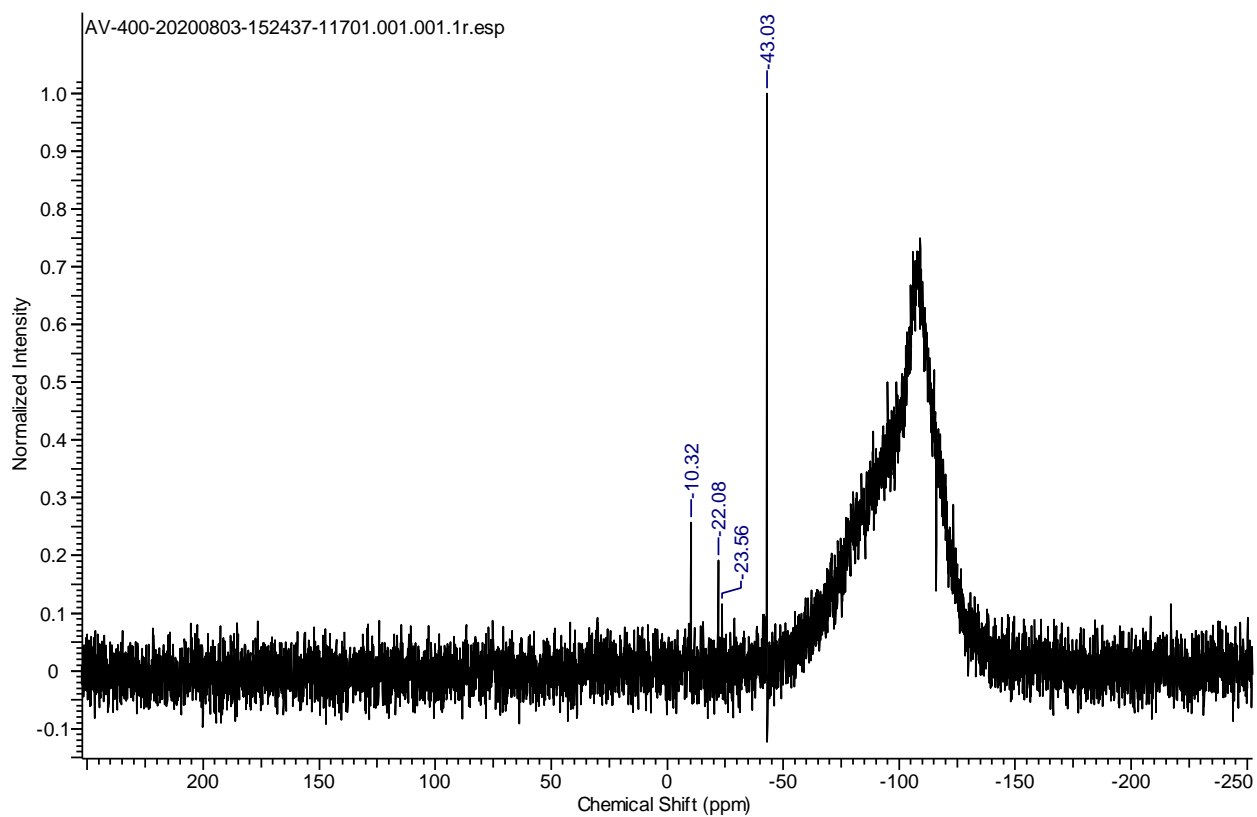
Figure S39. ¹¹B NMR of **2.11** (C₆D₆, 160.4 MHz, 298 K)Figure S40. ²⁹Si NMR of **2.11** (C₆D₆, 99.36 MHz, 298 K)

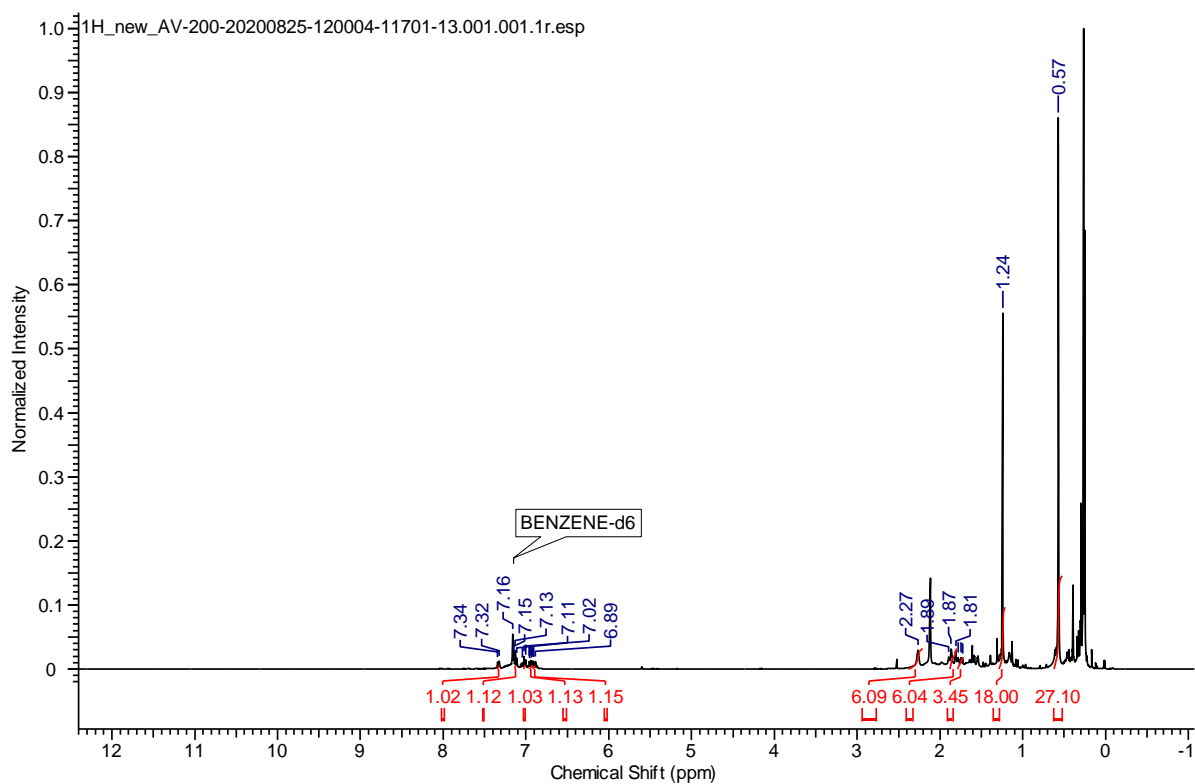
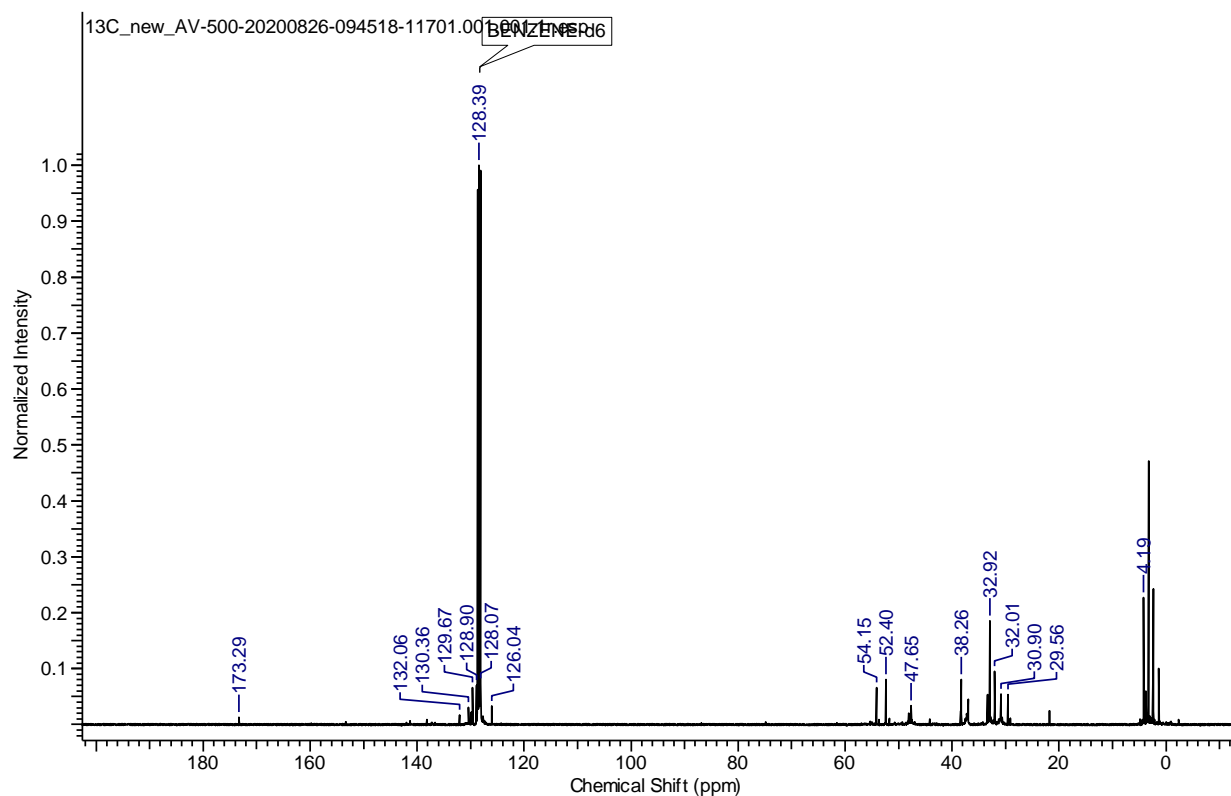
Figure S41. ^1H NMR Spectrum of **2.12** (C_6D_6 , 400 MHz, 298 K)Figure S42. ^1H NMR Spectrum of **2.13** (C_6D_6 , 400 MHz, 298 K)

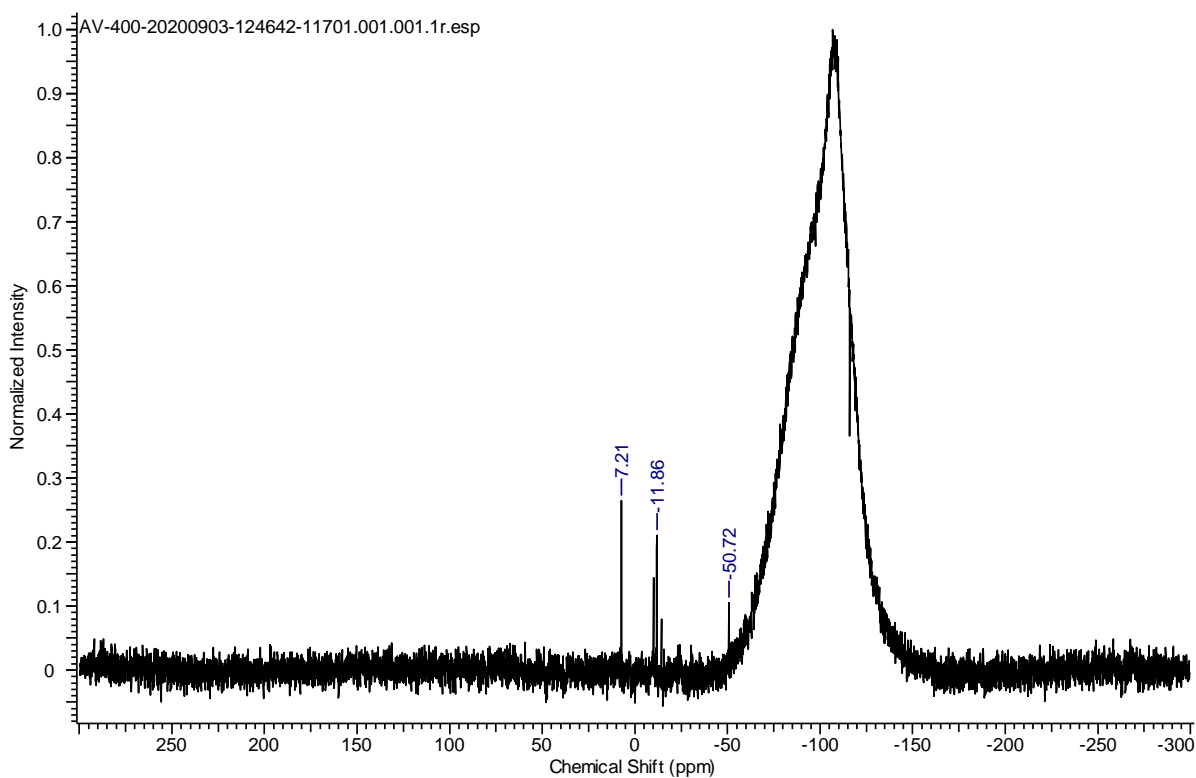
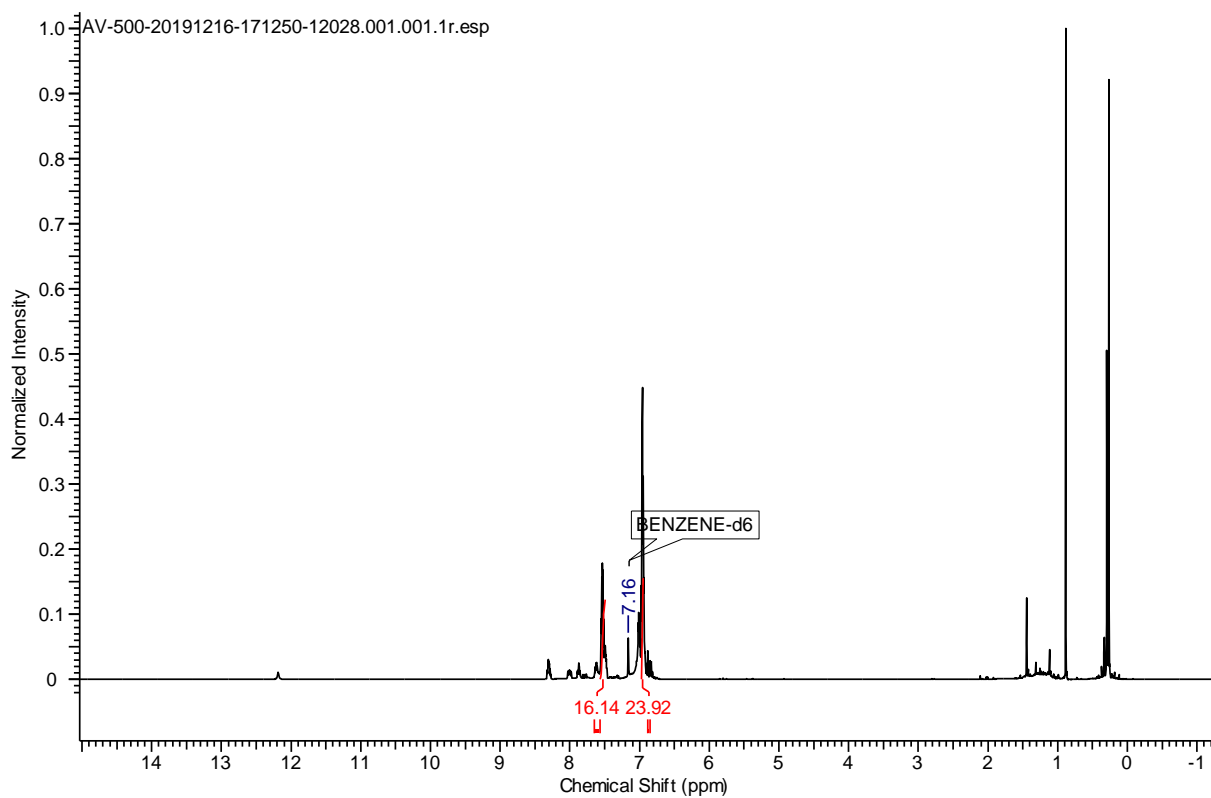
Figure S43. ^{11}B NMR Spectrum of **2.1** + **HBpin** (C_6D_6 , 128.4 MHz, 298 K)Figure S44. ^{29}Si NMR Spectrum of **2.1** + **HBpin** (C_6D_6 , 79.5 MHz, 298 K)

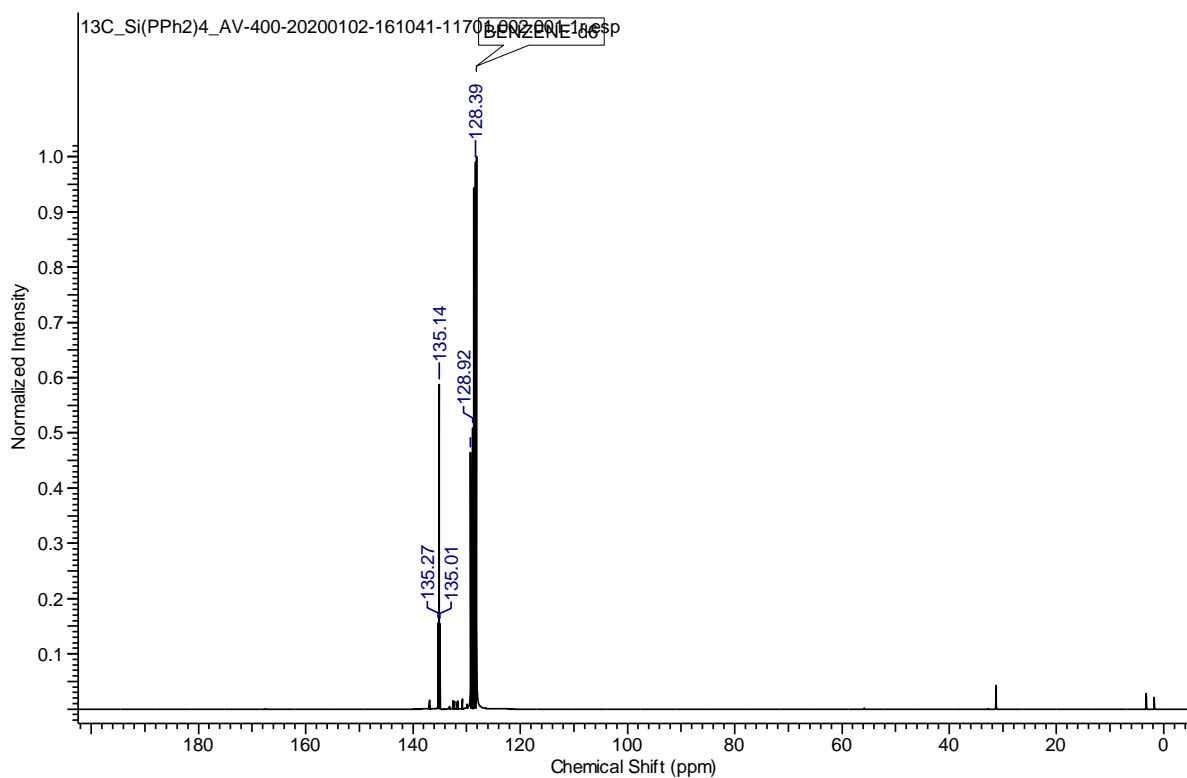
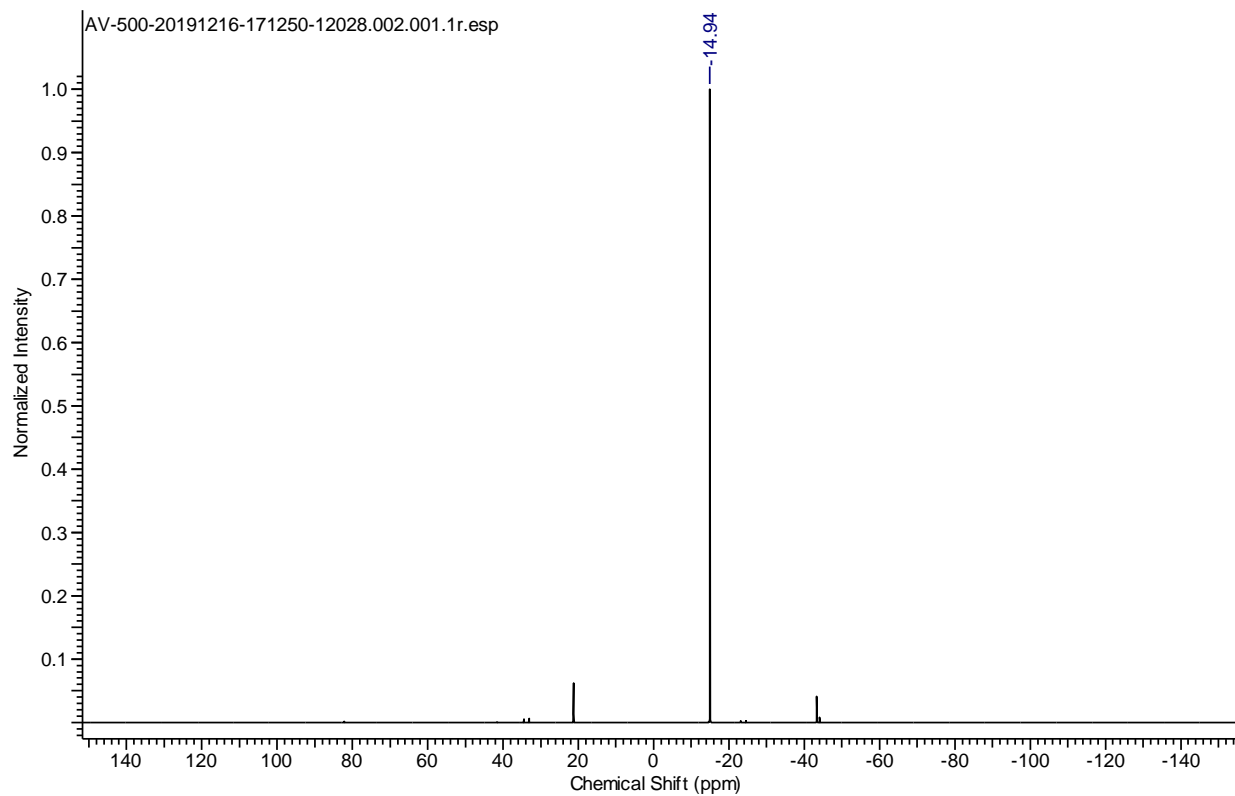
Figure S45. ¹H NMR Spectrum of **2.14** (CDCl₃, 200 MHz, 298 K)Figure S46. ¹³C NMR Spectrum of **2.14** (CDCl₃, 100.6 MHz, 298 K)

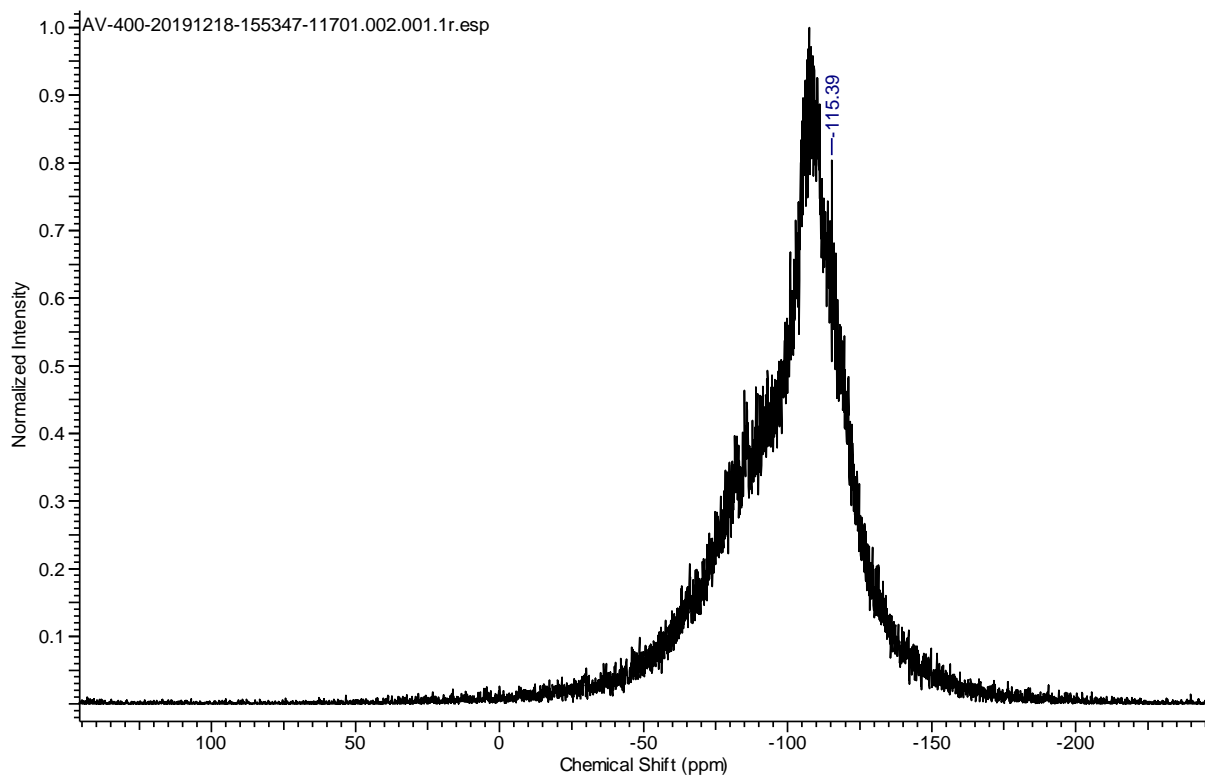
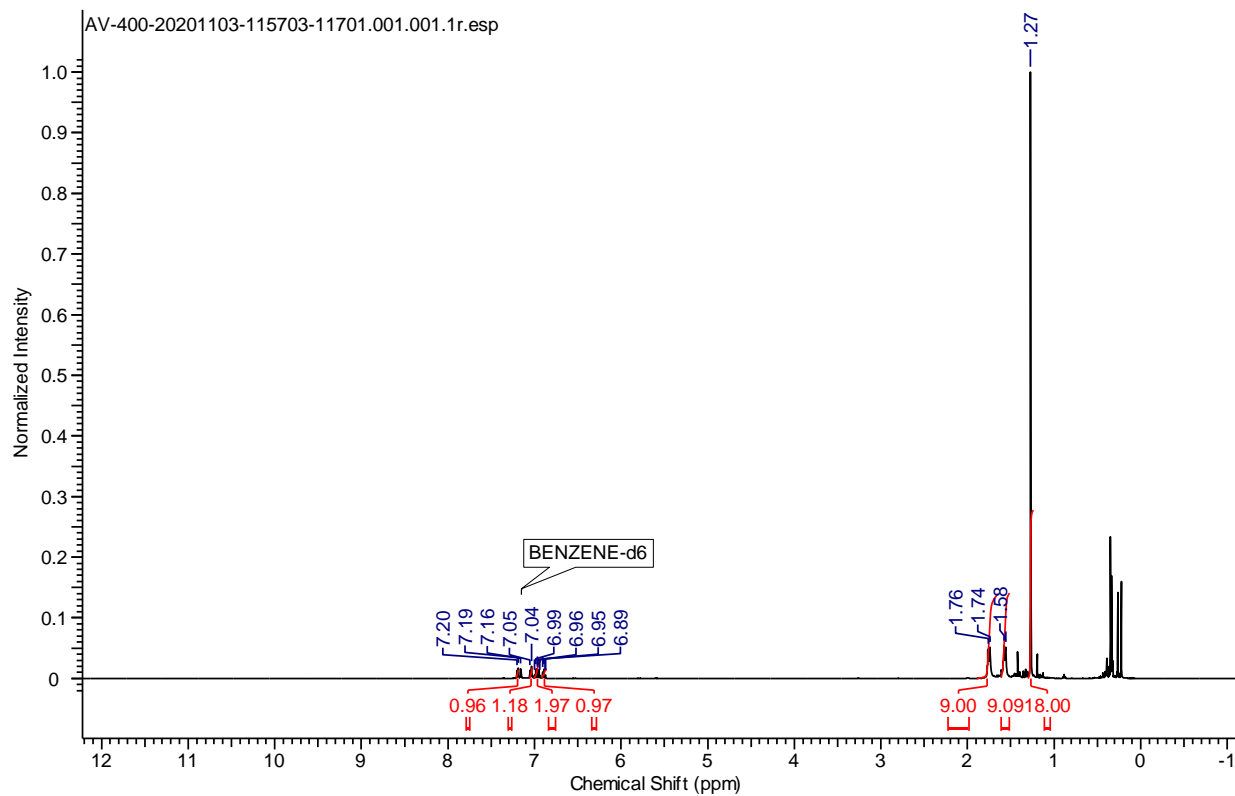
Figure S47. ¹¹B NMR Spectrum of **2.14** (CDCl₃, 160.4 MHz, 298 K)Figure S48. ¹H NMR Spectrum of **2.15** (C₆D₆, 200 MHz, 298 K)

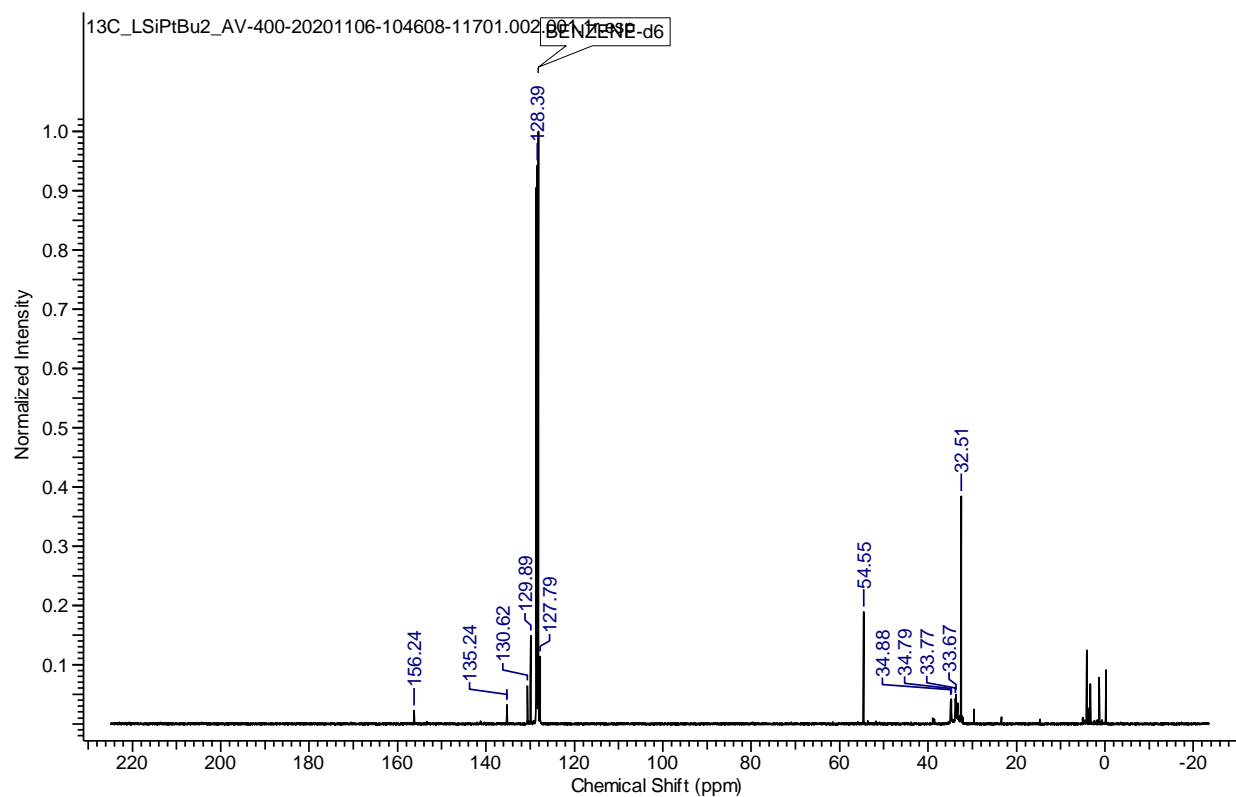
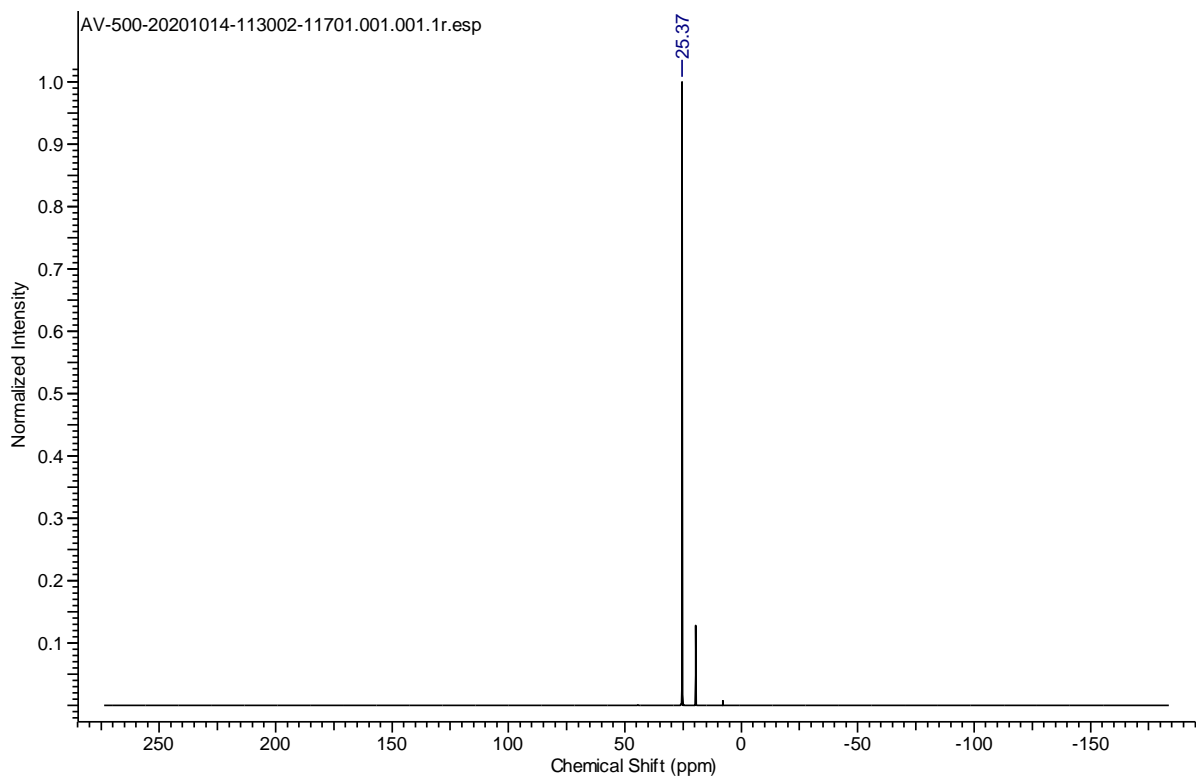
Figure S49. ¹³C NMR Spectrum of **2.15** (C₆D₆, 100.6 MHz, 298 K)Figure S50. ²⁹Si NMR Spectrum of **2.15** (C₆D₆, 99.3 MHz, 298 K).

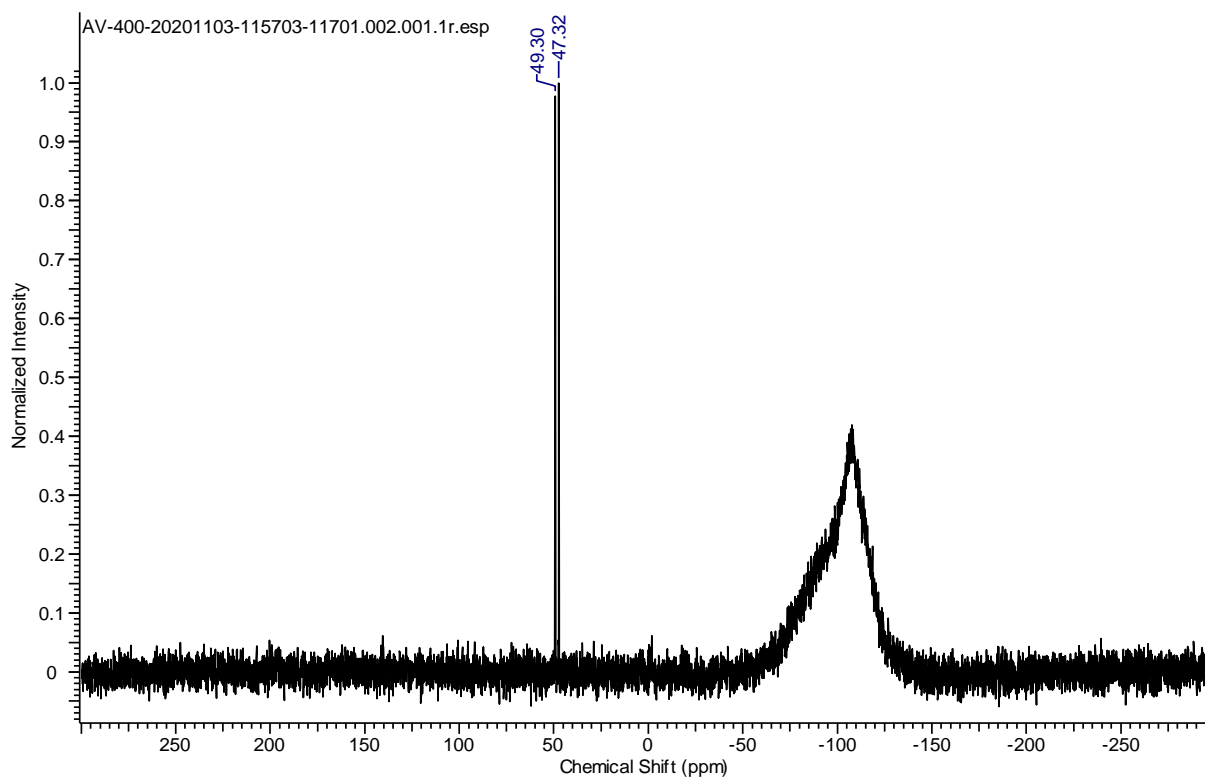
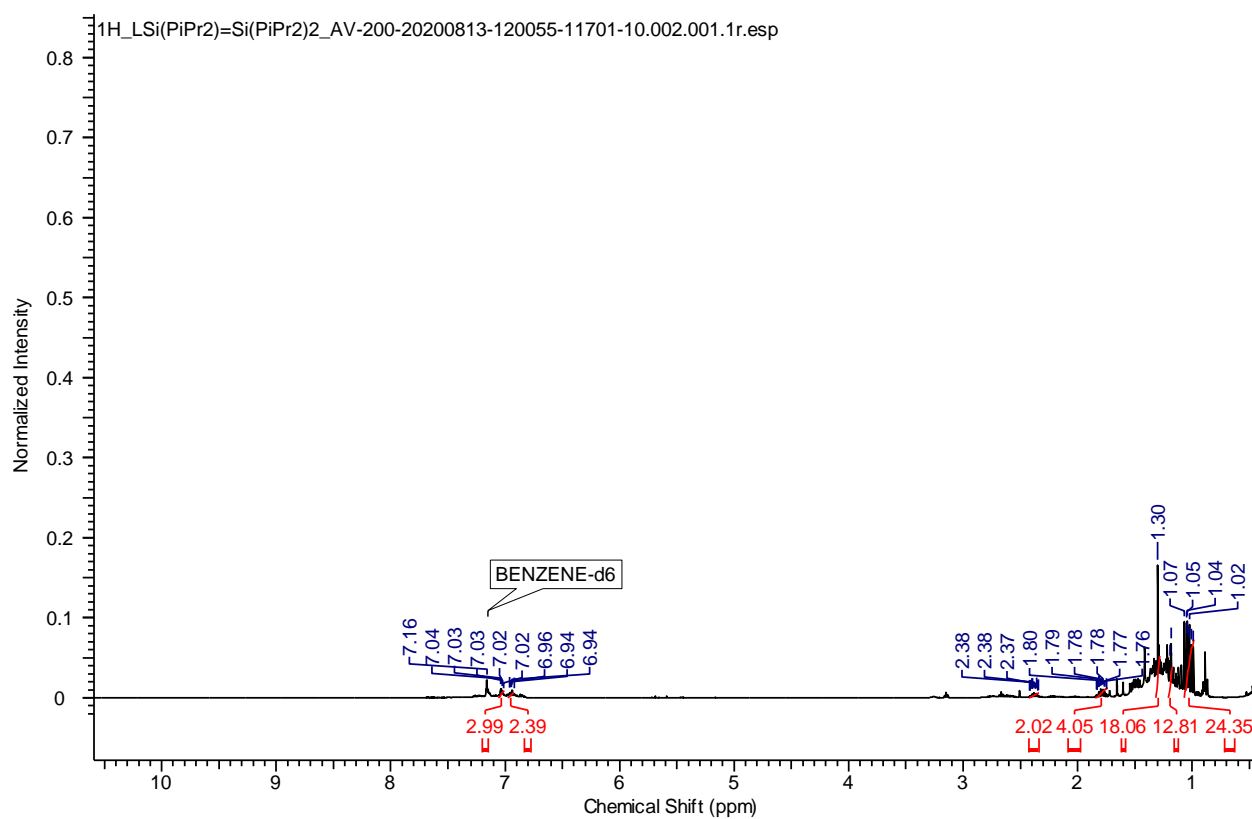
Figure S51. ¹H NMR Spectrum of **2.16** (C₆D₆, 200 MHz, 298 K)Figure S52. ¹³C NMR Spectrum of **2.16** (C₆D₆, 100.6 MHz, 298 K)

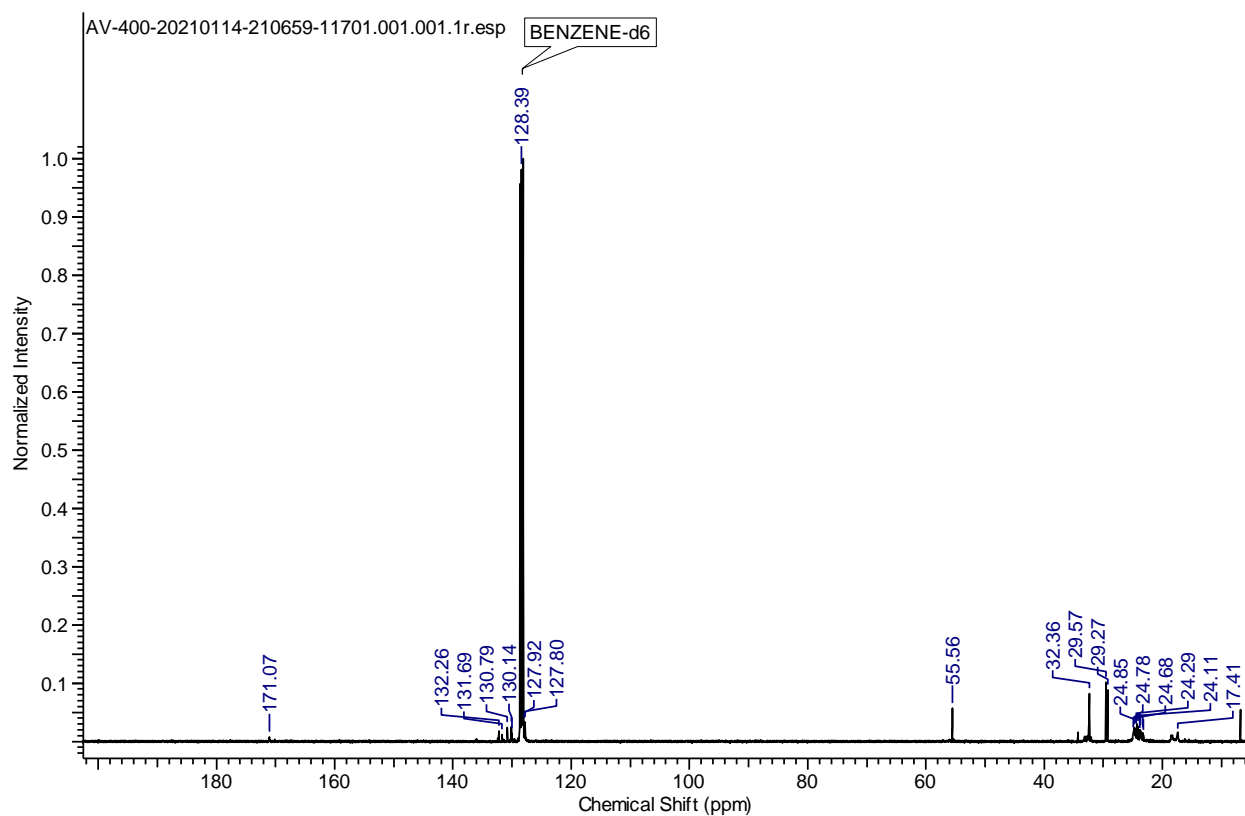
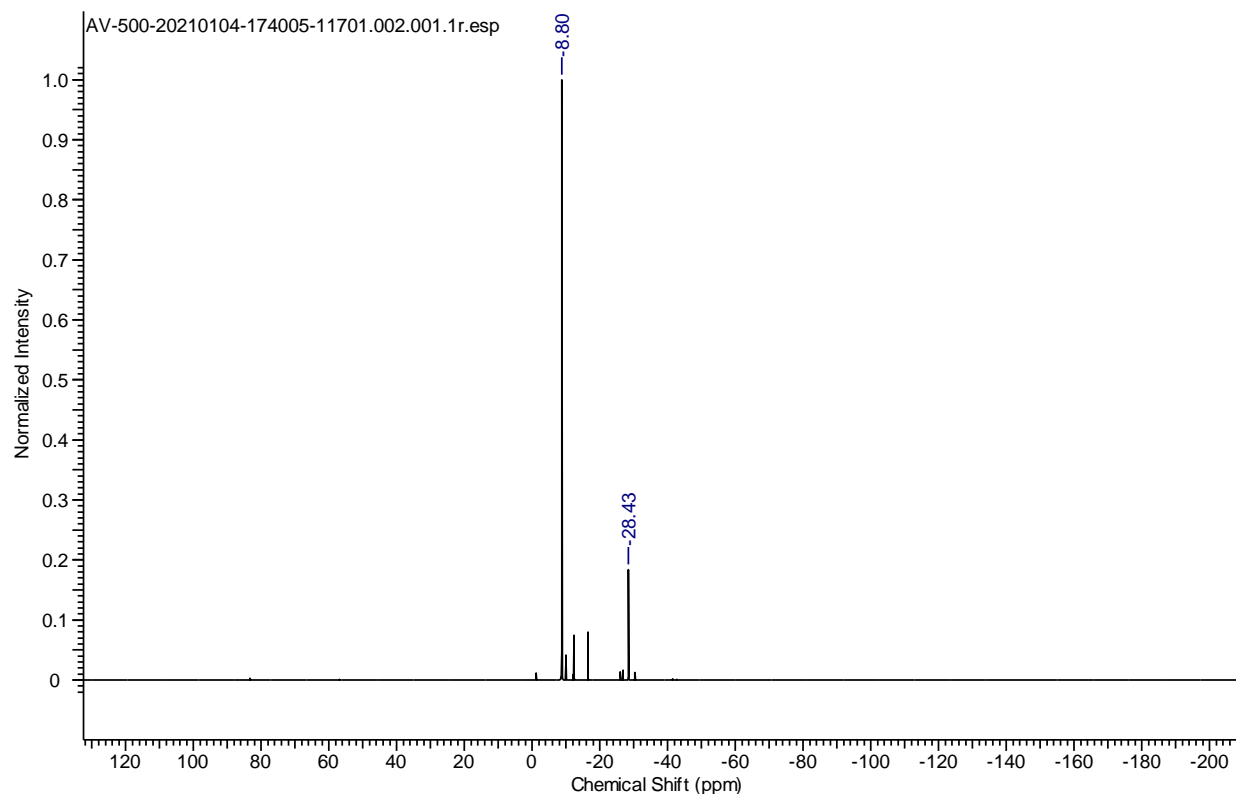
Figure S53. ²⁹Si NMR Spectrum of **2.16** (C₆D₆, 79.5 MHz, 298 K).Figure S54. ¹H NMR Spectrum of **2.17** (C₆D₆, 200 MHz, 298 K)

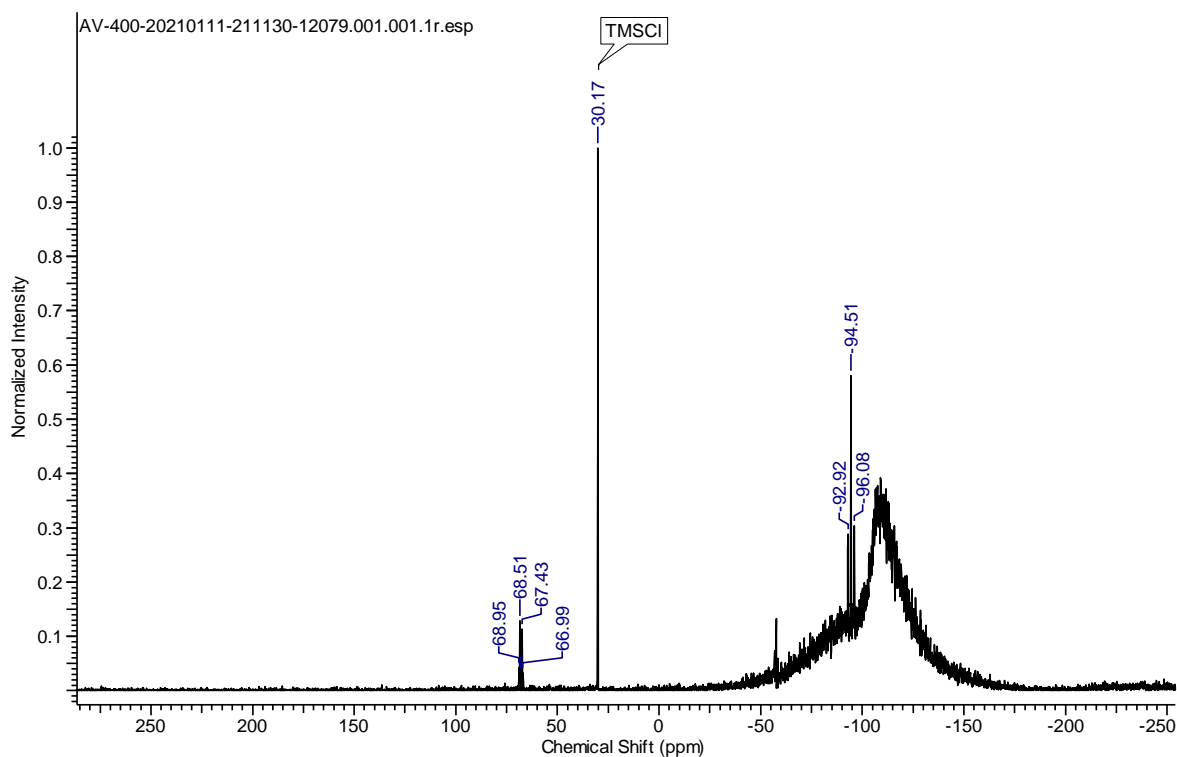
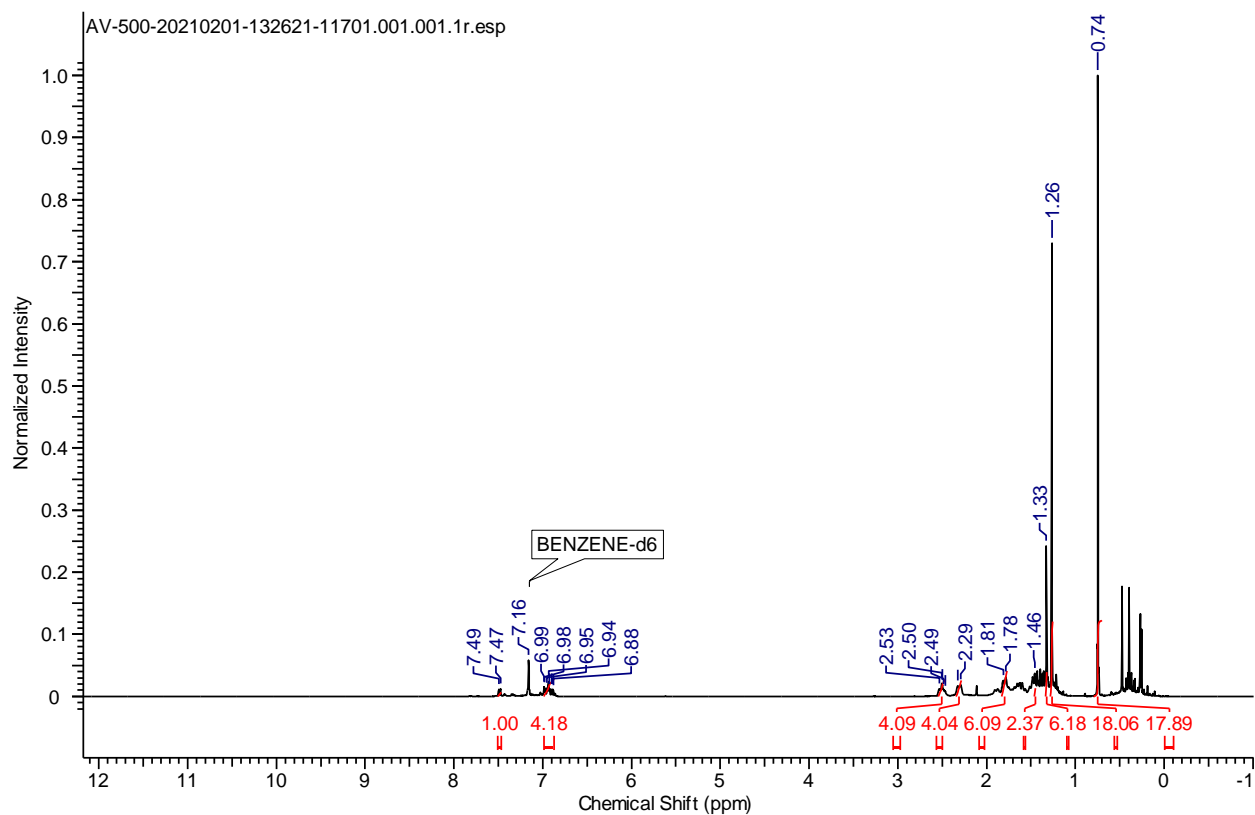
Figure S55. ¹³C NMR Spectrum of **2.17** (C₆D₆, 100.6 MHz, 298 K)Figure S56. ³¹P NMR Spectrum of **2.17** (C₆D₆, 161.9 MHz, 298 K)

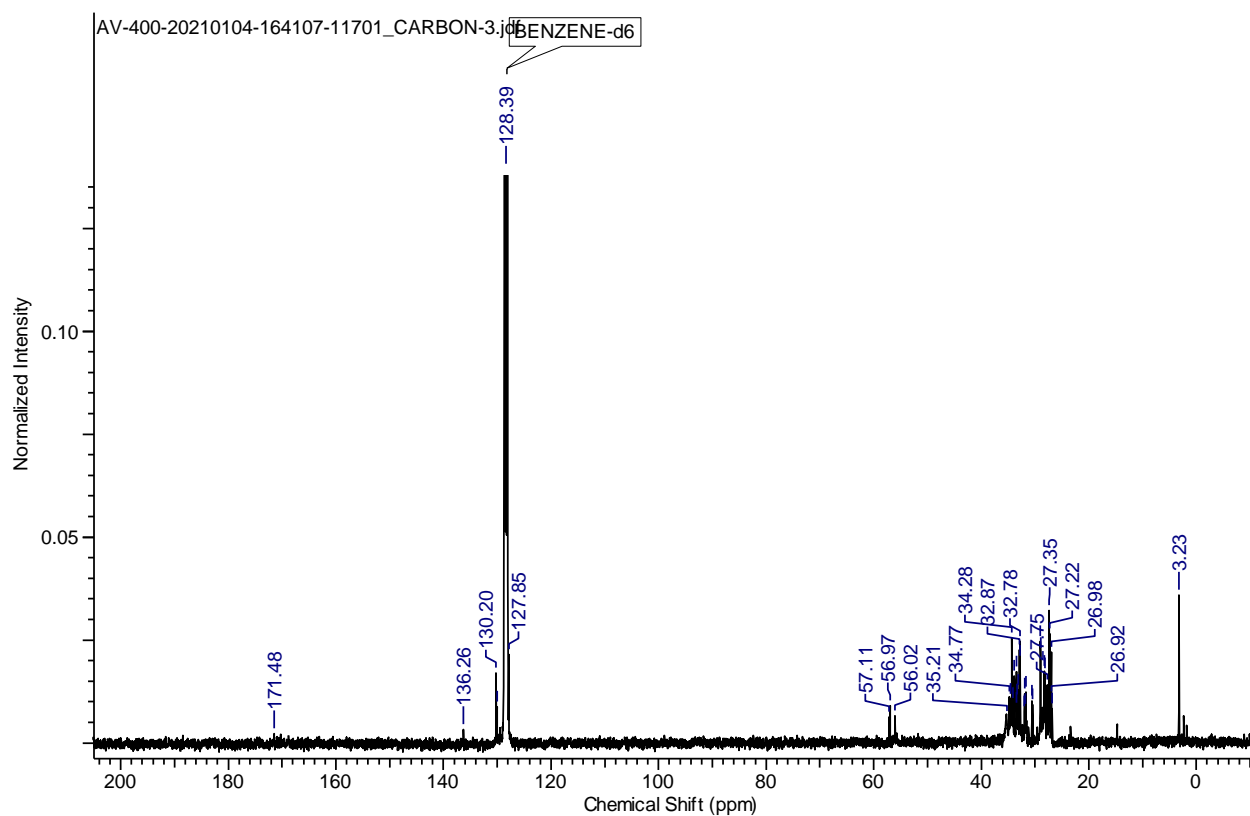
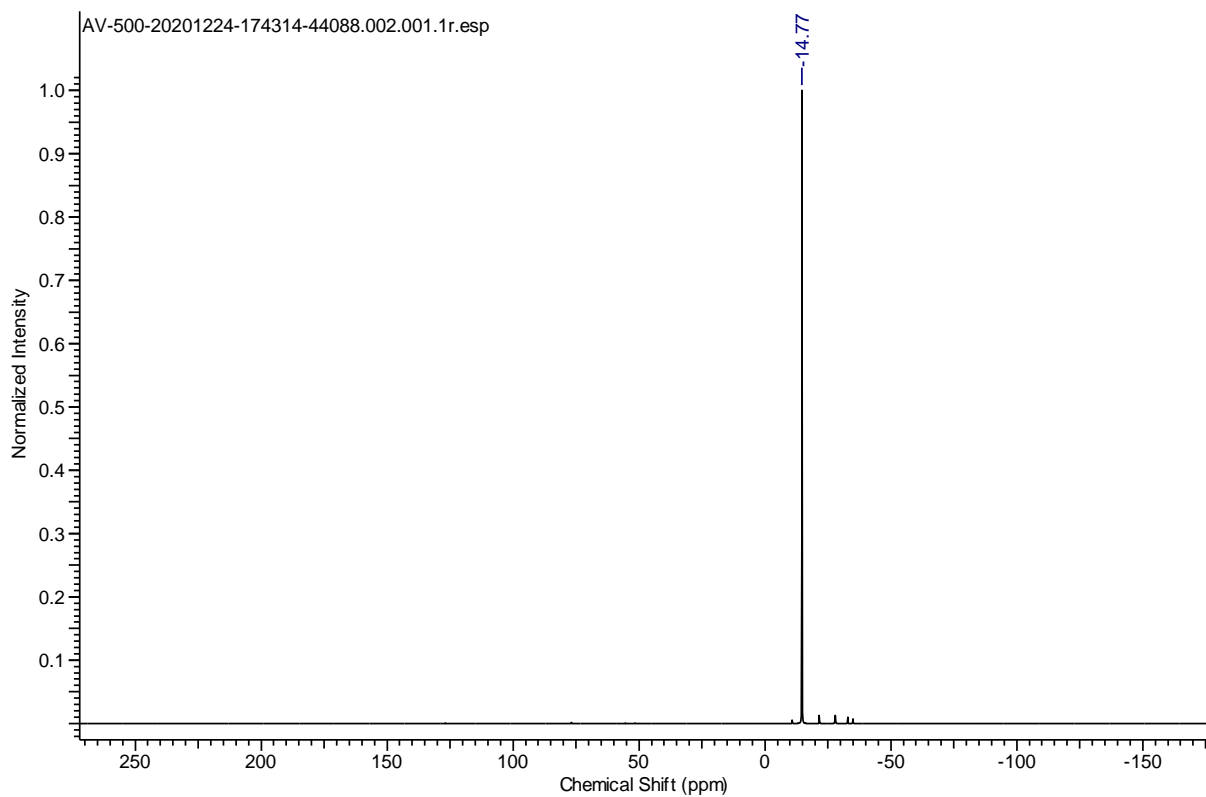
Figure S57. ²⁹Si NMR Spectrum of **2.17** (C₆D₆, 99.3 MHz, 298 K).Figure S58. ¹H NMR Spectrum of **2.18** (C₆D₆, 500 MHz, 298 K)

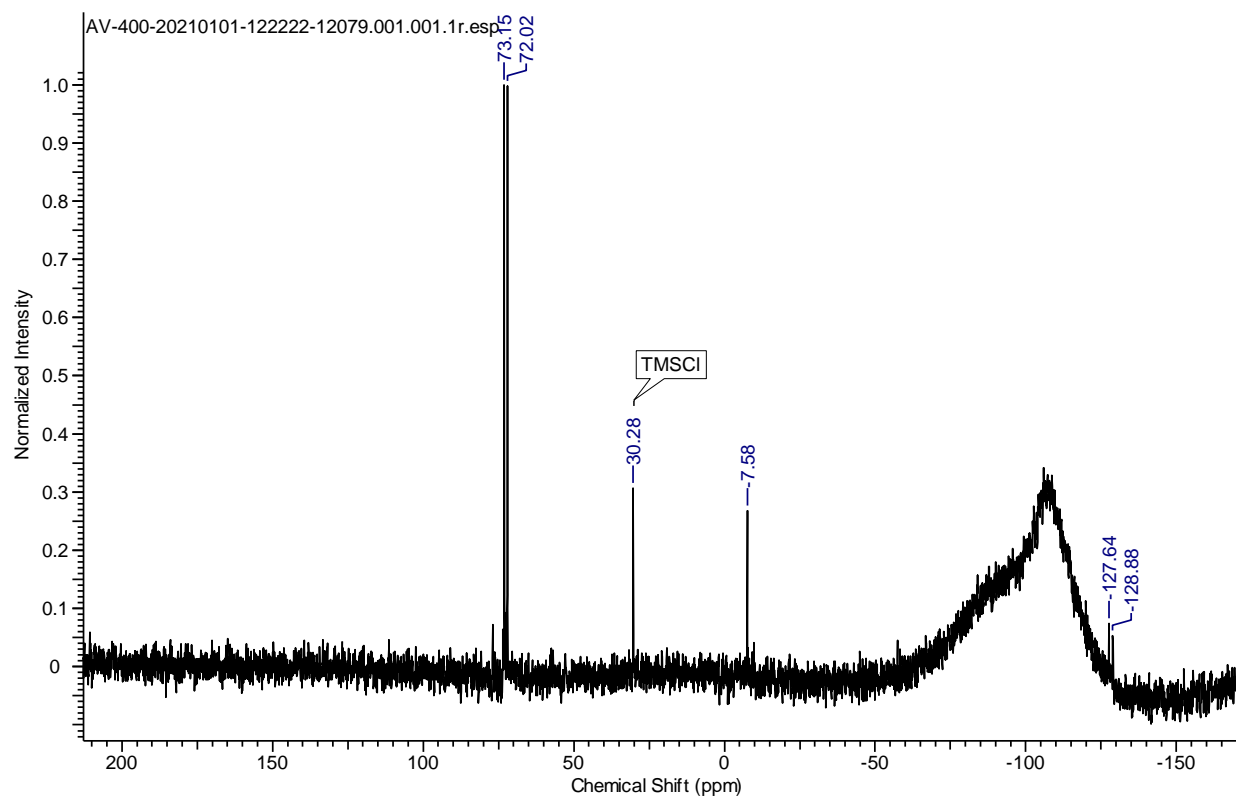
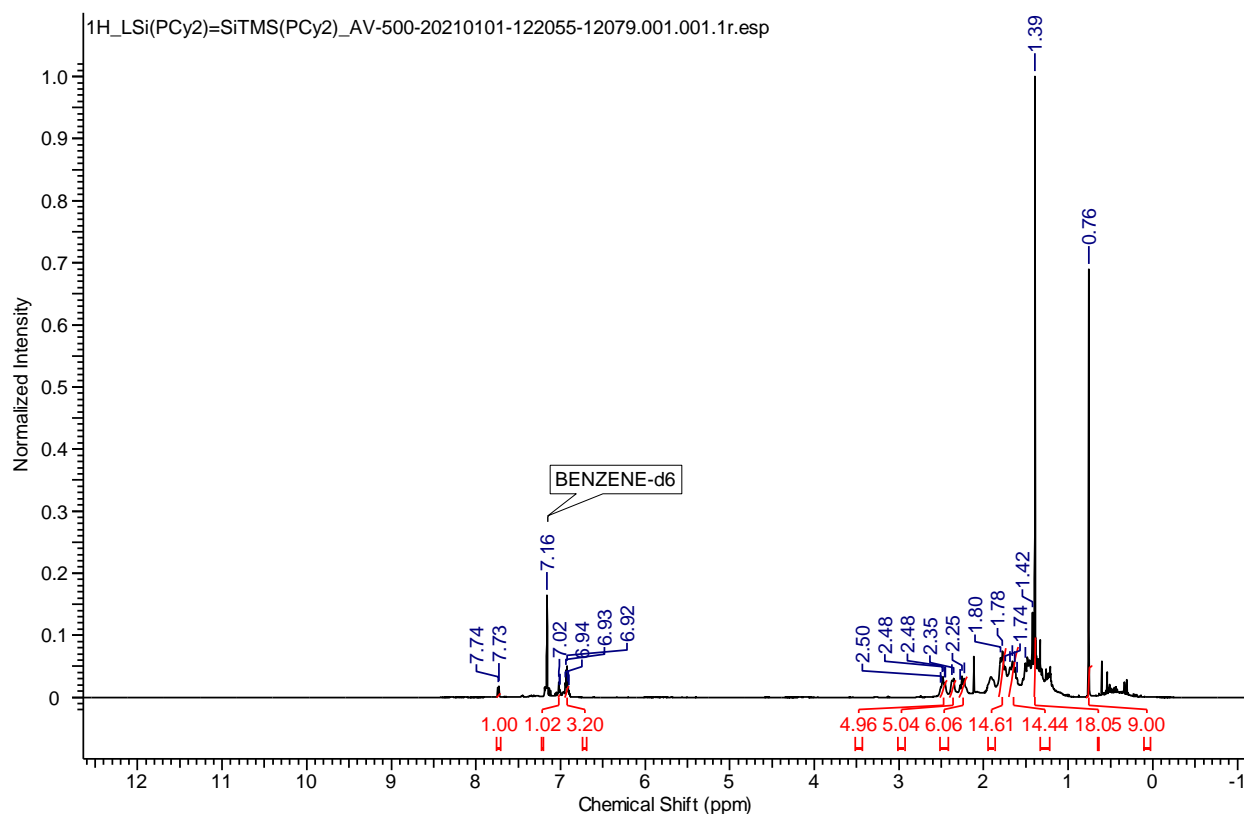
Figure S59. ¹³C NMR Spectrum of **2.18** (C₆D₆, 100.6 MHz, 298 K)Figure S60. ³¹P NMR Spectrum of **2.18** (C₆D₆, 202.4 MHz, 298 K)

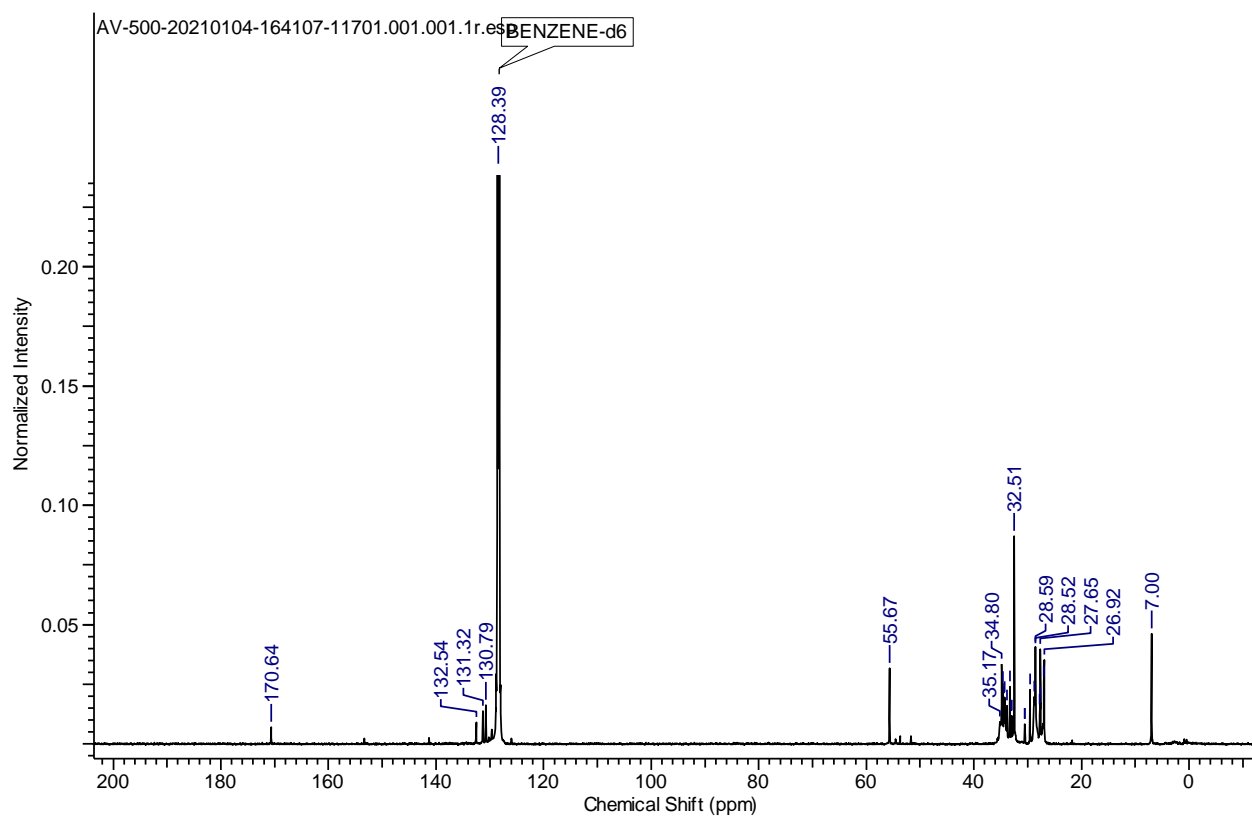
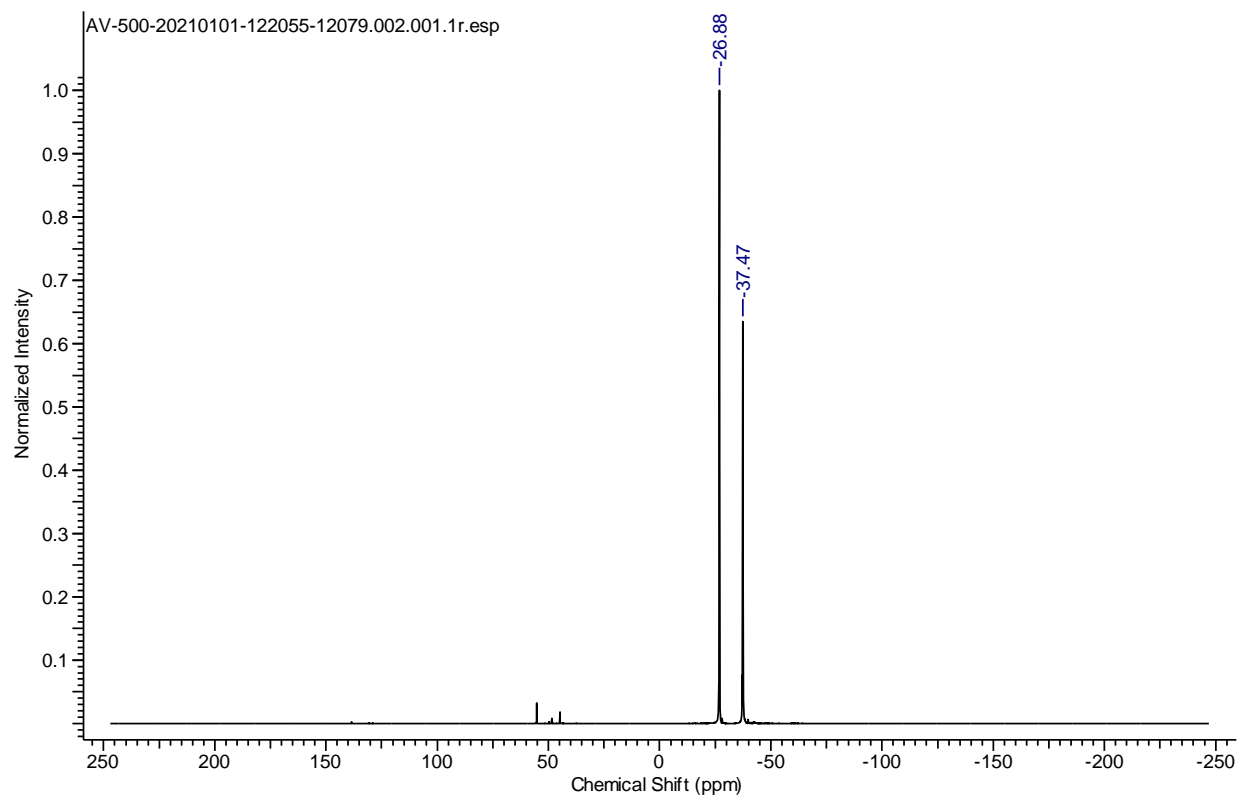
Figure S61. ²⁹Si NMR Spectrum of **2.18** (C₆D₆, 99.3 MHz, 298 K).Figure S62. ¹H NMR Spectrum of **2.19** (C₆D₆, 400 MHz, 298 K)

Figure S63. ¹³C NMR Spectrum of **2.19** (C₆D₆, 100.6 MHz, 298 K)Figure S64. ³¹P NMR Spectrum of **2.19** (C₆D₆, 202.4 MHz, 298 K)

Figure S65. ²⁹Si NMR Spectrum of **2.19** (C₆D₆, 99.3 MHz, 298 K)Figure S66. ¹H NMR Spectrum of **2.20** (C₆D₆, 500 MHz, 298 K)

Figure S67. ¹³C NMR Spectrum of **2.20** (C₆D₆, 100.6 MHz, 298 K)Figure S68. ³¹P NMR Spectrum of **2.20** (C₆D₆, 202.4 MHz, 298 K)

Figure S69. ²⁹Si NMR Spectrum of **2.20** (C₆D₆, 99.3 MHz, 298 K)Figure S70. ¹H NMR Spectrum of **2.21** (C₆D₆, 500 MHz, 298 K)

Figure S71. ¹³C NMR Spectrum of **2.21** (C₆D₆, 125.7 MHz, 298 K)Figure S72. ³¹P NMR Spectrum of **2.21** (C₆D₆, 202.4 MHz, 298 K)

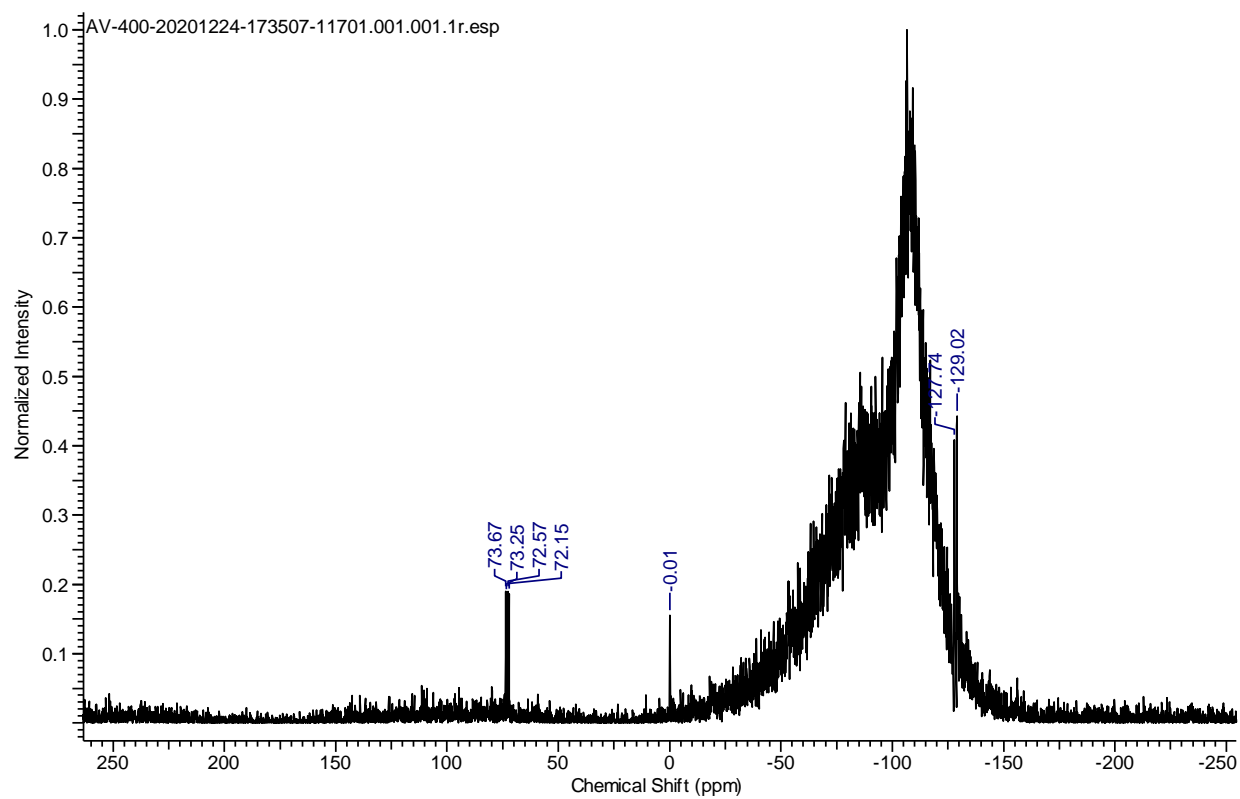


Figure S73. ^{29}Si NMR Spectrum of **2.21** (C_6D_6 , 99.3 MHz, 298 K)

ABSTRACT

Name of the Student: Milan Kumar Bisai

Registration No.: 10CC15A26020

Faculty of Study: Chemical Science

Year of Submission: 2020

AcSIR academic centre/CSIR Lab: CSIR-NCL **Name of the Supervisor:** Dr. Sakya S. Sen

Title of the thesis: Synthesis and Reactivity of Hypersilylsilylene and Catalytic Applications of Organosilicon and Lithium Compounds

The escalating need for environmentally benign and sustainability in chemical processes has led the compounds with main group elements as viable alternatives to sparse, expensive, and toxic transition metal catalysts. This thesis presents the synthesis and reactivity of a hypersilylsilylene and catalytic applications of organosilicon and easily accessible lithium compounds. The first chapter of the thesis describes the development of the chemistry of silylene and application of the compounds with main group elements in small molecule activation and catalysis with recent literature precedence. The second chapter describes the synthetic protocol of hypersilylsilylene and its applications for various small molecules activation, including boranes, organic azides, and chlorophosphines. In this chapter, hypersilylsilylene was shown as a new synthon to synthesize different unusual silicon compounds. In the third chapter, a neutral penta-coordinated Si(IV) compound has been utilized for the catalytic hydroboration of aldehydes and aldimines. We also discussed the practical applicability of simple and easily accessible lithium compounds for the catalytic hydroboration and cyanosilylation of aldehydes and ketones under ambient conditions; and this is depicted in the fourth chapter of the thesis. Besides, the catalytic activity was extended further for the other less activated and more important unsaturated compounds such as esters, amides, and carbodiimides. On the other hand, the fifth chapter explores the effectiveness of the same lithium compounds for the selective anti-Markovnikov hydroboration of alkenes and alkynes. The methodology was extended further to the reduction of biologically important terpenes.

List of publication(s) in SCI Journal(s) (published & accepted) emanating from the thesis work, with complete bibliographic details

1. **Bisai, M. K.**; Pahar, S.; Das, T.; Vanka, K.; Sen, S. S. Transition metal free catalytic hydroboration of aldehydes and aldimines by amidinato silane. *Dalton Trans.* **2017**, *46*, 2420–2424.
2. Bisai, M. K.; Das, T.; Vanka, K.; Sen, S. S. Easily accessible lithium compound catalyzed mild and facile hydroboration and cyanosilylation of aldehydes and ketones. *Chem. Commun.* **2018**, *54*, 6843–6846.
3. **Bisai, M. K.**; Swamy, V. S. V. S. N.; Das, T.; Vanka, K.; Gonnade, R. G.; Sen, S. S. Synthesis and Reactivity of a Hypersilylsilylene. *Inorganic Chemistry* **2019**, *58*, 10536–10542.
4. **Bisai, M. K.**; Yadav, S.; Das, T.; Vanka, K.; Sen, S. S. Lithium compounds as single site catalyst for hydroboration of alkenes and alkynes *Chem. Commun.* **2019**, *55*, 11711–11714.
5. **Bisai, M. K.**; Swamy, V. S. V. S. N.; Raj, K. V.; Vanka, K.; Sen, S. S. Diverse Reactivity of Hypersilylsilylene with Boranes and Three-Component Reactions with Aldehyde and HBpin *Inorganic Chemistry* **2021**, *60*, 1654–1663.
6. **Bisai, M. K.**; Gour, K.; Das, T.; Vanka, K.; Sen, S. S. Lithium compound catalyzed deoxygenative hydroboration of primary, secondary and tertiary amides. *Dalton Trans.* **2021**, *50*, 2354–2358.

Other publications:

1. Swamy, V. S. V. S. N.; **Bisai, M. K.**; Das, T.; Sen, S. S. Metal free mild and selective aldehyde cyanosilylation by a neutral penta-coordinate silicon compound. *Chem. Commun.* **2017**, *53*, 6910–6913.
2. Yadav, S.; Dixit, R.; **Bisai, M. K.**; Vanka, K.; Sen, S. S. Alkaline Earth Metal Compounds of Methylpyridinato β -Diketiminato Ligands and Their Catalytic Application in Hydroboration of Aldehydes and Ketones. *Organometallics* **2018**, *37*, 4576–4584.
3. Kundu, G.; Ajithkumar, V. S.; **Bisai, M. K.**; Tothadi, S.; Das, T.; Vanka, K.; Sen, S. S. Diverse reactivity of carbenes and silylenes towards fluoropyridines. *Chem. Commun.* **2021**, DOI:10.1039/D1CC01401C.

4. Dixit, R.; **Bisai, M. K.**; Yadav, S.; Yadav, V.; Sen, S. S.; Vanka, K. Substrate, Catalyst and Solvent: The Triune Nature of Multitasking Reagents in Hydroboration and Cyanosilylation. *Organometallics* **2021**, *Just Accepted*.
5. **Bisai, M. K.**; Das, T.; Vanka, K.; Gonnade, R. G.; Sen, S. S. Convenient Access to Unsymmetrically Substituted Disilenes from a Hypersilylsilylene. *Manuscript Communicated*.
6. **Bisai, M. K.**; Gour, K.; Das, T.; Vanka, K.; Sen, S. S. Hydroboration of Esters and Carbodiimides Using Simple Lithium Compounds. *Manuscript Communicated*.
7. **Bisai, M. K.**; Sharma, V.; Gonnade, R. G.; Sen, S. S. Synthesis and Reactivity of silaimines: Access to a Silylium Cation. *Manuscript Communicated*.

List of papers with abstract presented (oral/poster) at national/international conferences/seminars with complete details

1. Presented a virtual poster on “*Synthesis and Reactivity of a Hypersilylsilylene*” in international conference ‘*Global Inorganic Discussion Weekdays (GIDW)- online twitter poster event - July 9 & 10, 2020*’ and awarded Canadian Society of Chemistry- Inorganic Division Poster Award.
2. Presented poster on “*Easily Accessible Lithium Compounds for Catalytic Hydroboration: An Economical and Sustainable Catalysis*” in international conference ‘*Recent Trends in Catalysis RTC2020*’ at NIT Calicut, India, February 2020 and awarded a Catalysis Science & Technology poster prize from RSC.
3. Presented a virtual poster on “*Hypersilylsilylene: A new synthon for unusual silicon compounds*” in international conference ‘*#LatinXChem Twitter Conference 2020*’ on Sept 7th 2020.
4. Presented a contributed talk on “*Main Group Compounds for Catalytic Hydroboration and Cyanosilylation: An Economical and Sustainable Catalysis*” in ‘*NCL-RF Annual Students Conference- 2018*’ held at CSIR- National Chemical Laboratory, Pune, India and awarded for best oral presentation.
5. Presented poster on “*Catalytic Hydroboration by Main Group Elements: Cheap Elements for Noble Tasks*” in international conference ‘*Modern Trend in Inorganic Chemistry (MTIC- XVII)*’ Pune, India, December 2017.
6. Presented poster on “*Transition Metal Free Catalytic Hydroboration of Aldehydes and Aldimines by Amidinato Silane*”, during ‘*National Science Day Celebrations*’ at National Chemical Laboratory, Pune, India, February 2017.



Cite this: *Dalton Trans.*, 2017, **46**, 2420

Received 28th December 2016,
Accepted 26th January 2017

DOI: 10.1039/c6dt04893e

rsc.li/dalton

Transition metal free catalytic hydroboration of aldehydes and aldimines by amidinato silane†‡

Milan Kumar Bisai,^a Sanjukta Pahar,^a Tamal Das,^b Kumar Vanka^{*b} and Sakya S. Sen^{*a}

The transition metal free catalytic hydroboration of aldehydes and ketones is very limited and has not been reported with a well-defined silicon(IV) compound. Therefore, we chose to evaluate the previously reported silicon(IV) hydride [PhC(NtBu)₂SiHCl₂], (1) as a single component catalyst and found that it catalyzes the reductive hydroboration of a range of aldehydes with pinacolborane (HBpin) under ambient conditions. In addition, compound 1 can catalyze imine hydroboration. DFT calculation was carried out to understand the mechanism.

The addition of a B–H bond to the C=C, C=O, and C=N bonds requires a catalyst. Group 4 metallocenes¹ and precious metal compounds, particularly organometallic rhodium and iridium complexes² are the most studied catalysts for hydroboration reactions. Due to environmental concerns, limited terrestrial abundance, and the high cost of traditional transition metal catalysts, there is a recent surge in the exploration of compounds with main group elements as feasible alternatives to transition metal catalysts.^{3–6} Encouragingly, a number of research groups such as those of Hill, Roesky, Wesemann, Nembenna, Jones, Zhao, Kinjo, and others^{7–13} have started to use compounds with s- and p-block elements as single site catalysts for the catalytic hydroboration of aldehydes and ketones (Chart 1). However, when we look at the full gamut of single site neutral compounds reported for transition metal free hydroboration of aldehydes and ketones, there is one element missing that one might have expected to be there: silicon.

Being isosteres of carbon and owing to their larger covalent radius, electropositive nature, low toxicity and relative abundance, silicon compounds are highly sought after as single

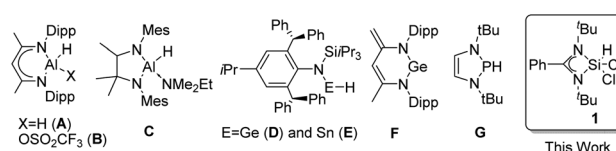


Chart 1 Single component compounds with heavier p-block elements that catalyze hydroboration of aldehydes (A–G); this work reports the first use of a neutral silicon(IV) compound (1) for aldehyde hydroboration.

component catalysts because a catalytic cycle based on silicon could be sustainable, economical and green. Silylium ion promoted catalytic imine reduction and Diels–Alder reactions,^{14a, b, g} and bis(perfluorocatecholato)silane [Si(cat^F)₂] catalyzed aldehyde hydrosilylation^{14c} have been lately reported, illustrating the potential of silicon compounds as catalysts. Besides, there are recent theoretical and experimental reports on formylation of amines using a combination of CO₂ and a silane as the formylating reagent.^{14d, e} Cantat *et al.* very recently reported the hydroboration of CO₂ using a well-defined guanidine substituted hydrosilane.^{14f} Boosted by the success of alanes (A–C) and phosphane (G), we were interested in exploring the catalytic potential of previously reported benz-amidinato dichlorosilane [PhC(NtBu)₂SiHCl₂], (1),^{15a} for hydroboration reaction. Our results are reported herein (Chart 1).

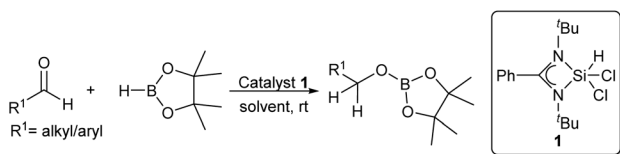
Compound 1 was previously reported by Roesky *et al.* as a precursor for silicon(II) chloride^{15a} and silicon(II) bis(trimethylsilyl)amide.^{15b} Compound 1 was chosen as a catalyst for hydroboration reaction because it can be synthesized in a single step with high yield.^{15a} Direct addition of HBpin to benzaldehyde in the absence of the catalyst only afforded a trace amount of PhCH₂OBpin; an observation also noted by others.^{7a, 8a, 11, 12} However, when the reaction was carried out in the presence of 1 mol% of 1, it led to quantitative conversion to PhCH₂OBpin at room temperature in an hour (Scheme 1). When the catalyst loading was reduced to 0.5 mol%, the conversion was still achieved albeit with a slightly lower yield (77%) (see ESI Table S1†). Therefore, each reaction was conducted at room

^aInorganic Chemistry and Catalysis Division, CSIR-National Chemical Laboratory, Dr. Homi Bhabha Road, Pashan, Pune 411008, India. E-mail: ss.sen@ncl.res.in

^bPhysical and Material Chemistry Division, CSIR-National Chemical Laboratory, Dr. Homi Bhabha Road, Pashan, Pune 411008, India. E-mail: k.vanka@ncl.res.in

†This paper is dedicated to Professor Didier Astruc on the occasion of his 70th birthday.

‡Electronic supplementary information (ESI) available: Experimental details, characterization data and details of computational methodology. See DOI: 10.1039/c6dt04893e

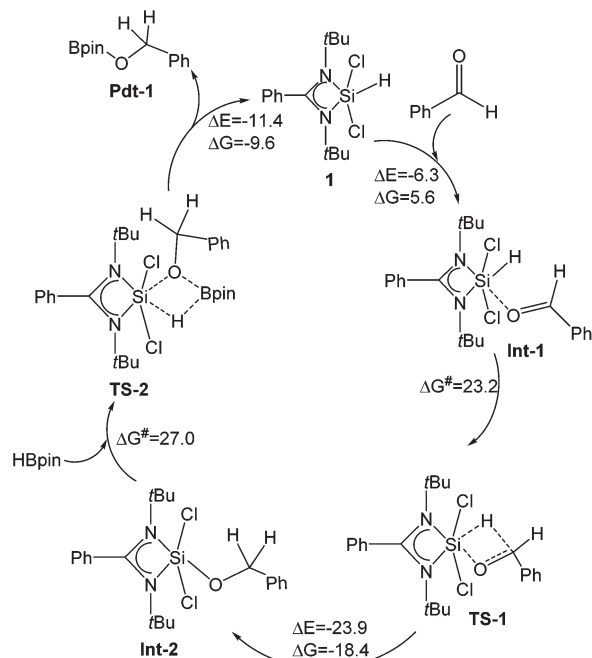


Scheme 1 Silicon(IV) hydride (**1**) catalyzed hydroboration of aldehydes.

temperature with 1 mol% of catalyst in an equimolar mixture of aldehyde and HBpin. We have also performed the reaction in the presence of only 1 mol% of HSiCl_3 as a catalyst, but only a trace amount of product formation was observed. We have explored the reactions in various solvents such as benzene, toluene, and dichloroethane and observed that the identity of the solvent had little effect on the yields. The products were identified by a combination of GC-MS, ^1H and ^{13}C NMR spectroscopies.

In order to understand the possible mechanistic pathway, simple NMR experiments were performed. As silicon is in the +4 oxidation state, it is expected that the catalysis will occur *via* σ -bond metathesis, which has a modicum of precedence for non-metal p-block elements.¹⁶ When a 1:1 mixture of **1** and benzaldehyde in CDCl_3 was monitored by ^1H NMR, the development of a new singlet at δ 5.05 ppm was observed with a concomitant disappearance of the aldehyde proton (δ 9.95 ppm) as well as the Si-H proton (δ 6.26 ppm).^{15a} The ^{13}C NMR spectrum was (in CDCl_3) also changed, with a new peak appearing at δ 66.00 ppm for a $[-\text{OCH}_2-]$ substituent, which was further confirmed by DEPT experiments. The ^{29}Si NMR spectrum showed a new resonance at δ -101.2 ppm, which is slightly upfield shifted compared with that in **1** (δ -96.6 ppm) but in good agreement with the previously reported penta-coordinate silicon compounds bearing a Si-O bond such as $[\text{PhC}(\text{N}t\text{Bu})_2\text{SiCl}_2\text{OR}]$, ($\text{R} = i\text{Pr}$ and $t\text{Bu}$).^{15c} Taken together, these data suggest the possible formation of an alkoxy compound $[\text{PhC}(\text{N}t\text{Bu})_2\text{SiCl}_2\text{OCH}_2\text{Ph}]$ (**Int-2**) as an intermediate. However, even after repeated attempts, we could not obtain single crystals of **Int-2**. In order to prove the formation of **Int-2** during the catalytic cycle, we performed a metathetical reaction between $[\text{PhC}(\text{N}t\text{Bu})_2\text{SiCl}_3]$ ¹⁷ and potassium phenylmethanolate, which also led to **Int-2**. Comparison of spectra obtained from two different reactions unequivocally confirms that **Int-2** was being formed during the catalytic cycle. The formation of a strong Si-O bond can be presumed as the driving force for the metathesis reaction.¹⁸

Full quantum mechanical calculations were done with density functional theory (DFT) at the dispersion and solvent corrected PBE/TZVP level of theory in order to understand the mechanism (Fig. S1† and Scheme 2) of the aldehyde hydroboration reaction in the presence of catalyst **1** [for further details, please see the ESI†]. In the first step of the reaction, a loosely bound complex (**Int-1**) is formed between catalyst **1** and benzaldehyde, with the benzaldehyde approaching the catalyst from the direction opposite the Si-N bond. The reaction energy (ΔE) and the Gibbs free energy (ΔG) for this step



Scheme 2 The catalytic cycle and reaction mechanism for the benzaldehyde hydroboration by catalyst **1**, calculated at the PBE/TZVP level of theory with DFT. ΔG and ΔG^\ddagger represent the Gibbs free energy of reaction and the Gibbs free energy of activation respectively. All values are in kcal mol^{-1} .

are $-6.3 \text{ kcal mol}^{-1}$ and $5.6 \text{ kcal mol}^{-1}$, respectively. This is the prelude to the nucleophilic attack by the carbonyl oxygen of benzaldehyde on the silicon centre of the catalyst, with the hydride being transferred from the silicon centre to the electrophilic carbonyl carbon of the benzaldehyde. This occurs through a four-membered transition state (**TS-1**) and leads to the formation of **Int-2** (see Scheme 2). The ΔE ($-23.9 \text{ kcal mol}^{-1}$) and ΔG ($-18.4 \text{ kcal mol}^{-1}$) values for this step are highly negative and the activation energy (ΔG^\ddagger) barrier corresponding to the transition state is $28.8 \text{ kcal mol}^{-1}$, which is moderate and explains why the reaction can take place at room temperature. This is also the slowest step of the overall hydroboration reaction. The silicon centre of catalyst **1** therefore acts as the hydride donor to the electrophilic carbonyl carbon centre.

In the next step, pinacolborane approaches the Si-O bond of **Int-2**, which then passes through a Si-O-B-H four membered cyclic transition state (**TS-2**), leading to the formation of the hydroboration product (**Pdt-1**) along with the regeneration of the catalyst. The regeneration of the catalyst has also been observed by ^1H NMR spectroscopy from the stoichiometric reaction between **Int-2** and HBpin with the reappearance of the Si-H resonance at δ 6.26 ppm in the reaction mixture with concomitant disappearance of the B-H protons. The four-membered cyclic transition state (**TS-2**) involves a H-bonding interaction between the Si and B atoms and in this transition state a significant amount of B-H bond activation takes place (1.27 \AA) in comparison with that in HBpin (1.19 \AA). Such

elongation allows hydride transfer from the boron to the silicon atom leading to simultaneous Si–O bond cleavage and B–O bond formation. A similar mechanistic proposal for the regeneration of an aluminum hydride catalyst was suggested by the groups of Zhi, Parameswaran, and Roesky. The driving force of the reaction can be attributed to the oxophilicity of the boron atom.¹⁹ The ΔE (-11.4 kcal mol⁻¹) and ΔG (-9.6 kcal mol⁻¹) values for this step are highly negative and the barrier (ΔG^\ddagger) is 27.0 kcal mol⁻¹. To confirm the slowest step, we have employed energetic span model (ESM) calculations²⁰ and found that the percentage contributions of the 1st and 2nd transition states are 95% and 5%, respectively. Hence the first step is seen to be the slowest step of the overall hydroboration process.

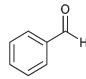
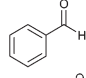
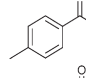
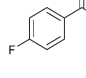
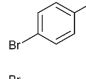
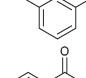
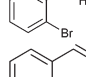
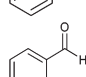
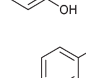
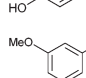
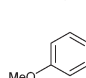
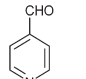
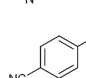
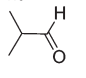
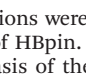
Subsequently, the scope of the catalytic reaction was examined with a range of aldehydes (Table 1). Reactions were monitored by ¹H NMR spectroscopy with the appearance of new upfield resonances corresponding to the α -protons of the boronate ester. Most of the aromatic aldehydes are converted to the corresponding boronate esters at room temperature in short reaction time in good yields (entries 1–15). No inhibitory effect was observed for *ortho* substituents (entries 7 and 9). The reaction showed tolerance towards fluoride groups, as demonstrated by the clean hydroboration of 4-fluorobenzaldehyde (entry 4). When salicylaldehyde or 4-hydroxybenzaldehyde was used, hydroboration occurred in the aldehyde functional group and double hydroboration occurred in the aldehyde and OH groups (minor products) (entries 9 and 10). However, only the hydroxylborane dehydrocoupled product has not been formed. Hydroboration of cinnamaldehyde led to 1,2-adducts, keeping the olefinic functionality intact (entry 8). The reaction of 4-pyridine-carboxaldehyde with HBpin led to exclusive hydroboration of the carbonyl functionality instead of pyridine dearomatization (entry 13).

We further examined the scope of hydroboration for ketones. However, even after increasing the mol% of the catalyst, reaction temperature, time, and changing the solvent did not lead to the hydroboration of ketone. In fact, no reaction was observed between **1** and ketone, which can be attributed to the higher coordination and sterics around the silicon atom. Consistent with that, theoretical calculations also reveal that both barriers are substantially higher for ketones than for aldehydes.

Silane catalyzed hydroboration has been extended to imines, which has been scarcely studied. The first transition metal-catalyzed imine hydroboration was reported by Baker and Westcott *et al.* using Au complexes,²¹ which were followed by few more reports.^{22–25} Transition metal free imine hydroboration was reported by the group of Hill using a magnesium compound [CH₂C(Me)NAr₂MgⁿBu] (Ar = 2,6-*i*-Pr₂C₆H₃)²⁶ and the group of Crudden using a Lewis adduct of DABCO and B(C₆F₅)₃.²⁷ It was observed that **1** catalyzes hydroboration of imines under slightly harsher conditions. Purification of products by SiO₂ column chromatography led exclusively to the corresponding secondary amines (Table 2).

We have also carried out quantum mechanical calculations to explore the reaction mechanism at the same level of theory

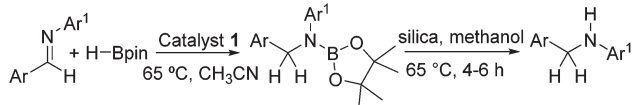
Table 1 Hydroboration of aldehydes catalyzed by **1**^a

Entry	Substrate	Cat. (mol%)	Time [h]	Yield ^b [%]
1		—	0.5	Trace
2		1	1	96
3		1	1	90
4		1	1	90
5		1	1	88
6		1	1	85
7		1	1	82
8		1	1.5	95
9		1	1	75
10		1	1	72
11		1	1	84
12		1	1	70
13		1	1	90
14		1	1	52
15		1	5	95

^a All reactions were carried out in benzene at room temperature using 1 equiv. of HBpin. ^b Conversion was determined by NMR spectroscopy on the basis of the consumption of the aldehyde and the identity of the product was confirmed by RCH₂OBpin or resonances.

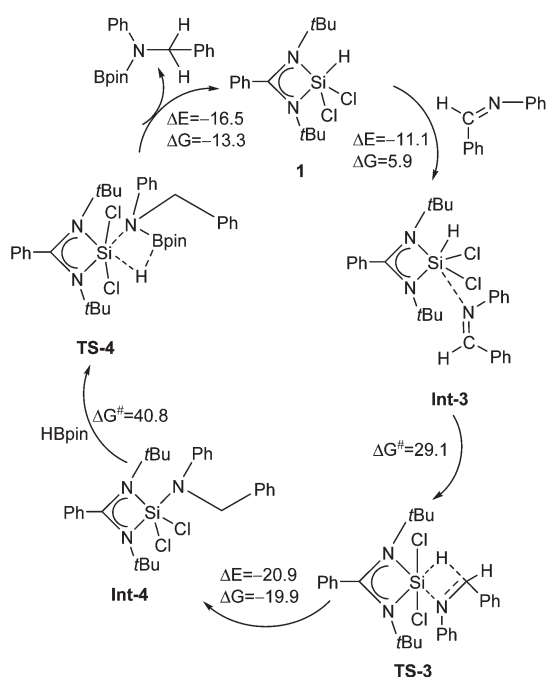
for imine hydroboration in the presence of a silane catalyst (Scheme 3 and Fig. S1†). Bond making and breaking between the Si–N and B–H bonds are involved in the transition state (**TS-4**) with significant B–H bond activation (1.28 Å). The only differences between this case and aldehydes are the energy barriers, especially at the second transition state (**TS-4**), with the barrier being 40.8 kcal mol⁻¹. This higher barrier explains why the reaction requires heating to 65 °C.

In summary, we have demonstrated the first use of a well-defined neutral silicon(IV) compound for catalytic hydroboration of aldehydes and aldimines. The initial step in the cata-

Table 2 Hydroboration of imines catalyzed by **1** and the conversion of amine boronate esters to secondary amines^a


Entry	Substrate	Cat. (mol%)	Time [h]	Yield ^b [%]
1		2	48	86
2		2	48	74
3		2	48	87
4		2	50	88
5		2	72	76
6		2	72	79
7		2	72	88
8		2	72	52

^a All reactions were carried out in acetonitrile at 65 °C using 1 equiv. of HBpin. ^b Yields are isolated yields of secondary amines.



Scheme 3 The catalytic cycle and reaction mechanism for the imine hydroboration by catalyst **1**, calculated at the PBE/TZVP level of theory with DFT. ΔG and ΔG^\ddagger represent the Gibbs free energy of reaction and the Gibbs free energy of activation respectively. All values are in kcal mol⁻¹.

lytic cycle is the facile addition of the Si–H bond to the C=O bond *via* a four-membered transition state. The second step involves the σ -bond metathesis between [PhC(N t Bu)₂SiCl₂OCH₂Ph] (**Int-2**) and HBpin, resulting in product formation along with the regeneration of the catalyst. The mechanism was further supported by DFT calculations. We believe that our findings will spur more interest among researchers to design many more silicon(IV) compounds as catalysts for various organic transformations.

This work was supported by the Science and Engineering Research Board (SERB), India (SB/S1/IC-10/2014). M. K. B. and T. D. thank CSIR, India for the research fellowships. K. V. acknowledges “MSM” (CSC0129) and DST (EMR/2014/000013) for funding. S. S. S. also thanks the Ramanujan research grant (SB/S1/RJN-073/2014). We thank Prof. Swadhin K. Mandal from the Indian Institute of Science Education and Research (IISER), Kolkata for providing us trichlorosilane (HSiCl₃). We are thankful to the reviewers for their critical suggestions to improve the manuscript.

Notes and references

- (a) X. He and J. F. Hartwig, *J. Am. Chem. Soc.*, 1996, **118**, 1696–1702; (b) J. F. Hartwig and C. N. Muhoro, *Organometallics*, 2000, **19**, 30–38.
- (a) K. Oshima, T. Ohmura and M. Sugimoto, *J. Am. Chem. Soc.*, 2012, **134**, 3699–3702; (b) J. Cid, J. J. Carbo and E. Fernandez, *Chem. – Eur. J.*, 2012, **18**, 1512–1521; (c) S. M. Smith and J. M. Takacs, *Org. Lett.*, 2010, **12**, 4612–4615; (d) S. M. Smith and J. M. Takacs, *J. Am. Chem. Soc.*, 2010, **132**, 1740–1741; (e) C. J. Lata and C. M. Crudden, *J. Am. Chem. Soc.*, 2010, **132**, 131–137; (f) B. Nguyen and J. M. Brown, *Adv. Synth. Catal.*, 2009, **351**, 1333–1343 and references therein.
- S. Yadav, S. Saha and S. S. Sen, *ChemCatChem*, 2016, **7**, 486–501.
- C. C. Chong and R. Kinjo, *ACS Catal.*, 2015, **5**, 3238–3259.
- For catalysis with alkaline earth metal, please see: (a) T. E. Stennett and S. Harder, *Chem. Soc. Rev.*, 2016, **45**, 1112–1128; (b) M. S. Hill, D. J. Liptrot and C. Weetman, *Chem. Soc. Rev.*, 2016, **45**, 972–988; (c) S. Harder, *Chem. Rev.*, 2010, **110**, 3852–3876.
- (a) Q.-L. Zhou, *Angew. Chem., Int. Ed.*, 2016, **55**, 5352–5353; (b) S. Bagherzadeh and N. P. Mankad, *Chem. Commun.*, 2016, **35**, 3844–3846; (c) D. Mukherjee, H. Osseili, T. P. Spaniol and J. Okuda, *J. Am. Chem. Soc.*, 2016, **138**, 10790–10793; (d) S. C. Sau, R. Bhattacharjee, P. K. Vardhanapu, G. Vijaykumar, A. Datta and S. K. Mandal, *Angew. Chem., Int. Ed.*, 2016, **55**, 15147–15151.
- (a) M. Arrowsmith, T. J. Hadlington, M. S. Hill and G. Kociok-Köhn, *Chem. Commun.*, 2012, **48**, 4567–4569; (b) C. Weetman, M. D. Anker, M. Arrowsmith, M. S. Hill, G. Kociok-Köhn, D. J. Liptrot and M. F. Mahon, *Chem. Sci.*, 2016, **7**, 628–641; (c) C. Weetman, M. S. Hill and

- M. F. Mahon, *Chem. Commun.*, 2015, **51**, 14477–14480; (d) K. Manna, P. Ji, F. X. Greene and W. Lin, *J. Am. Chem. Soc.*, 2016, **138**, 7488–7491; (e) D. Mukherjee, A. Ellern and A. D. Sadow, *Chem. Sci.*, 2014, **5**, 959–965; (f) L. Fohlmeister and A. Stasch, *Chem. – Eur. J.*, 2016, **22**, 10235–10246; (g) D. Mukherjee, S. Shirase, T. P. Spaniol, K. Mashima and J. Okuda, *Chem. Commun.*, 2016, **52**, 13155–13158.
- 8 (a) Z. Yang, M. Zhong, X. Ma, S. De, C. Anusha, P. Parameswaran and H. W. Roesky, *Angew. Chem., Int. Ed.*, 2015, **54**, 10225–10229; (b) Z. Yang, M. Zhong, X. Ma, K. Nijesh, S. De, P. Parameswaran and H. W. Roesky, *J. Am. Chem. Soc.*, 2016, **138**, 2548–2551.
- 9 J. Schneider, C. P. Sindlinger, S. M. Freitag, H. Schubert and L. Wesemann, *Angew. Chem., Int. Ed.*, 2017, **56**, 333–337.
- 10 V. K. Jakhar, M. K. Barman and S. Nembenna, *Org. Lett.*, 2016, **18**, 4710–4713.
- 11 T. J. Hadlington, M. Hermann, G. Frenking and C. Jones, *J. Am. Chem. Soc.*, 2014, **136**, 3028–3031.
- 12 Y. Wu, C. Shan, Y. Sun, P. Chen, J. Ying, J. Zhu, L(Leo). Liu and Y. Zhao, *Chem. Commun.*, 2016, **52**, 13799–13802.
- 13 C.-C. Chong, H. Hirao and R. Kinjo, *Angew. Chem., Int. Ed.*, 2015, **54**, 190–194.
- 14 (a) K. Mütter, J. Mohr and M. Oestreich, *Organometallics*, 2013, **32**, 6643–6646; (b) A. R. Nödling, K. Mütter, V. H. G. Rohde, G. Hilt and M. Oestreich, *Organometallics*, 2014, **33**, 302–308; (c) A. L. Liberman-Martin, R. G. Bergman and T. D. Tilley, *J. Am. Chem. Soc.*, 2015, **137**, 5328–5331; (d) L. Hao, Y. Zhao, B. Yu, Z. Yang, H. Zhang, B. Han, X. Gao and Z. Liu, *ACS Catal.*, 2015, **5**, 4989–4993; (e) Q. Zhou and Y. Li, *J. Am. Chem. Soc.*, 2015, **137**, 10182–10189; (f) N. von Wolff, G. Lefèvre, J.-C. Berthet, P. Thuéry and T. Cantat, *ACS Catal.*, 2016, **6**, 4526–4535; (g) K. Mütter and M. Oestreich, *Chem. Commun.*, 2011, **47**, 334–336.
- 15 (a) S. S. Sen, H. W. Roesky, D. Stern, J. Henn and D. Stalke, *J. Am. Chem. Soc.*, 2010, **132**, 1123–1126; (b) S. S. Sen, J. Hey, R. Herbst-Irmer, H. W. Roesky and D. Stalke, *J. Am. Chem. Soc.*, 2011, **133**, 12311–12316; (c) C.-W. So, H. W. Roesky, P. M. Gurubasavaraj, R. B. Oswald, M. T. Gamer, P. G. Jones and S. Blaurock, *J. Am. Chem. Soc.*, 2007, **129**, 12049–12054.
- 16 (a) Y. Wang, W. Chen, Z. Lu, Z.-H. Li and H. Wang, *Angew. Chem., Int. Ed.*, 2013, **52**, 7496–7499; (b) C.-C. Chong, H. Hirao and R. Kinjo, *Angew. Chem., Int. Ed.*, 2014, **53**, 3342–3346; (c) G. I. Nikonov, S. F. Vyboishchikov and O. G. Shirobokov, *J. Am. Chem. Soc.*, 2012, **134**, 5488–5491.
- 17 C.-W. So, H. W. Roesky, J. Magull and R. B. Oswald, *Angew. Chem., Int. Ed.*, 2006, **45**, 3948–3951.
- 18 One reviewer suggested that the actual catalyst could be silylium ions generated from the reaction of **1** with HBpin. So far we could not obtain any conclusive NMR spectroscopic evidence for the formation of silylium ions.
- 19 For comparison of oxophilicity, please see: K. S. Kepp, *Inorg. Chem.*, 2016, **55**, 9461–9470.
- 20 (a) S. Kozuch and S. Shaik, *Acc. Chem. Res.*, 2010, **44**, 101–110; (b) S. Kozuch and J. M. L. Martin, *ACS Catal.*, 2011, **1**, 246–253.
- 21 R. T. Baker, J. C. Calabrese and S. A. Westcott, *J. Organomet. Chem.*, 1995, **498**, 109–117.
- 22 L. Koren-Selfridge, H. N. Londino, J. K. Vellucci, B. J. Simmons, C. P. Casey and T. B. Clark, *Organometallics*, 2009, **28**, 2085–2090.
- 23 A. E. King, S. C. E. Stieber, N. J. Henson, S. A. Kozimor, B. L. Scott, N. C. Smythe, A. D. Sutton and J. C. Gordon, *Eur. J. Inorg. Chem.*, 2016, 1635–1640.
- 24 C. M. Vogels, P. O. O'Connor, T. E. Phillips, K. J. Watson, M. P. Shaver, P. J. Hayes and S. A. Westcott, *Can. J. Chem.*, 2001, **79**, 1898–1905.
- 25 A. Kaithal, B. Chatterjee and C. Gunanathan, *J. Org. Chem.*, 2016, **81**, 11153–11161.
- 26 M. Arrowsmith, M. S. Hill and G. Kociok-Köhn, *Chem. – Eur. J.*, 2013, **19**, 2776–2783.
- 27 P. Eisenberger, A. M. Bailey and C. M. Crudden, *J. Am. Chem. Soc.*, 2012, **134**, 17384–17387.

Cite this: *Chem. Commun.*, 2018, 54, 6843Received 23rd March 2018,
Accepted 24th April 2018

DOI: 10.1039/c8cc02314j

rsc.li/chemcomm

Easily accessible lithium compound catalyzed mild and facile hydroboration and cyanosilylation of aldehydes and ketones†

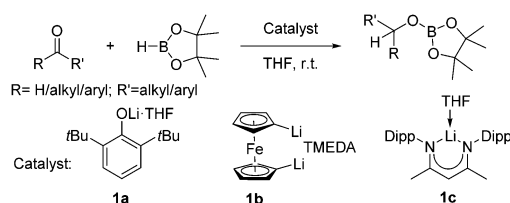
Milan Kumar Bisai,^a Tamal Das,^b Kumar Vanka^{ib} and Sakya S. Sen^{ib}*^a

Simple and readily accessible lithium compounds such as 2,6-*tert*-butyl phenolate lithium (**1a**), 1,1'-dilithioferrocene (**1b**) and nacnac lithium (**1c**) are found to be efficient single site catalysts for hydroboration of a range of aldehydes and ketones with HBpin at room temperature. The efficacy of **1a**–**1c** as catalysts is extended to the cyanosilylation of aldehydes and ketones with Me₃SiCN.

While the birth of lithium chemistry occurred one hundred years ago,¹ the growth of s-block compounds is still in its early days, finding its feet slowly and gradually from curiosity driven explorations to important catalytic transformations. Driven by the demand for catalytic processes with reduced environmental impact and low cost, numerous groundbreaking results have been achieved in molecular catalysis using complexes of the heavier alkaline earth metals.² Following the demonstration of the hydroboration of carbonyl compounds using a magnesium alkyl complex,³ there has been a flurry of research activity on hydroboration reactions using compounds with alkaline earth metals^{4–8} as well as p-block elements.^{9–16} For the heavier alkaline earth metal catalysts, Schlenk equilibrium is an issue, which is likely to impose a severe limitation on the preparation as well as the activity of the catalyst. In this context, group 1 complexes are advantageous over their adjacent neighbours as they are not involved in Schlenk-type equilibria. Moreover, as catalysts involving group 2 and p-block elements are usually prepared from the corresponding lithium compounds, the direct use of lithium compounds in catalysis would reduce the need for such additional transformations. In fact, group 1 complexes have been sporadically reported for hydrosilylation of alkenes¹⁷ or hydrogenation of aldimines,¹⁸ but they were not very efficient compared to their corresponding group 2 complexes in terms of reactivity or

selectivity or both. Hence, group 1 based complexes have remained largely unexplored in molecular catalysis. The paradigm has shifted with the two significant breakthroughs that recently came from the groups of Okuda^{19,20} and Mulvey.²¹ These breakthroughs have created a new avenue for lithium compounds to be used as single component catalysts for important organic transformations.

Okuda and co-workers noted that the success of lithium catalysts relies on the combination of the Lewis acidity of the Li atom and the hydridicity of the borate anions. A Li catalyst with a [HB(C₆F₅)₃] anion was reported to be inert, which was attributed to the diminished hydridicity of the borate anion.¹⁹ Thus, there remains scope for the study of the catalytic properties of lithium compounds with no hydridic hydrogen present in the counter anion. In light of our interests in developing catalytic methods for the reduction of carbonyl compounds,^{4,12,22,23} we attempted to use three popular and readily accessible lithium compounds with different electronegative substituents, 2,6-*tert*-butyl phenolate lithium (**1a**), nacnac lithium (**1c**) and 1,1'-dilithioferrocene (**1b**) (Scheme 1), for the reduction of aldehydes and ketones with HBpin under ambient conditions. The reason behind this selection is to examine how the Lewis acidity of the Li center influences the catalytic activity. For example, the Li atom in **1c** is purportedly more Lewis acidic than that in **1a**, as the Li atom in **1c** is bound to two nitrogen atoms, while the Li atom in **1a** is bound to only one oxygen atom. It is also interesting to compare the catalytic competence of **1b** with that of the other catalysts, as it possesses two active Li centres, although they are bound to less electronegative carbon atoms. Consistently with



Scheme 1 Hydroboration of aldehydes and ketones using **1a**, **1b** and **1c** as catalysts.

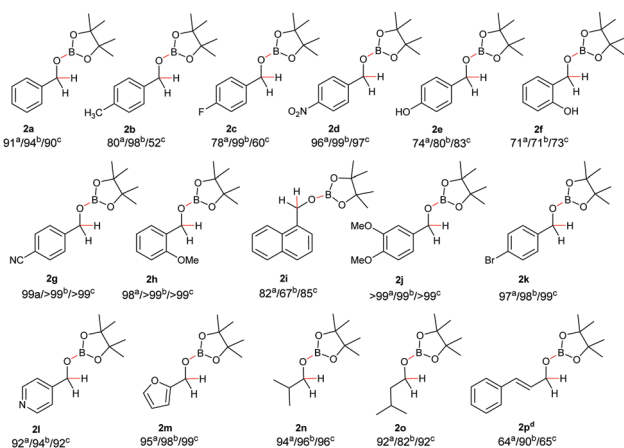
^a *Inorganic Chemistry and Catalysis Division, CSIR-National Chemical Laboratory, Dr. Homi Bhabha Road, Pashan, Pune 411008, India. E-mail: ss.sen@ncl.res.in*

^b *Physical and Material Chemistry Division, CSIR-National Chemical Laboratory, Dr. Homi Bhabha Road, Pashan, Pune 411008, India*

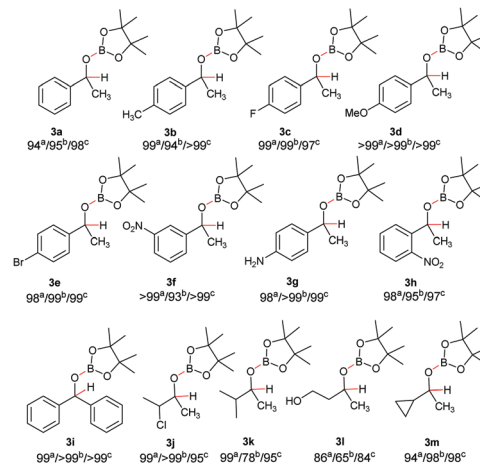
† Electronic supplementary information (ESI) available: Experimental details, details of DFT calculations, and representative NMR spectra. See DOI: 10.1039/c8cc02314j

our hypothesis, the catalytic activity (TOF) of **1c** is found to be better than that of **1a** or **1b**. To broaden the horizons of lithium compounds in catalysis, we have successfully employed **1a–1c** for the cyanosilylation of carbonyl compounds; a transformation thus far not known to be catalyzed by group 1 complexes.

The hydroboration reactions for a variety of aldehydes (Scheme 2, **2a–2p**) and ketones (Schemes 3, **3a–3m**) have been evaluated using **1a/1b/1c** as the catalyst (for optimization, please see the ESI,[†] Tables S1a–c and S3a–c). Both aliphatic and aromatic aldehydes underwent hydroboration within an hour with excellent TOFs (ESI,[†] Table S2), which reflects the high efficiency of the catalysts. Similarly, a wide range of aromatic and aliphatic ketones were converted to the corresponding boronate esters within 2–3 hours, keeping the mol% constant (ESI,[†] Table S4). Acetophenone derivatives bearing both electron-withdrawing and electron-donating functionalities (**3a–3h**) gave good yields, demonstrating a negligible electronic effect. Increasing the steric demands also has little effect on the yield, as seen in the case of hydroboration of benzophenone (**3i**). All of the catalysts show good functional group tolerance. The nitrile (**2g**), hydroxy (**2e** and **2f**), heterocycle (**2l** and **2m**), and amino (**3g**) containing substrates yielded the desired boronate esters. Furthermore, the bromo functionality (**2k** and **3e**) does not suffer from the lithium–bromide exchange. In some cases, the catalytic efficiencies vary, as **1c** gives the lowest yield for **2b** and **2c**. **1b** gives a quantitative yield in the most cases, presumably due to the presence of two Li centres, except for with **2i** and **3l**. Excellent chemoselectivity was observed in a competitive experiment with all three catalysts (ESI,[†] Scheme S1). We compared the catalytic activities of **1a–1c** for benzophenone and *trans*-cinnamaldehyde with those of some known catalysts. The most active one is lithium hydridotriphenylborate, which showed a remarkable TOF of 66 600 h^{−1} for benzophenone.¹⁹ Among rare earth catalysts, Marks' La^{NITMS} has the highest TOF of >40 000 h^{−1},^{21a}



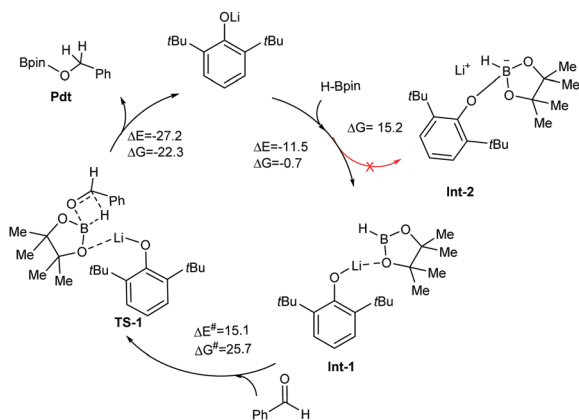
Scheme 2 Substrate scope for the hydroboration of aldehydes. Reaction conditions: 0.1 mol% catalyst and room temperature in THF. Reaction time (except *trans*-cinnamaldehyde): **1a**, 60 min; **1b**, 40 min; **1c**, 50 min. Yields are calculated based on the integration area of the product and starting material signals in the ¹H spectra using mesitylene as an internal standard. Superscripts a, b and c stand for the catalysts **1a**, **1b** and **1c**, respectively; d: the reaction time for *trans*-cinnamaldehyde reduction was 5 h.



Scheme 3 Substrate scope for the hydroboration of ketones. Reaction conditions: 0.1 mol% catalyst and room temperature in THF. Reaction time: **1a**, 3 h; **1b**, 2 h; **1c**, 2 h. Yields are calculated w.r.t. mesitylene as an internal standard.

while among transition metal catalysts, Mankad's copper carbene was reported to be the most active (TOF of 1000 h^{−1}).^{24b} Hill's magnesium alkyl complex was reported with a TOF of 500 h^{−1} for benzophenone,³ while Stasch's magnesium catalyst [(L)MgH]₄ (L = Ph₂PNDipp; Dipp = 2,6-*i*Pr₂C₆H₃) was recorded with a TOF of 1760 h^{−1}.⁵ We have found that **1c** shows very good efficiency with a TOF of 495 h^{−1}. Although **1b** gives the best yield, the activities of **1a** and **1b** are slightly poorer (TOF: 330 h^{−1} and 247 h^{−1}, respectively) than that of **1c**. The TOF of the *trans*-cinnamaldehyde reduction was calculated to be 130 h^{−1} for **1c**, which is second only to Okuda's lithium hydridotriphenylborate (210 h^{−1}).¹⁹ In comparison, **1a** and **1b** were recorded with TOFs of 128 and 90 h^{−1}, respectively, but their superiority was marked over the other reported main group catalysts for *trans*-cinnamaldehyde reduction (e.g. [Mg(thf)₆][HBPh₃]₂: 11.2 h^{−1},⁵ naenacAl(H)OTf: 16.5 h^{−1},¹⁴ PhC(N*t*Bu)₂SiHCl₂: 63.3 h^{−1},¹² and PhC(NiPr)₂CaI: 69 h^{−1}).⁴

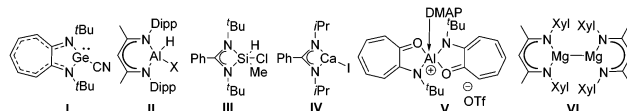
We have investigated the hydroboration mechanism for **1a** and **1c**. We found that **1a** reacts with HBpin but no change in the ¹H NMR spectrum was detected in the reaction of **1a** with an aldehyde. However, the NMR experiments indicate that no reaction takes place between **1c** and HBpin. Therefore, the catalytic pathways for **1a** and **1c** appear to be different. The reaction between **1a** and HBpin in toluene-*d*₈ shows a resonance at δ 4.7 ppm in the ¹¹B NMR spectrum, indicating a four-coordinated sp³ boron atom.^{25a} However, the prolonged time led to formation of trialkoxyborane [2,6-*t*Bu₂-C₆H₃-OBpin] and a BH₄[−] anion, as a singlet and a quintet started to appear at δ 21.62 and −39.83 ppm after 2–3 h, respectively.^{25b} To obtain mechanistic insights, full quantum chemical calculations were performed with density functional theory (DFT) at the dispersion and solvent corrected PBE/TZVP level of theory. The pathway is initiated with O-coordination of HBpin to the lithium atom of **1a**, resulting in the exergonic (ΔE = −11.5 kcal mol^{−1} and ΔG = −0.7 kcal mol^{−1}) formation of **Int-1**, which has an O··Li bond length of 1.92 Å. This binding mode is in agreement with the crystal structure of



Scheme 4 The catalytic cycle and reaction mechanism for aldehyde hydroboration by the catalyst **1a**, where ΔG and ΔG^\ddagger represent the Gibbs free energy of reaction and the Gibbs free energy of activation, respectively. All values are in kcal mol^{-1} .

[DippnacnacCa(H₂Bpin)]₃ where primary bonding between the anion and the metal cation proceeds through an O··Ca interaction.²⁶ The other possibility of coordinating the phenolate oxygen to the boron atom of HBpin leading to a four-coordinate boron complex (**Int-2**) was found to be thermodynamically unfavorable as the ΔG of the reaction was $15.2 \text{ kcal mol}^{-1}$. In the next step, the carbonyl oxygen atom of benzaldehyde attacks the boron centre of HBpin, with the hydride being transferred from the boron centre to the carbonyl carbon. This occurs through a four-membered transition state (**TS-1**), where a significant amount of the B–H bond activation (1.29 \AA) takes place, which leads to the formation of the hydroboration product (**Pdt**) along with the regeneration of **1a** (Scheme 4). The ΔE ($-27.2 \text{ kcal mol}^{-1}$) and ΔG ($-22.3 \text{ kcal mol}^{-1}$) values for this step are highly negative and the activation energy (ΔG^\ddagger) barrier corresponding to the transition state is calculated to be $25.7 \text{ kcal mol}^{-1}$.

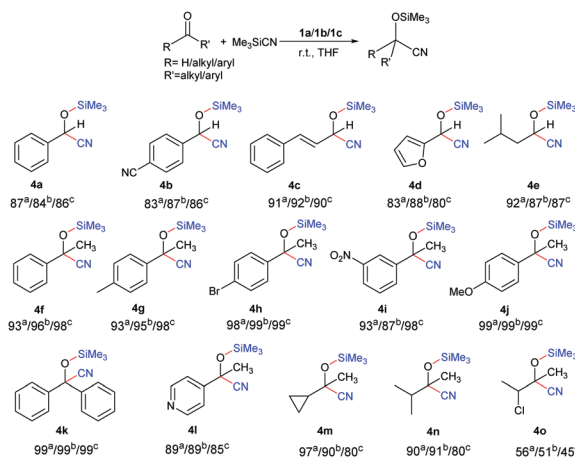
In the case of **1c**, a weakly bound complex (**Int-3**) is formed between **1c** and benzaldehyde, with the oxygen atom of benzaldehyde approaching the lithium atom of **1c** (ESI,† Scheme S3). The ΔE and ΔG for this step are -19.5 and $-5.5 \text{ kcal mol}^{-1}$, respectively. Subsequently, nucleophilic attack by the lone pair of the N atom of **1c** in **Int-3** to the vacant p orbital of the boron centre of HBpin takes place. A four-coordinated B centre is thus generated (**Int-4**). The ΔE and ΔG for this step are $-5.3 \text{ kcal mol}^{-1}$ and $7.2 \text{ kcal mol}^{-1}$, respectively. The activation free energy for the N··B bond formation is $24.1 \text{ kcal mol}^{-1}$. In the next step, the hydride is transferred from the boron centre to the electrophilic carbonyl carbon of the benzaldehyde through a three-membered transition state (**TS-3**), with a barrier of $21.6 \text{ kcal mol}^{-1}$. In this transition state, there is a significant amount of B–H bond activation (1.33 \AA vs. 1.19 \AA in the intermediate complex), which allows the hydride transfer from the boron to the carbonyl carbon centre. In the last step, the oxygen centre of the aldehyde attacks the boron centre of pinacolborane and simultaneously, B··N bond cleavage occurs along with N··Li bond formation. This takes place through a four-membered transition state (**TS-4**) and leads to the formation of the hydroboration product



Scheme 5 Examples of the reported main-group catalysts for the cyanosilylation of carbonyl compounds. This is the first report of group 1 catalysts for cyanosilylation of aldehydes and ketones.

(**Pdt-1**) along with the regeneration of the catalyst. The ΔE ($-14.5 \text{ kcal mol}^{-1}$) and ΔG ($-29.9 \text{ kcal mol}^{-1}$) values for this step are very favourable and the barrier (ΔG^\ddagger) corresponding to the transition state is $15.7 \text{ kcal mol}^{-1}$.

In contrast to the large number of publications on main group compound catalyzed hydroboration, only a few studies on main group compound catalyzed cyanosilylation have been reported (Scheme 5).^{12,22,23,27–32} The majority of them were reported to only catalyze aldehydes.^{22,27–30} The use of alkaline earth metal complexes in catalytic cyanosilylation is an emerging area. Recently, we and Ma *et al.* independently reported the cyanosilylation of aldehydes and ketones with a calcium complex, $\text{PhC}(\text{NiPr})_2\text{Ca}^{23}$ and a magnesium(i) complex, $\{(\text{Xyl})\text{nacnac}\}\text{Mg}\}_2$ ($\text{Xyl} = 2,6\text{-Me}_2\text{-C}_6\text{H}_3$),³² respectively. Nevertheless, to our knowledge, the use of lithium compounds as catalysts in cyanosilylation has not been reported so far. An initial screening of the catalytic effect of **1a–1c** revealed good conversion in most cases at room temperature in a reasonable amount of time (for aldehydes: 1 h & for ketones: 2 h) with 0.1 mol% catalyst loading (Scheme 6). The catalytic efficiencies and selectivity of **1a–1c** were found to be very similar. Benzaldehyde, acetophenone, and benzophenone (entries **4a**, **4f** and **4k**) were smoothly converted into the corresponding cyanohydrins. For the reduction of benzophenone, these lithium catalysts are superior to **IV** (3 mol%, 2 h, 82% yield). No other main group catalyst has been reported for cyanosilylation of benzophenone so far. In the case of α,β -unsaturated cinnamaldehyde, the 1,2 addition of Me_3SiCN took place selectively, and no Michael addition



Scheme 6 The scope of cyanosilylation with aldehyde and ketone substrates. Reaction conditions: 0.1 mol% catalyst and room temperature in THF. Reaction time for aldehydes: 1 h and for ketones: 2 h. Yields are calculated w.r.t. mesitylene as an internal standard.

product was formed (entry **4c**). Cyanation of aliphatic aldehydes and ketones (entries **4e**, **4m**, **4n** and **4o**) was found to proceed efficiently. Unlike other main group catalysts, which were reported to catalyze acetophenone substrates with either electron-withdrawing (**IV**²³ and **V**³¹) or electron-donating groups (**II**¹² and **VI**³²), it was observed that **1a–1c** can tolerate both electron-withdrawing as well as electron-donating substituents (**4g–4j**) for cyanosilylation. Heteroarenes (**4d** and **4l**) were tolerated under the reaction conditions to other substituents. ~30% chloride to cyanide exchange product, along with the formation of the desired cyanohydrin, was observed for **4o**.

Herein, we have demonstrated that the reduction of a variety of carbonyl compounds with HBpin and Me₃SiCN can be catalyzed rapidly by very simple lithium compounds (**1a–1c**) under mild and facile conditions with excellent functional group tolerance and TOFs. We have investigated the hydroboration mechanism for **1a** and **1c** and the mechanistic studies for cyanosilylation are currently ongoing. The methodologies described have clearly opened up new avenues for the catalytic application of lithium compounds, encouraged by the very economic and almost non-toxic nature of these reagents.

This work was supported by SERB (SB/S1/IC-10/2014), India and Ramanujan research grant (SB/S2/RJN-073/2014). MKB and TD thank CSIR, India for the research fellowships. We thank the reviewers for their critical feedback to improve the manuscript.

Conflicts of interest

There are no conflicts to declare.

Notes and references

- W. Schlenk and J. Holtz, *Ber. Dtsch. Chem. Ges.*, 1917, **50**, 262–274.
- (a) S. Harder, *Chem. Rev.*, 2010, **110**, 3852–3876; (b) T. E. Stennett and S. Harder, *Chem. Soc. Rev.*, 2016, **45**, 1112–1128; (c) M. S. Hill, D. J. Liptrot and C. Weetman, *Chem. Soc. Rev.*, 2016, **45**, 972–988; (d) K. Revunova and G. I. Nikonov, *Dalton Trans.*, 2015, **44**, 840–866.
- M. Arrowsmith, T. J. Hadlington, M. S. Hill and G. Kociok-Köhn, *Chem. Commun.*, 2012, **48**, 4567–4569.
- S. Yadav, S. Pahar and S. S. Sen, *Chem. Commun.*, 2017, **53**, 4562–4564.
- L. Fohlmeister and A. Stasch, *Chem. – Eur. J.*, 2016, **22**, 10235–10246.
- D. Mukherjee, S. Shirase, T. P. Spaniol, K. Mashima and J. Okuda, *Chem. Commun.*, 2016, **52**, 13155–13158.
- D. Mukherjee, A. Ellern and A. D. Sadow, *Chem. Sci.*, 2014, **5**, 959–965.
- K. Manna, P. Ji, F. X. Greene and W. Lin, *J. Am. Chem. Soc.*, 2016, **138**, 7488–7491.
- (a) T. J. Hadlington, M. Hermann, G. Frenking and C. Jones, *J. Am. Chem. Soc.*, 2014, **136**, 3028–3031; (b) J. Schneider, C. P. Sindlinger, S. M. Freitag, H. Schubert and L. Wesemann, *Angew. Chem., Int. Ed.*, 2017, **56**, 333–337; (c) Y. Wu, C. Shan, Y. Sun, P. Chen, J. Ying, J. Zhu, L. L. Liu and Y. Zhao, *Chem. Commun.*, 2016, **52**, 13799–13802.
- C.-C. Chong, H. Hirao and R. Kinjo, *Angew. Chem., Int. Ed.*, 2015, **54**, 190–194.
- M. K. Bisai, S. Pahar, T. Das, K. Vanka and S. S. Sen, *Dalton Trans.*, 2017, **46**, 2420–2424.
- Z. Yang, M. Zhong, X. Ma, S. De, C. Anusha, P. Parameswaran and H. W. Roesky, *Angew. Chem., Int. Ed.*, 2015, **54**, 10225–10229.
- (a) V. K. Jakhhar, M. K. Barman and S. Nembenna, *Org. Lett.*, 2016, **18**, 4710–4713; (b) J. R. Lawson, L. C. Wilkins and R. L. Melen, *Chem. – Eur. J.*, 2017, **23**, 10997–11000.
- (a) C. Weetman, M. D. Anker, M. Arrowsmith, M. S. Hill, G. Kociok-Köhn, D. J. Liptrot and M. F. Mahon, *Chem. Sci.*, 2016, **7**, 628–641; (b) C. Weetman, M. S. Hill and M. F. Mahon, *Chem. Commun.*, 2015, **51**, 14477–14480.
- (a) M.-A. Courtemanche, M.-A. Légaré, L. Maron and F.-G. Fontaine, *J. Am. Chem. Soc.*, 2013, **135**, 9326–9329; (b) D. Franz, L. Sirtl, A. Pöthig and S. Inoue, *Z. Anorg. Allg. Chem.*, 2016, **642**, 1245–1250; (c) J. L. Lortie, T. Dudding, B. M. Gabidullin and G. I. Nikonov, *ACS Catal.*, 2017, **7**, 8454–8459.
- For selected reviews on main group compound catalyzed hydroboration, please see: (a) C. C. Chong and R. Kinjo, *ACS Catal.*, 2015, **5**, 3238–3259; (b) G. I. Nikonov, *ACS Catal.*, 2017, **7**, 7257–7266; (c) D. Mukherjee and J. Okuda, *Angew. Chem., Int. Ed.*, 2018, **57**, 1458–1473; (d) S. Dagorne and R. Wehmschulte, *ChemCatChem*, 2018, DOI: 10.1002/cctc.201800045.
- (a) F. Buch, J. Brettar and S. Harder, *Angew. Chem., Int. Ed.*, 2006, **45**, 2741–2745; (b) V. Leich, T. P. Spaniol and J. Okuda, *Organometallics*, 2016, **35**, 1179–1182.
- H. Bauer, M. Alonso, C. Färber, H. Elsen, J. Pahl, A. Causero, G. Ballmann, F. De Proft and S. Harder, *Nat. Catal.*, 2018, **1**, 40–47.
- D. Mukherjee, H. Osseili, T. P. Spaniol and J. Okuda, *J. Am. Chem. Soc.*, 2016, **138**, 10790–10793.
- (a) H. Osseili, D. Mukherjee, K. Beckerle, T. P. Spaniol and J. Okuda, *Organometallics*, 2017, **36**, 3029–3034; (b) H. Osseili, D. Mukherjee, T. P. Spaniol and J. Okuda, *Chem. – Eur. J.*, 2017, **23**, 14292–14298.
- (a) R. McLellan, A. R. Kennedy, R. E. Mulvey, S. A. Orr and S. D. Robertson, *Chem. – Eur. J.*, 2017, **23**, 16853–16861; (b) V. A. Pollard, S. A. Orr, R. McLellan, A. R. Kennedy, E. Hevia and R. E. Mulvey, *Chem. Commun.*, 2018, **54**, 1233–1236.
- V. S. V. S. N. Swamy, M. K. Bisai, T. Das and S. S. Sen, *Chem. Commun.*, 2017, **53**, 6910–6913.
- S. Yadav, R. Dixit, K. Vanka and S. S. Sen, *Chem. – Eur. J.*, 2018, **24**, 1269–1273.
- (a) V. L. Weidner, C. J. Barger, M. Delferro, T. L. Lohr and T. J. Marks, *ACS Catal.*, 2017, **7**, 1244–1247; (b) S. Bagherzadeh and N. P. Mankad, *Chem. Commun.*, 2016, **52**, 3844–3846.
- (a) A. Bonet, H. Gulyás and E. Fernández, *Angew. Chem., Int. Ed.*, 2010, **49**, 5130–5134; (b) I. P. Query, P. A. Squier, E. M. Larson, N. A. Isley and T. B. Clark, *J. Org. Chem.*, 2011, **76**, 6452–6456.
- S. Harder and J. Spielmann, *J. Organomet. Chem.*, 2012, **698**, 7–14.
- Y. Li, J. Wang, Y. Wu, H. Zhu, P. P. Samuel and H. W. Roesky, *Dalton Trans.*, 2013, **42**, 13715–13722.
- R. K. Sitwatch and S. Nagendran, *Chem. – Eur. J.*, 2014, **20**, 13551–13556.
- A. L. Liberman-Martin, R. G. Bergman and T. D. Tilley, *J. Am. Chem. Soc.*, 2015, **137**, 5328–5331.
- Z. Yang, Y. Yi, M. Zhong, S. De, T. Mondal, D. Koley, X. Ma, D. Zhang and H. W. Roesky, *Chem. – Eur. J.*, 2016, **22**, 6932–6938.
- M. K. Sharma, S. Sinhababu, G. Mukherjee, G. Rajaraman and S. Nagendran, *Dalton Trans.*, 2017, **46**, 7672–7676.
- W. Wang, M. Luo, J. Li, S. A. Pullarkat and M. Ma, *Chem. Commun.*, 2018, **54**, 3042–3044.



Lithium compounds as single site catalysts for hydroboration of alkenes and alkynes†

Cite this: *Chem. Commun.*, 2019, 55, 11711

Received 25th July 2019,
Accepted 4th September 2019

DOI: 10.1039/c9cc05783h

rsc.li/chemcomm

Milan Kumar Bisai,^{ab} Sandeep Yadav,^{ab} Tamal Das,^{bc} Kumar Vanka^{bc} and Sakya S. Sen^{id}*^{ab}

The hydroboration of alkenes and alkynes using easily accessible lithium compounds [2,6-di-*tert*-butyl phenolatelithium (1a**) and 1,1'-dilithioferrocene (**1b**)] has been achieved with good yields, high functional group tolerance and excellent chemoselectivity. Deuterium-labeling experiments confirm the *cis*-addition of pinacolborane. The methodology has been further extended to myrcene, which undergoes selective 4,3-hydroboration. DFT calculations provide insights into the mechanism.**

Hydroboration of functionalized alkynes and alkenes using excess pinacolborane (HBpin) is known,¹ but their catalytic conversion usually requires a late transition metal catalyst.² Recently, the demand for supplanting the transition metal catalysts by more earth abundant and less toxic main group surrogates is ever increasing. Hydroboration using compounds with group 2 elements has been limited to the catalytic reduction of unsaturated polar bonds, such as aldehydes, ketones, imines, amides, esters *etc.*^{3–14} Although compounds with p-block elements are emerging as proficient catalysts for alkyne^{15–20} and alkene^{21–23} hydroboration, there are very limited reports on s-block metal catalyzed alkene or alkyne hydroboration. While Rueping and coworkers reported the first magnesium catalyzed hydroboration of terminal and internal alkynes,²⁴ the group of Parkin demonstrated styrene hydroboration by a terminal magnesium hydride.²⁵ Besides, Zhao and co-workers reported the hydroboration of carbonyl groups and styrene substrates using NaOH powder, although the scope of styrene substrates was somewhat limited.²⁶

The advantages of using lithium compounds are (i) cheap, (ii) moderately abundant (65 ppm in the Earth's crust),

(iii) readily accessible, and (iv) they do not involve in Schlenk equilibrium like group 2 elements. Moreover, as most of the main group catalysts are frequently prepared from the corresponding lithium reagents, taking advantage of the direct use of lithium compounds in catalysis would obviate the need for such additional transformations. In fact, the group of Mulvey demonstrated the use of lithium aluminates as catalysts for the hydroboration of aldehydes, ketones, and imines,^{27,28} and the group of Cowley and Thomas used LiAlH₄ for the hydroboration of alkenes.²³ However, it was aluminum which is the active catalyst in both these cases and lithium only influences the reactivity. This was confirmed by using AlEt₃ (a surrogate of AlH₃) as a single site catalyst to accomplish the hydroboration.

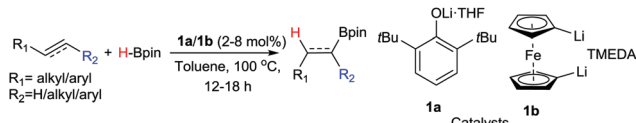
Hence, the utilization of lithium compounds as catalysts has been largely neglected. It is only recently that the groups of Okuda, Mulvey and our group have started to use lithium compounds as single site catalysts for hydroboration of aldehydes and ketones.^{29–33} Subsequently, *n*-BuLi was shown as an efficient catalyst for the hydroboration of alkynes with HBpin.³⁴ However, the substrate scope of the methodology was limited, and the mechanism was not elaborated. Thus, there remains a need for the development of alkene and alkyne hydroboration with lithium compounds as single site catalysts. Last year, we have reported the hydroboration and cyanosilylation of a range of aldehydes and ketones using 2,6-di-*tert*-butyl phenolate lithium (**1a**), 1,1'-dilithioferrocene (**1b**), and [Dipp₂nacnac]Li-THF (**1c**) and compared how the electronegativity of the ligand associated with the Li center influences the catalytic activity.³² The reason to select **1b** over monolithiated ferrocene can be attributed more to the sterics of the former as well as the ease of synthesis (monolithiated ferrocene preparation usually needs *t*BuLi, while **1b** can be prepared from *n*BuLi).³⁵ Although these compounds are prepared from alkyllithium reagents, they are solid in nature, easy to handle, and stable under inert conditions for a long time. Herein, we report efficient hydroboration of more challenging alkenes and alkynes by **1a** and **1b** (Scheme 1). Only a trace amount of conversion was observed when **1c** was used as the catalyst.

^a *Inorganic Chemistry and Catalysis Division, CSIR-National Chemical Laboratory, Dr Homi Bhabha Road, Pashan, Pune 411008, India. E-mail: ss.sen@ncl.res.in*

^b *Academy of Scientific and Innovative Research (AcSIR), Ghaziabad-201002, India*

^c *Physical and Material Chemistry Division, CSIR-National Chemical Laboratory, Dr Homi Bhabha Road, Pashan, Pune, 411008, India*

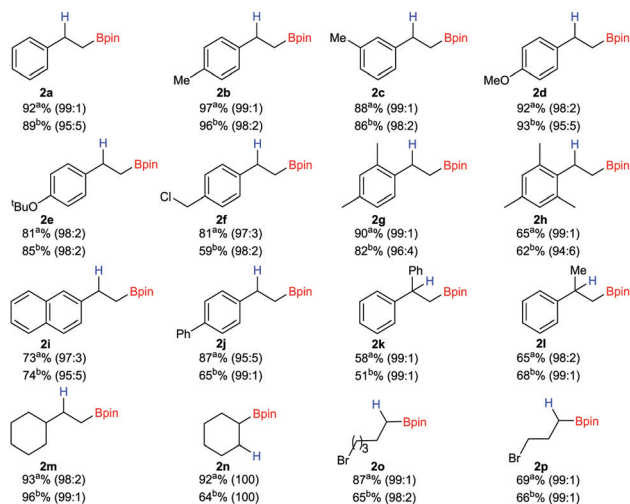
† Electronic supplementary information (ESI) available: Experimental details, theoretical calculations, kinetic analysis and representative NMR spectra. See DOI: 10.1039/c9cc05783h



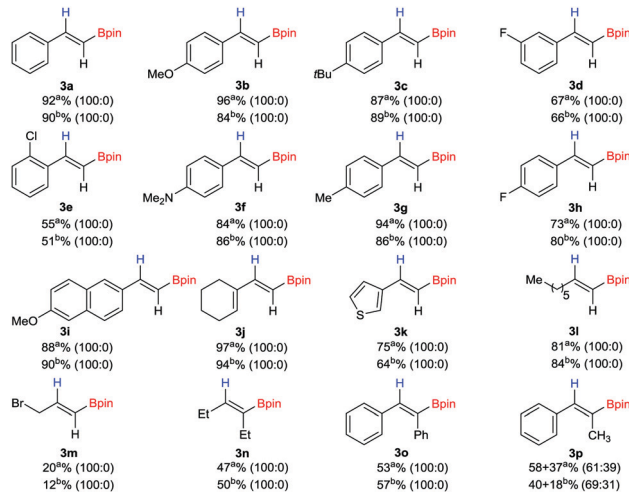
Scheme 1 Lithium compound catalyzed hydroboration of alkenes and alkynes.

A brief screening of catalyst loading, temperature and time has been carried out for the hydroboration of styrene or phenylacetylene with 1.1 equivalent of HBpin (see ESI,† Tables S1 and S3) to achieve the best conversion. For hydroboration of alkynes, the catalyst loadings were 2.0 mol% and the reactions were over around 12 h when heated at 100 °C. Note that, the catalyst loading is substantially lesser than that for *n*BuLi (10 mol%) catalyzed alkyne hydroboration.³⁵ For comparison purpose, cyclopentadienyllithium (CpLi) was employed as the catalyst. With 2.0 mol% catalyst loading CpLi afforded 65% yield under the same reaction conditions for the hydroboration of phenylacetylene (see ESI,† Table S3, entry 6). Slightly higher catalyst loadings (4.0 mol% for **1b** and 8.0 mol% for **1a**) and time (18 h) are required for the hydroboration of alkenes. Both aliphatic and aromatic alkenes/alkynes underwent hydroboration to form the corresponding alkyl or vinyl-boronates in good to excellent yields (Schemes 2 and 3), reflecting the high efficiency of the catalysts.

Smooth hydroboration of different aromatic alkenes or alkynes with electron donating or withdrawing substituents at *o/m/p* positions was observed. Both catalysts tolerate functional groups such as halogens (**2f**, **2o**, **2p**, **3d**, and **3h**), alkoxy (**2d**, **2e**, **3b**, and **3i**), heterocycle (**3k**), and amino (**3f**) containing substrates. However, in addition to alkyne hydroboration, lithium-halide exchange was also observed for **3e** in 29% yield. The lithium halide exchange was more pronounced for **3m** as the



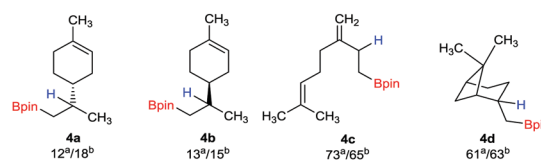
Scheme 2 Hydroboration scope with alkene substrates. Reaction conditions: alkene (0.50 mmol), HBpin (0.55 mmol, 1.1 equiv.), 4.0–8.0 mol% catalyst, 18 h reaction at 100 °C temperature in neat or in toluene. Yields were determined by ¹H NMR integration relative to mesitylene. Henceforth superscripts a and b stand for the catalysts **1a** and **1b** respectively. Ratios in parentheses indicate the distribution of regioisomers (linear vs. branched).



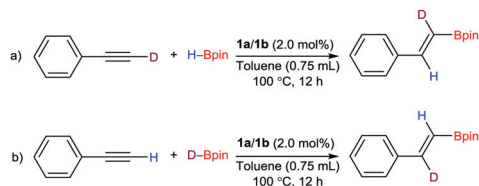
Scheme 3 Scope of hydroboration with alkyne substrates. Reaction conditions: alkyne (0.50 mmol), HBpin (0.55 mmol, 1.1 equiv), 2.0 mol% catalyst, 12 h reaction at 100 °C in toluene. Yields were determined by ¹H NMR integration relative to mesitylene.

metathesis product was obtained in more than 70% yield. Intramolecular chemoselective hydroboration of alkynes over alkenes was observed for **3j**. In contrast to terminal alkynes, internal alkynes (**3n**, **3o**, and **3p**) form their corresponding boronates in moderate yields under the optimization conditions. However, similar to Rueping's magnesium catalyst, by increasing the catalyst loading (5 mol%) and reaction time (36 h), good yields are achieved for **3o** (80%). We have also tested an unsymmetrical alkyne, phenylpropyne, for hydroboration which afforded a mixture of α - and β -vinyl boronates (**3p**) in 2:3 and 3:7 ratios for **1a** and **1b**, respectively. Aliphatic alkenes (**2m–2p**) or alkynes (**3l–3n**) were effectively converted to their corresponding products. Increase of the sterics has little effect on the yield as seen in the cases of hydroboration of **2h**, **2k**, **3n**, and **3o**.

To further explore the catalytic potential of **1a** and **1b**, naturally occurring terpenes have been chosen for the selective hydroboration of the olefinic bond. Although poor yields were obtained for *R*- or *S*-limonene (**4a** and **4b**), myrcene (**4c**) and β -pinene (**4d**) were converted to the corresponding alkyl boronate ester in good yield with excellent selectivity (Scheme 4). Interestingly, 4,3-selective hydroboration of 2-substituted 1,3-diene (**4c**) was observed for both the catalysts. Note that, hydroboration of dienes to access allylboranes is less-established, and only known with transition metals such as Fe,³⁶ Co,³⁷ Ni,³⁸ Ir,³⁹ etc. This is the first report of a main group element catalyzed selective hydroboration of myrcene.



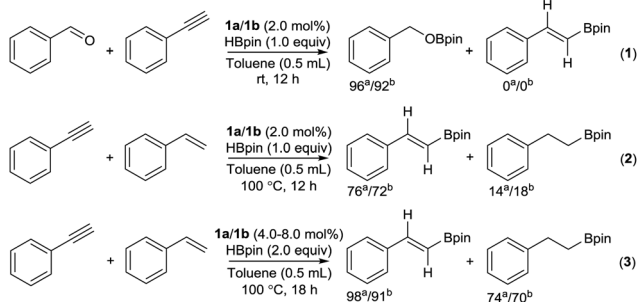
Scheme 4 Selective alkene hydroboration for terpenes.



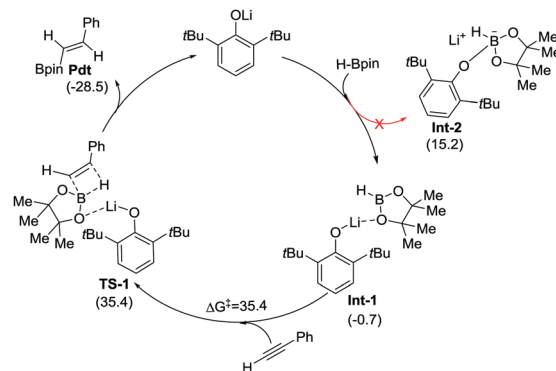
Scheme 5 Deuterium labelling experiment: (a) hydroboration of phenylacetylene- d with HBpin. (b) Hydroboration of phenylacetylene with DBpin.

Deuterium labelling experiments were carried out for the catalytic hydroboration of alkynes to understand the stereoselectivity. A sharp resonance at δ 6.18 ppm in the ^2H NMR for the catalytic reduction of $\text{PhC}\equiv\text{CD}$ with HBpin designates a *cis* configuration of the deuterium and phenyl ring [(a), Scheme 5]. Similarly, the *cis* arrangement of deuterium and the Bpin moiety was confirmed from the resonance at δ 7.28 ppm in the ^2H NMR spectrum for the catalytic reaction of $\text{PhC}\equiv\text{CH}$ and DBpin [(b), Scheme 5]. This experiment attests a *cis* stereoselectivity, which is in good agreement with ScOTf mediated alkyne hydroboration, reported by Geetharani and coworkers.⁴⁰ Intermolecular chemoselective hydroboration of aldehydes, alkenes and alkynes was also studied in three different sets of reactions and the results are summarized in Scheme 6.

No appreciable changes in the ^1H NMR was observed from the stoichiometric reaction of **1a** with styrene or phenylacetylene, even after heating at 100 °C overnight. However, the reaction between **1a** and HBpin in toluene- d_8 shows a new set of resonance in the ^{11}B NMR at δ 4.7 ppm, indicating the formation of an intermediate (**Int-1**)^{32,41} along with a singlet at δ 21.6 and a quintet at -39.8 ppm for the formation of a trialkoxyborane [$2,6\text{-}t\text{Bu}_2\text{-C}_6\text{H}_3\text{-OBpin}$] and BH_4^- anion, respectively. In addition, a singlet at δ 86.9 and a quartet at -25.4 ppm were also observed, probably due to the decomposition of HBpin and the Lewis base- BH_3 adduct.⁴² A white precipitate is formed in the NMR tube after 3–4 h and the filtrate part shows only three peaks at δ 4.7, 21.6 and -39.8 ppm in the ^{11}B NMR spectrum (see ESI,† Scheme S8). The elimination of LiH could lead to the formation of both trialkoxyborane and LiBH_4 .⁴³ However, due to the very high lattice energy and poor solubility, the involvement of LiH in the catalytic activity is very unlikely, which was also noted by the groups of Mulvey,³³ Thomas, and Cowley.²³ No conclusive NMR spectra



Scheme 6 Competitive experiments for chemoselective hydroboration.

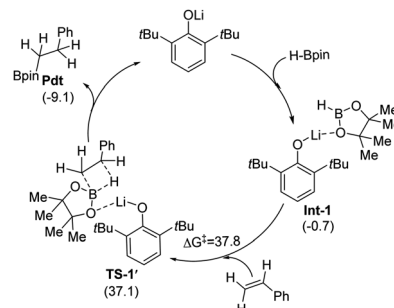


Scheme 7 The catalytic cycle and reaction mechanism for the alkyne hydroboration by catalyst **1a**, calculated at the PBE/TZVP level of theory with DFT. The relative free energy (ΔG) for each species is shown within parentheses in the catalytic cycle. ΔG^\ddagger represents the Gibbs free energy of activation respectively. All values are in kcal mol⁻¹.

were obtained from the stoichiometric reactions between **1b** and HBpin and peak broadening was always observed.

Full quantum chemical calculations were done with density functional theory (DFT) at the dispersion and solvent corrected PBE/TZVP level of theory in order to understand the mechanism (Schemes 7 and 8) of the alkene and alkyne hydroboration reactions in the presence of **1a** [please see the ESI,† Fig. S81 and S82 for further details].

In the first step of the reaction, a weakly coordinating complex (**Int-1**) is formed between catalyst **1a** and HBpin, with one of the oxygen atoms of pinacolborane approaching towards the lithium atom of **1a**. The reaction energy (ΔE) and the Gibbs free energy (ΔG) for this step are -11.5 kcal mol⁻¹ and -0.7 kcal mol⁻¹ respectively. Another possibility of coordinating phenolate oxygen to the boron atom of pinacolborane leading to a four-coordinate boron complex (**Int-2**) was found to be thermodynamically unfavorable due to the high ΔG (15.2 kcal mol⁻¹) of the reaction. Following this, the alkene or alkyne substrate approaches towards the B–H bond of **Int-1**. This is the overture to the nucleophilic attack by the C–C double or triple bond of the alkene or alkyne to the boron centre of the HBpin, with the hydride being transferred from the boron centre to the alkene or alkyne carbon centre having minimum hydrogen. This occurs through a four-membered transition state (**TS-1**)/(TS-1') and leads to the respective hydroboration



Scheme 8 The catalytic cycle and reaction mechanism for the alkene hydroboration by catalyst **1a**.

product along with the regeneration of the catalyst. The ΔE ($-32.8 \text{ kcal mol}^{-1}$ and $-11.9 \text{ kcal mol}^{-1}$) and ΔG ($-28.5 \text{ kcal mol}^{-1}$ and $-9.1 \text{ kcal mol}^{-1}$) values for these steps are highly negative and the barriers (ΔG^\ddagger s) corresponding to the transition states are moderate: $35.4 \text{ kcal mol}^{-1}$ and $37.8 \text{ kcal mol}^{-1}$ for the alkyne and alkene respectively. The moderate barriers explain the delicate feasibility of the reaction at 100°C . In the transition states, there is a significant amount of B–H bond activation (1.27 \AA vs. 1.19 \AA in the intermediate complex), which allows the hydride transfer from the boron to the alkene or alkyne carbon centre, along with the simultaneous C–C double and triple bond cleavage and B–O bond formation.

In summary, we are unwavering the utility of very simple, cost effective and almost non-toxic lithium compounds (**1a** and **1b**) for the catalytic hydroboration of a range of alkenes and alkynes including conjugated terpenes. The chemoselectivity and regioselectivity for the described catalytic process have been investigated. DFT calculations reveal that the role of the Li compounds could be interpreted in the binding of sterically demanding Lewis acids to one of the Lewis basic O atoms of HBpin, and thereby setting up a platform for the HBpin to offer its B–H bond to the unsaturated alkene and alkyne.

Science and Engineering Research Board (SERB), India (CRG/2018/000287) (SSS), and (EMR/2014/000013) (KV) are acknowledged for providing financial assistance. MKB, SY, and TD thank CSIR, India, for the research fellowships.

Conflicts of interest

There are no conflicts to declare.

Notes and references

- C. E. Tucker, J. Davidson and P. Knochel, *J. Org. Chem.*, 1992, **57**, 3483–3485.
- For reviews on transition metal catalyzed hydroboration: (a) I. Beletskaya and A. Pelter, *Tetrahedron*, 1997, **53**, 4957–5026; (b) N. Miyaura in *Catalytic Heterofunctionalization*, ed. A. Togni and H. Grützmacher, Wiley-VCH, Weinheim, 2001, pp. 1–46; (c) C. M. Vogels and S. W. Westcott, *Curr. Org. Chem.*, 2005, **9**, 687–699.
- M. Arrowsmith, T. J. Hadlington, M. S. Hill and G. Kociok-Köhn, *Chem. Commun.*, 2012, **48**, 4567–4569.
- M. Arrowsmith, M. S. Hill and G. Kociok-Köhn, *Chem. – Eur. J.*, 2013, **19**, 2776–2783.
- C. Weetman, M. S. Hill and M. F. Mahon, *Chem. Commun.*, 2015, **51**, 14477–14480.
- K. Manna, P. Ji, F. X. Greene and W. Lin, *J. Am. Chem. Soc.*, 2016, **138**, 7488–7491.
- D. Mukherjee, S. Shirase, T. P. Spaniol, K. Mashima and J. Okuda, *Chem. Commun.*, 2016, **52**, 13155–13158.
- L. Fohlmeister and A. Stasch, *Chem. – Eur. J.*, 2016, **22**, 10235–10246.
- C. Weetman, M. D. Anker, M. Arrowsmith, M. S. Hill, G. Kociok-Köhn, D. J. Liptrot and M. F. Mahon, *Chem. Sci.*, 2016, **7**, 628–641.
- S. Yadav, S. S. Pahar and S. S. Sen, *Chem. Commun.*, 2017, **53**, 4562–4564.
- S. Yadav, R. Dixit, M. K. Bisai, K. Vanka and S. S. Sen, *Organometallics*, 2018, **37**, 4576–4584.
- D. Mukherjee, A. Ellern and A. D. Sadow, *Chem. Sci.*, 2014, **5**, 959–964.
- N. L. Lampland, M. Hovey, D. Mukherjee and A. D. Sadow, *ACS Catal.*, 2015, **5**, 4219–4226.
- For reviews on main group compound carbonyl hydroboration, see: (a) M. L. Shegavi and S. K. Bose, *Catal. Sci. Technol.*, 2019, **9**, 3307–3336; (b) C. C. Chong and R. Kinjo, *ACS Catal.*, 2015, **5**, 3238–3259.
- Z. Yang, M. Zhong, X. Ma, K. Nijesh, S. De, P. Parameswaran and H. W. Roesky, *J. Am. Chem. Soc.*, 2016, **138**, 2548–2551.
- A. Bismuto, S. P. Thomas and M. J. Cowley, *Angew. Chem., Int. Ed.*, 2016, **55**, 15356–15359.
- J. S. McGough, S. M. Butler, I. A. Cade and M. J. Ingleson, *Chem. Sci.*, 2016, **7**, 3384–3389.
- M. Fleige, J. Möbus, T. V. Stein, F. Glorius and D. W. Stephan, *Chem. Commun.*, 2016, **52**, 10830–10833.
- (a) J. R. Lawson, L. C. Wilkins and R. L. Melen, *Chem. – Eur. J.*, 2017, **23**, 10997–11000; (b) J. L. Carden, L. J. Gierlichs, D. F. Wass, D. L. Browne and R. L. Melen, *Chem. Commun.*, 2019, **55**, 318–321.
- D. Franz, L. Sirtl, A. Pöthig and S. Inoue, *Z. Anorg. Allg. Chem.*, 2016, **642**, 1245–1250.
- Q. Yin, S. Kemper, H. F. T. Klare and M. Oestreich, *Chem. – Eur. J.*, 2016, **22**, 13840–13844.
- A. Prokofjevs, A. Boussonniere, L. Li, H. Bonin, E. Lacite, D. P. Curran and E. Vedejs, *J. Am. Chem. Soc.*, 2012, **134**, 12281–12288.
- A. Bismuto, M. J. Cowley and S. P. Thomas, *ACS Catal.*, 2018, **8**, 2001–2005.
- M. Magre, B. Maity, A. Falconnet, L. Cavallo and M. Rueping, *Angew. Chem., Int. Ed.*, 2019, **58**, 7025–7029.
- M. Rauch, S. Rucolo and G. Parkin, *J. Am. Chem. Soc.*, 2017, **139**, 13264–13267.
- Y. Wu, C. Shan, J. Ying, J. Su, J. Zhu, L. L. Liu and Y. Zhao, *Green Chem.*, 2017, **19**, 4169–4175.
- V. A. Pollard, M. A. Fuentes, A. R. Kennedy, R. McLellan and R. E. Mulvey, *Angew. Chem., Int. Ed.*, 2018, **57**, 10651–10655.
- L. E. Lemmerz, R. McLellan, N. R. Judge, A. R. Kennedy, S. A. Orr, M. Uzelac, E. Hevia, S. D. Robertson, J. Okuda and R. E. Mulvey, *Chem. – Eur. J.*, 2018, **24**, 9940–9948.
- D. Mukherjee, H. Osseili, T. P. Spaniol and J. Okuda, *J. Am. Chem. Soc.*, 2016, **138**, 10790–10793.
- H. Osseili, D. Mukherjee, K. Beckerle, T. P. Spaniol and J. Okuda, *Organometallics*, 2017, **36**, 3029–3034.
- H. Osseili, D. Mukherjee, T. P. Spaniol and J. Okuda, *Chem. – Eur. J.*, 2017, **23**, 14292–14298.
- M. K. Bisai, T. Das, K. Vanka and S. S. Sen, *Chem. Commun.*, 2018, **54**, 6843–6846.
- R. McLellan, A. R. Kennedy, R. E. Mulvey, S. A. Orr and S. D. Robertson, *Chem. – Eur. J.*, 2017, **23**, 16853–16861.
- D. Yan, X. Wu, J. Xiao, Z. Zhu, X. Xu, X. Bao, Y. Yao, Q. Shen and M. Xue, *Org. Chem. Front.*, 2019, **6**, 648–653.
- S. Bruña, A. M. González-Vadillo, M. Ferrández, J. Perles, M. M. Montero-Campillo, O. Mób and I. Cuadrado, *Dalton Trans.*, 2017, **46**, 11584–11597.
- J. Y. Yu, B. Moreau and T. Ritter, *J. Am. Chem. Soc.*, 2009, **131**, 12915–12917.
- R. J. Ely and J. P. Morken, *J. Am. Chem. Soc.*, 2010, **132**, 2534–2535.
- J. V. Obligation and P. J. Chirik, *J. Am. Chem. Soc.*, 2013, **135**, 19107–19110.
- D. Fiorito and C. Mazet, *ACS Catal.*, 2018, **8**, 9382–9387.
- S. Mandal, P. K. Verma and K. Geetharani, *Chem. Commun.*, 2018, **54**, 13690–13693.
- (a) A. Bonet, H. Gulyás and E. Fernández, *Angew. Chem., Int. Ed.*, 2010, **49**, 5130–5134; (b) R. Dasgupta, S. Das, S. Hiwase, S. Pati and S. Khan, *Organometallics*, 2019, **38**, 1429–1435.
- K. Burgess, W. A. vander Donk, S. A. Westcott, T. B. Marder, R. T. Baker and J. C. Calabrese, *J. Am. Chem. Soc.*, 1992, **114**, 9350–9359.
- I. P. Query, P. A. Squier, E. M. Larson, N. A. Isley and T. B. Clark, *J. Org. Chem.*, 2011, **76**, 6452–6456.

Synthesis and Reactivity of a Hypersilylsilylene

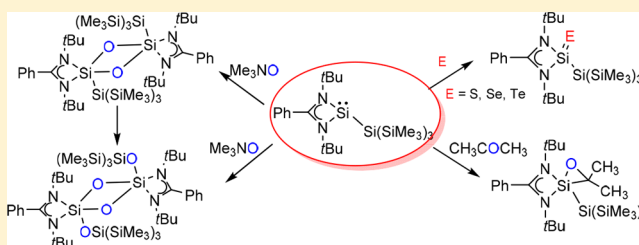
Milan Kumar Bisai,^{†,§} V. S. V. S. N. Swamy,^{†,§} Tamal Das,^{‡,§} Kumar Vanka,^{‡,§} Rajesh G. Gonnade,^{‡,§} and Sakya S. Sen^{*,†,§}

[†]Inorganic Chemistry and Catalysis Division and [‡]Physical and Material Chemistry Division, CSIR-National Chemical Laboratory, Dr. Homi Bhabha Road, Pashan, Pune 411008, India

[§]Academy of Scientific and Innovative Research, Ghaziabad 201002, India

Supporting Information

ABSTRACT: Stabilization of an amidinosilylene with a bulky tris(trimethylsilyl)silyl substituent was realized with the preparation of $\text{PhC}(\text{N}t\text{Bu})_2\text{Si}\{\text{Si}(\text{SiMe}_3)_3\}$ (**1**) from $\text{PhC}(\text{N}t\text{Bu})_2\text{SiHCl}_2$ with $\text{K}\{\text{Si}(\text{SiMe}_3)_3\}$ in more than 90% yield. The highly deshielded ^{29}Si NMR resonance ($\delta = 76.91$ ppm) can be attributed to the absence of a π -donating substituent. The molecular structure of **1** shows a trigonal-planar geometry around the Si^{II} center with a $\text{Si}^{\text{II}}\text{--Si}^{\text{IV}}$ bond length of 2.4339(13) Å. A series of reactions of **1** with Me_3NO , S, Se, and Te were performed. While siloxane derivatives (**2** and **3**) are obtained from reactions with Me_3NO , silachalcogenones (**4**–**6**) are formed with other chalcogens. The presence of $\text{Si}=\text{E}$ ($\text{E} = \text{S}, \text{Se}, \text{and Te}$) bonds in **4**–**6** have been confirmed by single-crystal X-ray studies. Silaoxirane (**7**) formation was observed when **1** was treated with acetone, demonstrating the importance of the tris(trimethylsilyl)silyl group to kinetically and thermodynamically protect the silaoxirane derivative with less bulky substituents on the C atom.



INTRODUCTION

The chemistry of silylenes continues to be a thriving and rapidly developing area in synthetic chemistry, driven primarily by the fundamental studies of structure and bonding but also encompassing more reactivity studies.¹ One of the most extensively studied silylenes is the benzamidinato-stabilized silylene of composition LSiX [$\text{L} = \text{PhC}(\text{N}t\text{Bu})_2$]^{1e–i,2} presumably because of their ease of synthesis and thermal stability.³ However, a closer look would reveal that the majority of amidinosilylenes contain an electron-rich π -donating functionalized group (X) such as Cl (**A**),³ Br (**B**),⁴ $\text{O}i\text{Pr}$ (**C**),⁵ NR_2 [$\text{R} = \text{Ph}$ (**D**),⁶ Cy (**E**),⁶ $i\text{Pr}$ (**F**),⁶ SiMe_3 (**G**)⁷], $\text{P}(\text{SiMe}_3)_2$ (**H**)⁸, etc. Replacement of the π -donor ligand with a σ -donor group may reduce the highest occupied molecular orbital (HOMO)–lowest unoccupied molecular orbital (LUMO) gap, but this would add more synthetic challenges. Nevertheless, the group of H. W. Roesky isolated the alkyl-functionalized amidinosilylene $\text{PhC}(\text{N}t\text{Bu})_2\text{Si}t\text{Bu}$ (**I**).⁹ Subsequently, the group of P. W. Roesky prepared the pentamethylcyclopentadienyl-functionalized amidinosilylene $\text{PhC}(\text{N}t\text{Bu})_2\text{SiCp}^*$ (**J**).¹⁰ However, their reactivity studies are not well-documented, apart from the use of **J** as a ligand for zinc complexes.¹⁰ Parallel to this, Driess and co-workers prepared bis(silylenyl)ferrocene (**K**)¹¹ from the reaction of amidinatochlorosilylene (**A**) with dilithiated ferrocene. Very recently, Cui et al. reported a tethered amidinosilylene, $\text{PhC}(\text{N}t\text{Bu})_2\text{SiCH}_2\text{C}(t\text{Bu})\text{NDipp}$ (**L**; $\text{Dipp} = 2,6\text{-}i\text{Pr}_2\text{-C}_6\text{H}_3$), where the Si^{II} unit is bound to the CH_2 moiety,¹² while Cabeza et al. prepared a mesityl-substituted amidinosilylene, PhC

$(\text{N}t\text{Bu})_2\text{SiMes}$ (**M**; $\text{Mes} = 2,4,6\text{-Me}_3\text{-C}_6\text{H}_2$).¹³ Silanides, being the heavier congeners to classical alkyl ligands, are of increasing importance because they have greater σ -donor strength than alkyl and π -donating ligands. However, access to silyl-substituted amidinosilylene has not been reported yet.

Since the pioneering work by Benkeser, Gilman, and Smith on the synthesis of tetrakis(trimethylsilyl)silane,¹⁴ there is an increasing use of the tris(trimethylsilyl)silyl group in the synthesis of numerous organometallic compounds^{15,16} because it possesses a pronounced steric effect. Apart from the steric bulk, another major factor is the strong σ -donor strength of the silyl ligand. The delicate balance between these two factors—strong σ donation and kinetic protection—has orchestrated a rapid development in low-valent main-group chemistry. The usefulness of the tris(trimethylsilyl)silyl group in low-valent silicon chemistry has been amply exemplified by Aldridge and co-workers in the isolation of a stable mixed (amido)-silylsilylene, $\text{Si}\{\text{Si}(\text{SiMe}_3)_3\}\{\text{N}(\text{SiMe}_3)\text{Dipp}\}$.¹⁷ While silylenes with π -donating ligands have not been reported for dihydrogen activation, the silylenes lacking π -donor ligands are found to split dihydrogen in a facile manner,^{17,18} which can be attributed to a decrease of π donation, leading to a reduction in the HOMO–LUMO gap. This significant result led us to study the synthesis of tris(trimethylsilyl)silylamidinosilylene

Special Issue: Celebrating the Year of the Periodic Table: Emerging Investigators in Inorganic Chemistry

Received: February 12, 2019

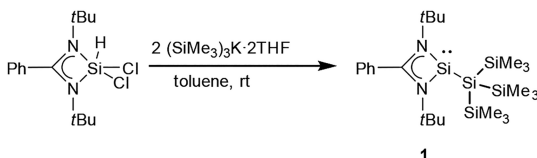
Published: April 24, 2019

(1). Subsequent to the synthesis of the silylene, we studied its reactivity toward S, Se, and Te, which led to silicon(IV) complexes with Si=E bonds. The reaction of **1** with acetone affords the first structurally authenticated silaoxirane derivative (**7**). Our results are reported herein.

RESULTS AND DISCUSSION

The treatment of $\text{PhC}(\text{N}t\text{Bu})_2\text{SiHCl}_2$ with 2 equiv of $\text{KSi}(\text{SiMe}_3)_3$ in toluene at room temperature for 8 h afforded a new monomeric hypersilylsilane(II) compound (**1**) in more than 90% yield (Scheme 1). **1** is stable at room temperature

Scheme 1. Synthesis of **1**



and is the first example of a system having a $\text{Si}^{\text{II}}\text{--Si}^{\text{IV}}$ bond with an amidinate moiety. **1** has been isolated as a pale-yellow crystalline solid with good solubility in toluene, tetrahydrofuran, diethyl ether, and *n*-hexane. Previously, Kira and co-workers reported the isomerization of dialkylsilylene to the corresponding silaethene via 1,2-trimethylsilyl migration.¹⁹ We have also heated **1** up to 100 °C, but no migration of the trimethylsilyl group was observed. The ¹H NMR spectrum of **1** displays a resonance at 0.51 ppm for the three SiMe₃ groups. The resonance for the *t*Bu protons of the amidinate moiety appears at 1.21 ppm, integrating for 18 protons. The ²⁹Si NMR of **1** exhibits three resonances at 76.91 ppm for the Si^{II} center, –8.36 ppm for SiMe₃ moieties, and –11.84 ppm for the silyl Si(SiMe₃)₃ moiety. The lack of π -donating substituents is reflected in the ²⁹Si NMR chemical shift of the Si^{II} center, which is significantly downfield with respect to those in **A–H**. The value is very close to that in $[\text{PhC}(\text{N}t\text{Bu})_2\text{Si}]_2$ (75.71 ppm).²⁰ In the high-resolution mass spectrometry spectrum, the molecular ion is observed as the most abundant peak, with the highest relative intensity at *m/z* 507.2883.

The molecular structure of **1** is shown in Figure 1, while the important bond lengths and angles are provided in the caption of Figure 1. **1** crystallizes in the monoclinic space group $P2_1/n$.

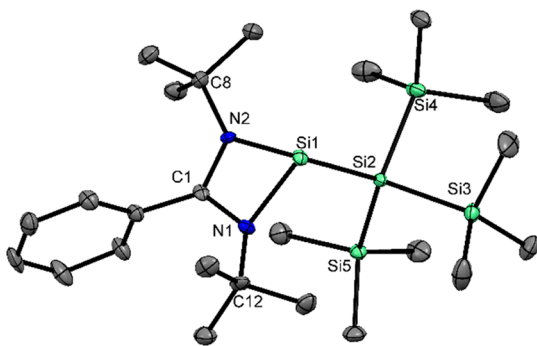
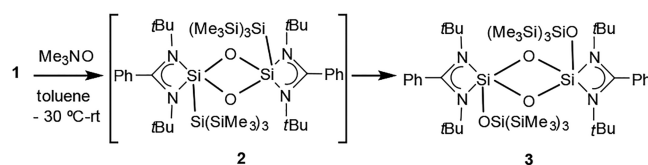


Figure 1. Molecular structure of **1**. Anisotropic displacement parameters are depicted at the 50% probability level. Selected bond lengths (Å) and angles (deg): Si1–Si2 2.4339(13), Si2–Si5 2.3472(12), Si2–Si4 2.3690(13), Si2–Si3 2.3746(12), Si1–N1 1.885(3), Si1–N2 1.873(3); N1–Si1–N2 69.27(11), N1–Si1–Si2 103.14(9), N2–Si1–Si2 105.49(9).

The Si atom is three-coordinate and features a trigonal-pyramidal geometry with a lone pair of electrons residing on the apex. The Si1–Si2 bond length in **1** is 2.433(13) Å, which is longer than the typical Si–Si single bond (2.35 Å), Aldridge's $\text{Si}\{\text{Si}(\text{SiMe}_3)_3\}\{\text{N}(\text{SiMe}_3)\text{Dipp}\}$ [2.386(1) Å],¹⁷ and the Si–Si bond length in interconnected amidinatobis(silylene) $[\text{PhC}(\text{N}t\text{Bu})_2\text{Si}]_2$ [2.413(2) Å].²⁰ The other Si–Si bond lengths vary from 2.3475(12) to 2.3740(13) Å, which are shorter than the Si1–Si2 bond. We have done geometry optimization of **1** for the ground-state singlet and triplet geometries using density functional theory (DFT) at the PBE/TZVP level (see the Supporting Information, SI). The singlet geometry is seen to be more stable than the triplet by 38.6 kcal mol^{–1}. The HOMO is located at the Si^{II} center of **1**, and the LUMO is spread over the phenyl ring of the amidinate ligand. The HOMO–LUMO energy gap for the silylene has been determined to be 3.7 eV. We have also calculated the HOMO–LUMO energy gaps for the known amidinatosilylenes using DFT studies, which reveal that the gaps are usually more than 4.00 eV [e.g., **A** (4.40 eV), **B** (4.35 eV), and **G** (4.13 eV)]; see the SI). The decrease in the HOMO–LUMO gap for **1** results from the lack of π donation from the substituent bound to the Si^{II} center.

The reactions of silylene with oxygen-containing substrates are always interesting because they pave the way for siloxanes, which are used as precursors for siloxane-high polymers by the reactions of ring-opening living polymerization with anionic initiators.²¹ The reaction of **1** with Me₃NO led to stepwise O insertion. In the first case, the O attacks the Si^{II} center, which leads to a cyclodisiloxane derivative (**2**), presumably resulting from dimerization of the putative $\text{LSi}(\text{=O})\text{Si}(\text{SiMe}_3)_3$.²² Subsequent insertion of O takes place at the Si–Si bond, leading to **3** (Scheme 2). It is of note here that the formation

Scheme 2. Reaction of **1** with Trimethyl *N*-Oxide and Formation of **2** and **3**



of **2** was serendipitous, and we were fortunate to characterize it by single-crystal X-ray diffraction studies. **2** crystallizes in the monoclinic space group $P2_1/n$. The molecular structure of **2** is shown in Figure 2. The structure consists of a four-membered Si₂O₂ ring with a five-coordinate Si atom. The Si1–Si2 bond distance in **2** [2.5099(18) Å] is significantly elongated in comparison to that in **1**. This bond elongation is probably a consequence of the increased coordination number and enhanced steric bulk at the Si center. However, we were not able to prepare **2** on a reasonable scale that allows for full spectroscopic characterization. Nevertheless, a variable-temperature NMR experiment in toluene-*d*₈ shows the shift of the SiMe₃ protons from 0.54 to 0.51 ppm and finally to 0.49 ppm, indicating the formation of **3** from **1** via **2** (Figure S23).

A substantial increase in the Si1–Si2 bond length in the molecular structure of **2** might facilitate the further insertion of another O atom, which led to the formation of **3**. The ²⁹Si NMR spectrum of **3** features a sharp resonance at –116.06 ppm, which is consistent with previously known five-coordinate Si atoms.¹⁸ The molecular structure of **3** is shown

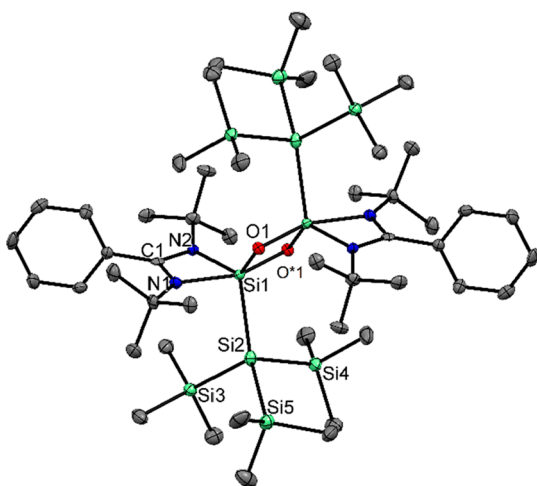


Figure 2. Molecular structure of **2**. Anisotropic displacement parameters are depicted at the 50% probability level. H atoms are omitted for clarity. Selected bond distances (Å) and angles (deg): Si1–N1 2.003(4), Si1–N2 1.849(4), Si1–O1 1.681(3), Si1–O1* 1.723(3), Si1–Si2 2.5099(18); N1–Si1–N2 67.56(17), N1–Si1–O1 91.43(16), N2–Si1–O1 122.58(16), O1–Si1–O1* 83.72(17).

in **Figure 3**. Like **2**, **3** also crystallizes in the monoclinic space group $P2_1/n$ and possesses a Si_2O_2 ring with a five-coordinate

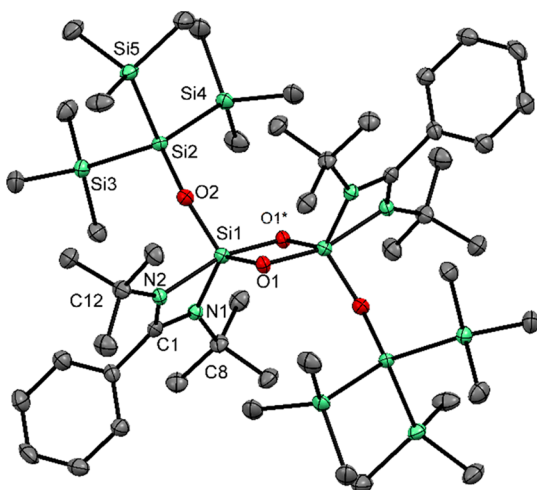


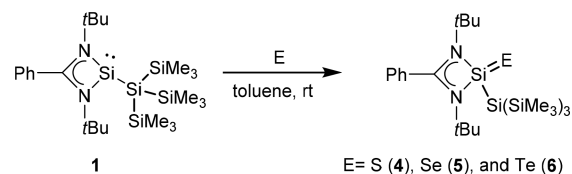
Figure 3. Molecular structure of **3**. Anisotropic displacement parameters are depicted at the 50% probability level. H atoms are omitted for clarity. Selected bond distances (Å) and angles (deg): Si1–N1 1.846(3), Si1–N2 1.965(3), Si1–O1 1.670(2), Si1–O1* 1.718(2), Si1–O2 1.646(2), Si2–O2 1.652(2); N1–Si1–N2 68.33(11), N1–Si1–O1 125.73(11), N2–Si1–O1 92.61(11), O1–Si1–O1* 84.79(11), O1–Si1–O2 119.41(11).

Si atom with three Si–O and two Si–N bonds. Here it is worth mentioning that the Si⋯Si and O⋯O separations in the cyclodisiloxane moiety are 2.53 and 2.27 Å, respectively, for **2**. In the case of **3**, the Si⋯Si and O⋯O separations are 2.50 and 2.28 Å. From these data, it can be understood that there is no bond between the two Si atoms in the cyclodisiloxane rings and they are best described as containing four equivalent localized Si–O bonds with no appreciable σ bonding between the Si atoms.^{22,23}

Generation of silathiones has been shown to be possible from the reaction of silylene with elemental S.^{24–26} However,

sometimes this leads to disilene derivatives,²⁷ for which steric factors have largely been held responsible because bulky substituents can only be introduced at the Si center. We have studied the reactions of **1** with S, Se, and Te, which led to compounds with Si=S (**4**), Si=Se (**5**), and Si=Te (**6**) bonds (**Scheme 3**). The ²⁹Si NMR spectra of **4–6** exhibit resonances

Scheme 3. Reactions of **1** with S, Se, and Te



at 27.50, 23.88, and 1.82 ppm, respectively, which are markedly deshielded from those in $\text{PhC}(\text{N}t\text{Bu})\text{Si}(=\text{E})\text{N}(\text{SiMe}_3)_2$ [–16.9 (S), –20 (Se), and –47.6 (Te) ppm],²⁶ reflecting the substitution of a π -donating NR_2 group with a σ -donating $\text{Si}(\text{SiMe}_3)_3$ moiety. The gradual upfield shift upon going from **4** to **6** is consistent with a decrease of the electronegativity from S to Te, and this trend was also observed for other silylenes.^{24,26} The $\text{Si}(\text{SiMe}_3)_3$ groups show high-field resonances at –123.13 (**4**), –119.99 (**5**), and –90.42 (**6**) ppm, which are in good agreement with that reported for the $\text{Si}(\text{SiMe}_3)_3$ group in Inoue's silepin (–138.2 ppm).²⁸ The molecular-ion peaks for **4–6** were detected at m/z 539.2630, 587.2041, and 637.1929, respectively, with the highest relative intensity.

4 crystallizes in the monoclinic space group $C2/c$. The molecular structure of **4** is shown in **Figure 4**. The Si=S bond

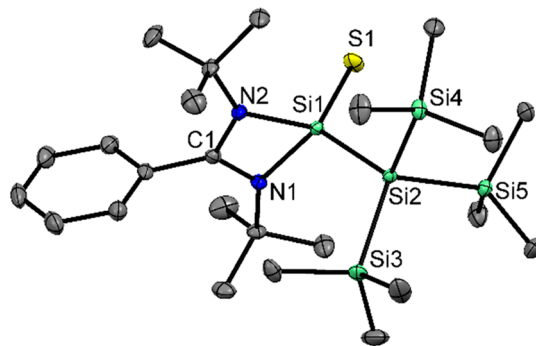


Figure 4. Molecular structure of **4**. Anisotropic displacement parameters are depicted at the 50% probability level. Selected bond lengths (Å) and angles (deg): Si1–N1 1.8538(13), Si1–N2 1.8578(14), Si1–S1 1.9996(6), Si1–Si2 2.3525(6); N1–Si1–N2 70.66(6), S1–Si1–Si2 113.82(2), N1–Si1–S1 118.23(5), N2–Si1–S1 117.29(5).

length in **4** is 1.9996(6) Å, which is consistent with a Si=S bond and in good agreement with the Si=S bond in $[\{\text{PhC}(\text{N}t\text{Bu})_2\}\text{Si}(\text{S})\text{N}(\text{SiMe}_3)_2]$ [1.987(8) Å], reported by Khan and co-workers.²⁵ However, the Si=S bond length in **4** is longer than that in the silanethiones with three-coordinate Si atoms [1.948(4) and 1.9575(7) Å]^{24,29} but marginally shorter than the Si=S bond with a five-coordinate Si atom [2.0193(9) Å].³⁰ Formation of the Si=S bond is accompanied by a decrease in the Si1–Si2 bond length [2.3525(6) Å].

5 crystallizes in the monoclinic space group $P2_1$. **Figure 5** depicts the molecular structure of **5**. The Si=Se bond length

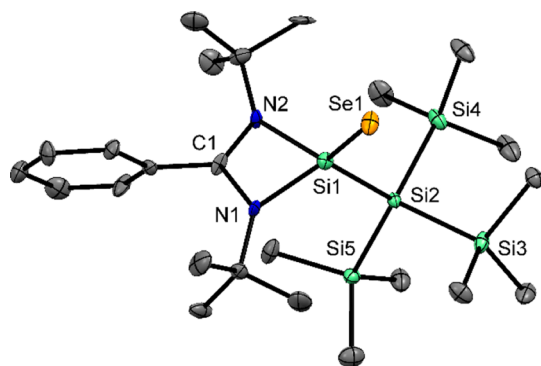


Figure 5. Molecular structure of **5**. Anisotropic displacement parameters are depicted at the 50% probability level. Selected bond lengths (Å) and angles (deg): Si1–N1 1.873(13), Si1–N2 1.857(13), Si1–Se1 2.139(4), Si1–Si2 2.357(6); N1–Si1–N2 70.1(6), Se1–Si1–Si2 114.3(2), N1–Si1–Se1 117.6(5), N2–Si1–Se1 118.4(5).

in **5** is 2.139(4) Å, which is consistent with the reported Si=Se bond length [2.136(9) Å] by Khan and co-workers,²⁵ and the Si=Se bond in [HC(CMeNAr){C(=CH₂)NAr}Si(NHC)=Se] [2.1457(9) Å] reported by Driess and co-workers.³¹ The Si=Se bond length in **5** is considerably longer than the Si=Se bond reported by Kira's group [2.0963(5) Å],²⁴ where the Si atom is three-coordinate and somewhat shorter than Tacke's silaneselenone with a five-coordinate Si atom [2.1632(7) Å],³⁰ illustrating the dependence of the Si=Se bond length on the coordination number of Si. The molecular structure of **6**, which crystallizes in the orthorhombic space group *P*2₁2₁1 is shown in Figure 6. Consistent

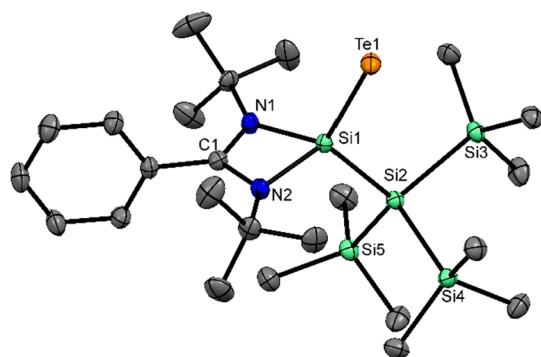


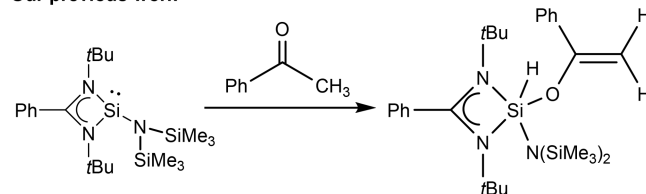
Figure 6. Molecular structure of **6**. Anisotropic displacement parameters are depicted at the 50% probability level. Selected bond lengths (Å) and angles (deg): Si1–N1 1.849(3), Si1–N2 1.855(3), Si1–Te1 2.3723(8), Si1–Si2 2.3620(12); N1–Si1–N2 70.97(12), Te1–Si1–Si2 115.23(4), N1–Si1–Te1 116.33(9), N2–Si1–Te1 116.62(9).

with this trend, the Si=Te bond length in **6** is 2.3723(8) Å, matching well with the other Si=Te bonds with four-coordinate Si atoms [HC(CMeNAr){C(=CH₂)NAr}Si(NHC)=Te, 2.383(2) Å;³¹ PhC(N*t*Bu)₂SiN{(SiMe₃)₂}=Te, 2.3720(15) Å²⁶], longer than Kira's three-coordinate Si=Te bonds [2.3210(6) Å],²⁴ but shorter than Tacke's five-coordinate Si=Te bonds [2.4017(6) Å].³⁰ It is of note here that the presence of the double bond in **4–6** is deduced from geometrical features obtained from the structural studies. Topological analysis of the experimentally determined charge density of these bonds will be a more realistic tool for elucidating the nature of the bonding.³²

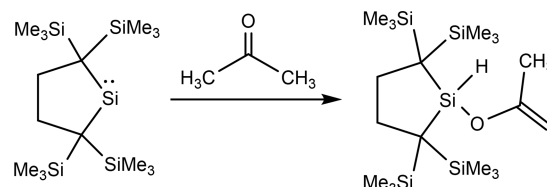
Up to this point, the installed tris(trimethylsilyl)silyl group did not have much of a role to play in all of the reactions that we have described. We were, therefore, looking for a reaction that is not successful with other functionalized amidinosilylenes and may illustrate the importance of the tris(trimethylsilyl)silyl group. One such reaction is formation of the silaoxirane derivative (**7**) with acetone. Silaoxirane, a heavier analogue of epoxides, has been prepared and studied recently because of its high reactivity. One protocol to access the silaoxiranes is the reaction of ketone with silylene. The methodology has been brought to the fore by Roesky and co-workers.³³ However, the formation of such silaoxiranes is feasible only when bulky ketones such as benzophenone and 2-adamantanone are employed.^{33,34} Interestingly, a ketone with a CH₃ unit has a propensity to undergo C–H activation with a silylene (Scheme 4). For example, the reaction of 2-

Scheme 4. Reactions of the Reported Silylenes with Methyl Ketones

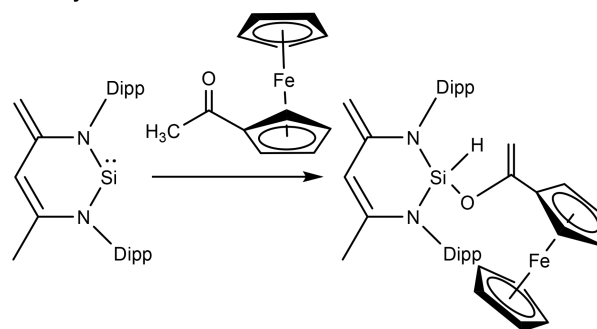
Our previous work



Kira & coworkers



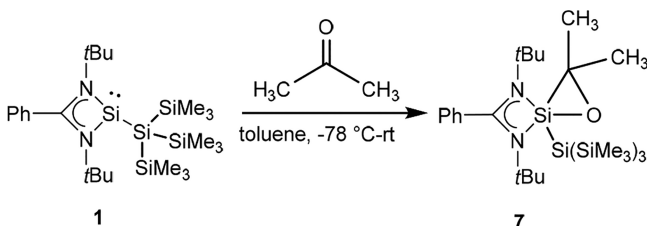
Roesky & coworkers



acylferrocene with Driess' silylene [CH{(C=CH₂)(CMe)(2,6-*i*Pr₂C₆H₃N)₂}Si],³⁴ the reaction of acetone with Kira's dialkylsilylene,³⁵ or the reaction of acetophenone with amidinosilylene PhC(N*t*Bu)₂N(SiMe₃)₂ (**G**)³⁶ led to C–H bond activation of the CH₃ motif. In fact, in 1999, Walsh and co-workers studied the reaction of the parent silylene with acetone using Rice–Ramsperger–Kassel–Marcus (RRKM) modeling and *ab initio* studies and concluded that 2-siloxypropene formation is more favorable than silaoxirane formation.³⁷ Because there is no report of a reaction of any amidinosilylene with acetone, we thought about investigating this reaction with **1** to see if (a) silaoxirane is formed or (b) C–H bond activation occurs. The reaction indeed led to

silaoxirane (7) formation, benefiting from steric protection as well as thermodynamic stability from the $-\text{Si}(\text{SiMe}_3)_3$ substituent (Scheme 5). Although the mechanism for

Scheme 5. Reaction of 1 with Acetone and the Formation of Silaoxirane 7



formation of 7 has not been definitively established, we presume that the attack at the Si electrophile by the O atom of acetone initiates the reaction with subsequent ring closure (Figure S24). 7 forms colorless crystals and shows durability in the solid state as well as in the solution state under an inert gas atmosphere with good benzene or toluene solubility. The ^{29}Si NMR spectrum of 7 shows a resonance at -96.42 ppm, consistent with a five-coordinate Si atom. 7 crystallizes in the monoclinic space group $P2_1/c$. The molecular structure of 7 is depicted in Figure 7. The Si atom in 7 is five-coordinate with

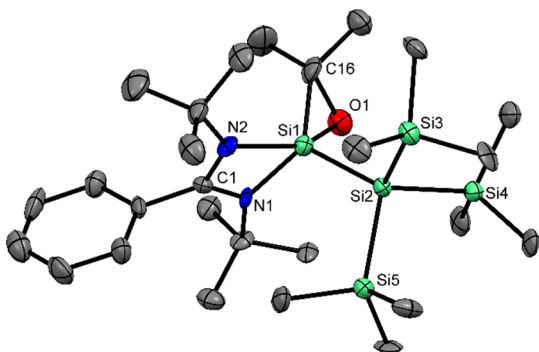


Figure 7. Molecular structure of 7. Anisotropic displacement parameters are depicted at the 50% probability level. Selected bond lengths (Å) and angles (deg): Si1–Si2 2.370(3), Si1–O1 1.729(5), Si1–C16 1.819(9), C16–O1 1.508(9), Si1–N1 1.843(6), Si1–N2 2.002(6); O1–Si1–C16 50.2(3), C16–O1–Si1 68.0(4), N1–Si1–N2 67.5(3), O1–Si1–Si2 104.5(2), O1–Si1–N2 148.0(3), C16–Si1–Si2 120.4(3), N1–Si1–Si2 117.9(2), C16–Si1–N1 119.7(4).

distorted trigonal-bipyramidal geometry, with $148.0(3)^\circ$ the largest bond angle for O1–Si1–N2. N1, Si2, and C16 reside in the equatorial positions, whereas N2 and O1 occupy the axial positions. The Si–O bond distance in the ring is $1.729(5)$ Å, which is in good agreement with the Si–O single bonds observed for 2 and 3. The Si–C bond length of $1.819(9)$ Å is typical for a Si–C single bond.³⁸

CONCLUSIONS

In summary, we have synthesized a new hypersilylsilylene (1) by using a bulky σ -donating $-\text{Si}(\text{SiMe}_3)_3$ substituent featuring the longest reported $\text{Si}^{\text{II}}-\text{Si}^{\text{IV}}$ bond. DFT studies revealed that the HOMO–LUMO energy gap is 3.7 eV. The attachment of a σ -donor ligand in the Si^{II} center is accompanied by a markedly downfield ^{29}Si NMR shift at 76.91 ppm. The reactivity of 1 with Me_3NO presented a stepwise O insertion to

form dimeric products (2 and 3) containing a Si_2O_2 unit. Subsequently, silachalcogenones (4–6) were synthesized by the oxidative addition of 1 with S, Se, or Te. Their X-ray structures are consistent with the silicon–chalcogen double-bond character in these compounds. The reaction of acetone with 1 represents the first example of the formation of a silaoxirane derivative (7) from a methyl ketone, which was previously known to undergo C–H bond activation upon reaction with silylene. The formation of 7 can be attributed to kinetic and thermodynamic protection provided by the bulky $-\text{Si}(\text{SiMe}_3)_3$ ligands.

ASSOCIATED CONTENT

Supporting Information

The Supporting Information is available free of charge on the ACS Publications website at DOI: 10.1021/acs.inorgchem.9b00418.

Synthesis and crystal description of 1–7, details of theoretical calculations (A, B, G, and 1), and representative NMR spectra (PDF)

Accession Codes

CCDC 1895534–1895537, 1895590, 1895596, and 1895606 contain the supplementary crystallographic data for this paper. These data can be obtained free of charge via www.ccdc.cam.ac.uk/data_request/cif, or by emailing data_request@ccdc.cam.ac.uk, or by contacting The Cambridge Crystallographic Data Centre, 12 Union Road, Cambridge CB2 1EZ, UK; fax: +44 1223 336033.

AUTHOR INFORMATION

Corresponding Author

*E-mail: ss.sen@ncl.res.in.

ORCID

Kumar Vanka: 0000-0001-7301-7573

Rajesh G. Gonnade: 0000-0002-2841-0197

Sakya S. Sen: 0000-0002-4955-5408

Notes

The authors declare no competing financial interest.

ACKNOWLEDGMENTS

This work was supported by the Science and Engineering Research Board, India (Grant CRG/2018/000287). M.K.B., V.S.V.S.N.S., and T.D. thank CSIR, India, for research fellowships. K.V. is grateful to the Department of Science and Technology (Grant EMR/2014/000013) for providing financial assistance, and R.G.G. acknowledges CSIR-National Chemical Laboratory for funding.

REFERENCES

- (1) For recent reviews on silylene, see: (a) Haaf, M.; Schmedake, T. A.; West, R. Stable Silylenes. *Acc. Chem. Res.* **2000**, *33*, 704–714. (b) Gehrhuis, B.; Lappert, M. F. Chemistry of Thermally Stable Bis(amino)silylenes. *J. Organomet. Chem.* **2001**, *617*–618, 209–223. (c) Nagendran, S.; Roesky, H. W. The Chemistry of Aluminum(I), Silicon(II), and Germanium(II). *Organometallics* **2008**, *27*, 457–492. (d) Kira, M. An Isolable Dialkylsilylene and its Derivatives. A Step Toward Comprehension of Heavy Unsaturated Bonds. *Chem. Commun.* **2010**, *46*, 2893–2903. (e) Yao, S.; Xiong, Y.; Driess, M. Zwitterionic and Donor-Stabilized N-Heterocyclic Silylenes (NHSis) for Metal-Free Activation of Small Molecules. *Organometallics* **2011**, *30*, 1748–1767. (f) Asay, M.; Jones, C.; Driess, M. N-Heterocyclic Carbene Analogues with Low-Valent Group 13 and Group 14

- Elements: Syntheses, Structures, and Reactivities of a New Generation of Multitalented Ligands. *Chem. Rev.* **2011**, *111*, 354–396. (g) Sen, S. S.; Khan, S.; Samuel, P. P.; Roesky, H. W. Chemistry of Functionalized Silylenes. *Chem. Sci.* **2012**, *3*, 659–682. (h) Sen, S. S.; Khan, S.; Nagendran, S.; Roesky, H. W. Interconnected Bis-Silylenes: A New Dimension in Organosilicon Chemistry. *Acc. Chem. Res.* **2012**, *45*, 578–587. (i) Ghadwal, R. S.; Azhakar, R.; Roesky, H. W. Dichlorosilylene: A High Temperature Transient Species to an Indispensable Building Block. *Acc. Chem. Res.* **2013**, *46*, 444–456. (j) Yadav, S.; Saha, S.; Sen, S. S. Compounds with Low-Valent p-Block Elements for Small Molecule Activation and Catalysis. *ChemCatChem* **2016**, *8*, 486–501. (k) Teichmann, J.; Wagner, M. Silicon Chemistry in Zero to Three Dimensions: From Dichlorosilylene to Silafullerene. *Chem. Commun.* **2018**, *54*, 1397–1412. (l) Chu, T.; Nikonov, G. I. Oxidative Addition and Reductive Elimination at Main-Group Element Centers. *Chem. Rev.* **2018**, *118*, 3608–3680.
- (2) (a) Blom, B.; Driess, M. In *Functional Molecular Silicon Compounds II*; Scheschke, D., Ed.; Springer, 2014. (b) Alvarez-Rodriguez, L.; Cabeza, J. A.; Garcia-Alvarez, P.; Polo, D. Transition-Metal Chemistry of Amidinatosilylenes, -Germynes and -Stannylenes. *Coord. Chem. Rev.* **2015**, *300*, 1–28. (c) Blom, D.; Gallego, D.; Driess, M. N-heterocyclic silylene complexes in catalysis: new frontiers in an emerging field. *Inorg. Chem. Front.* **2014**, *1*, 134–148. (d) Blom, D.; Stoelzel, M.; Driess, M. New Vistas in N-Heterocyclic Silylene (NHSi) Transition-Metal Coordination Chemistry: Syntheses, Structures and Reactivity towards Activation of Small Molecules. *Chem. - Eur. J.* **2013**, *19*, 40–62. (e) Zhou, Y.-P.; Driess, M., Isolable Silylene Ligands Can Boost Efficiencies and Selectivities in Metal-Mediated Catalysis. *Angew. Chem., Int. Ed.*, **2019**, *58*, 3715–3728.
- (3) (a) Sen, S. S.; Roesky, H. W.; Stern, D.; Henn, J.; Stalke, D. High Yield Access to Silylene RSiCl ($\text{R} = \text{PhC}(\text{N}t\text{Bu})_2$) and Its Reactivity toward Alkyne: Synthesis of Stable Disilacyclobutene. *J. Am. Chem. Soc.* **2010**, *132*, 1123–1126. (b) So, C.-W.; Roesky, H. W.; Magull, J.; Oswald, R. B. Synthesis and Characterization of $[\text{PhC}(\text{N}t\text{Bu})_2]\text{SiCl}$: A Stable Monomeric Chlorosilylene. *Angew. Chem., Int. Ed.* **2006**, *45*, 3948–3950.
- (4) Yeong, H.-X.; Lau, K.-C.; Xi, H.-W.; Hwa Lim, K.; So, C.-W. Reactivity of a Disilylene $[\{\text{PhC}(\text{N}t\text{Bu})_2\}\text{Si}]_2$ toward Bromine: Synthesis and Characterization of a Stable Monomeric Bromosilylene. *Inorg. Chem.* **2010**, *49*, 371–373.
- (5) So, C.-W.; Roesky, H. W.; Gurubasavaraj, P. M.; Oswald, R. B.; Gamer, M. T.; Jones, P. G.; Blaurock, S. Synthesis and Structures of Heteroleptic Silylenes. *J. Am. Chem. Soc.* **2007**, *129*, 12049–12054.
- (6) Azhakar, R.; Ghadwal, R. S.; Roesky, H. W.; Wolf, H.; Stalke, D. Facile Access to the Functionalized N-Donor Stabilized Silylenes $\text{PhC}(\text{N}t\text{Bu})_2\text{SiX}$ ($\text{X} = \text{PPh}_2, \text{NPh}_2, \text{NCy}_2, \text{NiPr}_2, \text{NMe}_2, \text{N}(\text{SiMe}_3)_2, \text{OtBu}$). *Organometallics* **2012**, *31*, 4588–4592.
- (7) Sen, S. S.; Hey, J.; Herbst-Irmer, R.; Roesky, H. W.; Stalke, D. Striking Stability of a Substituted Silicon(II) Bis(trimethylsilyl)amide and the Facile Si-Me Bond Cleavage without a Transition Metal Catalyst. *J. Am. Chem. Soc.* **2011**, *133*, 12311–12316.
- (8) Inoue, S.; Wang, W.; Präsang, C.; Asay, M.; Irran, E.; Driess, M. An Ylide-like Phosphasilene and Striking Formation of a 4 π -Electron, Resonance-Stabilized 2,4-Disila-1,3-diphosphacyclobutadiene. *J. Am. Chem. Soc.* **2011**, *133*, 2868–2871.
- (9) Azhakar, R.; Ghadwal, R. S.; Roesky, H. W.; Wolf, H.; Stalke, D. A Début for Base Stabilized Monoalkylsilylenes. *Chem. Commun.* **2012**, *48*, 4561–4563.
- (10) Schäfer, S.; Köppe, R.; Roesky, P. W. Investigations of the Nature of $\text{Zn}^{\text{II}}-\text{Si}^{\text{II}}$ Bonds. *Chem. - Eur. J.* **2016**, *22*, 7127–7133.
- (11) Wang, W.; Inoue, S.; Enthaler, S.; Driess, M. Bis(silylanyl)- and Bis(germylanyl)-Substituted Ferrocenes: Synthesis, Structure, and Catalytic Applications of Bidentate Silicon(II)-Cobalt Complexes. *Angew. Chem., Int. Ed.* **2012**, *51*, 6167–6171.
- (12) Bai, Y.; Zhang, Z.; Cui, C. An Arene-tethered Silylene Ligand Enabling Reversible Dinitrogen Binding to Iron and Catalytic Silylation. *Chem. Commun.* **2018**, *54*, 8124–8127.
- (13) Cabeza, J. A.; García-Álvarez, P.; González-Álvarez, L. Facile Cyclometallation of a Mesitylsilylene: Synthesis and Preliminary Catalytic Activity of Iridium(III) and Iridium(V) Iridasilacyclopentenes. *Chem. Commun.* **2017**, *53*, 10275–10278.
- (14) (a) Benkeser, R. A.; Severson, R. G. The Preparation and Reactions of Triphenylsilylpotassium. *J. Am. Chem. Soc.* **1951**, *73*, 1424–1427. (b) Gilman, H.; Wu, T. C. Cleavage of the Silicon-Silicon Bond in Hexaphenyldisilane. *J. Am. Chem. Soc.* **1951**, *73*, 4031–4033. (c) Gilman, H.; Smith, C. L. Tetrakis(trimethylsilyl)silane. *J. Organomet. Chem.* **1967**, *8*, 245.
- (15) Roddick, D. M.; Tilley, T. D.; Rheingold, A. L.; Geib, S. J. Coordinatively Unsaturated Tris(trimethylsilyl)silyl Complexes of Chromium, Manganese, and Iron. *J. Am. Chem. Soc.* **1987**, *109*, 945–946.
- (16) (a) Kornev, A. N. The Tris(trimethylsilyl)silyl Group in Organic, Coordination and Organometallic Chemistry. *Russ. Chem. Rev.* **2004**, *73*, 1065–1089. (b) Klinkhammer, K. W. Tris(trimethylsilyl)silanides of the Heavier Alkali Metals-A Structural Study. *Chem. - Eur. J.* **1997**, *3*, 1418–1431.
- (17) Protchenko, A. V.; Schwarz, A. D.; Blake, M. P.; Jones, C.; Kaltsoyannis, N.; Mountford, P.; Aldridge, S. A Generic One-Pot Route to Acyclic Two-Coordinate Silylenes from Silicon(IV) Precursors: Synthesis and Structural Characterization of a Silylsilylene. *Angew. Chem., Int. Ed.* **2013**, *52*, 568–571.
- (18) Protchenko, A. V.; Birjkumar, K. H.; Dange, D.; Schwarz, A. D.; Vidovic, D.; Jones, C.; Kaltsoyannis, N.; Mountford, P.; Aldridge, S. A Stable Two-Coordinate Acyclic Silylene. *J. Am. Chem. Soc.* **2012**, *134*, 6500–6503.
- (19) Kira, M.; Ishida, S.; Iwamoto, T.; Kabuto, C. The First Isolable Dialkylsilylene. *J. Am. Chem. Soc.* **1999**, *121*, 9722–9723.
- (20) Sen, S. S.; Jana, A.; Roesky, H. W.; Schulzke, C. A Remarkable Base-Stabilized Bis(silylene) with a Silicon(I)-Silicon(I) Bond. *Angew. Chem., Int. Ed.* **2009**, *48*, 8536–8538.
- (21) Unno, M.; Tanaka, R. *Silanols and Silsequioxanes in Efficient Methods for Preparing Silicon Compounds*; Roesky, H. W., Ed.; Academic Press/Elsevier, 2016.
- (22) (a) Sen, S. S.; Tavčar, G.; Roesky, H. W.; Kratzert, D.; Hey, J.; Stalke, D. Synthesis of a Stable Four-Membered Si_2O_2 Ring and a Dimer with Two Four-Membered Si_2O_2 Rings Bridged by Two Oxygen Atoms, with Five-Coordinate Silicon Atoms in Both Ring Systems. *Organometallics* **2010**, *29*, 2343–2347. (b) Tavčar, G.; Sen, S. S.; Roesky, H. W.; Hey, J.; Kratzert, D.; Stalke, D. Reactions of a Bis-silylene (LSi-SiL , $\text{L} = \text{PhC}(\text{N}t\text{Bu})_2$) and a Heteroleptic Chloro Silylene (LSiCl) with Benzil: Formation of Bis(siladioxolene) and Monosiladioxolene Analogue with Five-Coordinate Silicon Atoms in Both Ring Systems. *Organometallics* **2010**, *29*, 3930–3935.
- (23) (a) Kudo, T.; Nagase, S. Theoretical study on the dimerization of silanone and the properties of the polymeric products $(\text{H}_2\text{SiO})_n$ ($n = 2, 3$, and 4). Comparison with dimers $(\text{H}_2\text{SiS})_2$ and $(\text{H}_2\text{CO})_2$. *J. Am. Chem. Soc.* **1985**, *107*, 2589–2595. (b) Bachrach, S. M.; Streitwieser, A. Ab initio study of the reaction of silene with formaldehyde. *J. Am. Chem. Soc.* **1985**, *107*, 1186–1190. (c) Michalczyk, M. J.; Fink, M. J.; Haller, K. J.; West, R.; Michl, J. Structural and chemical properties of 1,3-cyclodisiloxanes. *Organometallics* **1986**, *5*, 531–536.
- (24) Iwamoto, T.; Sato, K.; Ishida, S.; Kabuto, C.; Kira, M. Synthesis Properties and Reactions of a Series of Stable Dialkyl-Substituted Silicon-Chalcogen Doubly Bonded Compounds. *J. Am. Chem. Soc.* **2006**, *128*, 16914–16920.
- (25) Parvin, N.; Pal, S.; Khan, S.; Das, S.; Pati, S. K.; Roesky, H. W. Unique Approach to Copper(I) Silylene Chalcogenone Complexes. *Inorg. Chem.* **2017**, *56*, 1706–1712.
- (26) Chan, Y.-C.; Li, Y.; Ganguly, R.; So, C.-W. Acyclic Amido-Containing Silanechalcogenones. *Eur. J. Inorg. Chem.* **2015**, *2015*, 3821–3824.
- (27) Khan, S.; Michel, R.; Koley, D.; Roesky, H. W.; Stalke, S. Reactivity Studies of a Disilene with N_2O and Elemental Sulfur. *Inorg. Chem.* **2011**, *50*, 10878–10883.

(28) Wendel, D.; Porzelt, A.; Herz, F. A. D.; Sarkar, D.; Jandl, C.; Inoue, S.; Rieger, B. From Si(II) to Si(IV) and Back - Reversible Intramolecular Carbon-Carbon Bond Activation by an Acyclic Iminosilylene. *J. Am. Chem. Soc.* **2017**, *139*, 8134–8137.

(29) Suzuki, H.; Tokitoh, N.; Nagase, S.; Okazaki, R. The First Genuine Silicon-Sulfur Double-Bond Compound: Synthesis and Crystal Structure of a Kinetically Stabilized Silanethione. *J. Am. Chem. Soc.* **1994**, *116*, 11578–11579.

(30) Junold, K.; Baus, J. A.; Burschka, C.; Auerhammer, D.; Tacke, R. Stable Five-Coordinate Silicon(IV) Complexes with SiN_4X Skeletons (X = S, Se, Te) and Si = X Double Bonds. *Chem. - Eur. J.* **2012**, *18*, 16288–16291.

(31) Yao, S.; Xiong, Y.; Driess, M. N-Heterocyclic Carbene (NHC)-Stabilized Silanochalcogenones: NHC-Si(R₂)=E (E = O, S, Se, Te). *Chem. - Eur. J.* **2010**, *16*, 1281–1288.

(32) Kocher, N.; Henn, J.; Gostevskii, B.; Kost, D.; Kalikhman, I.; Engels, B.; Stalke, D. Si-E (E = N, O, F) Bonding in a Hexacoordinated Silicon Complex: New Facts from Experimental and Theoretical Charge Density Studies. *J. Am. Chem. Soc.* **2004**, *126*, 5563–5568.

(33) Ghadwal, R. S.; Sen, S. S.; Roesky, H. W.; Granitzka, M.; Kratzert, D.; Merkel, S.; Stalke, D. Convenient Access to Monosilicon Epoxides with Pentacoordinate Silicon. *Angew. Chem., Int. Ed.* **2010**, *49*, 3952–3955.

(34) Azhakar, R.; Ghadwal, R. S.; Roesky, H. W.; Hey, J.; Stalke, D. Reactions of Stable N-Heterocyclic Silylenes with Ketones and 3,5-Di-tert-butyl-o-benzoquinone. *Organometallics* **2011**, *30*, 3853–3858.

(35) Ishida, S.; Iwamoto, T.; Kira, M. Reactions of an Isolable Dialkylsilylene with Ketones. *Organometallics* **2010**, *29*, 5526–5534.

(36) Swamy, V. S. V. S. N.; Parvin, N.; Vipin Raj, K.; Vanka, K.; Sen, S. S. C(sp³)-F, C(sp²)-F and C(sp³)-H Bond Activation at Silicon(II) Centers. *Chem. Commun.* **2017**, *53*, 9850–9853.

(37) Becerra, R.; Cannady, J. P.; Walsh, R. Gas-Phase Reaction of Silylene with Acetone: Direct Rate Studies, RRKM Modeling, and ab Initio Studies of the Potential Energy Surface. *J. Phys. Chem. A* **1999**, *103*, 4457–4464.

(38) Kaftory, M.; Kapon, M.; Botoshansky, M. In *The Chemistry of Organic Silicon Compounds*; Rappoport, Z., Apeloig, Y., Eds.; Wiley: Chichester, U.K., 1998; Vol. 2, Chapter 5.

Diverse Reactivity of Hypersilylsilylene with Boranes and Three-Component Reactions with Aldehyde and HBpin

Milan Kumar Bisai,^{||} V. S. V. S. N. Swamy,^{||} K. Vipin Raj, Kumar Vanka, and Sakya S. Sen^{*}Cite This: *Inorg. Chem.* 2021, 60, 1654–1663

Read Online

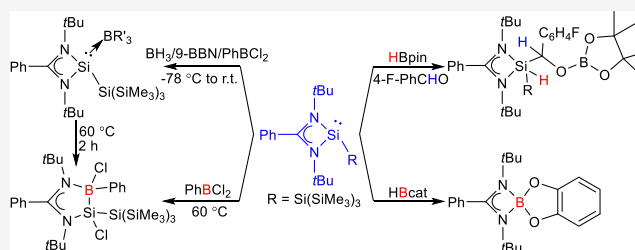
ACCESS |

Metrics & More

Article Recommendations

Supporting Information

ABSTRACT: The recently reported hypersilylsilylene $\text{PhC}(\text{NtBu})_2\text{SiSi}(\text{SiMe}_3)_3$ (**1**) reacts with BH_3 , 9-BBN, and PhBCl_2 to yield the respective Lewis acid base adducts **2–4**, respectively. Compound **4** undergoes isomerization to form a ring expansion product **5**. The same silylene was found to initially form an adduct with HBpin (**6**) and subsequently isomerized to **7** via the rupture of the B–H bond of HBpin (**7**), where the hydride was bound to the carbon atom of the amidinate ligand and the Bpin unit was attached to the silicon center. Surprisingly, the reaction of **1** with HBcat results in $\text{PhC}(\text{NtBu})_2\text{Bcat}$ (**8**). Subsequently, we have shown that HBcat forms the same product when it reacts with related silylene $\text{PhC}(\text{NtBu})_2\text{SiN}(\text{SiMe}_3)_3$ (**1'**). With all of these reactions in hand, we ponder if silylene can activate two small molecules at one time. In this work, we delineate the three-component reactions of silylenes **1** and **1'** with 4-fluorobenzaldehyde and HBpin, which afforded unusual coupling products, **9** and **10**, respectively. Note that **9** and **10** were prepared from the cleavage of the B–H and C=O bonds by silylene in a single reaction and are the first structurally attested Si–C–O–B coupled products.



INTRODUCTION

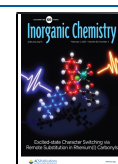
Bearing reactive lone pairs of electrons as well as vacant orbitals at silicon, silylenes can mimic transition metals in many reactions such as activation of H_2 ,¹ NH_3 ,² and P_4 ³ under mild conditions. Upon reaction with a Lewis acid such as borane, silylenes readily form adducts. The pioneering studies by several groups such as those of West, Driess, Tacke, Roesky, Braun, and their co-workers have significantly contributed to the initial advance in silylene-borane chemistry.^{4,5} Nonetheless, the reactivity of boron halides toward silylenes has been relatively less explored and reported only by the groups of Braunschweig,^{6,7} Iwamoto,⁸ So,⁹ and Roesky¹⁰ using a diverse range of silylenes. Kato and co-workers reported the reaction of a phosphine-stabilized bromosilylene with $\text{NHC}\cdot\text{BBr}_3$ that afforded a silyl-substituted phospho-bora-ylide.¹¹

Due to our current interest in the hydroboration of unsaturated substrates by compounds with main group elements,¹² we were interested in studying the reactivity of silylene with several boranes with a focus on the comparison of the reactivities of hydroboranes with the silylene. So and co-workers described the B–H bond activation of BH_2OTf by $\text{PhC}(\text{NtBu})_2\text{SiN}(\text{SiMe}_3)(\text{Dipp})$.¹³ Using a very similar Si(II) compound, $\text{PhC}(\text{NtBu})_2\text{SiN}(\text{SiMe}_3)_2$ (**1'**),¹⁴ we have demonstrated the scission of the B–H bond of HBpin in a cooperative manner, where the Bpin unit was attached to the silicon atom and the hydride was bonded to the remote carbon atom of the amidinate ligand.¹⁵ Very recently, we have synthesized a new hypersilylsilylene, $\text{PhC}(\text{NtBu})_2\text{SiSi}(\text{SiMe}_3)_3$ (**1**).¹⁶ The bulky $\text{Si}(\text{SiMe}_3)_3$ substituent on the Si(II) center

enabled the synthesis of a silaoxirane upon reaction with acetone,¹⁶ which is otherwise known to be involved in C–H bond cleavage with silylene.¹⁷ In this work, we have probed the reactivity of **1** with several boranes. While BH_3 and 9-BBN form adducts (**2** and **3**) with **1**, HBpin undergoes cooperative B–H bond activation (**7**), and HBcat led to the amidinate boron complex (**8**). It was observed that PhBCl_2 undergoes oxidative addition over the Si^{II} center of NHSi or amidinato bis-silylene followed by a ring expansion.^{6,9} However, we were able to isolate the adduct with PhBCl_2 (**4**), presumably due to the steric support provided by the $-\text{Si}(\text{SiMe}_3)_3$ moiety. **4** subsequently undergoes ring expansion to form **5** upon heating. Following this, we have studied the multicomponent reactions of 4-fluorobenzaldehyde and HBpin with **1** and **1'**, which resulted in Si(IV) species **9** and **10**, respectively. Note that **9** and **10**, which were prepared from activation of the B–H and C=O bonds by silylene in a single reaction, are the first structurally authenticated species featuring Si–C–O–B coupled products.

Received: October 23, 2020

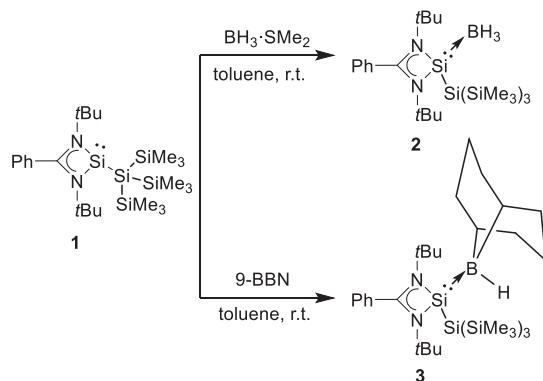
Published: January 19, 2021



RESULTS AND DISCUSSION

Silylene–borane adducts **2** and **3** were prepared by treatment of **1** with BH_3 and 9-BBN in toluene at room temperature (Scheme 1). The ^{11}B chemical shifts of **2** and **3** appear at

Scheme 1. Reactions of **1** with BH_3 and 9-BBN



−35.9 and −10.5 ppm, respectively. The analogous ^{29}Si NMR shifts are observed at 96.1 and 77.8 ppm, respectively, indicating adduct formation. The molecular diagrams from the X-ray determination of **2** and **3** are shown in Figures 1 and

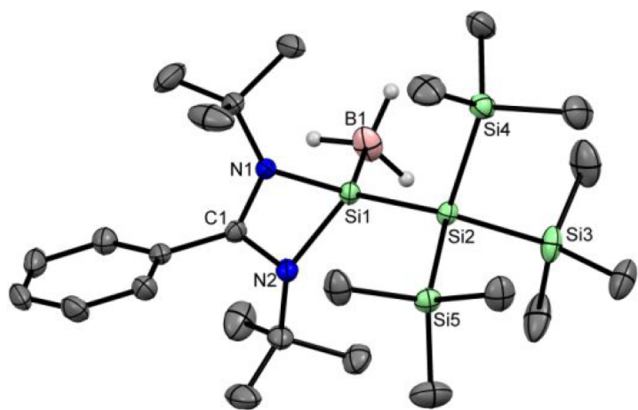


Figure 1. Molecular structure of **2**. The thermal ellipsoids are drawn at the 50% level of probability. The hydrogen atoms have been omitted (except the hydrogen atoms bonded to B) for the sake of clarity. Important bond lengths (angstroms) and angles (degrees): Si1–B1, 1.975(2); Si1–Si2, 2.3742(8); Si1–N1, 1.8433(13); Si1–N2, 1.8462(15); N1–Si1–N2, 70.75(6); N1–Si1–B1, 116.39(9); N2–Si1–B1, 116.28(9); B1–Si1–Si2, 119.53(7).

2, respectively. The geometries of the silicon and boron atoms in **2** and **3** are best described as tetrahedral with Si–B bond distances of 1.975(2) and 2.021(4) Å, respectively. These values are in good agreement with those of the previously reported amidinato and guanidinato silylene borane adducts.^{4c,d,i}

The reaction of PhBX_2 (X = Cl or Br) with a typical five-membered N-heterocyclic silylene led to six-membered silaborinines, where the boron atom was inserted into one of the Si–N bonds (Chart 1).⁶ The analogous reaction with amidinato bis(silylene), $[\text{PhC}(\text{N}t\text{Bu})_2\text{Si}]_2$, afforded a ring expansion product (Chart 1).⁹ In both of these cases, the initial formation of the silylene· PhBCl_2 adduct was proposed, but not structurally authenticated. Very recently, Zhu, Stalke, and Roesky reported the reaction of amidinato chlorosilylene,

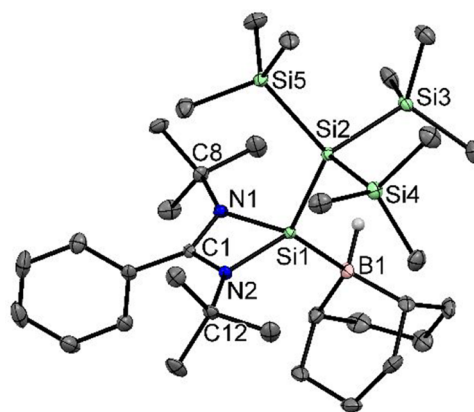


Figure 2. Molecular structure of **3**. The thermal ellipsoids are drawn at the 50% level of probability. The hydrogen atoms have been omitted (except the hydrogen atoms bonded to B) for the sake of clarity. Important bond lengths (angstroms) and angles (degrees): Si1–B1, 2.021(4); Si1–Si2, 2.3895(12); Si1–N1, 1.859(3); Si1–N2, 1.869(2); B1–H1, 1.17(4); N1–Si1–N2, 70.19(11); N1–Si1–B1, 110.05(14); N2–Si1–B1, 123.42(14); B1–Si1–Si2, 116.47(11).

$\text{PhC}(\text{N}t\text{Bu})_2\text{SiCl}$, with PhBCl_2 , which initially formed an adduct and subsequently isomerized to a borylsilane.¹⁰ It is of note here that the electron donating ability of silylene **1** is better than that of the related chlorosilylene, $\text{PhC}(\text{N}t\text{Bu})_2\text{SiCl}$, and West's two-coordinate silylene,¹⁸ which might facilitate the stabilization of adduct formation between **1** and PhBCl_2 .

Silylene–borane adduct **4** was afforded by the reaction of **1** with PhBCl_2 in toluene from −78 °C to room temperature (Scheme 2), which was isolated as a colorless crystal from toluene. The formation of **4** is likely caused by the enhanced electron donation by the silylene center as well as the steric constraints imposed by the bulky hypersilyl ligand. The ORTEP diagram of **4** is depicted in Figure 3. The four-coordinated B atom in **4** exhibits a distorted tetrahedral geometry with a Si1–B1 bond length of 2.065(5) Å, typical for a dative bond. The ^{11}B NMR resonance of **4** was observed at 3.13 ppm, which is slightly downfield from those of $\text{PhC}(\text{N}t\text{Bu})_2\text{Si}(\text{Cl}) \rightarrow \text{BPhCl}_2$ (−0.03 ppm).¹⁰

4 undergoes slow isomerization to the ring expansion product (**5**) via B–Cl bond activation at room temperature over a longer duration. The complete conversion of **4** to **5** can be accomplished by simply heating the toluene solution of **4** at 60 °C for 2 h (Scheme 2). There were two signals detected at 1.19 and 1.05 ppm for the *t*Bu groups. This is further reflected in the ^{13}C NMR spectrum of **5**, where two resonances for the − CMe_3 groups were detected at 34.9 and 35.5 ppm. The ^1H and ^{13}C NMR spectra suggest two chemically distinct *t*Bu groups in **5**. The ^{11}B NMR resonance (−0.45 ppm) is slightly upfield in comparison to that of **4** (56.6 ppm). The ^{29}Si NMR spectrum of **5** (39.3 ppm) is shifted upfield from that of **4** (56.6 ppm). Unlike in the case of Roesky's chlorosilylene (Chart 1), no 1,2-chloride migration takes place from **5**. For Roesky's chlorosilylene, the −I effect of the chloride ligands is assumed to be the main reason for the further nucleophilic attack by one of the amidinate N atoms on the boron atom of the putative five-membered ring and the ring contraction product (see Scheme S1). On the contrary, the stabilization of **5** is probably caused by the strong σ -donation from the $\text{Si}(\text{SiMe}_3)_3$ moiety, and its bulky nature, which hinders the migration of chloride from the B to the Si atom.

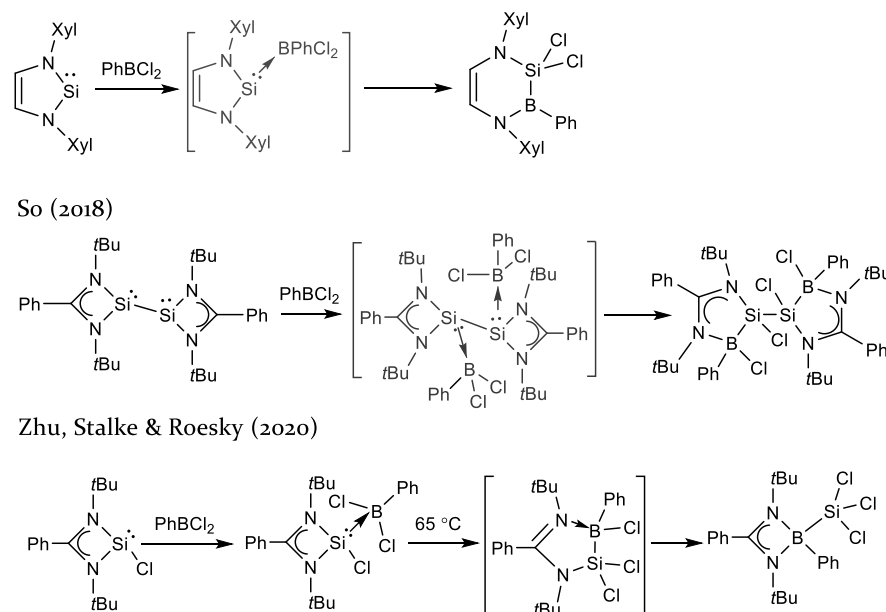
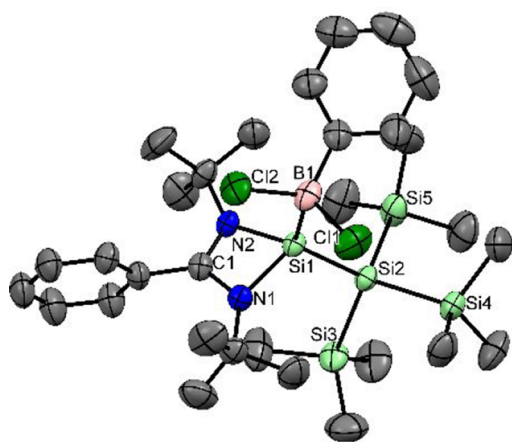
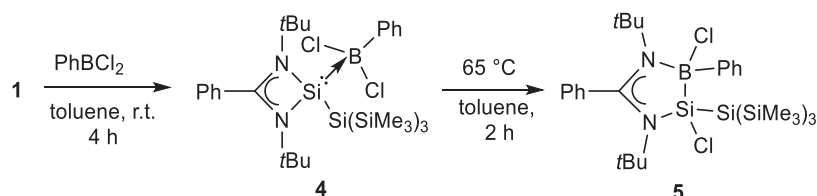
Chart 1. Selected Examples of Reactions between Silylenes and PhBCl₂Scheme 2. Formation of 4 and 5 from the Reaction of 1 with PhBCl₂

Figure 3. Molecular structure of 4. Anisotropic displacement parameters are depicted at the 50% probability level. Hydrogen atoms have been omitted for the sake of clarity. Selected bond distances (angstroms) and bond angles (degrees): Si1–B1, 2.065(5); Si1–Si2, 2.4031(13); Si1–N1, 1.836(3); Si1–N2, 1.831(3); B1–Cl1, 1.896(5); B1–Cl2, 1.891(5); N1–Si1–N2, 71.51(14); N1–Si1–B1, 108.56(18); N2–Si1–B1, 110.02(17); B1–Si1–Si2, 125.70(14).

Next, we reacted **1** with HBpin, which shows the formation of a silylene–borane adduct (**6**) (Scheme 3). The ¹¹B NMR spectrum shows a doublet at 21.3 ppm, reflecting the B–H linkage. **6** is not very stable and undergoes slow isomerization to **7** at room temperature, which is noted in the ¹H NMR spectrum from the appearance of a C–H proton signal at 5.81 ppm. Heating the benzene solution of **6** led to the complete

conversion to **7**. Noteworthy is the downfield ¹¹B resonance at 37.7 ppm, mirroring the transfer of the hydride from the boron to the amidinate carbon. The resonance at –59.9 ppm in the ²⁹Si NMR spectrum is consistent with a four-coordinated silicon atom. Along with **7**, the formation of the 1,1-oxidative addition product of HBpin (**7'**) was also detected in NMR spectroscopy, although with a very minor yield. Unfortunately, we could not grow the appropriate crystals required for X-ray diffraction studies for **6** and **7**.

The reaction of silylenes with HBcat is less known, presumably due to the latter being less stable than HBpin. Recently, Hadlington et al. reported an unusual reaction of the [bis(NHC)](silylene)Ni⁰ complex with HBcat,¹⁹ which leads to the formation of an unprecedented hydroborylene-coordinated (chloro)(silyl)nickel(II) complex. The reaction of HBcat with **1** at low temperatures afforded colorless single crystals of an amidinato borane, PhC(NtBu)₂Bcat (**8**), which was corroborated by X-ray structure determination (Scheme 4). Surprisingly, the product was also obtained when we reacted the related silylene, **1'**, with HBcat (Scheme 4). It is of note here that HBcat is more Lewis acidic than HBpin but sterically less bulky than the latter. Taking these points into account, we propose that HBcat also initially forms an adduct with **1** (**8'**). Subsequently, the N atom of the amidinate moiety attacks the electrophilic B atom of **8'**, leading to the formation of amidinato borane.

The ORTEP diagram of **8** is presented in Figure 4. The boron atom is tetracoordinate, adopting a distorted tetrahedral environment, with a B–N bond length of 1.58(3) Å. The ¹¹B NMR spectrum of **8** exhibits a resonance at 11.9 ppm. The fate

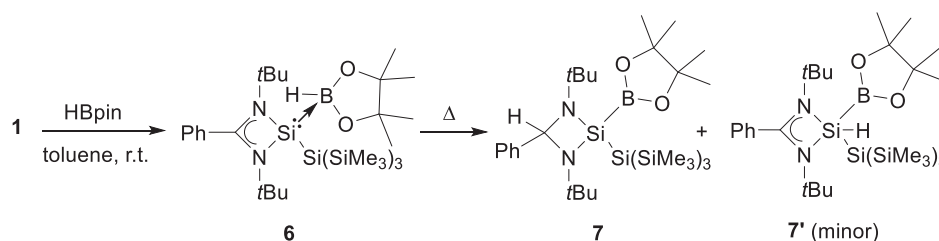
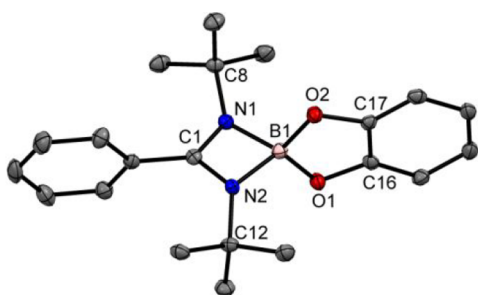
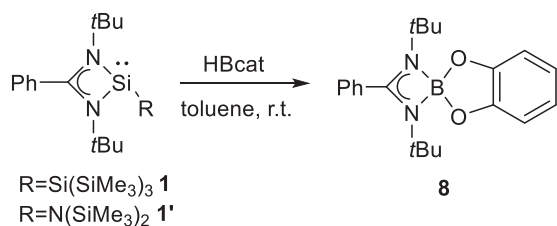
Scheme 3. Reaction of **1** with HBpin and Subsequent IsomerizationScheme 4. Reaction of **1** with HBcat

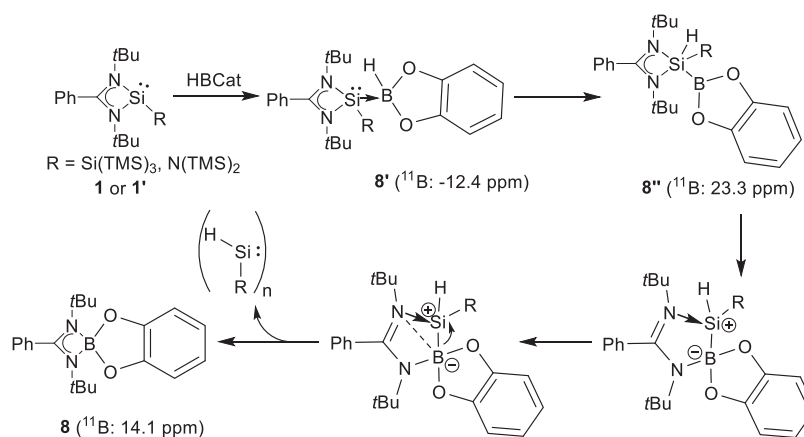
Figure 4. Molecular structure of **8**. The thermal ellipsoids are drawn at the 50% level of probability. The hydrogen atoms have been omitted for the sake of clarity. Important bond lengths (angstroms) and angles (degrees): B1–O1, 1.455(3); B1–O2, 1.459(3); B1–N1, 1.589(3); B1–N2, 1.583(3); O1–B1–O2, 107.12(19); N1–B1–N2, 81.74(16); O2–B1–N1, 115.90(19); O1–B1–N2, 116.86(19).

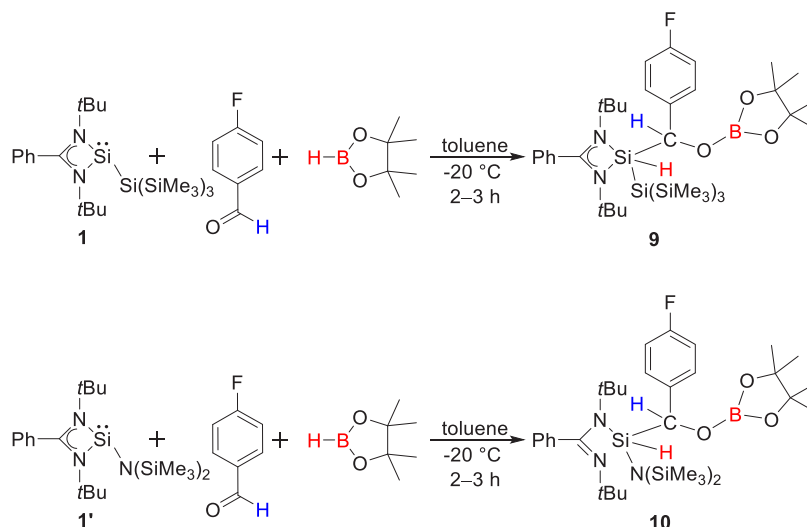
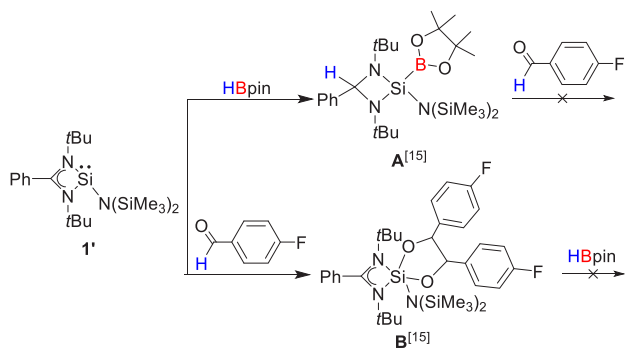
of the silicon unit is not clear. We have performed an NMR tube reaction, and after reaction for 6 h, a possible mixture of three compounds has been detected in ¹H and ¹¹B NMR spectra, indicating the formation of a Lewis acid–base adduct between HBcat and silylene (**8'**; ¹¹B –12.4 ppm), B–H activation on the Si center (**8''**; ¹¹B 23.3 ppm), and an isolated boron-inserted product (**8**; ¹¹B 14.1 ppm) in 31%, 16%, and

45% yields, respectively (see Figures S27–S29 and S42). Three resonances in the ²⁹Si NMR spectrum were observed at –11.8, –69.9, and –116 ppm. Taking these aforementioned experimental studies into account, we propose a possible mechanism for the formation of **8** (Scheme 5).

The three-component methodology is very attractive in organic chemistry as important complex molecules can be made using commercially available precursors in a single step. Minakata et al. reported the photolysis of bis(trimethylsilyl)bis mesityl silane (SiMe₃)₂SiMes₂ with aldehyde and an electron deficient alkyne to form cycloadducts, which were formed via in situ generation of silylene, Mes₂Si:.²⁰ The reaction is similar to those reported by Calad and Woerpel, who reported the silver-catalyzed transfer of the silylene moiety to α,β -unsaturated esters to access oxasila-cyclopentenes.²¹ However, stable silylene involved in the multicomponent reaction is not known. In this paper, we shall present multicomponent reactions of silylenes **1** and **1'** with 4-fluorobenzaldehyde and HBpin to form Si–C–O–B coupled products **9** and **10**, respectively, through activation of the B–H and C=O bonds by silylene in a single reaction (Scheme 6). These reactions are all the more remarkable given that combination of the three reagents results in the formation of the products, which are otherwise inaccessible. **9** and **10** were isolated in 45% and 40% yields, respectively, along with A and B types of side products (Scheme 7) in minor amounts.

The silicon atom in **9** is coordinated to two nitrogen atoms of the ligand and the tris(trimethylsilyl) substituent, one hydrogen atom, and one carbon atom (aldehydic carbon of 4-fluorobenzaldehyde) (Figure 5), thereby featuring a distorted trigonal bipyramidal geometry. The Si–H and Si–Si bond lengths in **9** are 1.40(2) and 2.367(7) Å, respectively. The Si–C bond length is 1.925(2) Å, slightly longer than those in PhC(N*t*Bu)₂SiH(Me)Cl (~1.85 Å)²² and the vinyl

Scheme 5. Tentative Mechanism for the Formation of **8**

Scheme 6. Three-Component Reactions of **1** or **1'**, Pinacolborane, and 4-FluorobenzaldehydeScheme 7. Stoichiometric Reactions of **1'** with HBpin and Aldehyde

silylsilylene species (~ 1.79 Å).^{3e} The binding of the oxygen atom of the aldehyde to boron instead of silicon can be attributed to the higher oxophilicity of the former.²³ The ^{11}B NMR spectrum displays a resonance at 20.4 ppm, consistent with a three-coordinate boron atom. The ^{29}Si NMR spectrum of **9** exhibits a resonance at -107.9 ppm, exemplifying the five coordination around the silicon atom.

The structure of **10** in the solid state (Figure 6) reveals that the only difference in the structural features of **9** and **10** is the geometry of the central silicon atom. We assume that the $\text{Si}(\text{SiMe}_3)_3$ group's steric effect plays a role in keeping the extra $\text{Si}-\text{N}$ coordination in **9**. The optimized geometries of **9** and **10** are shown in Figure S46. In both **9** and **10**, the hydride ligand is in a *trans* position to the nitrogen. However, because of the $\text{Si}(\text{SiMe}_3)_3$ ligand's bulkiness, in **9**, the hydride cannot push away the nitrogen entirely and thereby the geometry of the central silicon atom is nearly trigonal bipyramidal ($\angle\text{H}-\text{Si}-\text{Si} = 99.5^\circ$). On the contrary, in **10**, because of the presence of the less bulky $\text{N}(\text{SiMe}_3)_2$, the strong *trans* directing effect of the hydride leads to the complete removal of the nitrogen from the vicinity and makes the geometry around the silicon center nearly tetrahedral ($\angle\text{H}-\text{Si}-\text{N} = 106.2^\circ$). This is further reflected in the differing $\text{Si}-\text{H}$ bond lengths in **9** (1.40 Å) and **10** (0.98 Å). The cleavage of the amidinate $\text{Si}-\text{N}$ bonds was known for $\text{Si}(\text{II})$ compounds with π -donor substituents such as Cl and $\text{N}(\text{SiMe}_3)_2$ with C_6F_6 , COT.^{24,25} **10** resonates at -27.7 ppm in the ^{29}Si NMR spectrum, reflecting the four

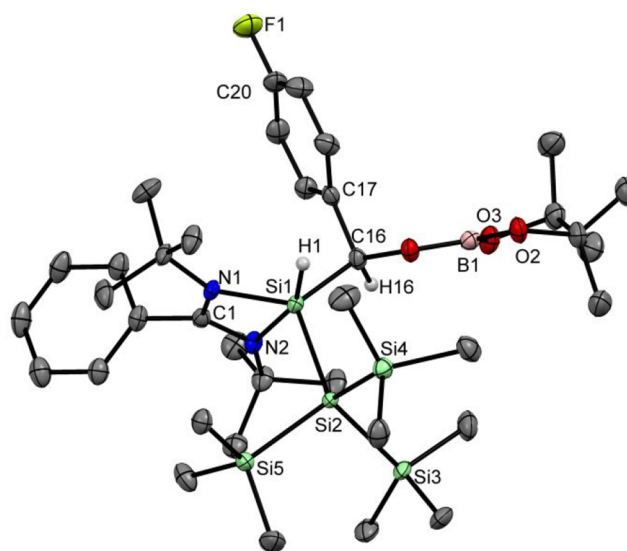


Figure 5. Molecular structure of **9**. The thermal ellipsoids are drawn at the 50% level of probability. The hydrogen atoms have been omitted (except H1 and H16 are bonded to Si1 and C16, respectively) for the sake of clarity. Important bond lengths (angstroms) and angles (degrees): Si1–N1, 1.815(2); Si1–N2, 2.319(2); Si1–Si2, 2.367(7); C16–Si1, 1.925(2); C16–O1, 1.459(3); O1–B1, 1.355(3); Si1–H1, 1.40(2); C16–H16, 1.000; N1–C1, 1.376(3); N2–C1, 1.294(3); C1–N1–Si1, 103.6(1); C1–N2–Si1, 83.4(1); N1–Si1–N2, 62.69(7); N1–Si1–H1, 98.2(9); N2–Si1–H1, 157.9(9); Si2–Si1–H1, 98.7(9); C16–Si1–H1, 92.6(9); Si2–Si1–C16, 116.22(6); Si1–C16–H16, 110.9(0).

coordination around the silicon atom. The ^{11}B NMR spectrum displays a resonance at 20.5 ppm. The $\text{Si1}-\text{H1}$ and $\text{Si1}-\text{C1}$ bond lengths of **10** are 0.979(4) and 1.90(4) Å, respectively, which are shorter than those in **9** [1.40(2) and 1.925(2) Å, respectively].

The next obvious question is how these compounds were formed. Compound **A** was obtained by reacting **1'** with HBpin, where the silylene and the remote carbon atom of the amidinate ligand were cooperatively involved in B–H bond scission (Scheme 7).¹⁵ Similarly, the reaction of **1'** with aldehydes afforded the dioxasilolane derivatives with C–C bond formation (**B**).^{12a} Nonetheless, both **A** and **B** are found

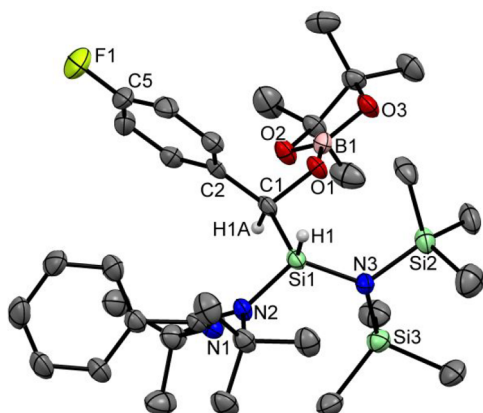


Figure 6. Molecular structure of **10**. The thermal ellipsoids are drawn at the 50% level of probability. The hydrogen atoms have been omitted (except H1 and H1A are bonded to Si1 and C1, respectively) for the sake of clarity. Important bond lengths (angstroms) and angles (degrees): Si1–N2, 1.744(3); Si1–N3, 1.729(4); C1–Si1, 1.90(4); C1–O1, 1.470(4); O1–B1, 1.343(6); Si1–H1, 0.980; C1–H1A, 0.980; N2–C8, 1.431(5); N1–C8, 1.270(5); N2–Si1–C1, 110.8(2); N3–Si1–C1, 110.3(2); Si1–C1–O1, 104.6(2); Si1–C1–C2, 117.3(3); C1–O1–B1, 119.8(3); N1–C8–N2, 115.6(3); H1–Si1–C1, 104.9(0); H1A–C1–Si1, 108.8(0); H1–Si1–N2, 105.0(0); H1–Si1–N3, 104.90(0); H1A–C1–C2, 108.80(0).

to be very stable and do not show any reactivity toward aldehyde and HBpin, respectively (Scheme 7). This indicates

that **A** and **B** are not the possible intermediates for the formation of **9** and **10**.

To understand the formation of **9** and **10** from silylene, we have performed variable-temperature-dependent NMR spectroscopy. No reaction was observed between **1'** and *p*-fluorobenzaldehyde at low temperatures. Similarly, the mixing of **1'** and HBpin at low temperatures presumably led to weak adduct formation as indicated from the slight shift of the methyl protons of HBpin and *t*Bu protons of silylene. In fact, when we have gradually increased the temperature from -35 to 25 °C, the beginning of the formation of product **A** was noted with the generation of a peak at 5.2 ppm (see Figure S43). Therefore, it can be surmised that the low temperature is imperative for the formation of **9** and **10**. It should also be noted that the formation of **9** and **10** was observed when **1** and **1'** were premixed with 4-F-benzaldehyde prior to the addition of HBpin.

To obtain further insight, we have conducted computational investigations with density functional theory (DFT), with the TZVP basis set and the PBE functional. For more information, see the Supporting Information. As shown in Figure 7, the first step involves a barrier of 8.1 kcal/mol, via transition state TS_1, in which the Si–C bond begins to form, and the C=O bond is transformed into a single bond. TS_1 leads to an intermediate Int_1, which is stable by 1.9 kcal/mol with respect to TS_1. The Int_1 immediately reacts with HBpin to form a stable intermediate Int_2, and this step is found to be barrier-less (confirmed using a linear transit search). The next

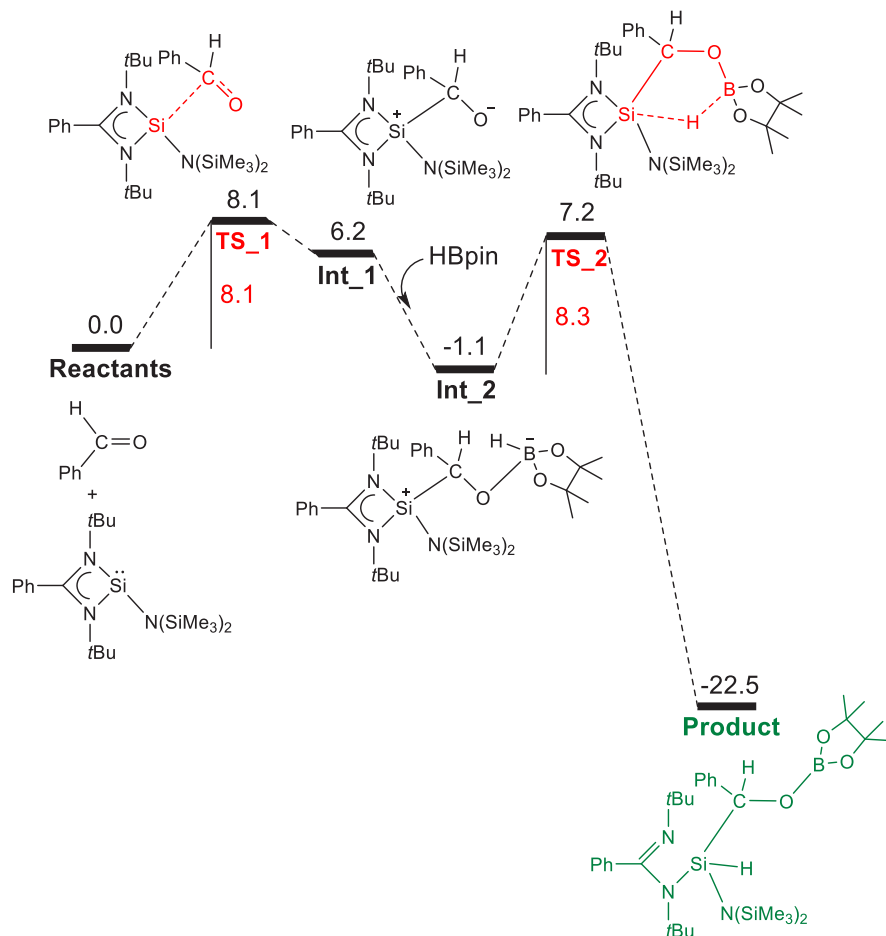


Figure 7. Free energy profile (in kilocalories per mole) for the formation of **10**.

step involves the five-membered transition state TS_2 (barrier of 8.3 kcal/mol), which proceeds through hydride transfer to the silicon center from the boron atom, giving rise to the formation of a very stable (29.7 kcal/mol stable with respect to TS_2) tetracoordinated Si(IV) species. Interestingly, this species has only two Si–N bonds. The third Si–N bond of silylene is broken as a result of the transfer of a hydride ion to silicon, which corroborates our experimental observations.

We have also considered an association between premixed **1'** and HBpin in the calculations. Our calculations suggest that the formation of an adduct between **1'** and HBpin is less favorable (see Figure S45) compared to the formation of Int_1 (see Figure 7), both from a thermodynamic and a kinetic point of view. Furthermore, to form coupled product **A**, the adduct has to surmount a barrier of 19.7 kcal/mol, whereas Int_1 can react with HBpin and form the stable Int_2. This would be a barrier-less process. Therefore, at a lower temperature, even though the interaction between **1'** and HBpin can take place, the reaction between **1'** and benzaldehyde will be more feasible if benzaldehyde is present in the mixture, because of the instability of the adduct and a high barrier to moving forward. An alternative pathway would proceed from the three reactants, the silylene, HBpin, and the benzaldehyde, approaching each other to produce a trimolecular reaction (see Figure S44). However, this was found to be less favorable than the mechanism shown here.

It is evident that **9** and **10** are coupled products obtained from the reactions of silylenes with HBpin and aldehyde. The next question is whether these Si(IV) species can undergo reductive elimination to yield the boronate ester product along with the regeneration of the corresponding silylene. A recent report has demonstrated that the steric congestion around the carbene center facilitates the reductive elimination step.²⁶ Very recently, the groups of Inoue and Rieger have demonstrated the reductive elimination of a Si(IV) compound.²⁷ Kato and co-workers have also shown facile redox reversible addition of hydrogen, Si–H, and other bonds.^{28,29} So and co-workers recently showed the use of a silicon(II) cation, [(I^{Me})₂SiH]I (I^{Me} = :C{N(Me)C(Me)}₂) as a catalyst for the hydroboration of ketones, CO₂, imines, and pyridine^{30a} as well as N-formylation of primary and secondary amines using CO₂ and phenylsilane.^{30b} Unfortunately, even after heating, we did not see any resonance at 4.8 ppm (characteristic of the CH₂ protons of the boronate esters), indicating that no reductive elimination takes place from **9** and **10**.

CONCLUSIONS

In this paper, we have reported a series of reactions of a hypersilylsilylene, PhC(NtBu)₂SiSi(SiMe₃)₃ (**1**), toward several hydro- and haloboranes. One forms stable adducts with BH₃ and 9-BBN. With PhBCl₂, an adduct is formed, which subsequently isomerizes to a ring expansion product. Extrusion of the silylene fragment was observed in the reaction with HBcat. In addition, we have shown that silylenes **1** and **1'** smoothly underwent three-component coupling reactions with 4-fluorobenzaldehyde and pinacolborane at low temperatures to afford Si(IV) species **9** and **10**, respectively. They are the first structurally characterized organosilicon–carbon–oxygen–boron coupled products synthesized by one-pot tandem reactions. DFT calculations were performed, which revealed the favorable formation of **10**.

EXPERIMENTAL SECTION

All experiments were performed under an argon atmosphere using standard Schlenk techniques or a glovebox. Toluene and *n*-hexane were purified by MBRAUN solvent purification system MB SPS-800. Benzene was dried and distilled over a Na/benzophenone mixture prior to use. The precursors [PhC(NtBu)₂SiSi(Si(CH₃)₃)₃] (**1**)¹⁶ and [PhC(NtBu)₂SiN(Si(CH₃)₃)₂] (**1'**)¹⁴ were synthesized as described in the literature. Other reagents were purchased either from Sigma-Aldrich or from TCI Chemicals and used without further purification. ¹H, ¹³C, ²⁹Si, and ¹¹B NMR spectra were recorded in C₆D₆ or CDCl₃ using a Bruker Advance DPX 200, Bruker Advance DPX 400, or a Bruker Advance DPX 500 spectrometer referenced to external SiMe₄. Microanalyses (C, H, N) were performed by the CSIR-National Chemical Laboratory. A Stuart SMP-30 melting point apparatus was used to measure melting points, which were uncorrected.

Synthesis of 2. BH₃·SMe₂ (200 μL, 2 M, 0.39 mmol) was added to the 10 mL toluene solution of **1** (0.200 g, 0.39 mmol) at –35 °C. The reaction mixture was stirred for a further 12 h at room temperature. Upon completion, all of the volatiles were removed in vacuum, and the residue was redissolved in toluene (10 mL) and filtered via cannula. The resulting filtrate was concentrated (3 mL) and stored overnight in a freezer at –4 °C to afford colorless crystals of **2** that are suitable for single-crystal X-ray analysis (0.172 g, 84.0% yield). Mp: 200–201 °C. ¹H NMR (200 MHz, C₆D₆, 298 K): δ 0.49 (s, 27H, SiMe₃), 1.17 (s, 18H, tBu), 6.87–7.00 (m, 3H, Ph), 7.08–7.14 (m, 1H, Ph), 7.28–7.32 (m, 1H, Ph). ¹³C{¹H} NMR (50.3 MHz, C₆D₆, 298 K): δ 4.3 (Si(SiMe₃)₃), 32.2 (CMe₃), 55.0 (CMe₃), 129.09, 130.26, 130.95, 132.21, 168.27 (NCN). ¹¹B NMR (128.4 MHz, C₆D₆, 298 K): δ –35.92. ²⁹Si{¹H} NMR (79.5 MHz, C₆D₆, 298 K): δ 96.14 (Si(BH₃)Si(SiMe₃)₃), –8.21 (SiSi(SiMe₃)₃), –128.13 (SiSi(SiMe₃)₃). ESI-HRMS: calcd for C₂₄H₅₄N₂Si₅B [M + H]⁺, *m/z* 521.3221; found, *m/z* 521.3036.

Synthesis of 3. Toluene (5 mL) and THF (3 mL) were added to the mixture of 9-BBN (0.048 g, 0.19 mmol) and **1** (0.10 g, 0.19 mmol) at room temperature and stirred for 12 h. The solution was filtered via cannula, and the filtrate was supersaturated to obtain colorless crystals of **3** that were suitable for single-crystal X-ray analysis (0.118 g, 80.0% yield). Mp: 221–223 °C. ¹H NMR (200 MHz, C₆D₆, 298 K): δ 0.49 (s, 27H, SiMe₃), 1.16 (s, 18H, tBu), 1.41–1.87 (br, 14H, CH), 6.89–7.16 (m, 5H, Ph). ¹³C{¹H} NMR (50.3 MHz, C₆D₆, 298 K): δ 4.7 (Si(SiMe₃)₃), 22.9, 23.4, 24.0, 27.3, 28.2, 29.5, 32.3, 33.3, 34.0 (CMe₃), 38.1, 54.7 (CMe₃), 126.0, 129.6, 130.3, 131.3, 138.1, 141.2, 167.5 (NCN). ¹¹B NMR (C₆D₆, 128.4 MHz, 298 K): δ –10.5. ²⁹Si{¹H} NMR (79.5 MHz, C₆D₆, 298 K): δ 77.81 (Si(9-BBN)Si(SiMe₃)₃), –3.26 (SiSi(SiMe₃)₃), –123.79 (SiSi(SiMe₃)₃). ESI-HRMS: calcd for C₃₂H₆₆N₂Si₅B [M + H]⁺, *m/z* 629.4160; found, *m/z* 629.4686.

Synthesis of 4. To a solution of **1** (0.300 g, 0.59 mmol) in toluene (5 mL) was added a PhBCl₂ (0.097 g, 0.59 mmol) solution in toluene (10 mL) dropwise via cannula at –78 °C. The reaction mixture was slowly warmed to room temperature and stirred for an additional 3 h. Upon completion, the reaction mixture was dried in vacuum and the residue was redissolved in toluene (10 mL). The solution was filtered via cannula, and the filtrate was concentrated *in vacuo* to ~3 mL and stored at –4 °C in a freezer overnight to obtain colorless crystals of **4** (0.283 g, 72% yield). Mp: 156–157 °C. ¹H NMR (400 MHz, CDCl₃, 298 K): δ 0.40 (s, 27H, SiMe₃), 1.16 (s, 18H, tBu), 7.17 (t, 1H, Ph), 7.29 (m, 1H, Ph), 7.41–7.48 (m, 4H, Ph), 7.52–7.56 (m, 2H, Ph), 7.89–7.91 (d, ³J_{H–H} = 8.13 Hz, 2H, Ph). ¹³C NMR (100.6 MHz, CDCl₃, 298 K): δ 4.09 (SiMe₃), 30.9 (CMe₃), 31.6 (CMe₃), 54.7 (CMe₃), 120.0 (Ph), 126.9 (Ph), 127.7 (Ph), 127.9 (Ph), 128.2 (Ph), 129.3 (Ph), 130.8 (Ph), 131.0 (Ph), 131.9 (Ph), 133.6 (Ph), 172.2 (NCN). ¹¹B NMR (160.4 MHz, CDCl₃, 298 K): δ 3.13. ²⁹Si{¹H} NMR (99.3 MHz, CDCl₃, 298 K): δ 55.62 (Si(PhBCl₂)₂Si(SiMe₃)₃), –7.91 (SiSi(SiMe₃)₃), –126.76 (SiSi(SiMe₃)₃).

Synthesis of 5. A solution of **4** (0.200 g, 0.30 mmol) in toluene (5 mL) was heated at 65 °C and stirred for 2 h. Then, the solution was filtered via cannula, and the resulting filtrate was dried *in vacuo* to

obtain a colorless powder of compound **5** (0.150 g, 75% yield). Mp: 126–127 °C. ¹H NMR (200 MHz, C₆D₆, 298 K): δ 0.48 (s, 27H, SiMe₃), 1.05 (s, 9H, tBu), 1.19 (s, 9H, tBu), 6.78–6.82 (t, 2H, Ph), 6.91–6.95 (t, 2H, Ph), 7.21–7.24 (t, 3H, Ph), 7.45–7.49 (t, 2H, Ph), 8.26–8.28 (m, 1H, Ph). ¹³C NMR (100.6 MHz, CDCl₃, 298 K): δ 4.6 (SiMe₃), 34.9 (CMe₃), 35.5 (CMe₃), 59.5 (CMe₃), 65.8 (CMe₃), 125.8 (Ph), 126.0 (Ph), 126.8 (Ph), 128.9 (Ph), 129.6 (Ph), 129.8 (Ph), 130.7 (Ph), 131.9 (Ph), 133.4 (Ph), 134.5 (Ph), 135.4 (Ph), 178.2 (NCN). ¹¹B NMR (160.4 MHz, CDCl₃, 298 K): δ –0.45. ²⁹Si{¹H} NMR (99.36 MHz, CDCl₃, 298 K): δ 39.00 (Si(PhBCl₂)-Si(SiMe₃)₃), –9.00 (SiSi(SiMe₃)₃), –103.74 (SiSi(SiMe₃)₃).

Synthesis of 6 and 7. To the 10 mL toluene solution of **1** (0.200 g, 0.39 mmol) was slowly added a toluene (5 mL) solution of HBpin (0.051 g, 0.39 mmol) at room temperature, and the mixture was stirred for 12 h. The volatiles were removed in vacuum to obtain a sticky reaction mixture of **6** (54% yield) and **7** (24% yield). ¹H NMR of **6** (200 MHz, C₆D₆, 298 K): δ 0.46 (s, 27H, SiMe₃), 1.01 (s, 12H, Bpin), 1.24 (s, 18H, tBu), 7.00–7.12 (m, 5H, Ph). ¹¹B NMR (C₆D₆, 128.4 MHz, 298 K): δ 21.7. ²⁹Si{¹H} NMR (79.5 MHz, C₆D₆, 298 K): δ 76.87 (SiSi(SiMe₃)₃), –9.10 (SiSi(SiMe₃)₃), –115.97 (SiSi(SiMe₃)₃). ¹H NMR of **7** (200 MHz, C₆D₆, 298 K): δ 0.48 (s, 27H, SiMe₃), 1.20 (s, 18H, tBu), 1.32 (s, 12H, Bpin), 5.81 (s, 1H, NCHN), 7.13–7.15 (m, 2H, Ph), 7.25–7.27 (m, 2H, Ph), 7.83–7.84 (d, J = 7.93 Hz, 1H, Ph). ¹¹B NMR (C₆D₆, 128.4 MHz, 298 K): δ 37.7. ²⁹Si{¹H} NMR (79.5 MHz, C₆D₆, 298 K): δ –0.01 (Si(SiMe₃)₃), –59.97 (Si(Bpin)(SiMe₃)₃), –96.03 (SiSi(SiMe₃)₃).

Synthesis of 8. To the 10 mL toluene solution of **1** (0.200 g, 0.39 mmol) was added dropwise an 8 mL toluene solution of HBcat (0.048 g, 0.39 mmol) at –78 °C. The reaction mixture was slowly warmed to room temperature and stirred overnight. Upon completion, all of the volatiles were removed in vacuum and the residue was redissolved in toluene (10 mL). The filtrate was separated via cannula and supersaturated to obtain colorless crystals of **8** (0.065 g, 47% yield). Mp: 117–118 °C. ¹H NMR of **8** (200 MHz, CDCl₃, 298 K): δ 0.98 (s, 18H, tBu), 6.69–6.73 (m, 2H, catechol-Ph), 6.75–6.80 (m, 2H, catechol-Ph), 7.30 (d, ³J_{H-H} = 8.38 Hz, 2H, Ph), 7.51 (t, 2H, Ph), 7.63 (t, 1H, Ph). ¹³C{¹H} NMR (100.6 MHz, CDCl₃, 298 K): δ 30.5 (CMe₃), 56.3 (CMe₃), 109.1, 118.6, 126.9, 128.2, 129.7, 132.3, 150.6, 166.8 (NCN). ¹¹B NMR (CDCl₃, 160.4 MHz, 298 K): δ 14.1. ¹H NMR of **8'** (200 MHz, C₆D₆, 298 K): δ 0.46 (s, 27H, SiMe₃), 1.13 (s, 18H, tBu), 6.74–7.15 (m, 10H, Ph). ¹¹B NMR (C₆D₆, 128.4 MHz, 298 K): δ –12.4 (d, J = 184.28 Hz). ¹H NMR of **8''** (200 MHz, C₆D₆, 298 K): δ 0.48 (s, 27H, SiMe₃), 1.04 (s, 18H, tBu), 5.53 (t, 1H, Si-H), 6.74–7.15 (m, 10H, Ph). ¹¹B NMR (C₆D₆, 128.4 MHz, 298 K): δ 23.3.

Synthesis of 9. The solution of 4-fluorobenzaldehyde (0.073 g, 0.059 mmol) in toluene (10 mL) was added dropwise to a solution of **1** (0.300 g, 0.059 mmol) and pinacolborane (0.075 g, 0.059 mmol) in toluene (10 mL) at low temperatures (<–20 °C) via cannula. After 2 h, the ¹H NMR spectrum was recorded to confirm the formation of compound **9**. The solvent was concentrated to 5 mL and kept at –30 °C. Colorless crystals of **9** were obtained after 5 days (0.091 g, 45.5% yield). Mp: 192.0 °C. Anal. Calcd for C₃₇H₆₈BFN₂O₃Si₃: C, 58.54; H, 9.03; N, 3.69. Found: C, 56.78; H, 8.53; N, 4.23. ¹H NMR (400 MHz, C₆D₆, 298 K): δ 0.56 (s, 27H, SiMe₃), 0.91 (s, 18H, tBu), 1.21 (s, 12H, Bpin), 5.19 (d, ³J_{H-H} = 4.40 Hz, 1H, CH), 5.51 (d, ³J_{H-H} = 4.40 Hz, 1H, SiH), 6.86–6.92 (m, 5H, Ph), 6.94–7.03 (d, 2H, Ph), 7.51 (d, 2H, Ph). ¹³C NMR (100.6 MHz, C₆D₆, 298 K): δ 4.3 (SiMe₃), 24.5, 25.3 (Bpin-Me), 33.6, 34.0 (tBu), 54.9, 55.0 (CtBu), 73.6 (CH), 82.7 (pin(OCMe₂)), 114.8, 115.0, 125.5, 127.5, 129.2, 129.5, 137.8, 138.3, 141.8, 141.8, 153.3, 161.2, 165.8 (Ph), 163.6 (NCN). ¹⁹F NMR (376.6 MHz, C₆D₆, 298 K): δ –116.66. ²⁹Si{¹H} NMR (79.5 MHz, C₆D₆, 298 K): δ –107.87 (SiSi(SiMe₃)₃), –37.22 (Si(SiMe₃)₂), –3.33 (Si(SiMe₃)₃). ¹¹B NMR (128.4 MHz, C₆D₆, 298 K): δ 20.35 (C(O)Bpin).

Synthesis of 10. A solution of 4-fluorobenzaldehyde (0.088 g, 0.71 mmol) in toluene (10 mL) was added dropwise to a solution of **1'** (0.3 g, 0.71 mmol) and pinacolborane (0.091 g, 0.71 mmol) in toluene at a low temperature (<–20 °C), via cannula. After 2 h, a ¹H NMR spectrum was recorded indicating the formation of compound

10. The solvent was then reduced *in vacuo* to ~5 mL and stored at –30 °C in a freezer for 5 days to obtain colorless crystals of compound **10** (0.076 g, 40.6% yield). Mp: 204.6 °C. Anal. Calcd for C₃₄H₅₉BFN₃O₃Si₃: C, 60.78; H, 8.85; N, 6.25. Found: C, 58.98; H, 8.33; N, 7.01. ¹H NMR (400 MHz, C₆D₆, 298 K): δ 0.64 (s, 18H, SiMe₃), 1.00 (s, 12H, Bpin), 1.19 (s, 18H, tBu), 5.36 (d, ³J_{H-H} = 4.40 Hz, 1H, CH), 5.57 (d, ³J_{H-H} = 4.40 Hz, 1H, SiH), 6.55–6.57 (d, 2H, Ph), 6.79–6.91 (m, 5H, Ph), 7.64–7.67 (d, 2H, Ph). ¹³C NMR (100.6 MHz, C₆D₆, 298 K): δ 5.9 (SiMe₃), 24.4, 25.1 (Bpin-Me), 32.9 (tBu), 55.5 (CtBu), 69.9 (CH), 82.5 (pin(OCMe₂)), 115.1, 126.3, 127.6, 127.9, 128.0, 131.4, 139.0, 140.0, 153.0, 160.7 (Ph), 163.6 (NCN). ¹³C-DEPT NMR (100.6 MHz, C₆D₆, 298 K): δ 5.6 (SiMe₃), 24.1, 24.8 (Me), 32.5 (tBu), 69.6 (CH), 114.9, 126.4, 127.7, 128.1, 130.2, 131.0, 131.1, 133.2 (Ph). ¹⁹F NMR (376.6 MHz, C₆D₆, 298 K): δ –115.47 (s, 1F, Ar-F). ²⁹Si{¹H} NMR (79.5 MHz, C₆D₆, 298 K): δ –27.70 (SiN(SiMe₃)₂), 9.05 (N(SiMe₃)₂). ¹¹B NMR (128.4 MHz, C₆D₆, 298 K): δ 20.55 (C(O)Bpin). ESI-HRMS: calcd for C₃₄H₆₀BFN₃O₃Si₃ [M + H]⁺, *m/z* 671.39; found, *m/z* 672.4016.

■ ASSOCIATED CONTENT

Supporting Information

The Supporting Information is available free of charge at <https://pubs.acs.org/doi/10.1021/acs.inorgchem.0c03137>.

Crystal descriptions of **2–4** and **8–10**, details of theoretical calculations, and representative NMR spectra (PDF)

Accession Codes

CCDC 1895594–1895595, 1952529, 1952537, 1993346, and 2039629 contain the supplementary crystallographic data for this paper. These data can be obtained free of charge via www.ccdc.cam.ac.uk/data_request/cif, or by emailing data_request@ccdc.cam.ac.uk, or by contacting The Cambridge Crystallographic Data Centre, 12 Union Road, Cambridge CB2 1EZ, UK; fax: +44 1223 336033.

■ AUTHOR INFORMATION

Corresponding Author

Sakya S. Sen – *Inorganic Chemistry and Catalysis Division, CSIR-National Chemical Laboratory, Pashan, Pune 411008, India; Academy of Scientific and Innovative Research (AcSIR), Ghaziabad 201002, India; orcid.org/0000-0002-4955-5408; Email: ss.sen@ncl.res.in*

Authors

Milan Kumar Bisai – *Inorganic Chemistry and Catalysis Division, CSIR-National Chemical Laboratory, Pashan, Pune 411008, India; Academy of Scientific and Innovative Research (AcSIR), Ghaziabad 201002, India*

V. S. V. S. N. Swamy – *Inorganic Chemistry and Catalysis Division, CSIR-National Chemical Laboratory, Pashan, Pune 411008, India; Academy of Scientific and Innovative Research (AcSIR), Ghaziabad 201002, India*

K. Vipin Raj – *Academy of Scientific and Innovative Research (AcSIR), Ghaziabad 201002, India; Physical and Material Chemistry Division, CSIR-National Chemical Laboratory, Pashan, Pune 411008, India; orcid.org/0000-0002-7178-264X*

Kumar Vanka – *Academy of Scientific and Innovative Research (AcSIR), Ghaziabad 201002, India; Physical and Material Chemistry Division, CSIR-National Chemical Laboratory, Pashan, Pune 411008, India; orcid.org/0000-0001-7301-7573*

Complete contact information is available at:

<https://pubs.acs.org/doi/10.1021/acs.inorgchem.0c03137>

Author Contributions

^{||}M.K.B. and V.S.V.S.N.S. contributed equally to this work.

Notes

The authors declare no competing financial interest.

ACKNOWLEDGMENTS

The authors thank the Science and Engineering Research Board, India (Grant CRG/2018/000287), and CSIR-Focused Basic Research (FBR) (Grant MLP101026) for supporting this work. The authors also thank CSIR, India, for research fellowships to M.K.B., V.S.V.S.N.S., and K.V.R.

REFERENCES

- (1) (a) Protchenko, A. V.; Birjumar, K. H.; Dange, D.; Schwarz, A. D.; Vidovic, D.; Jones, C.; Kaltsoyannis, N.; Mountford, P.; Aldridge, S. A Stable Two-Coordinate Acyclic Silylene. *J. Am. Chem. Soc.* **2012**, *134*, 6500–6503. (b) Protchenko, A. V.; Schwarz, A. D.; Blake, M. P.; Jones, C.; Kaltsoyannis, N.; Mountford, P.; Aldridge, S. A Generic One-Pot Route to Acyclic Two-Coordinate Silylenes from Silicon(IV) Precursors: Synthesis and Structural Characterization of a Silylsilylene. *Angew. Chem., Int. Ed.* **2013**, *52*, 568–571. (c) Reiter, D.; Holzner, R.; Porzelt, A.; Altmann, P. J.; Frisch, P.; Inoue, S. Disilene–Silylene Interconversion: A Synthetically Accessible Acyclic Bis(silyl)silylene. *J. Am. Chem. Soc.* **2019**, *141*, 13536–13546.
- (2) (a) Hadlington, T. J.; Abdalla, J. A. B.; Tirfoin, R.; Aldridge, S.; Jones, C. Stabilization of a Two-Coordinate, Acyclic DiaminoSilylene (ADASI): Completion of the Series of Isolable DiaminoTetrylenes, E-(NR₂)₂ (E = group 14 element). *Chem. Commun.* **2016**, *52*, 1717–1720. (b) Jana, A.; Schulzke, C.; Roesky, H. W. Oxidative Addition of Ammonia at a Silicon(II) Center and an Unprecedented Hydrogenation Reaction of Compounds with Low-Valent Group 14 Elements Using Ammonia Borane. *J. Am. Chem. Soc.* **2009**, *131*, 4600–4601.
- (3) For selected references, see: (a) Sen, S. S.; Khan, S.; Roesky, H. W.; Kratzert, D.; Meindl, K.; Henn, J.; Stalke, D.; Demers, J.-P.; Lange, A. Zwitterionic Si-C-Si-P and Si-P-Si-P Four-Membered Rings with Two-Coordinate Phosphorus Atoms. *Angew. Chem., Int. Ed.* **2011**, *50*, 2322–2325. (b) Khan, S.; Michel, R.; Sen, S. S.; Roesky, H. W.; Stalke, D. A P₄ Chain and Cage from Silylene-Activated White Phosphorus. *Angew. Chem., Int. Ed.* **2011**, *50*, 11786–11789. (c) Xiong, Y.; Yao, S.; Brym, M.; Driess, M. Consecutive Insertion of a Silylene into the P₄ Tetrahedron: Facile Access to Strained SiP₄ and Si₂P₄ Cage Compounds. *Angew. Chem., Int. Ed.* **2007**, *46*, 4511–4513. (d) Wang, Y.; Szilvási, T.; Yao, S.; Driess, M. A bis(silylene)-stabilized diphosphorus compound and its reactivity as a monophosphorus anion transfer reagent. *Nat. Chem.* **2020**, *12*, 801–807. (e) Roy, M. M. D.; Ferguson, M. J.; McDonald, R.; Zhou, Y.; Rivard, E. A Vinyl Silylsilylene and its Activation of Strong Homo- and Heteroatomic Bonds. *Chem. Sci.* **2019**, *10*, 6476–6481.
- (4) (a) Metzler, N.; Denk, M. Synthesis of a Silylene–Borane Adduct and its Slow Conversion to a Silylborane. *Chem. Commun.* **1996**, 2657–2658. (b) Ghadwal, R. S.; Roesky, H. W.; Merkel, S.; Stalke, D. Ambiphilicity of Dichlorosilylene in a Single Molecule. *Chem. - Eur. J.* **2010**, *16*, 85–88. (c) Azhakar, R.; Tavčar, G.; Roesky, H. W.; Hey, J.; Stalke, D. Facile Synthesis of a Rare Chlorosilylene–BH₃ Adduct. *Eur. J. Inorg. Chem.* **2011**, *2011*, 475–477. (d) Jana, A.; Azhakar, R.; Sarish, S. P.; Samuel, P. P.; Roesky, H. W.; Schulzke, C.; Koley, D. Reactions of Stable Amidinate Chlorosilylene and [1 + 4]-Oxidative Addition of N-Heterocyclic Silylene with N-Benzylideneaniline. *Eur. J. Inorg. Chem.* **2011**, *2011*, 5006–5013. (e) Jana, A.; Leusser, D.; Objartel, I.; Roesky, H. W.; Stalke, D. A Stable Silicon(II) Monohydride. *Dalton Trans.* **2011**, *40*, 5458–5463. (f) Al-Rafia, S. M. I.; Malcolm, A. C.; McDonald, R.; Ferguson, M. J.; Rivard, E. Efficient Generation of Stable Adducts of Si(II) Dihydride using a Donor–Acceptor Approach. *Chem. Commun.* **2012**, *48*, 1308–1310. (g) Rodriguez, R.; Troadec, T.; Kato, T.; Saffon-Merceron, N.; Sotiropoulos, J.-M.; Baceiredo, A. Synthesis and Characterization of an Isolable Base-Stabilized Silacycloprop-1-ylidene. *Angew. Chem., Int. Ed.* **2012**, *51*, 7158–7161. (h) Inoue, S.; Leszczynska, K. An Acyclic Imino-Substituted Silylene: Synthesis, Isolation, and its Facile Conversion into a Zwitterionic Silimine. *Angew. Chem., Int. Ed.* **2012**, *51*, 8589–8593. (i) Mück, F. M.; Baus, J. A.; Bertermann, R.; Burschka, C.; Tacke, R. Lewis Acid/Base Reactions of the Bis(amidinato)silylene [iPrNC(Ph)NiPr]₂Si and Bis(guanidinato)silylene [iPrNC(NiPr₂)NiPr]₂Si with ElPh₃ (El = B, Al). *Organometallics* **2016**, *35*, 2583–2588. (j) Pahar, S.; Karak, S.; Pait, M.; Raj, K. V.; Vanka, K.; Sen, S. S. Access to Silicon(II)- and Germanium(II)-Indium Compounds. *Organometallics* **2018**, *37*, 1206–1213.
- (5) Tacke, R.; Ribbeck, T. Bis(amidinato)- and bis(guanidinato)-Silylenes and Silylenes with One Sterically Demanding Amidinato or Guanidinato Ligand: Synthesis and Reactivity. *Dalton Trans.* **2017**, *46*, 13628–13659.
- (6) Gackstatter, A.; Braunschweig, H.; Kupfer, T.; Voigt, C.; Arnold, N. N-Heterocyclic Silylenes in Boron Chemistry: Facile Formation of Silylboranes and Silaborinines. *Chem. - Eur. J.* **2016**, *22*, 16415–16419.
- (7) Braunschweig, H.; Bruckner, T.; Deisenberger, A.; Dewhurst, R. D.; Gackstatter, A.; Gartner, A.; Hofmann, A.; Kupfer, T.; Prieschl, D.; Thiess, T.; Wang, S. R. Reaction of Dihalodiboranes(4) with a N-Heterocyclic Silylene: Facile Construction of 1-Aryl-2-Silyl-1,2-Diborainanes. *Chem. - Eur. J.* **2017**, *23*, 9491–9494.
- (8) Suzuki, Y.; Ishida, S.; Sato, S.; Isobe, H.; Iwamoto, T. An Isolable Potassium Salt of a Borasilene–Chloride Adduct. *Angew. Chem., Int. Ed.* **2017**, *56*, 4593–4597.
- (9) Khoo, S.; Shan, Y.-L.; Yang, M.-C.; Li, Y.; Su, M.-D.; So, C.-W. B–H Bond Activation by an Amidinate-Stabilized Amidosilylene: Non-Innocent Amidinate Ligand. *Inorg. Chem.* **2018**, *57*, 5879–5887.
- (10) Li, J.; Liu, Y.; Kundu, S.; Keil, H.; Zhu, H.; Herbst-Irmer, R.; Stalke, D.; Roesky, H. W. Reactions of Amidinate-Supported Silylene with Organoboron Dihalides. *Inorg. Chem.* **2020**, *59* (12), 7910–7914.
- (11) Rosas-Sánchez, A.; Alvarado-Beltran, I.; Baceiredo, A.; Hashizume, D.; Saffon-Merceron, N.; Branchadell, V.; Kato, T. The Lightest Element Phosphoranylidene: NHC-Supported Cyclic Bor-ylidene–Phosphorane with Significant B = P Character. *Angew. Chem., Int. Ed.* **2017**, *56*, 4814–4818.
- (12) (a) Bisai, M. K.; Yadav, S.; Das, T.; Vanka, K.; Sen, S. S. Lithium Compounds as Single Site Catalysts for Hydroboration of Alkenes and Alkynes. *Chem. Commun.* **2019**, *55*, 11711–11714. (b) Bisai, M. K.; Das, T.; Vanka, K.; Sen, S. S. Easily Accessible Lithium Compound Catalyzed Mild and Facile Hydroboration and Cyanosilylation of Aldehydes and Ketones. *Chem. Commun.* **2018**, *54*, 6843–6846. (c) Bisai, M. K.; Pahar, S.; Das, T.; Vanka, K.; Sen, S. S. Transition Metal Free Catalytic Hydroboration of Aldehydes and Aldimines by Amidinato Silane. *Dalton Trans.* **2017**, *46*, 2420–2424. (d) Yadav, S.; Pahar, S.; Sen, S. S. Benz-amidinato Calcium Iodide Catalyzed Aldehyde and Ketone Hydroboration with Unprecedented Functional Group Tolerance. *Chem. Commun.* **2017**, *53*, 4562–4564. (e) Yadav, S.; Dixit, R.; Bisai, M. K.; Vanka, K.; Sen, S. S. Alkaline Earth Metal Compounds of Methylpyridinato beta-diketiminato Ligands and their Catalytic Application in Hydroboration of Aldehydes and Ketones. *Organometallics* **2018**, *37*, 4576–4584.
- (13) Khoo, S.; Shan, Y.-L.; Yang, M.-C.; Li, Y.; Su, M.-D.; So, C.-W. B–H Bond Activation by an Amidinate-Stabilized Amidosilylene: Non-Innocent Amidinate Ligand. *Inorg. Chem.* **2018**, *57*, 5879–5887.
- (14) Sen, S. S.; Hey, J.; Herbst-Irmer, R.; Roesky, H. W.; Stalke, D. Striking Stability of a Substituted Silicon(II) Bis(trimethylsilyl)amide and the Facile Si–Me Bond Cleavage without a Transition Metal Catalyst. *J. Am. Chem. Soc.* **2011**, *133*, 12311–12316.
- (15) Swamy, V. S. V. S. N.; Raj, K. V.; Vanka, K.; Sen, S. S.; Roesky, H. W. Silylene Induced Cooperative B–H Bond Activation and Unprecedented Aldehyde C–H Bond Splitting with Amidinate Ring Expansion. *Chem. Commun.* **2019**, *55*, 3536–3539.
- (16) Bisai, M. K.; Swamy, V. S. V. S. N.; Das, T.; Vanka, K.; Gonnade, R. G.; Sen, S. S. Synthesis and Reactivity of a Hypersilylsilylene. *Inorg. Chem.* **2019**, *58*, 10536–10542.

(17) Ishida, S.; Iwamoto, T.; Kira, M. Reactions of an Isolable Dialkylsilylene with Ketones. *Organometallics* **2010**, *29*, 5526–5534.

(18) Takahashi, S.; Sekiguchi, J.; Ishii, A.; Nakata, N. An Iminophosphonamido-chlorosilylene as a Strong σ -Donating NHSi Ligand: Synthesis and Coordination Chemistry. *Angew. Chem., Int. Ed.* **2020**, DOI: 10.1002/anie.202013622.

(19) Hadlington, T. J.; Szilvási, T.; Driess, M. Silylene–Nickel Promoted Cleavage of B–O Bonds: From Catechol Borane to the Hydroborylene Ligand. *Angew. Chem., Int. Ed.* **2017**, *56*, 7470–7474.

(20) Minakata, S.; Ohashi, S.; Amano, Y.; Oderaotoshi, Y.; Komatsu, M. Three-Component Coupling of a Silylene, Aldehydes and Electron-Deficient Acetylenes via 1,3-Dipolar Cycloaddition. *Synthesis* **2007**, *16*, 2481–2484.

(21) Calad, S. A.; Woerpel, K. A. Silylene Transfer to Carbonyl Compounds and Subsequent Ireland-Claisen Rearrangements to Control Formation of Quaternary Carbon Stereocenters. *J. Am. Chem. Soc.* **2005**, *127*, 2046–2047.

(22) Swamy, V. S. V. S. N.; Bisai, M. K.; Das, T.; Sen, S. S. Metal Free Mild and Selective Aldehyde Cyanosilylation by a Neutral Penta-coordinate Silicon Compound. *Chem. Commun.* **2017**, *53*, 6910–6913.

(23) Kepp, K. S. A Quantitative Scale of Oxophilicity and Thiophilicity. *Inorg. Chem.* **2016**, *55*, 9461–9470.

(24) Swamy, V. S. V. S. N.; Parvin, N.; Vipin Raj, K.; Vanka, K.; Sen, S. S. C(sp³)–F, C(sp²)–F and C(sp³)–H Bond Activation at Silicon(II) Centers. *Chem. Commun.* **2017**, *53*, 9850–9853.

(25) Sen, S. S.; Khan, S.; Kratzert, D.; Roesky, H. W.; Stalke, D. Reaction of a Base-Stabilized Bis(silylene) [PhC(NtBu)₂Si]₂ with Cyclooctatetraene without Cleavage of the Si–Si Bond. *Eur. J. Inorg. Chem.* **2011**, *2011*, 1370–1373.

(26) Tolentino, D. R.; Neale, S. E.; Isaac, C. J.; Macgregor, S. A.; Whittlesey, M. K.; Jazzar, R.; Bertrand, G. Reductive Elimination at Carbon under Steric Control. *J. Am. Chem. Soc.* **2019**, *141*, 9823–9826.

(27) Wendel, D.; Porzelt, A.; Herz, F. A. D.; Sarkar, D.; Jandl, C.; Inoue, S.; Rieger, B. From Si(II) to Si(IV) and Back: Reversible Intramolecular Carbon–Carbon Bond Activation by an Acyclic Iminosilylene. *J. Am. Chem. Soc.* **2017**, *139*, 8134–8137.

(28) Rodriguez, R.; Contie, Y.; Mao, Y.; Saffon-Merceron, N.; Baceiredo, A.; Branchadell, V.; Kato, T. Reversible Dimerization of Phosphine-Stabilized Silylenes by Silylene Insertion into Si^{II}-H and Si^{II}-Cl σ -Bonds at Room Temperature. *Angew. Chem., Int. Ed.* **2015**, *54*, 15276–15279.

(29) Rodriguez, R.; Contie, Y.; Nogue, R.; Baceiredo, A.; Saffon-Merceron, N.; Sotiropoulos, J.-M.; Kato, T. Reversible Silylene Insertion Reactions into Si-H and P-H σ -Bonds at Room Temperature. *Angew. Chem., Int. Ed.* **2016**, *55*, 14355–14358.

(30) (a) Leong, B.-X.; Lee, J.; Li, Y.; Yang, M.-C.; Siu, C.-K.; Su, M.-D.; So, C.-W. A Versatile NHC-Parent Silyliumylidene Cation for Catalytic Chemo- and Regioselective Hydroboration. *J. Am. Chem. Soc.* **2019**, *141*, 17629–17636. (b) Leong, B.-X.; Teo, Y.-C.; Condamines, C.; Yang, M.-C.; Su, M.-D.; So, C.-W. A NHC-Silyliumylidene Cation for Catalytic N-Formylation of Amines Using Carbon Dioxide. *ACS Catal.* **2020**, *10*, 14824–14833.

Cite this: *Dalton Trans.*, 2021, 50, 2354Received 1st February 2021,
Accepted 5th February 2021

DOI: 10.1039/d1dt00364j

rsc.li/dalton

Lithium compound catalyzed deoxygenative hydroboration of primary, secondary and tertiary amides†‡

Milan Kumar Bisai,^{a,b} Kritika Gour,^{a,b} Tamal Das,^{b,c} Kumar Vanka^{b,c} and Sakya S. Sen^{b,a}*

A selective and efficient route for the deoxygenative reduction of primary to tertiary amides to corresponding amines has been achieved with pinacolborane (HBpin) using simple and readily accessible 2,6-di-*tert*-butyl phenolate lithium-THF (1a) as a catalyst. Both experimental and DFT studies provide mechanistic insight.

Reduction of amide to amine is a very important transformation because (a) amides are readily available as precursors and (b) amines are essential building blocks in the synthesis of many pharmaceuticals, natural products, and agrochemicals.¹ The electrophilicity of the amide carbonyl group is considerably lower than that of aldehydes and ketones, which makes the reduction of amides a challenging task. A variety of noble and non-noble metal based catalysts have been developed for the catalytic hydrosilylation of amides to amines.² However, dwindling noble metal reserves and their skyrocketing prices have led to significant focus on the development of compounds containing main group elements as homogeneous catalysts driven by their high terrestrial abundances and low cost. Meanwhile, the synthetic usefulness of hydroboration has been demonstrated for the chemoselective reduction of aldehydes, ketones, pyridines, alkenes, alkynes and nitriles by compounds with main-group elements.³ However, the development of catalytic hydroboration for the reduction of amides to amines remains cursory and mainly limited to only secondary and tertiary amides (Scheme 1). The reduction of primary amides to amines groups is more difficult than that of secondary and tertiary amides. Sadow and coworkers reported the catalytic reduction of amides by HBpin using a magnesium compound.⁴ Panda and coworkers prepared an aluminum

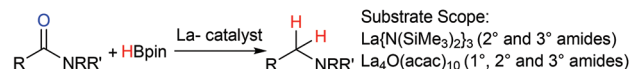
complex for amide hydroboration under ambient conditions.⁵ Lohr and Marks reported La[N(SiMe₃)₂]₃ catalyzed deoxygenative reduction of secondary and tertiary amides with HBpin,⁶ but reduction does not occur with the acetamide and benzamide. Nonetheless, Findlater and coworkers have recently shown that La₄O(acac)₁₀ can hydroborate 1°, 2° and 3° amides.⁷ Mandal and coworkers have also shown that the combination of an abnormal N-heterocyclic carbene and a potassium complex serve as an efficient cooperative catalyst for the hydroboration of a broad range of primary amides with HBpin.^{8a} Likewise, Yao and coworkers reported a combined KO^{*t*}Bu/BET₃ catalyst for the hydroboration of primary to tertiary amides.^{8b}

Lithium compounds are emerging as molecular catalysts, thanks to significant breakthroughs that have recently emerged from the groups of Okuda,^{9–11} Mulvey,^{12,13} Wangelin¹⁴ and others¹⁵ for the hydroboration of aldehydes, ketones, nitriles, and other organic substrates. We have been

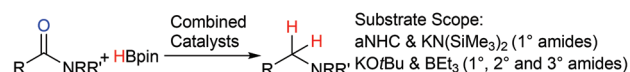
Amide hydroboration with main-group elements: Sadow,⁴ Panda⁵



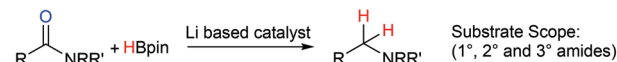
Amide hydroboration with lanthanides: Lohr and Marks⁶ & Findlater⁷



Amide hydroboration with combined main-group catalysts: Mandal^{8a} & Yao^{8b}



This work



Scheme 1 Previous approaches towards the hydroboration of amides to amines using single-site/combined catalysts involving main-group elements/lanthanides and the development of our strategy.

^aInorganic Chemistry and Catalysis Division, CSIR-National Chemical Laboratory, Dr Homi Bhabha Road, Pashan, Pune 411008, India. E-mail: ss.sen@ncl.res.in

^bAcademy of Scientific and Innovative Research (AcSIR), Ghaziabad-201002, India

^cPhysical and Material Chemistry Division, CSIR-National Chemical Laboratory, Dr Homi Bhabha Road, Pashan, Pune 411008, India

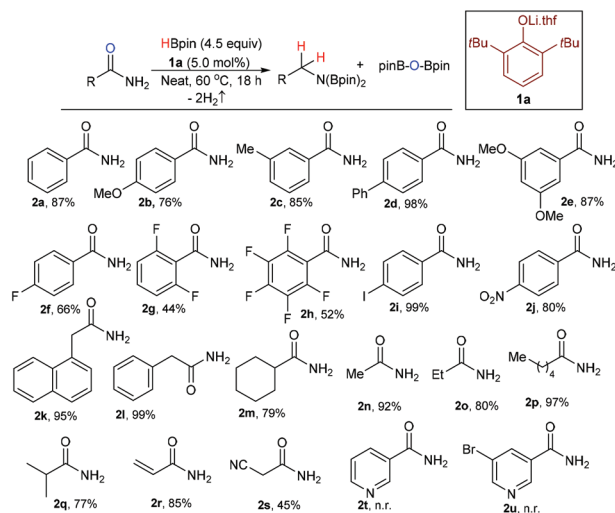
†Dedicated to Professor Herbert W. Roesky on the occasion of his 85th birthday.

‡Electronic supplementary information (ESI) available. See DOI: 10.1039/d1dt00364j

actively developing convenient methods for hydroboration of aldehydes, ketones, imines.^{16–18} We have demonstrated the use of readily accessible lithium compounds 2,6-di-*tert*-butyl phenolate lithium·THF (**1a**) and 1,1'-dilithioferrocene-TMEDA (**1b**) as catalysts for the reduction of aldehydes, ketones, alkenes, and alkynes.^{19,20} Herein, we report single-site chemo-selective hydroboration of 1°, 2° and 3° amides using HBpin in the presence of **1a**. However, a mixture of product formation was observed with **1b**.

A systematic study was carried out for the optimization of the catalytic reduction using benzamide as a model substrate with HBpin (see ESI, Table S1†). In the absence of any solvent, the reaction of benzamide (1 equiv., 0.25 mmol) and HBpin (4.5 equiv., 1.12 mmol) at 60 °C for 18 h in the presence of **1a** (5 mol%) afforded 87.0% of the corresponding borylamine (see entry 9, Table S1 in the ESI†). Although quantitative conversion of benzamide to the corresponding borylamine is achievable in the presence of 5 equiv. HBpin (entry 10), we have chosen entry 9 as the optimized condition to examine the electronic influence of the substituents. LiOtBu, LiCl, LiOPh and LiN(SiMe₃)₂ were also employed as the catalysts for comparison and afforded 68%, 48%, 45% and 66.5% yield, respectively for the hydroboration of benzamide in 18 h (see ESI, Table S1,† entries 11–14). Note that, the same reaction under catalyst free conditions produces only 55.0% yield in 20 h (see ESI, Table S1,† entry 15). Subsequently, the scope of the reaction was tested with a range of aromatic and aliphatic primary amides, and the corresponding borylated products were obtained in good to excellent yields (Scheme 2). Some of the corresponding borylated amines were converted to the corresponding primary amines and isolated as their hydrochloride salts upon hydrolysis and acidification. Smooth hydroboration was observed for the different aromatic amides with electron donating or withdrawing substituents at the *o*/*m*/*p* position (**2a–2j**). Under the optimized conditions, aromatic amides bearing electron-donating functional groups (Me, OMe, Ph, and I) provide better conversion compared to electron-withdrawing groups (F and NO₂). The catalyst shows very good tolerance towards the functional groups such as halogens (**2f–2i**), as well as alkoxy (**2b** and **2e**) and nitro (**2j**) containing substrates. Both electronic and steric influences was reflected on the moderate conversion of 2,6-difluorobenzamide (**2g**), and *per*fluorobenzamide (**2h**). No product formation was observed for the pyridine containing substrate such as nicotinamide (**2t**) and 3-bromo nicotinamide (**2u**), probably due to the coordination of the pyridine lone pair with HBpin.

It is of note here that the hydroboration of the aliphatic amides is also very important, as the aliphatic amines represent a privileged class in drug molecules. Herein, we employed the standard reaction conditions for the aliphatic amides bearing aromatic moiety such as 2-(naphthalen-1-yl)acetamide (**2k**) and 2-phenylacetamide (**2l**), and for both the cases, almost quantitative conversion of their corresponding borylated amines was observed. Furthermore, the cyclic (**2m**) and short to long chain aliphatic amides (**2n–2q**) were also tested and all of them afforded the desired products in good

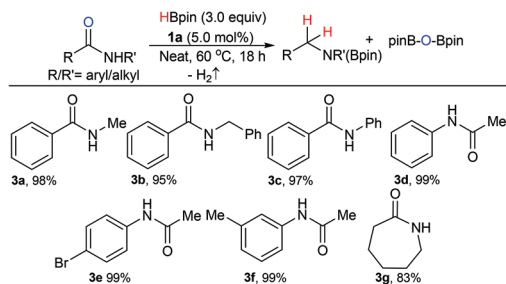


Scheme 2 Lithium compound catalyzed hydroboration of primary amides. Reaction conditions: Amide (0.25 mmol), HBpin (1.12 mmol, 4.5 equiv.), 5.0 mol% catalyst, 18 h reaction at 60 °C temperature in neat. Yields were determined by the ¹H NMR integration relative to mesitylene as an internal standard.

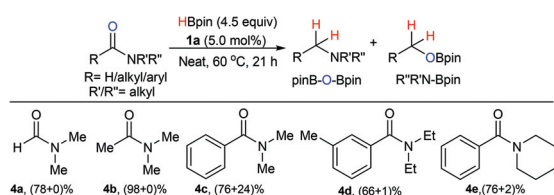
yields. Conjugated amides such as acrylamide (**2r**) undergo hydroboration in both the functional groups and form the same product as obtained from **2o**. However, in addition to amide hydroboration (45.0% yield), reduction of both cyano and amide functionality was also observed for **2s**, with 22.0% yield.

With good results in hand for the reduction of primary amides, the reactivity of secondary and tertiary amides was studied in the presence of **1a** under the optimized reaction conditions (Schemes 3 and 4). Here, *N*-methylbenzamide and *N,N*-dimethyl benzamide were employed as substrates for the optimization of secondary and tertiary amide hydroboration respectively (see ESI, entry 6, Table S3 and entry 6, Table S5† respectively). Similar to primary amide hydroboration, secondary amides also deoxygenated to secondary amines with subsequent release of dihydrogen in the presence of three equivalents of HBpin. Both aromatic and aliphatic *N*-alkyl or *N*-aryl substituted secondary amides (**3a–3h**) underwent hydroboration smoothly and formed the corresponding borylated secondary amines in good to excellent yields. Cyclic secondary amides, such as ϵ -caprolactam (**3g**), provide the corresponding borylated amine in good yield without suffering any polymerization.

The methodology works smoothly for the hydroboration of tertiary amide substrates as well. The slight excess of HBpin (4.5 equiv.) and longer reaction time (21 h) was found necessary to obtain good conversion over the selected temperature range and this was also noted by the groups by Lohr and Marks.⁶ In comparison to primary or secondary amides, moderate to good conversion was achieved for all five tertiary amides (**4a–4e**), probably due to greater steric around the nitrogen center. It is fair to mention here that selective formation of corresponding amine products was observed for all the sub-



Scheme 3 Scope of hydroboration with secondary amides. Reaction conditions: Amide (0.25 mmol), HBpin (0.75 mmol, 3.0 equiv.), 5.0 mol% catalyst, 18 h reaction at 60 °C temperature in neat.



Scheme 4 Scope of hydroboration with tertiary amides. Reaction conditions: Amide (0.25 mmol), HBpin (1.12 mmol, 4.5 equiv.), 5.0 mol% catalyst, 21 h reaction at 60 °C temperature in neat.

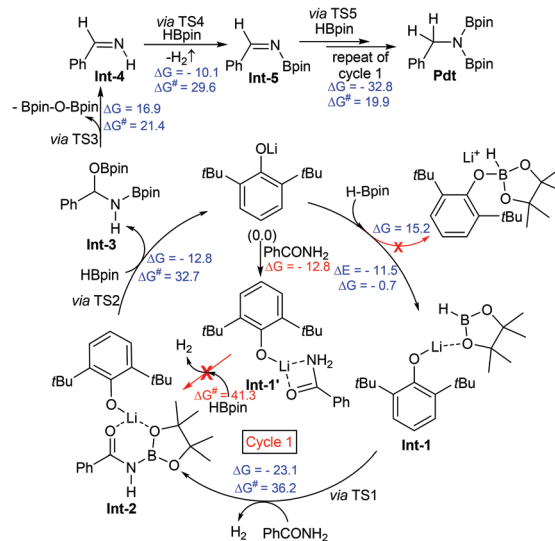
strates except *N,N*-dimethyl benzamide (**4c**), which produces both C–O and C–N bond cleavage product in 76.0% and 24.0% yield, respectively.

We have performed a series of stoichiometric reactions to gain mechanistic insight into primary amide hydroboration with **1a**. In the stoichiometric reaction of **1a** with benzamide in CDCl₃, a possible formation of **Int-1'** was observed at room temperature, as indicated by ¹H NMR spectroscopy. However, monitoring the reaction between **1a** and HBpin in toluene-d₈ showed a new set of resonance signals in ¹¹B NMR at δ 4.7 ppm, indicating the formation of an intermediate (**Int-1**)^{19,20} along with a singlet at δ 21.6 and a quintet at –39.8 ppm for a trialkoxyborane and BH₄[–] anion, respectively. In addition, a singlet at δ 86.9 and a quartet at –25.4 ppm were also observed, probably due to the decomposition of HBpin and the Lewis base–BH₃ adduct.^{21,22} Upon filtration of a white precipitate formed after 3–4 h, the filtrate part showed only three peaks at δ 4.7, 21.6 and –39.8 ppm in the ¹¹B NMR spectrum. The elimination of LiH would lead to the formation of both trialkoxyborane and LiBH₄, which was also observed by Thomas,^{21,22} Clark and coworkers.²³ However, due to the very high lattice energy and poor solubility, the involvement of LiH in the catalytic activity is very unlikely, which was also noted by the groups of Mulvey,¹² Thomas and Cowley.²⁴ Another set of reactions involving **1a**, HBpin and benzamide in toluene-d₈ showed a broad resonance at δ 3.8–3.5 ppm in ¹¹B NMR, indicating the possible formation of **Int-2** with the evolution of molecular dihydrogen. Also, to identify whether BH₃ was involved in hidden catalysis, as it may form by the decomposition of HBpin for the amide hydroboration,^{21,22} we have carried out the same reaction in the presence of

10 mol% TMEDA. Formation of the corresponding borylated amine with 73.0% yield for the benzamide substrate suggests negligible or low influence of BH₃ in catalysis (see ESI, Scheme S4†). Notably, although the evolution of molecular dihydrogen was observed for the non-catalytic reaction of benzamide and HBpin, the evolution was rapid in the presence of the catalyst and it was monitored by ¹H NMR resonance at δ 4.48 ppm (see ESI, Scheme S2†).⁷ Furthermore, the formation of *N*-borylated imine (**Int-5**) was detected with a sharp resonance in the ¹H NMR at δ 10.20 ppm, when hydroboration was carried out at room temperature in toluene, or by ceasing the standard heating reaction after 1 h (see ESI, Scheme S3†).⁷

Full quantum chemical calculations were done with density functional theory (DFT) at the dispersion corrected PBE/TZVP level of theory in order to understand the mechanism (Scheme 5 in the manuscript and Fig. S88 in the ESI†) of the primary amide hydroboration reaction in the presence of catalyst **1a**.

In the first step of the reaction, a weakly bound complex (**Int-1**) is formed between catalyst **1a** and HBpin, with one of the oxygen atoms of HBpin approaching towards the lithium atom of **1a** and making a weak coordinate bond. The first step of the mechanism is same as those reported for aldehyde, alkene or alkyne hydroboration.^{19,20} The reaction energy (ΔE) and the Gibbs free energy (ΔG) for this step are –11.5 kcal mol^{–1} and –0.7 kcal mol^{–1}, respectively. We cannot ignore the possibility of the binding of amide oxygen with the lithium atom of **1a**, which would lead to the formation of **Int-1'**. The corresponding reaction free energy for this step is favourable by 12.8 kcal mol^{–1}. Now, in the next step, either benzamide approaches the B–H bond of **Int-1** and makes a four-mem-



Scheme 5 The catalytic cycle and reaction mechanism for the benzamide hydroboration by catalyst **1a**, calculated at the PBE/TZVP level of theory with density functional theory (DFT). ΔG and ΔG^\ddagger represent the Gibbs free energy of reaction and the barrier, respectively. All values are in kcal mol^{–1}.

bered transition state **TS-1** involving N...H...H...B atoms where H₂ evolution takes place leading to the formation of **Int-2** with the free energy of activation barrier 36.2 kcal mol⁻¹, or HBpin approaches towards the N–H bond of **Int-1'** and similarly makes a four-membered transition state **TS-1'** involving N...H...H...B atoms, where H₂ extrusion occurs, leading to **Int-2**. The barrier for this step was calculated to be 41.3 kcal mol⁻¹ (shown in red in Scheme 5). During the experiments, we have observed the bubbling of H₂ gas in the initial phase of the reaction. Therefore, from our DFT calculations, we have excluded the H₂ evolution pathway *via* **TS-1'** due to the high energy barrier, which cannot be achieved under the reaction conditions. As the reaction proceeds through the **TS-1** pathway, in the next step, another molecule of HBpin comes towards the carbonyl group of **Int-2**. This is the prelude to the nucleophilic attack by the oxygen atom of the carbonyl group to the boron atom of HBpin, with the hydride being transferred to the carbonyl carbon atom of **Int-2**. This occurs through a four-membered transition state (**TS-2**) and leads to the formation of **Int-3**. The Gibbs free energy for this step is –12.8 kcal mol⁻¹, *i.e.*, the step is thermodynamically favourable. The activation free energy (ΔG^\ddagger) barrier corresponding to the transition state is 32.7 kcal mol⁻¹. Furthermore, the elimination of Bpin-O-Bpin from **Int-3** leads to the formation of the important intermediate imine (**Int-4**) *via* a four-membered transition state (**TS-3**) involving O...C...N...B atoms. The reaction free energy (ΔG) and the barrier (ΔG^\ddagger) for this step are 16.9 kcal mol⁻¹ and 21.4 kcal mol⁻¹, respectively. In the next step of the reaction, the imine (**Int-4**) reacts with a third molecule of HBpin, where the B–H bond of HBpin approaches towards the N–H bond of imine (**Int-4**), thereby making a four-membered transition state (**TS-4**) and leading to the formation of **Int-5** by evolution of one equivalent of H₂ gas. The reaction free energy (ΔG) and the barrier (ΔG^\ddagger) for this step are –10.1 kcal mol⁻¹ and 29.6 kcal mol⁻¹, respectively. In the last step of the reaction, **Int-5** reacts with a fourth molecule of HBpin, where the B–H bond of HBpin approaches towards the imine double bond of **Int-5**, making a four-membered transition state (**TS-5**) involving C...H...B...N atoms, which leads to the formation of Bpin substituted amine. In this case, both the B–H bond and the imine double bond activation takes place. The reaction free energy (ΔG) and the barrier (ΔG^\ddagger) for this step are –32.8 kcal mol⁻¹ and 19.9 kcal mol⁻¹, respectively. Further stepwise hydrolysis leads to the formation of final product benzylamine. The ΔG (–23.1 kcal mol⁻¹) value for the slowest step is significantly negative and the barrier corresponding to the transition state is 36.2 kcal mol⁻¹, which explains why the reaction takes place at 60 °C.

In summary, we have demonstrated the utility of easily accessible, cost effective and almost non-toxic lithium compounds for the catalytic hydroboration of a wide range of primary, secondary and tertiary amides. Furthermore, with the combined experimental and theoretical studies, we propose a mechanistic pathway, which reveals that the role of the lithium compound involves the binding of sterically demanding Lewis acids to one of the Lewis basic O atoms of HBpin, thereby

setting up a platform for the HBpin to offer its B–H bond to the unsaturated amide functionality.

Conflicts of interest

There are no conflicts to declare.

Acknowledgements

Science and Engineering Research Board (SERB), India (CRG/2018/000287) and Council of Scientific and Industrial Research (YSA000726) (SSS) are acknowledged for providing financial assistance. MKB, KG and TD thank CSIR, India for their research fellowships. The support and the resources provided by 'PARAM Brahma Facility' under the National Supercomputing Mission, Government of India at the IISER Pune are gratefully acknowledged.

Notes and references

- 1 A. Ricci, in *Amino Group Chemistry. From Synthesis to the Life Sciences*, ed. A. Ricci, Wiley-VCH: Weinheim, Germany, 2008.
- 2 (a) S. Hanada, E. Tsutsumi, Y. Motoyama and H. Nagashima, *J. Am. Chem. Soc.*, 2009, **131**, 15032–15040; (b) S. Park and M. Brookhart, *J. Am. Chem. Soc.*, 2012, **134**, 640–653; (c) C. Cheng and M. Brookhart, *J. Am. Chem. Soc.*, 2012, **134**, 11304–11307; (d) D. Addis, S. Das, K. Junge and M. Beller, *Angew. Chem.*, 2011, **123**, 6004–6011; (e) S. Das, Y. Li, K. Junge and M. Beller, *Chem. Commun.*, 2012, **48**, 10742–10744; (f) Y. Sunada, H. Kawakami, T. Imaoka, Y. Motoyama and H. Nagashima, *Angew. Chem., Int. Ed.*, 2009, **48**, 9511–9515; (g) S. Das, B. Wendt, K. Möller, K. Junge and M. Beller, *Angew. Chem., Int. Ed.*, 2012, **51**, 1662–1666; (h) M. G. Manas, L. S. Sharninghausen, D. Balcells and R. H. Crabtree, *New J. Chem.*, 2014, **38**, 1694–1700.
- 3 For a recent review: (a) M. L. Shegavi and S. K. Bose, *Catal. Sci. Technol.*, 2019, **9**, 3307–3336; (b) A. Sadow, Alkali and Alkaline Earth Element-Catalyzed Hydroboration Reactions, in *Early Main Group Metal Catalysis: Concepts and Reactions*, ed. S. Harder, Wiley-VCH Verlag GmbH, 2020.
- 4 N. L. Lampland, M. Hovey, D. Mukherjee and A. D. Sadow, *ACS Catal.*, 2015, **5**, 4219–4226.
- 5 S. Das, H. Karmakar, J. Bhattacharjee and T. K. Panda, *Dalton Trans.*, 2019, **48**, 11978–11984.
- 6 C. J. Barger, R. D. Dicken, V. L. Weidner, A. Motta, T. L. Lohr and T. J. Marks, *J. Am. Chem. Soc.*, 2020, **142**, 8019–8028.
- 7 S. R. Tamang, A. Singh, D. Bedi, A. R. Bazkiaei, A. A. Warner, K. Glogau, C. McDonald, D. K. Unruh and M. Findlater, *Nat. Catal.*, 2020, **3**, 154–162.
- 8 (a) M. Bhunia, S. R. Shao, A. Das, J. Ahmed, P. Sreejyothi and S. K. Mandal, *Chem. Sci.*, 2020, **11**, 1848–1854;

- (b) W. Yao, J. Wang, A. Zhong, S. Wang and Y. Shao, *Org. Chem. Front.*, 2020, 7, 3515–3520.
- 9 D. Mukherjee, H. Osseili, T. P. Spaniol and J. Okuda, *J. Am. Chem. Soc.*, 2016, 138, 10790–10793.
- 10 H. Osseili, D. Mukherjee, K. Beckerle, T. P. Spaniol and J. Okuda, *Organometallics*, 2017, 36, 3029–3034.
- 11 H. Osseili, D. Mukherjee, T. P. Spaniol and J. Okuda, *Chem. – Eur. J.*, 2017, 23, 14292–14298.
- 12 R. McLellan, A. R. Kennedy, R. E. Mulvey, S. A. Orr and S. D. Robertson, *Chem. – Eur. J.*, 2017, 23, 16853–16861.
- 13 L. E. Lemmerz, R. McLellan, N. R. Judge, A. R. Kennedy, S. A. Orr, M. Uzelac, E. Hevia, S. D. Robertson, J. Okuda and R. E. Mulvey, *Chem. – Eur. J.*, 2018, 24, 9940–9948.
- 14 P. Ghosh and A. J. v. Wanglein, *Org. Chem. Front.*, 2020, 7, 960–966.
- 15 (a) D. Yan, X. Wu, J. Xiao, Z. Zhu, X. Xu, X. Bao, Y. Yao, Q. Shen and M. Xue, *Org. Chem. Front.*, 2019, 6, 648–653; (b) T. K. Panda, I. Banerjee and S. Sagar, *Appl. Organomet. Chem.*, 2020, 34, e5765, 1–10. (c) B. Yan, X. He, C. Ni, Z. Yang and X. Ma, *ChemCatChem*, 2021, 13, 851–854.
- 16 S. Yadav, S. S. Pahar and S. S. Sen, *Chem. Commun.*, 2017, 53, 4562–4564.
- 17 S. Yadav, R. Dixit, M. K. Bisai, K. Vanka and S. S. Sen, *Organometallics*, 2018, 37, 4576–4584.
- 18 M. K. Bisai, S. Pahar, T. Das, K. Vanka and S. S. Sen, *Dalton Trans.*, 2017, 46, 2420–2424.
- 19 M. K. Bisai, T. Das, K. Vanka and S. S. Sen, *Chem. Commun.*, 2018, 54, 6843–6846.
- 20 M. K. Bisai, S. Yadav, T. Das, K. Vanka and S. S. Sen, *Chem. Commun.*, 2019, 55, 11711–11714.
- 21 A. D. Bage, T. A. Hunt and S. P. Thomas, *Org. Lett.*, 2020, 22, 4107–4112.
- 22 A. D. Bage, K. Nicholson, T. A. Hunt, T. Langer and S. P. Thomas, *ACS Catal.*, 2020, 10, 13479–13486.
- 23 I. P. Query, P. A. Squier, E. M. Larson, N. A. Isley and T. B. Clark, *J. Org. Chem.*, 2011, 76, 6452–6456.
- 24 A. Bismuto, M. J. Cowley and S. P. Thomas, *ACS Catal.*, 2018, 8, 2001–2005.